United States
Department of
Agriculture

Agricultural
Research
Service

Plum Island Animal Disease Center

Foreign Animal Disease Research Unit

Research Publications 2013

Foreign Animal Disease Research Unit
Plum Island Animal Disease Center
Luis L. Rodriguez, Research Leader

Foreword

"The science of today is the technology of tomorrow"

Edward Teller

Once again, I have the honor of presenting the collection of scientific publications by scientists and collaborators of the Foreign Animal Disease Research Unit (FADRU) at the Plum Island Animal Disease Center published in 2013. This year, as previous ones, was marked by significant achievements in the fields of pathogenesis, immune response and functional genomics of foot-and-mouth disease virus (FMDV) and classical swine fever virus (CSFV). However, FADRU scientists also made important contributions to understanding the pathogenesis of African Swine Fever Virus (ASFV). Research on this important pathogen, raging through the Caucasus region and threatening Europe's swine industry, was reinitiated at PIADC in 2010. An important aspect of ASFV is the fact that to date, there are no effective vaccines against this deadly disease of pigs. Furthermore, current methodology for vaccine evaluation in animals by challenge consists of intramuscular injection, a very unnatural route of infection. The work of Howey et. al. under the supervision of Dr. J. Arzt and Dr. M. Borca, showed that intra-naso-pharyngeal (INP) inoculation resulted in the most consistent progression of disease across the widest range of doses while preserving simulation of natural exposure. This route is proposed as a superior challenge system for pathogenesis and vaccine efficacy investigation. There were several manuscripts making important contributions to the understanding of FMDV pathogenesis using functional genomics approaches. Two examples of this are the description of FMDV protein 2C interactions with host proteins and their role in viral pathogenesis (Gladue et al) and the role of viral protein 3A in virulence to cattle (Pacheco et al). Other virus-host interactions of FMDV including receptor interactions (Lawrence et al) as well as the functional analysis of the leader protein (Uddowla et al) were also described. In the field of viral immunology there were important contributions including studies of the heterogeneity of the antibody response to vaccination in cattle of different genetic background (diGiacomo et al) as well as descriptions of cellular immune responses to FMD vaccination and infection in swine (Patch et al.) and protective innate responses induced by vector-delivered interferon genes in swine (Diaz-San Segundo et al). Finally, a bioinformatics approach to understanding FMDV tissue tropism based on differential gene expression was described by Zhu et al. This comprehensive study sets the stage for hypothesis driven research

addressing the molecular basis that not only define FMD as a disease but could also provide the evidence for development more effective countermeasures. The continued success of he FADRU research program would not have been possible without the strong support of the Department of Homeland Security Science and Technology Directorate. They not only provided all the necessary logistical support in terms of facilities and operational support, but also provided important support through various inter-agency agreement sin direct support of the research mission.

FADRU OVERVIEW

Foreign animal diseases such as foot-and-mouth disease, classical swine fever and African swine fever pose a major burden on the livelihoods of millions of people around the world, mostly in impoverished areas without adequate means to control them. Further, when these diseases incur into disease-free countries their economic and social impacts are immense and their control and eradication often involves the destruction of millions of animals, most of which may not even be infected. The mission of the USDA-ARS Foreign Animal Disease Research Unit (FADRU) at Plum Island is to carry out the research needed to understand the pathogenesis and the host response to foreign animal disease agents, and to translate this knowledge into useful interventions such as new diagnostic tools and vaccines for effective outbreak response, control and eradication.

This mission is accomplished by carrying out basic and applied research directed toward:

- understanding the genomic structure, viral factors determining virulence
- determining the pathogenesis and mechanism of defense and host resistance in livestock
- understanding the evolution and field epidemiology of FAD agents
- developing effective disease control strategies including novel agent detection methods, better vaccines, antiviral drugs and biotherapeutics

The collection of scientific publications presented here represents the product of FADRU scientist's research efforts over the past year (2012). This scientific knowledge is needed to develop better and more effective tools to prevent and control FAD. Other products include patents for inventions and funded research grants obtained by several FADRU researchers. Over the last year the FADRU also had a strong presence in international meetings and expert forums

on FAD, vaccines and animal health. Our international presence is also strong with ongoing research collaborations with over a dozen countries including: Argentina, Australia, Cameroon, India, Israel, Mexico, Pakistan, R. Georgia, Russia, Spain, South Africa, Uganda, UK, and Vietnam. This is the result of increased effort to connect our scientific program to the rest of the world, increase our international presence, leverage our resources and increase opportunities to apply our research to provide solutions to real-world situations.

2013 Highlights

- **Examination of Soluble Integrin Resistant Mutants of Foot-and-Mouth Disease Virus (FMDV):** In this study, we examined the effect of soluble foot-and-mouth disease virus (FMDV) receptor in the inhibition of virus growth in cell culture. We demonstrated that in the presence of soluble receptor FMDV mutants resistant to neutralization by soluble secreted bovine avb6 integrin could be selected. FMDV receptor resistant mutants were examined to determine the location of mutations in the virus capsid protein and to determine changes in receptor tropism, sensitivity to neutralization by the soluble receptor, and the established mode of entry into the cells.

- **Epidemiological Analysis, Serological Prevalence, and Genotypic Analysis of Foot-and-Mouth Disease in Nigeria 2008-2009**: Foot and mouth disease virus (FMDV) causes a highly contagious and economically devastating disease of cloven-hooved animals that affects the livelihoods of millions of people in some of the poorest regions of the world. Control of FMDV is a challenge due to the large genetic and antigenic variation which has led to the identification of seven FMDV serotypes, referred to as A,O,C, South African Territories (SAT) 1, SAT 2, SAT 3 and Asia 1; and multiple subtypes within each serotype. Each serotype requires a different vaccine to confer protection. Furthermore, little to no cross protection is also observed among subtypes within the same serotype, requiring that each region develops detailed knowledge of circulating strains of virus to find vaccines that are affective against them. Six FMDV serotypes (A, O, C, and the SATs) have been identified in Africa but submissions of FMDV samples to international reference laboratories for characterization are sporadic and knowledge of vaccine coverage for circulating strains is lacking. This study describes the genetic and epidemiological characterization of FMDV serotypes and strains circulating in Nigeria in recent years. Antibodies to five FMDV serotypes, (A, O, SAT1, SAT2 and SAT3) were detected in animals. This is the first report of the presence of FMDV SAT3 in Nigeria. Tissue samples collected from clinical cases in 2008-2009 were positive only for FMDV serotype A indicating that this serotype dominated in this period. This study provides knowledge on the epidemiological situation of FMD in Nigeria, and will ultimately help to develop effective control and preventive strategies for the disease in Nigeria and other countries in the West African sub region.

- **Theiler's Murine Encephalomyelitis Virus Contrasts with Encephalomyocarditis and Foot-and-Mouth Disease Viruses in its Functional Utilization of the StopGo Non-Standard Translation Mechanism**: Foot-and-mouth disease virus (FMDV) is a member of a group of viruses called "Picornaviruses". These viruses replicate inside the cell through the expression of a single polyprotein that is cleaved by viral proteins called proteases. In FMDV, an early cleavage event releases the capsid proteins (those protecting the viral RNA) along with a short protein called 2A by process known as 'StopGo'. Using genetic and biochemical analysis, we demonstrated the indispensability of the StopGo function for FMDV infectivity. That was not the case for Theiler's murine encephalomyelitis virus, another picornavirus from mice. This research identified parts of the protein 2A involved in the StopGo process that could be suitable targets for

antiviral interventions against FMDV disease for 6 days when challenged 24 hours post treatment by direct inoculation in the tongue with FMDV A24 Cruzeiro. Such protection was significantly improved –no disease until day 9- when treated cattle were challenged by an aerosol route with FMDV O1 Manisa. These results suggest that, in cattle, boIFNlambda3 plays a critical role in the innate immune response against infection with FMDV.

- **Venezuelan Equine Encephalitis Virus Replicon Particles can Induce Rapid Protection against Foot-and-Mouth Disease Virus:** Foot-and-Mouth Disease Virus (FMDV) is a variable virus consisting of 7 serotypes and multiple subtypes each requiring a separate vaccine to achieve protection. Vaccines produced by chemical inactivation of virus are available, but there are concerns about their safety and they do not induce protection prior to about 7 days post vaccination. In the event of an FMD outbreak in a disease-free country such as the U.S., it is necessary to induce immediate protection in order to limit or inhibit disease spread prior to induction of vaccine induced immunity. Production of interferons (IFNs) is the first host response to viral infection and it can rapidly control pathogen replication. We have previously constructed an adenovirus vector containing the gene for porcine type I IFN (Ad5-poIFNalpha) and demonstrated that swine inoculated with this vector are protected when challenged 1 day later with FMDV serotypes A24, O1 Manisa, or Asia-1. However, a relatively high dose of Ad5-poIFNalpha vector is required to induce protection. In this study we examined the potential of another rapid inducer of the host protective response. Venezuelan Equine Encephalitis Virus (VEE) replicon particles (VRPs) can induce a rapid protective response in cell culture and can protect mice against VEE and influenza virus infection. We found VRPs rapidly inhibit FMDV replication in cell culture. Furthermore, in an FMDV mouse model VRP pretreatment resulted in survival of all mice after challenge, while all nontreated mice died. These results suggest that it would be worthwhile to test the efficacy of VRP-poIFNalpha and VRP-bovine IFNalpha in naturally susceptible animals.

- **An Adenovirus Vectored Mucosal Adjuvant Augments Protection of Mice Immunized Intranasally with an Adenovirus-Vectored Foot-and-Mouth Disease Virus Subunit Vaccine**: Foot-and-mouth disease virus (FMDV) is an antigenically variable virus consisting of 7 serotypes and multiple subtypes and causes an economically devastating disease of cloven-hoofed animals. FMDV is a mucosal pathogen that enters the animal via the respiratory route.
  Vaccines produced by chemical inactivation of virus and a novel subunit vaccine which contains the coding region for the viral structural proteins but does not contain infectious FMDV are available. This subunit vaccine is delivered by a replication-defective human adenovirus (Ad5-FMD). Although both vaccines are effective in protecting animals neither induces mucosal immunity and therefore virus replication occurs at the initial site of FMDV infection. To address this limitation we cloned various mucosal adjuvants into the Ad5 vector. Mice vaccinated with the Ad5-FMD vaccine and the Ad5-adjuvant vector survived challenge with a lethal dose of FMDV and did not develop viremia, while mice given only the Ad5-FMD vaccine did not survive. These results suggest that induction of

mucosal immunity may enhance the protective effect of an FMD vaccine by blocking virus replication at the initial site of infection.

- **A Continuous Bovine Kidney Cell Line Constitutively Expressing Bovine Alpha v Beta 6 Integrin has Increased Susceptibility to Foot-and-Mouth Disease Virus**: Foot and mouth disease virus (FMDV) is highly contagious and can cause severe morbidity and mortality in livestock. Effective vaccines do currently exist for FMDV, but they are serotype-specific and do not confer long-term protection. Thus, the rapid detection and serotype determination of a circulating virus during an FMDV outbreak is critical to enable protective intervention to stop the spread of disease. FMDV is normally isolated from tongue tissue or vesicular lesions of infected animals by disrupting and filtering the tissues, then inoculating this filtrate onto susceptible cell culture. Historically, the most susceptible cells to field isolates of FMDV have been primary cells made directly from animal organs such as kidneys or thyroids, but these cells cannot be maintained in cell culture for more than a few days and lose their FMDV susceptibility after cryopreservation. To save resources, many laboratories use continuous cell lines for FMDV detection in clinical isolates but these cell lines are markedly less sensitive to FMDV field isolates, likely due to a lack of FMDV-specific receptors. In order to combine the high FMDV sensitivity of primary cells and the long-term stability of cell lines, we created a bovine kidney cell line that stably expresses a high-affinity FMDV receptor, the integrin alpha v Beta 6. These cells, designated LFBK- alpha v Beta 6, support the replication of all serotypes of FMDV from experimentally infected animals and can detect some FMDV strains with a tenfold higher sensitivity than even primary cells. LFBK- alpha v Beta 6 had excellent performance in a diagnostic setting, detecting field isolates of FMDV both quicker and more efficiently than other cell lines and a primary cell line. LFBK- alpha v Beta 6 cells also were able to detect other vesicular disease viruses, providing a more complete diagnostic result. The use of this cell line in a foreign animal disease diagnostic setting will add to the arsenal of tools for rapid vesicular disease virus detection and will help to reduce the use of animals for the production of primary cell cultures.

- **Repeated Exposure to 5D9, and Inhibitor of 3D Polymerase, Effectively Limits the Replication of Foot-and-Mouth Disease Virus in Host Cells:** Foot-and-mouth disease virus (FMDV) is the causal agent of an economically devastating disease affecting food animals (e.g. cattle, pigs). Besides the use of vaccines, there is no other therapeutic treatment approved for controlling the disease. Antivirals have been tested in the past with limited success due to the ability of the virus to easily mutate and escape the antiviral inhibition. In this study, we have examined the outcome of long-term exposure to the antiviral compound 5D9 that targets the viral 3D polymerase. This study builds up from the knowledge gained on our previous published work (Durk et al 2010) showing that 5D9 can inhibit FMDV infection in cells. Biological and biochemical assays demonstrated the lack of selection of escape mutants following treatment with 5D9 under the experimental conditions. Further efforts are warranted to test this compound in animals toward the development of an antiviral strategy against FMD.

- **Foot-and-Mouth Disease Virus Modulates Cellular Vimentin for Virus Survival**: Foot-and-mouth disease virus (FMDV) is the causative agent of foot-and-mouth disease. During infection with FMDV, the cell presents several areas where virus replication takes place. In these areas one of the virus proteins, 2C, appears to have multiple roles during virus replication. To better understand the role of 2C in the process of virus replication, we have been using a specific methodology, yeast two-hybrid, to identify cell host proteins that interact with virus 2C. Here, we report that a cellular protein, vimentin, specifically interacts with 2C. The 2C-vimentin interaction was confirmed to occur in cells infected with FMDV by using two different independent additional methodologies (co-immunoprecipitation and fluorescent microscopy). Manipulation of intracellular levels of vimentin showed that reduced levels of vimentin resulted in a significant decrease in viral yield, indicating that vimentin plays an important role in the replication cycle of FMDV. The use of Acrylamide, which causes disruption of intracellular vimentin filaments, also inhibited viral yield in FMDV infected cells. We also identified the areas of 2C being critical for vimentin binding. It also showed that the integrity of those areas in 2C are necessary for virus growth, suggesting that the interaction between FMDV 2C and cellular vimentin is essential for virus replication.

- **Analysis of SAT type Foot-and-Mouth Disease Virus Capsid Proteins and the Identification of Putative Amino Acid Residues in Virus Stability**: For reasons not well understood the South African Territory (SAT) FMDVs are difficult to adapt to tissue culture and typically render low amounts of stable antigen on formulated vaccines. In this study, we investigated the behavior and characterized SAT virus particles exposed to various environmental conditions. This is the first report that describes the identification of capsid determinants implicated in the stability of SAT viruses. Our findings are relevant as they could aid in the development of improved FMD vaccines, engineered to harbor these particular capsid modifications.

- **Mechanisms of Foot-and-Mouth Disease Virus Tropism Inferred from Differential Tissue Gene Expression**: Foot-and-mouth disease is a devastating disease of livestock caused by a virus (FMDV). In cattle, the virus targets specific sites to start the infection (primary sites) and then it spreads throughout the body via the bloodstream causing lesions at specific sites i.e. feet and mouth. After lesions heal, the virus can persist at the same sites where infection started. Why the virus targets these sites remains unknown. We utilized gene expression profiling to identify genes differentially expressed between FMDV-targeted and not targeted tissues and applied bioinformatics and statistical analyses to identify biological pathways\networks that could explain FMDV tissue tropism. Based on the knowledge in antiviral innate immunity and FMDV receptors, our results indicate that FMDV tissue tropism is strongly associated with differential expression of genes involved in non-specific (innate) immune responses, cell attachments, cell apoptosis, and cytokine signaling. Therefore, we hypothesize based our results that differences in the accessibility of cell receptors to FMDV, permissiveness for virus replication, and effectiveness in the clearance of infected cells play roles in determining FMDV tissue tropism. Understanding the mechanisms of disease will help design better vaccines.

- **Cell Mediated Innate Responses of Cattle and Swine are Diverse during Foot-and-Mouth Disease Virus (FMDV) Infection: A Unique Landscape of Innate Immunity:** Pathogens in general and pathogenic viruses in particular have evolved a myriad of mechanisms to escape the immune response of mammalian species. Viruses that cause acute disease and are rapidly cleared tend to bear characteristics that make them very contagious, as survival does not derive from chronicity of infection, but spread of disease throughout the herd. Foot-and-mouth disease virus (FMDV) is one of the most contagious viruses known. Upon infection of susceptible species, cloven-hoofed animals, the virus proliferates rapidly and causes a vesicular disease within 2-4 days. Disease symptoms resolve by 10 days to 2 weeks and in most cases, virus can no longer be detected. Periods of fever and viremia are usually brief, 1 to 3 days. In vivo control of virus infection and clearance of the virus during and following acute infection is of particular interest. The interaction of this virus with cells mediating the early, innate immune response has been analyzed in a number of recent studies. In most reports, the virus has a distinct inhibitory effect on the response of cells early in infection. Here we review these new data and discuss the dynamics of the interaction of virus with different cell types mediating the response to infection.

- **Foot-and-Mouth Disease Virus L Peptidase**: Foot-and-mouth disease virus (FMDV), equine rhinitis A virus (ERAV) and bovine rhinitis B virus (BRBV) comprise the genus Aphthovirus of the Picornaviridae family. Seven genera within this family, Aphthoviruses, Cardioviruses, Erboviruses (ERBV), Kobuviruses, Senecaviruses, Sapeloviruses, and Teschoviruses encode a leader (L) protein. The FMDV L-protein was originally identified as a papain-like proteinase by sequence homology and demonstration of catalytic activity. ERAV, BRBV, and ERBV L-proteins also have proteinase activity, whereas L proteins from the other Picornaviridae genera are proteolytically inactive. For FMDV there are two in-frame AUG codons at the beginning of the viral genome open reading frame, resulting in the synthesis of two L-proteins, Lab and Lb. Lb, the smaller of the two proteins, is the major synthesized species, and its sequence is highly conserved among the FMDV subtypes and serotypes. The ERAV and BRBV genomes also possess in-frame start sites in a similar position to the FMDV AUG codons. In contrast to FMDV, for ERAV the larger of the two L proteins, Lab, is the predominant species, while for BRBV, like for FMDV, the smaller Lb is the major protein found in infected cells. The active site residues of FMDV L proteinase have been identified and its crystal structure and solution structure have been determined at high resolution. A number of studies have contributed to the understanding of the role of L in virus replication. A genetic variant of FMDV, lacking the L protein coding region, was constructed and was significantly attenuated in naturally susceptible animals suggesting that while L is not required for growth in tissue culture it has a role in interacting with the host. The FMDV L protein has a number of functions related to blocking the host innate immune response including, 1) cleavage of the translation initiation factor eIF4G, 2) involvement in the cleavage of the transcription factor NF-kappaB, 3) degradation of the transcription factors interferon regulatory factors 3 and 7, and 4) ubiquitin (Ub)-protease activity responsible for removal of Ub moieties from cellular targets. In summary the FMDV L protein is a virulence

factor, or as recently defined a security protein, that has evolved multiple mechanisms to block the host response to viral infection.

- **Characterization of Cytotoxic T Lymphocyte Function following Foot-and-Mouth Disease Virus Infection and Vaccination:** Infection of livestock species with foot-and-mouth disease virus (FMDV) can be economically devastating as outbreaks in disease free countries can lead to strict quarantine of susceptible species and eventual cull and slaughter of exposed animals. Vaccines have become critical to control of disease following outbreaks as well as eradication of disease. The adaptive immune response to vaccination can be separated into two arms, the humoral or antibody response and the cellular response. Immunity to viral infection is commonly very dependent on the cellular immune response however the response to FMDV has been historically focused on neutralizing (virus blocking) antibody responses. The cellular immune response has been much more difficult to assess. We report vaccination strategies to induce the humoral or cellular response separately so we can determine the contribution of these different responses in protecting animals from infection. The experimental FMDV vaccine, vectored by human replication defective adenovirus 5, induces strong humoral immune responses but no cellular immunity. An altered Ad5-FMDV construct induces cellular immune responses and poor humoral immunity. Now, for the first time, we now show that the cellular response to FMDV, in the absence of significant humoral immunity, reduces clinical disease, most notably blocking virus spread via blood in animals challenged with live virus. This approach reveals the effect of cellular immunity alone and indicates that adding vaccination for cellular immune responses has the potential to improve the performance of the Ad5-FMDV vectored vaccine.

- **Heterogeneity in the Antibody Response to Foot-and-Mouth Disease Primo-Vaccinated Calves**: Foot-and-mouth disease (FMD) is an economically important viral disease of cattle and presents a major constraint to international trade of livestock and associated products. FMD vaccines are routinely used as effective control tools in large regions worldwide and to limit outbreaks during epidemics. Protection in cattle largely relates to the ability of vaccination to induce antibodies that can neutralize the virus and prevent its spread. Although there have been reports of cattle responding differently to vaccination, few studies have been done to determine the influence of the animal genetic background on their ability to respond to vaccination. Here investigated if the level of antibody response to FMD vaccination in cattle of different genetic lineages was related to their genetic background (breed of the parental sire). The analysis of 377 previously unvaccinated cattle showed lower immune responses in steers derived from Jersey sires compared to those derived from Holstein sires. This information is important to take into account during the implementation of vaccination programs to control FMD.

- **Characterization of a Chimeric Foot-and-Mouth Disease Virus bearing Bovine Rhinitis B Virus Leader Proteinase:** Foot and mouth disease virus (FMDV) causes a devastating disease (FMD) in livestock and represents a major threat to US agriculture exports and food security. Infection of cattle with FMDV usually initiates in the respiratory tract (throat and lungs) before generalizing and causing painful blisters in the mouth and feet. The closest genetic relative of FMDV is bovine rhinitis virus 2 (BRV2),

a virus that causes respiratory disease in cattle. In our search for effective FMDV vaccines, we substituted the FMDV leader proteinase (FMDV L^pro, a viral protein that determines viral virulence) with that of BRV2. The resulting virus grew well in tissue culture and caused attenuated FMD in animals, suggesting that BRV L^pro only partially replaced the FMDV L^pro functions. This information will ultimately be applied to the development of attenuated FMDV strains that could be utilized as potential vaccines.

- **A Partial Deletion in Non-Structural Protein 3A can Attenuate Foot-and-Mouth Disease Virus in Cattle:** Foot-and-mouth disease (FMD) continues to be one of the most economically devastating diseases of livestock worldwide. There is limited information regarding the specific role of FMD virus proteins in determining host susceptibility. This work deals with the role of one of the FMDV non-structural proteins (3A) in determining disease in cattle and swine. Previous reports had suggested a possible relationship between a deletion in a particular region of the 3A protein and inability to produce disease in cattle, but these results were not conclusive. Here we report the construction of a mutant FMDV of the O1Campos subtype, having deleted an area of 20 amino acids in protein 3A. This virus was fully attenuated in cattle but not in swine. The results presented here unequivocally demonstrated that a 20 amino acid region of the 3A protein is responsible for determining the attenuation of the virus in cattle. This information will be applied to future development of better vaccines against this important disease.

- **Pore-Forming Activity of Pestivirus pin a Minimal Model System Supports Genus-Specific Viroporin Function**: Classical Swine Fever Virus (CSFV) is a highly contagious and economically significant viral disease effecting pigs. Our research program is aimed at developing countermeasures against CSFV to minimize the economic impact of potential outbreaks. As part of this research we are studying the role of viral proteins in causing infection and disease. We previously characterized a viral protein called p7 and showed it is a viroporin, that is responsible for formation of pores in the membrane of the infected cells facilitating the egress of the virus. Here we have localized the area of p7 that actually mediates pore formation using a set of synthetic peptides. We also showed that blocking the viroporin function inhibited viral egress and the spread of the virus to surrounding cells. This viroporin thus constitutes a target in antiviral development that could be used in countermeasure development against this devastating disease of swine.

- **The Pathogenesis of Highly Virulent African Swine Fever Virus in Domestic Pigs Exposed via Intraoropharyngeal, Intranasopharyngeal, and Intramuscular Inoculation, and by Direct Contact with Infected Pigs:** The purpose of this study was to compare methods of experimental infection for African Swine Fever (ASF) in order to determine which method is optimal for future research and vaccine development. Groups of pigs were infected with African Swine Fever virus via the upper gastrointestinal tract (intraoropharyngeal), the upper respiratory tract (intranasopharyngeal) and intramuscular routes or through direct contact exposure to infected pigs. Within the first three infection routes, pigs were given either a low, mid, or high dose of virus. Pigs infected via direct contact were exposed to sick pigs for 24, 48 or 72 hours. Among the routes, doses and

exposure times, parameters such as clinical signs, the presence of virus within the blood and excretions collected from the tonsil and nasal cavity, as well as macroscopic and microscopic changes within tissues were examined and compared. Within all groups, animals that became infected had clinical signs and changes within tissues that were similar to previously described experimental and natural outbreaks of ASF. Differences amongst the percentage of animals infected per group and the onset and degree of virus within the blood and excretions suggest that the intranasopharyngeal route of infection is the most favorable method to be used for experimental research.

TABLE OF CONTENTS

SECTION	DESCRIPTION
1	Examination of Soluble Integrin Resistant Mutants of Foot-and-Mouth Disease Virus (FMDV)
2	Epidemiological Analysis, Serological Prevalence, and Genotypic Analysis of Foot-and-Mouth Disease in Nigeria 2008-2009
3	Theiler's Murine Encephalomyelitis Virus Contrasts with Encephalomyocarditis and Foot-and-Mouth Disease Viruses in its Functional Utilization of the StopGo Non-Standard Translation Mechanism
4	Venezuelan Equine Encephalitis Virus Replicon Particles can induce Rapid Protection against Foot-and-Mouth Disease Virus
5	An Adenovirus Vectored Mucosal Adjuvant Augments Protection of Mice Immunized Intranasally with an Adenovirus-Vectored Foot-and-Mouth Disease Virus Subunit Vaccine
6	A Continuous Bovine Kidney Cell Line Constitutively Expresssing Bovine Alpha V Beta 6 Integrin has Increased Susceptibility to Foot-and-Mouth Disease Virus
7	Repeated Exposure to 5D9, and Inhibitor of 3D Polymerase, Effectively Limits the Replication of Foot-and-Mouth Disease Virus in Host Cells.
8	Foot-and-Mouth Disease Virus Modulates Cellular Vimentin for Virus Survival.
9	Analysis of SAT type Foot-and-Mouth Disease Virus Capsid Proteins and the Identification of Putative Amino Acid Residues in Virus Stability
10	Mechanisms of Foot-and-Mouth Disease Virus Tropism Inferred from Differential Tissue Gene Expression
11	Cell-Mediated Innate Responses of Cattle and Swine are Diverse during Foot-and-Mouth Disease Virus (FMDV) Infection: A Unique Landscape of Innate Immunity
12	Foot-and-Mouth Disease Virus L Peptidase
13	Characterization of Cytotoxic T Lymphocyte Function following Foot-and-Mouth Disease Virus Infection and Vaccination

TABLE OF CONTENTS

SECTION	DESCRIPTION
14	Heterogeneity in the Antibody Response to Foot-and-Mouth Disease Primo-Vaccinated Calves
15	Characterization of a Chimeric Foot-and-Mouth Disease Virus bearing Bovine Rhinitis B Virus Leader Proteinase
16	A Partial Deletion in Non-Structural Protein 3A can Attenuate Foot-and-Mouth Disease Virus in Cattle
17	Pore-Forming Activity of Pestivirus P7 in a Minimal Model System Supports Genus-Specific Viroporin Function
18	The Pathogenesis of Highly Virulent African Swine Fever Virus in Domestic Pigs Exposed via Intraoropharyngeal, Intranasopharyngeal, and Intramuscular Inoculation, and by Direct Contact with Infected Pigs
Index	Author Index

Lawrence et al. Virology Journal 2013, 10:2
http://www.virologyj.com/content/10/1/2

VIROLOGY JOURNAL

RESEARCH Open Access

Examination of soluble integrin resistant mutants of foot-and-mouth disease virus

Paul Lawrence[†], Michael LaRocco[†], Barry Baxt and Elizabeth Rieder[*]

Abstract

Background: Foot-and-mouth disease virus (FMDV) initiates infection via recognition of one of at least four cell-surface integrin molecules $\alpha_v\beta_1$, $\alpha_v\beta_3$, $\alpha_v\beta_6$, or $\alpha_v\beta_8$ by a highly conserved Arg-Gly-Asp (RGD) amino acid sequence motif located in the G-H loop of VP1. Within the animal host, the $\alpha_v\beta_6$ interaction is believed to be the most relevant. Sub-neutralizing levels of soluble secreted $\alpha_v\beta_6$ ($ss\alpha_v\beta_6$) was used as a selective pressure during passages *in vitro* to explore the plasticity of that interaction.

Results: Genetically stable soluble integrin resistant (SIR) FMDV mutants derived from A24 Cruzeiro were selected after just 3 passages in cell culture in the presence of sub-neutralizing levels of $ss\alpha_v\beta_6$. SIR mutants were characterized by: replication on selective cell lines, plaque morphology, relative sensitivity to $ss\alpha_v\beta_6$ neutralization, relative ability to utilize $\alpha_v\beta_6$ for infection, as well as sequence and structural changes. All SIR mutants maintained an affinity for $\alpha_v\beta_6$. Some developed the ability to attach to cells expressing heparan sulfate (HS) proteoglycan, while others appear to have developed affinity for a still unknown third receptor. Two classes of SIR mutants were selected that were highly or moderately resistant to neutralization by $ss\alpha_v\beta_6$. Highly resistant mutants displayed a G145D substitution (RGD to RDD), while moderately resistant viruses exhibited a L150P/R substitution at the conserved RGD + 4 position. VP1 G-H loop homology models for the A-type SIR mutants illustrated potential structural changes within the integrin-binding motif by these 2 groups of mutations. Treatment of O1 Campos with $ss\alpha_v\beta_6$ resulted in 3 SIR mutants with a positively charged VP3 mutation allowing for HS binding.

Conclusions: These findings illustrate how FMDV particles rapidly gain resistance to soluble receptor prophylactic measures *in vitro*. Two different serotypes developed distinct capsid mutations to circumvent the presence of sub-neutralizing levels of the soluble cognate receptor, all of which resulted in a modified receptor tropism that expanded the cell types susceptible to FMDV. The identification of some of these adaptive mutations in known FMDV isolates suggests these findings have implications beyond the cell culture system explored in these studies.

Keywords: Soluble receptor, α_v-integrin heterodimers, Foot-and-mouth disease virus (FMDV)

Introduction

Foot-and-mouth disease virus (FMDV) is responsible for the most economically important viral disease of cattle and other cloven-hoofed animals [1-5]. FMDV, the prototypic member of the *Aphthovirus* genus of *Picornaviridae*, utilizes *in vitro* four integrin heterodimers ($\alpha_v\beta_1$, $\alpha_v\beta_3$, $\alpha_v\beta_6$, and $\alpha_v\beta_8$) for attachment to host cells and entry via clathrin-coated pits (CCPs) [6-14]. A prominent surface-exposed loop connecting the βG-βH strands (G-H loop) of the VP1 capsid protein contains a highly conserved Arg-Gly-Asp (RGD) motif, a recognition sequence for the α_v-integrin family of cell surface receptors [6,15-17]. Limited trypsin proteolysis removes the G-H loop, producing FMDV particles considerably less infectious relative to untreated virions, highlighting the importance of this region for productive infection [18-20]. Following integrin binding, CCPs internalize virus into acidic endosomes where uncoating occurs. FMDV field isolates continually passaged in cell culture adapt to utilize heparan sulfate (HS) as an alternative receptor, and exhibit attenuated pathogenicity [21-24].

Previously, soluble $\alpha_v\beta_3$ and $\alpha_v\beta_6$ lacking the transmembrane and cytoplasmic tail domains were shown to

* Correspondence: elizabeth.rieder@ars.usda.gov
[†]Equal contributors
Foreign Animal Disease Research Unit, United States Department of Agriculture, Agricultural Research Service, Plum Island Animal Disease Center, PO Box 848, Greenport, NY 11944-0848, USA

BioMed Central

© 2013 Lawrence et al.; licensee BioMed Central Ltd. This is an Open Access article distributed under the terms of the Creative Commons Attribution License (http://creativecommons.org/licenses/by/2.0), which permits unrestricted use, distribution, and reproduction in any medium, provided the original work is properly cited.

still function as FMDV receptors [25]. Pre-treatment of serotype A and O FMDV particles with soluble secreted bovine $\alpha_v\beta_3$ and $\alpha_v\beta_6$ prior to application on permissive cell lines was investigated as an antiviral therapy. Interestingly, only soluble $\alpha_v\beta_6$ limited FMDV attachment to host cells by competing for receptor binding sites on virus particles. Soluble $\alpha_v\beta_3$ exhibited a low affinity interaction with the virus particles and failed to attach to FMDV in the same manner as $\alpha_v\beta_6$ with no significant effect on infectivity. It remains to be determined whether binding to blocking molecules such as soluble receptor, will impact FMDV interaction with the cell-membrane receptor or affect viral growth.

Here, we conducted *in vitro* experiments to evaluate the selective pressure exerted by soluble receptor protein on FMDV attachment and examined the evolution of virus-host cell interactions. Studies conducted with poliovirus and its cognate receptor [26,27] showed that surface and internal capsid residues regulate attachment to the receptor and conformational change of the virus. Here, sub-neutralizing levels of soluble secreted bovine $\alpha_v\beta_6$ ($ss\alpha_v\beta_6$) were used to develop soluble receptor resistant mutants of FMDV A24 Cruzeiro. Of the 4 α_v-integrins used by FMDV for host cell attachment, the β_6 heterodimer was selected on the basis that $ss\alpha_v\beta_6$ most substantially impeded FMDV infection [25]. Additionally, the β_6 heterodimer was shown to be most responsible for the tissue tropism of FMDV in cattle [28]. Following 3 successive passages of FMDV (serotype A and serotype O) pre-treated and co-incubated with $ss\alpha_v\beta_6$ on the LFBK cell line, which is permissive to infection by all 7 serotypes of FMDV (Figure 1, Table 1) [29], virus was isolated that persisted despite the presence of soluble integrin (SI). The A-type isolates exhibited mutations in the normally conserved RGD motif or just outside of it within the G-H loop of VP1, while the O-type mutants displayed changes in VP3 and residues proximal to the VP1 RGD motif. SI resistant (SIR) FMDV mutants were further characterized for altered receptor tropism, relative sensitivity to neutralization by SI, as well as sequence and structural alterations in the G-H loop.

Table 1 Receptor repertoire of tested cell lines

Cell Line	αvβ1	αvβ3	αvβ6	αvβ8	HS	Reference
LFBK	+	+	+	*	+	Figure 1 (this paper); [29]
CHO K1	-	-	-	-	+	[30-37]
CHO 677	-	-	-	-	-	[21,30,38-41]
IBRS2	-	-	-	+	-	[16,42]
COS-1	*	-	-	-	+	Figures 3 and 6 (this paper); [7,36,37]

[+] Confirmed expression of the receptor molecule on the cell line indicated.
[-] Confirmed lack of expression of the receptor molecule on the cell line indicated.
[*] Unclear if the receptor molecule is expressed on the cell line indicated.
The receptor profile of $\alpha_v\beta_1$, $\alpha_v\beta_3$, $\alpha_v\beta_6$, $\alpha_v\beta_8$, and HS on 6 cell lines used was tabulated with references to studies that directly demonstrated the receptor profile or did so indirectly by virus growth profiles.

Results

Selection of FMDV serotype A SIR mutants

To examine the adaptability of serotype A FMDV (represented by A24 Cruzeiro) to the presence of soluble receptor during infection, we employed $ss\alpha_v\beta_6$, which is preferentially exploited by serotype A FMDV for host cell attachment [7,25]. As previously described, ectodomains of α_v and β_6 integrin subunits were secreted from stably transfected cells, which were properly folded and capable of heterodimerization (data not shown) [25]. The bovine kidney LFBK cell line was selected for these studies on the basis that it is susceptible to infection by all 7 FMDV serotypes, similar to primary bovine kidney cell culture and [29]. Western blot analysis confirmed that LFBK cells express both β_3 and β_6 integrins (Figure 1, Table 1). As expected, CHO 677 cells [30,38] did not express β_3 and β_6 integrins [21,30-33,39-41]. While BHK-21 cells expressed β_3 integrin, we were unable to detect the presence of β_6 integrin. As an additional control, RNA Helicase A (RHA), known to be expressed in all 3 cell lines, was also detected. By extension, these findings allowed for the potential that both $\alpha_v\beta_3$ and $\alpha_v\beta_6$ could be found on the surface of LFBK cells, which is consistent with repeated

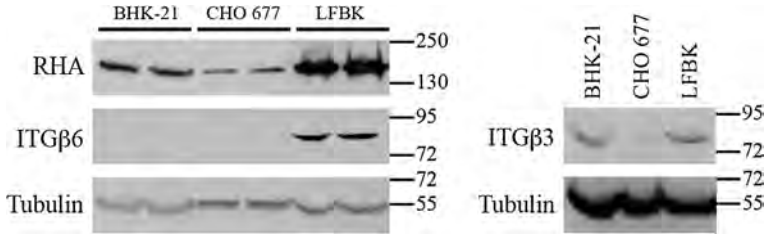

Figure 1 Integrin expression profile. BHK-21, CHO 677, and LFBK cell lysates were examined by Western blot probing with: anti-β_3 integrin (ITGβ3), anti-β_6 integrin (ITGβ6), and anti-RHA. Equivalent loading between lanes was confirmed by probing with anti-tubulin-α. Molecular weight ladder bands are indicated.

experiments showing the susceptibility of this cell line to non-HS-adapted field isolates of FMDV (data not shown).

Wild-type (WT) FMDV A24 Cruzeiro was pre-incubated with 10 μg/mL ssα$_v$β$_6$ (sub-neutralizing concentration for A24 Cruzeiro, Additional file 1: Figure S1) at 37°C for 1 hour prior to application of the coated virus on LFBK cells. As depicted in Figure 2A, LFBK cells were infected with ssα$_v$β$_6$ coated WT FMDV A24 Cruzeiro at a MOI of 1 at 37°C for 24 hours (P1). Thirty-five plaques were isolated and used for a second round (P2) of infection with ssα$_v$β$_6$. Only 17 of the 35 infections demonstrated cytopathic effects (CPE) at 24 hpi. Isolates from 17 P2 infections were individually used for a third selection (P3) with ssα$_v$β$_6$. This resulted in only 4 productive infections derived from A24 Cruzeiro numbered: 15, 23, 42, and 45. The 4 soluble integrin resistant (SIR) serotype A (A-type) isolates (designated A-SIR #15, A-SIR #23, A-SIR #42, and A-SIR #45) were subject to a final selection with ssα$_v$β$_6$, where by 24 hpi A-type SIR isolates 15, 23, and 45 produced 100% CPE and isolate 42 produced 50% CPE.

After multiple passages in cell culture, FMDV has been shown to gain the ability to attach to host cells via HS [14,21-24,43]. To determine if the A-type SIR mutants adapted to use HS for entry, replication of these viruses on LFBK and Chinese hamster ovary (CHO) K1 cells was compared. In contrast to LFBK cells, CHO K1 cells express HS, but not α$_v$β$_1$, α$_v$β$_3$ and α$_v$β$_6$ (Table 1) [24,30-35]. Of note,

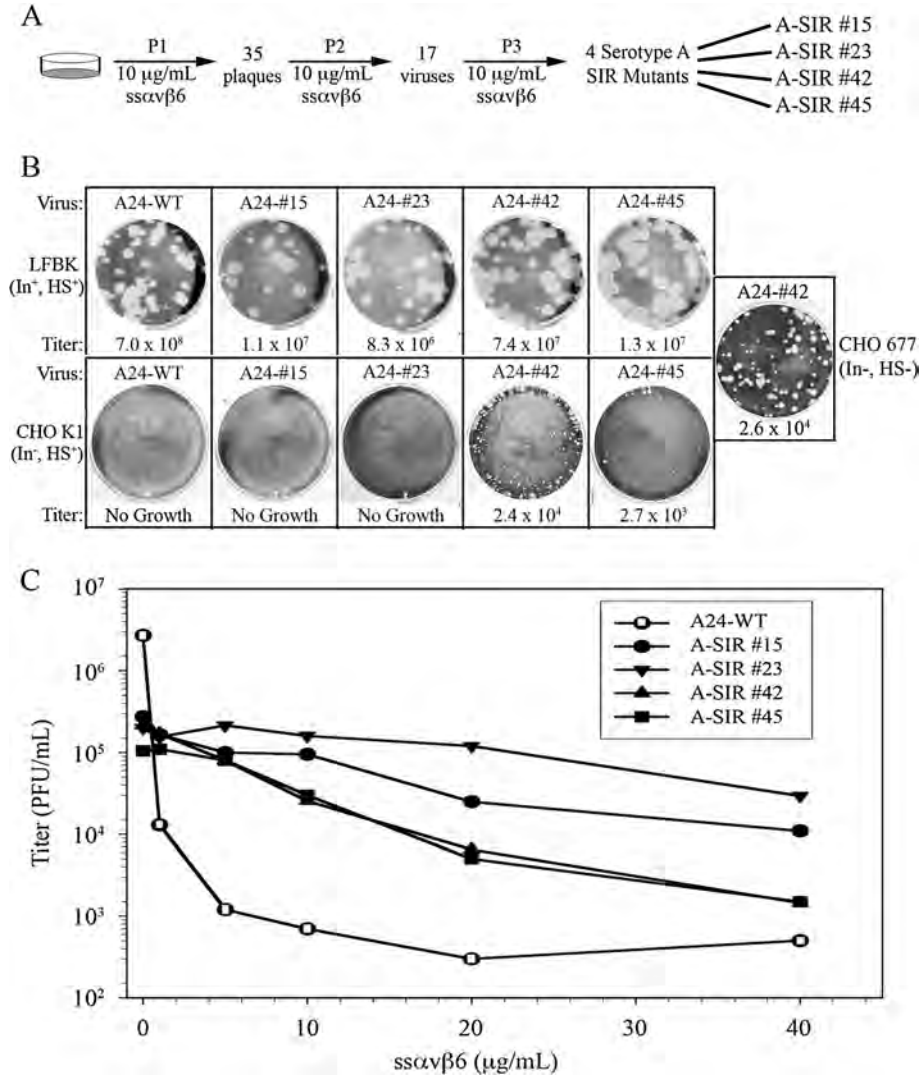

Figure 2 A-SIR mutant generation. A. Schematic of A-SIR mutant production. **B.** Comparison of the plaque morphology and titers achieved of A- SIRs relative to A24 Cruzeiro after pre-treatment and co-incubation with ssα$_v$β$_6$ on LFBK (top panel) and CHO K1 (bottom panel) cells for 24 h. SIR #42 was the only virus that amplified on CHO 677 cells (right box). Titers represent PFU/mL. **C.** WT and A-SIR viruses were co-incubated with increasing concentrations of ssα$_v$β$_6$ on LFBK monolayers for 24 h, and the calculated titers were subsequently plotted.

CHO K1 cells express 2 RGD-binding integrins ($\alpha_5\beta_1$ and $\alpha_v\beta_5$), but neither function as FMDV receptors [7,10,30]. WT and A-SIR viruses successfully infected LFBK cells (Figure 2B, top panel). However, WT and A-SIRs #15 and #23 were unable to infect CHO K1 cells. In contrast, A-SIRs #42 and #45 productively infected CHO K1 cells (Figure 2B, bottom panel). Thus, we suggest that A-SIRs #42 and #45 circumvented ss$\alpha_v\beta_6$ neutralization by expanding their receptor preference to include HS, as previously observed under other conditions with different FMDV serotypes [23,24].

The A-type SIR mutants diverged with respect to their plaque morphologies on different cell lines. WT and A-SIR mutants maintained relatively large plaque sizes on LFBK cells (Figure 2B, top panel). On CHO K1 monolayers, A-SIRs #42 and #45 showed reduced plaque size relative to LFBK cells (Figure 2B, lower panel). Comparative viral growth on LFBK and CHO K1 cells suggests some A-SIRs might utilize HS. To examine this further, the growth analysis was expanded to include the CHO 677 cell line (Figure 1, Table 1) [39,40,44]. In addition, the IBRS2 cell line with a unique receptor profile where FMDV infection is initiated via $\alpha_v\beta_8$ [9,16,42], was also examined (Table 1). IBRS2 cells were permissive to infection by WT and A-SIR viruses, growing to titers comparable to LFBK cells (Table 2). Interestingly, A-SIR #42 productively infected CHO 677 cells (Figure 2B, Table 2). SIR #42 grew to roughly equivalent titers on CHO 677 and CHO K1 cells (Figure 2B, Table 2). Viral growth on CHO 677 cells suggested this A-SIR mutant adapted to utilize an as yet unidentified and uncharacterized third FMDV receptor [21,41]. It was inferred that growth of A-SIR #45 on CHO K1 cells but not CHO 677 cells was indicative that this virus exploited HS. Different growth patterns for each A-SIR mutant on different cell lines also suggested these viruses are genetically distinct. These findings illustrated the rapid adaptability (after only 3 passages) of serotype A FMDV to overcome interference with host cell attachment.

A-SIR mutants exhibit reduced sensitivity to SI neutralization

Next, the relative sensitivities of A-SIR mutants to ss$\alpha_v\beta_6$ neutralization were examined relative to their WT counterpart. Each virus was pre-incubated with ss$\alpha_v\beta_6$ at gradually increasing concentrations (5, 10, 20, 30, and 40 μg/mL), applied to LFBK monolayers, and evaluated for reductions in virus titer. As shown in Figure 2C, the four A-SIR mutants could be divided into 2 classes with respect to sensitivity to neutralization by ss$\alpha_v\beta_6$: a highly resistant (#15 and #23, Class I) and a moderately resistant class (#42 and #45, Class II). A-SIRs #15 and #23 grew to titers 200–1000 fold higher than WT with increasing ss$\alpha_v\beta_6$, while mutants #42 and #45 exhibited titers 20–100 fold higher than WT (Figure 2C). Cumulatively, these findings reinforced the supposition that pre- and co-incubation of ss$\alpha_v\beta_6$ acts as a selective pressure forcing FMDV particles to quickly select for resistance to the treatment.

A-SIR mutants continue to utilize $\alpha_v\beta_6$

Since the A-SIR mutants exhibited reduced sensitivity to ss$\alpha_v\beta_6$ neutralization, we investigated whether they exhibit an altered integrin preference: shifting from $\alpha_v\beta_6$ to another integrin or a non-integrin receptor. The capability of A-SIRs to infect cells expressing distinct integrins was tested using a previously established transient transfection-infection assay [45]. COS-1 cells do not support FMDV infection and lack integrins used by FMDV (Table 1) [7]. These cells were co-transfected with plasmids encoding the full-length α_v-integrin subunit and 1 of 4 different full-length β subunits (β_1, β_3, β_5, or β_6). Expression was confirmed by immunocytochemical staining (Figure 3A). Of note, the antibody used to detect the $\alpha_v\beta_1$ only recognizes the β_1 subunit; as such, positive staining may be reflective of other β_1 containing integrin heterodimers.

WT virus and A-SIR mutants were incubated on the cells transiently expressing integrin with ^{35}S-methionine. After 24 hours, levels of viral protein synthesis were evaluated by radioimmunoprecipitation (RIP) (Figure 3B). Based on the sets where FMDV proteins (3D, VP0, VP1-3) were detected, it could be inferred as to which integrin heterodimers was/were used by WT and A-SIR viruses to gain entry to COS-1 cells for replication. Consistent with previous reports, viral protein synthesis was detected for A24 Cruzeiro WT in cells

Table 2 Growth comparison of A24 Cruzeiro WT and A-type SIRs on 6 cell lines

Virus	LFBK	CHO K1	CHO 677	CHO 677 αvβ6	IBRS2	COS-1
A24-WT	7×10^8	-	-	6.3×10^7	6×10^8	-
A-SIR #15	1.1×10^7	-	-	2.8×10^6	4×10^7	-
A-SIR #23	8.3×10^6	-	-	1.8×10^6	2×10^7	-
A-SIR #42	7.4×10^7	2.4×10^4	2.6×10^4	5.6×10^6	6.5×10^7	-
A-SIR #45	1.3×10^7	2.7×10^3	-	2×10^7	1×10^7	-

Numerical values represent virus titers in plaque forming units per milliliter (PFU/mL).
Dashes indicate no plaque detected at the lowest dilution of virus tested (1/10).

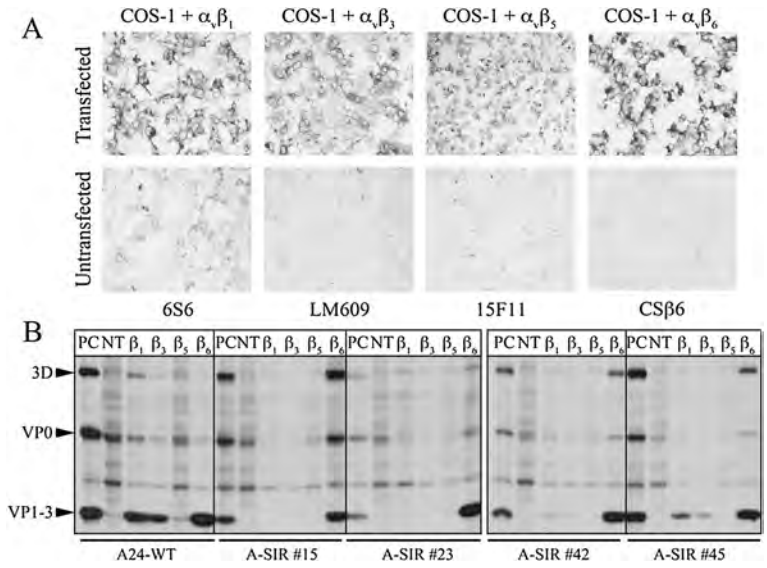

Figure 3 A-SIR mutants maintain $\alpha_v\beta_6$ affinity. A. Expression of α_v and β subunits (β_1, β_3, β_5, or β_6) examined by immuno-histochemical staining using indicated antibodies. Untransfected cells probed as a negative control. **B.** RIP analysis of transfected cells infected with: A24 Cruzeiro and A-SIRs in the presence of ^{35}S-methionine. NT, not transfected. PC, positive control: virus-infected LFBK cells.

expressing $\alpha_v\beta_1$, $\alpha_v\beta_3$ and $\alpha_v\beta_6$ (Figure 3B) [7,25]. A-SIRs #15 and #23 were only amplified on $\alpha_v\beta_6$ expressing cells. A-SIRs #42 and #45 infected cells displaying $\alpha_v\beta_1$ and $\alpha_v\beta_6$. However, the signal for virus proteins was noticeably lower for A-SIR #42 and #45 relative to WT, though we cannot exclude the possibility that this was partially due to differences in transfection efficiencies. Besides WT, A-SIR #45 was the only other virus able to infect via $\alpha_v\beta_3$. Interestingly, although resistant to neutralization by ss$\alpha_v\beta_6$, all 4 A-SIR viruses replicated on $\alpha_v\beta_6$ expressing COS-1 cells. Thus, it was inferred that all 4 A-SIR mutants maintained sufficient affinity for $\alpha_v\beta_6$ to continue to infect cells via this receptor.

To reinforce the supposition that the A-SIR viruses retained the ability to bind $\alpha_v\beta_6$, CHO 677 cells, which could not permit FMDV infection except for A-SIR #42, were transiently transfected with $\alpha_v\beta_6$ as was done for COS-1 cells (data not shown). The expression of $\alpha_v\beta_6$ restored infectivity of WT and A-SIR viruses, with titers within 0.5 to 1 log less than on LFBK cells (Table 2), with A-SIR #45 attaining a titer 1 log higher than both class I SIRs. Notably, A-SIR #42 achieved titers 2 logs higher than on untransfected CHO 677 cells, suggesting $\alpha_v\beta_6$ is the preferred surface receptor for this virus.

Amino acid substitutions detected in A-SIR mutants

To further distinguish A-SIR viruses from their parental counterpart, A-SIR mutants were examined for alterations in their nucleotide and amino acid sequences relative to WT (Accession #AY593768). No amino acid substitutions were detected in VP4, VP2, or VP3, with a single silent mutation detected in VP3. Interestingly, the 2 A-type SIR classes exhibited 2 corresponding types of mutations in VP1 summarized in Table 3 and Figure 4. Class I A-SIRs that were highly resistant to ss$\alpha_v\beta_6$ (#15 and #23) displayed a G145D amino acid substitution in the RGD motif considered essential for integrin interaction. The V154A substitution distinguished A-SIR #23 from #15. Class II A-type SIRs moderately resistant to ss$\alpha_v\beta_6$ (#42 and #45) exhibited substitutions at the RGD + 4 position with L150P for #42 and L150R for #45. Moreover, A-SIR #42 displayed 2 additional amino acid alterations upstream of the RGD motif: E95K and S96L. Previous reports have described the helical segment immediately C-terminal to the RGD motif as contributing to the interaction between FMDV and its cognate integrin receptor, specifically, amino acid positions RGD + 1 and RGD + 4. The RGD + 1 and RGD + 4 side chains face out like those of the RGD motif and are frequently occupied by leucine residues [8,14,46-49]. While proline substitution at the RGD + 4 position was previously detected in the A5 Westerwald FRG/58 field isolate ([50] b; [51]) and serially passaged populations of a serotype C FMDV strain [21], the arginine substitution at this position appears unprecedented. Cumulatively, the P1 sequences support the findings that 2 distinct classes of SIR mutants were derived from A24 Cruzeiro: where each class exhibited distinct forms of amino acid substitutions localized to the VP1 G-H loop.

Structural predictions of A-SIR mutant modifications

After defining the amino acid changes within VP1 in the A-SIR mutants (Figure 4), we explored how those changes might affect the overall structure of the

Table 3 Sequence comparison of the P1 region of A24 Cruzeiro and A-SIRs

Gene	A24 Cruzeiro WT			A-SIR #15 and #23 (Class I)			A-SIR #42 and #45 (Class II)		
	Nucleotide[a]	Codon[b]	Amino acid[c]	Nucleotide[a]	Codon[b]	Amino acid[c]	Nucleotide[a]	Codon[b]	Amino acid[c]
VP2	C50	cgG	——	——	——	——	G50[45]	cgA	Silent
VP1	G6	acG	——	C6	acC	Silent	C6	acC	Silent
VP1	G283	Gaa	E95	——	——	——	A283[42]	Aaa	K95
VP1	C287	tCa	S96	——	——	——	T287[42]	tTa	L96
VP1	G434	gGc	G145	A434	gAc	D145	——	——	——
VP1	T449	cTc	L150	——	——	——	C449[42]	cCc[42]	P150[42]
							G449[45]	cGc[45]	R150[45]
VP1	T461	gTc	V154	C461[23]	gCc	A154[23]	——	——	——

[a] Nucleotide differences between viruses followed by number indicating its position within the gene coding sequence.
[b] Lowercase letters indicate bases shared by the 2 viruses and capital letters indicate bases differing between the viruses.
[c] One-letter code of the encoded amino acid residues followed by number indicating residue position in the polypeptide.
P1 region of A24 Cruzeiro (Accession # AY596768) was compared against: Class I (#15 and #23) and Class II (#42 and #45) A-SIRs. Nucleotide changes relative to WT were indicated and codon positions. Silent mutations and amino acid substitutions are indicated. A-SIR mutant numerical designations were superscripted.

receptor-binding site in the G-H loop. The VP1 crystal structure has been solved for FMDV O1/BFS 1860/UK/67 (Accession 1FOD) [52]. Using the coordinates of 1FOD as a template, homology structures were generated of WT A24 Cruzeiro VP1 as well as those of the 4 A-SIR mutants using the Geno3D algorithm [53]. For each virus, 10 different "best fit" homology models were generated for VP1. Representative images of the G-H loop region were given particular scrutiny (Figure 5).

The RGD to RDD substitution detected in class I A-SIR mutants #15 and #23 placed a bulky negatively charged residue into the center of the integrin binding site, which can be seen projecting outward in the homology structures generated. The introduction of D145 "spread out" the adjacent side chains within the RGD motif, increasing the distance between the R144 and D146 side chains relative to WT (Figure 5). In all 10 of the predicted tertiary structures, the amino acid alteration failed to effect any significant change in the backbone structure of this region of VP1.

The previously undetected L150R substitution at the RGD + 4 position of class II A-SIR #45 replaces a linear non-polar amino acid side chain with a positively charged residue. Interestingly, Geno3D failed to predict a consensus structure for the A-SIR #45 G-H loop. Class II A-SIR mutant #42 exhibited a L150P substitution at RGD + 4, which was previously identified in FMDV A5 Westerwald FRG/58 [50,51]. The homology model of the A-SIR #42 G-H loop revealed the proline residue introducing a kink that "compressed" the RGD motif with the three side chains in much closer proximity than WT (Figure 5). This structural prediction was essentially the opposite of what was produced for the class I A-SIR mutants.

In addition to L150P, A-SIR #42 also displayed 2 substitutions upstream of the RGD: E95K and S96L, which are proximal to the VP1-VP3 interface. Using Geno3D, ribbon diagrams were generated of capsid protomers from WT and A-SIRs to determine if the protein interface was disrupted (Additional file 2: Figure S2). A short helical domain observed at the VP1-VP3 interface in the WT sequence was notably absent with the E95K/S96L substitution, replaced with a loop structure. With L150P previously detected in A5 Westerwald, E95K/S96L may be more significant to the adaptation of A_SIR #42. We concluded that the mutations elucidated in the A-SIR

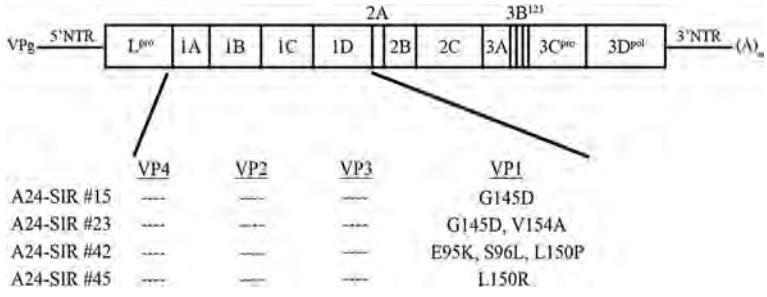

Figure 4 Amino acid substitutions within the P1 region of A-SIR mutants. Schematic of the FMDV genome summarizing the amino acid substitutions identified in the P1 region of A-SIR mutants after viral RNA from A24 Cruzeiro and A-SIRs was sequenced for amino acid substitutions in P1.

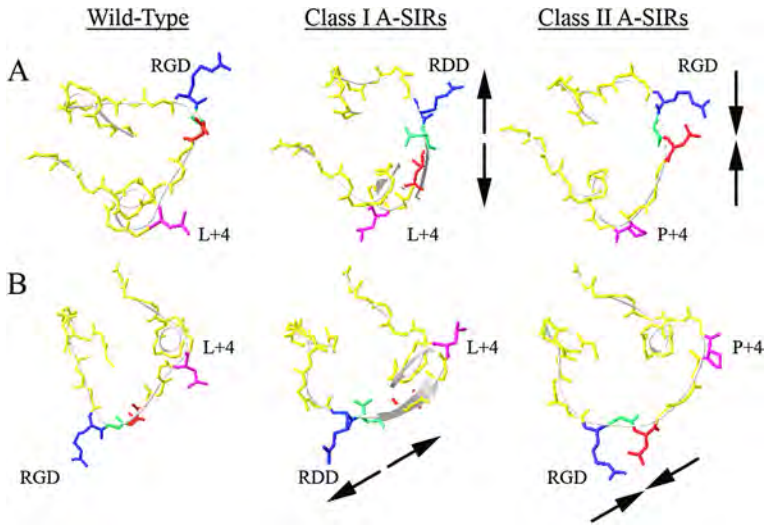

Figure 5 Structural prediction of the effect of the A-SIR amino acid substitutions on the G-H loop. Depicted are 2 angles (**A** and **B**) of models of the VP1 G-H loop of A24 Cruzeiro and representative class I and class II A-SIRs. RGD motif is indicated, and residues are colored: arginine (R), blue; glycine (G), green; aspartic acid (D), red. RGD + 4 position (L/P + 4) is violet. Black arrows indicate altered directionality of the amino acid side chains in A-SIR RGD/RDD sites.

mutants produce hypothetical structural alterations likely to affect cellular recognition.

O1 Campos derived SIR mutants circumvent ss$\alpha_v\beta_6$ by a different mechanism

A-SIR mutants derived from A24 Cruzeiro overcame the selective pressure introduced by ss$\alpha_v\beta_6$ by compensatory mutations targeted to the RGD motif or the RGD + 4 position within the VP1 G-H loop. In an effort to determine if a similar strategy would be exploited by a different FMDV serotype, the experiment was repeated whereby O1 Campos was pre-treated and passaged three times in the continued presence of 10 μg/mL ss$\alpha_v\beta_6$ (also a sub-neutralizing concentration for O1 Campos, data not shown). Three O-type SIR viruses were recovered designated O-SIR #1, O-SIR #9, and O-SIR #46 (Figure 6A). All three O-SIRs produced similar small plaque forming units on LFBK cells relative to their WT progenitor (Figure 6B, top panel). Unlike the WT virus, the O-SIRs productively infected CHO K1 cells (Figure 6B, bottom panel), achieving titers approximately 1 log lower than on LFBK cells (Table 4). This suggested that the O-SIRs adapted to the presence of ss$\alpha_v\beta_6$ by selecting an affinity for HS, which represents a well-characterized strategy employed by serotype O FMDV [22,23,54]. Each O-SIR mutant produced distinct plaque morphologies on CHO K1 cells; with large plaques for O-SIR #1, medium-sized plaques for O-SIR #9, and small pinprick plaques for O-SIR #46 (Figure 6B, bottom panel). Interestingly, like the A-type SIR mutant #42, O-SIR #9 could replicate, albeit to a limited titer, on CHO 677 cells (Figure 6B, right panel and Table 4). When CHO 677 cells transiently expressing $\alpha_v\beta_6$ were substituted in this assay, infectivity was restored for all O-SIR mutants and O1 Campos WT, with titers equivalent to or exceeding those on LFBK cells (Table 4). This particular finding was consistent with what was observed for the A-SIR viruses, where affinity for $\alpha_v\beta_6$ was maintained. Additionally, both O1 Campos and the O-SIR mutants demonstrated titers 1–2 logs higher on IBRS2 cells relative to LFBK cells (Table 4), which suggested that these viruses infect via $\alpha_v\beta_8$ with greater efficiency.

Further analysis revealed that all three O-SIRs were uniformly 2 logs more resistant to neutralization by ss$\alpha_v\beta_6$ up to 20 μg of ss$\alpha_v\beta_6$ (Figure 6C). However, while this resistance was maintained by O-SIR #1 and O-SIR #9 above 20 μg ss$\alpha_v\beta_6$, O-SIR #46 was inhibited by ss$\alpha_v\beta_6$ at concentrations above 20 μg. Initial examinations of the reliance of the O-SIRs on different integrin heterodimers revealed the presence of FMDV proteins in untransfected COS-1 cells infected with the O-SIR mutants, similar to the pattern observed for O-SIR infected LFBK cells (Figure 6D). No increase in viral protein synthesis was observed for cells transiently expressing integrins (data not shown). Like CHO K1 cells, COS-1 cells express HS, thus it was inferred that the O-SIR mutants had circumvented ss$\alpha_v\beta_6$ neutralization by adapting to utilize HS for host cell attachment.

Given the disparities in plaque morphology and sensitivity to soluble integrin neutralization, it was expected that the O-type SIR mutants would be genetically distinct. In contrast to A-SIRs, compensatory mutations

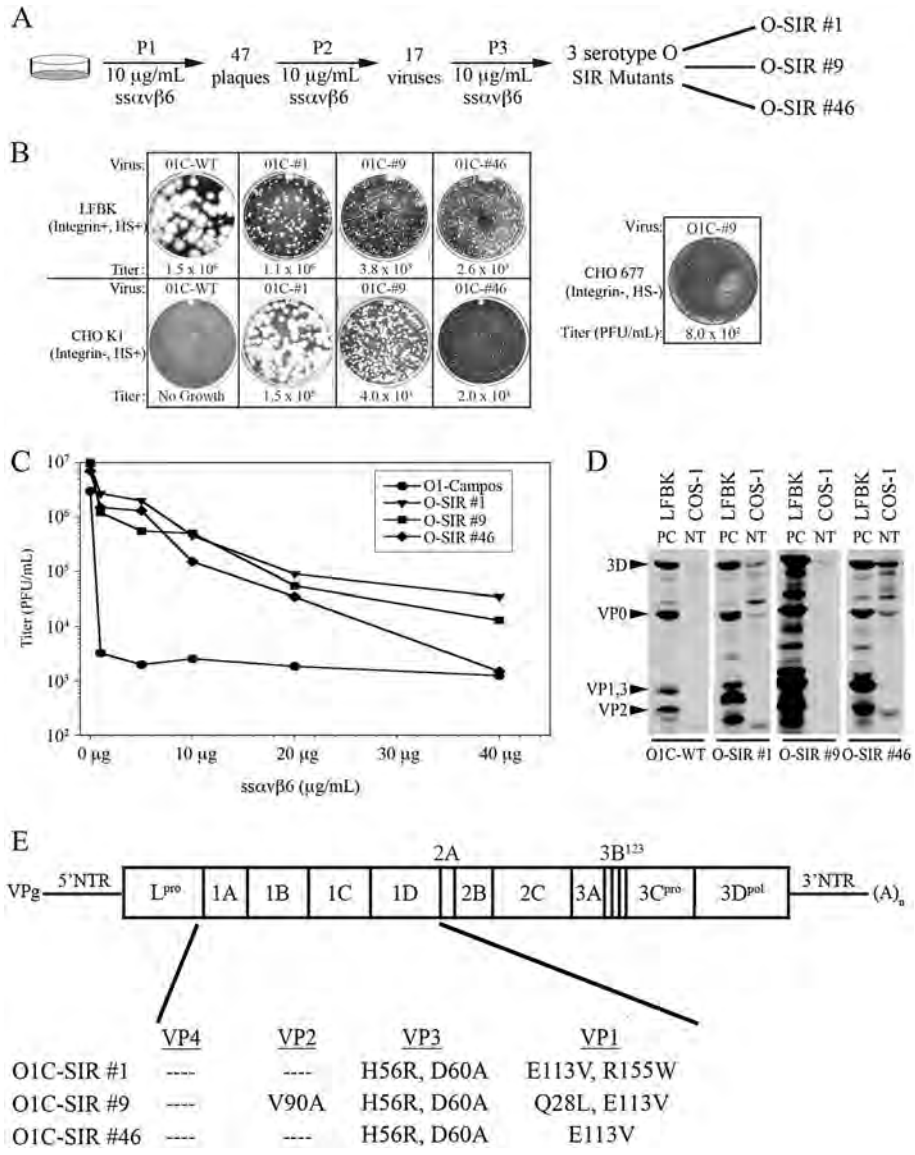

Figure 6 O1 Campos derived SIR mutants exhibit distinctive alterations. A. Schematic of O1 Campos derived O-SIR mutant production. **B.** Comparison of the growth characteristics of O-SIRs relative to O1 Campos after $ssa_v\beta_6$ co-incubation on LFBK and CHO K1 cells. O-SIR #9 was the only virus that amplified on CHO 677 cells. Titers represent PFU/mL. **C.** WT and O-SIR viruses were co-incubated with $ssa_v\beta_6$ on LFBK monolayers for 24 h, and the calculated titers were subsequently plotted. **D.** RIP analysis of untransfected LFBK and COS-1 cells infected with: O1 Campos and O-SIRs in the presence of ^{35}S-methionine. NT, not transfected (COS-1). PC, positive control (LFBK). **E.** FMDV genome depicting amino acid substitutions identified in the P1 region of O-SIR mutants.

Table 4 Growth comparison of O1 Campos WT and O-type SIRs on 6 cell lines

Virus	LFBK	CHO K1	CHO 677	CHO 677- αvβ6	IBRS2	COS-1
O1C-WT	1.5×10^6	-	-	4×10^8	8×10^7	-
O-SIR #1	1.1×10^6	1.5×10^5	-	9×10^5	1.9×10^8	*
O-SIR #9	3.8×10^5	4×10^4	8.0×10^2	1.5×10^6	5×10^8	*
O-SIR #46	2.6×10^5	2×10^4	-	1.5×10^6	1.6×10^8	*

Numerical values represent virus titers in plaque forming units per milliliter (PFU/mL).
Dashes indicate no plaque detected at the lowest dilution of virus tested (1/10).
Asterisks indicate limited abortive infection without plaque formation, indicated by thinning of the cell monolayer.

were not confined to VP1, but were also identified within VP3 (Figure 6E). The mutations detected in the O-SIRs were consistent with those previously found in HS-adapted serotype O FMDV passaged multiple times in cell culture with a signature H56R substitution in VP3 [22,23,54]. An additional D60A substitution in VP3 and an E113V substitution in the VP1 G-H loop were found in all O-SIR viruses. O-SIRs were distinguished from each other by 2 unique amino acid substitutions: R155W in the VP1 G-H loop of O-SIR #1 and Q28L in VP1 and V90A in VP2 of O-SIR #9. Notably, the conserved RGD motif and RGD + 4 amino acid positions were unchanged.

Cumulatively, the development and characterization of the A-SIR and O-SIR FMDV mutants and the evolution of the virus-host interaction under the selective pressure of soluble integrin treatment was determined in the present study.

Discussion

Distinct lineages of RNA viruses are frequently referred to as "quasi-species" due to their inherent mutability [47,55]. Their rapid adaptability stems from the lack of "proofreading" function in the RNA-dependent RNA polymerases responsible for amplification of RNA viral genomes. The poliovirus RNA polymerase delivers approximately 1 error in 2200 bases, which is significant for a virus genome of approximately 7500 nucleotides [56]. Constant variation with each duplicated RNA viral population represents a stumbling block in the development of anti-viral therapies. A previous study explored using soluble receptor treatments to impair FMDV infection [25,49]. Here, we investigated the effect of sub-neutralizing levels of soluble secreted $\alpha_v\beta_6$ ($ss\alpha_v\beta_6$) on FMDV replication in cells and documented the rapid emergence of resistant FMDV populations, how they circumvented the selective pressure of $ss\alpha_v\beta_6$, and the strategies deployed as they adapted.

Previous studies have investigated the effect of multiple passaging in cell culture on FMDV acquisition of alternative receptors, attenuated phenotypes, and for the dispensability of the RGD motif [21,49,57]. For instance, following 100 passages of a serotype C FMDV (C-S8c1) in cell culture, the virus was able to enter cells by an integrin-independent manner and multiple mutations were identified in the variant genomes [21]. For serotype A12 virus, it has been shown that mutations obtained during adaptation of field (bovine) isolates to cell culture localize downstream of the RGD and those mutations appear to alter the affinity for the integrin receptor [49].

Here, four SI resistant (SIR) FMD viruses derived from A24 Cruzeiro and three derived from O1 Campos were rapidly selected after only 3 rounds of cell culture selection in the continued presence of $ss\alpha_v\beta_6$. The A-SIR mutants could be separated into 2 classes that were either highly or moderately resistant to neutralization by $ss\alpha_v\beta_6$. Highly resistant A-SIRs (Class I) did not select HS as a secondary receptor and maintained $\alpha_v\beta_6$ affinity. These variants displayed a G145D substitution in the highly conserved VP1 RGD motif. The moderately resistant A-SIRs (Class II) also retained $\alpha_v\beta_6$ affinity and appeared to either utilize HS or an as yet unidentified and uncharacterized third FMDV receptor. Moreover, similar to A24 Cruzeiro, all 4 A-SIR mutants were amplified on IBRS2 cells, indicating that the A-SIRs have maintained the ability to infect and replicate on cells expressing an abundance of $\alpha_v\beta_8$, which can also function as a FMDV receptor [9,16,42].

Class I A-SIR Mutants

A-SIR mutants appear to have circumvented $ss\alpha_v\beta_6$ treatment by 2 different routes. Substitution of an aspartic acid (G145D) in the RGD motif (Figure 4) rendered A-SIR #15 and 23 (Class I) highly resistant to $ss\alpha_v\beta_6$ (Figure 2C) while paradoxically maintaining use of $\alpha_v\beta_6$ for infection (Figure 3B). Notably, class I A-SIRs did not adapt to utilize HS. Interestingly, this RDD mutation in the cell receptor binding site has been detected in a field strain of Asia1 virus (Asia1/JS/CHA/05) after just 2 passages, one *in vivo* and one *in vitro* [57]. RDD Asia1 variants showed no change in their ability to replicate in established cell lines, nor did it alter clinical onset of disease in animals tested [57]. While the environmental pressure that selected for RDD Asia1 variants is unknown, it suggests that this mutation might be a natural adaptation mechanism that could manifest across different FMDV serotypes. This hypothesis is supported by the observation that natural outbreaks of serotype A FMDV featuring the RDD amino acid substitution have occurred in Argentina on two occasions: A25-Arg/59 (GenBank #AY593769) and A25-Arg/61 (GenBank #AY593789).

The likely reason for the selection of a modified RGD was also investigated using homology models of the VP1 G-H loop structure and position of the RDD side chains (Figure 5). The data showed an additional negative charge provided by G145D widened the gap between the side chains of R144 and D146. Potentially, the widening of the RDD side chains or the introduction of an additional negatively charged side chain might diminish the affinity of the motif for the integrin by sterically complicating the binding of $ss\alpha_v\beta_6$, which is not anchored to a membrane, to the virus particle during pre-treatment in solution. Correspondingly, by reducing the affinity but not ablating the interaction with $\alpha_v\beta_6$ (Figure 3B, Table 2), unoccupied RDD sites on the virus particle after pre-treatment and subsequent co-incubation with $ss\alpha_v\beta_6$ likely allow infection of host cells via $\alpha_v\beta_6$.

Class II A-SIR Mutants

In contrast, moderately resistant Class II A-SIRs left the RGD intact, but substituted a key amino acid at the RGD + 4 position [8,14,46-48], with the conserved leucine replaced with proline for A-SIR #42 and arginine for A-SIR #45. L150P was previously identified in FMDV A5 Westerwald FRG/58 [50,51] as well as a multiply passaged serotype C FMDV [21,58]. However, L150R appears unprecedented. Interestingly, while both viruses replicated in CHO K1 cells, only A-SIR #42 infected CHO 677 cells. However, both class II A-SIRs exhibited preference for $\alpha_v\beta_6$ over alternative surface molecules (Figure 2, Table 2). Given L150P was previously detected in the WT field strain A5 Westerwald [51], it will be interesting to explore in the future whether this amino acid alteration was solely responsible for shifting receptor tropism to allow infection of cells devoid of FMDV integrin receptors and HS [21,30,38,41]. However, two additional mutations detected in VP1, E95K and S96L, might also contribute or be exclusively responsible for the A-SIR #42 phenotype.

Homology modeling was also employed to illustrate how Class II amino acid substitutions affected both the G-H loop (Figure 5) and the capsid protomer (Additional file 2: Figure S2). In contrast to Class I A-SIRs, L150P appears to compress the side chains projecting from the RGD motif, where R144 and D146 are in closer proximity than in A24 Cruzeiro or Class I A-SIRs (Figure 5). The unique E95K/S96L substitutions localized to the VP1-VP3 interface, potentially altering capsid protomer stability (Additional file 2: Figure S2). Modeling algorithms failed to generate a consensus structure for the G-H loop of A-SIR #45, where multiple potential side chain angles for L150R altered the shape and presentation of the RGD motif (data not shown).

O-SIR mutants

When the approach used to generate the A-SIRs was applied to O1 Campos, this resulted in three distinctive O-SIR mutants that bind to HS and that carried a signature H56R mutation. This particular mutation has been observed in attenuated HS-adapted FMDVs [22,23,54]. Similar to their A-type counterparts, the O-SIRs also could be amplified on IBRS2 cells suggesting that the selective pressure of co-incubation with ss$\alpha_v\beta_6$ did not abrogate the affinity for $\alpha_v\beta_8$. However, unlike A24 Cruzeiro and the A-SIRs, O1 Campos and the O-type SIR mutants amplified 2–3 logs more in IBRS2 cells relative to LFBK cells, thus it could be inferred that serotype O FMDV may have a preference for $\alpha_v\beta_8$ as a receptor. As such it would be intriguing to explore the effects of successive passages of O1 Campos in the presence of ss$\alpha_v\beta_8$ in the future. Lastly, it is interesting to note that the mutations accumulated by the O-SIRs were not in the VP1 RGD motif, but rather peripheral to it and at locations in VP3, separate from the primary site of attachment to the host cell.

Conclusions

Together the results of this study have shed light on the plasticity of FMDV serotype A and O interactions with its primary cognate receptor: $\alpha_v\beta_6$. Amino acid substitutions detected in SIR mutants were rapidly selected to overcome soluble receptor neutralization. Thus, the tolerance of the VP1 G-H loop to amino acid substitutions plays an essential role in cell receptor adaptability of FMDV. Interestingly, mutations identified in the current study have been also identified in FMDV field isolates causing outbreaks suggesting that similar selective pressures may exist in the natural host environment. The mode and relative speed with which FMDV was able to adapt to a selective pressure, represented here by ss$\alpha_v\beta_6$, highlights both the evolutionary advantage of highly mutable RNA viruses and the challenges of designing effective antiviral therapies against these pathogens.

Materials and methods

Materials

Fugene-6 was purchased from Roche (Nutley, NJ). Mouse monoclonal anti-β_3 integrin (ITGβ3) was purchased from Abcam (Cambridge, MA). Rabbit polyclonal anti-β_6 integrin (ITGβ6) was purchased from Sigma (St. Louis, MO). Mouse monoclonal anti-β_1 integrin (6S6), anti-$\alpha_v\beta_3$ integrin (LM609), anti-$\alpha_v\beta_5$ integrin (15 F11), and anti-β_6 integrin (CSβ6) was purchased from Millipore (Billerica, MA). Rabbit polyclonal anti-RHA was purchased from Bethyl Laboratories (Montgomery, TX).

Cells, viruses, and plasmids

IBRS2, COS-1, and 293a cell lines purchased from American Tissue Collection Company (ATCC; Manassas, VA) were cultured in Dulbecco's minimal eagle medium (DMEM) with 10% fetal bovine serum (FBS) at 37°C with 5% CO_2. LFBK cell line was previously described [29], and cultured in DMEM with 10% FBS at 37°C with 5% CO_2. CHO K1 and 677 cell lines were acquired from Dr. Jeffrey Esko [39] and cultured in Ham's MEM (Gibco) with 10% FBS at 37°C with 5% CO_2. FMDV A24 Cruzeiro field strain was derived from pA24-Cru [59]. FMDV O1 Campos field strain was previously described [24].

SI production

Expression and purification of ss$\alpha_v\beta_3$ and ss$\alpha_v\beta_6$ was previously described [25]. Plasmids encoding ectodomains of integrin subunits (α_v, β_3, and β_6) were transfected using Fugene-6 (Roche) per manufacturer's instructions. Stable expression was selected by incubating with G418 (α_v gene sub-cloned into pcDNA3.1-G418) and zeomycin (β_3 and

β_6 gene sub-cloned into pcDNA3.1-Zeo). Supernatants were collected and concentrated 10-fold using Centricon Plus-70 filter devices (Millipore, Billerica, MA). Subsequent protein concentration measured between 125–250 μg/mL.

Radio-immunoprecipitation (RIP)

Virus-infected cells grown overnight in the presence of ^{35}S-methionine were lysed with 1% Triton X100. Aliquots of each sample were precipitated with 20% trichloroacetic acid (TCA) to determine the counts per minute (cpm). Lysates were mixed with Protein A/G agarose beads, tumbled 15 minutes, centrifuged at 1500 rpm 10 minutes, and the supernatants collected. Recovered supernatant was tumbled with indicated antibodies (6S6, LM609, 15 F11, and CSβ6) 1 hour at 4°C. The mixture was tumbled overnight at 4°C with fresh Protein A/G agarose. Afterwards, the agarose was washed 3 times with NET/NP40 buffer (NaCl, EDTA, Tris, Nonidet-P40). Finally, the agarose was boiled in sample buffer without β-mercaptoethanol, pelleted, the supernatants separated by SDS-PAGE, and the gel examined by autoradiography.

Transient transfection-infection assay

Assay was conducted as previously described [45]. Two sets of COS-1 or CHO 677 cells were transfected with 2 plasmids: one encoding full-length α_v-integrin subunit and the other encoding 1 of 4 different full-length β subunits (β_1, β_3, β_5, or β_6). The first sets were examined by immuno-histochemical staining to confirm expression, using antibodies: 6S6 ($\alpha_v\beta_1$), LM609 ($\alpha_v\beta_3$), 15 F11 ($\alpha_v\beta_5$), and CSβ6 ($\alpha_v\beta_6$). 6S6 binds the β_1 subunit and COS-1 cells express $\alpha_5\beta_1$, which is not a cellular receptor for FMDV [11,12,21]. The other sets were infected with WT and SIR viruses at a MOI of 1 in ^{35}S-methionine containing media. Subsequently, virus-infected cell lysates were examined by RIP for virus-specific bands: 3D, VP0, and VP1-3.

Virus titer assay

One hour post-adsorption, the inoculum was removed, and cells washed in a mild acid solution followed by virus growth media (VGM, DMEM containing L-glutamine). VGM was then added and cells incubated 24 hours at 37°C. Afterwards, virus-infected cells were harvested and titers determined by plaque assay as previously described [60]. Plates were fixed, stained with crystal violet (0.3% in Histochoice; Amresco, Solon, OH), and plaques counted. Values calculated for number of plaque-forming units (PFUs) per milliliter (mL) were plotted using Microsoft Excel (Microsoft Corporation, Redmond, WA). Assays were performed in triplicate.

Western blot

Protein samples were separated by Nu-PAGE® pre-cast gel system (Invitrogen), and electro-blotted onto nitrocellulose (Sigma). After blocking with 5% milk, proteins were detected with indicated primary integrin antibodies (anti-β_3, Abcam and anti-β_6, Sigma) followed by HRP-conjugated goat-anti-mouse or goat-anti-rabbit antibodies (Bethyl Laboratories), respectively. Cellular tubulin, employed as a loading control, was detected with HRP-conjugated anti-tubulin-α (Abcam, Cambridge, MA). HRP was reacted with WestDura SuperSignal chemiluminescent reagent (Pierce) and visualized on X-ray film (X-Omat; Kodak, N.Y., USA).

Sequencing of the FMDV P1 Region

The P1 region in twenty FMDV isolates were sequenced from PCR product with sequencing primers providing at least 3X coverage across 3,000 base pairs. PCR products were purified with QIAQuick spin columns (Qiagen) in accordance with the manufacturer's instructions. Sequencing reaction mixtures (10 μl) contained 2.5 μM primer, 20 ng of PCR product, and 0.75 μl of Big Dye (Applied Biosystems) in molecular biology-grade water. The sequence cycling conditions were 30 s of pre-incubation at 85°C; 25 cycles of 10 s at 96°C, 5 s at 50°C, and 4 min at 60°C; and a 10-min 60°C final extension. The sequencing reaction mixtures were purified with Agencourt's CleanSEQ system in accordance with the manufacturer's instructions (Beckman Coulter).

Structural analysis

Amino acid sequences of SIRs were used to construct homology models of the G-H loop and capsid protomers using the Geno3D algorithm [53]. Ten most likely structures were generated using a solved structure as a template. Two X-ray crystal structures for the major immunogenic site of FMDV designated 1FOD [52] and 1ZBE [61] in the Protein Data Bank (PDB) were selected as templates. Hypothetical structures were examined using DeepView [62,63], and a consensus structure for each sequence was selected.

Additional files

Additional file 1: Figure S1. Soluble integrin neutralization assay. Titration experiment performed where A24 Cruzeiro was pre-incubated with gradually increasing amounts of ssαvβ6 to determine a suitable sub-neutralizing soluble receptor concentration.

Additional file 2: Figure S2. Structural prediction of the effect of the A-SIR amino acid substitutions on the capsid protomer. Depicted are 3 ribbon models of the FMDV capsid protomer (excluding VP4) of A24 Cruzeiro (A) and class I (B) and class II (C) A-SIRs. Black arrows indicate the RGD motif and the RGD + 4 position. Blue arrows indicate the VP1-VP3 interface. VP1 is yellow, VP2 is blue, and VP3 is red.

Competing interests

The authors declare that they have no competing interests.

Authors' contributions

PL: evaluated the integrin expression on the tested cell lines, organized the sequencing data and performed the sequencing alignments, constructed the structural models, and drafted the manuscript. ML: produced the FMDV SIR mutants, evaluated SIR plaque morphologies and growth kinetics on indicated cell lines, and performed the radio-immunoprecipitation analysis. BB: co-conceived the study and participated in its design and implementation. ER: co-conceived the study and participated in its design, implementation, and coordination. All authors have read and approved the final version of the manuscript.

Acknowledgments

We wish to thank Bill Hurtle for his expertise sequencing the capsid region of FMDV SIR mutants. We also wish to thank Drs. Devendra Rai and Francois Maree for fruitful discussions regarding structural analyses of the SIR mutants. Dr. Paul Lawrence was sponsored by the Plum Island Animal Disease Research Participation Program administered by the Oak Ridge Institute for Science and Education through an interagency agreement between the U.S. Department of Energy and the U.S. Department of Agriculture.

Received: 5 July 2012 Accepted: 11 December 2012
Published: 2 January 2013

References

1. Domingo E, Baranowski E, Escarmis C, Sobrino F: **Foot-and-mouth disease virus.** *Comp Immunol Microbiol Infect Dis* 2002, **25:**297–308.
2. Grubman MJ, Baxt B: **Foot-and-mouth disease.** *Clin Microbiol Rev* 2004, **17:**465–493.
3. Mason PW, Grubman MJ, Baxt B: **Molecular basis of pathogenesis of FMDV.** *Virus Res* 2003, **91:**9–32.
4. Saiz M, Nunez JI, Jimenez-Clavero MA, Baranowski E, Sobrino F: **Foot-and-mouth disease virus: biology and prospects for disease control.** *Microbes Infect* 2002, **4:**1183–1192.
5. Sobrino F, Saiz M, Jimenez-Clavero MA, Nunez JI, Rosas MF, Baranowski E, Ley V: **Foot-and-mouth disease virus: a long known virus, but a current threat.** *Vet Res* 2001, **32:**1–30.
6. Baxt B, Becker Y: **The effect of peptides containing the arginine-glycine-aspartic acid sequence on the adsorption of foot-and-mouth disease virus to tissue culture cells.** *Virus Genes* 1990, **4:**73–83.
7. Duque H, Baxt B: **Foot-and-mouth disease virus receptors: comparison of bovine alpha(V) integrin utilization by type A and O viruses.** *J Virol* 2003, **77:**2500–2511.
8. Jackson T, Blakemore W, Newman JW, Knowles NJ, Mould AP, Humphries MJ, King AM: **Foot-and-mouth disease virus is a ligand for the high-affinity binding conformation of integrin alpha5beta1: influence of the leucine residue within the RGDL motif on selectivity of integrin binding.** *J Gen Virol* 2000, **81:**1383–1391.
9. Jackson T, Clark S, Berryman S, Burman A, Cambier S, Mu D, Nishimura S, King AM: **Integrin alphavbeta8 functions as a receptor for foot-and-mouth disease virus: role of the beta-chain cytodomain in integrin-mediated infection.** *J Virol* 2004, **78:**4533–4540.
10. Jackson T, Mould AP, Sheppard D, King AM: **Integrin alphavbeta1 is a receptor for foot-and-mouth disease virus.** *J Virol* 2002, **76:**935–941.
11. Jackson T, Sheppard D, Denyer M, Blakemore W, King AM: **The epithelial integrin alphavbeta6 is a receptor for foot-and-mouth disease virus.** *J Virol* 2000, **74:**4949–4956.
12. Neff S, Sa-Carvalho D, Rieder E, Mason PW, Blystone SD, Brown EJ, Baxt B: **Foot-and-mouth disease virus virulent for cattle utilizes the integrin alpha(v)beta3 as its receptor.** *J Virol* 1998, **72:**3587–3594.
13. O'Donnell V, LaRocco M, Duque H, Baxt B: **Analysis of foot-and-mouth disease virus internalization events in cultured cells.** *J Virol* 2005, **79:**8506–8518.
14. Ruiz-Saenz J, Goez Y, Tabares W, Lopez-Herrera A: **Cellular receptors for foot and mouth disease virus.** *Intervirology* 2009, **52:**201–212.
15. Brown F, Benkirane N, Limal D, Halimi H, Newman JF, Van Regenmortel MH, Briand JP, Muller S: **Delineation of a neutralizing subregion within the immunodominant epitope (GH loop) of foot-and-mouth disease virus VP1 which does not contain the RGD motif.** *Vaccine* 1999, **18:**50–56.
16. Burman A, Clark S, Abrescia NG, Fry EE, Stuart DI, Jackson T: **Specificity of the VP1 GH loop of Foot-and-Mouth Disease virus for alphav integrins.** *J Virol* 2006, **80:**9798–9810.
17. Fox G, Parry NR, Barnett PV, McGinn B, Rowlands DJ, Brown F: **The cell attachment site on foot-and-mouth disease virus includes the amino acid sequence RGD (arginine-glycine-aspartic acid).** *J Gen Virol* 1989, **70**(Pt 3):625–637.
18. Robertson BH, Morgan DO, Moore DM: **Location of neutralizing epitopes defined by monoclonal antibodies generated against the outer capsid polypeptide, VP1, of foot-and-mouth disease virus A12.** *Virus Res* 1984, **1:**489–500.
19. Strohmaier K, Franze R, Adam KH: **Location and characterization of the antigenic portion of the FMDV immunizing protein.** *J Gen Virol* 1982, **59:**295–306.
20. Wild TF, Brown F: **Nature of the inactivating action of trypsin on foot-and-mouth disease virus.** *J Gen Virol* 1967, **1:**247–250.
21. Baranowski E, Ruiz-Jarabo CM, Sevilla N, Andreu D, Beck E, Domingo E: **Cell recognition by foot-and-mouth disease virus that lacks the RGD integrin-binding motif: flexibility in aphthovirus receptor usage.** *J Virol* 2000, **74:**1641–1647.
22. Fry EE, Lea SM, Jackson T, Newman JW, Ellard FM, Blakemore WE, Abu-Ghazaleh R, Samuel A, King AM, Stuart DI: **The structure and function of a foot-and-mouth disease virus-oligosaccharide receptor complex.** *EMBO J* 1999, **18:**543–554.
23. Jackson T, Ellard FM, Ghazaleh RA, Brookes SM, Blakemore WE, Corteyn AH, Stuart DI, Newman JW, King AM: **Efficient infection of cells in culture by type O foot-and-mouth disease virus requires binding to cell surface heparan sulfate.** *J Virol* 1996, **70:**5282–5287.
24. Sa-Carvalho D, Rieder E, Baxt B, Rodarte R, Tanuri A, Mason PW: **Tissue culture adaptation of foot-and-mouth disease virus selects viruses that bind to heparin and are attenuated in cattle.** *J Virol* 1997, **71:**5115–5123.
25. Duque H, LaRocco M, Golde WT, Baxt B: **Interactions of foot-and-mouth disease virus with soluble bovine alphaVbeta3 and alphaVbeta6 integrins.** *J Virol* 2004, **78:**9773–9781.
26. Colston E, Racaniello VR: **Soluble receptor-resistant poliovirus mutants identify surface and internal capsid residues that control interaction with the cell receptor.** *EMBO J* 1994, **13:**5855–5862.
27. Colston EM, Racaniello VR: **Poliovirus variants selected on mutant receptor-expressing cells identify capsid residues that expand receptor recognition.** *J Virol* 1995, **69:**4823–4829.
28. Monaghan P, Gold S, Simpson J, Zhang Z, Weinreb PH, Violette SM, Alexandersen S, Jackson T: **The alpha(v)beta6 integrin receptor for Foot-and-mouth disease virus is expressed constitutively on the epithelial cells targeted in cattle.** *J Gen Virol* 2005, **86:**2769–2780.
29. Swaney LM: **A continuous bovine kidney cell line for routine assays of foot-and-mouth disease virus.** *Vet Microbiol* 1988, **18:**1–14.
30. Weinacker A, Chen A, Agrez M, Cone RI, Nishimura S, Wayner E, Pytela R, Sheppard D: **Role of the integrin alpha v beta 6 in cell attachment to fibronectin. Heterologous expression of intact and secreted forms of the receptor.** *J Biol Chem* 1994, **269:**6940–6948.
31. Gianni T, Cerretani A, Dubois R, Salvioli S, Blystone SS, Rey F, Campadelli-Fiume G: **Herpes simplex virus glycoproteins H/L bind to cells independently of {alpha}V{beta}3 integrin and inhibit virus entry, and their constitutive expression restricts infection.** *J Virol* 2010, **84:**4013–4025.
32. Gianni T, Gatta V, Campadelli-Fiume G: **{alpha}V{beta}3-integrin routes herpes simplex virus to an entry pathway dependent on cholesterol-rich lipid rafts and dynamin2.** *Proc Natl Acad Sci USA* 2010, **107:**22260–22265.
33. Xu X, Nagarajan H, Lewis NE, Pan S, Cai Z, Liu X, Chen W, Xie M, Wang W, Hammond S, Andersen MR, Neff N, Passarelli B, Koh W, Fan HC, Wang J, Gui Y, Lee KH, Betenbaugh MJ, Quake SR, Famili I, Palsson BO, Wang J: **The genomic sequence of the Chinese hamster ovary (CHO)-K1 cell line.** *Nat Biotechnol* 2011, **29:**735–741.
34. Esko JD, Stewart TE, Taylor WH: **Animal cell mutants defective in glycosaminoglycan biosynthesis.** *Proc Natl Acad Sci USA* 1985, **82:**3197–3201.
35. Esko JD, Weinke JL, Taylor WH, Ekborg G, Roden L, Anantharamaiah G, Gawish A: **Inhibition of chondroitin and heparan sulfate biosynthesis in Chinese hamster ovary cell mutants defective in galactosyltransferase I.** *J Biol Chem* 1987, **262:**12189–12195.
36. Maree FF, Blignaut B, Aschenbrenner L, Burrage T, Rieder E: **Analysis of SAT1 type foot-and-mouth disease virus capsid proteins: influence of receptor usage on the properties of virus particles.** *Virus Res* 2011, **155:**462–472.
37. Maree FF, Blignaut B, de Beer TA, Visser N, Rieder EA: **Mapping of amino acid residues responsible for adhesion of cell culture-adapted foot-and-mouth disease SAT type viruses.** *Virus Res* 2010, **153:**82–91.

38. Lidholt K, Weinke JL, Kiser CS, Lugemwa FN, Bame KJ, Cheifetz S, Massague J, Lindahl U, Esko JD: **A single mutation affects both N-acetylglucosaminyltransferase and glucuronosyltransferase activities in a Chinese hamster ovary cell mutant defective in heparan sulfate biosynthesis.** *Proc Natl Acad Sci USA* 1992, **89:**2267–2271.
39. Esko JD, Rostand KS, Weinke JL: **Tumor formation dependent on proteoglycan biosynthesis.** *Science* 1988, **241:**1092–1096.
40. Stephens RS, Poteralski JM, Olinger L: **Interaction of Chlamydia trachomatis with mammalian cells is independent of host cell surface heparan sulfate glycosaminoglycans.** *Infect Immun* 2006, **74:**1795–1799.
41. Zhao QZ, Pacheco JM, Mason PW: **Evaluation of genetically engineered derivatives of a Chinese strain of foot-and-mouth disease virus reveals a novel cell-binding site which functions in cell culture and in animals.** *J Virol* 2003, **77:**3269–3280.
42. Johns HL, Berryman S, Monaghan P, Belsham GJ, Jackson T: **A dominant-negative mutant of rab5 inhibits infection of cells by foot-and-mouth disease virus: implications for virus entry.** *J Virol* 2009, **83:**6247–6256.
43. O'Donnell V, Larocco M, Baxt B: **Heparan sulfate-binding foot-and-mouth disease virus enters cells via caveola-mediated endocytosis.** *J Virol* 2008, **82:**9075–9085.
44. O'Donnell CD, Shukla D: **A novel function of heparan sulfate in the regulation of cell-cell fusion.** *J Biol Chem* 2009, **284:**29654–29665.
45. Neff S, Mason PW, Baxt B: **High-efficiency utilization of the bovine integrin alpha(v) beta(3) as a receptor for foot-and-mouth disease virus is dependent on the bovine beta(3) subunit.** *J Virol* 2000, **74:**7298–7306.
46. Dicara D, Burman A, Clark S, Berryman S, Howard MJ, Hart IR, Marshall JF, Jackson T: **Foot-and-mouth disease virus forms a highly stable, EDTA-resistant complex with its principal receptor, integrin alphavbeta6: implications for infectiousness.** *J Virol* 2008, **82:**1537–1546.
47. Domingo E, Escarmis C, Martinez MA, Martinez-Salas E, Mateu MG: **Foot-and-mouth disease virus populations are quasispecies.** *Curr Top Microbiol Immunol* 1992, **176:**33–47.
48. Mateu MG, Valero ML, Andreu D, Domingo E: **Systematic replacement of amino acid residues within an Arg-Gly-Asp-containing loop of foot-and-mouth disease virus and effect on cell recognition.** *J Biol Chem* 1996, **271:**12814–12819.
49. Rieder E, Baxt B, Mason PW: **Animal-derived antigenic variants of foot-and-mouth disease virus type A12 have low affinity for cells in culture.** *J Virol* 1994, **68:**5296–5299.
50. Nunez JI, Martin MJ, Piccone ME, Carrillo E, Palma EL, Dopazo J, Sobrino F: **Identification of optimal regions for phylogenetic studies on VP1 gene of foot-and-mouth disease virus: analysis of types A and O Argentinean viruses.** *Vet Res* 2001, **32:**31–45.
51. Weddell GN, Yansura DG, Dowbenko DJ, Hoatlin ME, Grubman MJ, Moore DM, Kleid DG: **Sequence variation in the gene for the immunogenic capsid protein VP1 of foot-and-mouth disease virus type A.** *Proc Natl Acad Sci USA* 1985, **82:**2618–2622.
52. Logan D, Abu-Ghazaleh R, Blakemore W, Curry S, Jackson T, King A, Lea S, Lewis R, Newman J, Parry N, *et al*: **Structure of a major immunogenic site on foot-and-mouth disease virus.** *Nature* 1993, **362:**566–568.
53. Combet C, Jambon M, Deleage G, Geourjon C: **Geno3D: automatic comparative molecular modelling of protein.** *Bioinformatics* 2002, **18:**213–214.
54. Borca MV, Pacheco JM, Holinka LG, Carrillo C, Hartwig E, Garriga D, Kramer E, Rodriguez L, Piccone ME: **Role of arginine-56 within the structural protein VP3 of foot-and-mouth disease virus (FMDV) O1 Campos in virus virulence.** *Virology* 2011, **422:**37–45.
55. Ojosnegros S, Perales C, Mas A, Domingo E: **Quasispecies as a matter of fact: Viruses and beyond.** *Virus Res* 2011, In press.
56. Wells VR, Plotch SJ, DeStefano JJ: **Determination of the mutation rate of poliovirus RNA-dependent RNA polymerase.** *Virus Res* 2001, **74:**119–132.
57. Li P, Lu Z, Bao H, Li D, King DP, Sun P, Bai X, Cao W, Gubbins S, Chen Y, Xie B, Guo J, Yin H, Liu Z: **In-vitro and in-vivo phenotype of Asia1 foot-and-mouth disease viruses utilizing two non-RGD receptor recognition sites.** *BMC Microbiol* 2011, **11:**1–12.
58. Gutierrez-Rivas M, Pulido MR, Baranowski E, Sobrino F, Saiz M: **Tolerance to mutations in the foot-and-mouth disease virus integrin-binding RGD region is different in cultured cells and in vivo and depends on the capsid sequence context.** *J Gen Virol* 2008, **89:**2531–2539.
59. Rieder E, Henry T, Duque H, Baxt B: **Analysis of a foot-and-mouth disease virus type A24 isolate containing an SGD receptor recognition site in vitro and its pathogenesis in cattle.** *J Virol* 2005, **79:**12989–12998.
60. Rieder E, Bunch T, Brown F, Mason PW: **Genetically engineered foot-and-mouth disease viruses with poly(C) tracts of two nucleotides are virulent in mice.** *J Virol* 1993, **67:**5139–5145.
61. Fry EE, Newman JW, Curry S, Najjam S, Jackson T, Blakemore W, Lea SM, Miller L, Burman A, King AM, Stuart DI: **Structure of Foot-and-mouth disease virus serotype A10 61 alone and complexed with oligosaccharide receptor: receptor conservation in the face of antigenic variation.** *J Gen Virol* 2005, **86:**1909–1920.
62. Guex N, Peitsch MC: **SWISS-MODEL and the Swiss-PdbViewer: an environment for comparative protein modeling.** *Electrophoresis* 1997, **18:**2714–2723.
63. Kaplan W, Littlejohn TG: **Swiss-PDB Viewer (Deep View).** *Brief Bioinform* 2001, **2:**195–197.

doi:10.1186/1743-422X-10-2
Cite this article as: Lawrence *et al.*: Examination of soluble integrin resistant mutants of foot-and-mouth disease virus. *Virology Journal* 2013 **10**:2.

Submit your next manuscript to BioMed Central and take full advantage of:

- **Convenient online submission**
- **Thorough peer review**
- **No space constraints or color figure charges**
- **Immediate publication on acceptance**
- **Inclusion in PubMed, CAS, Scopus and Google Scholar**
- **Research which is freely available for redistribution**

Submit your manuscript at
www.biomedcentral.com/submit

BioMed Central

Transboundary and Emerging Diseases

Transboundary and Emerging Diseases

ORIGINAL ARTICLE

Epidemiological Analysis, Serological Prevalence and Genotypic Analysis of Foot-and-Mouth Disease in Nigeria 2008–2009

D. O. Ehizibolo[1], A. M. Perez[2,3], C. Carrillo[4], S. Pauszek[5], M. AlKhamis[3], I. Ajogi[6], J. U. Umoh[6], H. M. Kazeem[7], P. O. Ehizibolo[8], A. Fabian[4], M. Berninger[4], K. Moran[4], L. L. Rodriguez[5] and S. A. Metwally[4,9]

1 Viral Research Division, National Veterinary Research Institute, Vom, Nigeria
2 CONICET/CECSA-Facultad de Ciencias Veteinarias UNR, Rosario, Argentina
3 Center for Animal Disease Modeling and Surveillance, UC Davis, Davis, CA, USA
4 Foreign Animal Disease Diagnostic Laboratory, APHIS, USDA, Plum Island Animal Disease Center (PIADC), Greenport, NY, USA
5 Agricultural Research Service, USDA, PIADC, Greenport, NY, USA
6 Department of Veterinary Public Health and Preventive Medicine, Ahmadu Bello University (ABU), Zaria, Nigeria
7 Department of Veterinary Microbiology and Pathology, ABU, Zaria, Nigeria
8 Department of Veterinary Physiology and Pharmacology, ABU, Zaria, Nigeria
9 Food and Agriculture Organization of the United Nations, Rome, Italy

Keywords:
FMD; genotype; epidemiology; serology; West Africa; Nigeria

Correspondence:
D. Ehizibolo. Foot-and-Mouth Disease Laboratory, Viral Research Division, National Veterinary Research Institute, Vom, Plateau State, Nigeria.
Tel.: +2348035924859;
E-mail: kingdavid_e@yahoo.com

Received for publication April 14, 2011

doi:10.1111/tbed.12054

Summary

The epidemiological situation of foot-and-mouth disease virus (FMDV) is uncertain in Nigeria, where the disease is endemic, and the majority of outbreaks are unreported. Control measures for FMD in Nigeria are not being implemented due to the absence of locally produced vaccines and an official ban on vaccine importation. This study summarizes the findings of a 3-year study aimed at quantifying the seroprevalence of FMD, its distribution in susceptible species and the genetic diversity of FMDV isolated from the Plateau State of Nigeria. A 29% FMD prevalence was estimated using 3ABC enzyme-linked immunosorbent assay (3ABC ELISA). Farms with suspected FMD nearby, with contact with wildlife, that used drugs or FMD vaccines or with >100 animals, and animals of large ruminant species and in pastures other than nomadic grazing were significantly ($P < 0.05$) associated with FMD. Antibodies against five FMDV serotypes, (A, O, SAT1, SAT2 and SAT3) were detected by the virus neutralization test (VNT) at various titres (<100–>800) from all tested sera from most parts of the region. This is probably the first report of the presence of FMDV SAT3 in Nigeria. Further studies to investigate the potential probable presence and prevalence of SAT 3 virus in Nigeria are required. Tissue samples collected from clinical animals were positive for FMDV. Virus isolates were sequenced and confirmed as serotype A. All of the isolates showed marked genetic homogeneity with >99% genetic identity in the VP1 region and were most closely related to a previously described virus collected from Cameroon in 2000. This study provides knowledge on the epidemiological situation of FMD in Plateau State, Nigeria, and will probably help to develop effective control and preventive strategies for the disease in Nigeria and other countries in the West African subregion.

Introduction

Foot-and-mouth disease (FMD) is a highly contagious viral disease of cloven-footed animals caused by the foot-and-mouth disease virus (FMDV), which is a member of the Aphthovirus genus of the Picornaviridae family (King, 2000). The FMDV is a small, non-enveloped, icosahedral, positive-sense, single-stranded RNA virus, with an

© 2013 Blackwell Verlag GmbH • Transboundary and Emerging Diseases.

approximately 8.5-kb genome that encodes for structural proteins (SP) as well as non-structural proteins (NSPs) (Carroll et al., 1984; Forss et al., 1984; Grubman et al., 1984). The FMDV exhibits a high potential for genetic and antigenic variation, which has led to the identification of seven FMDV serotypes, referred to as A, O, C, South African Territories (SAT) 1, SAT 2, SAT 3 and Asia 1 (Domingo et al., 2003). Arguably, FMD is one of the most important livestock diseases in the world in terms of its economic impact (James and Rushton, 2002). Losses arise from the direct effects of the disease on production, costs of disease control and restrictions imposed to international trade.

Six FMDV serotypes (A, O, C and the SATs) have been identified in Africa (Vosloo et al., 2002). Although the disease is considered endemic in most of Sub-Saharan Africa (Bronsvoort et al., 2006), there are only sporadic submissions of FMDV samples to international reference laboratories (Vosloo et al., 2002). Recent reviews of reports submitted to the FMD World Reference Laboratory (WRL) in Pirbright, United Kingdom, between 1958 and 1992 (Ferris and Donaldson, 1992) and from 1948 to 2002 (Vosloo et al., 2002), have shown that at least four FMDV serotypes (SAT 1, SAT 2, O and A) have been identified in Western and Central Africa. In Western Africa, FMD outbreaks occur regularly in the absence of any known wildlife hosts. It is, therefore, possible that the disease is maintained in small ruminants and even cattle during inter-epidemic periods (Sangare et al., 2003). Genetic studies of serotype A, O and SAT 2 suggested that a single epidemic in West Africa often affects two or more neighbouring countries (Knowles et al., 1998; Bastos and Sangare, 2001; Sangare et al., 2001). Migrating nomads and trade cattle markets may also play a major role in spreading infection across borders in the region. Several factors, including absence of effective control and surveillance programmes, lack of farm biosecurity, insufficient infrastructural facilities, lack of financial resources for disease diagnosis and absence of effective vaccines, contribute to the disease endemicity in Western Africa.

Foot-and-mouth disease was first reported in Nigeria in 1924 as sporadic outbreaks attributed to serotype O FMDV incursions (Libeau, 1960). Serotypes A, SAT 1 and SAT 2 FMDV outbreaks have subsequently been reported in the country (Owolodun, 1971; Nawathe and Goni, 1976; Durojaiye, 1981). Prior to the last decade, serotypes O and A were identified in the country for the last time in 1963 and 1979, respectively, whereas SAT 1 and SAT 2 outbreaks were reported for the last time in 1981 and 1982, respectively (Ferris and Donaldson, 1992). Recently, however, serotypes O, A and SAT 2 were identified from samples submitted to the WRL (Knowles, 2008; OIE/FAO, 2010).

The epidemiological situation of FMD in Nigeria is quite uncertain. There is no routine prophylactic vaccination programme in place in the country due to the absence of locally produced FMD vaccines and the lack of permission for vaccine importation. A few dairy farms in the country with exotic breeds, however, use occasionally imported vaccine. There is a need to understand the current situation and epidemiology of the disease in Nigeria with a view to planning an effective control strategy and to enhance efficient livestock production necessary to ensure food security. This article summarizes the findings from a 3-year long study aimed at quantifying the seroprevalence of FMD and its distribution in susceptible species, the association between seroprevalence and epidemiological factors and the genetic diversity of FMDV isolates from the Plateau state of Nigeria, which is considered to be a major route for cattle movements, linking the north-east and part of the north-central part of Nigeria to the eastern, western and southern regions.

Materials and Methods

Study area

The Plateau state of Nigeria lies between longitude 8°22′N, 8°35′E and latitude 10°26′N, 10°40′E, with a total land area of 26 899 square kilometres (NBS, 2009). The state falls largely within the Northern Guinea savannah zone, which consists mainly of short trees, grasses and the plateau-type mosaic vegetation. The human population was estimated at 3.5 million people, including over 30 ethnic groups, a large percentage of which are mostly engaged in farming. Livestock production, which accounts for 25% of the agricultural contribution to the GDP of the state, is typically conducted following a familiar management system, although there are a few commercial farms. Administratively, the state is divided into 17 local government areas (LGA) grouped into three federal senatorial zones referred to as northern, central and southern zones (NBS, 2009). The study was designed in 2007, samples were collected through 2008 and 2009, and laboratory and statistical analyses were conducted through 2009 and 2010.

Data collection and sampling

A structured questionnaire was developed through discussion with field extension workers, researchers and livestock owners, in order to capture information related to epidemiological factors potentially associated with FMD incidence in the region. The questions covered a variety of aspects, including herd information; production system; previous/recent FMD outbreak; herd movement; grazing system; number of contacts between herds and wildlife; number of contacts at watering point; animal purchases from the markets; how herdsmen respond to outbreak situation; and additional relevant questions. A total of 198 questionnaires

 © 2013 Blackwell Verlag GmbH • Transboundary and Emerging Diseases.

were distributed to livestock owners/herdsmen across 10 of the 17 LGAs (Bokkos, Shendam, Mangu, Pankshin, Kanam, Wase, Riyom, Barkin Ladi, Bassa and Jos South) of the Plateau State (Fig. 1). The questionnaire was composed in English and translated to the Fulani herdsmen in Hausa language. Each questionnaire took about 25–40 min to be answered by interview conducted by some of the authors.

Blood samples (n = 532) were collected from apparently healthy and clinically ill animals using a two-stage sampling design. Because no accurate data on population size and distribution were available to us, the population size was assumed to approximate infinite, and the expected seroprevalence for cattle was 27% (Abegunde, 1987). Assuming an error level of 5% in the predictions and a 99% confidence interval (CI), the number of samples required was 524 (Mahajan, 1997). To increase representativeness of the sampling design and in the absence of population data to distribute the samples proportionally, at least one LGA from each of the three senatorial zones was randomly selected for sampling, and from each selected LGA, samples were collected from at least two cattle herds. Samples were collected from traditional Fulani (nomadic) herds, from a cattle market, and from two commercial farms from Bassa (Miango and Kwall); Barkin Ladi; Jos South (Bukuru, Kwata and Vom); and Mangu and Shendam LGAs (Table 1). Apart from a commercial farm in Vom in which 166 of the sampled cattle had history of previous vaccination for FMD, the remaining 366 samples were obtained from non-vaccinated animals. Within the herds, individual animals selected for sampling were properly restrained. The mouth, teat and feet for each animal were carefully examined for any sign of active or previous FMD-like lesions. Five millilitres of blood was collected via the jugular vein in a syringe and allowed to clot. Samples were then kept in a cold box and transported to the laboratory in National Veterinary Research Institute Vom and centrifuged at 1100 ***g*** for 10 min. Serum was aliquoted into 1.8 ml cryovials (Nunc), frozen and stored at −20°C. Clinical materials (epithelial tissue) from outbreaks (n = 30) (collected from four separate locations: Miango, Kwata, Bukuru and Barkin Ladi), in Plateau State, Nigeria, were collected from oral and foot lesions of cattle and sheep into appropriate transport medium for confirmatory diagnosis and characterization of FMDV serotype(s). All laboratory tests were conducted at the Plum Island Animal Disease Center (PIADC), USA.

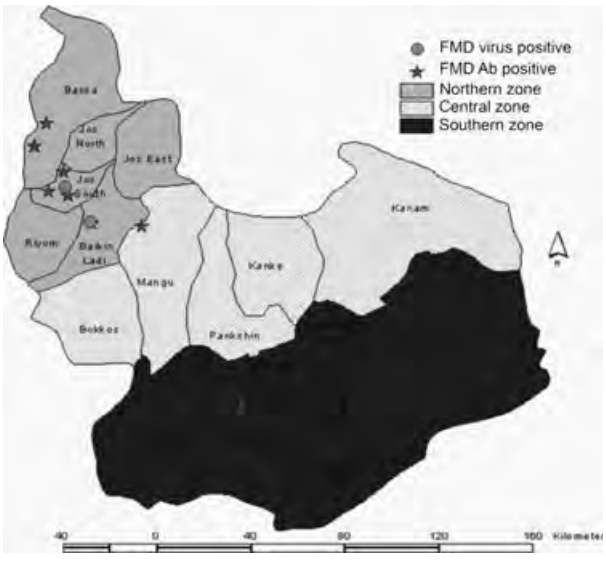

Fig. 1. Map of Plateau state, Nigeria showing the 17 local government areas, the distribution of foot-and-mouth disease (FMD) antibodies and FMD virus positive results.

Serological analysis

VIAA assay for non-structural protein 3D

An agar gel immunodiffusion (AGID) assay was used for the detection of antibodies to the non-structural 3D RNA-dependent RNA polymerase protein, the major component of the 'virus infection-associated antigen' (VIAA) of the FMDV (Morgan et al., 1978; Newman et al., 1979). The FMD VIAA AGID reaction is an indication of FMDV replication in a host (Fernandez et al., 1975; Lobo et al., 1976), and the test has been useful in detecting FMDV infection in the absence of vaccination (McVicar and Sutmoller, 1970; Rosenberg et al., 1976; Dawe and Pinto, 1978; Abu Elzein et al., 1987). The use of vaccine that has not been completely purified could have residual 3D protein eliciting antibody response. A batch of 0.6% agarose gel (agarose Type-II-A, Sigma™) was prepared with 0.86% sodium chloride in a sodium barbital buffer (0.025 M sodium 5,5-diethylbarbiturate, 0.437 M glycine, 0.1% NaN_3, pH 7.8), plated into petri dishes and stored at 4°C. As needed, wells were cut into and aspirated from an agarose gel plate in a predetermined pattern of well clusters, a total of seven clusters per plate each consisting of a circle of six wells surrounding a central well. The 3D antigen was placed in the central well, and the reference serum, containing an antibody to the 3D antigen, was added into the peripheral wells alternating with the test or control sera samples. Antigen-positive control/reference sera and weak positive control were produced from infected bovine by the PIADC. Bovine calf serum was used as a negative control. Plates were placed in a humidified container and incubated at room temperature (20–25°C) overnight, after which the test and control wells were read and interpreted based on precipitin lines and points of identity. Foot-and-mouth disease 3D positives sera were tested on 3ABC ELISA.

Table 1. Summary of sera collected from Plateau State, Nigeria, for foot-and-mouth disease (FMD) 3D-VIAA and 3ABC enzyme-linked immunosorbent assay (3ABC ELISA) assays in 2008–2009

Location	Number of herds	Herd vaccination status	Herd history	Sample	VIAA positive	3ABC ELISA positive
Barkin ladi	5	NV	Reported FMD outbreak in the area	24	8	5
Bukuru	NR	NV	Trade cattle market, lesions of FMD seen	6	6	5
Kwall	3	NV	Surveillance on in-contact herds	28	13	11
Kwata	5	NV	In-contact and affected herds	51 (40, 11, 0)	14 (13, 1, 0)	12 (11, 1, 0)
Mangu	5	NV	Report of previous outbreak in the area. In-contact herds	41	32	32
Miango	5	NV	Herds had recovered from infection. In-contact herds	30 (17, 13, 0)	20 (12, 8, 0)	16 (9, 7, 0)
Shendam	5	NV	Herds had just recovered from an outbreak	16	15	15
Vom	2	V/NV	Surveillance on commercial/institutional farms on semi-intensive management system	336 (224, 72, 40)	89 (83, 0 ,6)	59 (59, NA, 0)
				532	197	154

NR, not recorded; NV, not vaccinated; V, vaccinated; VIAA, virus infection-associated antigen; NA, non-applicable.
For locations in which samples were collected from species other than cattle, the species-specific number of samples and results are indicated (bovine, ovine and caprine).

Fmd 3abc elisa

The PrioCHECK® FMDV NS Antibody test ELISA kit (Prionics Lelystad B.V., Lelystad, The Netherlands, product code 7610450) was used according to the manufacturer's instructions for detection of antibodies to the highly conserved non-structural 3ABC protein of FMDV (Sorensen et al., 1998). Briefly, the ELISA kit contains plates precoated with the FMDV 3ABC non-structural antigen captured by anti-3ABC monoclonal antibody (mAb). Test and control sera were added to plates as directed, followed by the addition of a secondary mAb-HRPO detector and substrate. Anti-3ABC antibodies, if present in sample sera, block the binding of the secondary mAb-HRPO detector thereby decreasing colour development. Results are determined based on per cent inhibition. 3ABC ELISA positives were tested on virus neutralization test (VNT).

Virus neutralization test

The VNT was performed on serum samples according to OIE (2008), using the following FMDV strains belonging to 6 serotypes: A Iraq 4/90, O1 Manisa, C1 Noville, SAT-1 Rho 5/66, SAT-2 Zim 5/81 and SAT-3/Rho 7/34. Briefly, an equal volume of sera diluted 2-fold was incubated at 37°C 5% CO_2 for 60' with a standardized quantity of each virus, between 32 and 63 $TCID_{50}$. Following the addition of MVPK cells, the test was incubated at 37°C 5% CO_2 for 3 days. Due to the nature of the VNT where cross-reactivity amongst serotypes is known to occur, full titration of each serum against above virus strains was conducted. Serum samples were considered positive to the virus strain that produce the highest neutralizing titres. The Spearman–Karber method was used to determine the 50% endpoint antibody titre.

Analysis of tissues

Virus isolation

Tissues were prepared as 10% w/v homogenates in Hank's minimal essential media with antibiotics using Teflon disposable pestles. Virus isolation was performed using secondary lamb kidney (LK) and permanent cell line of Instituto Biologico Rim Suino-2 swine kidney (IBRS-2). Confluent monolayers of cell culture in 24-well plates (Corning #3524) containing 0.5 ml of reserved media (Hank's minimal essential media with antibiotics) were inoculated with 250 μl of a 0.45-μ sample filtrate for the first passage and absorbed for 30–60 min; then, 1 ml/well of Hank's minimal essential media with antibiotics with 4% foetal bovine serum was added. The monolayers were monitored daily for the presence of cytopathic effect (CPE). After 3 days, the plates were frozen at −70°C and thawed to lyse the cells, and 500 μl of this lysate was inoculated on confluent monolayers in 25-cm^2 cell culture flasks containing 0.5 ml of reserved media and absorbed for 60 min; then, 5 ml/flask of Hank's minimal essential media was added. Cells were monitored daily for the presence of CPE. After 3 days, cultures with CPE were frozen at −70°C until tested by real-time RT-PCR for FMDV identification and by antigen capture ELISA (AgELISA) for virus serotyping

FMDV AgELISA

The cell culture isolates were serotyped using an in-house AgELISA test. This method is based on the methodology and reagents developed at the FMD World Reference Laboratory at Pirbright Laboratory (Roeder and Le Blanc Smith,

 © 2013 Blackwell Verlag GmbH • Transboundary and Emerging Diseases.

1987; Ferris and Dawson, 1988) with some modification described in Dulac et al., 1993. Rabbit polyclonal anti-sera to FMDV types O1 BFS 1860 and 01 Manisa, A5/22/24 (Combination) and A Col 85, C3 Resende, SAT 1 BOT 1/68, SAT 2 ZIM 5/81, SAT 3 ZIM 4/81 and Asia 1 CAM 9/80 were used to coat the wells, and guinea pig polyclonal anti-sera to the same FMDV serotypes were used as detector antibodies in the assays. The conjugate, MP (ICN Kappel), was a commercial rabbit anti-guinea pig conjugate with horseradish peroxidase (catalogue # 55392). The normal bovine serum was from Hyclone Cosmic CalfTM (catalogue # SH30087.02) or equivalent. The normal rabbit serum was obtained from Sigma (catalogue # R9133 or equivalent).

Real-time RT-PCR assay

The cell culture isolates were analysed for FMDV RNA using real-time reverse transcription-polymerase chain reaction (rRT-PCR). RNA was extracted from 140 μl of the respective samples using the Qiagen RNeasy extraction kit (Qiagen, Stanford, CA, USA) following the manufacturer's protocol for extraction of total RNA from animal tissues. RNA was eluted in 40 μl of RNase-free water and stored at −70°C until the PCR was performed. Samples were tested for the presence of nucleic acid of FMDV, using oligonucleotide primers and probe targeting a conserved region within the FMDV RNA polymerase (3D) gene (Callahan et al., 2002) as described in the published reference. The location and sequence of the primers and probes were as follows: forward primer starting with base position 6769 (GenBank AF189157) 5′ACT GGG TTT TAC AAA CCT GTG A; reverse primer, base 6875, 5′-GCG AGT CCT GCC ACG GA; and probe, base 6820, 5′-TCC TTT GCA CGC CGT GGG AC. The probe was labelled with a 5′-reporter dye, 6-carboxyfluorescein and a 3′-quencher, tetramethylrhodamine.

Sequence analysis

Products were purified from RT-PCR using QIA quick PCR purification kits (Qiagen). PCR amplicons were sequenced by dideoxy sequencing using a BigDye Terminator Sequencing kit, version 3.1, on a 3703A automated sequencer (Applied Biosystems, Foster City, CA, USA). SEQUENCER software v4.1 (Gene Codes Corporation, Ann Arbor, MI, USA) was used to analyse the chromatograms. Alignments were performed using CLUSTAL_X (Thompson et al., 1997).

Phylogenetic analysis

Either the entire amplified product (Fig. 2/Tree 1) or the complete VP1 (Fig. 3/Tree 2) was used for phylogenetic analysis, which was performed using the maximum-likelihood optimality criterion as implemented in PAUP* version β10 (Swofford, 1998). Additional previously determined complete VP1 sequences (n = 49) from GenBank were included in the analysis. Parameters of nucleotide substitution were estimated using Modeltest, version 3.7 (Posada and Crandall, 1998). The sequences of 21 isolates reported here for the first time were submitted to GenBank (Accession numbers: JN 680709–JN 680729).

Statistical analysis

Questionnaire responses were used to identify factors associated with FMD prevalence at a herd level (herd-level model), whereas the results of the serological tests were used to assess the association between exposure to FMDV and epidemiological factors at the individual level (individual-level model). Records with incomplete information were not included in the statistical analysis, and for that reason, the herd-level model included the information from 194 of 198 questionnaires, whereas the individual-level model included data and results of analysis from 408 of 532 serological tests.

The dependent variables were FMD status (present and absence), as reported in the questionnaires by cattle farmers, for the herd-level model and antibody status for FMD (positive and negative) detected by 3ABC ELISA for the individual-level model. Epidemiological factors included in the questionnaires were considered independent variables for the analysis. A threshold value of $P < 0.1$ was used in a

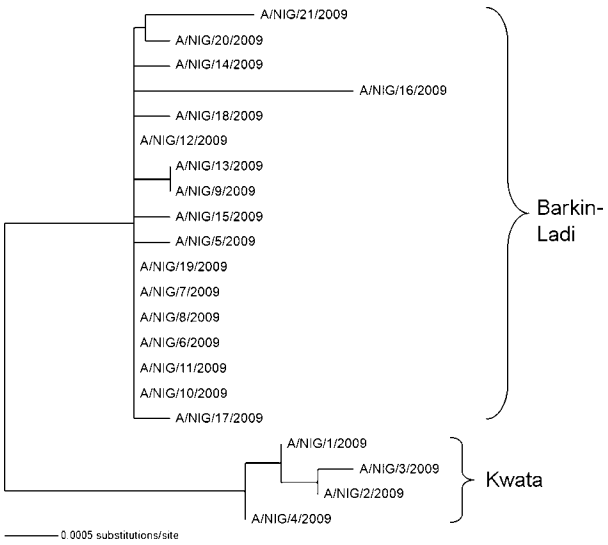

Fig. 2. Mid-point rooted maximum likelihood analysis of 21 foot-and-mouth disease viruses causing disease in Nigeria in 2009. The analysis was conducted on a 2983nt stretch from the 5′UTR through 2A. Viruses form monophyletic groups according to the local government area of origin.

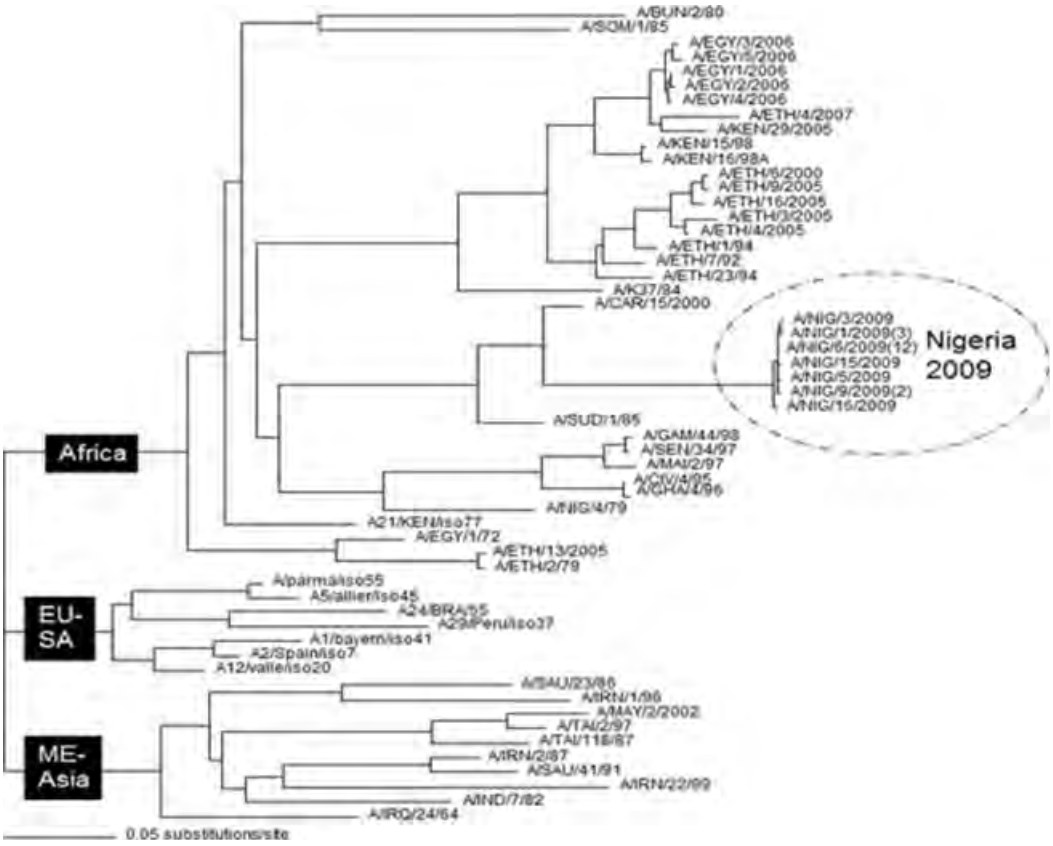

Fig. 3. Mid-point rooted maximum likelihood analysis of the 2009 Nigerian isolates based on the complete VP1 sequence. Full-length VP1 sequences of additional Serotype A viruses available in GenBank were included in the analysis (EU, Europe; SA, South America; ME, Middle East). The total number of viruses with identical VP1 sequences collected from the same local government area is indicated in parentheses.

two-by-two (bivariate) chi-squared test to screen out independent variables unlikely associated with the dependent variables. Variables that passed this initial screening were included in multivariate model using a backward-elimination procedure starting with the least statistically significant from the bivariate analysis. As each variable was removed from the saturated model, which includes all variables that passed the bivariate screening, the model has been reassessed using a likelihood ratio test (LLR). The LLR test compares the saturated model with the model with terms removed and assumes that the assessed model is nested within the saturated model. Variables that were no longer significant were dropped, and the deviance and its effect on other variables were reassessed. If the coefficient for a variable was altered by more than 10% (suggesting confounding), the variable was reentered into the model (Hosmer and Lemeshow, 2000). Interaction between pairs of variables was assessed in the final models. The variables included in the final model were assessed for collinearity following the suggestion from Hosmer and Lemeshow (2000) that any variable with a correlation >0.9 should be further assessed. The Akaike information criteria (AIC) and the Bayesian information criteria (BIC) were used to compare between the non-nested competitive models as a final confirmation process, and the final model was the one with the smallest AIC and BIC values.

The overall fit of the final models was assessed using Pearson's chi-squared statistic and the Hosmer-Lemeshow chi-squared statistic (Hosmer and Lemeshow, 2000). The regression diagnostics delta D (ΔD) and influence ($\Delta\beta$) were calculated and plotted against the predicted probability of disease from the models. Statistical analyses were conducted using both 'STATA 10' software package (Stata Corporation, College Station, TX, USA) and 'SPSS 17' software package (SPSS Corporation, Chicago, IL, USA).

Results

Laboratory analysis

Morbidity rate of sampled animals varied from as low as 12.5% to as high as 100%, and case-fatality was reported to be nil. Foot-and-mouth disease prevalence, as measured by the 3ABC ELISA, in the Plateau region of Nigeria was estimated at 29% (154 of 532), with a 95% CI = 25–33%. The

 © 2013 Blackwell Verlag GmbH • Transboundary and Emerging Diseases.

largest proportions of positive animals were obtained in Bukuru, Mangu and Shendam, representing the three senatorial zones of the state (Table 1, Fig. 1). The proportion of positive results was higher in adult cattle (0.54) compared with calves (0.07): 108 of 168 and 89 of 364 sera collected from traditional/nomadic (free-range) herds and from commercial/institutional farms on semi-intensive (enclosed grazing) systems tested positive to the 3D antibody test, respectively. Amongst vaccinated animals, 64 of 166 and 50 of 64 were VIAA and 3ABC positive, respectively. All sera tested from the various regions showed evidence of virus-neutralizing antibodies at various titres (range, <100–>800) to more than one serotype of FMDV, with the exception of Vom region (Table 2). In sheep during 2008, antibody to serotype O was reported in Kwata, whilst antibody to SAT 1, SAT 2 and SAT 3 was predominant in Miango. Lower titres to serotype O than those to SAT 1, SAT 2 and SAT 3 were detected in sheep sera. In cattle, antibody to serotype O was more prevalent as detected in regions surveyed during 2008 and 2009, whilst antibody to serotype A was detected in Bukuru in 2008 and in Mangu and Shendam in 2009. Additionally, antibody to SAT 1 and SAT 3 was detected in 2008 and to SAT 1, SAT 2 and SAT 3 in 2009 in cattle sera. In contrast to sheep, highest antibody titres were detected against serotype O in cattle sera. Collectively, antibodies against five FMDV serotypes, A, O, SAT 1, SAT 2 and SAT 3 were detected by the VNT in Plateau State, Nigeria. All isolated viruses belonged to the serotype A (Table 3). The distribution of VNT- and rRT-PCR-positive results is shown in Fig. 1.

Statistical analysis

Herd-level risk factors

Ten variables passed the bivariate screening (P-value < 0.1) and were included as candidate variables in the multivariable model. Those ten variables were movement type (settled, nomadic and trade), herd size (≤ 50, 51–100 and >100), grazing type (enclosed, common pastures grazing and nomadic), suspected FMD nearby (yes and no), transhumance (yes and no), contact with wildlife (yes and no), overnight practice (open field, fenced field and cattle market pens), number of contacts within a herd (<3, 3–4 contacts and >4), use of drugs or FMD vaccines (yes and no) and presence of concomitant diseases (yes and no). The final model included five variables. Farms with suspected FMD nearby [odds ratio (OR): 9.5, 95% CI: 4.4–20.4, $P < 0.01$], with contact with wildlife (OR: 1.9, 95% CI: 0.9–4.1, $P < 0.01$), that used drugs or FMD vaccines (OR: 3.2, 95% CI: 1.4–7.6, $P < 0.01$) and with >100 animals (OR: 5.8, 95% CI: 1.5–22.5, $P < 0.01$) were significantly ($P < 0.05$) associated with FMD (Table 4). Although not significantly associated with the outcome, grazing type was also retained in the final model because its removal caused a >10% change in the estimates of OR. No significant interactions were detected, and the final model fitted the data well (Hosmer–Lemeshow chi-squared P-value = 0.987).

Individual-level risk factors

Large ruminants (OR: 9.8, 95% CI: 5.2–18.4, $P < 0.01$), rather than small ruminants, and enclosed (OR: 3.4, 95% CI: 1.6–7.1, $P < 0.01$) or common pastures grazing (OR: 10.8, 95% CI: 5.1–22.3, $P < 0.01$), rather than nomadic grazing were associated with FMD-positive status to the 3ABC ELISA test (Table 5). The interaction between both variables was not significant, and the final model fitted the data well (Hosmer–Lemeshow chi-squared P-value = 0.11).

Phylogenetic analysis

Genetic analysis of the entire RT-PCR product showed a clear separation of viruses causing disease in Barkin Ladi from those in Kwata, with each forming monophyletic groups (Fig. 2). These monophyletic groups were maintained in separate analyses of the leader and the individual P1 proteins (data not shown). The complete VP1 protein, most commonly used for molecular analysis of FMDV isolates, was used to discern the genetic relationship of the 2009 Nigerian viruses with other serotype A isolates (Fig. 3). The Nigerian isolates showed 99.2–100% nucleotide (nt) identity between themselves and 89.5–89.8% nt identity with a virus from Cameroon. The 2009 Nigerian viruses formed a monophyletic group with the nearest genetic neighbour a virus isolated from neighbouring Cameroon in 2000. Based on previously defined limits of nucleotide differences (Knowles and Samuel, 2003), the 2009 Nigerian isolates do not represent a new topotype (data not shown).

Discussion

Foot-and-mouth disease prevalence estimated here (29%, 95% CI: 25–33%) was similar to the 27% recorded by Abegunde (1987) in abattoir samples from the same study area and larger than the 13% reported by Dawe and Durojaiye (1986) in a serological survey of livestock conducted in Oyo State, western Nigeria; these previous studies were conducted based on VIAA test. Noteworthy, prevalence here was computed considering only 3ABC-positive results, given that some false-positive results may be obtained with the 3D antibody test. However, false-positive results for the 3D test are typically due to vaccine usage, and it is likely that most of the animals sampled here have not been vaccinated. For that reason, it is possible that the true disease prevalence in the region may be larger than the 29% estimated computing only

Table 2. Indication of levels of foot-and-mouth disease virus (FMDV) serotype-neutralizing antibodies in cattle and sheep by region in Plateau State, Nigeria

	Cattle 2009				Cattle 2008				Sheep 2008	
VNT Titre Range	Kwall	Kwata	Mangu	Shendam	Bukuru Market	Barkin Ladi	Miango	Vom	Kwata	Miango
<100			A, SAT-2	SAT-2	A			O	O	
100–200	SAT-3	SAT-3	A		A	O				SAT-1, SAT-3
200–400	O			A, O		O, SAT-1	SAT-3			
400–800							O			SAT-2
>800		O	O	O	O					

VNT, virus neutralization test.

Table 3. Diagnostic results on tissue samples from a vesicular disease outbreak in ruminants in Nigeria 2008–2009

Location	Species	Sample type	Number positive/tested VI	rRT-PCR	AgELISA
Kwata	Bovine	Foot	2/3	2/2	FMDV A
	Bovine	Gum	2/2	2/2	FMDV A
Miango	Bovine	Foot	0/2	0/0	NT
	Ovine	Foot	0/1	0/0	NT
Bukuru	Bovine	Foot	0/5	0/0	NT
Barkin Ladi	Bovine	Gum	3/3	3/3	FMDV A
	Bovine	Tongue	14/14	14/14	FMDV A

VI, virus isolation on lamb kidney and porcine kidney epithelial cell line (IBRS2); rRT-PCR, real-time reverse transcription-polymerase chain reaction; AgELISA, antigen capture enzyme-linked immunosorbent assay; NT, not tested.

Table 4. Adjusted multivariate logistic model reporting the OR with 95% CI for risk factors associated with the prevalence of foot-and-mouth disease (FMD) reported by cattle farmers in the Plateau state of Nigeria (N = 194)

Variables in the equation	OR	Sig.	95% CI for OR Lower	Upper
Suspected FMD nearby	9.48	<0.01	4.41	20.4
Wildlife contact	1.94	0.077	0.932	4.06
Use of Drugs/vaccines to control FMD	3.21	0.008	1.36	7.58
Herd Size				
≤ 50	1.00	–	–	–
≤ 100	1.10	0.813	0.505	2.39
≥ 101	5.81	0.011	1.50	22.5
Grazing Type				
Zero	1.00	–	–	–
Common	7.76	0.086	0.7	80.4
Enclosed	0.358	0.602	0.007	17.1

Cox & Snell R^2 = 0.276; Pearson's chi-squared P-value < 0.001; Hosmer–Lemeshow chi-squared P-value = 0.987; Akaike information criteria = 205.8; Bayesian information criteria = 231.9.

Table 5. Adjusted multivariate logistic model reporting the OR with 95% CI for foot-and-mouth disease categorical risk factors associated with the serological results of livestock herds in the Plateau state of Nigeria (N = 508)

Variables in the equation	OR	Sig.	95% CI for OR Lower	Upper
Species (Large ruminants)	9.81	<0.01	5.23	18.39
Grazing Type				
Zero	1.00	–	–	–
Enclosed	3.38	<0.01	1.60	7.12
Common	10.78	<0.01	5.07	22.9

Cox and Snell R^2 = 0.255; Pearson's chi-squared P-value < 0.001; Hosmer–Lemeshow chi-squared P-value = 0.11; Akaike information criteria = 471.1; Bayesian information criteria = 488.

the 3ABC ELISA results. The high prevalence reported in certain regions (Bukuru, Mangu and Shendam) and the finding that FMD-infected animals were identified throughout the state confirms the perceived endemic status of the disease in the region.

Interestingly, the highest proportion of FMD 3D-positive results was obtained in animals sampled from a trade cattle market in Bukuru, stressing the importance of trade markets in disease spread in the region. Previous reports of FMD serotypes detected in Nigeria have been associated with trade cattle entering Nigeria from neighbouring countries (Libeau, 1960; Owolodun, 1971; Nawathe and Goni, 1976; Durojaiye, 1981). Furthermore, because of the cross-sectional nature of the study, results reported here are the reflection of the situation observed at the time when samples were collected; indeed, disease prevalence and incidence fluctuate in association with changes in epidemiological conditions of the setting, such as introduction of trade cattle from neighbouring countries, for example. Therefore, and although purchases for markets did not show up as a significant predictor for FMD risk in the final model, perhaps, due to a recall bias, the role of markets in disease spread should not be ignored. With Nigeria as one of Western Africa's main cattle market, this influx of cattle from neighbouring countries may serve as a confounding source of disease spread within the country. These results suggest that trade markets are a key component of FMD transmission in the Plateau State and that implementation

 © 2013 Blackwell Verlag GmbH • Transboundary and Emerging Diseases.

of control measures, such as inspection and selective restriction of movements and effective disinfection in markets, may help to reduce the disease incidence in the region. This may be implemented through the establishment of quarantine posts at markets, which would certainly require agreement and cooperation from traders (particularly middle men) and cattle suppliers. There was evidence of virus-neutralizing antibodies to FMDV serotypes A, O, SAT 1, SAT 2 and SAT 3 in the sera tested by VNT. This is the first report of the probable presence of FMDV serotype SAT 3 in sheep and cattle in three regions of Plateau State, Nigeria, which may be associated to extensive cross-border animal movements and inter-regional animal trades. Further studies to investigate the potential presence and prevalence of SAT3 virus in Nigeria are required. Farms with suspected FMD nearby (OR: 9.5, 95% CI: 4.4–20.4, $P < 0.01$) were at high risk for FMD, which is a consequence of the infectious nature of the disease and reflects the expected spatial correlation of disease prevalence. Farms that used drugs or vaccines were also likely to be FMD positive (OR: 3.2, 95% CI: 1.4–7.6, $P < 0.01$), suggesting that farmers may treat their animals with drugs and emergency vaccination in response to the detection of FMD-like clinical signs. Herds with >100 animals were also more likely to be FMD positive than small farms (OR: 5.8, 95% CI: 1.5–22.5, $P < 0.01$), likely because large herds have higher probability of adequate contacts, introduction of animals and, consequently, spread of FMD than small herds. Although not significantly associated with the outcome, cattle grazing type and contacts with wildlife (e.g. African buffalo, antelope) improved the model fitness, indicating that those factors may be assessed in future studies to elucidate whether they play any role on the epidemiology of the disease in the region. The association between risk for FMD and contact with wildlife may have different explanations. Although role of wildlife hosts for FMD has not been proved in Western Africa, it could be possible that some susceptible wildlife may simply be a proxy for another factor, such as openness of the farm borders and feasibility of the contact between susceptible and infected animals. Large ruminants and animals kept in non-nomadic systems were more likely to be 3 ABC ELISA positive than small ruminants ($P < 0.01$). Cattle are more susceptible to FMDV especially via aerosol because of their larger respiratory volume compared with sheep and goats (Donaldson, 1987). Settled herds were more FMD positive than nomadic system due to faster spread of the virus via aerosol and increased contact that may be evident at common pasture and water sources they share particularly during scarcity.

Results of the phylogenetic analysis suggest a strong relation amongst and between collected samples. Kwata is located in the Jos South LGA, whereas B/LADI is in the B/LADI LGA. These two areas share a common boundary. Clinical samples were obtained 5 days apart from fulani nomads (pastoralist) who normally move around and beyond the state in search of pasturage and water. Thus, it is likely that the phylogenetic differences identified between those two regions were just an anecdotic evidence of the changes in biodiversity with time that one would expect for viruses circulating in an endemic region, rather than a reflection of true topographic boundaries for different FMD strains.

In conclusion, this article provides report on the prevalence, geographical distribution, association with epidemiological factors and genetic diversity of FMD in Plateau State, Nigeria. These results provide knowledge on the epidemiological situation of FMD in Plateau State and which could probably help to develop effective control and prevention strategies for FMD in Nigeria and other countries of the region.

Acknowledgements

We thank the fulani herdsmen and farm owners for their hospitality and for allowing samples to be collected from their herds. We also thank Drs Damina, Manasa and Shedrach and Mr Abdullahi for linking us with the fulanis, and the staff of diagnostic services section, foreign animal disease diagnostic laboratory, for technical support with diagnostic analyses. This project was funded in part by the USDA/ARS-UC Davis specific cooperative agreement SCA 58-1940-9-970.

References

Abegunde, A. A. 1987: **S**tudies on the epidemiology of foot – and- mouth disease in Nigeria. PhD Thesis, Ahmadu Bello University, Zaria, Nigeria.

Abu Elzein, E. M. E., B. J. Newman, J. R. Crowther, I. T. R. Barnett and J. J. McGrane, 1987: The prevalence of antibodies against foot-and-mouth disease in various species of Sudanese livestock following natural infection. *Rev. Elev. Med. Vet. Pays Trop.* 40, 7–12.

Bastos, A. D. S. and O. Sangare, 2001: Geographic distribution of SAT 2 type foot-and-mouth disease virus genotypes in Africa. *Proceedings of Southern African Society for Veterinary Epidemiology and Preventive Medicine (SASVEPM), 10–11 May, Onderstepoort, South Africa. SASVEMPM, Pretoria* 20–26.

Bronsvoort, B. M. D. E. C., J. Anderson, A. Corteyn, P. Hamblin, R. P. Kitching, C. Nfon, V. N. Tanya and K. L. Morgan, 2006: Geographical and age-stratified distributions of foot –and-mouth disease virus- seropositive and probang- positive cattle herds in the Adamawa province of Cameroon. *Vet. Rec.* 159, 299–308.

Callahan, J. D., F. Brown, F. A. Osorio, J. H. Sur, E. Kramer, G. W. Long, J. Lubroth, S. J. Ellis, K. S. Shoulars, K. L. Gaffney,

D. L. Rock, and W. M. Nelson, 2002: Use of a portable real-time reverse transcriptase-polymerase chain reaction assay for the rapid detection of foot-and-mouth disease virus. *J. Am. Vet. Med. Assoc.* 220, 1636–1642.

Carroll, A. R., D. J. Rowlands and B. E. Clarke, 1984: The complete nucleotide sequence of the RNA coding for the primary translation product of foot-and-mouth disease virus. *Nucleic Acids Res.* 12, 2461–2472.

Dawe, P. S. and O. A. Durojaiye, 1986: A preliminary survey of antibody to VIA antigen of foot and mouth disease virus in Nigerian Livestock. *Rev. Sci. Tech.* 5, 711–714.

Dawe, P. S. and A. A. Pinto, 1978: Antibody responses to type-specific and virus-infection-associated antigens in cattle vaccinated with inactivated polyvalent foot and mouth disease virus in north Malawi. *Brit. Vet. J.* 134, 504–510.

Domingo, E., C. Escarmis, E. Baronowski, C. M. Ruiz-Jarabo, E. Carrillo, J. I. Neun˜z and F. Sobrino, 2003: Evolution of foot-and-mouth disease virus. *Virus Res.* 9, 47–63.

Donaldson, A. I., 1987: Foot-and-mouth disease: the principal features. *Irish Vet. J.* 41, 325–327.

Dulac, G. C., R. A. Heckert, A. Afshar, J. Bosse, W. White, A. Torres, J. A. House, N. P. Ferris, C. Dubuc, and A. A. Alonso, 1993: Application of the double antibody sandwich ELISA test for the diagnosis of vesicular disease virus. *Proceeding of 97th Annual Meeting of the United States Animal Health Association. 25–29 October*, Las Vegas, Nevada: USAHA, 225–237.

Durojaiye, A. O., 1981: Incidence of foot-and-mouth disease in Oyo State of Nigeria 1967–1981. *Nig. Vet. J.* 10, 7–13.

Fernandez, A. A., P. Mello, I. Auge de Gomes, and F. Rosenberg, 1975: The use of virus-infection-associated antigen (VIA) in the detection of cattle exposed to FMDV. *Bol. Centr. Panam. Fiebre Aftosa* 17–18, 17–22.

Ferris, N. P. and M. Dawson, 1988: Routine application of enzyme-linked immunosorbent assay in comparison with complement fixation for the diagnosis of foot-and-mouth and swine vesicular diseases. *Vet. Microbiol.* 16, 201–209.

Ferris, N. P. and A. I. Donaldson, 1992: The World Reference Laboratory for Foot and Mouth Disease: a review of thirty-three years of activity (1958–1991). *Rev. Sci. Tech.* 11, 657–684.

Forss, S., K. Strebel, E. Beck and H. Schaller, 1984: Nucleotide sequence and genome organisation of foot-and-mouth disease virus. *Nucleic Acids Res.* 12, 6587–6601.

Grubman, M. J., B. H. Robertson, D. O. Morgan, D. M. Moore and D. Dowbenko, 1984: Biochemical map of polypeptides specified by foot-and-mouth disease virus. *J. Virol.* 50, 579–586.

Hosmer, D. N. and S. Lemeshow, 2000: Assessing the Fit of the Model in Applied Logistic Regression, pp. 143–202. Wiley, New York.

James, A. D. and J. Rushton, 2002: The economics of foot and mouth disease. *Rev. Sci. Tech.* 21, 637–644.

King, A. M. Q., 2000: Picornaviridae. In: Van Regenmortel, M. H. V., C. M. Fauquet, and D. H. L. Bishop (eds), Virus Taxonomy: Classification and Nomenclature of Viruses, pp. 657–673. Academic Press, San Diego, CA.

Knowles, N. J., 2008: Molecular epidemiology report on foot-and-mouth disease virus serotypes O and SAT 2 from Nigeria in 2007–2008. Molecular epidemiology report form IAH-P-EP-MEG-FOR-005-1, FAO, WRLFMD.

Knowles, N. J. and A. R. Samuel, 2003: Molecular epidemiology of foot-and-mouth disease virus. *Virus Res.* 91, 65–80.

Knowles, N. J., D. M. Ansell, and A. R. Samuel, 1998: Molecular comparison of recent foot-and-mouth disease type A viruses from West Africa with historical and reference virus strains. Paper presented to the session of the research group of the standing technical committee of the European Commission for the control of foot-and-mouth disease (EUFMD), 14–18 September, Pirbright, United Kingdom. EUFMD, Rome, 1–6.

Libeau, J., 1960: Foot and mouth disease in Africa south of the Sahara-the present situation. *Bull. Epizoot. Dis. Afr.* 8, 152–158.

Lobo, C. A., R. P. Hanson, A. Gutierrez and L. E. Beltran, 1976: Serological detection of natural foot-and-mouth disease infection in cattle and pigs. *Bull. Off. Int. Epizoot.* 85, 1075–1104.

Mahajan, B. K., 1997: Methods in Biostatistics For Medical Students and Research Workers. 6th edn, pp. 88–94. Jaypee brothers medical publisher Ltd, India.

McVicar, J. W. and P. Sutmoller, 1970: Foot-and-mouth disease: the agar gel immunodiffusion precipitin test for antibody to virus-infection-associated (VIA) antigen as a tool for epizootiologic surveys. *Am. J. Epidemiol.* 92, 273–278.

Morgan, D. O., D. M. Moore, and P. D. McKercher, 1978: Purification of foot-and-mouth disease virus infection- associated antigen. *Proceeding of 82nd Annual Meeting of the United States Animal Health Association. 29–31 October, 1–3 November, Buffalo, NY*. Richmond, Virginia: USAHA, 277–283.

National Bureau of Statistic (NBS) 2009: Information on plateau state. http://www.nigeriastat.gov.ng/idex.php/stateinformation (accessed 07 August 2009).

Nawathe, D. R. and M. Goni, 1976: Foot and mouth disease in Nigeria. *Bull. Anim. Health. Prod. Afr.* 24, 1–4.

Newman, J. F. E., B. Cartwright, T. R. Doel, and F. Brown, 1979: Purification and identification of the RNA-dependent RNA polymerase of foot-and-mouth disease virus. *J. Gen. Virol.* 45, 497–507.

OIE 2008: Foot and Mouth Disease. *Manual of Diagnostic Tests and Vaccines for Terrestrial Animals (Mammals, Birds, and Bees)*, 6th Edn, Volume 1, Chapter 2.1.5., pp. 190–217. World Organization for Animal Health, Paris, France, http://www.oie.int/eng/publicat/en_standards.htm (accessed 16 October 2011).

OIE/FAO Annual Report 2010: Foot and mouth disease reference laboratory network. www.fao.org/ag/againfo/commissions/docs/OIE-FAO-FMD_Reference-Laboratory-Network_2010 (accessed 12 October 2011).

Owolodun, B. Y., 1971: Foot and mouth disease and virus type distribution in Nigeria. *Bull. Epizoot. Dis. Afr.* 19, 152–158.

Posada, D. and K. A. Crandall, 1998: Modeltest: testing the model of DNA substitution. *Bioinformatics* 14, 817–818.

 © 2013 Blackwell Verlag GmbH • Transboundary and Emerging Diseases.

Roeder, P. L. and P. M. Le Blanc Smith, 1987: Detection and typing of foot-and-mouth disease virus by enzyme-linked immunosorbent assay: a sensitive, rapid and reliable technique for primary diagnosis. *Res. Vet. Sci.* 43, 225–232.

Rosenberg, F. J., H. M. Cruz, A. A. Fernandez, T. Martinez and A. Barreto, 1976: Prevalence of antibodies against foot-and-mouth disease virus-infection-associated antigen (VIA) in cattle of the Paraguayan Chaco. *Bol. Centr. Panam. Fiebre Aftosa* 21–22, 1–8, 9–16.

Sangare, O., O. Bastos, E. H. Marquardt, and W. Venter, 2001: Molecular epidemiology of serotype O foot-and-mouth disease virus with emphasis on West and South Africa. *Virus Genes* 22, 345–351.

Sangare, O., A. D. S. Bastos, E. H. Venter and W. Vosloo, 2003: Retrospective genetic analysis of SAT 1 type foot-and-mouth disease outbreaks in West Africa 1975–1981. *Vet. Microbiol.* 93, 279–289.

Sorensen, K. J., C. M. Hansen, E. S. Madsen, and K. G. Madsen, 1998: Blocking ELISAs using the FMDV non-structural proteins 3D, 3AB, and 3ABC produced in baculovirus expression system. *Vet. Q.* 20, S17–S20.

Swofford, D. L., 1998: PAUP*. Phylogenetic Analysis Using Parsimony, Version 4. Sinauer Associates, Sunderland, MA.

Thompson, J. D., T. J. Gibson, F. Plewniak, F. Jeanmogin and D. G. Higgins, 1997: The CLUSTER_X windows interface flexible strategies for multiple sequence alignment aided by quality analysis tools. *Nucleic Acids Res.* 24, 4876–4882.

Vosloo, W., A. D. S. Bastos, O. Sangare, S. K. Hargreaves and G. R. Thomson, 2002: Review of the status and control of foot and mouth disease in Sub-Saharan Africa. *Rev. Sci. Tech.* 21, 437–449.

Journal of General Virology (2013), **94**, 348–353 DOI 10.1099/vir.0.047571-0

Short Communication

Theiler's murine encephalomyelitis virus contrasts with encephalomyocarditis and foot-and-mouth disease viruses in its functional utilization of the StopGo non-standard translation mechanism

G. Loughran,[1] J. E. Libbey,[2] S. Uddowla,[3] M. F. Scallan,[4] M. D. Ryan,[5] R. S. Fujinami,[2] E. Rieder[3] and J. F. Atkins[1,4,6]

Correspondence
John F. Atkins
J.atkins@ucc.ie

[1]Department of Biochemistry, Western Gateway Building, University College Cork, Cork, Ireland

[2]Department of Pathology, University of Utah, Salt Lake City, UT 84132, USA

[3]Foreign Animal Disease Research Unit, United States Department of Agriculture, Agricultural Research Service, Plum Island Animal Disease Center, Greenport, NY 11944, USA

[4]Department of Microbiology, University College Cork, Cork, Ireland

[5]Centre for Biomolecular Sciences, University of St Andrews, St Andrews, Scotland, UK

[6]Department of Human Genetics, University of Utah, Salt Lake City, UT 84112, USA

Received 28 August 2012
Accepted 20 October 2012

The picornaviruses' genome consists of a positive-sense ssRNA. Like many picornaviruses, cardioviruses synthesize two distinct polyprotein precursors from adjacent but non-overlapping genome segments. Both the [L-1ABCD-2A] and the [2BC-3ABCD] polyproteins are proteolytically processed to yield mature capsid and non-structural proteins, respectively. An unusual translational event, known as 'StopGo' or 'Stop-Carry on', is responsible for the release of the [L-1ABCD-2A] polyprotein from the ribosome and synthesis of the N-terminal amino acid of the [2BC-3ABCD] polyprotein. A common feature of these viruses is the presence of a highly conserved signature sequence for StopGo: –D(V/I)ExNPG↓P–, where –D(V/I)ExNPG are the last 7 aa of 2A, and the last P- is the first amino acid of 2B. Here, we report that, in contrast to encephalomyocarditis virus and foot-and-mouth disease virus, a functional StopGo does not appear to be essential for Theiler's murine encephalomyelitis virus viability when tested *in vitro* and *in vivo*.

The genus *Cardiovirus* belongs to the family *Picornaviridae* of positive-sense ssRNA viruses. Currently, two cardiovirus species are recognized – encephalomyocarditis virus (EMCV) (including mengovirus) and *Theilovirus*. The latter species encompasses a number of divergent clades and isolates, including Theiler's murine encephalomyelitis virus (TMEV), Thera virus, Vilyuisk human encephalomyelitis virus and human Saffold viruses. The cardiovirus genome comprises a single RNA molecule of ~8 kb that contains a single long ORF, which is translated as two polyproteins each of which is cleaved by the virus-encoded 3C protease (Palmenberg *et al.*, 1984; Jackson, 1986; Palmenberg, 1990). Like many picornaviruses, cardioviruses use an unusual proteolysis-independent but ribosome-dependent mechanism, termed 'StopGo' or 'Stop-Carry on', to release the [L-1ABCD-2A] polyprotein from the ribosome and to specify the N-terminal amino acid of the [2BC-3ABCD] polyprotein (Batson & Rundell, 1991; Palmenberg *et al.*, 1992; Atkins *et al.*, 2007; Brown & Ryan, 2010). The C-terminal amino acid of the [L-1ABCD-2A] polyprotein and the N-terminal amino acid of the [2BC-3ABCD] polyprotein are encoded by adjacent codons – no stop codon or proteolytic processing is involved. StopGo is mediated by a highly conserved amino acid motif –D(V/I)ExNPG↓P– which, together with upstream amino acids that have a strong α-helical propensity, prevents formation of a peptide bond between Asn–Pro–Gly and Pro, but allows the continuation of translation with up to near-100 % efficiency (Ryan & Drew, 1994; Hahn & Palmenberg, 1996; Donnelly *et al.*, 1997; Hahn & Palmenberg, 2001; Donnelly *et al.*, 2001a; Doronina *et al.*, 2008; Brown & Ryan, 2010).

Previous analysis of StopGo translational activity has been performed *in vitro* with either reporter sequences flanking StopGo-encoding sequences (Ryan *et al.*, 1991; Ryan & Drew, 1994; Donnelly *et al.*, 2001a) or using cDNAs encoding partial virus sequences, including and surrounding StopGo

Supplementary tables are available with the online version of this paper.

 047571 © 2013 SGM *Printed in Great Britain*

(Roos *et al.*, 1989; Batson & Rundell, 1991; Palmenberg *et al.*, 1992). Mutational analysis indicated that the highly conserved –NPGP– motif is indispensable for StopGo activity (Hahn & Palmenberg, 1996; Donnelly *et al.*, 2001b). Hahn & Palmenberg (1996) also determined a critical role for StopGo activity for normal viral infection. In that study, HeLa monolayers infected with StopGo-mutated EMCV failed to form plaques.

To establish whether a general requirement for StopGo activity exists in other cardiovirus species/clades and in an aphthovirus species, we set out to investigate the effects of StopGo mutations in TMEV and foot-and-mouth disease virus (FMDV) on virus viability and polyprotein processing. Although there are no previous reports describing mutations engineered within the TMEV StopGo motif, an –NPGP– to –NAGP– mutation (PA mutation) has been shown to inhibit FMDV StopGo activity using a reporter system (Donnelly *et al.*, 2001b). However, mutation of a proline codon (CCX) to an alanine codon (GCX) necessarily requires only a single base change; therefore, to reduce the possibility of reversion, we made a second StopGo mutation, –NPGP– to –NPLV– (LV mutation) that would require at least four base changes for complete reversion. To determine whether these StopGo mutations can disable TMEV StopGo activity, mutations were first introduced into partial virus cDNA subclones encoding 1D2A2B and part of 2C (1D2A2B2Cmid) (Fig. 1a). This sequence is devoid of other virus processing events (in particular cleavage by 3C protease). StopGo mutations (PA and LV) to 1D2A2B2Cmid were engineered by a standard two-step PCR (Phusion polymerase; NEB) using primers 1–6 (Table S1, available in JGV Online), with pSK-GDVII as template. pSK-GDVII is a full-length infectious cDNA clone of TMEV [virus GDVII (GenBank accession no. NC_001366) is a virulent strain of TMEV]. As a control, we also mutated mengovirus –NPGP– to –NPLV– (LV mutation) in the context of 1D2A2B2Cmid by two-step PCR (primers 7–10, Table S1), with mengovirus cDNA (pMC0) as template. pMC0 is a full-length infectious recombinant mengovirus (vMC0) identical to GenBank accession no. DQ294633 except in the 5′UTR where vMC0 has the poly(C) tract deleted (Duke *et al.*, 1990). All amplicons were cloned *Bam*HI/*Xba*I into pcDNA3.1 (Invitrogen) using standard cloning procedures, and all clones were confirmed by sequencing.

DNA encoding wild-type and StopGo-mutated TMEV and mengovirus 1D2A2B2Cmid were used to programme coupled *in vitro* transcription–translation reactions in rabbit reticulocyte extracts with [^{35}S] methionine according to the manufacturer's (Promega) instructions (Fig. 1b). As expected for translation of a functional StopGo, both TMEV and mengovirus wild-type constructs expressed 1D2A and 2B2Cmid as separate proteins (Fig. 1b). All StopGo-mutated constructs expressed a 1D2A2B2Cmid fusion, indicating that these mutations (PA and LV) disable StopGo activity. Densitometry (ImageQuant) of radiolabelled 1D2A and 2B2Cmid and normalization for

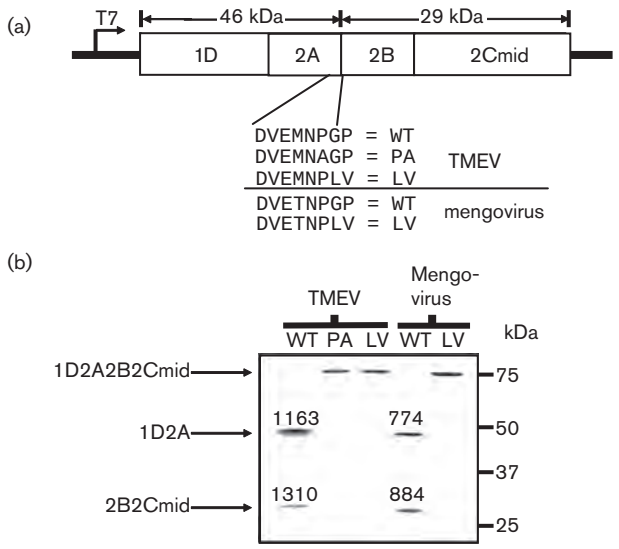

Fig. 1. (a) Schematic representation of the wild-type and mutant TMEV and mengovirus region expressed by *in vitro* translation. (b) Coupled *in vitro* transcription–translation. Each plasmid (100 ng) in a 10 μl reaction volume was incubated at 30 °C for 60 min before resolving by SDS-PAGE (12 %). Arbitrary values above each band in lanes marked 'WT' correspond to relative intensity per encoded methionine.

encoded methionines, indicated that, as previously reported for FMDV (Donnelly *et al.*, 2001a), active StopGo results in an equimolar ratio of N- and C-terminal products. Together, these results show that in TMEV, mutating the highly conserved StopGo motif completely inhibits StopGo activity, which is in complete agreement with previous *in vitro* StopGo mutagenesis studies in FMDV (Donnelly *et al.*, 2001a) and EMCV (Hahn & Palmenberg, 1996).

We next set out to determine the effect that disabling StopGo might have on virus viability and polyprotein processing by replicating these mutations in the context of full-length virus. Recombinant TMEV genomes containing mutations in the StopGo motif were made by subcloning the *Acc*III/*Bsg*I region of the mutant TMEV 1D2A2B2Cmid cDNAs into pSK-GDVII. Similarly, mutant mengovirus genomes were engineered by subcloning the *Bgl*II/*Afl*II region of the mutant mengovirus 1D2A2B2Cmid cDNAs into pMC0. In addition, a full-length infectious FMDV cDNA clone, A24 Cruzeiro, [pA24-WT (Rieder *et al.*, 2005)] was used to derive A24-PA and A24-LV mutant RNAs by two-step PCR by using primers 13–16 (Table S1). PCR amplicons were digested with *Sna*BI/*Mfe*I and cloned into pA24-WT digested with the same enzymes. Again standard cloning procedures were used throughout, and all clones were confirmed by sequencing.

Plasmids encoding full-length wild-type and StopGo-mutated infectious TMEV, FMDV and mengovirus cDNAs were linearized with either *Xba*I (TMEV), *Swa*I (FMDV) or

*Bam*HI (mengovirus) and transcribed with T7 RNA polymerase (Megascript; Ambion) for 3 h at 37 °C. Equivalent amounts of RNA (TMEV and mengovirus) were transfected into BHK-21 cells (ATCC) using DMRIE-C (Invitrogen) according to the manufacturer's recommendations. BHK-21 cells were maintained in Dulbecco's modified Eagle medium (DMEM) supplemented with 10 % FBS, 1 mM L-glutamine and antibiotics and incubated at 37 °C with 5 % CO_2. Twenty-four hours after transfection, virus titres were quantified by plaque assay. Transfected cells were subjected to three freeze–thaw cycles followed by centrifugation (1800 ***g***) to pellet cell debris. Supernatants were collected then aliquoted and stored at −80 °C. BHK-21 monolayers (90 % confluent) were infected with 10-fold dilutions of each supernatant for 1 h at 37 °C. The virus inocula were removed, and cells overlaid with 1.0 % agarose containing MEM. After 48 h incubation (72 h for mengovirus-LV) at 37 °C, cells were fixed with 2.5 % formalin, and plaques visualized by crystal violet staining. Surprisingly, even though we fully expected inhibition of StopGo activity with the two TMEV mutants (PA and LV), virus titres were similar to wild-type, whereas we observed at least a 3 log decrease in virus titre between wild-type and StopGo-inactivated mengovirus (Fig. 2a). One-step growth curves comparing wild-type and mutant TMEV showed little difference (Fig. 2b). For one-step growth curves, BHK-21 monolayers were infected as above at an m.o.i. of 1.0 and then infected cells collected and viruses recovered by freeze–thawing 6, 12 and 24 h post-infection. Virus titres from each time point were determined by plaque assay. To rule out the possibility that these surprising results for TMEV could be explained by reversion or contamination, RNA was extracted from 200 µl of each virus stock using the Trizol (Invitrogen) method, then reverse transcribed (Superscript III; Invitrogen) with primer 2 (Table S1). The sequence surrounding the 2A–2B junction was amplified by PCR using primers 11 and 12 (Table S1) and amplicons sequenced on both strands to confirm that reversion had not occurred. For FMDV, electroporation was used to transfect BHK-21 cells as described previously (Rieder *et al.*, 1993). Blind passages were carried out resulting in the absence of cytopathic effects (CPE). Therefore, StopGo-mutated FMDV produced no viable progeny even after several passages (Fig. 2c).

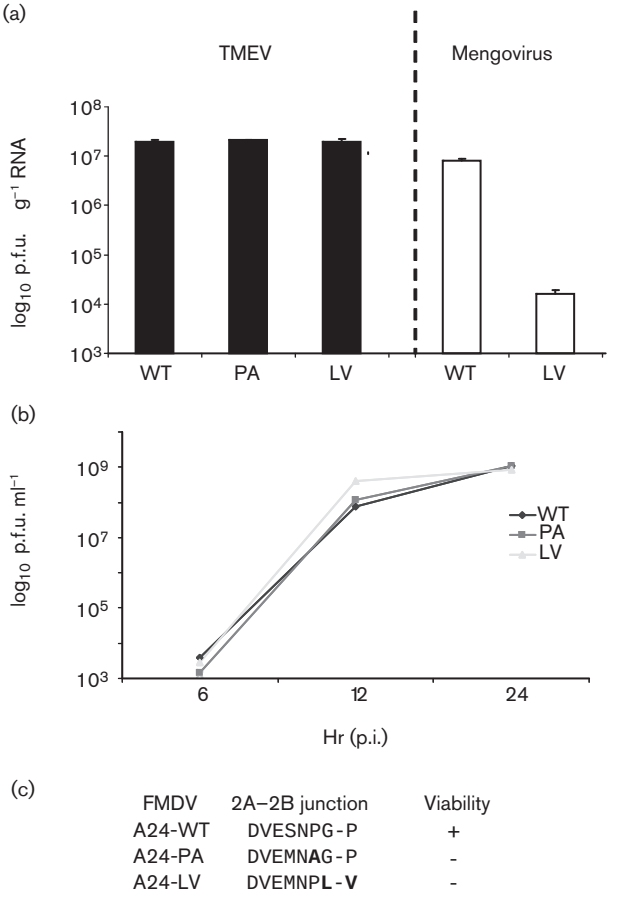

Fig. 2. (a) Virus titres expressed as p.f.u. per µg RNA determined by plaque assay after harvesting virus from BHK-21 cells transfected with RNA encoding either wild-type or mutant TMEV and mengovirus. (b) One-step growth curves of wild-type and StopGo-mutated TMEV. Cells were infected at an m.o.i. of 1.0 and virus collected at 6, 12 and 24 h post-infection (p.i.) then virus titres determined by plaque assay. (c) Viability of wild-type and mutant FMDVs. After four blind passages, no CPE (represented by '–') was observed in StopGo mutants. '+' Indicates CPE >95 % cells infected with wild-type FMDV.

While we clearly observed StopGo inhibition by *in vitro* translation experiments (Figs 1b and 3b), replicating these same mutations into the full-length infectious cDNAs resulted in stark differences between TMEV, FMDV and mengovirus. Again consistent with a previous report in which StopGo was mutated in EMCV (Hahn & Palmenberg, 1996), StopGo-mutated mengovirus was severely attenuated (Fig. 2a). This contrasted dramatically with StopGo-mutated TMEV, which appeared completely normal under the conditions tested (Fig. 2a, b).

Although we observed little effect of inhibiting StopGo on TMEV in cultured cells, we next tested the possibility that the mutant TMEV may lose virulence in a more natural setting (*in vivo*). Rodents are the natural host of TMEV, and intracerebral GDVII virus infections of mice cause acute and fatal encephalitis (Villarreal *et al.*, 2006). We injected intracerebrally 1000 p.f.u. of wild-type and LV mutant TMEV into SJL/J mice (13 animals for each group) and then monitored the number of days post-injection for death to occur. All mice injected with wild-type or StopGo-mutated TMEV were dead by the end of day 7 at the expected time (Table S2), indicating that these mutant viruses were completely viable even though they did not have StopGo activity.

Since inactivating StopGo in TMEV does not affect viral infectivity or replication in BHK-21 cells, we were able to monitor the effect of disrupting StopGo on TMEV

polyprotein processing by pulse-labelling. BHK-21 cells (90–100 % confluent) in 35 mm dishes were infected with wild-type or mutant TMEV (m.o.i. 10). After 60 min of adsorption at 37 °C, the virus inocula were removed. The cells were washed once with methionine-free DMEM and incubated in 0.25 ml methionine-free DMEM. Cells were labelled with [^{35}S] methionine (50 μCi ml^{-1}) at 37 °C for 30 min, washed once in PBS, lysed by suspension in 0.2 ml of sample buffer and heated at 95 °C for 5 min. Lysates were then analysed by SDS-PAGE. After electrophoresis, gels were processed for fluorography with Amplify (Amersham) before drying and exposure to a phosphorscreen. Mutating TMEV StopGo in the context of full-length infectious clones would be expected to produce 2A–2B fusion proteins of ~34 kDa. However, as shown in Fig. 3(a), there was no ~34 kDa 2A–2B fusion protein detected in cells infected with mutant TMEV. Instead, a protein very similar in molecular mass to wild-type 2A (~16 kDa) was detected (2A* in Fig. 3a). Furthermore, unlike polyprotein processing in StopGo-mutated EMCV (Hahn & Palmenberg, 1996) where the P1 proteins were not properly processed, processing of the TMEV P1 proteins appears to be unaffected when StopGo is mutated. The effect of mutating FMDV StopGo was determined by *in vitro* transcription and translation of FMDV cDNAs and indicates that, as expected, polyprotein processing is severely impaired when StopGo is mutated (Fig. 3b).

One possible explanation for these unexpected TMEV polyprotein processing data could be that phylogenetically conserved Gln and Gly residues just 9 aa downstream of the StopGo site may act as a cryptic 3C protease cleavage site. In general, the consensus picornavirus 3C cleavage site is hydrophobic-x-x-Q/(G, A or S) (Leong *et al.*, 2002), and in TMEV and EMCV, the putative cryptic 3C cleavage sites are FQPQ/G and FQTQ/G, respectively. No consensus 3C protease cleavage site exists in this region of FMDV. Therefore, TMEV and EMCV with StopGo mutated would synthesize 2A fused to 2B and subsequent 3C cleavage at the cryptic site would leave the N-terminal 9 aa of 2B still fused to 2A (2A*). The absence of 2A* in the absence of 3C protease (Fig. 1b) also supports this explanation. The possibility of an EMCV cryptic 3C cleavage site near this position has been suggested previously in several other reports (Parks & Palmenberg, 1987; Palmenberg *et al.*, 1992). Furthermore, *in vitro* translation of StopGo-mutated EMCV RNA still appeared to synthesize L-P1-2A (Hahn & Palmenberg, 1996). These authors also failed to detect a ~34 kDa 2A–2B fusion protein during polyprotein processing of StopGo-mutated EMCV. In this regard it is interesting to note that in hepatoviruses the equivalent primary cleavage in this region of the polyprotein (between 2A and 2B) is mediated by the 3C protease (Harmon *et al.*, 1992).

Another possible explanation for the observed heavier 2A species (2A* in Fig. 3a) when StopGo is mutated could be that it is a 2A–2B* fusion. 2B* is a recently identified transframe protein (Loughran *et al.*, 2011) that is a fusion resulting from a programmed −1 frameshift into a conserved overlapping ORF within the 2B region of EMCV. The conserved EMCV ribosome slip site (G GUU UUY) is also conserved in TMEV and all other cardioviruses. While

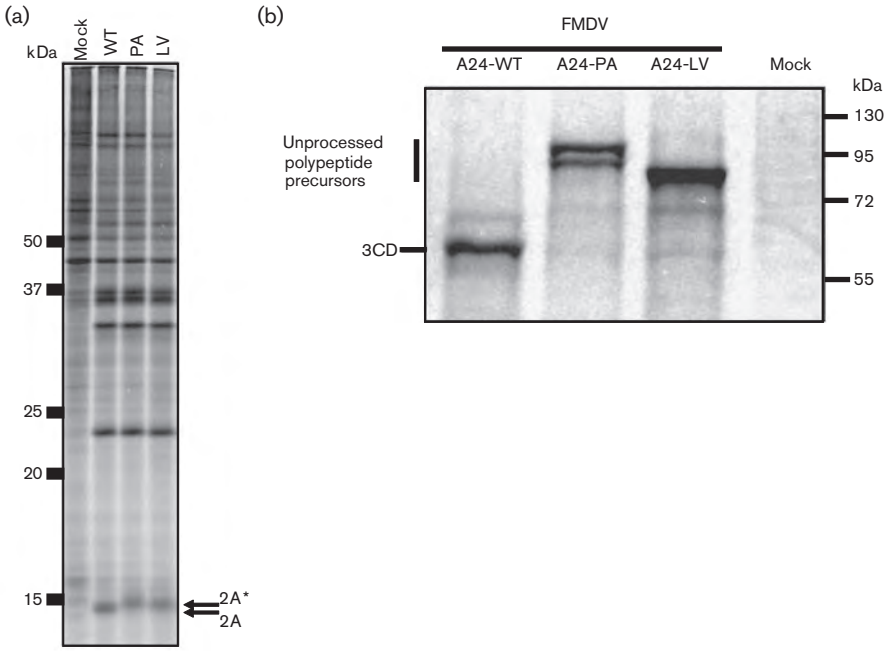

Fig. 3. (a) 4–20 % SDS-PAGE of TMEV infected (m.o.i. 10) BHK-21 cell extracts from a pulse-labelling experiment. Lysates were prepared 6 h post-infection. (b) *In vitro* translation reactions of FMDV wild-type and its StopGo mutants.

2B* in EMCV is ~130 aa it is only predicted to encode 11 aa in TMEV. While this possibility might explain the greater mass of 2A in cells infected with the mutant TMEV, it does not adequately explain the absence of the ~34 kDa protein (unless fusion of 2B has a dramatic protein destabilizing effect), which would still be expected regardless of frameshifting.

Why does mutating StopGo have such dramatic differences on virus viability between TMEV and mengovirus? One clue is the major difference that mutating StopGo has on polyprotein processing. As can be seen in Fig. 3(a), polyprotein processing appears identical in the P1 region between TMEV wild-type and mutant viruses. This is in contrast to *in vitro* translation of StopGo-mutated EMCV RNA where polyprotein processing of the L-P1-2A precursor by 3C protease was impaired, suggesting a critical role for a primary 'cleavage' event to allow proper folding of the P1 precursor in a manner that is compatible with efficient 3C cleavage (Hahn & Palmenberg, 1996). Consistent with this hypothesis, one of the EMCV mutations made by Hahn and Palmenberg, in which the wild-type –DIETNPGP– was mutated to –DIEvNPGP–, was completely efficient at StopGo but was still unable to properly process the P1 proteins.

StopGo is extremely highly conserved (Luke *et al.*, 2008). It is unclear to us at this stage why StopGo appears to be dispensable in TMEV, but not in EMCV or FMDV. It seems likely that we simply have not found those conditions in which StopGo provides a clear advantage for TMEV.

Acknowledgements

We are extremely grateful for the assistance generously volunteered by Professor Ray Gesteland. We also wish to thank Maurice O'Donoghue for technical assistance. This work was supported by Science Foundation Ireland grant 08/IN.1/B1889 and NIH R03 MH098688 to J. F. A., NIH 1R01NS065714 to R. S. F. Work conducted on FMDV was supported by CRIS project no. 1940-32000-053-00D, Agricultural Research Service (ARS), US Department of Agriculture (Dr Elizabeth Rieder).

References

Atkins, J. F., Wills, N. M., Loughran, G., Wu, C. Y., Parsawar, K., Ryan, M. D., Wang, C. H. & Nelson, C. C. (2007). A case for "StopGo": reprogramming translation to augment codon meaning of GGN by promoting unconventional termination (Stop) after addition of glycine and then allowing continued translation (Go). *RNA* **13**, 803–810.

Batson, S. & Rundell, K. (1991). Proteolysis at the 2A/2B junction in Theiler's murine encephalomyelitis virus. *Virology* **181**, 764–767.

Brown, J. D. & Ryan, M. D. (2010). Ribosome "skipping": "Stop-Carry On" or "StopGo" translation. In *Recoding: Expansion of Decoding Rules Enriches Gene Expression*, pp. 101–121. Edited by J. F. Atkins & R. F. Gesteland. Heidelberg: Springer.

Donnelly, M. L., Gani, D., Flint, M., Monaghan, S. & Ryan, M. D. (1997). The cleavage activities of aphthovirus and cardiovirus 2A proteins. *J Gen Virol* **78**, 13–21.

Donnelly, M. L., Hughes, L. E., Luke, G., Mendoza, H., ten Dam, E., Gani, D. & Ryan, M. D. (2001a). The 'cleavage' activities of foot-and-mouth disease virus 2A site-directed mutants and naturally occurring '2A-like' sequences. *J Gen Virol* **82**, 1027–1041.

Donnelly, M. L., Luke, G., Mehrotra, A., Li, X., Hughes, L. E., Gani, D. & Ryan, M. D. (2001b). Analysis of the aphthovirus 2A/2B polyprotein 'cleavage' mechanism indicates not a proteolytic reaction, but a novel translational effect: a putative ribosomal 'skip'. *J Gen Virol* **82**, 1013–1025.

Doronina, V. A., Wu, C., de Felipe, P., Sachs, M. S., Ryan, M. D. & Brown, J. D. (2008). Site-specific release of nascent chains from ribosomes at a sense codon. *Mol Cell Biol* **28**, 4227–4239.

Duke, G. M., Osorio, J. E. & Palmenberg, A. C. (1990). Attenuation of Mengo virus through genetic engineering of the 5′ noncoding poly(C) tract. *Nature* **343**, 474–476.

Hahn, H. & Palmenberg, A. C. (1996). Mutational analysis of the encephalomyocarditis virus primary cleavage. *J Virol* **70**, 6870–6875.

Hahn, H. & Palmenberg, A. C. (2001). Deletion mapping of the encephalomyocarditis virus primary cleavage site. *J Virol* **75**, 7215–7218.

Harmon, S. A., Updike, W., Jia, X. Y., Summers, D. F. & Ehrenfeld, E. (1992). Polyprotein processing in cis and in trans by hepatitis A virus 3C protease cloned and expressed in *Escherichia coli*. *J Virol* **66**, 5242–5247.

Jackson, R. J. (1986). A detailed kinetic analysis of the *in vitro* synthesis and processing of encephalomyocarditis virus products. *Virology* **149**, 114–127.

Leong, L. E.-C., Cornell, C. T. & Semler, B. L. (2002). Processing determinants and functions of cleavage products of picornavirus polyproteins. In *Molecular Biology of Picornaviruses*, pp. 187–197. Edited by B. L. Semler & E. Wimmer. Washington, D.C.: American Society for Microbiology.

Loughran, G., Firth, A. E. & Atkins, J. F. (2011). Ribosomal frameshifting into an overlapping gene in the 2B-encoding region of the cardiovirus genome. *Proc Natl Acad Sci U S A* **108**, E1111–E1119.

Luke, G. A., de Felipe, P., Lukashev, A., Kallioinen, S. E., Bruno, E. A. & Ryan, M. D. (2008). Occurrence, function and evolutionary origins of '2A-like' sequences in virus genomes. *J Gen Virol* **89**, 1036–1042.

Palmenberg, A. C. (1990). Proteolytic processing of picornaviral polyprotein. *Annu Rev Microbiol* **44**, 603–623.

Palmenberg, A. C., Kirby, E. M., Janda, M. R., Drake, N. L., Duke, G. M., Potratz, K. F. & Collett, M. S. (1984). The nucleotide and deduced amino acid sequences of the encephalomyocarditis viral polyprotein coding region. *Nucleic Acids Res* **12**, 2969–2985.

Palmenberg, A. C., Parks, G. D., Hall, D. J., Ingraham, R. H., Seng, T. W. & Pallai, P. V. (1992). Proteolytic processing of the cardioviral P2 region: primary 2A/2B cleavage in clone-derived precursors. *Virology* **190**, 754–762.

Parks, G. D. & Palmenberg, A. C. (1987). Site-specific mutations at a picornavirus VP3/VP1 cleavage site disrupt *in vitro* processing and assembly of capsid precursors. *J Virol* **61**, 3680–3687.

Rieder, E., Bunch, T., Brown, F. & Mason, P. W. (1993). Genetically engineered foot-and-mouth disease viruses with poly(C) tracts of two nucleotides are virulent in mice. *J Virol* **67**, 5139–5145.

Rieder, E., Henry, T., Duque, H. & Baxt, B. (2005). Analysis of a foot-and-mouth disease virus type A24 isolate containing an SGD receptor recognition site *in vitro* and its pathogenesis in cattle. *J Virol* **79**, 12989–12998.

Roos, R. P., Kong, W. P. & Semler, B. L. (1989). Polyprotein processing of Theiler's murine encephalomyelitis virus. *J Virol* **63**, 5344–5353.

Ryan, M. D. & Drew, J. (1994). Foot-and-mouth disease virus 2A oligopeptide mediated cleavage of an artificial polyprotein. *EMBO J* **13**, 928–933.

Ryan, M. D., King, A. M. & Thomas, G. P. (1991). Cleavage of foot-and-mouth disease virus polyprotein is mediated by residues located within a 19 amino acid sequence. *J Gen Virol* **72**, 2727–2732.

Villarreal, D., Young, C. R., Storts, R., Ting, J. W. & Welsh, C. J. (2006). A comparison of the neurotropism of Theiler's virus and poliovirus in CBA mice. *Microb Pathog* **41**, 149–156.

JVI Journals.ASM.org

Venezuelan Equine Encephalitis Replicon Particles Can Induce Rapid Protection against Foot-and-Mouth Disease Virus

Fayna Diaz-San Segundo,[a] Camila C. A. Dias,[a,b] Mauro P. Moraes,[c]* Marcelo Weiss,[a,b] Eva Perez-Martin,[a,b] Gary Owens,[d]* Max Custer,[d]* Kurt Kamrud,[d]* Teresa de los Santos,[a] Marvin J. Grubman[a]

Plum Island Animal Disease Center, North Atlantic Area, Agricultural Research Service, U.S. Department of Agriculture, Greenport, New York, USA[a]; Oak Ridge Institute for Science and Education, PIADC Research Participation Program, Oak Ridge, Tennessee, USA[b]; Department of Pathobiology and Veterinary Science, University of Connecticut, Storrs, Connecticut, USA[c]; AlphaVax, Research Triangle Park, North Carolina, USA[d]

Downloaded from http://jvi.asm.org/ on May 15, 2013 by DigiTop -USDA's Digital Desktop Library

We have previously shown that delivery of the porcine type I interferon gene (poIFN-α/β) with a replication-defective human adenovirus vector (adenovirus 5 [Ad5]) can sterilely protect swine challenged with foot-and-mouth disease virus (FMDV) 1 day later. However, the need of relatively high doses of Ad5 limits the applicability of such a control strategy in the livestock industry. Venezuelan equine encephalitis virus (VEE) empty replicon particles (VRPs) can induce rapid protection of mice against either homologous or, in some cases, heterologous virus challenge. As an alternative approach to induce rapid protection against FMDV, we have examined the ability of VRPs containing either the gene for green fluorescent protein (VRP-GFP) or poIFN-α (VRP-poIFN-α) to block FMDV replication *in vitro* and *in vivo*. Pretreatment of swine or bovine cell lines with either VRP significantly inhibited subsequent infection with FMDV as early as 6 h after treatment and for at least 120 h posttreatment. Furthermore, mice pretreated with either 10^7 or 10^8 infectious units of VRP-GFP and challenged with a lethal dose of FMDV 24 h later were protected from death. Protection was induced as early as 6 h after treatment and lasted for at least 48 h and correlated with induction of an antiviral response and production of IFN-α. By 6 h after treatment several genes were upregulated, and the number of genes and the level of induction increased at 24 h. Finally, we demonstrated that the chemokine IP-10, which is induced by IFN-α and VRP-GFP, is directly involved in protection against FMDV.

Foot-and-mouth disease (FMD) is a highly contagious viral disease of cloven-hoofed animals that has significant economic consequences in affected countries. The infectious agent, FMD virus (FMDV), is a member of the *Aphthovirus* genus of the *Picornaviridae* family and contains a single-stranded positive-sense RNA genome of about 8,500 nucleotides encapsidated by 60 copies each of four structural proteins (1). FMDV is an antigenically variable virus consisting of seven serotypes (A, O, C, Asia, and South African Territories 1, 2, and 3 [SAT 1-3]) and multiple subtypes (1, 2). In the event of an outbreak in a previously disease-free country, FMD is controlled by restriction of animal movement, slaughter of infected and in-contact susceptible animals, and in some cases vaccination with an inactivated whole virus vaccine followed by slaughter of these animals (1). However, in countries in which the disease is enzootic, vaccination is used, and in general these animals are not slaughtered.

Infection of animals with FMDV results in rapid replication and spread and subsequent shedding of virus into the environment. Administration of the inactivated vaccine or an experimental vaccine based on a replication-defective human adenovirus 5 (Ad5) vector containing the FMDV capsid and 3C proteinase coding regions requires approximately 7 days to induce protective immunity in animals (3–5). As a result, vaccinated animals exposed to virus within the first 7 days after vaccination are still susceptible to the disease. To address the need of protecting vaccinated animals during this window of susceptibility, we have used an approach that induces the innate immune response. We have shown that FMDV replication is inhibited by prior treatment of cells with interferon type I (IFN-α/β), II, or III (6–8). Based on this information, we constructed Ad5 vectors containing porcine type I IFN genes (Ad5-poIFN-α/β) and demonstrated that swine inoculated with Ad5-poIFN-α/β are protected from challenge with FMDV A24 Cruzeiro as early as 1 day after Ad5-poIFN-α/β administration (4, 9, 10). Protection can last for 3 to 5 days (4). We further showed that this approach is also protective against several other FMDV serotypes, e.g., O1, Manisa, and Asia-1 (10). However, when this approach was used to rapidly protect cattle, we found that only one of six treated animals did not develop vesicular lesions; although all of the other treated animals developed disease, it was delayed and less severe than that in control animals (11). More recently, we found that cattle respond best to type III IFN delivered by an Ad5 vector; in a group of three animals treated with an Ad5 vector containing bovine IFN-λ3 (Ad5-boIFN-λ3), one animal did not develop disease after aerosol challenge with FMDV O1 Manisa while the other two animals developed disease 6 or 9 days later than the control challenged animals (12).

It is known that animals initially detect pathogens through pattern recognition receptors (PRRs), molecules that recognize specific nonhost molecules, e.g., pathogen-associated molecular patterns (PAMPs), such as single- and double-stranded viral RNA (13–15). Host PRRs include Toll-like receptors (TLRs), present

Received 18 December 2012 Accepted 26 February 2013
Published ahead of print 6 March 2013
Address correspondence to Marvin J. Grubman, marvin.grubman@ars.usda.gov.
* Present address: Mauro P. Moraes, Ceva Biomune, Shawnee Mission, Kansas, USA; Gary Owens, Liquidia Technologies, Research Triangle Park, North Carolina, USA; Max Custer, Novartis, Holly Springs, North Carolina, USA; Kurt Kamrud, Harrisvaccines, Ames, Iowa, USA.
F.D.-S.S. and C.C.A.D. contributed equally to this article.
Copyright © 2013, American Society for Microbiology. All Rights Reserved.
doi:10.1128/JVI.03462-12

on the plasma membrane or on endosomal membranes, as well as cytoplasmic soluble receptors. Recognition of PAMPs by PRRs triggers a series of events, which may differ for each PRR engaged, and results in the induction of a protective IFN-dependent antiviral response. The events involved in the induction of the antiviral IFN response include the activation of a series of transcription factors, i.e., IFN regulatory factors (IRFs), nuclear factor κB (NF-κB), etc. Activated IRFs and NF-κB are required for IFN induction as well as upregulation of additional antiviral genes, some of which are induced by mechanisms independent of type I IFN (15). So far, our strategy has been to directly utilize type I, II, or III IFNs to induce rapid protection through upregulation of various IFN-stimulated genes (ISGs). However, this approach bypasses the natural pathway of pathogen induction of the host innate immune response, including the activation of constitutively expressed and induced transcription factors. We hypothesize that treatment of animals with both IFN and various PAMPs may result in a broader, enhanced, and prolonged antiviral response than with Ad5-IFN treatment alone.

Venezuelan equine encephalitis virus (VEE) is a positive-sense RNA virus belonging to the *Alphavirus* genus, *Togaviridae* family. It is an arthropod-borne virus that has been associated with epidemics and equine epizootics. Pushko et al. (16) have constructed VEE replicon particles (VRPs) that contain a defective VEE genome lacking the genes for the structural proteins. As a result, while the viral genome is replicated, it is not packaged, and only a single round of infection occurs. VRPs have been used as vaccine vectors for various foreign genes (16–18) including FMDV (unpublished data). Recently, Konopka et al. (19, 20) demonstrated that null VRPs, VRPs lacking any foreign gene, induce an early innate immune response in mice within 1 to 3 h postinfection (hpi), resulting in the upregulation of a number of ISGs and the production of type I IFN protein. Furthermore, null-VRP-inoculated mice are protected from lethal challenge with VEE as early as 6 h after VRP administration as well as 24 h later, and this pretreatment induced protection against heterologous challenge with influenza virus but not vesicular stomatitis virus (VSV) (20).

In this study, we demonstrated that pretreatment of cells with VRPs containing green fluorescent protein (VRP-GFP) as well as porcine IFN-α (VRP-poIFN-α) significantly reduced FMDV replication in infected porcine or bovine cells, and inhibition lasted for at least 5 days. A number of genes were upregulated after treatment of swine cells with either VRP-GFP or VRP-poIFN-α. We also examined the effectiveness of VRP treatment in a small-animal model. Adult C57BL/6 mice, which can be lethally infected with FMDV, survived challenge when pretreated with VRP-GFP. The chemokine 10-kDa IFN-γ-inducible protein 10 (IP-10) was significantly upregulated in IFN- or VRP-treated cells and in mice at early times after VRP treatment, as well as in swine or cattle after IFN treatment. While 100% of wild-type (WT) mice pretreated with murine IFN-α (muIFN-α) survived FMDV challenge, only 30% of IP-10 knockout (KO) mice pretreated with muIFN-α were protected, demonstrating a role for IP-10 in protection against FMDV.

These results suggest that VRP treatment is an effective approach to rapidly protect against FMD. In addition, we found that VRP-induced protection against FMDV requires a functional type I IFN system that is directly dependent on IP-10.

MATERIALS AND METHODS

Cells and viruses. Porcine kidney cell lines (IB-RS-2 and SK6) and bovine kidney cells (LF-BK) (21) were used for the experiments. These cells were maintained in minimal essential medium (MEM; Gibco-BRL/Invitrogen, Carlsbad, CA) containing 10% fetal bovine serum (FBS; HyClone, Logan, UT) and supplemented with 1% antibiotics and nonessential amino acids. BHK-21 cells (baby hamster kidney cells strain 21, clone 13; ATCC CL10) obtained from the American Type Culture Collection (Rockville, MD) were used to propagate virus stocks and to measure virus titers. BHK-21 cells were maintained in MEM containing 10% calf serum and 10% tryptose phosphate broth supplemented with 1% antibiotics and nonessential amino acids (Gibco-BRL/Invitrogen). Murine L929 fibroblasts were maintained in MEM containing 10% horse serum supplemented with 1% antibiotics and nonessential amino acids and used to test antiviral activity of mouse serum after encephalomyocarditis virus (EMCV) infection. Cell cultures were incubated at 37°C in 5% CO_2. FMDV serotypes A12 and A24 Cruzeiro were used in the experiments. Human 293 cells (ATCC CRL-1573) were used to generate and propagate recombinant adenoviruses and determine virus titer (22). A certified Vero cell line derived from a master cell bank prepared from cells obtained from the World Health Organization was used to generate VRPs. Vero cells were maintained at 37°C in an atmosphere containing 5% CO_2. The cells were grown in MEM supplemented with 5% fetal bovine serum, nonessential amino acids, and antibiotic-antimycotic solution (Gibco-BRL/Invitrogen).

Replicon construction. The pVEK replicon vector is based on the current investigational new drug (IND) VEE virus vaccine (TC-83) (18, 23). The poIFN-α and GFP genes were PCR amplified from existing DNA plasmids (9, 24). Each PCR product coded for XbaI restriction sites at the 5′ and 3′ end. The PCR products were then cloned into the XbaI site of the transfer vector pcDNA3.3 (25). The orientations of the poIFN-α and GFP genes in pcDNA3.3 were determined by restriction analysis, and positive clones were sequenced to ensure that no errors were introduced into the gene during PCR amplification. Each of the genes was then subcloned as an AscI fragment into the AscI site of the pVEK replicon plasmid. The orientation of the gene was determined by restriction analysis, and clones in the sense orientation were selected.

RNA transcription, electroporation, and VRP production. The methods used to *in vitro* transcribe replicon RNA, electroporate RNA into Vero cells, and produce and purify VRP vaccines were described previously (25). The infectious titer (in infectious units [UI]) of VRP-poIFN-α was determined by immunofluorescence assay (IFA) using goat anti-VEE nsP2-specific polyclonal antiserum as the primary antibody and donkey anti-goat Alexa Fluor 488 (Invitrogen) as the secondary antibody on methanol-fixed cells using a Nikon Eclipse TE300 fluorescence microscope. The infectious titer of VRP-GFP was determined directly from infected cells without the use of antibody reagents. The VRPs were tested for the presence of contaminating replication-competent VRP (RCV) using two blind passages on Vero cells, as described previously (25).

Ad5 vector construction. The Ad5-Blue, Ad5-VSVG (containing the glycoprotein gene of vesicular stomatitis virus-NJ), and Ad5-poIFN-α vectors were constructed as previously described (9, 26). Ad5-GFP and an Ad5 vector containing a small interfering RNA (siRNA) directed against GFP (Ad5-siGFP) were produced using the pAd5-Blue direct ligation system (26). All vectors were purified as previously described and tested for foreign gene expression in IB-RS-2 cells (27).

Expression of poIFN-α. Vero cells were infected with VRP-poIFN-α, and 24 h later supernatants were obtained, centrifuged at 14,000 rpm to remove cellular debris, and filtered through a Centricon-100 filter to remove VRPs. Concentrated supernatants were examined for the presence of IFN protein by Western blot analysis.

Virus infection. Cells were infected with VRPs at a multiplicity of infection (MOI) of 1 for 1 h washed with MEM, and 1 ml of MEM was added per well. At various times (see figure legends) the medium was removed, centrifuged, and filtered through a Centricon-100 filter at 4,000 rpm for 10 min in a Sorvall centrifuge. Samples were stored at −70°C until

Downloaded from http://jvi.asm.org/ on May 15, 2013 by DigiTop -USDA's Digital Desktop Library

assayed for antiviral activity or the presence of poIFN-α by enzyme-linked immunosorbent assay (ELISA). The cells were then infected with FMDV A12 at an MOI of 1 for 1 h, and unabsorbed virus was inactivated by washing the cells with 150 mM NaCl–20 mM morpholineethanesulfonic acid (MES) (pH 6.0). MEM was added, and incubation continued for 24 h. Virus was released by one freeze-thaw cycle. As a control, to measure infectious FMDV remaining after the acid wash, infected cells were frozen and thawed at 1 h postinfection. FMDV yields were determined by plaque assay on BHK-21 cells as previously described (5) and expressed by subtracting the titers of virus in cells infected for 1 h from the 24-h titers. The detection level of this assay is 5 PFU per ml (PFU/ml).

Analysis of mRNA. Total RNA was isolated from SK6 or IB-RS-2 cells, infected with VRPs or treated with poly(I · C), using an RNeasy isolation kit (Qiagen, Valencia, CA) following the manufacturer's directions. RNA yield and quality were determined in a NanoDrop 1000 spectrophotometer (Thermo Fisher, Waltham, MA) and in a Bioanalyzer (Agilent Technologies, Santa Clara, CA). A quantitative real-time reverse transcription-PCR (qRT-PCR) assay was used to evaluate the mRNA levels of a number of porcine genes as previously described (28). Glyceraldehyde-3-phosphate dehydrogenase (GAPDH) was used as the internal control to normalize the values of each sample. Primer and probe sequences were previously described (29). Reactions were performed in an ABI Prism 7500 sequence detection system (Applied Biosystems). Relative mRNA levels were determined by comparative cycle threshold analysis (30) utilizing as a reference the samples at 0 dpi from the control groups. We considered genes upregulated only if there was a 2-fold or greater induction.

RNA was also extracted from spleen cells of mice inoculated for 3, 6, and 24 h with VRP-GFP. Spleens were incubated with RPMI 1640 complete medium containing 10% fetal bovine serum (FBS), L-glutamine, 0.05 M β-mercaptoethanol, and antibiotic/antimycotic solutions. Single-cell suspensions were obtained by mechanical disruption pressing the whole spleen through a plastic grid (BD Bioscience, Franklin Lakes, NJ). Contaminating erythrocytes were removed by lysis with 0.83% ammonium chloride. Single-cell suspensions were washed twice in phosphate-buffered saline (PBS) and once with complete RPMI 1640 medium, and cells were counted. A total of 1×10^7 cells were lysed with 700 μl of RLT buffer (Qiagen) containing β-mercaptoethanol and stored at −70°C until RNA extraction using an RNeasy isolation kit (Qiagen). qRT-PCR was performed using the RT^2 Profiler PCR modified antiviral response pathway from SA Bioscience-Super Array (Qiagen), following the manufacturer's instructions from cDNA synthesis to data analysis. Reactions were performed in an ABI Prism 7500 sequence detection system (Applied Biosystems). We analyzed a total of 84 genes (Table 1), and only those that showed changes were reported.

Interferon biological assay. Antiviral activity was evaluated in supernatants as previously described (4). Samples were diluted and incubated on IB-RS-2 cells for approximately 24 h. Supernatants were removed, and the cells were infected for 1 h with approximately 100 PFU of FMDV serotype A12 and overlaid with gum tragacanth. Plaques were visualized 24 h later by staining with 1% crystal violet. Antiviral activity (U/ml) was reported as the reciprocal of the highest supernatant dilution that resulted in a 50% reduction in the number of plaques relative to the number of plaques in the mock-treated infected cells.

Serum samples of mice inoculated with VRP-GFP at different time points (3, 6, and 24 h) were collected, and antiviral activity was tested in L929 cells as previously described (20). Briefly, serum samples were diluted 1:10 in medium and acidified to pH 2.0 for 24 h. Following neutralization to pH 7.4, the samples were titrated by 2-fold dilutions and added to confluent monolayers of L929 cells. Twenty-four hours after the addition of the serum, IFN-sensitive EMCV (2×10^5 PFU) was added to each well and incubated at 37°C. At 18 to 24 h postinfection, the remaining cells were then stained with 1% crystal violet. The percent cytopathic effect (CPE) in each well was scored by direct observation. The antiviral titers (IU/ml) were calculated based on the standard curves generated with commercial IFN-α/β; the endpoint titer was calculated from the dilution of IFN-α/β required to protect 50% of the cell monolayer from EMCV-induced CPE.

IFN-α ELISA. An ELISA was performed as previously described (4). Porcine IFN-α concentrations in SK6 cell supernatants were expressed in picograms per milliliter and calculated by linear regression analysis of a standard curve generated with serial 2-fold dilutions of recombinant poIFN-α (PBL Biomedical Laboratories, NJ). All samples were assayed in duplicate. Levels of poIFN-α protein of <200 pg/ml were not considered meaningful.

Serum from mice infected with VRP-GFP at different time points (6 and 24 h) and control mice inoculated with PBS were tested for the presence of IFN-α, IFN-β, and IFN-λ with VeriKine mouse IFN-α, IFN-β, and IFN-λ 2/3 ELISAs (PBL Interferon Source, Piscataway, NJ) following the manufacturer's directions. All ELISAs were developed with 3,3′,5,5′-tetramethylbenzidine (TMB) from KPL (Gaithersburg, MD). The absorbance at 450 nm was measured in an ELISA reader (VersaMax, Molecular Devices, Sunnyvale, CA). Cytokine concentrations were calculated based on the optical densities obtained with the standards and are expressed in relative levels with respect to the levels observed at day 0 postinfection.

Mouse challenge studies. C57BL/6 WT or IP-10 KO (C57BL/6 background) 6- to 7-week-old female mice were purchased from Jackson Laboratory (Bar Harbor, ME) and were acclimated for 1 week. All animal work was conducted in compliance with the Animal Welfare Act (AWA), the 2011 Guide for Care and Use of Laboratory Animals, 2002 PHS Policy for the Humane Care and Use of Laboratory Animals, and U.S. Government Principles for Utilization and Care of Vertebrates Animal Used in Testing, Research and Training (IRAC 1985), as well as a specific animal protocol (protocol number 204-09-R) reviewed and approved by the Institutional Animals Care and Use Committee (IACUC) of Plum Island Animal Disease Center (PIADC) (USDA/APHIS/AC certificate number 21-F-0001).

For virus infection experiments, groups of 5 C57BL/6 mice were anesthetized with isoflurane (Webster Veterinary, Devens, MA) and immediately infected subcutaneously (s.c.) in the left/right rear footpad with 10^4, 10^5, or 10^6 PFU of FMDV A24 or O1 Campos or PBS in 50 μl. Animals were monitored for 7 days, and blood was taken at day 0 and on alternate days until the end of the experiment. Viremia was determined by plaque assay on BHK-21 cells as described above.

To test the *in vivo* effect of VRP-GFP, groups of five mice were anesthetized as described above and immediately infected s.c. in the right rear footpad with 10^6, 10^7, or 10^8 IU of VRP-GFP or PBS in 50 μl. One day after VRP-GFP treatment, mice were anesthetized and challenged with 5×10^4 PFU/mouse FMDV A24 in 50 μl in the left rear footpad.

In a second experiment, groups of five mice were inoculated with 10^7 or 10^8 IU of VRP-GFP and challenged at 6, 24, or 48 h with 5×10^4 PFU/mouse FMDV A24 as above. A PBS-inoculated control group was challenged with FMDV 24 h later. In this experiment groups of mice were also inoculated with 10^8 IU of VRP-GFP and euthanized at 3, 6, or 24 h later. A control group was inoculated with PBS and euthanized 24 h later. Serum was obtained, and the spleen was isolated from each animal; red blood cells were lysed, and the cells were washed. The cells were resuspended in RLT buffer (Qiagen). RNA was extracted using an RNeasy miniprep kit following the manufacturer's instructions (Qiagen). The serum was examined for the production of a number of proteins by ELISA (IFN-α, IFN-β, IFN-γ, and IFN-λ3/2, [all from PBL]), following the manufacturer's instructions, and RNA was examined for the induction of various genes as described above.

Finally, groups of 10 C57BL/6 IP-10 KO mice and WT mice were treated with 10^4 U of murine IFN-α (muIFN-α) by intraperitoneal (i.p.) inoculation and challenged s.c. with 5×10^4 PFU of FMDV A24 at 4 or 18 h after treatment. Ten untreated C57BL/6 WT or IP-10 KO mice were included as a control group. Animals were monitored for 7 days, and blood taken at day 0 and on alternate days until the end of the experiment.

Downloaded from http://jvi.asm.org/ on May 15, 2013 by DigiTop -USDA's Digital Desktop Library

TABLE 1 Complete list of analyzed genes in spleen lymphocytes after treatment of mice with VRP-GFP for different times

Symbol	Gene name	Other name(s)	Description	GenBank
Aim2	Gm1313	Ifi210	Absent in melanoma 2	NM_001013779
Atg12	4931423H11Rik	A330058M13Rik, Apg12l, Atg12l	Autophagy-related 12 (yeast)	NM_026217
Atg5	2010107M05Rik	3110067M24Rik, AW319544, Apg5l, Atg5l, C88337, Paddy	Autophagy-related 5 (yeast)	NM_053069
Azi2	AA410145	AZ2	5-Azacytidine-induced gene 2	NM_013727
Card9	Gm782		Caspase recruitment domain family, member 9	NM_001037747
Casp1	ICE	Il1bc	Caspase 1	NM_009807
Casp8	CASP-8	FLICE, MACH, Mch5	Caspase 8	NM_009812
Ccl3	MIP-1α	AI323804, G0S19-1, LD78α, MIP1-(a), MIP1-α, Mip1a, Scya3	Chemokine (C-C motif) ligand 3	NM_011337
Ccl4	MIP-1B	AT744.1, Act-2, Mip1b, Scya4	Chemokine (C-C motif) ligand 4	NM_013652
Ccl5	MuRantes	RANTES, SISd, Scya5, TCP228	Chemokine (C-C motif) ligand 5	NM_013653
Cd40	AI326936	Bp50, GP39, HIGM1, IGM, IMD3, T-BAM, TRAP, Tnfrsf5, p50	CD40 antigen	NM_011611
Cd80	B71	Cd28l, Ly-53, Ly53, MIC17, TSA1	CD80 antigen	NM_009855
Cd86	B7	B7-2, B7.2, B70, CLS1, Cd28l2, ETC-1, Ly-58, Ly58, MB7, MB7-2, TS, A-2	CD86 antigen	NM_019388
Chuk	AI256658	Chuk1, Fbx24, Fbxo24, IKBKA, IKK1, Ikka, MGC25325, NFKBIKA	Conserved helix-loop-helix ubiquitous kinase	NM_007700
Cnpy3	1600025D17Rik	2410050O22Rik, AI413153, CAG4A, ERDA5, PRAT4A, Tnrc5	Canopy 3 homolog (zebrafish)	NM_028065
Ctsb	CB		Cathepsin B	NM_007798
Ctsl	1190035F06Rik	Ctsl1, MEP, fs, nkt	Cathepsin L	NM_009984
Ctss			Cathepsin S	NM_021281
Cxcl10	IP-10	IP10, Ifi10, Scyb10, gIP-10, mob-1, C7, CRG-2, INP10	Chemokine (C-X-C motif) ligand 10	NM_021274
Cxcl11	Cxc11	H174, I-tac, Ip9, Itac, Scyb11, Scyb9b, b-R1, betaR1	Chemokine (C-X-C motif) ligand 11	NM_019494
Cxcl9	BB139920	CMK, Mig, MuMIG, Scyb9, crg-10	Chemokine (C-X-C motif) ligand 9	NM_008599
Cyld	2010013M14Rik	2900009M21Rik, C130039D01Rik, CDMT, CYLD1, EAC, mKIAA0849	Cylindromatosis (turban tumor syndrome)	NM_173369
Dak	BC021917	MGC28742	Dihydroxyacetone kinase 2 homolog (yeast)	NM_145496
Ddx3x	D1Pas1-rs2	Ddx3, Fin14	DEAD/H (Asp-Glu-Ala-Asp/His) box polypeptide 3, X-linked	NM_010028
Ddx58	RIG-I	6430573D20Rik, C330021E21	DEAD (Asp-Glu-Ala-Asp) box polypeptide 58	NM_172689
Dhx58	Lgp2	B430001I08Rik, D11Lgp2e, LPG2	DEXH (Asp-Glu-X-His) box polypeptide 58	NM_030150
Fadd	FADD	Mort1	Fas (TNFRSF6)-associated via death domain	NM_010175
Fos	cFos	D12Rfj1, c-*fos*	FBJ osteosarcoma oncogene	NM_010234
Hsp90aa1	86kDa	89kDa, AL024080, AL024147, Hsp86-1, Hsp89, Hsp90, Hspca, hsp4	Heat shock protein 90, alpha (cytosolic), class A member 1	NM_010480
Ifih1	MDA5	9130009C22Rik, Helicard, Hlcd, MGC90959	Interferon induced with helicase C domain 1	NM_027835
Ifna2	Ifa2		Interferon alpha 2	NM_010503
Ifnar1	Infar	CD118, Ifar, Ifrc	Interferon (alpha and beta) receptor 1	NM_010508
Ifnb1	IFN-beta	IFNB, Ifb	Interferon beta 1, fibroblast	NM_010510
Ikbkb	IKKbeta	AI132552, IKK-2, IKKβ, IKK2, IKKβ	Inhibitor of kappaB kinase beta	NM_010546
Il12a	IL-12p35	Il-12a, Ll12a, MGC151228, MGC151232, p35	Interleukin-12A	NM_008351
Il12b	Il-12b	Il-12p40, Il12p40, p40	Interleukin-12B	NM_008352
Il15	AI503618		Interleukin-15	NM_008357
Il18	Il-18	Igif	Interleukin-18	NM_008360
Il1b	IL-1beta	Il-1b	Interleukin-1 beta	NM_008361
Il6	Il-6		Interleukin-6	NM_031168
Irak1	IRAK	AA408924, IRAK-1, IRAK1-S, Il1rak, Plpk, mPLK	Interleukin-1 receptor-associated kinase 1	NM_008363
Irf3	IRF-3	C920001K05Rik, MGC91046	Interferon regulatory factor 3	NM_016849
Irf5	mirf5	AW491843	Interferon regulatory factor 5	NM_012057
Irf7			Interferon regulatory factor 7	NM_016850
Isg15	IGI15	G1p2, IP17, Irfp, MGC103144 MGC130321, MGC18616, UCRP	ISG15 ubiquitin-like modifier	NM_015783
Jun	AP-1	JunC, c-jun	Jun oncogene	NM_010591
Map2k1	MAPKK1	MEKK1, Mek1, Prkmk1	Mitogen-activated protein kinase kinase 1	NM_008927
Map2k3	AW212142	MEK3, MKK3, Prkmk3, mMKK3b	Mitogen-activated protein kinase kinase 3	NM_008928
Map3k1	MAPKKK1	MEKK1, Mekk	Mitogen-activated protein kinase kinase kinase 1	NM_011945
Map3k7	B430101B05	C87327, Tak1	Mitogen-activated protein kinase kinase kinase 7	NM_172688
Mapk1	9030612K14Rik	AA407128, AU018647, C78273, ERK, Erk2, MAPK2, PRKM2, Prkm1, p41mapk, p42mapk	Mitogen-activated protein kinase 1	NM_011949
Mapk14	CSBP2	Crk1, Csbp1, MGC102436, Mxi2, PRKM14, PRKM15, p38, p38-alpha, p38MAPK, p38a, p38alpha	Mitogen-activated protein kinase 14	NM_011951
Mapk3	Erk-1	Erk1, Ert2, Esrk1, Mnk1, Mtap2k, Prkm3, p44, p44erk1, p44mapk	Mitogen-activated protein kinase 3	NM_011952
Mapk8	AI849689	JNK, JNK1, Prkm8, SAPK1	Mitogen-activated protein kinase 8	NM_016700
Mavs	IPS-1	D430028G21Rik, MGC25836, Visa, cardif	Mitochondrial antiviral signaling protein	NM_144888
Mefv	FMF	MGC124344, MGC124345, TRIM20, pyrin	Mediterranean fever	NM_019453
Mx1	Mx-1	AI893580, Mx	Myxovirus (influenza virus) resistance 1	NM_010846
Myd88			Myeloid differentiation primary response gene 88	NM_010851
Nfkb1	NF-KB1	NF-κB, NF-κB1, p105, p50, p50, p105	Nuclear factor of kappa light polypeptide gene enhancer in B-cells 1, p105	NM_008689
Nfkbia	Nfkbi	AI462015	Nuclear factor of kappa light polypeptide gene enhancer in B-cells inhibitor, alpha	NM_010907
Nlrp3	AGTAVPRL	AII, AVP, Cias1, FCAS, FCU, MGC129375, MWS, Mmig1, NALP3, Pypaf1	NLR family, pyrin domain containing 3	NM_145827
Nod2	ACUG	BLAU, CD, Card15, F830032C23Rik, IBD1, Nlrc2	Nucleotide-binding oligomerization domain containing 2	NM_145857

(Continued on following page)

Downloaded from http://jvi.asm.org/ on May 15, 2013 by DigiTop -USDA's Digital Desktop Library

TABLE 1 (Continued)

Symbol	Gene name	Other name(s)	Description	GenBank
Oas2	Oasl11		2′,5′-oligoadenylate synthetase 2	NM_145227
Pin1	0610025L01Rik	D9Bwg1161e	Protein (peptidyl-prolyl cis/trans isomerase) NIMA-interacting 1	NM_023371
Pstpip1	CD2BP1	def-2	Proline-serine-threonine phosphatase-interacting protein 1	NM_011193
Pycard	9130417A21Rik	Asc, CARD5, TMS-1, TNS1, masc	PYD and CARD domain containing	NM_023258
Rela	p65		V-rel reticuloendotheliosis viral oncogene homolog A (avian)	NM_009045
Ripk1	D330015H01Rik	RIP, Rinp, Rip1	Receptor (TNFRSF)-interacting serine-threonine kinase 1	NM_009068
Spp1	2AR	Apl-1, BNSP, BSPI, Bsp, ETA-1, Eta, OP, Opn, Opnl, Ric, Spp-1	Secreted phosphoprotein 1	NM_009263
Stat1	2010005J02Rik	AA408197	Signal transducer and activator of transcription 1	NM_009283
Sugt1	2410174K12Rik	SGT1	SGT1, suppressor of G2 allele of SKP1 (*Saccharomyces cerevisiae*)	NM_026474
Tank	C86182	E430026L09Rik, I-TRAF	TRAF family member-associated Nf-kappa B activator	NM_011529
Tbk1	1200008B05Rik	AI462036, AW048562, MGC150301, MGC150302	TANK-binding kinase 1	NM_019786
Tbkbp1	3110043L15Rik	ProSAPiP2, SINTBAD	TBK1 binding protein 1	NM_198100
Ticam1	AW046014	AW547018, TICAM-1, TRIF	Toll-like receptor adaptor molecule 1	NM_174989
Tlr3	AI957183		Toll-like receptor 3	NM_126166
Tlr7			Toll-like receptor 7	NM_133211
Tlr8			Toll-like receptor 8	NM_133212
Tlr9			Toll-like receptor 9	NM_031178
Tnf	TNF-α	DIF, MGC151434, TNFSF2, TNF-α, Tnfa, Tnfsf1a	Tumor necrosis factor	NM_013693
Tradd	9130005N23Rik	AA930854	TNFRSF1A-associated via death domain	NM_001033161
Traf3	AI528849	CAP-1, CD40bp, CRAF1, LAP1, T-BAM, amn	Tnf receptor-associated factor 3	NM_011632
Traf6	2310003F17Rik	AI851288, C630032O20Rik	Tnf receptor-associated factor 6	NM_009424
Trim25	AA960166	AL022677, EFP, Zfp147	Tripartite motif-containing 25	NM_009546
Gusb	AI747421	Gur, Gus, Gus-r, Gus-s, Gus-t, Gus-u, Gut, asd, g	Glucuronidase, beta	NM_010368
Hprt	C81579	HPGRT, Hprt1, MGC103149	Hypoxanthine guanine phosphoribosyl transferase	NM_013556
Hsp90ab1	90kDa	AL022974, C81438, Hsp84, Hsp84-1, Hsp90, Hspcb, MGC115780	Heat shock protein 90 alpha (cytosolic), class B member 1	NM_008302
Gapdh	Gapd	MGC102544, MGC102546, MGC103190, MGC103191, MGC105239	Glyceraldehyde-3-phosphate dehydrogenase	NM_008084
Actb	Actx	E430023M04Rik, beta-actin	Actin, beta	NM_007393
MGDC	MIGX1B		Mouse Genomic DNA Contamination	SA_00106
RTC	RTC		Reverse Transcription Control	SA_00104
Ifng	IFN-g	Ifg	Interferon gamma	NM_008337
Ifn7				
Ifna4	Ifa4	MGC143607	Interferon alpha 4	NM_010504
Il28ra				
PPC	PPC		Positive PCR Control	SA_00103
Aim2	Gm1313	Ifi210	Absent in melanoma 2	NM_001013779

Statistical analyses. Data handling, analysis, and graphic representation were performed by using Prism, version 5.0 (GraphPad Software, San Diego, CA), or Microsoft Excel. Statistical differences were determined using a Student *t* test.

RESULTS

Synthesis of IFN by VRP-poIFN-α. Previous work has shown that alphavirus replicon vectors efficiently deliver significant amounts of foreign proteins into mammalian cells (25). We therefore constructed VRPs that express poIFN-α under the control of the alphavirus 26S promoter element (Fig. 1A). Vero cells were infected with VRP-poIFN-α, and 24 h later supernatants were assayed for the presence of active IFN protein. Western blot analysis revealed high levels of IFN expression (Fig. 1B) which correlated with the detection of significant antiviral activity against FMDV as measured by a plaque reduction neutralization assay (unpublished data). To determine if VRP replicons could infect cells derived from the FMDV natural host, swine (SK6 and IB-RS-2) and bovine (LF-BK) cell lines were treated with 50 IU of a reporter VRP-GFP replicon. A similar level of GFP fluorescence was detected in all three cell lines (Fig. 1C), indicating that they were equally susceptible to infection with VRPs.

Pretreatment with VRPs inhibits FMDV replication. SK6 cells were infected with either VRP-GFP or VRP-poIFN-α, and at 6, 24, or 48 h posttreatment (hpt) supernatants were removed, and cells were washed and infected with FMDV A12. After 24 h, virus yields were determined by plaque assay. The FMDV yield was reduced greater than 1,000-fold as early as 6 h posttreatment with VRP-poIFN-α relative to cells treated with medium (Fig. 2A). A 5-fold reduction was detected in the cells pretreated with VRP-GFP. Inhibition was significantly increased after 24 h of VRP-GFP treatment (1,000-fold) and was maintained for at least 48 h. To examine the duration of protection provided by a 24-h treatment with VRPs, we infected SK6 cells with FMDV at 0, 24, 48, 96, and 120 h posttreatment (Fig. 2B). The level of inhibition of FMDV remained essentially the same throughout the experiment. Furthermore, similar results were obtained in bovine LF-BK cells (unpublished data). These results indicated that treatment with either VRP-poIFN-α or VRP-GFP can significantly inhibit FMDV replication for a considerable length of time.

The presence of poIFN-α protein was measured by ELISA, and FMDV antiviral activity was measured by a biological assay. Su-

Downloaded from http://jvi.asm.org/ on May 15, 2013 by DigiTop -USDA's Digital Desktop Library

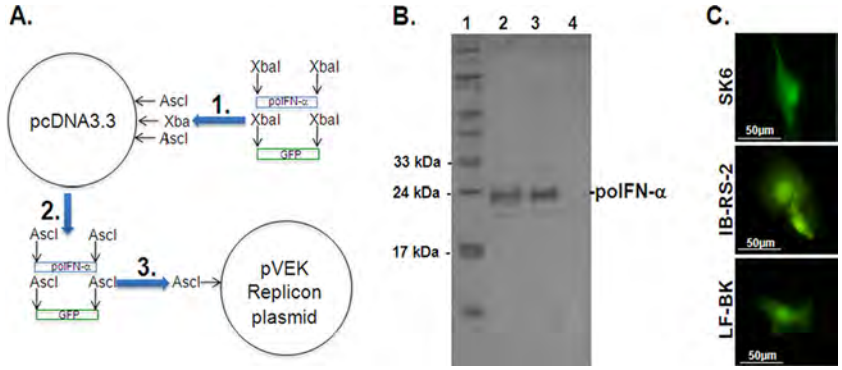

FIG 1 (A) Schematic diagram of construction of VRP replicon vectors. Genes were PCR amplified with XbaI restriction enzyme recognition sites engineered at the 5′ and 3′ ends (step 1). The genes were cloned into the unique XbaI site in pcDNA3.3. The genes were removed from the intermediate plasmid by digestion with the AscI restriction enzyme (step 2). The fragments were cloned into the unique AscI restriction site in the pVEK replicon vector (step 3). (B) Expression of poIFN-α in cells infected with VRP-poIFN-α. Vero cells were infected with 50 IU of VRP-poIFN-α, and 24 h later the supernatant was centrifuged to remove cell debris, filtered through a Centricon-100 filter, treated at pH 2 overnight, and neutralized to ~pH 7. IB-RS-2 cells were infected at an MOI of 20 with Ad5-poIFN-α, and supernatants were collected at ~24 h and treated as above. The supernatants were run on a 12% SDS-PAGE gel, transferred to a membrane, probed with a 1:250 dilution of rabbit anti-poIFN-α, and detected with a 1:2,000 dilution of goat anti-rabbit alkaline phosphatase. Lane 1, molecular size markers; lane 2, Ad5-poIFN-α-infected IB-RS-2 cell supernatant; lane 3, VRP-poIFN-α-infected Vero cell supernatant; lane 4, supernatant from mock-infected cells. (C) Expression of GFP in cells infected with VRP-GFP. Different porcine (SK-6 and IB-RS-2) or bovine (LF-BK) cell lines were infected with VRP-GFP for 24 h, and GFP expression was examined.

pernatants from VRP-poIFN-α-treated cells had high levels of poIFN-α protein (28,000 to 48,000 pg/ml) at both 24 and 48 h, consistent with significant levels of antiviral activity (3,000 to 6,000 U/ml) (Fig. 2C). Low levels of poIFN-α protein and no antiviral activity were detected in the supernatants of VRP-GFP-treated cells at 24 and 48 h.

We have previously reported that Ad5 vectors containing the gene for poIFN-α/β can sterilely protect swine when challenged 1

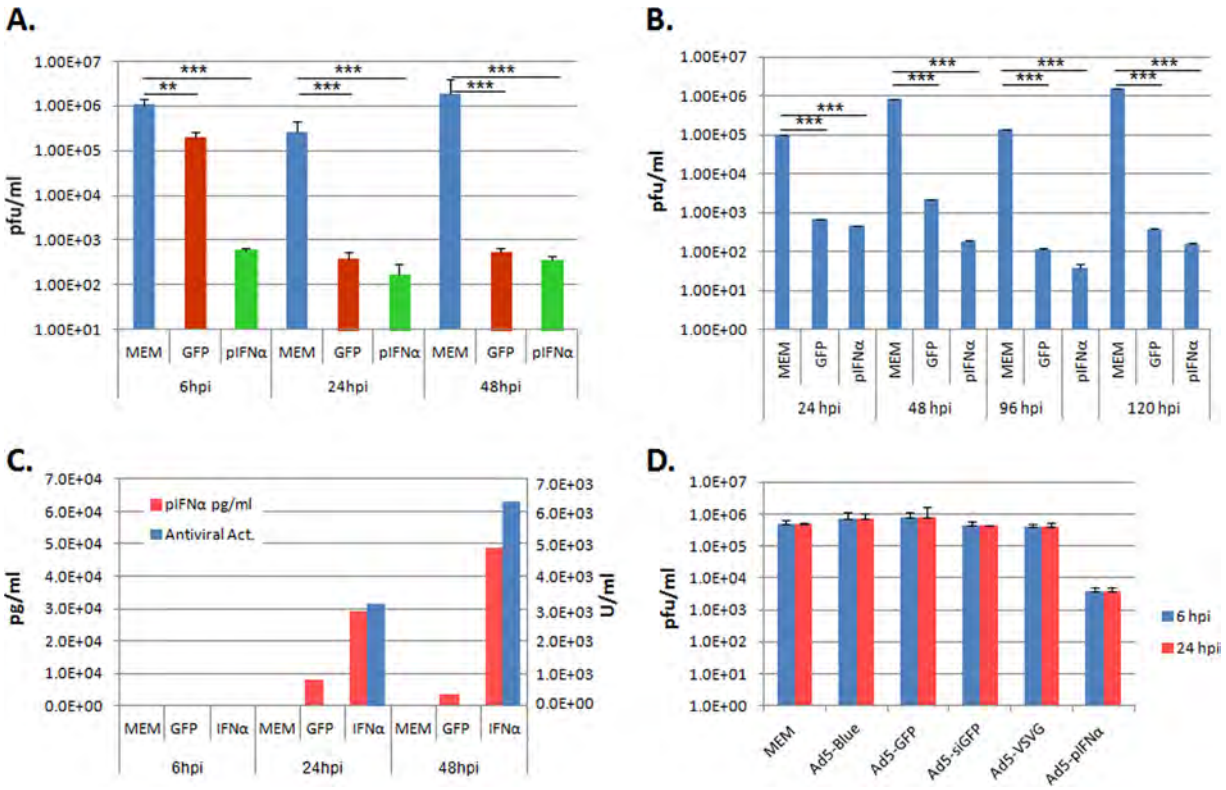

FIG 2 Effect of VRP or Ad5 infection on FMDV replication in SK6 cells. SK6 cells were infected at an MOI of 1 with either VRP-GFP or VRP-poIFN-α and at 6, 24, or 48 h (A) or 24, 48, 96, or 120 h (B) after VRP infection, supernatants were removed, and cells were washed and subsequently infected at an MOI of 1 with FMDV A12 for 24 h. Virus yields were determined by plaque assay and are expressed in PFU/ml. (C) Supernatants of SK6 cells infected with VRP-GFP or VRP-poIFN-α at an MOI of 1 for at 6, 24, or 48 h were examined for the presence of poIFN-α by ELISA (expressed in pg/ml) or antiviral activity by plaque reduction assay (expressed in U/ml). (D) SK6 cells were treated with various Ad5 vectors including Ad5-Blue, Ad5-GFP, Ad5-siGFP, Ad5-VSVG, and Ad5-poIFN-α; 6 or 24 h later supernatants were removed, and cells were washed and infected with FMDV A12 at an MOI of 1 for 24 h. Virus yields were determined by plaque assay and are expressed in PFU/ml. *, $P \leq 0.05$; **, $P \leq 0.01$; ***, $P \leq 0.001$.

Downloaded from http://jvi.asm.org/ on May 15, 2013 by DigiTop -USDA's Digital Desktop Library

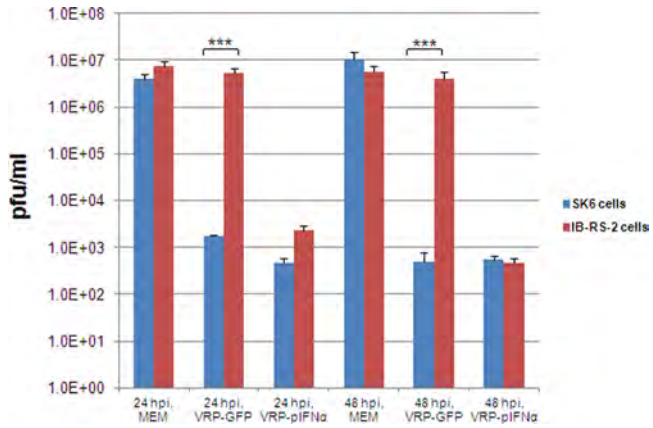

FIG 3 Effect of VRP infection on FMDV replication in SK6 or IB-RS-2 cells. SK6 or IB-RS-2 cells were infected at an MOI of 1 with either VRP-GFP or VRP-poIFN-α; 24 h later supernatants were removed, and cells washed and subsequently infected with FMDV A12 at an MOI of 1 for 24 h. Virus yields were determined by plaque assay and are expressed in PFU/ml. *, $P \leq 0.05$; **, $P \leq 0.01$; ***, $P \leq 0.001$.

day later with FMDV (4, 9, 10). To determine if, similar to VRP-GFP, Ad5 vectors in addition to Ad5-poIFN-α could inhibit FMDV replication, we tested various vectors including Ad5-Blue (an Ad5 vector containing the β-galactosidase α gene fragment [26]), Ad5-GFP, Ad5-siGFP (containing a GFP siRNA), Ad5-VSVG (containing the glycoprotein gene of vesicular stomatitis virus New Jersey which is a known ligand of TLR4) (31), and Ad5-poIFN-α. SK6 cells were transduced with these Ad5 vectors followed by infection with FMDV 6 or 24 h later. Only cells pretreated with Ad5-poIFN-α reduced the yield of FMDV, with an approximately 100- to 200-fold decrease at each time point (Fig. 2D), consistent with the detection of high levels of antiviral activity (unpublished data). Similar results were obtained in Ad5-transduced bovine LF-BK cells (unpublished data).

IB-RS-2 cells do not respond to VRP-GFP infection. Konopka et al. (20) have shown that signaling through the IFN-α/β receptor is required for both antiviral gene induction by VRP replicons and protection against VEE and influenza virus challenge. We have previously shown that the porcine cell line IB-RS-2 is sensitive to type I IFN protein but does not express type I IFN mRNA (6), and thus presumably treatment of these cells with VRP-GFP would not induce protection from subsequent FMDV challenge. IB-RS-2 cells were pretreated with VRP-GFP or VRP-poIFN-α for 24 h and then infected with FMDV immediately or 24 h later. A control experiment was run in parallel in SK6 cells. As previously shown, FMDV yields in either VRP-GFP- or VRP-poIFN-α-pretreated SK6 cells were reduced approximately 10,000-fold at both 24 and 48 h compared to yields in an untreated control (Fig. 3). In IB-RS-2 cells pretreated with VRP-poIFN-α, FMDV yield was reduced by approximately 2,000-fold at 24 h and 10,000-fold at 48 h. However, in VRP-GFP-pretreated IB-RS-2 cells, there was no reduction in FMDV yield compared to mock-pretreated cells at either time. These results support the data of Konopka et al. (20) indicating that a functional type I IFN system is required for the antiviral response induced by VRPs.

Effect of VRP treatment on gene induction. SK6 and IB-RS-2 cells were treated with VRP-poIFN-α or VRP-GFP for 24 h, and RNA was extracted and assayed by qRT-PCR for induction of a number of genes including ISGs and chemokines (Table 2). Treatment of SK6 cells with either VRP resulted in the induction of the same genes although VRP-poIFN-α generally induced higher levels. However, significant differences between the two VRPs were detected in the number and levels of genes induced in IB-RS-2 cells. All genes, except for IFN-λ3, were more upregulated in VRP-poIFN-α-treated than in VRP-GFP-treated cells. These included a number of ISGs (ISG15, Mx1, and OAS), chemokines (IP-10, CCL2, and CCL5) as well as cytoplasmic PRRs (RIG-I and MDA-5). As a control of gene induction, we treated each cell line with 10 μg/ml of synthetic double-stranded RNA (dsRNA) [poly(I · C)]. In SK6 cells the number of genes upregulated was the same after either VRP treatment but for most genes to a lower extent than gene induction after poly(I · C) treatment. In IB-RS-2 cells poly(I · C) gene induction mimicked VRP-poIFN-α treatment although the level of gene induction varied for individual genes (Table 2).

Treatment with VRP-GFP protects C57BL/6 mice against FMDV infection. To examine the ability of VRP-GFP to induce an innate protective response against FMDV *in vivo*, we used an FMDV mouse model system. Salguero et al. (32) demonstrated that certain strains of adult mice, including C57BL/6, are susceptible to FMDV when infected subcutaneously in the footpad. Infected animals develop a significant viremia and die within a few days of infection. To confirm that C57BL/6 mice are susceptible to the strains of FMDV that we use in our lab, we infected groups of five mice with 10^4, 10^5, or 10^6 PFU of FMDV A24 Cruzeiro or O1 Campos per mouse. Mice infected with 10^4 or 10^5 PFU of A24 developed very high levels of viremia, with levels of 10^7 to 10^8 PFU/ml (unpublished data), and 80% died by 2 days postchallenge. All animals in the group infected with 10^6 PFU of FMDV A24 died by 2 days postchallenge (Fig. 4A). Infection with FMDV O1 Campos resulted in a more severe phenotype. All mice infected with 10^4 PFU of FMDV O1 Campos had high levels of viremia (unpublished data) and died by 2 days postchallenge, while 100% of the animals in groups infected with 10^5 or 10^6 PFU FMDV died

TABLE 2 Gene expression in IB-RS-2 or SK6 cells after treatment with poly(I · C), VRP-GFP, or VRP- poIFN-α[a]

Genes	IB-RS-2 cells			SK6 cells		
	Poly IC	VRP-GFP	VRP-poIFNα	Poly IC	VRP-GFP	VRP-poIFNα
IFNβ	243.8	49.2	58.6	5329.7	1043.8	2555.9
IFNλ3	8661.3	244.3	127.0	251572.6	587.6	1848.5
IFNλR	8.1	0.6	1.9	1.4	0.0	0.0
IFNαR	1.1	0.8	1.9	1.5	0.8	0.5
ISG15	25.6	1.3	7.5	667.4	817.6	896.9
IRF1	73.1	9.5	37.3	15.3	7.0	8.3
IRF3	1.3	0.6	1.5	5.6	2.1	1.5
IRF7	2.3	1.0	7.8	16.0	18.5	26.4
MX-1	10.5	1.0	5.4	1532.5	1361.4	962.4
OAS	111.1	1.0	123.9	116.1	244.7	259.8
CCL2	501.7	16.0	1884.3	1997.3	106.4	314.7
CCL5	13.9	8.1	140.0	7027.3	1437.4	2881.4
IP-10	531.0	3.2	23889.6	3598.9	67.8	605.7
IL1	7.5	51.5	112.8	17.9	8.0	3.7
IL6	114.6	8.6	40.5	724.3	14.4	27.6
IL10	3625.9	27.5	68.3	4082.1	8.4	17.0
RIG-I	17.5	1.5	14.1	277.8	1389.5	1938.4
MDA-5	27.4	0.9	4.0	82.9	36.7	46.2
TBK1	0.8	0.9	2.0	0.9	0.8	1.0
TRAF-6	2.4	0.9	2.1	3.3	0.7	0.6
TNF-α	1352.7	23.4	80.6	5492.5	7.4	14.5

[a] Numbers in red indicate upregulation (≥2) compared with the value for mock-infected cells.

Downloaded from http://jvi.asm.org/ on May 15, 2013 by DigiTop -USDA's Digital Desktop Library

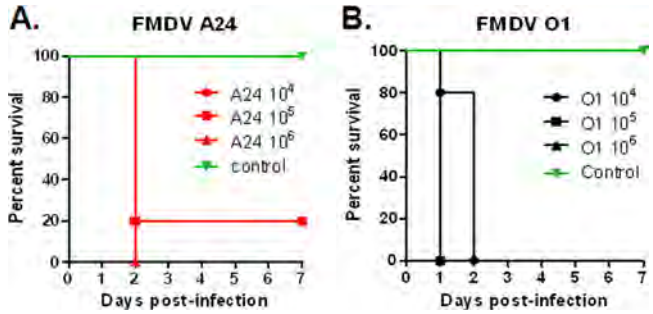

FIG 4 Survival curve of C57BL/6 mice infected with different serotypes of FMDV. Groups ($n = 5$) of 7-week-old mice were infected with different doses (10^4, 10^5, or 10^6 PFU) of FMDV serotype A24 (A) or O1 Campos (B) in the rear footpad. Percent survival was evaluated at the indicated times.

at 1 day postchallenge (Fig. 4B). Based on these results we decided to use FMDV A24 in subsequent experiments.

Groups of five mice were inoculated with 10^6, 10^7, or 10^8 infectious units (IU) of VRP-GFP or PBS (control group) followed by challenge 1 day later with 5×10^4 PFU of FMDV A24. All animals in the control group died between 2 and 3 days after challenge (Fig. 5A), displaying high levels of viremia (4×10^7 to 7×10^8 PFU/ml) (Fig. 5B). In the group inoculated with 10^6 IU of VRP-GFP, 20% died by day 2, and 100% were dead by 3 days postchallenge (Fig. 5A). In this group, all the animals developed viremia, but the levels were slightly lower than in the animals of the control group (Fig. 5B). Interestingly, 100% survival was observed in the groups inoculated with 10^7 or 10^8 IU of VRP-GFP. Furthermore, three of five animals in the 10^7-IU VRP-GFP group and only one of five animals in the 10^8-IU VRP-GFP group developed viremia at levels 2 to 3 logs lower (10^4 to 10^6 PFU/ml) than the control group (Fig. 5B; also unpublished data). In fact, the levels of viremia at 2 days postchallenge of the different VRP-GFP-treated groups were statistically significantly different than the levels of the control group (10^6 IU of VRP-GFP, $P \leq 0.05$; 10^7 and 10^8 IU of VRP-GFP, $P \leq 0.01$).

In the next experiment we examined how rapidly and for how long VRP-GFP-inoculated mice would be protected from subsequent FMDV challenge (Fig. 6). Groups of five mice were inoculated with either 10^7 or 10^8 IU of VRP-GFP and challenged 6, 24, or 48 h later with FMDV A24. A control group was inoculated with PBS and challenged with FMDV 24 h later. As expected 100% of the animals in the control group died by 3 days postchallenge (Fig. 6A), and all animals in this group developed levels of viremia from 1×10^6 to 2.5×10^7 PFU/ml (Fig. 6B). Two out of five mice in the two groups inoculated with 10^7 IU of VRP-GFP and challenged 6 and 48 h later survived (Fig. 6A). In these groups, the levels of viremia were slightly lower than in the control group (Fig. 6B) although there was not a statistically significant difference, and one animal in each group never developed viremia (data not shown). In the group challenged at 24 h, only the animal that developed viremia (1.3×10^6 PFU/ml) died (Fig. 6B; also unpublished data), and the levels of viremia at 2 days postchallenge were different from those of the control group ($P \leq 0.05$). In contrast, all groups inoculated with 10^8 IU of VRP-GFP survived the challenge (Fig. 6A). Although 6 out of the 15 animals in these groups developed viremia, the levels were considerably lower than in the animals that died in the other groups ($P \leq 0.05$ to $P \leq 0.01$), with viremia levels, e.g., of 1×10^4 to 3.7×10^5 PFU/ml.

Inoculation of C57BL/6 mice with VRP-GFP induces an IFN-α-mediated antiviral state. The experiments described above demonstrated the ability of VRP-GFP to rapidly induce a protective response against FMDV. Konopka et al. (20) have previously shown that BALB/c mice infected with null VRPs (replicons that do not express any foreign gene) display high systemic levels of biologically active IFN as early as 3 to 6 h postinfection. Furthermore, a robust upregulation of four host antiviral genes was detected in several organs. To determine if VRP-GFP treatment induces a similar response in C57BL/6 mice, groups of animals were inoculated with 10^8 IU of VRP-GFP and sacrificed at 3, 6, or 24 h after treatment. A control group was inoculated with PBS and euthanized at 24 h. Animals were not challenged with FMDV. Sera were assayed for antiviral activity and for the production of muIFNs by ELISA, and gene analysis was performed on RNA extracted from purified spleen lymphocytes (Fig. 6C and D; Table 3).

Mice inoculated with VRP-GFP developed significant antiviral activity by 3 h postinfection, reaching a peak at 6 h followed by a decline at 24 h (Fig. 6C). A similar kinetics was observed for induction of muIFN-α protein (Fig. 6D). However, we did not detect any significant levels of muIFN-β, -γ, and -λ in the sera of VRP-treated animals (data not shown), suggesting that all the observed antiviral activity was presumably due to IFN-α.

Effect of VRP-GFP treatment on systemic gene induction in mice. Pathogens express various PAMPs that are detected by the host through different PRRs, potentially inducing a number of pathways that are involved in the host antiviral response. As demonstrated above, VRP inoculation induced a strong IFN response.

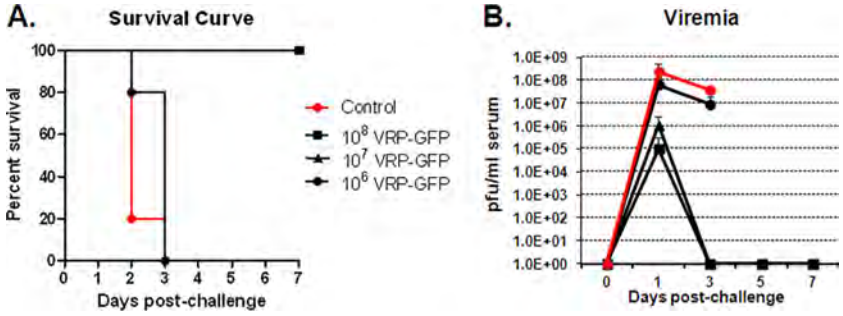

FIG 5 Effect of VRP-GFP treatment on FMDV infection in mice. C57BL/6 mice ($n = 5$/group) were inoculated with different doses (10^6, 10^7 or 10^8 PFU) of VRP-GFP in the right rear footpad and challenged 24 h later in the left rear footpad with 5×10^4 PFU of FMDV A24. Disease was followed (A), and serum samples were collected for 7 days after challenge to assay for viremia (B).

Downloaded from http://jvi.asm.org/ on May 15, 2013 by DigiTop -USDA's Digital Desktop Library

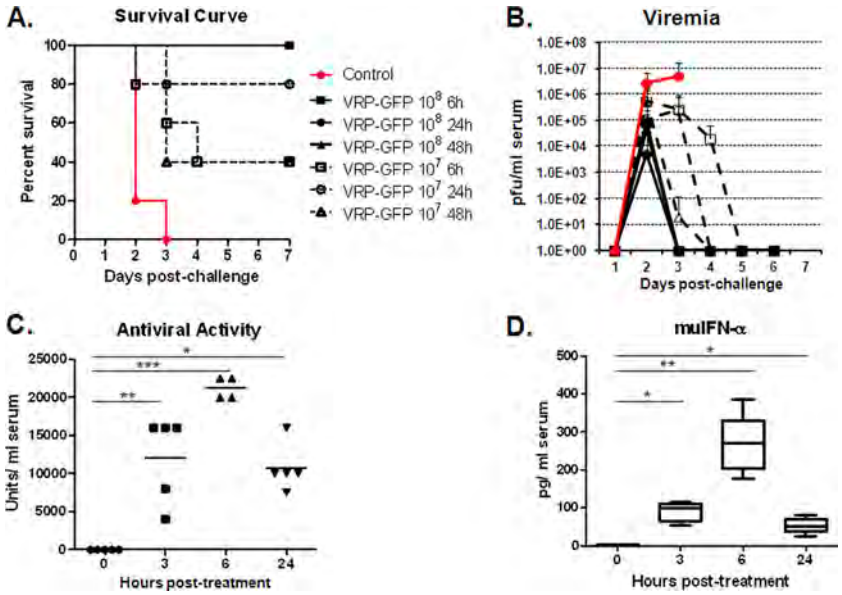

FIG 6 Duration of effect of VRP-GFP treatment on FMDV infection in mice. C57BL/6 mice ($n = 5$/group) were inoculated with different doses (10^7 or 10^8 PFU) of VRP-GFP in the right rear footpad and challenged 6, 24, and 48 h later in the left rear footpad with 5×10^4 PFU of FMDV A24. Disease was followed (A), and serum samples were collected for 7 days after challenge to assay for viremia (B). Serum of mice was tested for antiviral activity (C) and presence of IFN-α (D) at different time points (3, 6, and 24 h) after VRP-GFP treatment before FMDV challenge. *, $P \leq 0.05$; **, $P \leq 0.01$; ***, $P \leq 0.001$.

To identify the genes induced by VRP treatment that may lead to the protective antiviral response, splenic lymphocytes were isolated from treated animals, RNA was purified, and the expression of 84 genes was analyzed by real-time RT-PCR using an RT^2 Profiler PCR custom-modified antiviral response pathway kit (Table 1). RNA from a PBS-inoculated group euthanized at the beginning of the experiment was used as a control. At 3 h only a few genes were induced, including the three IFN-α subtypes in our array and IFN-β, although induction was not statistically significant (Table 3). However, by 6 h, a number of genes were statistically significantly upregulated (fold induction of ≥2; $P \leq 0.05$). These included the following: (i) PRRs TLR3, TLR7, TLR8, TLR9, RIG-I, MDA-5, and LPG2; (ii) proinflammatory cytokines interleukin-15 (IL-15), IL-18 and IL-6; (iii) costimulatory molecule CD86; (iv) transcription factors involved in the IFN pathway including IRF7, MYD88, and Stat1; (v) ISGs ISG15, Mx1, and OAS2; and (vi) chemokines MIP-1α, IP-10, CXCL-9, and CXCL-11 (Table 2). No IFNs were upregulated at 6 h. The most upregulated gene at 6 h was IP-10. Twenty-four hours after treatment, most of these genes remained upregulated but at reduced levels compared to levels at 6 h (Table 3). Furthermore, a number of other genes were induced at this time, including the three IFN-α subtypes and IFN-β, which were all significantly upregulated, and the type III IFN receptor subunit present in our array.

IP-10 is directly involved in the type I IFN-induced protective response. Thus far, we have demonstrated that inoculation of mice with VRP-GFP induced a strong protective antiviral response against FMDV which correlated with increased levels of IFN-α in serum. This is in accordance with the demonstrated antiviral and protective effect of type I IFN against FMDV in the natural host (4, 9, 10). To confirm the antiviral effect of IFN-α against FMDV in the mouse model, we treated groups of five mice with 10^4 U of muIFN-α followed by challenge with 5×10^4 PFU of FMDV A24 at 4 or 18 h after treatment. Five untreated mice were included as a control group. As expected, the presence of IFN protein was detected in serum, with the level peaking at 4 h after IFN treatment (Fig. 7A) and correlated with detectable levels of antiviral activity (Fig. 7B). All (100%) of the animals treated with IFN-α survived FMDV challenge (Fig. 7C). Interestingly, none of the animals treated 4 h prior to challenge developed viremia, and only two of five animals in the group treated with IFN-α for 18 h developed viremia, which was 100-fold lower than that in the control animals ($P \leq 0.01$) (Fig. 7D). These results demonstrated that recombinant muIFN-α is able to inhibit FMDV replication in C57BL/6 mice.

In the previous experiment we demonstrated that mice inoculated with VRP-GFP had high levels of IFN-α in sera and induction of numerous ISGs in splenocytes. Some of these genes might be involved in the IFN protection conferred against FMDV. IP-10 was the most upregulated gene at 6 h after treatment. This chemokine is of particular interest because we have previously demonstrated that swine or cattle inoculated with Ad5-poIFN-α or Ad5-boIFN-λ3, respectively, and protected against FMD display selective upregulation of IP-10 (7, 8, 12, 33). To determine if IP-10 has a role in the IFN-induced protection against FMDV, we treated IP-10 KO mice (10 per group) with muIFN-α or PBS 4 h prior to challenge. As controls, we included WT C57BL/6 mice that were treated similarly. The IFN-treated IP-10 KO mice had detectable but lower levels of IFN-α and antiviral activity than the WT IFN-treated mice (Fig. 8A and B, compare with 7A and B). Ninety percent of PBS-treated WT mice died 2 to 4 days after challenge (Fig. 8C) and developed high levels of viremia (Fig. 8D). All WT muIFN-α-treated mice survived FMDV A24 challenge and did not develop viremia (Fig. 8C and D). In contrast, IP-10 KO mice did not respond to muIFN-α treatment, displaying a survival rate of 30%, similar to the survival rate of the IP-10 KO or WT mice treated with PBS (20% and 10%, respectively). Overall, the levels of viremia were the same for muIFN-α-treated IP-10 KO

Downloaded from http://jvi.asm.org/ on May 15, 2013 by DigiTop -USDA's Digital Desktop Library

TABLE 3 Gene expression in spleen lymphocytes after treatment of mice with VRP-GFP for different times

	Genes	3 h		6 h		24 h	
		Fold induction	P value	Fold induction	P value	Fold induction	P value
IFN & IFN pathway	IFNα2	2.63[a]	0.246191	0.86	0.466226	22.50	0.071424
	IFNα4	5.6	0.206939	1.22	0.608305	62.95	0.092891
	IFNα7	4.27	0.213146	0.57	0.343659	35.32	0.084141
	IFNb1	3.91	0.250578	0.48[b]	0.351841	25.03	0.059114
	IFNγ	1.35	0.237723	1.97	0.053467	3.97	0.000751
	IL28ra	2.13	0.234084	0.55	0.226972	9.66	0.049797
	IRF3	1.75	0.253831	0.62	0.191625	5.16	0.050329
	IRF7	0.83	0.140633	15.81	0.000117	8.69	0.005479
	Stat1	0.75	0.044758	4.92	0.000000	1.78	0.006905
ISGs	ISG15	0.97	0.943103	32.59	0.000011	10.07	0.001302
	Mx1	1.44	0.314996	34.62	0.000311	17.4	0.000029
	OAS2	0.67	0.271944	18.33	0.000054	11.23	0.000009
Pro-inflammatory cytokines & proteins	IL12b	1.52	0.246191	0.79	0.156999	6.71	0.031207
	IL15	1.53	0.175364	7.23	0.001103	5.51	0.000004
	IL18	1.53	0.004976	2.75	0.005214	1.99	0.000117
	IL1b	2.78	0.002358	1.45	0.206729	2.18	0.020273
	IL6	2.38	0.198424	3.52	0.008270	12.91	0.057188
	Mefv	0.99	0.797361	1.53	0.203894	4.03	0.007090
	Nlrp3	1.69	0.113898	1.44	0.176663	3.67	0.001961
	Spp1	1.56	0.254452	1.26	0.272122	9.85	0.026040
Chemokines	CCL3	1.2	0.317019	1.82	0.147049	2.41	0.008493
	MIP-1b	1.23	0.347210	2.55	0.029841	2.76	0.010919
	IP-10	1.46	0.119504	124.73	0.000117	14.73	0.000918
	Cxcl11	5.32	0.207501	2.67	0.003416	53.22	0.060117
	Cxcl9	1.18	0.094395	4.52	0.000033	2.40	0.004760
Cell prolif.[c]	CD80	1.26	0.323187	0.97	0.915370	2.51	0.040226
	CD86	1.23	0.098300	2.29	0.005785	1.29	0.062576
	Aim2	1.4	0.334853	1.76	0.086456	4.01	0.049203
PRRs	RIG-I	0.93	0.241102	6.47	0.000129	2.35	0.001207
	mda-5	0.98	0.246191	28.41	0.000396	9.05	0.000119
	Lpg2	1.01	0.51479	9.37	0.000032	3.82	0.000297
	Nod2	1.12	0.368251	1.89	0.067574	5.51	0.006049
	TLR3	0.78	0.284456	4.55	0.000125	3.18	0.001224
	TLR7	0.91	0.451904	2.7	0.000245	2.19	0.000104
	TLR8	0.98	0.925725	2.54	0.050990	3.77	0.000669
	TLR9	0.59	0.000059	2.3	0.000619	1.23	0.070618
Adap.[d]	Trim25	0.66	0.067851	4.52	0.000334	1.45	0.090908
	Myd88	0.97	0.699230	3.77	0.000195	2	0.000738
	Tbkbp1	0.88	0.528735	1.12	0.634106	3.04	0.013323
Apoptosis	Card9	1.1	0.474987	1.03	0.786197	3.46	0.005801
	Casp1	1.49	0.127514	2.35	0.006339	1.26	0.096922
	Casp8	1.2	0.173247	1.15	0.386998	2.92	0.063306
	Fadd	1.93	0.225227	0.94	0.598978	6.65	0.082939

[a] Numbers in red indicate upregulation (≥2) compared with the level in mock-infected animals.
[b] Numbers in blue indicate downregulation (<0.5) compared with the level in mock-infected animals.
[c] Cell prolif, cell proliferation.
[d] Adap, adaptor proteins.

Downloaded from http://jvi.asm.org/ on May 15, 2013 by DigiTop -USDA's Digital Desktop Library

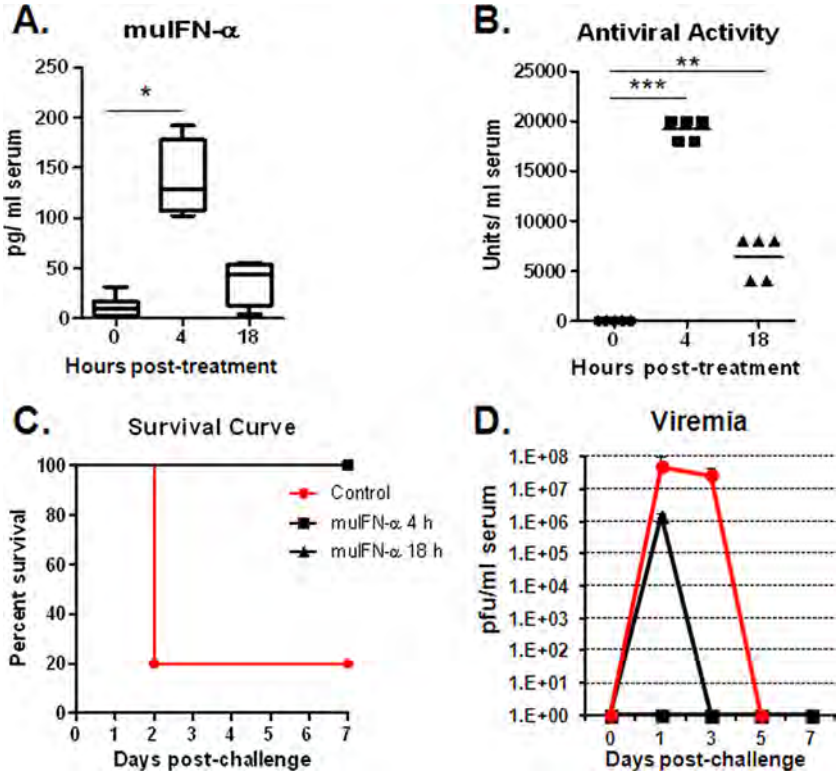

FIG 7 Effect of IFN-α treatment on FMDV infection in mice. C57BL/6 mice ($n = 5$/group) were treated with 10^4 U of muIFN-α and challenged with 5×10^4 PFU of FMDV A24 in the rear left footpad at different times (4 or 18 h) after treatment. Serum of the mice was tested for the presence of IFN-α (A) and antiviral activity (B). Disease was followed (C) and serum samples were collected for 7 days after challenge to assay for viremia (D). *, $P \leq 0.05$; **, $P \leq 0.01$; ***, $P \leq 0.001$.

mice and PBS-treated IP-10 KO or WT mice (Fig. 8D). These results indicated that in our C57BL/6 mouse model, IP-10 mediates at least one of the IFN-α-induced mechanisms of protection against FMD.

DISCUSSION

We have previously demonstrated that swine inoculated with Ad5-poIFN-α are rapidly protected when challenged 1 day later with FMDV (4, 9, 10). More recently we also showed that treatment of bovines with Ad5-boIFN-λ3 can significantly delay and reduce clinical disease (12). However, in each case the protective dose is relatively high, limiting the applicability of such a strategy in the livestock industry. To overcome these limitations, we hypothesized that a broader and more robust innate immune response could be obtained by adding to IFN treatment a mimic of natural viral infection. We found that treatment of cell cultures with poly(I · C) or swine with poly(IC) stabilized with poly-L-lysine and carboxymethyl cellulose [poly(ICLC)], both mimics of dsRNA produced during virus infection, inhibits FMDV replication and induces a rapid protective response (29). Others have shown that the baculovirus *Autographa californica* nuclear polyhedrosis virus (AcNPV) can induce a rapid innate immune response in animals (34). Recently, Molinari et al. (35) demonstrated that mice pretreated with AcNPV as early as 3 h and up to 3 days prior to challenge with FMDV survived. The authors speculated that protection was presumably a result of induction of IFN but did not directly assay for the initiation of an antiviral response.

In this article we examined the potential of VEE replicons as an alternative approach to induce rapid protection against FMDV. Empty VRPs have recently been shown to induce a rapid innate response in mice and protect against challenge with homologous VEE virus as well as the heterologous influenza virus but did not protect against VSV (20). We demonstrated that treatment of the SK6 swine cell line with either VRP-poIFN-α or VRP-GFP rapidly inhibited subsequent FMDV replication and that the duration of inhibition lasted for at least 5 days. In agreement with Konopka et al. (20), we found that VRP-induced protection requires a functional type I IFN system. Swine IB-RS-2 cells, which do not produce type I IFN, are not protected from FMDV infection by VRP-GFP treatment but are protected after VRP-poIFN-α treatment.

Treatment of SK6 cells with either VRP induced a broad array of genes (17 to 18 of 21 genes examined), but in VRP-poIFN-α-treated cells the majority of these genes were induced to higher levels that in VRP-GFP-treated cells (Table 2). It is important to note that in SK6 cells VRP-GFP as well as poly(I · C) induces the upregulation of both type I and III IFNs as well as various ISGs. We previously obtained similar results in bovine cells treated with poly IC, but treatment of these cells with boIFN-α or boIFN-λ3 only upregulated ISGs and not IFNs (8; also unpublished data), indicating that this new approach is inducing a broader response.

While both VRP-GFP- and VRP-poIFN-α-treated SK6 cells were protected from subsequent FMDV infection, only supernatants from VRP-poIFN-α-treated cells contained significant levels of poIFN-α protein and antiviral activity at 24 and 48 hpi (Fig. 2C). However, even supernatants from VRP-GFP- or VRP-poIFN-α-treated cells containing undetectable or low levels of poIFN-α protein or antiviral activity could still significantly re-

Downloaded from http://jvi.asm.org/ on May 15, 2013 by DigiTop -USDA's Digital Desktop Library

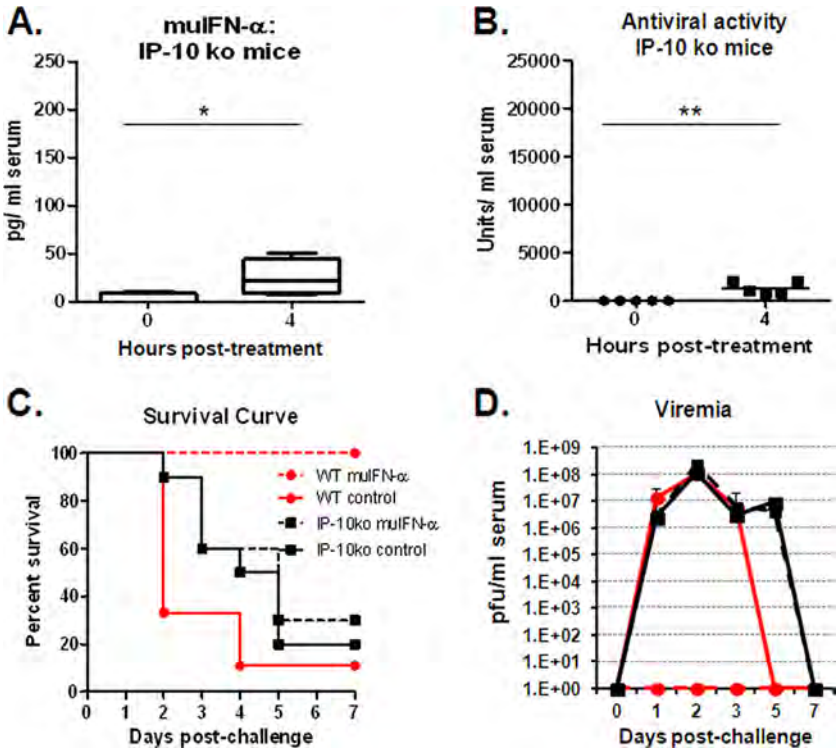

FIG 8 Effect of IFN-α treatment on FMDV infection in IP-10 KO mice. WT and IP-10 KO mice were treated with 10^4 U of muIFN-α and challenged with 5×10^4 PFU of FMDV A24 in the rear left footpad at 4 h after treatment. Serum of the mice was tested for the presence of IFN-α (A) and antiviral activity (B). Disease was followed (C), and serum samples were collected for 7 days after challenge to assay for viremia (D). *, $P \leq 0.05$; **, $P \leq 0.01$.

duce virus yield (as much as 1,000-fold) (Fig. 2A and C). These results suggest that the observed inhibition of viral replication could be due to a cytokine other than poIFN-α or that the IFN-α ELISA or our method of measuring antiviral activity is much less sensitive than the evaluation of a reduction in viral replication. The gene induction data in Table 2 indicated that poIFN-β and poIFN-λ3 were both upregulated in cells treated with the VRPs. It should be pointed out, however, that our antiviral assays were performed in IB-RS-2 cells which we know lack a functional IFN-λ receptor (E. Perez-Martin et al., unpublished data). Therefore, the absence of antiviral activity at 6, 24, and 48 h in the supernatants of VRP-GFP-treated SK6 cells and at 6 h in the supernatants of VRP-poIFN-α-treated cells may as well be due to the presence of low levels of poIFN-α/β proteins undetectable by our relatively low sensitivity assay or to poIFN-λ to which IB-RS-2 cells are insensitive. In any case, all the antiviral activity observed *in vivo* in mice was consistent with the detected serum levels of IFN-α, suggesting that this cytokine primarily mediates the VRP-GFP-induced effect. However, it is possible that other cytokines may also be involved.

It has been reported by numerous investigators that adenovirus vectors can induce a very rapid innate immune response both in cell culture and in mice (36–39). We have also demonstrated that inoculation of swine with an Ad5-VSVG vector induces a very rapid systemic antiviral response and high levels of poIFN-α as early as 4 hpi; but the antiviral response essentially is not detectable by 24 hpi, and animals inoculated with this vector are not protected from FMD when challenged 1 day after administration (4). Therefore, we examined the ability of various Ad5 vectors, including Ad5-GFP, to induce an FMDV-protective response in SK6 and LF-BK cells. Surprisingly, only the Ad5-poIFN-α vector inhibited FMDV replication (Fig. 2D). Although we currently do not understand the molecular basis of this difference, the results in the cell lines used in this study suggest that VRPs have the ability to induce a more potent protective innate response than Ad5 vectors.

The cell culture results prompted us to examine the effectiveness of VRP-GFP in protecting adult mice from FMDV infection. Although it would have been preferable to directly compare the two constructs used *in vitro*, we did not use VRP-poIFN-α in these studies because our cell culture data indicated that poIFN-α was not effective in mouse cells (unpublished data). Nevertheless, the main purpose of these experiments was to determine if VRPs are able to activate a protective innate immune response against FMDV. Confirming our hypothesis, we observed that mice treated with VRP-GFP survived FMDV challenge as early as 6 h posttreatment (hpt) and for at least 48 h. As shown by Konopka et al. (20) and confirmed in our study, the effectiveness of treatment is dependent on the dose of the VRP. After VRP treatment there is a very rapid rise in antiviral activity, which appears to be attributed to the induction of muIFN-α since we were unable to detect the presence of IFN-β, IFN-γ, or IFN-λ. To confirm this data, we demonstrated that animals treated with recombinant muIFN-α and challenged at different times after treatment were completely protected from FMDV. Similarly to the gene induction data in cell culture, a number of genes were upregulated in mice treated with VRP-GFP. As early as 3 hpt several of the 84 genes analyzed were induced, including the three subtypes of muIFN-α present in our array as well as IFN-β. Marie et al. (40) have found that muIFN-α4

Downloaded from http://jvi.asm.org/ on May 15, 2013 by DigiTop -USDA's Digital Desktop Library

is the most rapidly induced IFN in mouse fibroblasts infected with Newcastle disease virus, and our results indicate that this subtype along with muIFN subtypes 2 and 7 were all detectable by 3 hpt. By 6 hpt many genes were induced at a statistically significant level, including genes with direct antiviral activity, transcription factors, chemokines, and PRRs. In particular, IP-10 was upregulated over 124-fold. By 24 hpt more genes were upregulated, but the level of induction of most of the genes first detectable at 6 hpt was reduced. Furthermore, type I IFN genes were significantly induced.

In our previous studies in swine and cattle, as well as in the current mouse study, we demonstrated a significant induction of IP-10 by type I, II, or III IFN or VRP treatment (12, 33). IP-10 is a chemokine involved in the recruitment, proliferation, and activation of natural killer (NK) cells (41). In the swine study we demonstrated that in animals treated with Ad5-poIFN-α, protection against FMDV challenge correlated with recruitment of dendritic cells (DCs) and NK cells to the skin and lymph nodes, respectively (33). Furthermore, 1 day after Ad5-poIFN-α administration, there was a significant upregulation of IP-10 in the skin and lymph nodes. Using a mouse model, we confirmed that IP-10 plays a role *in vivo* in protecting animals from subsequent FMDV infection. As expected, less than 20% survival was observed in WT and IP-10 KO mice after FMDV challenge. However, while preadministration of muIFN-α protected 100% of WT mice against virus challenge, only 30% survival was observed when IP-10 KO mice were treated similarly. These results demonstrated that IP-10 plays a critical role in the IFN-induced protection against FMDV although presumably other ISGs may also be involved in inhibition of FMDV replication. As mentioned before, we have previously demonstrated in cell culture that PKR and the OAS/RNase L system control FMDV replication (6, 28). It will be useful to examine the role of additional ISG products in this process. Testing other KO mice, performing ISG-overexpression or -downregulation screens, etc., will help elucidate the IFN-dependent mechanisms of FMDV inhibition.

As we previously demonstrated, administration of Ad5-poIFN-α sterilely protected swine from FMDV infection (10). Since our results in cell culture indicate that VRPs containing an IFN gene induce an enhanced protective response and higher levels of ISGs than VRP-GFP treatment, we plan to initiate studies in naturally susceptible animals with different doses of VRP-po/boIFN-α/β and examine their efficacy against FMDV challenge.

ACKNOWLEDGMENTS

This research was supported in part by the Plum Island Animal Disease Research Participation Program administered by the Oak Ridge Institute for Science and Education through an interagency agreement between the U.S. Department of Energy and the U.S. Department of Agriculture (appointments of C.C.A.D., M.W., and E.P.-M.), by CRIS project number 1940-32000-057-00D, ARS, USDA (M.J.G. and T.D.L.S.), and by grants through an interagency agreement with the Science and Technology Directorate of the U.S. Department of Homeland Security under Award Numbers HSHQDC-09-X00373 and HSHQDC-11-X-00189 (M.J.G. and T.D.L.S).

We thank Diego Sturza and Beatriz Matias for maintaining cells for *in vitro* experiments and the animal care staff at PIADC for their professional support and assistance.

REFERENCES

1. **Grubman MJ, Baxt B.** 2004. Foot-and-mouth disease. Clin. Microbiol. Rev. **17**:465–493.
2. **Domingo E, Escarmís C, Baranowski E, Ruiz-Jarabo CM, Carrillo E, Nunez JI, Sobrino F.** 2003. Evolution of foot-and-mouth disease virus. Virus Res. **91**:47–63.
3. **Golde WT, Pacheco JM, Duque H, Doel T, Penfold B, Ferman GS, Gregg DR, Rodriguez LL.** 2005. Vaccination against foot-and-mouth disease virus confers complete clinical protection in 7 days and partial protection in 4 days: use in emergency outbreak response. Vaccine **23**: 5775–5782.
4. **Moraes MP, Chinsangaram J, Brum MCS, Grubman MJ.** 2003. Immediate protection of swine from foot-and-mouth disease: a combination of adenoviruses expressing interferon alpha and a foot-and-mouth disease virus subunit vaccine. Vaccine **22**:268–279.
5. **Pacheco JM, Brum MCS, Moraes MP, Golde WT, Grubman MJ.** 2005. Rapid protection of cattle from direct challenge with foot-and-mouth disease virus (FMDV) by a single inoculation with an adenovirus vectored FMDV subunit vaccine. Virology **337**:205–209.
6. **Chinsangaram J, Koster M, Grubman MJ.** 2001. Inhibition of L-deleted foot-and-mouth disease virus replication by alpha/beta interferon involves double-stranded RNA-dependent protein kinase. J. Virol. **75**: 5498–5503.
7. **Moraes MP, de los Santos T, Koster M, Turecek T, Wang H, Andreyev VG, Grubman MJ.** 2007. Enhanced antiviral activity against foot-and-mouth disease virus by a combination of type I and II porcine interferons. J. Virol. **81**:7124–7135.
8. **Díaz-San Segundo F, Weiss M, Perez-Martín E, Koster MJ, Zhu J, Grubman MJ, de los Santos T.** 2011. Antiviral activity of bovine type III interferon against foot-and-mouth disease virus. Virology **413**:283–292.
9. **Chinsangaram J, Moraes MP, Koster M, Grubman MJ.** 2003. Novel viral disease control strategy: adenovirus expressing alpha interferon rapidly protects swine from foot-and-mouth disease. J. Virol. **77**:1621–1625.
10. **Dias CCA, Moraes MP, Diaz-San Segundo F, de los Santos T, Grubman MJ.** 2011. Porcine type I interferon rapidly protects swine against challenge with multiple serotypes of foot-and-mouth disease virus. J. Interferon Cytokine Res. **31**:227–236.
11. **Wu Q, Brum MCS, Caron L, Koster M, Grubman MJ.** 2003. Adenovirus-mediated type I interferon expression delays and reduces disease signs in cattle challenged with foot-and-mouth disease virus. J. Interferon Cytokine Res. **23**:359–368.
12. **Perez-Martin E, Weiss M, Diaz-San Segundo F, Pacheco JM, Arzt J, Grubman MJ, de los Santos T.** 2012. Bovine type III interferon significantly delays and reduces severity of foot-and-mouth disease in cattle. J. Virol. **86**:4477–4487.
13. **Medzhitov R, Janeway CA, Jr.** 1998. Innate immune recognition and control of adaptive immune responses. Semin. Immunol. **10**:351–353.
14. **Honda K, Taniguchi T.** 2006. IRFs: master regulators of signaling by Toll-like receptors and cytosolic pattern-recognition receptors. Nat. Rev. Immunol. **6**:644–658.
15. **Kawai T, Akira S.** 2011. Toll-like receptors and their crosstalk with other innate receptors in infection and immunity. Immunity **34**:637–650.
16. **Pushko P, Parker M, Ludwig GV, Davis NL, Johnston RE.** 1997. Replicon-helper systems from attenuated Venezuelan equine encephalitis virus: expression of heterologous genes in vitro and immunization against heterologous pathogens in vivo. Virology **239**:389–401.
17. **Lee JS, Hadjipanayis AG, Welkos SL.** 2003. Venezuelan equine encephalitis virus-vectored vaccines protect mice against anthrax spore challenge. Infect. Immun. **71**:1491–1496.
18. **Hooper JW, Ferro AM, Golden JW, Silvera P, Dudek J, Alterson K, Custer M, Rivers B, Morris J, Owens G, Smith JF, Kamrud KI.** 2009. Molecular smallpox vaccine delivered by alphavirus replicons elicits protective immunity in mice and non-human primates. Vaccine **28**:494–511.
19. **Konopka JL, Penalva LO, Thompson JM, White LJ, Beard CW, Keene JD, Johnston RE.** 2007. A two-phase innate host response to alphavirus infection identified by mRNP-tagging in vivo. PLoS Pathog. **3**:e199. doi: 10.1371/journal.ppat.0030199.
20. **Konopka JL, Thompson JM, Whitmore AC, Webb DL, Johnston RE.** 2009. Acute infection with Venezuelan equine encephalitis virus replicon particles catalyzes a systemic antiviral state and protects from lethal virus challenge. J. Virol. **83**:12432–12442.
21. **Swaney LM.** 1988. A continuous bovine kidney cell line for routine assays of foot-and-mouth disease virus. Vet. Microbiol. **18**:1–14.
22. **Graham F, Prevec L.** 1991. Manipulation of adenovirus vectors, p 109–128. *In* Murray EJ (ed), Gene transfer and expression protocols. Methods in molecular biology, vol 7. Humana Press, Clifton, NJ.

Downloaded from http://jvi.asm.org/ on May 15, 2013 by DigiTop -USDA's Digital Desktop Library

23. **Kinney RM, Johnson BJ, Welch JB, Tsuchiya KR, Trent DW.** 1989. The full-length nucleotide sequences of the virulent Trinidad donkey strain of Venezuelan equine encephalitis virus and its attenuated vaccine derivative, strain TC-83. Virology **170**:19–38.
24. **Bernstein DI, Reap EA, Katen K, Watson A, Smith K, Norberg P, Olmsted RA, Hoeper A, Morris J, Negri S, Maughan MF, Chulay JD.** 2009. Randomized, double-blind, phase 1 trial of an alphavirus replicon vaccine for cytomegalovirus in CMV seronegative adult volunteers. Vaccine **28**:484–493.
25. **Kamrud KI, Custer M, Dudek JM, Owens G, Alterson KD, Lee JS, Groebner JL, Smith JF.** 2007. Alphavirus replicon approach to promoterless analysis of IRES elements. Virology **360**:376–387.
26. **Moraes MP, Mayr GA, Grubman MJ.** 2001. pAd5-Blue: an easy to use, efficient, direct ligation system for engineering recombinant adenovirus constructs. Biotechniques **31**:1050–1056.
27. **Moraes MP, Mayr GA, Mason PW, Grubman MJ.** 2002. Early protection against homologous challenge after a single dose of replication-defective human adenovirus type 5 expressing capsid proteins of foot-and-mouth disease virus (FMDV) strain A24. Vaccine **20**:1631–1639.
28. **de los Santos T, de Avila Botton S, Weiblen R, Grubman MJ.** 2006. The leader proteinase of foot-and-mouth disease virus inhibits the induction of beta interferon mRNA and blocks the host innate immune response. J. Virol. **80**:1906–1914.
29. **Dias CC, Moraes MP, Weiss M, Diaz-San Segundo F, Perez-Martin E, Salazar AM, de los Santos T, Grubman MJ.** 2012. Novel antiviral therapeutics to control foot-and-mouth disease. J. Interferon Cytokine Res. **32**:462–473.
30. **Applied Biosystems.** 1997. User bulletin 2. ABI Prism 7700 sequence detection system: relative quantification of gene expression (P/N 4303859). Applied Biosystems, Foster City, CA.
31. **Georgel P, Jiang Z, Kunz S, Janssen E, Mols J, Hoebe K, Bahram S, Oldstone MBS, Beutler B.** 2007. Vesicular stomatitis virus glycoprotein G activates a specific antiviral Toll-like receptor 4-dependent pathway. Virology **362**:304–313.
32. **Salguero FJ, Sanchez-Martin MA, Diaz-San Segundo F, de Avila A, Sevilla N.** 2005. Foot-and-mouth disease virus (FMDV) causes an acute disease that can be lethal for adult laboratory mice. Virology **332**:384–396.
33. **Diaz-San Segundo F, Moraes MP, de los Santos T, Dias CCA, Grubman MJ.** 2010. Interferon-induced protection against foot-and-mouth disease virus correlates with enhanced tissue specific innate immune cell infiltration and interferon stimulated gene expression. J. Virol. **84**:2063–2077.
34. **Abe T, Takahashi H, Hamazaki H, Miyano-Kurosaki N, Matsuura Y, Takaku H.** 2003. Baculovirus induces an innate immune response and confers protection from lethal influenza virus infection in mice. J. Immunol. **17**:1133–1139.
35. **Molinari P, Garcia-Nunez S, Gravisaco MJ, Carrillo E, Berinstein A, Taboga O.** 2010. Baculovirus treatment fully protects mice against a lethal challenge of FMDV. Antiviral Res. **87**:276–279.
36. **Hartman ZC, Black EP, Amalfitano A.** 2007. Adenoviral infection induces a multi-faceted innate cellular immune response that is mediated by the toll-like receptor pathway in A549 cells. Virology **358**:357–372.
37. **Muruve DA.** 2004. The innate immune response to adenovirus vectors. Hum. Gene Ther. **15**:1157–1166.
38. **Muruve DA, Barnes MJ, Stillman IE, Libermann TA.** 1999. Adenoviral gene therapy leads to rapid induction of multiple chemokines and acute neutrophil-dependent hepatic injury in vivo. Hum. Gene Ther. **10**:965–976.
39. **Zhang Y, Chirmule N, Gao GP, Qian R, Croyle M, Joshi B, Tazelaar J, Wilson JM.** 2001. Acute cytokine response to systemic adenoviral vectors in mice is mediated by dendritic cells and macrophages. Mol. Ther. **3**:697–707.
40. **Marie I, Durbin JE, Levy DE.** 1998. Differential viral induction of distinct interferon-α genes by positive feedback through interferon regulatory factor-7. EMBO J. **17**:6660–6669.
41. **Taub DD, Sayers TJ, Carter CR, Ortaldo JR.** 1995. α and β chemokines induce NK cell migration and enhance NK-mediated cytolysis. J. Immunol. **155**:3877–3888.

Downloaded from http://jvi.asm.org/ on May 15, 2013 by DigiTop -USDA's Digital Desktop Library

Vaccine 31 (2013) 2302–2309

Contents lists available at SciVerse ScienceDirect

Vaccine

journal homepage: www.elsevier.com/locate/vaccine

An adenovirus vectored mucosal adjuvant augments protection of mice immunized intranasally with an adenovirus-vectored foot-and-mouth disease virus subunit vaccine

Diana M. Alejo[a], Mauro P. Moraes[b,d,1], Xiaofen Liao[b], Camila C. Dias[c], Edan R. Tulman[b], Fayna Diaz-San Segundo[d], Debra Rood[e], Marvin J. Grubman[d], Lawrence K. Silbart[e,*]

[a] Department of Animal Science, University of Connecticut, Storrs, CT 06269, United States
[b] Department of Pathobiology and Veterinary Science, University of Connecticut, Storrs, CT 06269, United States
[c] Oak Ridge Institute for Science and Education, PIADC Research Participation Program, Oak Ridge, TN 37831, United States
[d] Plum Island Animal Disease Center, U.S. Department of Agriculture, Agriculture Research Service, NAA, P.O. Box 848, Greenport, NY 11944, United States
[e] Department of Allied Health Sciences, University of Connecticut, Storrs, CT 06269, United States

ARTICLE INFO

Article history:
Received 28 September 2012
Received in revised form 8 February 2013
Accepted 27 February 2013
Available online 13 March 2013

Keywords:
Adenovirus
FMDV
Mucosal immunity
E. coli enterotoxin
Adjuvants
Mice

ABSTRACT

Foot-and-mouth disease virus (FMDV) is a highly contagious pathogen that causes severe morbidity and economic losses to the livestock industry in many countries. The oral and respiratory mucosae are the main ports of entry of FMDV, so the stimulation of local immunity in these tissues may help prevent initial infection and viral spread. *E. coli* heat-labile enterotoxin (LT) has been described as one of the few molecules that have adjuvant activity at mucosal surfaces. The objective of this study was to evaluate the efficacy of replication-defective adenovirus 5 (Ad5) vectors encoding either of two LT-based mucosal adjuvants, LTB or LTR72. These vectored adjuvants were delivered intranasally to mice concurrent with an Ad5-FMDV vaccine (Ad5-A24) to assess their ability to augment mucosal and systemic humoral immune responses to Ad5-A24 and protection against FMDV. Mice receiving Ad5-A24 plus Ad5-LTR72 had higher levels of mucosal and systemic neutralizing antibodies than those receiving Ad5-A24 alone or Ad5-A24 plus Ad5-LTB. The vaccine plus Ad5-LTR72 group also demonstrated 100% survival after intradermal challenge with a lethal dose of homologous FMDV serotype A24. These results suggest that Ad5-LTR72 could be used as an important tool to enhance mucosal and systemic immunity against FMDV and potentially other pathogens with a common route of entry.

© 2013 Elsevier Ltd. All rights reserved.

1. Introduction

Foot-and-mouth disease (FMD) is one of the most economically devastating and highly contagious diseases of cloven-hoofed animals including cattle, sheep and pigs [1]. The etiologic agent, FMD virus (FMDV), is classified in the family *Picornaviridae* in the genus *Aphthovirus*.

Susceptible livestock become infected through contact with infected animals or a virus-contaminated environment. FMDV is a mucosal pathogen that typically enters via the respiratory route as aerosolized virus or by mechanical transfer [2–5]. The dorsal soft palate and the roof of the pharynx have been established as an initial site of FMDV replication in cattle [2,3], reflecting the mucosal route of exposure.

Control of outbreaks in countries normally free from disease is achieved by slaughter of infected animals, complete restriction of movement of susceptible animals, and the use of a parenterally administered, chemically inactivated, whole virus vaccine [6]. Chemical inactivation is not without risk and the final preparation can be contaminated with viral non-structural proteins, making it difficult to distinguish vaccinated from infected animals using currently approved diagnostic tests [7,8]. High containment facilities are required for vaccine production, and there is also a risk of escape of live virus as occurred in the 2007 FMD outbreak in the U.K. [9]. The current vaccine induces little mucosal immunity, potentially allowing vaccinated animals to harbor sub-clinical and often chronic infection; providing time and opportunity for mutation and the generation of escape variants [10,11].

An alternative vaccine strategy that overcomes some of the disadvantages of the inactivated vaccine has been developed which involves cloning the FMDV serotype A24 Cruzeiro capsid

* Corresponding author.
E-mail addresses: Silbart@uconn.edu, lsilbart@yahoo.com (L.K. Silbart).
[1] Present address: CEVA Biomune, 8906 Rosehill Rd. Lenexa, KS 66215, United States.

0264-410X/$ – see front matter © 2013 Elsevier Ltd. All rights reserved.
http://dx.doi.org/10.1016/j.vaccine.2013.02.060

polyprotein (P1-2A) coding region and the serotype A12 3C^{pro} coding region into a replication-defective human adenovirus type 5 (Ad5) vector (Ad5-A24) [12]. Studies in swine using this vaccine demonstrated that after one intramuscular inoculation (IM), animals developed FMDV-specific neutralizing antibodies that conferred protection upon direct inoculation with homologous virus at 7, 14, and 42 days post-vaccination [12]. Others have shown that intranasal, oral gavage and enteric vaccination strategies with adeno-based vectors can induce antigen-specific systemic and mucosal responses and in some cases overcome preexisting Ad5 immunity [13–15].

Several enterotoxin adjuvants have been shown to augment respiratory immunity when co-administered intranasally (IN) with proteins or peptides. These adjuvants include the heat labile enterotoxin of *E. coli* (LT) and its associated non-toxic B subunit (LT-B) [16,17]. Attempts to reduce LT toxicity and maintain adjuvanticity have generated several LT mutants, including LTK63 and LTR72, which have been described elsewhere [18–20]. Co-administration of attenuated LT-toxins with candidate vaccines has enhanced the cytotoxic T cell response to HIV gag-p55 [21] and respiratory syncytial virus matrix protein [22]. When delivered via the respiratory tract, the efficacy of the group C meningococcal conjugate vaccine [23] was improved, as was immunity to the SAG1 Ag of *Toxoplasma gondii* [24] and FMDV peptides [25]. Overall, the effect of LT mutants is based on an improvement in the co-stimulatory activity of APCs, in part due to an up-regulation of CD80/86 that in turn leads to the proliferation of antigen-specific CD4$^+$ T cells [26]. LT has effects on Th populations, activating Th1 and Th2 cells and inducing a long lasting immunoglobulin production of IgG1, IgG2a, IgG2b and mucosal IgA from plasma cells [26,27]. Reports of retrograde transport of the B-subunit to the brain by olfactory nerves have dampened enthusiasm for the use of mucosal adjuvants in nasal vaccines for use in humans [28,29], however adverse effects are not observed in all animals [30].

The natural tropism of Ad5 for mucosal surfaces makes it an ideal choice as a mucosal vaccine delivery vector. Moreover, the co-administration of a mucosal adjuvant delivered by Ad5 is hypothesized to increase the immunological response at the site of FMDV entry. Taken together, this approach may provide a dual benefit; an antigen-sparing effect based on lower doses of Ad5-A24 needed to induce immunity and elicitation of mucosal immunity in respiratory secretions and tissues, a known site of FMDV replication. The objective of this study was to evaluate the efficacy of Ad5 vectored mucosal adjuvants for augmenting immunity and protection in mice when co-administered IN with Ad5-A24.

2. Materials and methods

2.1. Adenovirus vector

The recombinant replication-defective human adenovirus type 5 (Ad5) vector with deletions in the E1 and E3 coding regions was used in this study. Genes of interest were ligated downstream of a cytomegalovirus (CMV) promoter in the E1 region and upstream of a simian virus 40 (SV40) polyadenylation signal in a directional manner as described previously [31].

2.1.1. Construction of recombinant LTB, LTK63 and LTR72 adenoviruses

The LT sequence was obtained from Genebank Accession Number DQ778054. The final sequence for the LT-B subunit was 410 bp after addition of a porcine IFNα-1 secretion signal sequence for plasma membrane translocation (Fig. 1a).

LTK63 and LTR72 adjuvants, as mutated heat-labile enterotoxins, require that two separate polypeptide subunits (A and B) be expressed at different levels for formation of functional AB_5 holotoxins. The synthetic genes were engineered in a cassette which included, in the following order, the IFNα-1 signal sequence, LT-B subunit, an internal ribosomal entry site (IRES) from FMDV-serotype A12, a second IFNα-1 signal sequence, and the LT-A subunit of either LTK63 or LTR72 (Fig. 1b,c).

After cloning the different synthetic genes into bacterial plasmid vectors, plasmids were double digested with *ClaI* and *XbaI*, and expression cassettes ligated into the similarly digested pAd5-Blue vector plasmid. The presence of the inserted sequences in the new constructs were confirmed by restriction enzyme analysis and sequencing. The resulting vector plasmids were linearized with *PacI* and transfected into HEK-293 cells using an MBS Mammalian Transfection Kit (Stratagene, La Jolla, CA). Recombinant viruses were collected and purified as described by Moraes *et al.* [31,32].

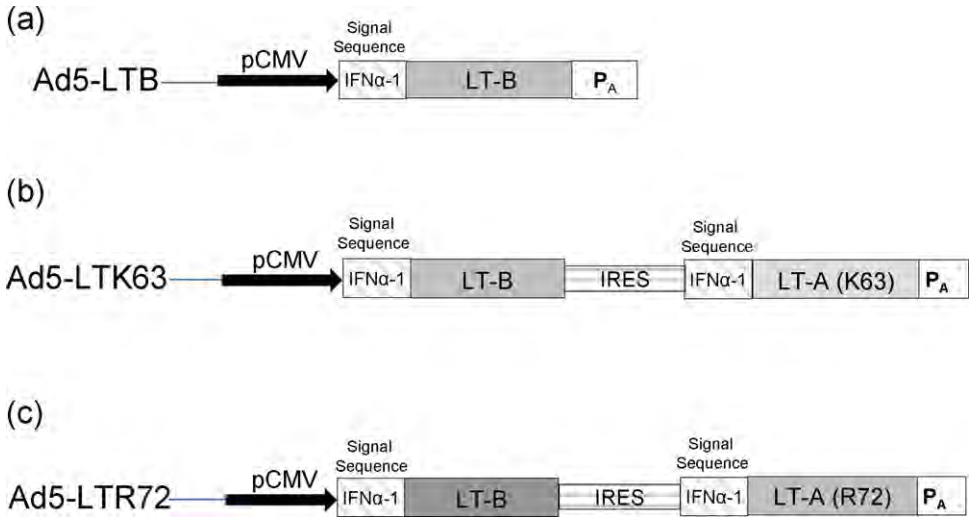

Fig. 1. Schematic representation of the adenovirus-vectored LT adjuvant expression cassettes used in this study. (a) cDNA containing IFNα-1 signal sequence and LT-B subunit coding region incorporated in the E1/E3 deleted Ad5 vector, under the control of CMV promoter (pCMV) and SV40 polyadenylation signal (P_A). (b) and (c) cDNA containing IFNα-1 signal sequence and LT-B subunit coding region followed by IRES, IFNα-1 and LT-A subunit containing K63S substitution in b), and R72A substitution in (c), under the control of pCMV and P_A.

2.2. In vitro assessment of Ad5-vectored adjuvant expression

2.2.1. Protein expression

Swine kidney cells (IBRS-2 cells) were utilized to check LT-B and LT-A transgene expression following infection with Ad5 constructs. Cells were infected at a multiplicity of infection (MOI) of 20 with the different Ad5 constructs, using Ad5-Blue as a negative control, in the presence or absence of tunicamycin (Sigma–Aldrich, St. Louis, MO) at a final concentration of 100 μg/ml to determine if the expressed proteins were glycosylated. Tunicamycin inhibits the transfer of *N*-acetylglucosamine 1-phosphate to the intermediate lipid carrier, dolichol phosphate, thereby blocking the synthesis of N-linked glycoproteins [33]. After 24 h of incubation, supernatants and cells were collected as described by Moraes et al. [34] and analyzed by SDS-PAGE followed by Western blot using antisera and conditions noted in each figure legend (Fig. 2).

2.2.2. GM1 ELISA

96-well polystyrene Immunolo-4 HBX plates were coated with 50 μl of 10 μg/ml GM1 (Sigma–Aldrich) and incubated with 50 μl of diluted supernatant or cell lysate as described in the figure legend (Fig. 3).

2.3. Vaccination and challenge experiments

All animal experiments were conducted in the high-containment facility of the USDA Plum Island Animal Disease Center. Sixty one C57BL/6 female mice, 6 weeks old and weighing 30 grams, from Jackson Labs (Bar Harbor, ME), were randomly divided into 4 groups of 14 animals each. The remaining 5 animals were sacrificed at day 0 as negative controls to perform nasal and oral washes.

2.3.1. Vaccination

All animals were inoculated IN, using plastic pipette tips, with a total volume of 25 μl of PBS containing 5×10^8 pfu of each Ad5 construct. Small volumes (<10 ul) of the inoculums were placed in the nares of each animal until the total volume was inhaled. Group 1 was vaccinated with Ad5-Blue, which expresses the α gene fragment of β-galactosidase [31], as a negative control. Group 2 was vaccinated with Ad5-A24 FMDV and Ad5-Blue. The dose of Ad5-Blue was matched to that of the mucosal adjuvants to serve as an Ad5 total dose control. Group 3 received Ad5-A24 and Ad5-LTB, encoding the wild-type B subunit of *E. coli* enterotoxin (LT). Group 4 received Ad5-A24 plus Ad5-LTR72, encoding the detoxified LT-A subunit containing the A72R mutation [18]. Ad5-LTK63 was excluded from this experiment because previous inoculation in mice showed a significantly lower immune response relative to Ad5-LTR72 (data not shown). At day 14, 7 animals in each group received a IN booster with the same dose of vaccine used at day 0. Animals were bled at 0, 14, 28 days post-vaccination (dpv). The seven animals per group that were not boosted were euthanized at 14 dpv to perform nasal washes as explained below.

2.3.2. FMDV challenge

Boosted animals were challenged at 28 dpv with a lethal dose of FMDV-A24 (2.5×10^5 pfu/animal in a 50 μl volume) by intradermal inoculation in the footpad. C57BL/6 mice have been shown to be susceptible to FMDV with signs of the disease characterized by apathy, ruffled fur, humped posture, mild wasting, and developing

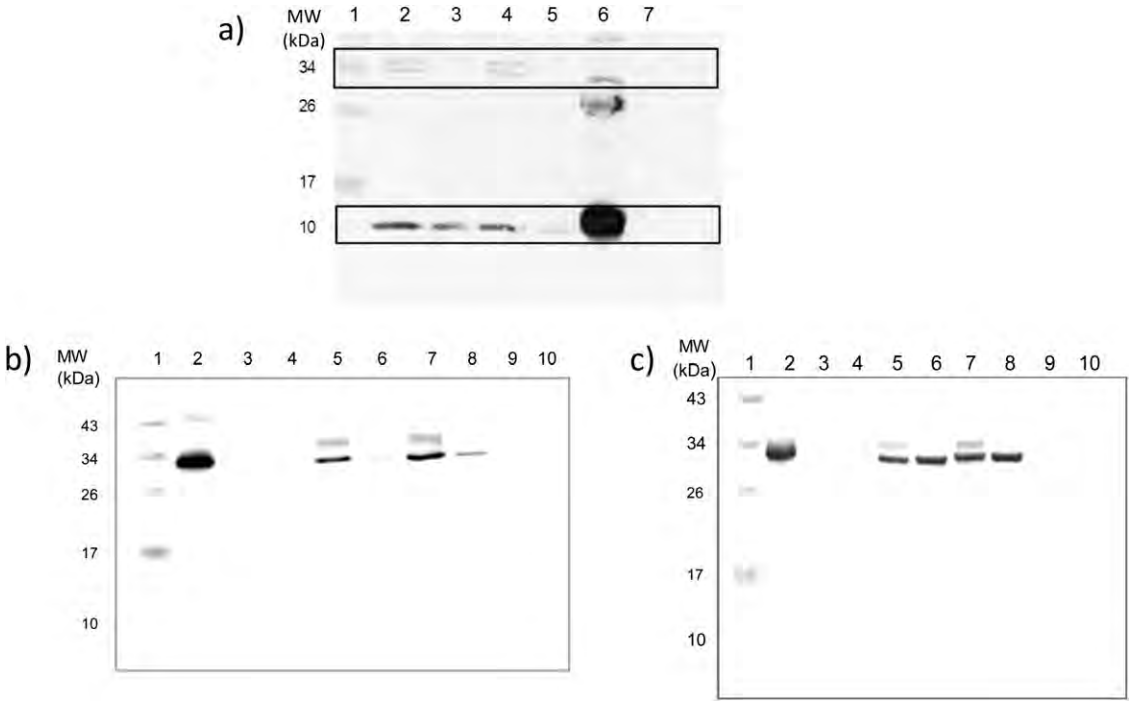

Fig. 2. Expression of LT in supernatant and cell lysates of IBRS-2 cells after infection with Ad5-Blue, Ad5-LTK63, or Ad5-LTR72 analyzed by Western blot. (a) Proteins were probed with a 1:200 dilution of hyperimmune serum from a pig previously inoculated with an LT mutant, followed by a goat anti-pig IgG antibody conjugated to horseradish peroxidase (HRP) (Bethyl Laboratories, Montgomery, TX). LT-B subunit is expressed as a band of approximately 10 kDa (lower box) while LT-A is shown as a band of approximately 28–30 kDa (upper box). (a) Lane 1: molecular weight marker (MWM), Lane 2: Ad5-LTR72 cell lysate, Lane 3: Ad5-LTR72 supernatant, Lane 4: Ad5-LTK63 cell lysate, Lane 5: Ad5-LTK63 supernatant, Lane 6: LT positive control, Lane 7: Ad5-Blue negative control. (b) and (c) Expression of LT-A in LT-mutants in IBRS-2 supernatants and cell lysates, respectively, treated or non-treated with tunicamycin (TN). Proteins were probed with a 1:500 dilution of monoclonal anti-LTA subunit (Abcam, Cambridge, MA) followed by a 1:2500 dilution of phosphatase labeled goat anti-mouse IgG (KPL labs, Gaithersburg, Maryland). For both panels: Lane 1: MWM, Lane 2: LT positive control, Lane 3: Ad5-LTB, Lane 4: Ad5-LTB with TN, Lane 5: Ad5-LTK63, Lane 6: Ad5-LTK63 with TN, Lane 7: Ad5-LTR72, Lane 8: Ad5-LTR72 with TN, Lane 9: Ad5-Blue negative control, Lane 10: Ad5-Blue negative control with TN.

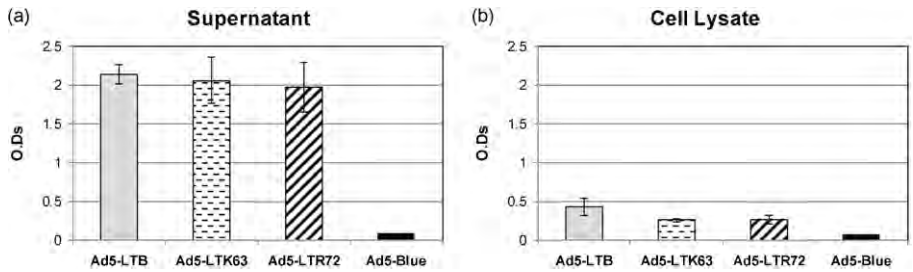

Fig. 3. Expression of LTB in supernatant (a) and cell lysates (b) in IBRS-2 cells infected with Ad5-LTB, Ad5-LTK63, Ad5-LTR72, and Ad5-Blue tested by GM1 ELISA. Samples were probed with 50 μl of pig hyperimmune serum against LT mutant (1:2000), followed by an HRP conjugated goat anti-pig antibody (1:1000) (Bethyl laboratories), and developed with TMB substrate (KPL labs). O.Ds were measured at 450 nm. O.D.s represent average of protein produced at 24, 48, and 72 h post-transfection (±S.D.) for each mutant.

neurological signs such as ataxia in the hindlimb at the late stages of the disease. The rapid development of the disease led to death of most animals within 48–72 h post-inoculation [35]. Animals were clinically evaluated daily post-challenge. Sick animals were bled and humanely euthanized. Serum samples were collected at 1, 3, and 5 days post-challenge (dpc) to assess viremia. At 14 dpc, a final bleeding was performed to determine serum antibody conversion and then animals were euthanized.

2.3.3. Tissue sampling

Oral mucosa was sampled at 14 and 28 dpv to detect the presence of IgA. Oral samples were obtained under anesthesia, animals received an IP injection of 125 μl of pilocarpine (Sigma–Aldrich), 0.05 mg/ml, to induce salivary secretion. Saliva was collected by direct aspiration and by using Whatman # 2 filter paper strips as described by Amuguni *et al.* [36]. Protease inhibitor leupeptin (Sigma–Aldrich), 1 μg/ml, was added to the samples which were subsequently stored at -70 °C. At 28 dpv, 2 animals in Group 4 died following administration of anesthetics.

The seven animals in each group that were challenged were sacrificed at 14 dpc to perform nasal washes for IgA detection. Nasal washes were collected by flushing 250 μl of PBS into the nasal cavity from the trachea to the nares as described by Morris et al. [37]. Once the sample was recovered, it was stored as described for oral washes.

2.4. Evaluation of humoral immune response

2.4.1. Determination of neutralizing antibody titer

Sera samples were tested in 96-well plates for the presence of FMDV-specific neutralizing antibodies as $TCID_{50}$ considering a $\log_{10}$ value of the reciprocal of the dilution that neutralizes 50% of the wells [38].

2.4.2. Detection of FMDV-specific antibody responses by ELISA

The presence of specific IgM and IgG antibodies in serum, and IgA antibodies in nasal and oral washes against FMDV were tested by indirect antibody sandwich immunoassay as described previously [39] with modifications noted in figure legends (Fig. 5).

2.5. Statistical analysis

Data were analyzed using SAS 9.3 for Microsoft Windows. Analysis of variance (ANOVA) was applied for comparison of the differences among experimental groups. Values of $p < 0.05$ were considered to be statistically significant. Data of animal survival was analyzed using the Log-rank test, values of $p < 0.05$ were considered to be statistically significant.

3. Results

3.1. Expression of LT mutants

Ad5-LTB, Ad5-LTK63, or Ad5-LTR72 IBRS-2 infected ce;; supernatants and cell lysates were evaluated by Western blot and ELISA for LT-mutant expression. LT-B subunit was observed as a band migrating close to the 10 kDa molecular marker in supernatants and cell lysates in all three LT constructs. LT-B functional form was confirmed by GM1 binding ELISA (Fig. 3). The LT-A subunit was observed as a very faint 28-34 kDa doublet in cell lysates from Ad5-LTK63 and Ad5-LTR72 infections (Fig. 2a). In order to confirm the presence of the LT-A subunit, a second Western blot was probed with a monoclonal antibody against LT-A. Two bands at a molecular weight of 28-34 kDa representing the LT-A subunit were observed in the supernatant and cell lysate from cells infected with Ad5-LTK63 and Ad5-LTR72. The slightly higher molecular weight band disappeared when the cells were treated with tunicamycin, indicating that the protein was glycosylated. As expected, the 28 kDa band representing the LT-A subunit was absent in the supernatant and cell lysate from cells infected with Ad5-LTB (Fig. 2b, c).

3.2. Antibody response in serum after immunization with Ad5-vaccines

Animals inoculated with Ad5-A24 + Ad5-LTR72 (Group 4) started producing serum neutralizing antibodies against FMDV at 14 dpv and sustained levels through day 28. Animals inoculated with Ad5-A24 (Group 2) showed a weak response at the same time points. No neutralizing antibodies were detected for the Ad5-Blue (Group 1) or Ad5-A24 + Ad5-LTB (Group 3) before challenge (Fig. 4).

Consistent with the serum neutralization results, Group 4 had a significantly higher IgM response at 14 dpv than the rest of the groups ($p < 0.01$). At 28 dpv, the IgM production in Group 4 was significantly higher than in Group 1 ($p < 0.05$) but no significant differences were observed with Groups 2 or 3. At 14 dpc there was a decline in IgM production in Group 4. In contrast, Group 2 showed the highest level of IgM production followed by Group 3 (Fig. 5a).

The analysis of the IgG isotype showed that IgG production in Group 4 at 14 and 28 dpv were significantly higher than the rest of the groups ($p < 0.0001$). No differences in IgG production was observed among the surviving groups at 14 dpc (Fig. 5b).

3.3. Antibody response in nasal and oral washes

Nasal washes were performed at 14 dpv and 14 dpc. Even though no IgA antibody was detected in any of the groups after the first vaccination or the booster, there was a peak of IgA production after the challenge in Group 4 that is significantly higher than for the rest of the groups in the experiment ($p < 0.0001$) (Fig. 5c).

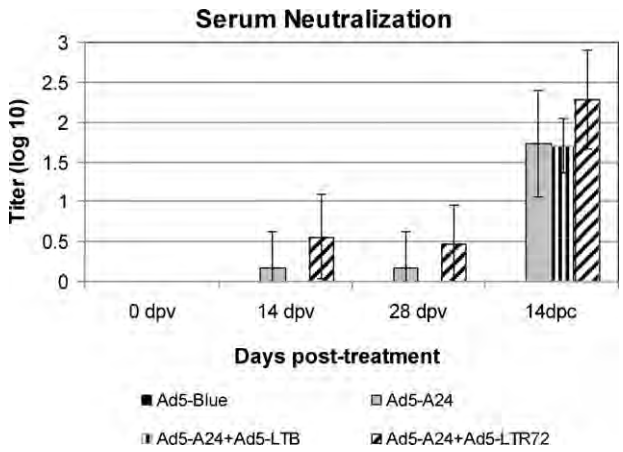

Fig. 4. Neutralizing antibodies against FMDV-A24 in mice vaccinated with Ad5 vectors and challenged at 28 dpv with FMDV. Serum samples were collected at 0, 14, and 28 dpv, and 14 dpc. Neutralizing antibodies are expressed as $TCID_{50}$ considering a $\log_{10}$ value of the reciprocal of the dilution that neutralizes 50% of the wells. Results are expressed as the mean (±S.D.) for each group.

Oral washes were collected at 14 and 28 dpv. Even though IgA production was undetectable in all groups after the first Ad5 vaccination, there was an increase in IgA level after the booster (28 dpv) in Group 4 that was not observed in the other groups (Fig. 5d).

3.4. FMDV challenge, animal survival and viremia

In order to evaluate the level of protection in the different groups of animals after Ad5 vaccination, all the animals were challenged with a lethal dose of FMDV-A24 at 28 dpv. As expected, all animals inoculated with Ad5-Blue died 72 h after the lethal challenge. Four animals out of 7 (57%) survived in the group inoculated with Ad5-A24 and 3 mice out of 7 (43%) survived in the group inoculated with Ad5-A24 + Ad5-LTB. In contrast, all animals (5 out of 5) in the group inoculated with Ad5-A24 + Ad5-LTR72 survived the challenge. The survival rate in Ad5-A24 + Ad5-LTR72 group was significantly higher than the Ad5-Blue group ($p < 0.05$) (Fig. 6a).

Consistent with the animal survival results, no FMDV was detected in sera from mice in the Ad5-A24 + Ad5-LTR72 group at any of the days assayed. Only one surviving animal in the Ad5-A24 group had viremia at 1 and 3 dpc (3.6×10^3 pfu/ml), which was undetectable at 5 dpc. No FMDV was detected in any of the surviving animals vaccinated with Ad5-A24 + Ad5-LTB (Fig. 6b).

4. Discussion

Parenterally administered vaccines are generally poor inducers of mucosal immunity and therefore less effective against infection at mucosal surfaces. For this reason, most mucosal vaccines target inductive lymphoepithelial tissues associated with the mucosae,

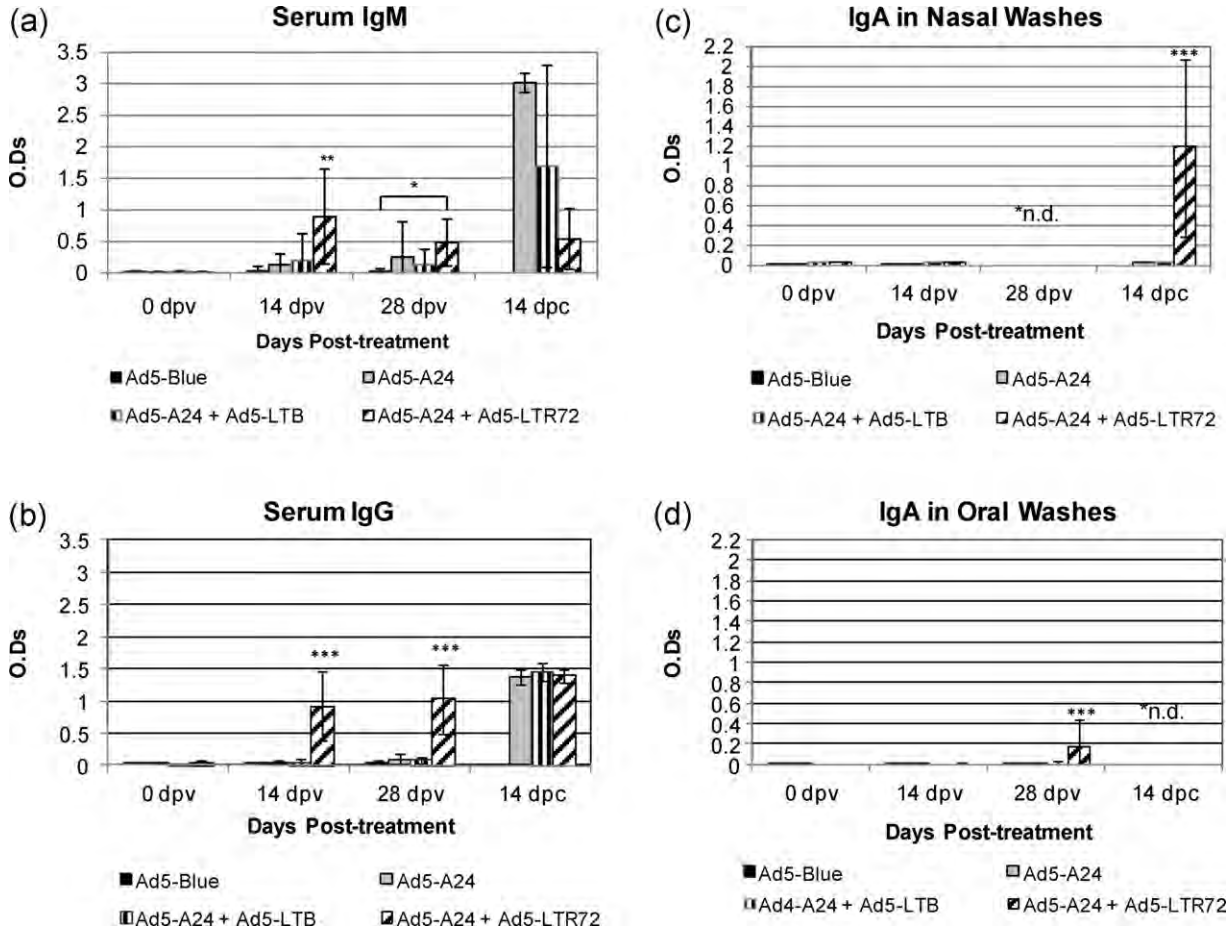

Fig. 5. Antibody isotype in mice serum after immunization with Ad5 vectors. FMDV-specific IgM was detected using a goat anti-mouse IgM-HRP (Sigma–Aldrich) at a 1:2000 dilution. (a) and IgG was detected using a polyclonal goat anti-mouse IgG-HRP (Bethyl Laboratories) (b), responses were analyzed in serum samples (1:50) collected at 0, 14, and 28 dpv and 14 dpc. (c) IgA response in nasal washes (1:2) sampled at 0 and 14 dpv, and 14 dpc. (d) IgA response in oral washes (1:2) sampled at 0, 14, and 28 dpv. IgA in nasal and oral washes was detected using a goat anti-mouse IgA-HRP at a 1:10,000 dilution (Bethyl Laboratories). Responses are expressed as the mean (±S.D.) for each group. *n.d. (not done): samples were not collected at that time point. Statistical analysis was performed using ANOVA test, $^{*}p < 0.05$, $^{**}p < 0.01$, and $^{***}p < 0.0001$.

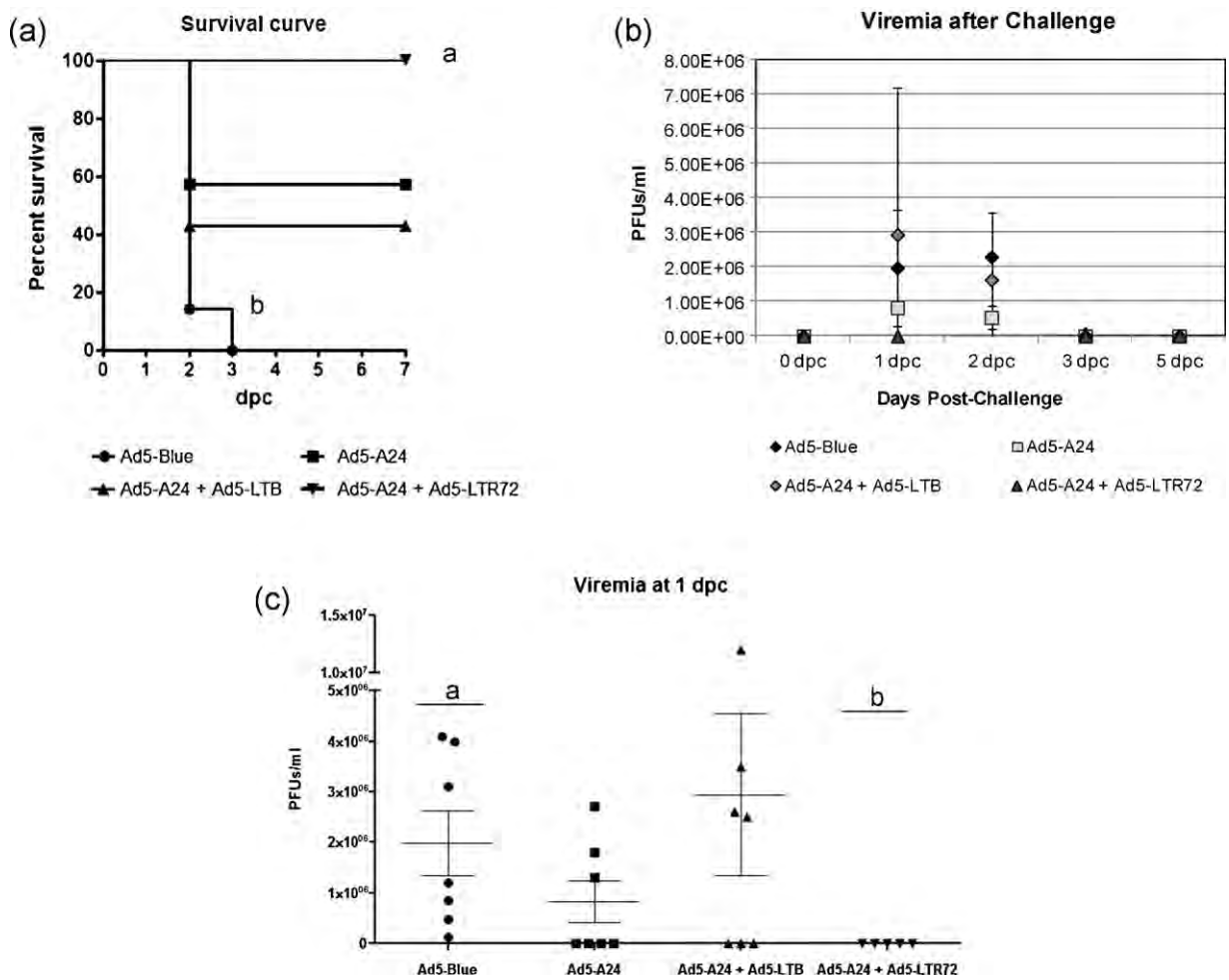

Fig. 6. (a) Survival of immunized mice following a lethal FMDV challenge, a differs from b at $p < 0.05$. (b) Detection of viremia after lethal FMDV challenge at 28 dpv. Serum samples were collected at 0, 1, 3, and 5 dpc. At 2 dpc, 5 animals were bled and euthanized. (c) Viremia at 1 dpc, a differs from b at $p < 0.05$. Plaque assay limit of detection 5 pfu.

which ultimately gives rise to antigen-specific lymphocyte trafficking to a variety of mucosal surfaces [40,41]. The establishment of a local mucosal immunity in these primary sites of entry of FMDV could block the invading virus, thereby preventing or limiting replication, reducing viral load as well as dissemination to other tissues during the initial stage of infection. The natural tropism of adenovirus vector for the mucosal epithelium makes it an ideal choice as a mucosal vaccine platform [42].

In the current study, mice that received Ad5-A24 plus Ad5-LTR72 developed markedly greater antibody responses than did those vaccinated with Ad5-A24 alone, as animals not receiving the LTR72 adjuvant developed only weak serum neutralizing antibodies after priming vaccination and booster. In contrast, the group vaccinated with Ad5-A24 plus Ad5-LTB did not show any systemic antibody response, which is consistent with previous observations [43]. These results indicate that the adjuvant effect of LT derivatives is mainly determined by the presence of the nontoxic AB complex and the modest ADP-ribosyltransferase activity of the A subunit present in Ad5-LTR72 adjuvant [18,44].

Consistent with the serum neutralization results, the group of animals inoculated with Ad5-A24 plus Ad5-LTR72 had the highest IgM and IgG production in blood, indicating that intranasal inoculation was able to elicit a systemic immune response as reported by Croyle and Du [13,45]. Although the role of cell mediated immunity to FMDV remains potentially important yet poorly explored [34,46], immunity to FMDV is primarily mediated by circulating antibodies that are relatively efficient in clearing virus from circulation by opsonization and uptake by phagocytes located in the liver, spleen, and elsewhere that rapidly reduce or prevent viremia [2,47]. Part of the protective effect of attenuated LT mutants may have been due to cellular responses that limit virus replication, as has been reported by others [48]. In the present study, the co-administration of Ad5-A24 and Ad5-LTR72 induced neutralizing antibodies that were, at least in part, responsible for the reduction in viremia, illness and death.

Many studies in rodents indicate that systemic immunization is able to produce strong-antiviral systemic responses, while mucosal vaccination can stimulate both the systemic and the mucosal immune system. This immune response can confer long-term immunological memory against a given pathogen, even though the magnitude of these responses is often reported to be rather weak [41,49,50]. Similar results were observed in our experiment at the mucosal level, in which there was a low or undetectable amount of IgA in the oral and nasal washes after the priming inoculation and booster immunizations prior to challenge.

Also notable in the current work, intranasal immunization with Ad5-A24 plus Ad5-LTR72 induced both systemic and mucosal immune responses and provided complete protection against a lethal FMDV challenge, with 100% survival and the complete absence of viremia. These results are consistent with previous reports showing protection against challenge following intranasal inoculation using an Ad5 vectored antigen [13,45].

These results establish a benefit of Ad5-vectored LT-based adjuvants in stimulating protective anti-FMDV immunity. They also provide a sound rationale for further evaluation of specific immune responses and protective efficacy of Ad5-LTR72 adjuvanticity when co-administered with Ad5-A24 intranasally to susceptible livestock species.

Acknowledgements

We thank Marla Koster for her technical support in the development of the Ad5-mutants, Dr. T. Hoagland, R. Ramanathan, and Dr. R. Mancini for their help and advice in the statistical analysis of the data, and the Plum Island animal caretakers for their assistance with the care and handling of the animals. This work was supported by USDA-ARS under cooperative agreement 58-1940-5-520 to the University of Connecticut Center of Excellence for Vaccine Research. Any opinions, findings, conclusion, or recommendations expressed in this publication are those of the authors and do not necessarily reflect the view of the U.S. Department of Agriculture.

References

[1] Bachrach HL. Foot-and-mouth disease: world-wide impact and control measures. In: Kurstak E, Maramorosch K, editors. Viruses and environment. New York: Academic Press; 1978.
[2] Alexandersen S, Zhang Z, Donaldson AI, Garland AJ. The pathogenesis and diagnosis of foot-and-mouth disease. J Comp Pathol 2003 Jul;129(1):1–36.
[3] Arzt J, Pacheco JM, Rodriguez LL. The early pathogenesis of foot-and-mouth disease in cattle after aerosol inoculation. Identification of the nasopharynx as the primary site of infection. Vet Pathol 2010 Nov;47(6):1048–63.
[4] Alexandersen S, Brotherhood I, Donaldson AI. Natural aerosol transmission of foot-and-mouth disease virus to pigs: minimal infectious dose for strain O1 Lausanne. Epidemiol Infect 2002 Apr;128(2):301–12.
[5] Alexandersen S, Donaldson AI. Further studies to quantify the dose of natural aerosols of foot-and-mouth disease virus for pigs. Epidemiol Infect 2002 Apr;128(2):313–23.
[6] Saraiva V. Vaccines and foot-and-mouth disease eradication in South America. Dev Biol (Basel) 2003;114:67–77.
[7] Barnett PV, Pullen L, Williams L, Doel TR. International bank for foot-and-mouth disease vaccine: assessment of Montanide ISA 25 and ISA 206, two commercially available oil adjuvants. Vaccine 1996 Sep;14(13):1187–98.
[8] Lubroth J, Lopez A, Ramalho AK, Meyer RF, Brown F, Darsie GC. Cattle response to foot-and-mouth disease virus nonstructural proteins as antigens within vaccines produced using different concentrations. Vet Q 1998;20(Suppl. 2):S13–7.
[9] Defra FMD in Surrey, UK, 2007. Epidemiology report on the probable release of FMD virus at the Pirbright site and the transmission of infection to the first infected cattle herd, from investigations up to 29 August 2007 (Day 26). In: Department for Environment Food and Rural Affairs U; 2007.
[10] Brown F. The importance of antigenic variation in vaccine design. Arch Virol (Suppl) 1963;9:1–8.
[11] Eble PL, Bouma A, Weerdmeester K, Stegeman JA, Dekker A. Serological and mucosal immune responses after vaccination and infection with FMDV in pigs. Vaccine 2007 Jan 22;25(6):1043–54.
[12] Moraes MP, Mayr GA, Mason PW, Grubman MJ. Early protection against homologous challenge after a single dose of replication-defective human adenovirus type 5 expressing capsid proteins of foot-and-mouth disease virus (FMDV) strain A24. Vaccine 2002 Feb 22;20(11-12):1631–9.
[13] Croyle MA, Patel A, Tran KN, Gray M, Zhang Y, Strong JE, et al. Nasal delivery of an adenovirus-based vaccine bypasses pre-existing immunity to the vaccine carrier and improves the immune response in mice. PLoS One 2008;3(10):e3548.
[14] Lemiale F, Kong WP, Akyurek LM, Ling X, Huang Y, Chakrabarti BK, et al. Enhanced mucosal immunoglobulin A response of intranasal adenoviral vector human immunodeficiency virus vaccine and localization in the central nervous system. J Virol 2003;77(Sep (18)):10078–87.
[15] Xiang ZQ, Gao GP, Reyes-Sandoval A, Li Y, Wilson JM, Ertl HC. Oral vaccination of mice with adenoviral vectors is not impaired by preexisting immunity to the vaccine carrier. J Virol 2003;77(Oct (20)):10780–9.
[16] Pizza M, Giuliani MM, Fontana MR, Monaci E, Douce G, Dougan G, et al. Mucosal vaccines: non toxic derivatives of LT and CT as mucosal adjuvants. Vaccine 2001;19(Mar (17–19)):2534–41.
[17] Rappuoli R, Pizza M, Douce G, Dougan G. Structure and mucosal adjuvanticity of cholera and Escherichia coli heat-labile enterotoxins. Immunol Today 1999;20(Nov (11)):493–500.
[18] Giuliani MM, Del Giudice G, Giannelli V, Dougan G, Douce G, Rappuoli R, et al. Mucosal adjuvanticity and immunogenicity of LTR72, a novel mutant of Escherichia coli heat-labile enterotoxin with partial knockout of ADP-ribosyltransferase activity. J Exp Med 1998;187(Apr (7)):1123–32.
[19] Pizza M, Domenighini M, Hol W, Giannelli V, Fontana MR, Giuliani MM, et al. Probing the structure-activity relationship of Escherichia coli LT-A by site-directed mutagenesis. Mol Microbiol 1994;14(Oct (1)):51–60.
[20] Dickinson BL, Clements JD. Dissociation of Escherichia coli heat-labile enterotoxin adjuvanticity from ADP-ribosyltransferase activity. Infect Immun 1995;63(May (5)):1617–23.
[21] Neidleman JA, Vajdy M, Ugozzoli M, Ott G, O'Hagan D. Genetically detoxified mutants of heat-labile enterotoxin from Escherichia coli are effective adjuvants for induction of cytotoxic T-cell responses against HIV-1 gag-p55. Immunology 2000;101(Sep (1)):154–60.
[22] Simmons CP, Hussell T, Sparer T, Walzl G, Openshaw P, Dougan G. Mucosal delivery of a respiratory syncytial virus CTL peptide with enterotoxin-based adjuvants elicits protective, immunopathogenic, and immunoregulatory antiviral CD8+ T cell responses. J Immunol 2001;166(Jan (2)):1106–13.
[23] Baudner BC, Morandi M, Giuliani MM, Verhoef JC, Junginger HE, Costantino P, et al. Modulation of immune response to group C meningococcal conjugate vaccine given intranasally to mice together with the LTK63 mucosal adjuvant and the trimethyl chitosan delivery system. J Infect Dis 2004;189(Mar (5)):828–32.
[24] Bonenfant C, Dimier-Poisson I, Velge-Roussel F, Buzoni-Gatel D, Del Giudice G, Rappuoli R, et al. Intranasal immunization with SAG1 and nontoxic mutant heat-labile enterotoxins protects mice against Toxoplasma gondii. Infect Immun 2001;69(Mar (3)):1605–12.
[25] Barrette RW, Szczepanek SM, Rood D, Challa S, Avery N, Vajdy M, et al. Use of inactivated Escherichia coli enterotoxins to enhance respiratory mucosal adjuvanticity during vaccination in swine. Clin Vaccine Immunol 2011;18(Nov (11)):1996–8.
[26] Yamamoto M, Kiyono H, Kweon MN, Yamamoto S, Fujihashi K, Kurazono H, et al. Enterotoxin adjuvants have direct effects on T cells and antigen-presenting cells that result in either interleukin-4-dependent or -independent immune responses. J Infect Dis 2000;182(Jul (1)):180–90.
[27] Takahashi I, Marinaro M, Kiyono H, Jackson RJ, Nakagawa I, Fujihashi K, et al. Mechanisms for mucosal immunogenicity and adjuvancy of Escherichia coli labile enterotoxin. J Infect Dis 1996;173(Mar (3)):627–35.
[28] Mutsch M, Zhou W, Rhodes P, Bopp M, Chen RT, Linder T, et al. Use of the inactivated intranasal influenza vaccine and the risk of Bell's palsy in Switzerland. N Engl J Med 2004;350(Feb (9)):896–903.
[29] van Ginkel FW, Jackson RJ, Yuki Y, McGhee JR. Cutting edge: the mucosal adjuvant cholera toxin redirects vaccine proteins into olfactory tissues. J Immunol 2000;165(Nov (9)):4778–82.
[30] Zurbriggen R, Metcalfe IC, Gluck R, Viret JF, Moser C. Nonclinical safety evaluation of Escherichia coli heat-labile toxin mucosal adjuvant as a component of a nasal influenza vaccine. Expert Rev Vaccines 2003;2(Apr (2)):295–304.
[31] Moraes MP, Mayr GA. Grubman MJ. pAd5-Blue: direct ligation system for engineering recombinant adenovirus constructs. Biotechniques 2001;31(Nov (5)):1050, 2, 4–6.
[32] Graham FL, Prevec L. Manipulation of adenovirus vectors. Methods Mol Biol 1991;7:109–28.
[33] Savage KE, Baur PS. Effect of tunicamycin, an inhibitor of protein glycosylation, on division of tumour cells in vitro. J Cell Sci 1983;64(Nov):295–306.
[34] Moraes MP, Diaz-San Segundo F, Dias CC, Pena L, Grubman MJ. Increased efficacy of an adenovirus-vectored foot-and-mouth disease capsid subunit vaccine expressing nonstructural protein 2B is associated with a specific T cell response. Vaccine 2011 Nov 28;29(51):9431–40.
[35] Salguero FJ, Sanchez-Martin MA, Diaz-San Segundo F, de Avila A, Sevilla N. Foot-and-mouth disease virus (FMDV) causes an acute disease that can be lethal for adult laboratory mice. Virology 2005 Feb 5;332(1):384–96.
[36] Amuguni JH, Lee S, Kerstein KO, Brown DW, Belitsky BR, Herrmann JE, et al. Sublingually administered Bacillus subtilis cells expressing tetanus toxin C fragment induce protective systemic and mucosal antibodies against tetanus toxin in mice. Vaccine 2011;29(Jun (29–30)):4778–84.
[37] Morris JB, Stanek J, Gianutsos G. Sensory nerve-mediated immediate nasal responses to inspired acrolein. J Appl Physiol 1999;87(Nov (5)):1877–86.
[38] Crespo Leon F, Gutierrez Diez F, Rodriguez Ferri F, Leon Vizcaino L, Cuello Gijon F, Gimeno EJ, et al. The translation into Spanish of the OIE Manual of diagnostic tests and vaccines for terrestrial animals (mammals, birds and bees): problems, solutions and conclusions. Rev Sci Tech 2005;24(Dec (3)):1095–104.
[39] de Avila Botton S, Brum MC, Bautista E, Koster M, Weiblen R, Golde WT, et al. Immunopotentiation of a foot-and-mouth disease virus subunit vaccine by interferon alpha. Vaccine 2006;24(Apr (17)):3446–56.
[40] Lycke N. Recent progress in mucosal vaccine development: potential and limitations. Nat Rev Immunol 2012;12(Aug (8)):592–605.
[41] Neutra MR, Kozlowski PA. Mucosal vaccines: the promise and the challenge. Nat Rev Immunol 2006;6(Feb (2)):148–58.
[42] Santosuosso M, McCormick S, Xing Z. Adenoviral vectors for mucosal vaccination against infectious diseases. Viral Immunol 2005;18(2):283–91.
[43] Clements JD, Hartzog NM, Lyon FL. Adjuvant activity of Escherichia coli heat-labile enterotoxin and effect on the induction of oral tolerance in mice to unrelated protein antigens. Vaccine 1988;6(Jun (3)):269–77.
[44] Simmons CP, Ghaem-Magami M, Petrovska L, Lopes L, Chain BM, Williams NA, et al. Immunomodulation using bacterial enterotoxins. Scand J Immunol 2001;53(Mar (3)):218–26.
[45] Du L, Zhao G, Lin Y, Sui H, Chan C, Ma S, et al. Intranasal vaccination of recombinant adeno-associated virus encoding receptor-binding domain of severe acute respiratory syndrome coronavirus (SARS-CoV) spike protein induces strong mucosal immune responses and provides long-term protection against SARS-CoV infection. J Immunol 2008;180(Jan (2)):948–56.
[46] Guzman E, Taylor G, Charleston B, Skinner MA, Ellis SA. An MHC-restricted CD8+ T-cell response is induced in cattle by foot-and-mouth disease virus (FMDV)

infection and also following vaccination with inactivated FMDV. J Gen Virol 2008;89(Mar (Pt 3)):667–75.
[47] McCullough KC, De Simone F, Brocchi E, Capucci L, Crowther JR, Kihm U. Protective immune response against foot-and-mouth disease. J Virol 1992;66(Apr (4)):1835–40.
[48] Simmons CP, Mastroeni P, Fowler R, Ghaem-maghami M, Lycke N, Pizza M, et al. MHC class I-restricted cytotoxic lymphocyte responses induced by enterotoxin-based mucosal adjuvants. J Immunol 1999;163(Dec (12)):6502–10.
[49] Kiyono H, Fukuyama S. NALT- versus Peyer's-patch-mediated mucosal immunity. Nat Rev Immunol 2004;4(Sep (9)):699–710.
[50] Patel A, Zhang Y, Croyle M, Tran K, Gray M, Strong J, et al. Mucosal delivery of adenovirus-based vaccine protects against Ebola virus infection in mice. J Infect Dis 2007;196(Nov (Suppl 2)):S413–20.

JCM
Journals.ASM.org

A Continuous Bovine Kidney Cell Line Constitutively Expressing Bovine $\alpha_V\beta_6$ Integrin Has Increased Susceptibility to Foot-and-Mouth Disease Virus

Michael LaRocco,[a] Peter W. Krug,[a] Ed Kramer,[b] Zaheer Ahmed,[a] Juan M. Pacheco,[a] Hernando Duque,[c] Barry Baxt,[a] Luis L. Rodriguez[a]

Foreign Animal Disease Research Unit, United States Department of Agriculture, Agricultural Research Service, Plum Island Animal Disease Center, Greenport, New York, USA[a]; The McConnell Group, Inc., Rockville, Maryland, USA[b]; Foreign Animal Disease Diagnostic Laboratory, United States Department of Agriculture, Animal and Plant Health Inspection Service, Plum Island Animal Disease Center, Greenport, New York, USA[c]

Foot-and-mouth disease (FMD) is a worldwide problem limiting the trade of animals and their products from affected countries. The rapid isolation, serotyping, and vaccine matching of FMD virus from disease outbreaks is critical for enabling the implementation of effective vaccination programs and to stop the spread of infection during outbreaks. Some primary cells have been shown to be highly susceptible to most strains of FMD virus (FMDV) but are difficult and expensive to prepare and maintain. Since the $\alpha_V\beta_6$ integrin is a principal receptor for FMDV, we transduced a bovine kidney cell line to stably express both the α_V and β_6 bovine integrin subunits. This stable cell line (LFBK-$\alpha_V\beta_6$) showed β_6 expression and enhanced susceptibility to FMDV infection for ≥100 cell passages. LFBK-$\alpha_V\beta_6$ cells were highly sensitive for detecting all serotypes of FMDV from experimentally infected animals, including the porcinophilic FMDV strain O/TAW/97. In comparison to other cell types that are currently used for virus isolation, LFBK-$\alpha_V\beta_6$ cells were more effective at detecting FMDV in clinical samples, supporting their use as a more sensitive tool for virus isolation.

Foot-and-mouth disease virus (FMDV) is a severe economic concern for meat-producing nations since the trade of animal products is limited in the countries where the virus is present. The rapid spread of the virus among susceptible animals results in severe morbidity and, in some cases, death, especially in young animals (reviewed in reference 1). Infection or vaccination with one of the seven different serotypes does not confer cross-protection to other serotypes or even to some subtypes of the same serotype. Vaccines for FMDV are widely used to prevent clinical disease, but since vaccines are serotype and subtype specific, the virus(es) causing outbreaks must be isolated and serologically characterized for vaccine matching prior to selecting the appropriate vaccine antigen to be used in vaccine formulations (reviewed in reference 2).

Although molecular techniques, such as PCR coupled with genomic sequencing, can be used in samples containing enough virus to rapidly identify the virus serotype and its relationship to other FMDV strains, appropriate vaccine prediction requires virus growth in cell culture to carry out neutralization tests using reference sera. Inefficient recovery of virus from animal samples can delay diagnosis and vaccine selection, hampering the rapid implementation of control measures; thus, virus isolation protocols are designed for maximum sensitivity. Some primary cells, such as bovine thyroid (BTY), are highly susceptible to a wide range of FMDV serotypes (3), but they are difficult and costly to prepare and lose FMDV susceptibility after multiple passages (4). Primary lamb kidney (LK) cells are also very sensitive to FMDV, and unlike BTY cells, LK cells maintain their sensitivity to FMDV infection after cryopreservation (5). Immortalized cell lines (e.g., baby hamster kidney [BHK-21] fibroblasts and porcine kidney epithelial cells), while much easier to maintain, are in many cases less susceptible to specific animal-derived FMDV serotypes (6–9). There is a need for a cell line that is easily maintained and is highly susceptible to all serotypes and subtypes of FMDV.

Integrins of the α_V subgroup have been demonstrated by several laboratories to be FMDV receptors, including our laboratory (reviewed in reference 10). Of the many α_V integrins that have been shown to mediate FMDV attachment, the integrin $\alpha_V\beta_6$ has been shown to be one of the most efficient receptors for all FMDV serotypes (11, 12), and the sites of infection in cattle show high levels of $\alpha_V\beta_6$ expression on epithelial cells (13, 14). BTY cells, considered the most sensitive primary cells for FMDV isolation, have high levels of $\alpha_V\beta_6$ integrin surface expression (15). Moreover, the transient expression of bovine α_v and β_6 integrin subunits in baby hamster kidney cells (BHK3-$\alpha_V\beta_6$) (16) greatly increased the susceptibility of this cell line to a cow-passaged FMDV A24 Cruzeiro strain that contains an SGD motif in the VP1 capsid protein (17). Although initially more permissive to the A24-SGD virus than BHK-21 cells, the BHK3-$\alpha_V\beta_6$ cells lost integrin expression and sensitivity to this virus after multiple passages (E. Rieder, personal communication).

Swaney (18) derived an immortalized line of fetal bovine kidney (LFBK) cells that had high susceptibility to most FMDV serotypes that was maintained over many passages. Compared to BTY cells, LFBK cells had similar susceptibilities to most FMDV serotypes and had equal or better susceptibility than MVPK, IB-RS-2, and fetal bovine kidney cells in the same experiments (18). In the work presented here, we combined the long-lived FMDV suscep-

Received 20 December 2012 Returned for modification 6 February 2013
Accepted 14 March 2013
Published ahead of print 20 March 2013
Address correspondence to Peter W. Krug, peter.krug@ars.usda.gov.
M.L. and P.W.K. contributed equally to this article.
Supplemental material for this article may be found at http://dx.doi.org/10.1128/JCM.03370-12.
Copyright © 2013, American Society for Microbiology. All Rights Reserved.
doi:10.1128/JCM.03370-12

Downloaded from http://jcm.asm.org/ on May 28, 2013 by DigiTop -USDA's Digital Desktop Library

tibility of the LFBK cell line with a principal bovine receptor for FMDV to derive a stable cell line that is highly susceptible to FMDV. We characterize the FMDV susceptibility of this transduced cell line by infection with animal-derived FMDV from all 7 serotypes, as well as from recent diagnostic field samples, and compared its susceptibility to those of other cell types used for diagnostic FMDV virus isolation. Our results indicate that LFBK-αvβ6 cells are highly permissive for all FMDV serotypes and have excellent performance in a diagnostic setting.

MATERIALS AND METHODS

Cells. LFBK cells (18) were propagated in Dulbecco's modified Eagle medium (DMEM) supplemented with 10% fetal bovine serum and antibiotics as described previously (19) and were used for these experiments between passages 64 and 71. LFBK-$\alpha_V\beta_6$ cells were propagated in DMEM (catalog no. 11965092; Gibco) supplemented with 10% fetal bovine serum (catalog no. SH30071.03; HyClone) and antibiotics (catalog no. 15240062; Gibco) and were used at the passage indicated in each figure. BHK-21 cells, used between passages 62 and 67, were propagated in minimal essential medium (MEM) supplemented with 10% calf serum, 10% tryptose phosphate broth, nonessential amino acids, and antibiotics. Primary lamb kidney (LK) cells, generously supplied by the APHIS Diagnostic Service Section at the Plum Island Animal Disease Center (PIADC), were propagated in DMEM supplemented with 10% fetal bovine serum, antibiotics, and sodium pyruvate and were used directly from cryovials or at passage 1. IB-RS-2 cells were used between passages 129 and 137 and MVPK cells were used between passages 38 and 41; both of these cell lines were propagated in MEM supplemented with 10% fetal calf serum, nonessential amino acids, and antibiotics.

Transduction of LFBK cells with α_V and β_6 integrin subunits. Individual retroviruses expressing the bovine α_V (GenBank accession no. AF239958) or bovine β_6 (GenBank accession no. AF468060) integrin subunits (16) were created using the Pantropic retroviral expression system (PT3346-5; Clontech) as per the manufacturer's protocol. LFBK cells at passage 145 were infected with the α_V-expressing retrovirus, and neomycin selection was used to select against nontransduced cells. A pool of these cells was infected with the β_6-expressing retrovirus and was cloned to single cells by terminal dilution. A clone was chosen that showed consistent expression of the β_6 subunit by immunohistochemistry as described below.

Plaque assays. Cells were seeded 72 h before infection in 6-well cell culture plates unless otherwise noted. Ten-fold virus dilutions were made using phosphate-buffered saline containing calcium and magnesium supplemented with 1% bovine serum. The inoculum volume was 200 μl per well. One hour postadsorption, the inoculum was removed and the cells were overlaid with 50/50 1.2% gum tragacanth-2× MEM supplemented with antibiotic-antimycotic. Plates were incubated for 24 h unless otherwise indicated and simultaneously fixed and stained with HistoChoice tissue fixative (AMRESCO) containing crystal violet, and plaques were counted. Where indicated, statistical analysis was performed on log-transformed titer values using one-way analysis of variance (ANOVA) in Prism (GraphPad Software, Inc.).

Multistep growth curve. LFBK-$\alpha_V\beta_6$ or LFBK cells were seeded in 24-well plates 72 h before infection with either FMDV A24-BHK (a cell culture-passaged virus containing the wild-type RGD motif in VP1) or FMDV A24-SGD (vesicular fluid from the second bovine passage of the SGD-containing A24-B9 virus described in reference 17) at a multiplicity of 0.01 PFU/cell. Virus stocks were diluted in maintenance medium (DMEM supplemented with 1% fetal bovine serum and antibiotics) and absorbed for 1 h with rocking at 37°C. The cells were then acid washed (25 mM 2-(*N*-morpholino)ethanesulfonic acid [MES] [pH 5.5] in 145 mM NaCl), washed once with DMEM, and incubated at 37°C in 0.5 ml maintenance medium per well. At the indicated time, cells were frozen at −70°C and thawed, and the virus titer was determined by plaque assay on LFBK-$\alpha_V\beta_6$ cells.

Immunohistochemistry. The Vectastain ABC kit (PK-6102; Vector Laboratories) and Vector VIP peroxidase substrate kit (SK-4600; Vector Laboratories) were used according to the manufacturer's protocols. Mouse anti-human β_6 (MAB2076Z; Chemicon) was used to detect the bovine integrin subunit β_6 at a 1:300 dilution. The mouse monoclonal antibody F19-51 (20) was used to detect the FMDV 3D protein at a 1:200 dilution.

Detection of FMDV in diagnostic tissue samples. LK, BHK-21, IB-RS-2, and LFBK-$\alpha_V\beta_6$ cells were seeded onto 48-well cell culture plates 48 h prior to infection. LK cells were seeded directly from storage cryovials. LFBK-$\alpha_V\beta_6$ cells were seeded at passage 32, IB-RS-2 at passage 136, and BHK-21 at passage 66. Diagnostic lesion tissues were disrupted, and the virus was isolated after centrifugation through a Spin-X purification column (Costar) as described in reference 21. These tissue macerates were diluted 10-fold in DMEM supplemented with 25 mM HEPES and 0.5% fetal calf serum, and 100 μl was then used to infect each cell type for 1 h at 37°C. After adsorption, 200 μl of maintenance medium was added to each well and the plates were incubated at 37°C. Starting at 4 h postinfection (hpi), visual evidence of cytopathic effects was recorded every 2 h until 20 hpi and then at 24, 28, and 48 hpi. At 48 hpi, all wells were fixed with 50% acetone to 50% methanol and wells that were negative for cytopathic effects were immunostained with a monoclonal antibody to FMDV 3D protein to confirm the negative results.

RESULTS

Characterization of LFBK cells expressing bovine $\alpha_v\beta_6$ integrin. The integrin $\alpha_V\beta_6$ is an important receptor for FMDV in relevant tissues *in vivo*. LFBK cells are a transformed cell line that has high sensitivity to most FMDV serotypes but does not express high levels of β_6 integrin protein. In order to merge the enhanced susceptibility of $\alpha_V\beta_6$ expression with the transformed phenotype of LFBK cells, the bovine α_V and β_6 integrin subunits were transduced into LFBK cells as described in Materials and Methods. Immunohistochemical staining demonstrated long-term maintenance of enhanced β_6 expression in the LFBK-$\alpha_V\beta_6$ cells for ≥102 cell passages compared to the nontransduced LFBK cells (Fig. 1A to C).

FMDV A24-SGD, an FMDV A24 Cruzeiro strain serially passed in cattle, has an SGD motif in the G-H loop of VP1 and an enhanced infectivity in cells expressing the $\alpha_V\beta_6$ integrin (17). LFBK-$\alpha_V\beta_6$ cells at various subculture passages and nontransduced LFBK cells were infected with A24-SGD or a cell culture-grown control virus (A24-BHK) to confirm the long-term functional maintenance of the $\alpha_V\beta_6$ integrin. These experiments demonstrate that the LFBK-$\alpha_V\beta_6$ cells have a 2.5-log-increased susceptibility to A24-SGD compared to LFBK cells and that this increased susceptibility is maintained for >100 passages (Fig. 1D). The expression of surface proteins can be delayed due to trypsin treatment during cell subculture. To determine if increasing the time between seeding and infecting the cells had an effect on susceptibility, LFBK and LFBK-$\alpha_V\beta_6$ cells were seeded on plates at 24, 48, or 72 h prior to infection with the A24-SGD or A24-BHK virus. It was found that seeding the LFBK-$\alpha_V\beta_6$ cells 72 h prior to infection provided only slightly better sensitivity than seeding 24 h prior to infection (Fig. 1E). This result indicates that the LFBK-$\alpha_V\beta_6$ cells can be infected early after trypsin treatment with only a minimal loss in susceptibility. In order to show that the LFBK-$\alpha_V\beta_6$ cells support the normal growth progression of FMDV, a multistep growth curve analysis was performed (Fig. 1F). In this experiment, the replication of A24-BHK was similar in both LFBK and LFBK-$\alpha_V\beta_6$ cells. While A24-SGD replicated slowly in the nontransduced LFBK cells, this virus grew normally in LFBK-

Downloaded from http://jcm.asm.org/ on May 28, 2013 by DigiTop -USDA's Digital Desktop Library

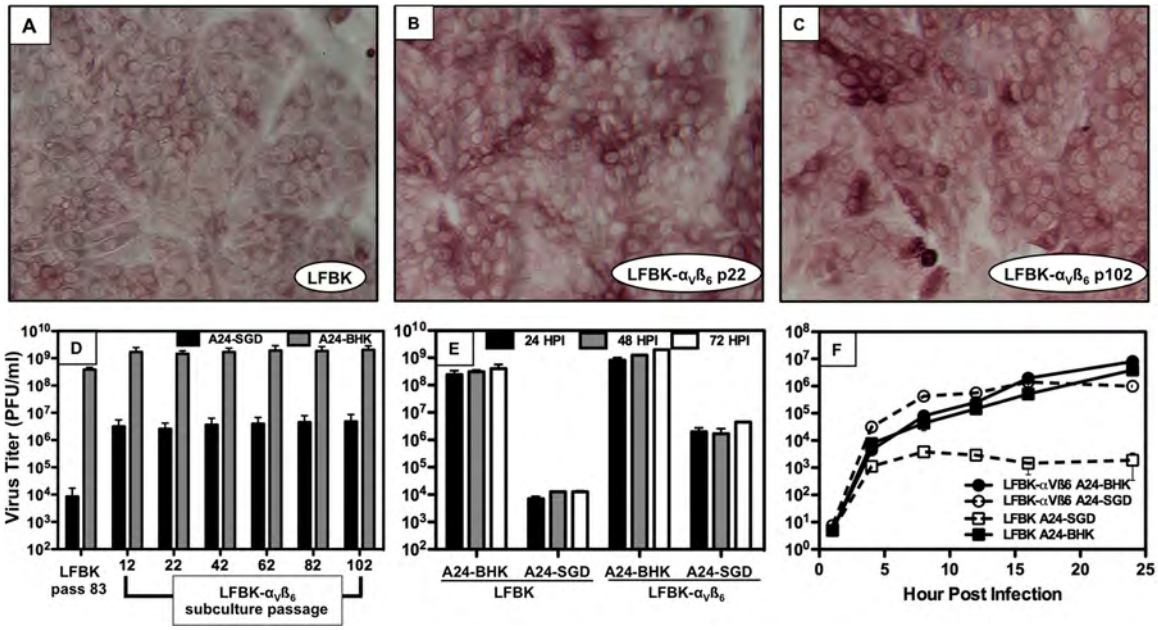

FIG 1 LFBK-$\alpha_V\beta_6$ cell characterization. LFBK-$\alpha_V\beta_6$ cells maintain long-term expression of β_6. Mouse anti-human β_6 was used to detect the bovine integrin subunit β_6 in LFBK at passage 83 (A), LFBK-$\alpha_V\beta_6$ at passage 22 (B), or passage 102 (C). Dark staining indicates β_6 expression. (D) LFBK-$\alpha_V\beta_6$ cells maintain long-term susceptibility to A24-SGD. The indicated cells were infected with serial dilutions of either A24-BHK or A24-SGD for plaque titration as described in Materials and Methods. (E) Relationship between susceptibility and time after seeding. Cells were seeded at the indicated time prior to infection and then infected with serial dilutions of the indicated virus for plaque titration as described in Materials and Methods. (F) Comparison of FMDV A24-BHK and A24-SGD growth in LFBK and LFBK-$\alpha_V\beta_6$ cells. LFBK and LFBK-$\alpha_V\beta_6$ cells were seeded in 24-well plates and infected 72 h later with either A24-BHK or A24-SGD at a multiplicity of infection (MOI) of 0.01. After 1 h, the monolayers were acid washed and fresh medium was added. At the indicated times after infection, the plates were frozen at −70°C, thawed, and titrated on LFBK-$\alpha_V\beta_6$ cells.

$\alpha_V\beta_6$ cells, demonstrating that the expression of $\alpha_V\beta_6$ in LFBK cells complements the defect of nontransduced LFBK cells to support efficient A24-SGD virus replication.

Susceptibility of LFBK-αVβ6 cells to animal-derived FMDV of all serotypes. In order to determine the susceptibility of LFBK-$\alpha_V\beta_6$ cells to animal-derived FMDV strains and compare it with those of LFBK, primary lamb kidney, BHK-21, and two swine kidney cells lines (IB-RS-2 and MVPK), each cell type was infected with serial dilutions of infected tissue macerates or vesicular fluid obtained from animals that were experimentally infected with each of the FMDV serotypes. The viruses used in this experiment were passaged twice in cattle or swine and are listed in Table 1. For each strain of virus, the LFBK-$\alpha_V\beta_6$ cells had equal or higher sensitivity to animal-derived FMDV than the other cells that we tested. In some cases, especially with the FMDV serotype O strains, the LFBK-$\alpha_V\beta_6$ cells supported FMDV replication that was >10-fold higher than most cell types tested (Fig. 2; see also Table S1 in the supplemental material). Overall, these data confirm that LFBK-$\alpha_V\beta_6$ cells can readily detect all FMDV serotypes in tissues from experimentally infected animals.

Detection of FMDV in diagnostic tissue samples using LFBK-$\alpha_V\beta_6$ cells. Samples from experimentally infected animals tend to have a high titer and better integrity than do field samples. To more closely mimic diagnostic conditions, we obtained field

TABLE 1 Experimentally infected animal-derived viruses used in this study

Virus strain	Sample species[a]	Sample type	Reference/source
A24 Cruzeiro/55	Swine	Vesicular fluid	Pacheco et al. (22)
A24 Cruzeiro/55	Bovine	Pool of bovine tongue and vesicular fluid	Uddowla et al. (23)
O1 Manisa/69	Bovine	Tongue tissue homogenate	Arzt et al. (24)
O1 Manisa/69	Swine	Vesicular fluid	Pacheco et al. (22)
Asia1 Shamir/89	Bovine	Tongue tissue homogenate	Science and Technology Directorate, DHS
Asia1 Shamir/89	Swine	Vesicular fluid	Pacheco et al. (22)
C3 Resende/55	Swine	Vesicular fluid	Nfon et al. (25)
C3 Resende/55	Bovine	Tongue tissue homogenate	Foreign Animal Disease Diagnostic Lab, APHIS
O/Taiwan/97	Swine	Vesicular fluid	Pacheco and Mason (29)
O/UK/35/01	Swine	Vesicular fluid	Pacheco and Mason (29)
SAT1/Zimbabwe/79	Bovine	Tongue tissue homogenate	Foreign Animal Disease Diagnostic Lab, APHIS
SAT2 Saudi Arabia/2000	Bovine	Vesicular fluid	Science and Technology Directorate, DHS
SAT3/Zimbabwe/83	Bovine	Tongue tissue homogenate	Science and Technology Directorate, DHS

[a] Each virus was collected from the indicated tissue(s) during the second round of infection in the indicated species.

Downloaded from http://jcm.asm.org/ on May 28, 2013 by DigiTop -USDA's Digital Desktop Library

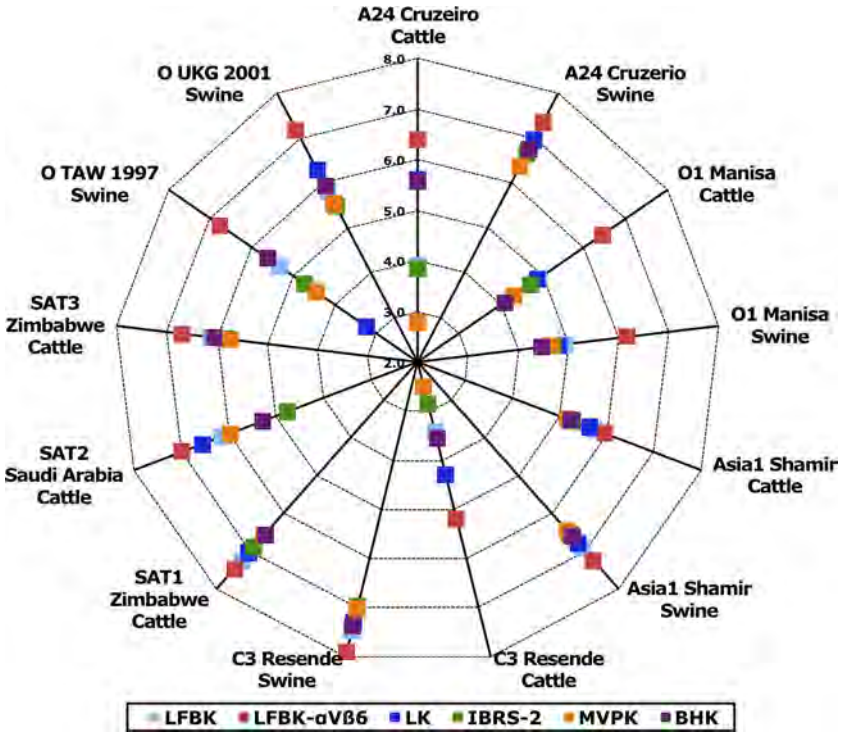

FIG 2 Susceptibility of 6 cell types to animal-derived FMDV. Cells were infected with the indicated viruses (Table 1), and virus titers were determined on each cell type by plaque assay. Each solid line is the axis for titers generated from the indicated virus strain. Colored points on the solid lines indicate the mean titer of that virus strain in a single cell type (see Table S1 in the supplemental material for sample range). Dashed lines specify the $\log_{10}$ scale of the virus titer in PFU/ml; points located outside the plot correspond to higher virus titers (10^8) than those located toward the center (10^2). Each point corresponds to the mean of $\geq$3 replicates.

diagnostic samples from Afghanistan, Bolivia, and Pakistan (see Table S2 in the supplemental material). These samples were processed from tissues according to standard virus isolation procedures and were used to infect LFBK-$\alpha_V\beta_6$ cells, as well as cells commonly used for FMDV diagnostics, including LK, IB-RS-2, and BHK-21 cells. Figure 3A shows the time point at which each diagnostic isolate first showed visible cytopathic effects (CPE) in each cell line. We observed that LFBK-$\alpha_V\beta_6$ was the only cell type in which all clinical samples were positive based on the presence of CPE by 24 h postinfection. A few of the samples yielded virus in all 4 cell lines, 12 samples were able to show CPE in only LFBK-$\alpha_V\beta_6$ or LK cells, and 3 of the 38 isolates tested grew only in LFBK-$\alpha_V\beta_6$ cells. These data show that LFBK-$\alpha_V\beta_6$ is the most permissive to these FMDV field isolates among all the cells tested. In order to rule out the presence of FMDV in noncytopathic infection, all CPE-negative wells were stained for FMDV 3D antigen after 48 hpi; none of the CPE-negative LK and IB-RS-2 wells reacted with the antibody. Five CPE-negative BHK-21 wells had individual nonrounded cells that stained positive for antigen (data not shown), indicating that these particular FMDV isolates were able to enter BHK-21 cells but were not spread efficiently in the culture by 48 h.

Figure 3B shows the overall CPE progression over time in all 38 virus isolates by plotting the mean CPE score of each isolate at each time point per cell type. On average, the LK and LFBK-$\alpha_V\beta_6$ cells performed very similarly, both being much more permissive to the diagnostic isolates than the IB-RS-2 and BHK-21 cells. While the LFBK-$\alpha_V\beta_6$ cells had slightly faster overall early detection of the isolates than the LK cells, the higher mean CPE score at later times indicates a faster progression of virus replication in the LFBK-$\alpha_V\beta_6$ cells. Taken together, the enhanced susceptibility, rapid initial detection of CPE, and faster progression of CPE strongly suggest that LFBK-$\alpha_V\beta_6$ cells are superior to many cells that are currently used for FMDV diagnostics from tissue specimens.

Susceptibility of LFBK-αVβ6 cells to other vesicular disease-causing viruses. Animals exhibiting vesicular lesions might be infected with other agents besides FMDV. In order to determine if LFBK-$\alpha_V\beta_6$ cells could detect other viruses causing vesicular disease, we inoculated BHK-21, LK, IB-RS-2, LFBK, or LFBK-$\alpha_V\beta_6$ cells with each of 5 non-FMD viruses that cause vesicular disease. We found that vesicular exanthema of swine virus (VESV) and swine vesicular disease virus (SVDV) replicated as well in LFBK-$\alpha_V\beta_6$ cells as they did in IB-RS-2 (Table 2). Vesicular stomatitis virus serotype New Jersey (VSV-NJ) grew to similar titers in all the cell lines. LK, LFBK, and LFBK-$\alpha_V\beta_6$ cells supported the growth of bovine papular stomatitis virus (BPSV), as evidenced by the formation of plaques; BPSV grew to a slightly higher titer in LK cells than in LFBK-$\alpha_V\beta_6$ cells. Infection with bluetongue virus induced cytopathic effects in only IB-RS-2 and LK cells by 96 hpi.

DISCUSSION

Here, we report the characterization of a bovine kidney cell line that is stably transduced with the bovine α_V and β_6 integrin subunits. The expression of the β_6 integrin subunit and the enhanced susceptibility to FMDV containing an SGD domain in VP1 were

Downloaded from http://jcm.asm.org/ on May 28, 2013 by DigiTop -USDA's Digital Desktop Library

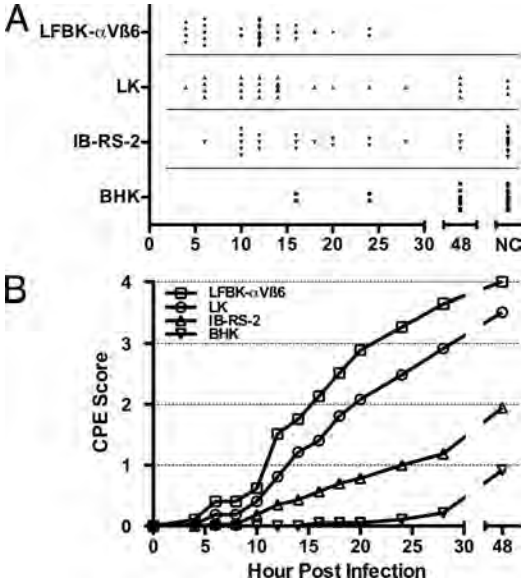

FIG 3 Detection of FMDV in diagnostic samples. Wells of 48-well plates seeded with the indicated cells were infected with 38 FMDV-suspect tissue homogenates from Afghanistan, Bolivia, and Pakistan (see Table S2 in the supplemental material for isolate information). Beginning at 4 h postinfection, each well was scored for the presence of cytopathic effects. (A) Each point on the scatter plot represents the time after infection that a cytopathic effect was first detected in a given well for one diagnostic isolate. NC denotes the diagnostic samples that did not induce visible cytopathic effects by 48 h in the indicated cells. (B) Each point on the graph represents the average CPE score for all 38 diagnostic isolates at each time point. 1+, ≤25% of the cell monolayer exhibited visual CPE; 2+, approximately 50% of the cell monolayer exhibited CPE; 3+, approximately 75% of the cell monolayer exhibited CPE; 4+, 100% of the cell monolayer exhibited CPE.

both maintained for ≥100 cell passages. We found that the LFBK-$\alpha_V\beta_6$ cells were more susceptible to all FMDV serotypes derived from experimentally infected animals than were other commonly used cells for FMDV isolation. In a diagnostic sensitivity assay, LFBK-$\alpha_V\beta_6$ cells were more sensitive than primary lamb kidney, IBRS-2, and BHK-21 cells. LFBK-$\alpha_V\beta_6$ cells were also able to detect other vesicular disease viruses. Our results support the use of LFBK-$\alpha_V\beta_6$ cells for FMDV diagnostic purposes.

Our data also indicate that the LFBK-$\alpha_V\beta_6$ cells are highly effective for the detection of FMDV serotype O isolates. A previous study (21) showed that LFBK cell sensitivity to FMDV O1 Manisa isolated from cattle was close to that of bovine tongue inoculation, and in our hands, the LFBK-$\alpha_V\beta_6$ cells detected O1 Manisa >1-$\log_{10}$-more efficiently than LFBK cells. Further, Burman and coworkers (26) showed that the integrin-binding domain on the VP1 capsid protein from O1 FMDV binds $\alpha_V\beta_6$ with the highest affinity among the $\alpha_V\beta_3$, $\alpha_V\beta_6$, and $\alpha_V\beta_8$ integrins. In our experiments (Fig. 2), O1 Manisa viruses were detected at titers nearly 2 logs better in LFBK-$\alpha_V\beta_6$ than in IB-RS-2 cells that do not express high levels of $\alpha_V\beta_6$ (15).

BHK-21 cells are widely used for FMDV propagation in research laboratory settings due to their rapid growth properties and sufficient susceptibility to most serotypes of FMDV. BHK-21 cells generally performed well in our sensitivity experiments (Fig. 2), detecting cattle-derived A24, as well as primary LK cells; O1 Manisa (from both swine and cattle) was the only serotype where BHK-21 had the least efficient FMDV detection of the cell lines tested. In contrast, low-passage-number BHK cells were able to detect FMDV from only 18 out of 40 diagnostic tissue samples, and in five of those cases, the detection of a few single infected BHK-21 cells (most with no obvious cytopathic morphology) was done by immunohistochemistry. Taken together, our results clearly indicate that BHK-21 cells are not as susceptible to animal-derived FMDV isolates as LFBK-$\alpha_V\beta_6$ cells.

FMDV strain O/TAW/97 does not grow well in primary bovine thyroid cells (BTY) or in cattle, and historically, its detection requires the use of swine cells, such as IB-RS-2 (27). As such, O/TAW/97 has been referred to as a porcinophilic virus (27–29). In our experiments, this virus grew poorly in primary LK cells, forming extremely small plaques. Interestingly, in our hands, O/TAW/97 grew better in the bovine-derived LFBK cells than in the swine-derived MVPK and IB-RS-2 cell lines. This suggests that the growth defect of O/TAW/97 in BTY (and possibly LK) cells is a postattachment step, since BTY cells express the $\alpha_V\beta_6$ integrin, indicating that other cell-specific factors are involved. Indeed, alterations in the 3A protein of O/TAW/97 have been identified (28), and while the function of 3A is not clear (30–32), it seems to be involved in host range specificity (33, 34). The reason that LFBK and LFBK-$\alpha_V\beta_6$ support the replication of this virus is unknown, but we can speculate that these cells have lost a factor that is present in bovine cells that restricts O/TAW/97 growth. Although we have not made a direct comparison, the results presented here suggest that LFBK-$\alpha_V\beta_6$ cells can support the replication of O/TAW/97 more efficiently than BTY cells.

IB-RS-2 cells have been shown to be less sensitive to some serotypes of FMDV than primary bovine thyroid cells (7), possibly due to low levels of $\alpha_V\beta_6$ integrin on the surface of the cells (15). In our experiments, the IB-RS-2 and MVPK cells had poor sensitivities to certain serotypes from bovine tissues, especially A24 Cruzeiro, O1 Manisa, and C3 Resende, whereas the A24 and C3 viruses from porcine tissues were efficiently detected by both swine origin cell lines. Interestingly, IB-RS-2, but not MVPK, cells were specifically less sensitive to SAT2 virus isolated from cattle; unfortunately, a comparison to swine-derived SAT2 was not available. While many laboratories include IB-RS-2 cells for the detection of swine vesicular diseases and swine-adapted FMDV strains, one concern with the diagnostic use of these cells is that they can test positive for classical swine fever (35), potentially confounding the results in array-based diagnostic assays.

Recently, Brehm and coworkers demonstrated the sensitivity of a fetal goat tongue cell line (36) that supports the replication of all FMDV strains tested, with the exception of the porcinophilic

TABLE 2 Growth of selected animal-derived vesicular disease viruses in various cell types

Virus (strain)	Titer[a] of the indicated virus in the following cell types:				
	LFBK	LFBK-$\alpha_V\beta_6$	IB-RS-2	BHK-21	LK
VESV (A48ET305)	6.15[a]	6.55	5.8	ND[b]	3.05
SVDV (UKG72)	6.2	6.2	6.3	ND	3.05
BSPV (New York 2004)	3.2	3.05	3.2	ND	3.8
BTV-1 (S. Africa 1993)	ND	ND	3.2	ND	3.05
VSV (New Jersey[c])	7.3	7.05	6.55	6.3	5.8

[a] Virus titers in $\log_{10}$ 50% tissue culture infective dose ($TCID_{50}$)/ml.
[b] ND, not detected. Limit of detection in this assay is 1.8 $\log_{10}$ $TCID_{50}$/ml.
[c] This virus was obtained from a pool of experimentally infected animal tissues.

Downloaded from http://jcm.asm.org/ on May 28, 2013 by DigiTop -USDA's Digital Desktop Library

O/TAW/97 strain. According to the authors, this cell line expresses the $\alpha_V\beta_6$ integrin and is equal to primary BTY cells in its sensitivity to FMDV. Although these cells were reported to grow slowly in culture, the monolayers of these goat tongue cells take days to become confluent but then are stable for a period of weeks once established. In contrast, the LFBK-$\alpha_V\beta_6$ cells grow very quickly in culture and are readily susceptible to infection within 24 h after seeding.

LFBK-$\alpha_V\beta_6$ cells have been used for FMDV research for several years at PIADC. They support the replication of animal-derived virus strains that do not grow well in other cell types (e.g., O1 Manisa and O/TAW/97) and maintain a high sensitivity to FMDV for >100 subculture passages. They do not require the extraction of animal organs to make primary cells, they grow as efficiently as standard LFBK cells, and they have no special medium requirements. Based on the data presented here, LFBK-$\alpha_V\beta_6$ is an excellent cell line for FMDV diagnostic- and research-based cell applications. LFBK-$\alpha_V\beta_6$ cells have been deposited in the American Type Culture Collection (PTA-13047).

ACKNOWLEDGMENTS

We thank the following groups for their assistance obtaining the viruses and for other reagents used in this study: the APHIS Foreign Animal Disease Diagnostics Laboratory at PIADC for primary lamb kidney cells, field isolates of FMDV, and field isolates of VESV, SVDV, bluetongue virus 1 (BTV-1), and BPSV, the Department of Homeland Security Science and Technology Directorate for experimentally infected animal-derived isolates of FMDV, and Khalid Naeem of the National Agricultural Research Center in Islamabad, Pakistan, for field isolates of FMDV. We thank Steve Pauszek (ARS) for serotype determination of the field isolates from Pakistan.

The LFBK-$\alpha_V\beta_6$ cell line is the subject of a U.S. patent application.

REFERENCES

1. **Grubman MJ, Baxt B.** 2004. Foot-and-mouth disease. Clin. Microbiol. Rev. **17**:465–493.
2. **Rodriguez LL, Gay CG.** 2011. Development of vaccines toward the global control and eradication of foot-and-mouth disease. Expert Rev. Vaccines **10**:377–387.
3. **Snowdon WA.** 1966. Growth of foot-and-mouth disease virus in monolayer cultures of calf thyroid cells. Nature **210**:1079–1080.
4. **House JA, Yedloutschnig RJ.** 1982. Sensitivity of seven different types of cell cultures to three serotypes of foot-and-mouth disease virus. Can. J. Comp. Med. **46**:186–189.
5. **House C, House JA.** 1989. Evaluation of techniques to demonstrate foot-and-mouth disease virus in bovine tongue epithelium: comparison of the sensitivity of cattle, mice, primary cell cultures, cryopreserved cell cultures and established cell lines. Vet. Microbiol. **20**:99–109.
6. **Swaney LM.** 1976. Susceptibility of a new fetal pig kidney cell line (MVPK-1) to foot-and-mouth disease virus. Am. J. Vet. Res. **37**:1319–1322.
7. **Ferris NP, King DP, Reid SM, Hutchings GH, Shaw AE, Paton DJ, Goris N, Haas B, Hoffmann B, Brocchi E, Bugnetti M, Dekker A, De Clercq K.** 2006. Foot-and-mouth disease virus: a first inter-laboratory comparison trial to evaluate virus isolation and RT-PCR detection methods. Vet. Microbiol. **117**:130–140.
8. **Ferris NP, Hutchings GH, Moulsdale HJ, Golding J, Clarke JB.** 2002. Sensitivity of primary cells immortalised by oncogene transfection for the detection and isolation of foot-and-mouth disease and swine vesicular disease viruses. Vet. Microbiol. **84**:307–316.
9. **De Castro MP.** 1964. Behaviour of the foot-and-mouth disease virus in cell cultures: susceptibility of the IB-RS-2 line. Arch. Inst. Biol., São Paulo. **31**:63–78.
10. **Ruiz-Sáenz J, Goez Y, Tabares W, López-Herrera A.** 2009. Cellular receptors for foot and mouth disease virus. Intervirology **52**:201–212.
11. **Jackson T, Sheppard D, Denyer M, Blakemore W, King AMQ.** 2000. The epithelial integrin $\alpha_V\beta_6$ is a receptor for foot-and-mouth disease virus. J. Virol. **74**:4949–4956.
12. **Ferris NP, Abrescia NGA, Stuart DI, Jackson T, Burman A, King DP, Paton DJ.** 2005. Utility of recombinant integrin $\alpha_V\beta_6$ as a capture reagent in immunoassays for the diagnosis of foot-and-mouth disease. J. Virol. Methods **127**:69–79.
13. **Monaghan P, Gold S, Simpson J, Zhang Z, Weinreb PH, Violette SM, Alexandersen S, Jackson T.** 2005. The alpha(v)beta6 integrin receptor for foot-and-mouth disease virus is expressed constitutively on the epithelial cells targeted in cattle. J. Gen. Virol. **86**:2769–2780.
14. **O'Donnell V, Pacheco JM, Gregg D, Baxt B.** 2009. Analysis of foot-and-mouth disease virus integrin receptor expression in tissues from naïve and infected cattle. J. Comp. Pathol. **141**:98–112.
15. **King DP, Burman A, Gold S, Shaw AE, Jackson T, Ferris NP.** 2011. Integrin sub-unit expression in cell cultures used for the diagnosis of foot-and-mouth disease. Vet. Immunol. Immunopathol. **140**:259–265.
16. **Duque H, LaRocco M, Golde WT, Baxt B.** 2004. Interactions of foot-and-mouth disease virus with soluble bovine alphaVbeta3 and alphaV-beta6 integrins. J. Virol. **78**:9773–9781.
17. **Rieder E, Henry T, Duque H, Baxt B.** 2005. Analysis of a foot-and-mouth disease virus type A24 isolate containing an SGD receptor recognition site *in vitro* and its pathogenesis in cattle. J. Virol. **79**:12989–12998.
18. **Swaney LM.** 1988. A continuous bovine kidney cell line for routine assays of foot-and-mouth disease virus. Vet. Microbiol. **18**:1–14.
19. **Piccone ME, Feng Y, Chang AC, Mosseri R, Lu Q, Kutish GF, Lu Z, Burrage TG, Gooch C, Rock DL, Cohen SN.** 2009. Identification of cellular genes affecting the infectivity of foot-and-mouth disease virus. J. Virol. **83**:6681–6688.
20. **Yang M, Clavijo A, Li M, Hole K, Holland H, Wang H, Deng MY.** 2007. Identification of a major antibody binding epitope in the non-structural protein 3D of foot-and-mouth disease virus in cattle and the development of a monoclonal antibody with diagnostic applications. J. Immunol. Methods **321**:174–181.
21. **Pacheco JM, Arzt J, Rodriguez LL.** 2010. Early events in the pathogenesis of foot-and-mouth disease in cattle after controlled aerosol exposure. Vet. J. **183**:46–53.
22. **Pacheco JM, Tucker M, Hartwig E, Bishop E, Arzt J, Rodriguez LL.** 2012. Direct contact transmission of three different foot-and-mouth disease virus strains in swine demonstrates important strain-specific differences. Vet. J. **193**:456–463.
23. **Uddowla S, Hollister J, Pacheco JM, Rodriguez LL, Rieder E.** 2012. A safe foot-and-mouth disease vaccine platform with two negative markers for differentiating infected from vaccinated animals. J. Virol. **86**:11675–11685.
24. **Arzt J, Pacheco JM, Rodriguez LL.** 2010. The early pathogenesis of foot-and-mouth disease in cattle after aerosol inoculation. Identification of the nasopharynx as the primary site of infection. Vet. Pathol. **47**:1048–1063.
25. **Nfon CK, Toka FN, Kenney M, Pacheco JM, Golde WT.** 2010. Loss of plasmacytoid dendritic cell function coincides with lymphopenia and viremia during foot-and-mouth disease virus infection. Viral Immunol. **23**:29–41.
26. **Burman A, Clark S, Abrescia NG, Fry EE, Stuart DI, Jackson T.** 2006. Specificity of the VP1 GH loop of foot-and-mouth disease virus for alphav integrins. J. Virol. **80**:9798–9810.
27. **Dunn CS, Donaldson AI.** 1997. Natural adaption to pigs of a Taiwanese isolate of foot-and-mouth disease virus. Vet. Rec. **141**:174–175.
28. **Knowles NJ, Davies PR, Henry T, O'Donnell V, Pacheco JM, Mason PW.** 2001. Emergence in Asia of foot-and-mouth disease viruses with altered host range: characterization of alterations in the 3A protein. J. Virol. **75**:1551–1556.
29. **Pacheco JM, Mason PW.** 2010. Evaluation of infectivity and transmission of different Asian foot-and-mouth disease viruses in swine. J. Vet. Sci. **11**:133–142.
30. **Moffat K, Howell G, Knox C, Belsham GJ, Monaghan P, Ryan MD, Wileman T.** 2005. Effects of foot-and-mouth disease virus nonstructural proteins on the structure and function of the early secretory pathway: 2BC but not 3A blocks endoplasmic reticulum-to-Golgi transport. J. Virol. **79**:4382–4395.
31. **García-Briones M, Rosas MF, González-Magaldi M, Martín-Acebes MA, Sobrino F, Armas-Portela R.** 2006. Differential distribution of non-structural proteins of foot-and-mouth disease virus in BHK-21 cells. Virology **349**:409–421.
32. **O'Donnell VK, Pacheco JM, Henry TM, Mason PW.** 2001. Subcellular

Downloaded from http://jcm.asm.org/ on May 28, 2013 by DigiTop -USDA's Digital Desktop Library

distribution of the foot-and-mouth disease virus 3A protein in cells infected with viruses encoding wild-type and bovine-attenuated forms of 3A. Virology **287**:151–162.

33. **Rosas MF, Vieira YA, Postigo R, Martín-Acebes MA, Armas-Portela R, Martínez-Salas E, Sobrino F.** 2008. Susceptibility to viral infection is enhanced by stable expression of 3A or 3AB proteins from foot-and-mouth disease virus. Virology **380**:34–45.
34. **Pacheco JM, Henry TM, O'Donnell VK, Gregory JB, Mason PW.** 2003. Role of nonstructural proteins 3A and 3B in host range and pathogenicity of foot-and-mouth disease virus. J. Virol. **77**:13017–13027.
35. **Bolin SR, Black JW, Frey ML, Katz JB, Ridpath JF, Roblin RO.** 1994. Detection of a cell line contaminated with hog cholera virus. J. Am. Vet. Med. Assoc. **205**:742–745.
36. **Brehm KE, Ferris NP, Lenk M, Riebe R, Haas B.** 2009. Highly sensitive fetal goat tongue cell line for detection and isolation of foot-and-mouth disease virus. J. Clin. Microbiol. **47**:3156–3160.

Downloaded from http://jcm.asm.org/ on May 28, 2013 by DigiTop -USDA's Digital Desktop Library

Supplemental table 1. Strain Susceptibility of 6 Cell Types to Animal-Derived FMDV Samples. (log_{10} PFU/ml ± max-min)

Virus Strain (Species)	LFBK-$\alpha_V ß_6$	LFBK	LK	IBRS-2	MVPK	BHK-21
A24 Cruzerio (Cattle)	6.4 ± 0.4	3.9 ± 0.4**	5.6 ± 0.1*	3.9 ± 0.2**	2.8 ± 0.6**	5.6 ± 0.7*
A24 Cruzerio (Swine)	7.4 ± 0.2	6.9 ± 0.4	7.0 ± 0.6	6.7 ± 0.4	6.4 ± 0.3	6.8 ± 0.6
O1 Manisa (Cattle)	6.4 ± 0.5	4.9 ± 0.4**	4.9 ± 0.8*	4.7 ± 0.6**	4.3 ± 0.5**	4.1 ± 0.6**
O1 Manisa (Swine)	6.2 ± 0.5	4.9 ± 0.5**	4.8 ± 0.5**	4.7 ± 0.5**	4.6 ± 0.3**	4.5 ± 0.2**
Asia1 Shamir (Cattle)	6.0 ± 0.4	5.7 ± 0.3	5.6 ± 0.3	5.3 ± 0.1	5.2 ± 0.3	5.2 ± 0.2
Asia1 Shamir (Swine)	7.2 ± 0.2	6.9 ± 0.2	6.8 ± 0.1	6.6 ± 0.3	6.5 ± 1.1	6.6 ± 0.3
C3 Resende (Cattle)	5.2 ± 0.6	3.4 ± 0.3**	4.3 ± 0.6*	2.9 ± 0.4**	2.5 ± 0.2**	3.6 ± 0.1**
C3 Resende (Swine)	7.9 ± 0.1	7.5 ± 0.4	7.3 ± 0.1	7.0 ± 0.2	7.0 ± 0.7	7.4 ± 0.1
SAT1/ZIM (Cattle)	7.5 ± 0.5	7.2 ± 0.4	7.0 ± 0.4	6.9 ± 0.1	6.6 ± 0.8	6.6 ± 0.5
SAT2/SAU (Cattle)	7.0 ± 0.4	6.1 ± 0.3	6.6 ± 0.7	4.8 ± 0.9	6.0 ± 0.8	5.3 ± 0.5
SAT3/ZIM (Cattle)	6.7 ± 0.2	6.1 ± 0.3	5.9 ± 0.3	5.8 ± 0.5	5.7 ± 0.1	6.1 ± 0.5
O/TAW/1997 (Swine)	6.8 ± 0.6	5.3 ± 0.1*	3.2 ± 0.1**	4.7 ± 0.1**	4.4 ± 0.6**	5.6 ± 0.6*
O/UKG/2001 (Swine)	7.2 ± 0.3	5.8 ± 1.4*	6.3 ± 0.3	5.5 ± 0.2**	5.6 ± 1.0**	5.9 ± 0.1*

* The comparison to the LFBK-$\alpha_V ß_6$ titer is statistically different ($p < 0.05$)
** The comparison to the LFBK-$\alpha_V ß_6$ titer is statistically different ($p < 0.01$)

Supplemental Table 2. Field isolates used for diagnostic assay.

Virus Designation	Species
A/AFG/156/2005	Cattle
A/AFG/160/2005	Cattle
O/AFG/210/2004	Cattle
O/BOL/741/2000	Cattle
O/BOL/758/2001	Cattle
A/BOL/803/2001	Cattle
A/BOL/812/2001	Cattle
O/Sargodha/PAK/9/2010	Cattle
O/Islamabad/PAK/10/2010	Cattle
O/Bahawalpur/PAK/11/2010	Cattle
O/Bahawalpur/PAK/12/2010	Buffalo
O/Bahawalpur/PAK/13/2010	Buffalo
O/Rawalpindi/PAK/14/2010	Buffalo
O/Rawalpindi/PAK/15/2010	Buffalo
O/Sahiwal/PAK/16/2010	Buffalo
O/Sargodha/PAK/17/2010	Buffalo
O/Sargodha/PAK/18/2010	Cattle
Asia1/Sargodha/PAK/22/2011	Cattle
Asia1/Sargodha/PAK/23/2011	Cattle
Asia1/Sargodha/PAK/24/2011	Cattle
Asia1/Sargodha/PAK/25/2011	Cattle
Asia1/Sargodha/PAK/26/2011	Cattle
Asia1/Sargodha/PAK/27/2011	Cattle
Asia1/Sargodha/PAK/28/2011	Cattle
Asia1/Sargodha/PAK/29/2011	Cattle
Asia1/Sargodha/PAK/30/2011	Cattle
Asia1/Karachi/PAK/31/2011	Buffalo
Asia1/Karachi/PAK/32/2011	Buffalo
Asia1/Karachi/PAK/33/2011	Buffalo
O/Karachi/PAK/34/2011	Buffalo
Asia1/Karachi/PAK/35/2011	Buffalo
Asia1/Karachi/PAK/36/2011	Buffalo
Asia1/Karachi/PAK/37/2011	Buffalo
O/Karachi/PAK/38/2011	Buffalo
Asia1/Karachi/PAK/39/2011	Buffalo
O/Karachi/PAK/40/2011	Buffalo
O/Karachi/PAK/41/2011	Buffalo
O/Karachi/PAK/42/2011	Buffalo

Antiviral Research 98 (2013) 380–385

Contents lists available at SciVerse ScienceDirect

Antiviral Research

journal homepage: www.elsevier.com/locate/antiviral

Short Communication

Repeated exposure to 5D9, an inhibitor of 3D polymerase, effectively limits the replication of foot-and-mouth disease virus in host cells

Devendra K. Rai [a], Elizabeth A. Schafer [a], Kamalendra Singh [b,c], Mark A. McIntosh [c], Stefan G. Sarafianos [b,c,d,*], Elizabeth Rieder [a,*]

[a] Foreign Animal Disease Research Unit, United States Department of Agriculture, Agricultural Research Service, Plum Island Animal Disease Center, Greenport, NY, USA
[b] Christopher Bond Life Sciences Center, University of Missouri School of Medicine, Columbia, MO, USA
[c] Department of Molecular Microbiology and Immunology, University of Missouri School of Medicine, Columbia, MO, USA
[d] Department of Biochemistry, Columbia, MO, USA

ARTICLE INFO

Article history:
Received 7 January 2013
Revised 11 March 2013
Accepted 28 March 2013
Available online 8 April 2013

Keywords:
Foot-and-mouth disease virus (FMDV)
5D9 compound
3D polymerase inhibitor
FMDV therapeutic treatment
Antiviral

ABSTRACT

Foot-and-mouth disease (FMD) is a highly contagious disease of livestock caused by a highly variable RNA virus (FMDV) that has seven serotypes and more than sixty subtypes. Both prophylactic and post-infection means of controlling the disease outbreak, including universally applicable vaccines and emergency response measures such as therapeutic treatments, are on high demand. In this study, we analyzed the long-term exposure outcome to a previously identified inhibitor of 3D polymerase (FMDV 3Dpol) for controlling FMDV infection and for the selection of resistance mutants. The results showed that no escape mutant viruses were isolated from FMDV A24 Cruzeiro infections in cell culture treated with gradually increasing concentrations of the antiviral compound 5D9 (4-chloro-N′-thieno, [2,3-d]pyrimidin-4-ylbenzenesulfonohydrazide) over ten passages. Biochemical and plaque assays revealed that when 5D9 was used at concentrations within a non-toxic range in cells, it drove the virus to undetectable levels at passage eight to ten. This is in contrast with observations made on parallel control (untreated) passages exhibiting fully viable and stable virus progenies. Collectively, the results demonstrated that under the experimental conditions, treatment with 5D9 does not confer a resistant phenotype and the virus is unable to evade the antiviral effect of the inhibitor. Further efforts using quantitative structure–property relationship (QSPR) based modifications of the 5D9 compound may result in the successful development of an effective in vivo antiviral drug targeting FMDV.

© 2013 Elsevier B.V. All rights reserved.

Foot-and-mouth disease virus (FMDV) is the etiologic agent of a highly contagious vesicular disease that affects cattle, sheep, goats, and other cloven-hoofed animals. While mortality rates are low in infected animals, morbidity can reach extremely high levels leading to loss of productivity, culling of infected and susceptible animals, and great personal and financial detriments due to both the loss of livestock and the international trade capabilities (Mort et al., 2008; Paarlberg et al., 2002). Recent outbreaks in South Korea, Japan, Egypt, and the UK have brought to the forefront the importance of controlling this disease, as well as the devastating local and global effects both during and post-outbreak (Ghoneim et al., 2010; Knowles et al., 2012; Reid et al., 2009).

FMDV belongs to the Picornaviridae family of the genus Aphthovirus. It has seven distinct serotypes (A, C, O, Asia 1, Sat 1, Sat 2, and Sat 3) (Bachrach, 1968; Grubman and Baxt, 2004) and more than 60 subtypes. Due to such a high level of diversity the development of a universal vaccine against FMDV has been a challenging task (Paton et al., 2005). The current most-effective vaccines are serotype-specific and consist of chemically inactivated whole-virus FMDV, offering protection only after seven days of vaccination (Grubman, 2005). The combined efforts including both vaccination and antivirals have been proposed as one strategy to more

Abbreviations: FMD, foot-and-Mouth Disease; FMDV, foot-and-mouth disease virus; 3Dpol, 3D polymerase; 5D9, 4-chloro-N′-thieno [2,3-d]pyrimidin-4-ylbenzenesulfonohydrazide; QSPR, quantitative structure–property relationship; RdRp, RNA dependent RNA polymerase; RNA, ribonucleic acid; NTP, nucleoside triphosphate; MTT, 3-(4,5-dimethylthiazol-2-yl)-2,5-diphenyltetrazolium bromide; BME, eagle's medium basal; ATCC, American Type Culture Collection; BHK, baby hamster kidney; MOI, multiplicity of infection; hpi, hours post infection; PBST, Phosphate Buffered Saline with Tween-20; DMSO, Dimethylsulphoxide; RT-PCR, reverse transcriptase-polymerase chain reaction; RIPA, radioimmunoprecipitation assay.

* Corresponding authors. Address: Plum Island Animal Disease Center, USDA/ARS/NAA, P.O. Box 848, Greenport, NY 11944-0848, USA. Tel. +1 (631) 323 3177; fax: +1 (631) 323 3006 (E. Rieder), 471d Christopher Bond Life Sciences Center, 1201 Rollins Street, Columbia, MO 65211, USA. Tel. +1 573 882 4338 (S.G. Sarafianos).

E-mail addresses: sarafianoss@missouri.edu (S.G. Sarafianos), elizabeth.rieder@ars.usda.gov (E. Rieder).

0166-3542/$ - see front matter © 2013 Elsevier B.V. All rights reserved.
http://dx.doi.org/10.1016/j.antiviral.2013.03.022

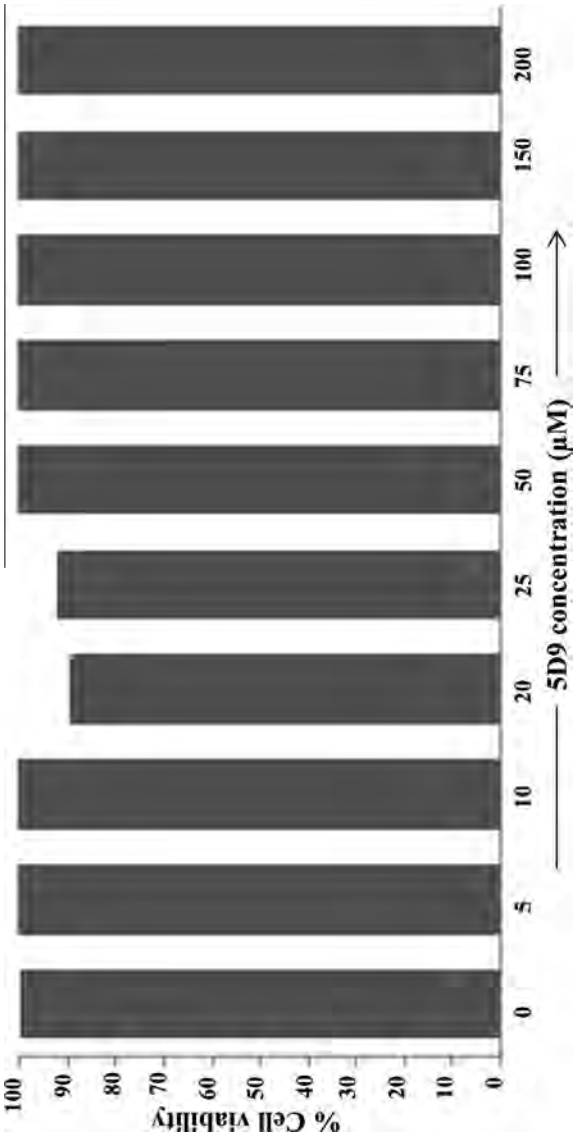

Fig. 1. Determination of cytotoxicity of 5D9: 10 × 104 baby hamster kidney (BHK) cells were seeded in BHK growth medium in the presence of either 4% DMSO only (vehicle control) or 5–200 μM 5D9. 24 h later MTT assay was conducted to determine the cellular viability. The numbers on *X*-axis represent the 5D9 concentration and *Y*-axis values represent %viability of the cells in comparison to 4% DMSO treated cells.

effectively treat FMD-infected animals and contain the spread of disease.

The FMDV genome consists of an 8.5 kb long single-stranded, positive sense RNA genome that is translated into a single polyprotein, which is processed into four structural and ten non-structural proteins (Grubman and Baxt, 2004). The non-structural RNA-dependent RNA polymerase (RdRp) protein also known as 3Dpol is coded within the 3′ end of the FMDV genome. It is essential for the synthesis of viral RNA and pivotal to the virus lifecycle. A number of crystal structures of apo enzyme, enzyme complexes containing template-primer (Ferrer-Orta et al., 2004), Vpg (Ferrer-Orta et al., 2006), RNA template-primer and incoming NTP or mutagenic nucleotides ribavirin triphosphate (RTP) and 5-fluorouridine triphosphate (FUTP) (Ferrer-Orta et al., 2007, 2010) and biochemical studies (Arias et al., 2008; Belsham, 1992; Bentham et al., 2012; Ferrer-Orta et al., 2004, 2007; Nayak et al., 2006) have provided significant insights into the RNA replication mechanism of 3Dpol over the years. Although a number of approaches have been pursued to develop anti-FMD therapies (Airaksinen et al., 2003; Dias et al., 2011, 2012; Uddowla et al., 2012; Vagnozzi et al., 2007) no clinically approved antiviral compounds are available for treatment of FMDV infection. This is in contrast with other viral diseases for which there are approved antiviral drugs that specifically target their polymerases (Airaksinen et al., 2003; Crotty et al., 2000; De Clercq, 2005; Parniak and Sluis-Cremer, 2000; Sarafianos et al., 2009).

In a previous study we identified seven compounds that inhibit 3Dpol at low micromolar concentrations. One of these inhibitors, 5D9 inhibited both FMDV 3Dpol enzyme and virus with comparable IC50 for the enzyme and the EC50 for the virus in cell-based assay suggesting that 5D9 acts by a single mechanism of action, inhibition of 3Dpol. The crystal structure of FMDV 3Dpol containing RNA template-primer, UTP and leaving PPi (after AMP incorporation) (PDB entry 2E9Z) as well as apo enzyme (PDB entry 1U09) was used to dock 5D9 in a cavity close to but distinct from the NTP binding site (Durk et al., 2010). This pocket consists of amino acid residues V55, I56, S58, K59, R168, G176, K177, T178, R179 and I180. The binding of 5D9 in this pocket was confirmed by site-directed mutagenesis of K59 and K177, which are located at two sides of the binding pocket (Durk et al., 2010). K59 is located near the junction of fingers (index finger, Ferrer-Orta et al., 2004) and palm subdomains of 3Dpol, whereas K177 and R168 belongs to motif F in the fingers subdomain (Bruenn, 2003; Ferrer-Orta

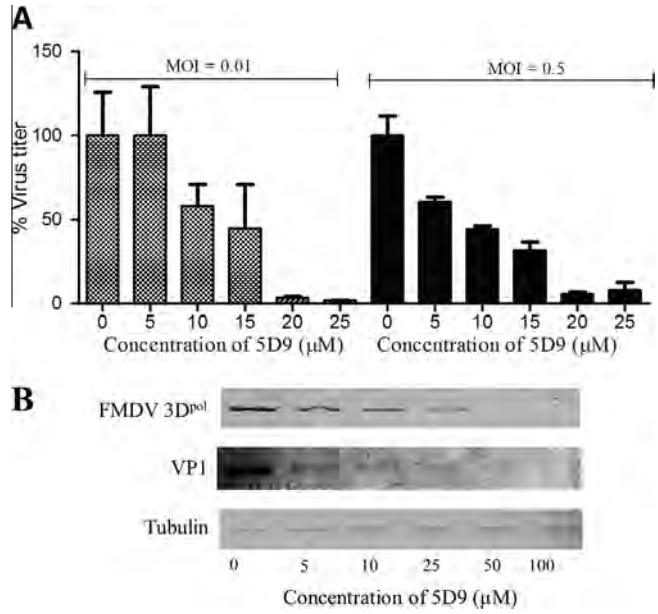

Fig. 2. Antiviral effect of 5D9: (A) Virus titer reduced upon treatment with 5D9. 0–25 μM 5D9 was administered in the presence on 4% DMSO to a confluent monolayer of BHK-21 cells prior to infection with FMDV. After 1 h cells were infected with A24 Cruzeiro strain of FMDV at 0.01 and 0.5 MOI. After 1 hpi the unadsorbed viruses were washed and the compound was re-administered and incubated for another 24 h at 37 °C and 5% CO_2. Following this incubation, samples were taken and plaque assays were performed. Results are reported as percent inhibition compared to a sample without inhibitor, and demonstrate a dose-dependent inhibition of virus replication. At the highest concentrations of 5D9 (25 μM) there was a greater than 90% inhibition of virus replication. Error bars represent standard deviation for two independent experiments. (B) 5D9 caused dose-dependent reduction in the expression of FMDV 3Dpol and VP1. Compound treatment and virus infections were performed as described as above. The numbers bellow each lane represent μM concentration of 5D9. The FMDV A24 Cruzeiro strain was used at a MOI of 10 for the infection. After 5 h of treatment cells were harvested, washed with PBS, pH 7.4 supplemented with complete protease inhibitor cocktail, lysed with RIPA buffer and viral genomic RNA was degraded using benzonase nuclease; equal protein was loaded in each lane as reflected by tubulin expression. The details of antibody concentrations and protocol for western blot analysis are described in the main text.

et al., 2004; Poch et al., 1989). None of these two residues bind to either RNA template-primer or NTP. In fact, only one residue of the inhibitor binding pocket (R168) has additional interaction with substrate (incoming NTP). In the ternary complex of FMDV 3Dpol, NH2 atom of R168 interacts with β-phosphate (distance NH2 – **βPO4 = 3.2 Å) of incoming UTP (Ferrer-Orta et al., 2007; PDB entry 2E9Z). R168 is also neighbor to P169, which associated to fidelity changes in fmdv and Coxacivirus 3Dpol (Gnadig et al., 2012). It is possible that the interaction of 5D9 with R168 (due to its proximity to residue P169) may have an impact on the fidelity of FMDV 3Dpol (Agudo et al., 2010).

The goal of this study was to examine the outcome of long-term exposure of FMDV to 5D9, which had exhibited the highest level of reduction in FMDV replication in our earlier work. The antiviral potency of 5D9 in terms of therapeutic index compares favorable (~80-fold higher) over ribavirin (EC50 = 970 μM, EC90 = 1697 μM), and comparable to 2′-C-methylcytidine (EC50 = 10 μM, EC90 = 15 μM) (Durk et al., 2010; Goris et al., 2007). Here, we serially passed the A24 Cruzeiro parental virus in the presence of a gradually increasing dosage of 5D9 and this led to a reduction of viral titers to undetectable levels after eight passages, while control passages in the absence of treatment grew similar to parental levels. Western blot analysis indicated a dose-dependent decrease in the expression of 3Dpol when 5D9 was present.

First we determined the cytotoxicity of 5D9. To this end, 1×10^4 BHK-21 cells/well were seeded in a 96-well plate in BHK growth medium (BME containing 10% fetal calf serum, L-glutamine, sodium-pyruvate and 1X antibiotic, antimycotic). 5D9 was added to confluent cell monolayers at concentrations of 0–200 μM and incubated at 370C for 24 h in a total volume of 100 μL in the presence of 4% DMS° (Fig. 1). After 24 h cell viability/proliferation was evaluated with the 3-(4,5-dimethylthiazol-2-yl)-2,5-diphenyltetrazolium bromide (MTT) Cell Proliferation Assay method (American Type Culture Collection, ATCC) according to the manufacturer's instructions. Values were compared with those obtained from untreated control cells. 80% cell viability was set as cut off for the determination of cytotoxicity of the compound. As shown in Fig. 1 the inhibitor did not cause any significant change in the cell viability at these concentrations.

In order to assess the antiviral activity of 5D9 on FMDV infection under different compound dose and multiplicity of infection (MOI, ratio of number of infectious virus particles in plaque forming units per cell) conditions, a confluent monolayer of BHK-21 cells pretreated with concentrations of 5D9 within the 0–25 μM range (Fig. 2A) was infected with FMDV A24 Cruzeiro at 0.01 and 0.5 MOI and incubated at 37 °C. One hour post infection (hpi), unadsorbed viruses were inactivated by two acidic washes [25 mM MES (2-morpholinoethanesulfonic acid) pH 6.0; 145 mM NaCl] and then neutralized with virus growth medium, VGM [(Eagle's basal medium (BME) (Life Technologies, Gaithersburg, MD), 1% antibiotic/antimycotic]. The compound was re-administered in a total volume of 500 μl VGM containing 4% DMSO. Twenty-four hours post infection the plates were frozen, then freeze–thawed and viral plaque assays were performed for the quantification of infectious virus in treated and untreated samples as described (Rieder et al., 1993). Fig. 2A shows the effects of 5D9 on the replication of FMDV A24 Cruzeiro. The compound inhibited virus replication both at 0.01 and 0.5 MOIs to similar extent

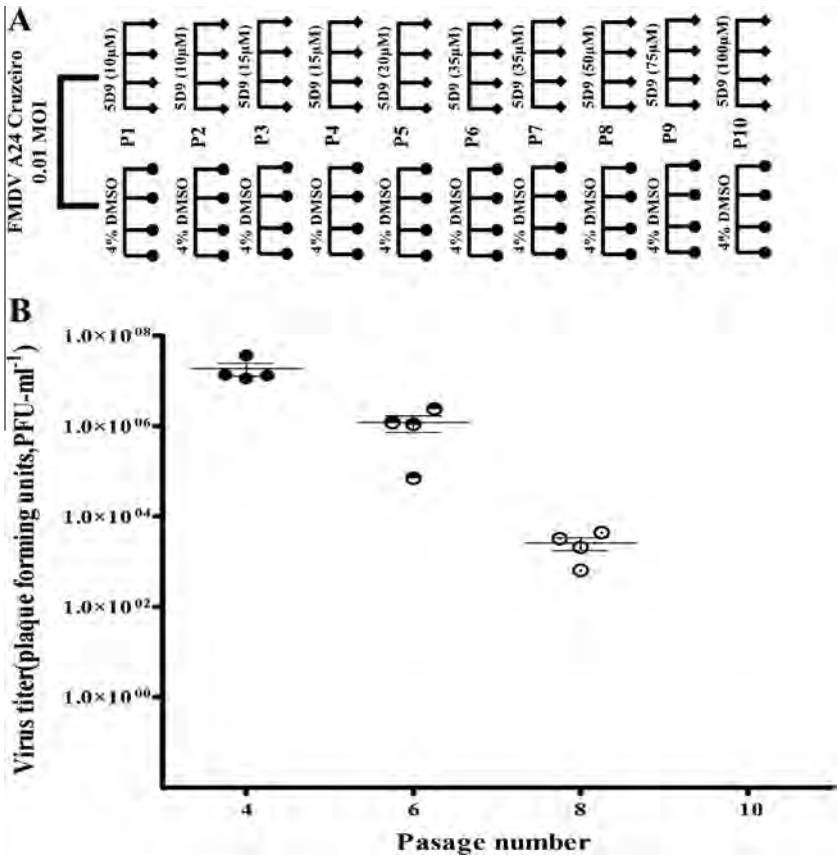

Fig. 3. Continued treatment with 5D9 drove virus to undetectable levels. (A) Scheme of virus passage. FMDV A24 Cruzeiro strain was passaged in the presence of gradually increasing concentrations of 5D9 in quadruplicates (right panel shown with filled diamonds as arrowhead), 4% DMSO used as to dissolve 5D9 was run as control (in quadruplicate) throughout passage (left panel shown with filled circles as arrowhead). (B) Effect of 5D9 on the virus titer over the passage. Zero PFU/ml was set the detection limit. At passage 10, the virus in the compound treated group was not detectable by plaque assay.

(~50% reduction in viral titer at 10 μM concentration). The specific effect of 5D9 on FMDV replication in the cells was also demonstrated by a reduction in 3Dpol expression in western blot analysis when BHK cells were infected with A24 Cruzeiro in the presence of the compounds at a MOI of ten. (Fig. 2B). Reduction in 3Dpol expression also correlated with lower expression of the viral structural protein VP1, which suggests that the decrease in viral protein expression observed is indeed due to the inhibition of viral replication and not to the misfolding or degradation of 3Dpol. For western blot analysis, first the cell lysates were electrophoresed on SDS–PAGE (sodium dodecyl sulfate–polyacrylamide gel electrophoresis) using a 12% Nu-PAGE® pre-cast gel system (Invitrogen) to separate the proteins. Subsequently, the separated proteins were electro-blotted onto a nitrocellulose membrane (Sigma). After blocking with 5% milk in PBS, FMDV 3Dpol and VP1 were probed with mouse-monoclonal anti-FMDV 3Dpol antibody (a gift from A. Clavijo at the National Centre for Foreign Animal Disease, Winnipeg, Manitoba, Canada) and rabbit polyclonal anti-VP1 sera (a gift from M. Grubman, ARS, USDA, USA) at 1:500 and 1:1000 dilutions, respectively in 1% milk and PBST (Phosphate Buffered Saline with Tween 20). Primary antibodies reacted with alkaline phosphatase (ALKP)-conjugated secondary antibodies and the blot was developed with SIGMAFASTTMB-CIP®/NBT (5-bromo-4-chloro-3-indolyl phosphate/nitro blue tetrazolium). Cellular tubulin, employed as an internal loading control protein, was detected with anti-tubulin-α (Sigma). The 5D9 dose-dependent disappearance of 3Dpol corroborated the dose-dependent inhibitory effect of this compound observed in plaque assays (Fig. 2B). Tubulin controls were included to ensure equal loading in each of the test wells.

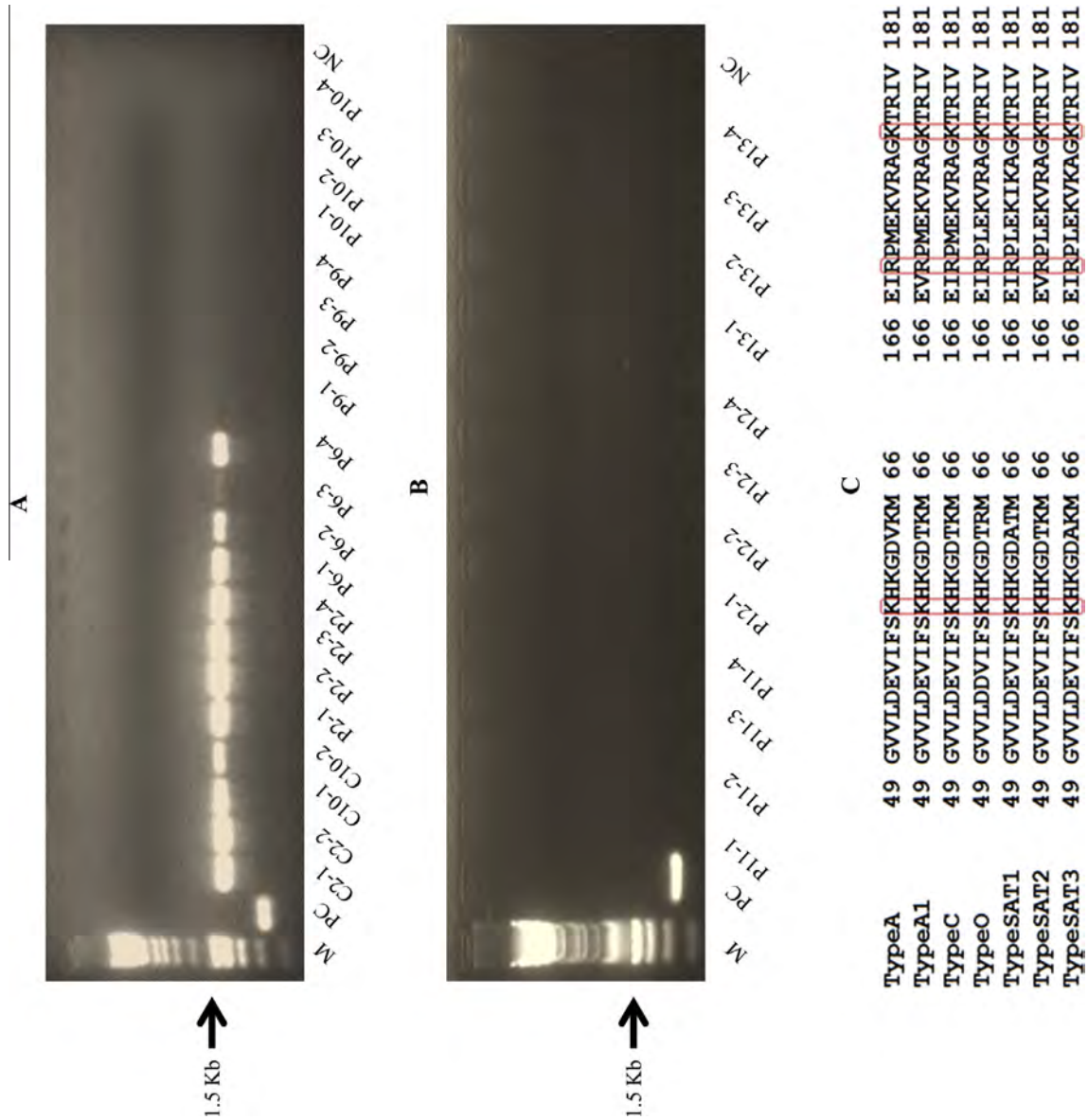

Fig. 4. Reverse transcriptase-polymerase chain reaction (RT-PCR) detection of viral RNA. (A) Viral RNA was not detectable at and after passage 9 in the presence of 5D9. C2 and C10 represent control (vehicle only) treated viral RNA from passage 2 and 10, respectively. The numbers after (–) represent sample replicate. Similarly, P1-P10 represent 5D9 treated viral RNA from passage numbers, P1–P10, respectively. PC is positive control for the PCR reaction with HeLa RNA template and negative control (NC) represents the PCR reaction without RNA. Lane M is marker lane showing 1 Kb DNA ladder. (B) In order to recover (if any present) viral RNA from passage 10 of 5D9 treatment group, the lysates from were further passaged for three generations in the absence of 5D9. As the gel shows there was no detection of viral RNA. The numbering and denotations are similar to figure A. (C) Alignment of 3Dpol sequences from seven FMDV serotypes. Sequence alignment shows absolute conservation (highlighted with red bar) of K59, R168 and K177 residues critical to 5D9 binding (Durk et al., 2010). The text starting each line indicates the serotype, the numbers at left and right hand side of each sequence denote the position of sequence in 3Dpol protein. (For interpretation of the references to colour in this figure legend, the reader is referred to the web version of this article.)

On the basis of similar antiviral effects of 5D9 at the two different MOIs observed in Fig. 2 and the role of 3Dpol in virus replication, we next pursued an experimental design to evaluate viral fitness in the presence of 5D9 and the selection of resistant mutants. To this end FMDV A24 Cruzeiro was used to infect BHK-21 cells at a MOI of 0.01 and exposed to a low (5 μM) compound concentration in the first passage. Further passages were performed using a fraction (1/5) of total volume of freeze–thawed cell lysates at MOIs calculated within a range of 2–5 (passages 2–7). Compound treatment was performed as described earlier and the plates containing virus were freeze–thawed for further passages or analysis. The MOI was calculated by dividing plaque forming units (PFUs) by the cell number (4.5×10^5). The passage scheme presented in Fig 3A shows that each virus passage was conducted in parallel quadruplicates. At passages 4, 6, and 8, samples were processed for sequencing and quantitative analysis. For sequencing the viral genome and RT-PCR of viral RNA, the RNA extraction was carried out using the RNeasy Mini Kit column method (Qiagen, Catalog Number 74014, Valencia, CA). Post-RNA extraction, cDNA was produced using the SuperScript III First-Strand Synthesis System for RT-PCR (Invitrogen, Catalog Number 18080-051) and PCR was subsequently performed using the Phusion High-Fidelity PCR KIT (New England Biolabs, Catalog Number E0553L, Ipswich, MA). Sequencing was performed on an ABI sequencer (Applied Biosystems, Bedford, MA, USA). Fig. 3B shows that the compound treatment reduced the virus titer gradually from 10^7 PFU/ml at passage four to 10^3 PFU/ml at passage 8. In contrast, no significant changes in viral titers were observed in mock-treated virus passages, except for a slight increase (<1 log) after 10 passages (data not shown). This suggests that ten passages of FMDV A24 Cruzeiro in the absence of compound was not detrimental to the virus. Virus titration (Fig. 3B) and RT-PCR results (Fig. 4) show that no detectable virus is present at and after passage nine.

To determine the sequence of the viruses passaged in the presence or absence of 5D9, samples at passages 4 and 8 were examined by RT-PCR and sequenced as previously described (Rieder et al., 2005). In addition, individual clones from infected cell culture monolayers at passage 5 were isolated under low melting point agarose (SeaPlaque) overlay followed by RT-PCR and sequencing. Analysis of whole viral population showed that no predominant mutations were fixed in the region coding for 3Dpol within the 5D9-treated viruses (at passage 4 and passage 8). Interestingly, one out of 12 randomly picked clones at 5D9-treated passage 5 displayed a P169Q change in 3Dpol and another clone exhibited multiple mutations within the 3Dpol sequence [(amino acid substitutions P44R, E259 V, S335F and L376F) and one silent mutation ($C \gg T$) at nucleotide position 7585]. Based on the fact that under the experimental conditions no mutant viruses became predominant in subsequent parallel passages, it can be suggested that none of these mutations were able to confer a selective advantage to the virus against the antiviral compound. Although these residues are not part of the validated 5D9 binding pocket (Durk et al., 2010), evidence suggests that P44 and P169 are important determinants of RdRp fidelity whereas S335 is important for RdRp function (Castro et al., 2005; Gnadig et al., 2012; Gong and Peersen, 2010; Korneeva and Cameron, 2007; Verdaguer and Ferrer-Orta, 2012; Weeks et al., 2012). In particular, Agudo et al. reported changes at P44 and P169 in response to ribavirin treatment for FMDV 3Dpol affecting the enzyme fidelity (Agudo et al., 2010). However, failure of these mutants to adapt to 5D9 compound challenge could possibly be explained in two ways: (I) If the mutations increase the fidelity, the virus quasispecies may be critically reduced in size leading to its extinction; (II) The decrease in fidelity could lead the virus towards another extreme, where virus will accumulate too many errors in its genome and will eventually be unable to survive. It should be noted that the isolation/emergence of resistant mutants is an important step in the determination of target specificity for an antiviral drugs and deciding the antiviral therapy (Aloia et al., 2012; Koev and Kati, 2008), (Wainberg and Friedland, 1998). In addition to intrinsic error rate of viral RdRPs (10^{-3}-10^{-5}/copy for a 10 Kb genome), a number of other factors including the host environment contribute to the virus evolution (Domingo, 1989, 1997; Domingo et al., 1996; Elena et al., 2006; Elena and Sanjuan, 2005; Furio et al., 2005; Sanjuan et al., 2007, 2010). In this context, we cannot absolutely exclude the possibility that using higher virus inputs and/or different conditions resistance mutants to 5D9 may emerge.

In conclusion, the results demonstrated that compound 5D9 is a very efficient inhibitor of FMDV replication, and long-term exposure of FMDV A24 Cruzeiro to this compound did not result in the selection of resistant mutants in cell culture. The fact that the drug-binding pocket in FMDV 3Dpol targeted by 5D9 (via a single mechanism of action, see Durk et al., 2010) is conserved among different serotypes (Fig. 4C) suggests that this compound could potentially be developed as a broad-spectrum inhibitor of FMDV. Clinically effective inhibitors acting either alone or in conjunction with current vaccines may be very helpful as an emergency response measure in controlling the spread of disease in the outbreaks.

Disclosure statement

The authors declare no competing interests.

Acknowledgements

This research was supported in part by CRIS project no. 1940-32000-057-00D, Agricultural Research Service (ARS), U.S. Department of Agriculture (Elizabeth Rieder) and USDA-ARS-58-1940-5-519. USDA-ARS-58-1940-8-868; NIH grants AI076119, AI099284, and AI100890 (Stefan G. Sarafianos). Dr D. Rai is the recipient of a fellowship by the Plum Island Animal Disease Research Participation Program administered by the Oak Ridge Institute for Science and Education through an interagency agreement between the U.S. Department of Energy and the U.S. Department of Agriculture. We thank A. Clavijo (National Centre for Foreign Animal Disease, 1015 Arlington Street, Winnipeg, Manitoba, Canada) for the gift of monoclonal antibodies targeting the FMDV 3D polymerase protein.

References

Agudo, R., Ferrer-Orta, C., Arias, A., de la Higuera, I., Perales, C., Perez-Luque, R., Verdaguer, N., Domingo, E., 2010. A multi-step process of viral adaptation to a mutagenic nucleoside analogue by modulation of transition types leads to extinction-escape. PLoS Pathog. 6 (8), e1001072.

Airaksinen, A., Pariente, N., Menendez-Arias, L., Domingo, E., 2003. Curing of foot-and-mouth disease virus from persistently infected cells by ribavirin involves enhanced mutagenesis. Virology 311 (2), 339–349.

Aloia, A.L., Locarnini, S., Beard, M.R., 2012. Antiviral resistance and direct-acting antiviral agents for HCV. Antivir. Ther. 17 (6 Pt B), 1147–1162.

Arias, A., Arnold, J.J., Sierra, M., Smidansky, E.D., Domingo, E., Cameron, C.E., 2008. Determinants of RNA-dependent RNA polymerase (in)fidelity revealed by kinetic analysis of the polymerase encoded by a foot-and-mouth disease virus mutant with reduced sensitivity to ribavirin. J. Virol. 82 (24), 12346–12355.

Bachrach, H.L., 1968. Foot-and-mouth disease. Annu. Rev. Microbiol. 22, 201–244.

Belsham, G.J., 1992. Dual initiation sites of protein synthesis on foot-and-mouth disease virus RNA are selected following internal entry and scanning of ribosomes in vivo. EMBO J. 11 (3), 1105–1110.

Bentham, M., Holmes, K., Forrest, S., Rowlands, D.J., Stonehouse, N.J., 2012. Formation of higher-order foot-and-mouth disease virus 3D(pol) complexes is dependent on elongation activity. J. Virol. 86 (4), 2371–2374.

Bruenn, J.A., 2003. A structural and primary sequence comparison of the viral RNA-dependent RNA polymerases. Nucl. Acids Res. 31 (7), 1821–1829.

Castro, C., Arnold, J.J., Cameron, C.E., 2005. Incorporation fidelity of the viral RNA-dependent RNA polymerase: a kinetic, thermodynamic and structural perspective. Virus Res. 107 (2), 141–149.

Crotty, S., Maag, D., Arnold, J.J., Zhong, W., Lau, J.Y., Hong, Z., Andino, R., Cameron, C.E., 2000. The broad-spectrum antiviral ribonucleoside ribavirin is an RNA virus mutagen. Nat. Med. 6 (12), 1375–1379.
De Clercq, E., 2005. Antiviral drug discovery and development: where chemistry meets with biomedicine. Antiviral Res. 67 (2), 56–75.
Dias, C.C., Moraes, M.P., Segundo, F.D., de los Santos, T., Grubman, M.J., 2011. Porcine type I interferon rapidly protects swine against challenge with multiple serotypes of foot-and-mouth disease virus. J. Interferon Cytokine Res. 31 (2), 227–236.
Dias, C.C., Moraes, M.P., Weiss, M., Diaz-San Segundo, F., Perez-Martin, E., Salazar, A.M., de los Santos, T., Grubman, M.J, 2012. Novel antiviral therapeutics to control foot-and-mouth disease. J Interferon Cytokine Res 32 (10), 462–473.
Domingo, E., 1989. RNA virus evolution and the control of viral disease. Prog. Drug Res. 33, 93–133.
Domingo, E., 1997. RNA virus evolution, population dynamics, and nutritional status. Biol. Trace Elem. Res. 56 (1), 23–30.
Domingo, E., Escarmis, C., Sevilla, N., Moya, A., Elena, S.F., Quer, J., Novella, I.S., Holland, J.J., 1996. Basic concepts in RNA virus evolution. FASEB J. 10 (8), 859–864.
Durk, R.C., Singh, K., Cornelison, C.A., Rai, D.K., Matzek, K.B., Leslie, M.D., Schafer, E., Marchand, B., Adedeji, A., Michailidis, E., Dorst, C.A., Moran, J., Pautler, C., Rodriguez, L.L., McIntosh, M.A., Rieder, E., Sarafianos, S.G., 2010. Inhibitors of foot and mouth disease virus targeting a novel pocket of the RNA-dependent RNA polymerase. PLoS ONE 5 (12), e15049.
Elena, S.F., Sanjuan, R., 2005. RNA viruses as complex adaptive systems. Biosystems 81 (1), 31–41.
Elena, S.F., Carrasco, P., Daros, J.A., Sanjuan, R., 2006. Mechanisms of genetic robustness in RNA viruses. EMBO Rep. 7 (2), 168–173.
Ferrer-Orta, C., Arias, A., Perez-Luque, R., Escarmis, C., Domingo, E., Verdaguer, N., 2004. Structure of foot-and-mouth disease virus RNA-dependent RNA polymerase and its complex with a template-primer RNA. J. Biol. Chem. 279 (45), 47212–47221.
Ferrer-Orta, C., Arias, A., Agudo, R., Perez-Luque, R., Escarmis, C., Domingo, E., Verdaguer, N., 2006. The structure of a protein primer-polymerase complex in the initiation of genome replication. EMBO J. 25 (4), 880–888.
Ferrer-Orta, C., Arias, A., Perez-Luque, R., Escarmis, C., Domingo, E., Verdaguer, N., 2007. Sequential structures provide insights into the fidelity of RNA replication. Proc. Natl. Acad. Sci. USA 104 (22), 9463–9468.
Ferrer-Orta, C., Sierra, M., Agudo, R., de la Higuera, I., Arias, A., Perez-Luque, R., Escarmis, C., Domingo, E., Verdaguer, N., 2010. Structure of foot-and-mouth disease virus mutant polymerases with reduced sensitivity to ribavirin. J. Virol. 84 (12), 6188–6199.
Furio, V., Moya, A., Sanjuan, R., 2005. The cost of replication fidelity in an RNA virus. Proc. Natl. Acad. Sci. USA 102 (29), 10233–10237.
Ghoneim, N.H., Abdel-Karim, A.K., El-Shehawy, L., Abdel-Moein, K.A., 2010. Foot and mouth disease in animals in Sharkia governorate – Egypt. Transbound Emerg. Dis. 57 (1–2), 19–21.
Gnadig, N.F., Beaucourt, S., Campagnola, G., Borderia, A.V., Sanz-Ramos, M., Gong, P., Blanc, H., Peersen, O.B., Vignuzzi, M., 2012. Coxsackievirus B3 mutator strains are attenuated in vivo. Proc. Natl. Acad. Sci. USA 109 (34), E2294–E2303.
Gong, P., Peersen, O.B., 2010. Structural basis for active site closure by the poliovirus RNA-dependent RNA polymerase. Proc. Natl. Acad. Sci. USA 107 (52), 22505–22510.
Goris, N., De Palma, A., Toussaint, J.F., Musch, I., Neyts, J., De Clercq, K., 2007. 2′-C-methylcytidine as a potent and selective inhibitor of the replication of foot-and-mouth disease virus. Antiviral Res. 73 (3), 161–168.
Grubman, M.J., 2005. Development of novel strategies to control foot-and-mouth disease: marker vaccines and antivirals. Biologicals 33 (4), 227–234.
Grubman, M.J., Baxt, B., 2004. Foot-and-mouth disease. Clin. Microbiol. Rev. 17 (2), 465–493.
Knowles, N.J., He, J., Shang, Y., Wadsworth, J., Valdazo-Gonzalez, B., Onosato, H., Fukai, K., Morioka, K., Yoshida, K., Cho, I.S., Kim, S.M., Park, J.H., Lee, K.N., Luk, G., Borisov, V., Scherbakov, A., Timina, A., Bold, D., Nguyen, T., Paton, D.J., Hammond, J.M., Liu, X., King, D.P., 2012. Southeast Asian foot-and-mouth disease viruses in eastern Asia. Emerg. Infect. Dis. 18 (3), 499–501.
Koev, G., Kati, W., 2008. The emerging field of HCV drug resistance. Expert Opin. Investig. Drugs 17 (3), 303–319.
Korneeva, V.S., Cameron, C.E., 2007. Structure-function relationships of the viral RNA-dependent RNA polymerase: fidelity, replication speed, and initiation mechanism determined by a residue in the ribose-binding pocket. J. Biol. Chem. 282 (22), 16135–16145.
Mort, M., Convey, I., Baxter, J., Bailey, C., 2008. Animal disease and human trauma: the psychosocial implications of the 2001 UK foot and mouth disease disaster. J. Appl. Anim. Welf. Sci. 11 (2), 133–148.
Nayak, A., Goodfellow, I.G., Woolaway, K.E., Birtley, J., Curry, S., Belsham, G.J., 2006. Role of RNA structure and RNA binding activity of foot-and-mouth disease virus 3C protein in VPg uridylylation and virus replication. J. Virol. 80 (19), 9865–9875.
Paarlberg, P.L., Lee, J.G., Seitzinger, A.H., 2002. Potential revenue impact of an outbreak of foot-and-mouth disease in the United States. J. Am. Vet. Med. Assoc. 220 (7), 988–992.
Parniak, M.A., Sluis-Cremer, N., 2000. Inhibitors of HIV-1 reverse transcriptase. Adv. Pharmacol. 49, 67–109.
Paton, D.J., Valarcher, J.F., Bergmann, I., Matlho, O.G., Zakharov, V.M., Palma, E.L., Thomson, G.R., 2005. Selection of foot and mouth disease vaccine strains – a review. Rev. Sci. Tech. 24 (3), 981–993.
Poch, O., Sauvaget, I., Delarue, M., Tordo, N., 1989. Identification of four conserved motifs among the RNA-dependent polymerase encoding elements. EMBO J. 8 (12), 3867–3874.
Reid, S.M., Ebert, K., Bachanek-Bankowska, K., Batten, C., Sanders, A., Wright, C., Shaw, A.E., Ryan, E.D., Hutchings, G.H., Ferris, N.P., Paton, D.J., King, D.P., 2009. Performance of real-time reverse transcription polymerase chain reaction for the detection of foot-and-mouth disease virus during field outbreaks in the United Kingdom in 2007. J. Vet. Diagn. Invest. 21 (3), 321–330.
Rieder, E., Bunch, T., Brown, F., Mason, P.W., 1993. Genetically engineered foot-and-mouth disease viruses with poly(C) tracts of two nucleotides are virulent in mice. J. Virol. 67 (9), 5139–5145.
Rieder, E., Henry, T., Duque, H., Baxt, B., 2005. Analysis of a foot-and-mouth disease virus type A24 isolate containing an SGD receptor recognition site in vitro and its pathogenesis in cattle. J. Virol. 79 (20), 12989–12998.
Sanjuan, R., Cuevas, J.M., Furio, V., Holmes, E.C., Moya, A., 2007. Selection for robustness in mutagenized RNA viruses. PLoS Genet. 3 (6), e93.
Sanjuan, R., Nebot, M.R., Chirico, N., Mansky, L.M., Belshaw, R., 2010. Viral mutation rates. J. Virol. 84 (19), 9733–9748.
Sarafianos, S.G., Marchand, B., Das, K., Himmel, D.M., Parniak, M.A., Hughes, S.H., Arnold, E., 2009. Structure and function of HIV-1 reverse transcriptase: molecular mechanisms of polymerization and inhibition. J. Mol. Biol. 385 (3), 693–713.
Uddowla, S., Hollister, J., Pacheco, J.M., Rodriguez, L.L., Rieder, E., 2012. A safe foot-and-mouth disease vaccine platform with two negative markers for differentiating infected from vaccinated animals. J. Virol. 86 (21), 11675–11685.
Vagnozzi, A., Stein, D.A., Iversen, P.L., Rieder, E., 2007. Inhibition of foot-and-mouth disease virus infections in cell cultures with antisense morpholino oligomers. J. Virol. 81 (21), 11669–11680.
Verdaguer, N., Ferrer-Orta, C., 2012. Conformational changes in motif D of RdRPs as fidelity determinant. Structure 20 (9), 1448–1450.
Wainberg, M.A., Friedland, G., 1998. Public health implications of antiretroviral therapy and HIV drug resistance. JAMA 279 (24), 1977–1983.
Weeks, S.A., Lee, C.A., Zhao, Y., Smidansky, E.D., August, A., Arnold, J.J., Cameron, C.E., 2012. A Polymerase mechanism-based strategy for viral attenuation and vaccine development. J. Biol. Chem. 287 (38), 31618–31622.

JVI Journals.ASM.org

Foot-and-Mouth Disease Virus Modulates Cellular Vimentin for Virus Survival

D. P. Gladue,[a] V. O'Donnell,[a] R. Baker-Branstetter,[a] L. G. Holinka,[a] J. M. Pacheco,[a] I. Fernández Sainz,[a] Z. Lu,[b] X. Ambroggio,[c] L. Rodriguez,[a] M. V. Borca[a]

Plum Island Animal Disease Center, ARS, USDA, Greenport, New York, USA[a]; Plum Island Animal Disease Center, DHS, Greenport, New York, USA[b]; Bioinformatics and Computational Biosciences Branch, NIAID, NIH, Bethesda, Maryland, USA[c]

Foot-and-mouth disease virus (FMDV), the causative agent of foot-and-mouth disease, is an Aphthovirus within the *Picornaviridae* family. During infection with FMDV, several host cell membrane rearrangements occur to form sites of viral replication. FMDV protein 2C is part of the replication complex and thought to have multiple roles during virus replication. To better understand the role of 2C in the process of virus replication, we have been using a yeast two-hybrid approach to identify host proteins that interact with 2C. We recently reported that cellular Beclin1 is a natural ligand of 2C and that it is involved in the autophagy pathway, which was shown to be important for FMDV replication. Here, we report that cellular vimentin is also a specific host binding partner for 2C. The 2C-vimentin interaction was further confirmed by coimmunoprecipitation and immunofluorescence staining to occur in FMDV-infected cells. It was shown that upon infection a vimentin structure forms around 2C and that this structure is later resolved or disappears. Interestingly, overexpression of vimentin had no effect on virus replication; however, overexpression of a truncated dominant-negative form of vimentin resulted in a significant decrease in viral yield. Acrylamide, which causes disruption of vimentin filaments, also inhibited viral yield. Alanine scanning mutagenesis was used to map the specific amino acid residues in 2C critical for vimentin binding. Using reverse genetics, we identified 2C residues that are necessary for virus growth, suggesting that the interaction between FMDV 2C and cellular vimentin is essential for virus replication.

Foot-and-mouth disease (FMD), a highly contagious viral disease of cattle, pig, sheep, goats, and wild cloven-hoofed animals, is caused by foot-and-mouth disease virus (FMDV), a single-stranded positive-sense RNA virus. There are seven serotypes (A, O, C, Asia, SAT1, SAT2, and SAT3) of FMDV that do not offer cross-protection (1, 2). Four structural proteins (VP1, VP2, VP3, and VP4) comprise the infectious nonenveloped icosahedral virion. The genome has a single large open reading frame (ca. 7,000 nucleotide [nt]), which is translated to make the polyprotein which is processed by the two viral proteases Lpro and 3C and by a ribosomal skip mechanism in 2A into the polypeptide products L, P1-2A, P2 (2B and 2C), and P3 (3A, 3B1-3, 3Cpro, and 3Dpol). Further cleavage of these regions yields 14 mature virus proteins, along with several protein intermediates, that are critical for viral replication (3, 4).

During replication, FMDV causes several rearrangements of intracellular membranes, resulting in vesicular structures that contain viral proteins, which are part of the replication complex. Replication complexes have been associated with many other positive-strand RNA virus infections (5–11). FMDV has been shown to modulate the autophagosome pathway through the interaction of FMDV 2C with a central cell regulator of autophagy, Beclin1 (12). FMDV 2C, a 318-amino-acid protein, has also been shown to play a role in disruption of the Golgi-ER secretory pathway (13). However, it is possible that 2C can play multiple roles in the process of virus replication and that 2C may interact with several host cellular factors during infection. To gain insight into possible cellular factors that could interact with 2C helping to form these replication structures, we have been utilizing a yeast two-hybrid approach to identify host cell proteins that interact with 2C. We recently reported that cellular Beclin1 is a natural ligand of 2C and that it is involved in the process of autophagy which was shown to be important for FMDV replication (12, 14). We now report that cellular vimentin is also a specific binding partner for viral 2C. Vimentin is a class III intermediate filament (IF), a predominant IF in cells of the vascular endothelium. Vimentin has been shown to be associated with several cellular organelles, including autophagosomes, and to have a role in lysosomal degradation of proteins (15, 16).

Vimentin has been shown to be important during the replication cycle of various viruses. It is involved in the process of viral entry of cowpea mosaic virus (17) and Japanese encephalitis virus (18) and in the viral egress of bluetongue virus (19). It has also been implicated in the process of viral replication of vaccinia virus (20) and dengue virus (21). Although the significance is not clear, vimentin is cleaved in cells infected with human immunodeficiency viruses (22) and adenovirus type 2 (23), and its transcription significantly increases during infection with human T-cell leukemia virus type I (24). In addition, in cells infected with African swine fever virus (25) or iridovirus frog virus 3 (26), vimentin surrounds virus factories. These vimentin "cage-like" structures containing viral proteins have been shown to be important for virus survival (25). It is also possible that vimentin serves a potential protective host function, as vimentin has been implicated to be involved in the isolation and clearance of misfolded proteins in cells (15, 27). In addition, vimentin has a possible involvement in

Received 26 February 2013 Accepted 29 March 2013
Published ahead of print 10 April 2013
Address correspondence to M. V. Borca, pmanuel.borca@ars.usda.gov.
Copyright © 2013, American Society for Microbiology. All Rights Reserved.
doi:10.1128/JVI.00448-13

Downloaded from http://jvi.asm.org/ on June 3, 2013 by DigiTop -USDA's Digital Desktop Library

the autophagy pathway since it plays an important role in positioning autophagosomes, lysosomes, and the Golgi complex within the cell (15).

In this report we further examine the 2C-vimentin interaction identified by yeast two-hybrid analysis, confirming by coimmunoprecipitation that this interaction occurs in FMDV-infected cells. Immunofluorescence staining in FMDV-infected cells revealed transient formation of a vimentin cage structure that surrounds FMDV protein 2C. Importantly, expressing a dominant-negative (DN) form of vimentin resulted in the disruption of the physiological disposition of vimentin and in a significantly decreased ability for FMDV to replicate, suggesting that interaction with vimentin plays an important and necessary role during viral infection. In addition, the site of interaction in the 2C protein that is responsible for binding to vimentin was mapped by alanine scanning mutagenesis. Using reverse genetics it was shown that changes to amino acid residues of 2C responsible for binding vimentin are clearly detrimental for virus replication. This further supports the hypothesis that 2C binding to vimentin may play a significant and necessary role for virus replication.

MATERIALS AND METHODS

Cell lines, viruses, and plasmids. Human mammary gland epithelial cells (MCF-10A) were obtained from the American Type Culture Collection (catalogue no. CRL-10317) and maintained in a mixture of Dulbecco minimal essential medium (DMEM; Life Technologies) and F-12 Ham media (1:1; Life Technologies, Grand Island, NY) containing 5% heat-inactivated fetal bovine serum (HI-FBS, Thermo Scientific, Waltham, MA), 20 ng of epidermal growth factor (Sigma-Aldrich, St. Louis, MO)/ml, 100 ng of cholera toxin (Sigma-Aldrich)/ml, 10 μg of insulin (Sigma-Aldrich)/ml, and 500 ng of hydrocortisone (Sigma-Aldrich)/ml.

FMDV type O1 strain Campos (FMDV O1C) was derived from the vesicular fluid of an experimentally infected steer. The virus was amplified once in baby hamster kidney-21 (BHK-21) cells, and the titer determined by plaque assay on (BHK) cells using standard techniques (14).

Plasmids vimentin-HA and vimentin DN-HA were generously donated by Stewart Martin's laboratory (University of Maryland School of Medicine, Baltimore, MD). Plasmid phrGFP II-N mammalian expression vector is commercially available (Agilent Technologies, Santa Clara, CA).

For viral replication studies, MCF-10A cells were plated at a density of 10^6 per well in a six-well plate (Falcon; Becton Dickinson Labware, Franklin Lakes, NJ). Indicated plasmids were transfected into cells using FuGene (Roche Applied Science, Indianapolis, IN) according to the manufacturer's protocol. After 24 h, the cells were infected with FMDV O1C at the specified multiplicity of infection (MOI) or mock infected. Virus was allowed to adsorb for 1 h, followed by an acid wash with ice-cold 145 mM NaCl–25 mM MES (morpholineethanesulfonic acid; pH 5.5) to remove residual virus particles and the addition of fresh medium containing 0.5% HI-FCS. Samples were taken at the indicated time points.

Antibodies and reagents. Monoclonal antibody (MAb) 3D10, directed against the FMDV O1 nonstructural protein 2C, was developed in the Istituto Zooprofilattico Sperimentale della Lombardia e dell Emilia-Romagna, Brescia, Italy. The vimentin-specific MAb for staining and coimmunoprecipitation was from Sigma-Aldrich (V6630). The MAb specific for the hemagglutinin (HA) tag used for Western blot analyses was produced by Millipore (clone DW2). The actin-specific MAb was from Millipore (MAb1501). Acrylamide (Sigma-Aldrich) was made as a 4 M stock in water and diluted in media to the indicated concentrations. Nocodazole (Sigma-Aldrich) was made as a 40 mM stock and diluted to the indicated concentrations. Cell proliferation kit I (MTT; Roche catalog no. 11465007001) analysis was performed according to the manufacturer's instructions.

Infection and transfection of cells for immunofluorescence staining. Subconfluent monolayers of MCF-10A cells grown on 12-mm glass coverslips in 24-well tissue culture dishes were transfected with the indicated plasmids. After 24 h, they were infected with FMDV O1C at an MOI of 10 in minimum essential medium (MEM; Life Technologies, Grand Island, NY) containing 0.5% HI-FBS, 25 mM HEPES (pH 7.4), and 1% antibiotics. After the 1-h adsorption period, the supernatant was removed, and the cells rinsed with ice-cold 2-morpholinoethanesulfonic acid (MES) buffered saline (25 mM MES [pH 5.5], 145 mM NaCl) to remove unadsorbed virus. The cells were washed once with medium before fresh medium was added and then incubated at 37°C and 5% CO_2. At the indicated time points after infection, the cells were fixed with 4% paraformaldehyde (EMS, Hatfield, PA) and analyzed by immunofluorescence staining. To express HA-vimentin, HA-DN-vimentin, or green fluorescent protein (GFP) protein, monolayers of MCF-10A cells were transfected with 0.5 μg of plasmid DNA using FuGene (Roche, Mannheim, Germany), according to the manufacturer's recommendations. At 19 to 24 h posttransfection, the cells were infected as described above and then fixed with 4% paraformaldehyde (EMS) at the appropriate times.

After 15 min of fixation, the paraformaldehyde was removed, and the cells were permeabilized with 0.5% Triton X-100 for 5 min at room temperature, followed by incubation in blocking buffer (phosphate-buffered saline [PBS], 5% normal goat serum, 2% bovine serum albumin, 10 mM glycine, 0.01% Thimersal) for 1 h at room temperature. The fixed cells were then incubated with the primary antibodies overnight at 4°C. When double labeling was performed, cells were incubated with both antibodies together. After being washed three times with PBS, the cells were incubated with the appropriate secondary antibody, goat anti-rabbit immunoglobulin G (IgG) (1/400; Alexa Fluor 594 or Alexa Fluor 647; Molecular Probes), goat anti-mouse isotype-specific IgG (1/400; Alexa Fluor 488 or Alexa Fluor 594; Molecular Probes), for 1 h at room temperature. After this incubation, the coverslips were washed three times with PBS, counterstained with the nuclear stain TOPRO-iodide 642/661 (Molecular Probes) or DAPI (4′,6′-diamidino-2-phenylindole; Life Technologies, Grand Island, NY) for 5 min at room temperature, washed as before, mounted, and examined using a Nikon Eclipse 90i microscope. The data were collected utilizing appropriate prepared controls lacking the primary antibodies, as well as using anti-FMDV antibodies in uninfected cells to give the negative background levels and to determine channel crossover settings. The captured images were adjusted for contrast and brightness using Adobe Photoshop software.

Coimmunoprecipitation of FMDV 2C and vimentin. MCF-10A cells were grown to 90% confluence and then infected with a MOI of 10 or mock infected. Cells were lysed at 2.5 h postinfection using protease inhibitors (Protea Biosciences, Morgantown, WV) and radioimmunoprecipitation assay (RIPA) buffer (Teknova, Hollister, CA). For immunoprecipitation the protein lysate was incubated with protein G-beads (Sigma-Aldrich) precoupled to a MAb directed against vimentin (Sigma-Aldrich V6630). The cell lysate was incubated with anti-vimentin antibody for 2.5 h and then incubated with the antibody and beads overnight at 4°C. The beads were washed five times using RIPA buffer, and then protein elutes were collected for each sample and examined by Western blotting probing for anti-2C (3D10).

Library screening. A bovine cDNA expression library was constructed (12), where cellular proteins were expressed as GAL4-AD fusion proteins. The GAL4-based yeast two-hybrid system provides a transcriptional assay for detection of protein-protein interactions (28, 29). The bait protein, FMDV O1C 2C protein, was expressed with an N-terminus fusion to the GAL4-binding domain (BD). Full-length 2C protein (amino acids 1082 to 1399 of the FMDV polyprotein) was used for screening and for full-length mutant protein construction. Screening used FMDV 2C as bait and testing of positive clones recovered from the bovine library was done (12). The vimentin recovered from the library matched bovine vimentin (NCBI reference sequence NP_776394.2).

Western blot quantification. To quantify Western blots, we used ImageJ software provided by http://imagej.nih.gov/ij/ (30). Actin was used as a loading control. To calculate the percentage of vimentin in each sample the relative density of vimentin was divided by the relative density of actin.

Downloaded from http://jvi.asm.org/ on June 3, 2013 by DigiTop -USDA's Digital Desktop Library

Site-directed mutagenesis. Full-length pO1Ca (31) or 2C-BD was used as a template in which amino acids were substituted with alanine, introduced by site-directed mutagenesis using QuikChange XL site-directed mutagenesis (Stratagene, Cedar Creek, TX) performed according to the manufacturer's instructions (12).

Primers were designed using the manufacturer's primer design program (https://www.genomics.agilent.com/CollectionSubpage.aspx?PageType=Tool&SubPageType=ToolQCPD&PageID=15), which limited us to a maximum of seven amino acid changes and provided the rationale for deciding on the regions to be mutated.

Construction of mutant FMDV viruses. Plasmid pO1Ca or its mutant version was used as a template for RNA synthesis (12). BHK-21 cells were transfected with these synthetic RNAs by electroporation (Electrocell Manipulator 600; BTX, San Diego, CA) (31, 32). The supernatants from transfected cells were passed in LF-BK αVβ6 cells until a cytopathic effect (CPE) appeared or until a minimum of four blind passages was performed and no evidence of CPE was observed. After successive passages in these cells, virus stocks were prepared and the viral genome completely sequenced using the Prism 3730xl automated DNA sequencer (Applied Biosystems) (31).

Bioinformatic analysis of FMDV 2C. The FMDV 2C amino acid sequence was queried with BLAST (33) and HHpred (34) against the PDB and HHpred PDB70 database, respectively. The BLAST search of the 2C amino acids sequence against the PDB resulted in a match between residues 85 and 177 of 2C with residues 4 to 91 of a putative fructose transport system kinase protein from *Silicibacter* (*Silicibacter* fructokinase) with an E value of 0.17. HHpred identified two viral AAA+ ATPases, the simian virus 40 large T antigen (simian virus 40 LT) and adeno-associated virus 2 REP40 (Aav2 Rep40) protein, with E values of 2.5E−08 and 2.5E−06, respectively. For the former, the identified region of homology began at amino acid 109 of 2C, whereas for the latter, it began at amino acid 18. We used a structural alignment of the monomeric units of *Silicibacter* fructokinase (PDB ID 3C8U), SV40 LT (PDB ID 1SVM), and Aav2 Rep40 (1U0J) and the sequence alignment of 2C with *Silicibacter* fructokinase and Aav2 Rep40. These crystal structures were superposed using LSQMAN, from which a structure-based sequence alignment was extracted. Alanine scanning blocks 12 and 13 were mapped, respectively, to the exposed loop preceding helix 0 of the AAA+ domain of the SV40 LT crystal structure (residues 395 to 400) and the first half of this helix (residues 401 to 407).

RESULTS

FMDV nonstructural 2C protein interacts with the bovine host protein vimentin. Nonstructural FMDV 2C is a highly conserved (>85% identity) 318-amino-acid protein, essential for virus replication (1, 31). This high degree of conservation suggests a possible essential function during virus infection.

A yeast two-hybrid system (35) was used to identify interactions between host cellular proteins and FMDV 2C protein (12). An N-terminal fusion of the Gal4 protein DNA-binding domain (BD) with FMDV 2C protein from FMDV O1C was used as "bait". For "prey" we used a custom cDNA library that was derived from RNA extracted from FMDV-susceptible bovine tissues expressed as N-terminal fusion of the Gal4 activation domain (AD). Library screening was performed as described by Gladue et al. (35). One specific protein binding partner for 2C, vimentin (NCBI reference sequence NP_776394.2) (Fig. 1A), was selected for further study due to its potential involvement in the rearrangement of intracellular membranes (36–38) and positioning of autophagosomes (15, 39), both processes known to be important in FMDV replication (12–14).

Coimmunoprecipitation and immunofluorescence staining were used to confirm that the interaction identified using the two-hybrid system in yeast actually occurs during FMDV infection of host cells. Coimmunoprecipitation experiments were performed using cell lysates from FMDV-infected human epithelial cell line MCF-10A, an FMDV-susceptible cell line which allows for use of MAbs recognizing human proteins, and MAbs specifically recognizing FMDV 2C and vimentin. MCF-10A cells were infected with an MOI of 1 of FMDV O1C, and samples were harvested at 1.5 to 2 h postinfection (hpi), the time point when 2C is beginning to accumulate in MCF-10A cells as previously confirmed by Western blotting (12). MCF-10A cell lysates were collected from infected

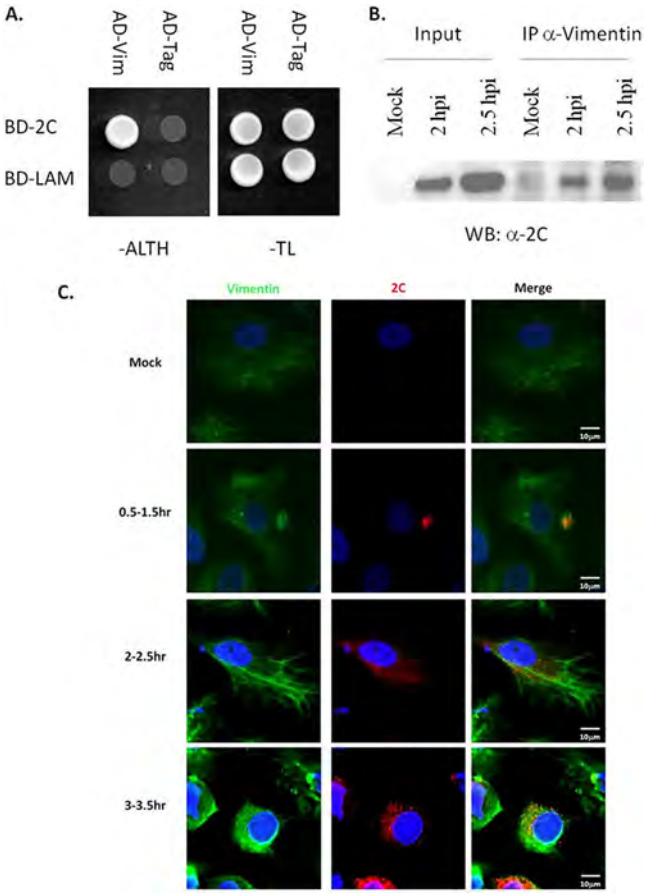

FIG 1 Protein-protein interaction of FMDV 2C with bovine vimentin in the yeast two-hybrid system (A), coimmunoprecipitation (B), and immunofluorescence staining (C). (A) Yeast strain AH109 was transformed with GAL4-binding domain (BD) fused to FMDV 2C (BD-2C) or a negative control, human lamin C (BD-LAM). These strains were then transformed with GAL4 activation domain (AD) fused to vimentin (AD-Vim) or T antigen (AD-Tag) as indicated above each lane. Spots of strains expressing the indicated constructs containing 2×10^6 yeast cells were spotted on selective media to screen for protein-protein interaction in the yeast two-hybrid system: either SD Ade/His/Leu/Trp plates (ALTH) or nonselective SD_Leu/Trp (_TL) for plasmid maintenance only. (B) Western blot probing for FMDV 2C (~40 kDa). Input cell lysate from mock-infected or FMDV-infected (at 2 and 2.5 hpi) preparations. Coimmunoprecipitation of FMDV 2C from mock-infected or FMDV O1C-infected (at 2 and 2.5 hpi) cell lysates performed using a MAb specific to vimentin. (C) Analysis of the distribution of vimentin and FMDV 2C proteins in MCF-10A cells. Cells were infected or mock infected with FMDV O1C and processed by immunofluorescence staining as described in Materials and Methods. FMDV 2C was detected with MAb 3D10 and visualized with Alexa Fluor 594 (red). Vimentin was detected with MAb V6630 and visualized with Alexa Fluor 488 (green). Yellow indicates colocalization of Alexa Flour 594 and 488 in the merged image.

Downloaded from http://jvi.asm.org/ on June 3, 2013 by DigiTop -USDA's Digital Desktop Library

or mock-infected cells and immunoprecipitated with an anti-vimentin MAb (V6630), followed by a Western blot specific for FMDV 2C protein (3D10). A single band was observed at the correct molecular mass (40 kDa) for 2C, indicating that 2C and vimentin interact during FMDV infection, confirming the results obtained by the yeast two-hybrid methodology (Fig. 1B). Several attempts were made to do the reverse coimmunoprecipitation methodology by pulling down FMDV protein 2C and blotting for vimentin; however, the vimentin band is masked by a background band belonging to the immunoglobulin heavy chain of the MAb used in the immunoprecipitation step, so the results were inconclusive.

Vimentin forms a cage-like structure around 2C. To further confirm that vimentin interacts with 2C during FMDV infection, we analyzed the location of both proteins at different times postinfection by using double-label immunofluorescence in cells that were infected with FMDV. MCF-10A cells were infected with an MOI of 10 or mock infected with FMDV O1C. Cells were then fixed on glass coverslips at 30-min intervals after infection up to 4 hpi and stained using MAbs that exhibit specific fluorescence for either FMDV 2C or vimentin (3D10 and V6630, respectively). The results indicated that there was a clear transitory colocalization of FMDV 2C and vimentin proteins between 0.5 and 1.5 hpi, with vimentin forming a cage-like structure around 2C in all cells infected with FMDV (Fig. 1C). Interestingly, similar cage-like structures formed by vimentin-associated virus proteins have been observed in cells infected with African swine fever virus, vaccinia virus, and some iridoviruses (25, 40, 41). Therefore, initial results obtained by yeast two-hybrid showing interaction between virus 2C and cellular vimentin were confirmed in FMDV-infected cells by two independent methodologies.

Vimentin is degraded in FMDV-infected cells. To determine whether FMDV infection by itself has an effect on the levels of vimentin expression, MCF-10A cells were infected with an MOI of 1 with FMDV O1C, and cell lysates were collected every 30 min during the course of infection up to 4 hpi. Samples were tested by Western blotting (Fig. 2A), and the expression levels of vimentin in the cell lysates were quantified using ImageJ software (obtained from the National Center for Biotechnology Information) using the recommended procedure to calculate relative density compared to a treated control (Fig. 2B). Expression of endogenous levels of actin was used to normalize vimentin values. The results demonstrated transitory increasing amounts (~20 to 40%) of vimentin in the infected cells between 1.5 to 3 hpi, with a decrease after 3 hpi. Accordingly, vimentin degradation products (50, 46, and 29 kDa) began to appear at 2.5 hpi, increasing for the remainder of the infection, possibly suggesting that this degradation could be how the vimentin cage is resolved after the initial formation around 2C.

Expression of dominant-negative forms of vimentin decrease viral yield. To assess the role of vimentin in FMDV replication we attempted to manipulate the levels of vimentin in infected cells. MCF-10A cells were transfected with either a plasmid encoding a full-length vimentin gene (HA-vimentin), used to increase cellular levels of vimentin, or a truncated form of the vimentin gene (HA-DN-vimentin, truncated at amino acid residue 134 compared to the full-length vimentin at 466 amino acids) that acts as a dominant-negative form of vimentin (42–44), to disrupt vimentin function. Both constructs had an HA tag for detection of the respective protein products by Western blotting. Cell lysates

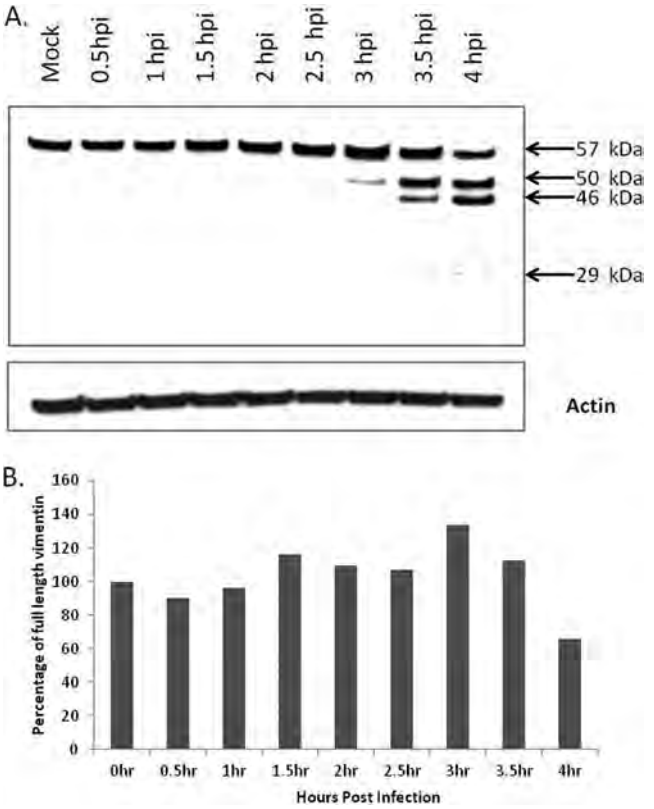

FIG 2 Analysis of vimentin expression in FMDV-infected MCF-10A cells. (A) Cells were infected with FMDV O1C and at different times postinfection, cell were lysed in RIPA buffer and assessed by Western blotting with a specific MAb V6630 vimentin. Full-length Vimentin is ~57 kDa, and the breakdown fragments are 50, 46, and 29 kDa, as indicated by the arrows. Actin (MAb1501) is shown as a loading control. (B) Quantification of vimentin bands in a representative Western blot shown in panel A using ImageJ analysis software using actin levels to normalize each sample.

were taken 19 h after transfection and assessed by Western blotting for HA (Fig. 3B), demonstrating the expression of either construct (Fig. 3B). Furthermore, MCF-10A cells overexpressing HA-vimentin, HA-DN-vimentin or a control plasmid containing GFP were infected 19 h posttransfection infected with an MOI of 0.1 with FMDV O1C and virus yields in the extracellular medium were assessed at 0, 5, and 24 hpi. The results demonstrated that while overexpression of vimentin does not affect virus replication, cells overexpressing the dominant-negative form of vimentin presented a significant reduction (>2 logs) in virus titer compared to cells overexpressing full-length vimentin or an GFP-expressing control (Fig. 3A).

To determine whether the decrease in viral replication in the presence of a dominant-negative form of vimentin was related to the inability of the vimentin cage to form around 2C during infection, double-label immunofluorescence microscopy against 2C and vimentin in cells overexpressing truncated forms of vimentin and infected with FMDV was performed. HA-DN-vimentin-transfected MCF-10A cells were infected with an MOI of 10 or mock infected with FMDV O1C. Cells were then fixed on glass coverslips at the indicated time points and stained using MAbs that demonstrate specific fluorescence for either FMDV 2C or vimentin (Fig. 3C). The results indicated that the vimentin cage

Downloaded from http://jvi.asm.org/ on June 3, 2013 by DigiTop -USDA's Digital Desktop Library

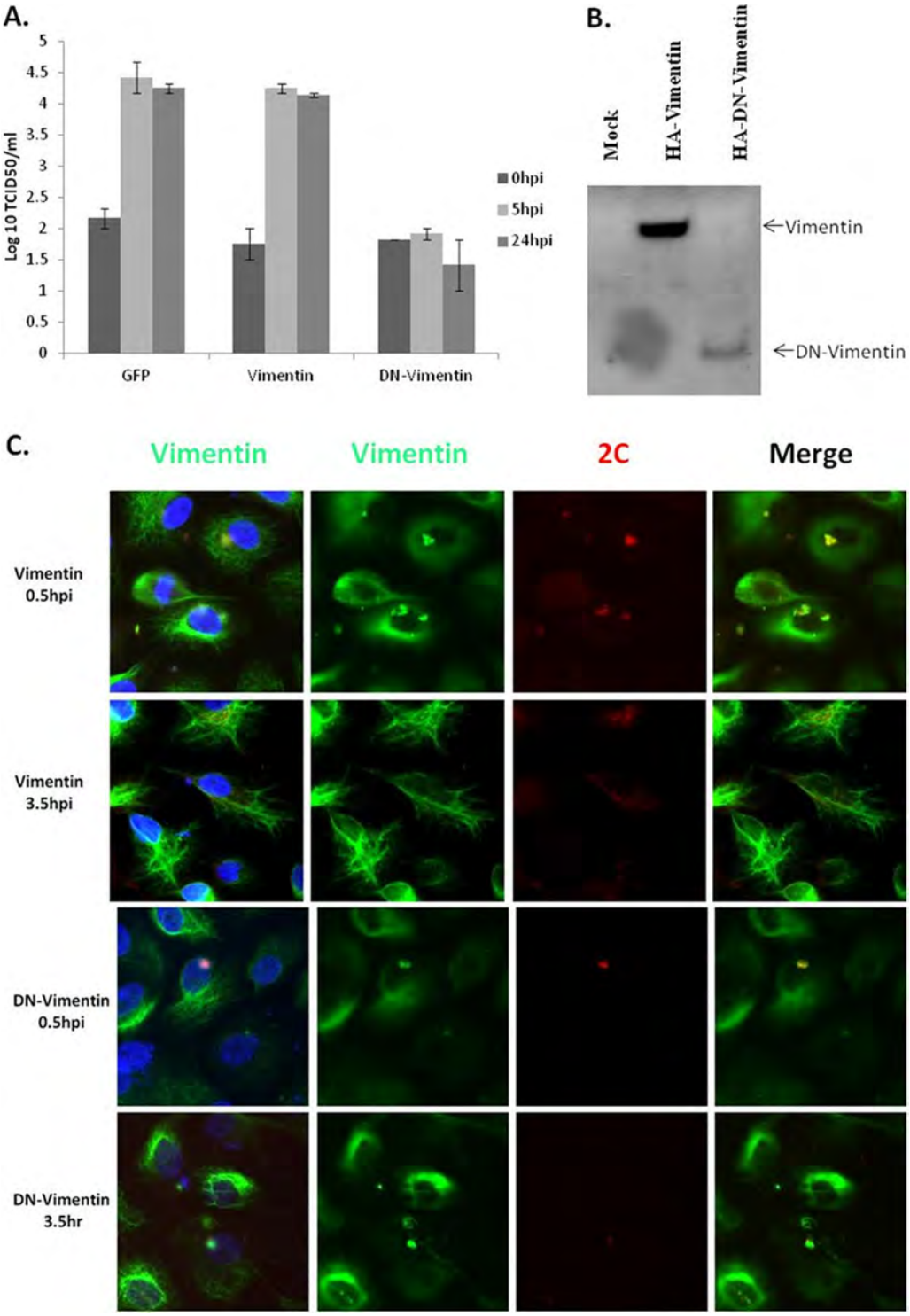

FIG 3 Effect of vimentin or truncated forms of vimentin on FMDV replication. MCF-10A cells were transfected with a plasmid encoding vimentin (pvimentin-HA), DN-vimentin (pDN-vimentin-HA), or GFP (pGFP) and then at 19 h posttransfection were infected with an MOI of 10 with FMDV O1C. (A) Virus yield is expressed as the $\log_{10}$ 50% tissue culture infective doses ($TCID_{50}$)/ml. Each value represents the mean and standard deviation from two independent experiments. The sensitivity of virus detection was $\geq\log_{10}$ 1.8 $TCID_{50}$/ml. (B) Expression levels of vimentin and DN-vimentin detected by Western blotting using an anti-HA MAb (DW2), with the correct predicted sizes of ~57 kDa for vimentin and 15 kDa for DN-vimentin. (C) Analysis of the distribution of vimentin and FMDV 2C proteins at different times postinfection. Cells were processed by immunofluorescence staining as described in Materials and Methods. FMDV 2C was detected with MAb 3D10 and visualized with Alexa Fluor 594 (red). Vimentin was detected with MAb V6630 and visualized with Alexa Fluor 488 (green). Yellow indicates colocalization of Alexa Flour 594 and 488 in the merged image.

Downloaded from http://jvi.asm.org/ on June 3, 2013 by DigiTop -USDA's Digital Desktop Library

was formed in the presence of a dominant-negative form of vimentin at 0.5 hpi as it happens in a normal viral infection. However, the vimentin cage, which is normally resolved by 2 hpi, remained unaltered in cells containing the DN form of vimentin at least until 4 hpi. At 4 hpi, an apparent decrease in the intensity of 2C fluorescence was observed in vimentin cages, with some vimentin cages having undetectable levels of 2C, suggesting that 2C could be degraded if the cage is not resolved. Therefore, expression of a DN form of vimentin appears to correlate with permanence of the vimentin cage and a significant reduction in viral yield.

An intact vimentin but not microtubule pathway is required for FMDV replication. Vimentin has a radial organization, where filaments typically extend outward from the cell center and it has been shown that vimentin structures can move on microtubules (45, 46). Since expression of truncated forms of vimentin has a significant effect on virus replication, it is interesting to evaluate whether the integrity of the endogenous vimentin and associated structures directly affect FMDV replication. To assess this issue, we carried out pharmacological experiments using nocodazole and acrylamide, which specifically disrupt the microtubules and the vimentin intermediate filament networks, respectively (47, 48). Mock-treated MCF-10A cells present an intact vimentin structure dispersed throughout the cytoplasm, while in the presence of nocodazole there was a redistribution of vimentin toward the nucleus (Fig. 4B). This observation concurs with a previous study showing that vimentin intermediate filaments are organized by the microtubule network (48). The addition of acrylamide causes the disruption of vimentin. This effect was observed in MCF-10A cells treated with acrylamide (Fig. 4B).

To test the effect of the changes of vimentin distribution on virus replication, MCF-10A cells were pretreated for 30 min with either nocodazole or acrylamide and then infected with an MOI of 0.1 of FMDV O1C (Fig. 4A). Interestingly, treatment with nocodazole had no significant effect on viral replication, agreeing with previous studies (49). However, treatment with 400 μM acrylamide resulted in a consistent 10-fold decrease in virus titers. Assessment of cell viability after acrylamide treatment demonstrated a viability of 94.5% ± 0.03%, by using an MTT assay. Thus, vimentin disruption resulted in decreased virus titers, supporting the hypothesis that an intact vimentin network is required for viral replication while disruption of the microfilament network has no effect on FMDV replication.

Alanine scanning of FMDV 2C reveals binding site for vimentin. To evaluate the importance of the binding between 2C and vimentin to FMDV replication, we tried to identify amino acid residues within 2C that directly mediate the interaction with vimentin. To determine the binding site(s) for vimentin present in 2C, an alanine scanning mutagenesis approach was used. Using site-directed mutagenesis, 46 mutant 2C proteins were constructed (35) in the yeast two-hybrid system to contain a stretch of seven amino acids that were changed from their native amino acid to alanine residues (Fig. 5A). Each of these mutated 2C proteins were assessed in their ability to bind vimentin in the yeast two-hybrid system. 2C proteins containing mutations in areas 12 and 13 were unable to bind vimentin (Fig. 5B). To ensure that all 2C alanine mutants were still able to be expressed in the yeast two-hybrid system, protein Beclin-AD (12) (another host protein that was detected as a binding partner for 2C) was used as an internal control. Beclin-AD was able to interact with all 2C mutants lacking vimentin binding, demonstrating that mutating these areas specifically interrupted the binding between vimentin and 2C.

Binding between FMDV 2C and host vimentin appears critical for virus replication. Reverse genetics was used to assess the effect of 2C mutations identified as critical in mediating the interaction between 2C and vimentin. Infectious clones (ICs) of FMDV O1C (31) containing areas of 2C harboring the same alanine substitutions shown to alter 2C-vimentin reactivity in the yeast two-hybrid were constructed. Those IC constructs were then used to produce the corresponding RNAs by *in vitro* transcription, which were then used in cell transfections to produce their respective FMDV progeny. Although transfection with parental FMDV O1C RNA produced viable virus progeny, mutants 2C-12 and 13 (Fig. 5A) consistently produced nonviable virus. It is possible that these mutations, besides altering the reactivity with vimentin, could be detrimental to the virus for other as yet unidentified reasons. Therefore, a more detailed mapping of the area of interaction between vimentin and 2C was performed with the aim of reducing the number of amino acids mutated and still disrupt the interaction. The regions in 2C-12 and 13 were further subdivided into three separate subareas (comprising two to three residues each), which were individually assessed in their reactivity with vimentin in the yeast two-hybrid system (Fig. 5C). However, none of the smaller mutated regions resulted in the lost ability to bind vimentin, suggesting that multiple contact points within the seven residue stretch is needed for disruption of 2C binding to vimentin.

DISCUSSION

The complex cellular pathways and mechanisms that FMDV manipulates to facilitate viral replication and to evade host defenses are not completely understood. One potential mechanism FMDV may use to manipulate the host cell involves interaction with cellular proteins to modify their function, thus changing the natural cellular pathway. For example, we previously demonstrated that FMDV 2C could manipulate the autophagy pathway by binding to Beclin1, resulting in the inability of autophagosomes to fuse with lysosomes, favoring virus survival. We report here that FMDV nonstructural protein 2C binds to host class III intermediate filament vimentin. A yeast two-hybrid model was used to identify vimentin as a specific protein binding partner for viral 2C. We also demonstrated coimmunoprecipitation of 2C with vimentin from FMDV-infected cell extracts as well as colocalization of 2C with vimentin in cells infected with FMDV.

The importance of vimentin during viral infection has been described in a wide range of viruses. For example, in cowpea mosaic virus and Japanese encephalitis virus (JEV), surface-expressed vimentin is necessary for efficient viral entry (18, 50, 51). An increase of vimentin expression is observed during infection with Hepatitis C virus (HCV) (52), T-cell leukemia virus type I (24) and rabies virus (RV) (53). Alternatively, during infection with retroviruses, including human immunodeficiency viruses and bovine leukemia virus (BLV), the viral-encoded protease specifically cleaves vimentin; however, the function of vimentin cleavage is still unknown (22, 54, 55). It is possible that vimentin is cleaved to change the global cell structure or to prevent intracellular cell signaling as seen with Epstein-Barr virus protein LMP1 which causes the disruption of vimentin to modulate cell signaling (56). Studies of other viruses have shown that viral proteins directly bind vimentin as observed with dengue virus nonstructural protein 1, where vimentin binding is critical for virus replication (57),

Downloaded from http://jvi.asm.org/ on June 3, 2013 by DigiTop -USDA's Digital Desktop Library

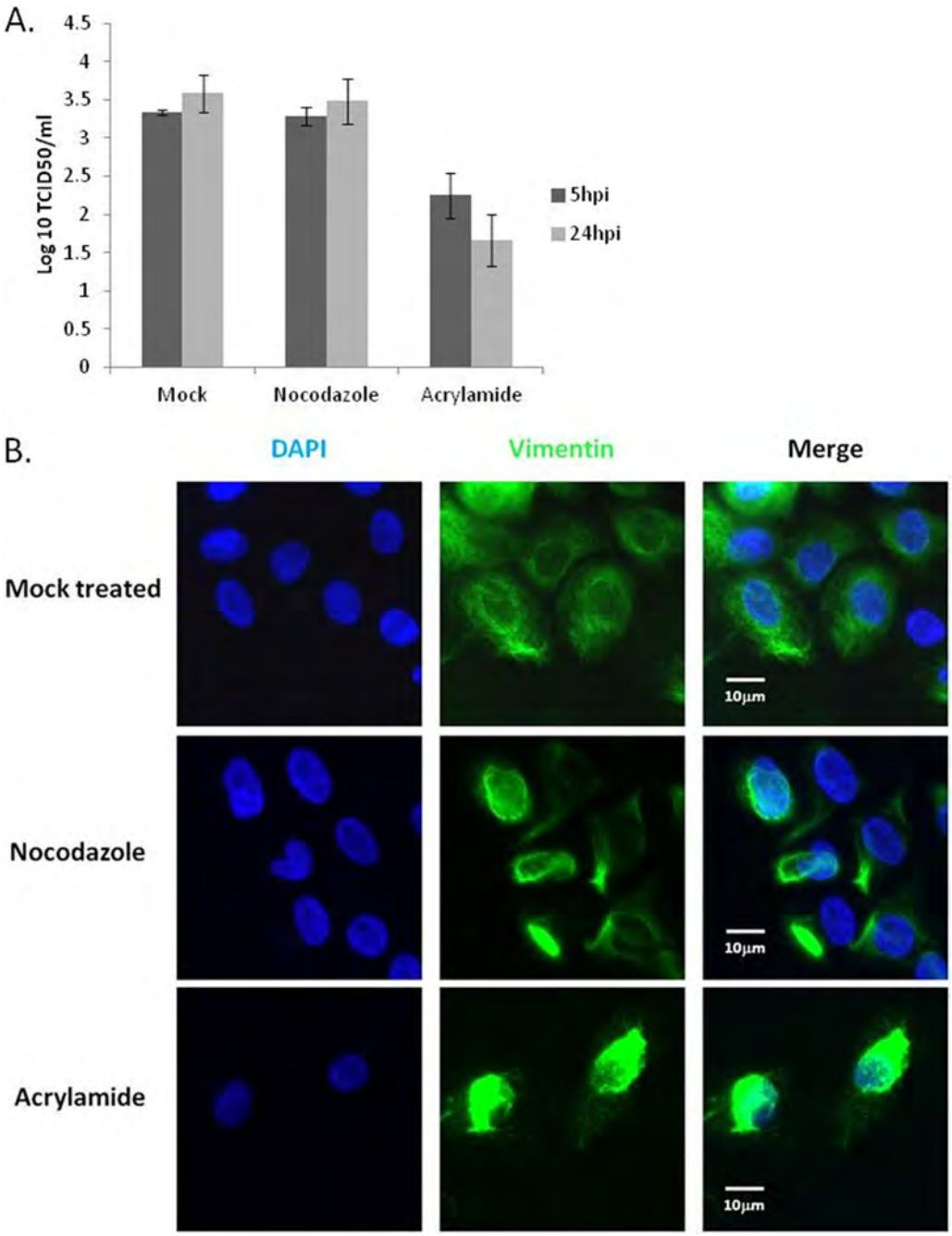

FIG 4 Effect of nocodazole and acrylamide treatment on MCF-10A cell cultures infected with FMDV. MCF-10A cell cultures were treated with either drug for 1 h and then infected with FMDV 01C infected with an MOI of 0.1. (A) Virus yield was assessed at the indicated times postinfection and expressed as $\log_{10}$ $TCID_{50}$/ml. Each value represents the mean and standard error from two independent experiments. The sensitivity of virus detection was $\geq\log_{10}$ 1.8 $TCID_{50}$/ml. (B) Analysis of the distribution of vimentin in MCF-10A cells treated with either nocodazole (5 μm) or acrylamide (400 μm). Cells were treated and then processed by immunofluorescence staining as described in Materials and Methods using a vimentin-specific MAb (V6630) and visualized with Alexa Fluor 488 (green).

and in bluetongue virus protein VP2, where binding of vimentin is necessary for viral egress (19). In African swine fever virus, it has been shown that vimentin is arranged around viral factories, forming a cage-like structure, which may aid to isolate viral proteins from the rest of the cell (25).

In previous studies by Armer et al. (5), some degree of vimentin rearrangement was observed with FMDV, but their studies were limited to time points late during infection, where they observed a lack of vimentin in areas of the cell cytoplasm where virus was being produced. We observed that early during infection, starting at 0.5 hpi, cellular vimentin colocalized and formed a cage-like structure around FMDV protein 2C, and that later during infection this cage-like structure disappeared as viral infection progressed. We also observed that as infection progressed, vimen-

Downloaded from http://jvi.asm.org/ on June 3, 2013 by DigiTop -USDA's Digital Desktop Library

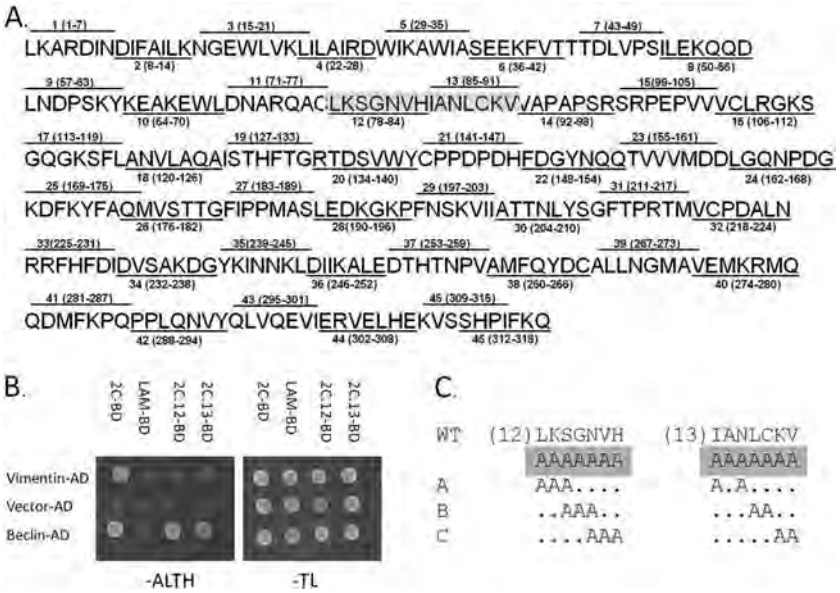

FIG 5 Scheme showing FMDV 2C alanine mutants used in the present study. (A) Each alanine 2C mutant name is followed, in parentheses, by the amino acid residues mutated for that mutant. All indicated residues were mutated to an alanine. The highlighted 2C mutants represent mutations that resulted in lack of binding of 2C to vimentin in the yeast two-hybrid system. (B) Yeast strain AH109 was transformed with either GAL4-binding domain (BD) fused to FMDV 2C (2C-BD), the indicated FMDV 2C mutation, or as a negative control human lamin C (LAM BD). These strains were then transformed with GAL4 activation domain (AD) fused to vimentin (Vimentin-AD) or Beclin1 (Beclin1-AD) as indicated above. Strains expressing the indicated constructs containing 2×10^6 yeast cells were spotted onto selective media to evaluate protein-protein interaction in the yeast two-hybrid system, using either SD−Ade/His/Leu/Trp plates (−ALTH) or nonselective SD−Leu/Trp plates (−TL) for plasmid maintenance only. (C) Subdivisions (labeled A, B, and C) of the original alanine scanning mutants 12 and 13.

tin degradation occurred, possibly explaining the previously observed vimentin rearrangement at late time points during infection (33).

To determine whether an intact vimentin pathway is required for FMDV infection, we utilized overexpression plasmids containing either the wild-type or a truncated form of vimentin and showed that in the presence of truncated vimentin the virus exhibited reduced virus replication. Along with this observation, cells expressing the truncated vimentin form still contained vimentin cages but, in contrast to what is observed in cells containing wild-type vimentin, cages were never able to be resolved. It may be that the formation of the vimentin cage is part of an initial cellular response to isolate the virus from the rest of the cell, consequently serving as an initial site of replication. If so, then it is possible that once enough viral replication or viral protein 2C is produced the vimentin cage may be resolved. However, in the presence of truncated vimentin one possibility is that 2C gets bound to the truncated vimentin, and this could affect the ability for the vimentin cage to be resolved, which could allow the virus proteins in the vimentin cage to eventually be degraded by the host cell. However, it is still unclear how the vimentin cage is able to form in the presence of a dominant-negative form of vimentin; it is possible that the formation of the cage does not rely on full-length vimentin or the normal vimentin pathway and that an intact vimentin pathway is only required to resolve the vimentin cage.

Chemical disruption of vimentin using acrylamide resulted in decreased viral yield, supporting the hypothesis that an intact vimentin network is required for viral replication. Conversely, in agreement with previous reports (49), chemical disruption of microfilaments using nocodazole does not affect viral replication, which is surprising since disruption of the microfilament network also disrupts the vimentin filament network, as noted in Fig. 4B. However, this fact is not unique to FMDV, since a similar observation has been seen with dengue virus (21), where the virus requires an intact vimentin network, but not a microtubule network, for efficient viral replication.

Although it appears that the 2C-vimentin interaction is necessary for virus replication and that an intact vimentin pathway is required for a successful FMDV infection, the precise mechanism governing vimentin cage formation and its later resolution, allowing FMDV to progress with replication, remains to be elucidated. During ASFV infection, it has been shown that vimentin recruits the virus to the microtubule-organizing center (MTOC); however, the specific reason for this is unknown. As a marker for MTOC we tested if the vimentin cage colocalizes with γ-tubulin; no clear colocalization with the vimentin cage formed by FMDV and γ-tubulin could be observed (data not shown), suggesting that the formation of the vimentin cage during FMDV infection may play a different role than that of the vimentin cage during ASFV infection. This is in agreement with previous studies from Armer et al. (5) that show the MTOC remains intact during FMDV infection while γ-tubulin is lost from the MTOC later in infection, suggesting that the MTOC is not involved in FMDV replication. Although the precise role played by the formation of the vimentin cage is unknown, it is possible that its initial formation is to protect the cell from the accumulation of 2C or, conversely, to prevent 2C from being degraded by the cellular defense machinery. Alternatively, it could also be possible that the vimentin cage may provide a physical scaffold that is required for the

Downloaded from http://jvi.asm.org/ on June 3, 2013 by DigiTop -USDA's Digital Desktop Library

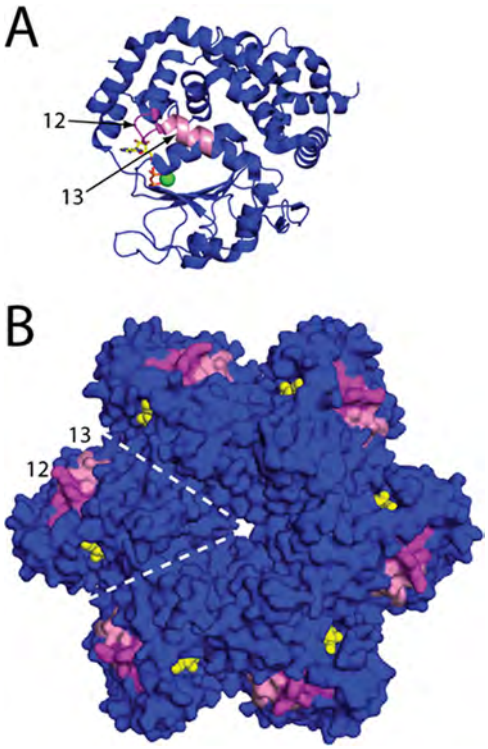

FIG 6 Mapping the alanine scanning blocks 12 (magenta, labeled) and 13 (pink, labeled) effecting vimentin binding with FMDV 2C to corresponding regions on the crystal structure of the AAA+ homolog SV40 LT (PDB ID 1SVM) to assess potential accessibility and localize the blocks in the context of the AAA+ fold. The bound ATP is shown in a yellow/orange and the associated magnesium ion in green. (A) Richardson diagram of an SV40 LT monomer with bound ATP in stick representation. (B) Accessible surface diagram of the SV40 LT hexamer with bound ATP as a van der Waals surface. Dashed white lines give the approximate bounds of one monomer within the hexamer.

initial virus replication, preventing viral proteins from diffusing out into the cytoplasm. Further work is necessary to better characterize this phenomenon.

To gain some potential insight into how the alanine mutations in 2C could affect the binding to vimentin, we performed bioinformatic analysis to map to corresponding regions of homologous proteins with known crystal structures to assess potential accessibility and their location in the context of the AAA+ fold. The regions in 2C responsible for vimentin binding map to a region that could be potentially exposed in the previously determined hexameric state of 2C (58), suggesting that these two areas may be directly accessible for vimentin binding in 2C (Fig. 6). We also note that the region of SV40 LT corresponding to alanine scanning block 12 makes direct contact with ATP in the SV40 LT crystal structure (59) (Fig. 6). However, in order to determine exactly how vimentin interacts structurally and functionally with these potential areas of 2C, further experiments, and perhaps the crystal structure of FMDV 2C would have to be performed.

The results reported here identify, for the first time, cellular host protein vimentin as an interaction partner for FMDV viral protein 2C. This interaction appears to be critical for virus growth since FMDV genomes harboring 2C mutations that disrupted the interaction between 2C and vimentin resulted in viruses unable to replicate in cell cultures. Importantly, the 2C-vimentin interaction appears to somehow modulate the host cell environment to allow for viral replication. This presents new possibilities of exploration for FMDV pathogenesis, and perhaps new insights into how the virus is able to form and later resolve the vimentin cage, providing novel starting points toward designing novel therapeutic strategies that target the cellular vimentin pathway. In addition, further work still needs to be done to understand other host protein-viral protein relationships and how the virus utilizes or avoids specific cellular pathways for its own survival.

ACKNOWLEDGMENTS

We thank Stewart Martin and Rebecca Whipple for the vimentin-HA and DN-vimentin-HA plasmids and Emiliana Brocchi (Istituto Zooprofilattico Sperimentale della Lombardia e dell'Emilia Romagne, Brescia, Italy) for the 2C MAb. We thank Elizabeth Bishop, Ethan Hartwig, and Steven Pauszek for help with RNA *in vitro* transcription, cell transfections, and sequencing of mutant viruses. We also thank Melanie Prarat for editing the manuscript.

REFERENCES

1. **Carrillo C, Tulman ER, Delhon G, Lu Z, Carreno A, Vagnozzi A, Kutish GF, Rock DL.** 2005. Comparative genomics of foot-and-mouth disease virus. J. Virol. **79**:6487–6504.
2. **Kitching RP, Knowles NJ, Samuel AR, Donaldson AI.** 1989. Development of foot-and-mouth disease virus strain characterization: a review. Trop. Anim. Health Prod. **21**:153–166.
3. **Grubman MJ, Baxt B.** 2004. Foot-and-mouth disease. Clin. Microbiol. Rev. **17**:465–493.
4. **Grubman MJ, Baxt B.** 1982. Translation of foot-and-mouth disease virion RNA and processing of the primary cleavage products in a rabbit reticulocyte lysate. Virology **116**:19–30.
5. **Armer H, Moffat K, Wileman T, Belsham GJ, Jackson T, Duprex WP, Ryan M, Monaghan P.** 2008. Foot-and-mouth disease virus, but not bovine enterovirus, targets the host cell cytoskeleton via the nonstructural protein 3Cpro. J. Virol. **82**:10556–10566.
6. **Bienz K, Egger D, Pasamontes L.** 1987. Association of polioviral proteins of the P2 genomic region with the viral replication complex and virus-induced membrane synthesis as visualized by electron microscopic immunocytochemistry and autoradiography. Virology **160**:220–226.
7. **Bienz K, Egger D, Wolff DA.** 1973. Virus replication, cytopathology, and lysosomal enzyme response of mitotic and interphase Hep-2 cells infected with poliovirus. J. Virol. **11**:565–574.
8. **Egger D, Wolk B, Gosert R, Bianchi L, Blum HE, Moradpour D, Bienz K.** 2002. Expression of hepatitis C virus proteins induces distinct membrane alterations including a candidate viral replication complex. J. Virol. **76**:5974–5984.
9. **Monaghan P, Cook H, Jackson T, Ryan M, Wileman T.** 2004. The ultrastructure of the developing replication site in foot-and-mouth disease virus-infected BHK-38 cells. J. Gen. Virol. **85**:933–946.
10. **Pedersen KW, van der Meer Y, Roos N, Snijder EJ.** 1999. Open reading frame 1a-encoded subunits of the arterivirus replicase induce endoplasmic reticulum-derived double-membrane vesicles which carry the viral replication complex. J. Virol. **73**:2016–2026.
11. **Schwartz M, Chen J, Lee WM, Janda M, Ahlquist P.** 2004. Alternate, virus-induced membrane rearrangements support positive-strand RNA virus genome replication. Proc. Natl. Acad. Sci. U. S. A. **101**:11263–11268.
12. **Gladue DP, O'Donnell V, Baker-Branstetter R, Holinka LG, Pacheco JM, Fernandez-Sainz I, Lu Z, Brocchi E, Baxt B, Piccone ME, Rodriguez L, Borca MV.** 2012. Foot-and-mouth disease virus nonstructural protein 2C interacts with beclin1, modulating virus replication. J. Virol. **86**:12080–12090.
13. **Moffat K, Knox C, Howell G, Clark SJ, Yang H, Belsham GJ, Ryan M, Wileman T.** 2007. Inhibition of the secretory pathway by foot-and-mouth disease virus 2BC protein is reproduced by coexpression of 2B with 2C, and the site of inhibition is determined by the subcellular location of 2C. J. Virol. **81**:1129–1139.
14. **O'Donnell V, Pacheco JM, LaRocco M, Burrage T, Jackson W, Rodriguez LL, Borca MV, Baxt B.** 2012. Foot-and-mouth disease virus utilizes an autophagic pathway during viral replication. Virology **410**:142–150.

Downloaded from http://jvi.asm.org/ on June 3, 2013 by DigiTop -USDA's Digital Desktop Library

15. **Earl RT, Mangiapane EH, Billett EE, Mayer RJ.** 1987. A putative protein-sequestration site involving intermediate filaments for protein degradation by autophagy: studies with transplanted Sendai-viral envelope proteins in HTC cells. Biochem. J. **241**:809–815.
16. **Mayer RJ, Gaskell MJ, Earl R, Billett EE, Mangiapane HE, Fernig D, Doherty FJ.** 1986. Intracellular protein catabolism: evidence for sequestration of proteins into an intermediate-filament fraction before lysosomal degradation. Biomed. Biochim. Acta **45**:1591–1602.
17. **Koudelka KJ, Destito G, Plummer EM, Trauger SA, Siuzdak G, Manchester M.** 2009. Endothelial targeting of cowpea mosaic virus (CPMV) via surface vimentin. PLoS Pathog. **5**:e1000417. doi:10.1371/journal.ppat.1000417.
18. **Das S, Ravi V, Desai A.** 2011. Japanese encephalitis virus interacts with vimentin to facilitate its entry into porcine kidney cell line. Virus Res. **160**:404–408.
19. **Bhattacharya B, Noad RJ, Roy P.** 2007. Interaction between Bluetongue virus outer capsid protein VP2 and vimentin is necessary for virus egress. Virol. J. **4**:7.
20. **Risco C, Rodriguez JR, Lopez-Iglesias C, Carrascosa JL, Esteban M, Rodriguez D.** 2002. Endoplasmic reticulum-Golgi intermediate compartment membranes and vimentin filaments participate in vaccinia virus assembly. J. Virol. **76**:1839–1855.
21. **Chen W, Gao N, Wang JL, Tian YP, Chen ZT, An J.** 2008. Vimentin is required for dengue virus serotype 2 infection but microtubules are not necessary for this process. Arch. Virol. **153**:1777–1781.
22. **Shoeman RL, Mothes E, Honer B, Kesselmeier C, Traub P.** 1991. Effect of human immunodeficiency virus type 1 protease on the intermediate filament subunit protein vimentin: cleavage, in vitro assembly and altered distribution of filaments in vivo following microinjection of protease. Acta Histochem. Suppl. **41**:129–141.
23. **Belin MT, Boulanger P.** 1987. Processing of vimentin occurs during the early stages of adenovirus infection. J. Virol. **61**:2559–2566.
24. **Lilienbaum A, Duc Dodon M, Alexandre C, Gazzolo L, Paulin D.** 1990. Effect of human T-cell leukemia virus type I tax protein on activation of the human vimentin gene. J. Virol. **64**:256–263.
25. **Stefanovic S, Windsor M, Nagata KI, Inagaki M, Wileman T.** 2005. Vimentin rearrangement during African swine fever virus infection involves retrograde transport along microtubules and phosphorylation of vimentin by calcium calmodulin kinase II. J. Virol. **79**:11766–11775.
26. **Murti KG, Chen M, Goorha R.** 1985. Interaction of frog virus 3 with the cytomatrix III. Role of microfilaments in virus release. Virology **142**:317–325.
27. **Johnston JA, Ward CL, Kopito RR.** 1998. Aggresomes: a cellular response to misfolded proteins. J. Cell Biol. **143**:1883–1898.
28. **Chien CT, Bartel PL, Sternglanz R, Fields S.** 1991. The two-hybrid system: a method to identify and clone genes for proteins that interact with a protein of interest. Proc. Natl. Acad. Sci. U. S. A. **88**:9578–9582.
29. **Fields S, Song O.** 1989. A novel genetic system to detect protein-protein interactions. Nature **340**:245–246.
30. **Schneider CA, Rasband WS, Eliceiri KW.** NIH Image to ImageJ: 25 years of image analysis. Nat. Methods **9**:671–675.
31. **Borca MV, Pacheco JM, Holinka LG, Carrillo C, Hartwig E, Garriga D, Kramer E, Rodriguez L, Piccone ME.** 2011. Role of arginine-56 within the structural protein VP3 of foot-and-mouth disease virus (FMDV) O1 Campos in virus virulence. Virology **422**:37–45.
32. **Mason PW, Rieder E, Baxt B.** 1994. RGD sequence of foot-and-mouth disease virus is essential for infecting cells via the natural receptor but can be bypassed by an antibody-dependent enhancement pathway. Proc. Natl. Acad. Sci. U. S. A. **91**:1932–1936.
33. **Altschul SF, Gish W, Miller W, Myers EW, Lipman DJ.** 1990. Basic local alignment search tool. J. Mol. Biol. **215**:403–410.
34. **Soding J.** 2005. Protein homology detection by HMM-HMM comparison. Bioinformatics **21**:951–960.
35. **Fields S, Sternglanz R.** 1994. The two-hybrid system: an assay for protein-protein interactions. Trends Genet. **10**:286–292.
36. **Gao Y, Sztul E.** 2001. A novel interaction of the Golgi complex with the vimentin intermediate filament cytoskeleton. J. Cell Biol. **152**:877–894.
37. **Styers ML, Kowalczyk AP, Faundez V.** 2005. Intermediate filaments and vesicular membrane traffic: the odd couple's first dance? Traffic **6**:359–365.
38. **Styers ML, Salazar G, Love R, Peden AA, Kowalczyk AP, Faundez V.** 2004. The endo-lysosomal sorting machinery interacts with the intermediate filament cytoskeleton. Mol. Biol. Cell **15**:5369–5382.
39. **Doherty FJ, Wassell JA, Mayer RJ.** 1987. A putative protein-sequestration site involving intermediate filaments for protein degradation by autophagy. Studies with microinjected purified glycolytic enzymes in 3T3-L1 cells. Biochem. J. **241**:793–800.
40. **Ferreira LR, Moussatche N, Moura Neto V.** 1994. Rearrangement of intermediate filament network of BHK-21 cells infected with vaccinia virus. Arch. Virol. **138**:273–285.
41. **Heath CM, Windsor M, Wileman T.** 2001. Aggresomes resemble sites specialized for virus assembly. J. Cell Biol. **153**:449–455.
42. **Goldman RD, Khuon S, Chou YH, Opal P, Steinert PM.** 1996. The function of intermediate filaments in cell shape and cytoskeletal integrity. J. Cell Biol. **134**:971–983.
43. **Kural C, Serpinskaya AS, Chou YH, Goldman RD, Gelfand VI, Selvin PR.** 2007. Tracking melanosomes inside a cell to study molecular motors and their interaction. Proc. Natl. Acad. Sci. U. S. A. **104**:5378–5382.
44. **Whipple RA, Balzer EM, Cho EH, Matrone MA, Yoon JR, Martin SS.** 2008. Vimentin filaments support extension of tubulin-based microtentacles in detached breast tumor cells. Cancer Res. **68**:5678–5688.
45. **Gyoeva FK, Gelfand VI.** 1991. Coalignment of vimentin intermediate filaments with microtubules depends on kinesin. Nature **353**:445–448.
46. **Liao G, Gundersen GG.** 1998. Kinesin is a candidate for cross-bridging microtubules and intermediate filaments. Selective binding of kinesin to detyrosinated tubulin and vimentin. J. Biol. Chem. **273**:9797–9803.
47. **Arocena M.** 2006. Effect of acrylamide on the cytoskeleton and apoptosis of bovine lens epithelial cells. Cell Biol. Int. **30**:1007–1012.
48. **Vasquez RJ, Howell B, Yvon AM, Wadsworth P, Cassimeris L.** 1997. Nanomolar concentrations of nocodazole alter microtubule dynamic instability *in vivo* and *in vitro*. Mol. Biol. Cell **8**:973–985.
49. **O'Donnell V, Larocco M, Baxt B.** 2008. Heparan sulfate-binding foot-and-mouth disease virus enters cells via caveola-mediated endocytosis. J. Virol. **82**:9075–9085.
50. **Liang JJ, Yu CY, Liao CL, Lin YL.** 2011. Vimentin binding is critical for infection by the virulent strain of Japanese encephalitis virus. Cell Microbiol. **13**:1358–1370.
51. **Plummer EM, Thomas D, Destito G, Shriver LP, Manchester M.** Interaction of cowpea mosaic virus nanoparticles with surface vimentin and inflammatory cells in atherosclerotic lesions. Nanomedicine (Lond.) **7**:877–888.
52. **Ghosh S, Ahrens WA, Phatak SU, Hwang S, Schrum LW, Bonkovsky HL.** Association of filamin A and vimentin with hepatitis C virus proteins in infected human hepatocytes. J. Viral Hepat. **18**:e568–e577.
53. **Wang X, Zhang S, Sun C, Yuan ZG, Wu X, Wang D, Ding Z, Hu R.** Proteomic profiles of mouse neuro N2a cells infected with variant virulence of rabies viruses. J. Microbiol. Biotechnol. **21**:366–373.
54. **Shoeman RL, Honer B, Stoller TJ, Kesselmeier C, Miedel MC, Traub P, Graves MC.** 1990. Human immunodeficiency virus type 1 protease cleaves the intermediate filament proteins vimentin, desmin, and glial fibrillary acidic protein. Proc. Natl. Acad. Sci. U. S. A. **87**:6336–6340.
55. **Snasel J, Shoeman R, Horejsi M, Hruskova-Heidingsfeldova O, Sedlacek J, Ruml T, Pichova I.** 2000. Cleavage of vimentin by different retroviral proteases. Arch. Biochem. Biophys. **377**:241–245.
56. **Meckes DG, Jr, Menaker NF, Raab-Traub N.** EBV LMP1 modulates lipid raft microdomains and the vimentin cytoskeleton for signal transduction and transformation. J. Virol., in press.
57. **Kanlaya R, Pattanakitsakul SN, Sinchaikul S, Chen ST, Thongboonkerd V.** 2010. Vimentin interacts with heterogeneous nuclear ribonucleoproteins and dengue nonstructural protein 1 and is important for viral replication and release. Mol. Biosyst. **6**:795–806.
58. **Sweeney TR, Cisnetto V, Bose D, Bailey M, Wilson JR, Zhang X, Belsham GJ, Curry S.** 2010. Foot-and-mouth disease virus 2C is a hexameric AAA+ protein with a coordinated ATP hydrolysis mechanism. J. Biol. Chem. **285**:24347–24359.
59. **Gai D, Zhao R, Li D, Finkielstein CV, Chen XS.** 2004. Mechanisms of conformational change for a replicative hexameric helicase of SV40 large tumor antigen. Cell **119**:47–60.

Downloaded from http://jvi.asm.org/ on June 3, 2013 by DigiTop -USDA's Digital Desktop Library

Analysis of SAT Type Foot-And-Mouth Disease Virus Capsid Proteins and the Identification of Putative Amino Acid Residues Affecting Virus Stability

Francois F. Maree[1,2]*, Belinda Blignaut[1,3], Tjaart A. P. de Beer[4,5], Elizabeth Rieder[6]

1 Transboundary Animal Diseases Programme, Onderstepoort Veterinary Institute, Agricultural Research Council, Onderstepoort, Pretoria, South Africa, **2** Department of Veterinary Tropical Diseases, Faculty of Veterinary Sciences, University of Pretoria, Onderstepoort, South Africa, **3** Department of Microbiology and Plant Pathology, Faculty of Agricultural and Natural Sciences, University of Pretoria, Pretoria, South Africa, **4** Bioinformatics and Computational Biology Unit, University of Pretoria, Pretoria, South Africa, **5** European Bioinformatics Institute, Wellcome Trust Campus, Hinxton, Cambridge, United Kingdom, **6** Foreign Animal Disease Research Unit, United States Department of Agriculture, Agricultural Research Service, Plum Island Animal Disease Center, Greenport, New York, United States of America

Abstract

Foot-and-mouth disease virus (FMDV) initiates infection by adhering to integrin receptors on target cells, followed by cell entry and disassembly of the virion through acidification within endosomes. Mild heating of the virions also leads to irreversible dissociation into pentamers, a characteristic linked to reduced vaccine efficacy. In this study, the structural stability of intra- and inter-serotype chimeric SAT2 and SAT3 virus particles to various conditions including low pH, mild temperatures or high ionic strength, was compared. Our results demonstrated that while both the SAT2 and SAT3 infectious capsids displayed different sensitivities in a series of low pH buffers, their stability profiles were comparable at high temperatures or high ionic strength conditions. Recombinant vSAT2 and intra-serotype chimeric viruses were used to map the amino acid differences in the capsid proteins of viruses with disparate low pH stabilities. Four His residues at the inter-pentamer interface were identified that change protonation states at pH 6.0. Of these, the H145 of VP3 appears to be involved in interactions with A141 in VP3 and K63 in VP2, and may be involved in orientating H142 of VP3 for interaction at the inter-pentamer interfaces.

Citation: Maree FF, Blignaut B, de Beer TAP, Rieder E (2013) Analysis of SAT Type Foot-And-Mouth Disease Virus Capsid Proteins and the Identification of Putative Amino Acid Residues Affecting Virus Stability. PLoS ONE 8(5): e61612. doi:10.1371/journal.pone.0061612

Editor: Jianming Qiu, University of Kansas Medical Center, United States of America

Received December 19, 2012; **Accepted** March 11, 2013; **Published** May 22, 2013

Copyright: © 2013 Maree et al. This is an open-access article distributed under the terms of the Creative Commons Attribution License, which permits unrestricted use, distribution, and reproduction in any medium, provided the original author and source are credited.

Funding: Research findings documented in this manuscript are in part the result of a cooperative research and development agreement between the Agricultural Research Council, Onderstepoort Veterinary Institute of South Africa and the United States Department of Agriculture, Agricultural Research Service, entitled, ''Genetic engineering of antigenically stable strains of foot-and-mouth disease virus for vaccine production'', agreement number 58-3K95-M-894. Additional financial support was received from the Red meat Research and Development trust of SA and MSD Animal Health (previously Intervet/Schering Plough), The Netherlands. The funders had no role in study design, data collection and analysis, or preparation of the manuscript. The funders were consulted in regards to the publication of the results and approved the manuscript for publication.

Competing Interests: The authors state that the research findings documented in this manuscript are in part the result of a cooperative research and development agreement between the Agricultural Research Council, Onderstepoort Veterinary Institute of South Africa and the United States Department of Agriculture, Agricultural Research Service, (agreement number 58-3K95-M-894). Additional financial support was received from the Red meat Research and Development trust of SA and MSD Animal Health (previously Intervet/Schering Plough), The Netherlands. This does not alter the authors' adherence to all the PLOS ONE policies on sharing data and materials.

* E-mail: mareef@arc.agric.za

Introduction

Control of highly contagious diseases such as foot-and-mouth disease (FMD) by means of vaccination relies strongly on the chemical inactivation of complete viral particles. One of the principle factors which influences the potency of vaccine preparations and permits the induction of a protective antibody response, is the structural integrity of the intact virion typified by a sedimentation rate of 146S [1]. Other characteristics that play a role in vaccine efficacy include the productivity and replication efficiency of the vaccine strain in the production cell line, a close antigenic relationship to field viruses circulating in current outbreaks, and the ability to provide protection against a wide range of antigenic variants in the field [2,3]. However, adaptation of new vaccine strains in the production cell line (BHK-21) is difficult and hampered by low amounts of stable antigen, often rendering this method inefficient for commercial vaccine manufacturing purposes [4–6]. In addition, the hot climate in sub-Saharan Africa, where the South African Territories (SAT) types are prevalent, also calls for vaccines with improved stability which are less reliant on a cold chain during storage and handling.

The aetiological agent, FMD virus (FMDV), is a single-stranded (ss) positive-sense RNA virus belonging to the genus *Aphthovirus* in the family *Picornaviridae* and exists as seven serotypes, *i.e.* A, C, O, SAT1, 2, 3, and Asia-1, with absence of cross protection [7–10]. Elucidation of the crystal structure of FMDV over 20 years ago [11] enabled assessment of the effects of acid and heat on the virus capsid structure and identification of protein-protein interactions that may correlate with enhanced acid or heat stability [12–14]. Reverse genetics combined with targeted mutagenesis of residues involved in the stability of the capsid is a powerful tool for the improvement of vaccines [15,16], given that thermostability was linked to vaccine potency since the 1980s [1]. The self-assembly and stability of a multimeric protein capsid, such as FMDV, depends on the occurrence of numerous non-covalent interactions

between multiple polypeptide subunits [11,12,14,17–20]. The non-enveloped, icosahedral virion of FMDV is composed of 60 repetitions of four viral structural proteins, VP1-4. The three surface-exposed proteins, VP1, VP2 and VP3, assemble into a protomeric subunit, with the smaller VP4 located internally [9,11,12]. Subsequently, five protomers assemble into a pentameric intermediate and finally, 12 pentamers self-assemble through complex protein-protein interactions into a complete capsid [12–14,21].

Even though FMDV, especially the SAT types, exhibit large intra- and inter-serotype genetic variability [22–25], the multiple and repetitive intersubunit interactions appear to have evolved under stringent and selective constraints [11,13,26,27]. As a result the viral properties of each serotype are constrained within fundamental structural requirements of the virus capsid [26–29]. Viral capsid inter-subunit interactions are required to be sufficiently robust in order to provide stability to the capsid under environmental denaturing conditions [12,13], whilst still permitting intracellular uncoating and release of viral RNA. Acidification of FMDV within cellular endosomes disrupts the interactions between VP2 and VP3 at the pentemeric interfaces leading to dissociation of the structure into pentamers, thereby releasing the viral RNA [30–34]. Mild heating of FMDV virions also leads to irreversible dissociation into pentamers, a characteristic associated with poor vaccine performance. This phenomenon, therefore, highlights the importance of a cold chain in the preservation of FMD vaccines [1,13,14].

The amino acid residues involved in protein-protein interactions at the pentameric interfaces and their intolerance to variation within serotype A and C viruses have previously been demonstrated [13,14]. However, very little is known about residues located at the SAT pentameric interfaces involved in structural stability. Furthermore, by comparison to isolates from serotypes A, O and C, the SAT viral capsids are generally considered to be less stable [1]. Consequently, the principle aim of this study was to investigate the stability of SAT2 and SAT3 isolates in mildly acidic, heat or high ionic strength conditions. Interestingly, we showed that the SAT2 virions display similar acid lability compared to virions from serotypes A, O and C. In addition, our results demonstrate that amino acid residues at the pentameric interfaces may also contribute to acid stability of the SAT2 and SAT3 viruses. This is the first report that describes the identification of residues in the SAT virus capsids that may be replaced to allow the engineering of more stable capsids and consequently improved recombinant FMD vaccines.

Materials and Methods

Cells and viruses

Baby hamster kidney (BHK) clone 13 cells (strain 21; ATCC CCL-10) were maintained as described previously [35]. Virus stocks were prepared and titrated in BHK-21 cells using the plaque assay method [35]. Cultured BHK-21 cells were also used for RNA transfection and virus recovery. In addition, plaque assays were performed in either IB-RS-2 (Instituto Biologico renal suino) cells or Chinese hamster ovary (CHO) cells (strain K1; ATCC CCL-61), respectively propagated in RPMI medium (Sigma) and Ham's F-12 medium (Invitrogen) supplemented with 10% foetal calf serum (FCS, Delta Bioproducts). The GAG-deficient CHO derivative, pgsA-677 (CRL-2242), was also maintained in Ham's F-12 medium containing 10% FCS. COS-1 cells, transiently expressing the bovine integrin α_V subunit and either the β1, β3 or β6 subunits were used for cell binding studies [36,37].

The wild-type SAT2 viruses used in this study were kindly provided by either the Transboundary Animal Diseases Programme (TADP, ARC-Onderstepoort Veterinary Institute, SA) or the FMD World Reference Laboratory at the Institute for Animal Health (IAH, Pirbright, UK). These viruses were subsequently either isolated on primary pig kidney (PK) or bovine thyroid (BTY) cells as part of the strategic stock maintenance and the passage history of the isolates have been described previously [16]. The viruses selected for this study included (1) three SAT2 viruses isolated from buffalo which originated from western Zimbabwe (SAT2/ZIM/7/83, SAT2/ZIM/17/91 and SAT2/ZIM/14/90); (2) a SAT2 virus from cattle outbreak in Zambia, (SAT2/ZAM/7/96); (3) a SAT3 virus isolated from buffalo originating in Zambia, (SAT3/ZAM/4/96). The passage history, host, country of origin and topotype are summarised in Table 1. For serial passages, infected or transfected 35-mm BHK-21 cell monolayers were frozen and thawed, and $1/10^{th}$ of the volume was used to inoculate a fresh BHK-21 monolayer. Following virus adsorption (with periodical rocking for 60 min at 37°C), virus growth medium (VGM; Eagle's basal medium (BME) with 1% FCS, 1% HEPES and antibiotics) was added, and the culture was incubated for no longer than 48 h at 37°C, after which the infected cells were frozen for subsequent passaging of the viruses.

Table 1. Summary of the different virus strains used in this study and their passage history.

FMDV strain	Host	Passage history	Country of origin	Topotype[a]	Chimeric virus[b] and amino acid differences[c]
SAT2/ZIM/7/83	Bovine	B1BHK5B1	Zimbabwe	II (SAT2)	**vSAT2;** Y1169H, E1181A, L1182V
SAT2/ZIM/14/90	Buffalo	BTY1RS3	southern Zimbabwe	II (SAT2)	**vSAT2^{ZIM14}SAT2;** V2015L, N3067I, S3087I, T3182A, K1174N
SAT2/ZIM/17/91	Buffalo	BTY2RS4	southern Zimbabwe	II (SAT2)	**vSAT2^{ZIM17}SAT2;** V2015L, A2077T, C2164G, C1134G, E1179K
SAT2/ZAM/7/96	Buffalo	BTY1RS2	Zambia	III (SAT2)	**vSAT2^{ZAM7}SAT2;** G2020R, E2214K, E1083K,
SAT3/ZAM/4/96	Buffalo	BTY1RS1	Zambia	4 (SAT3)	**vSAT3^{ZAM4}SAT2**

The amino acid differences between the 1B/C/D-2A chimeric viruses and the parental isolates are indicated.
[a]Topotypes refers to genotypes distributed to specific geographic regions. The topotypes for the SAT serotypes were previously described [24,25].
[b]Viruses recovered by transfection of BHK-21 cells with chimeric plasmids are designated "v" followed by the parental isolate number and the SAT2 plasmid used for cloning purposes. The amino acid residues have been numbered independently for each protein. For each residue, the first digit indicates the protein (VP1, VP2 or VP3) and the last three digits the amino acid position.
[c]The amino acid differences within the 1B/C/D-2A region of chimeric viruses and the parental viruses are indicated next to each respective viral protein.
doi:10.1371/journal.pone.0061612.t001

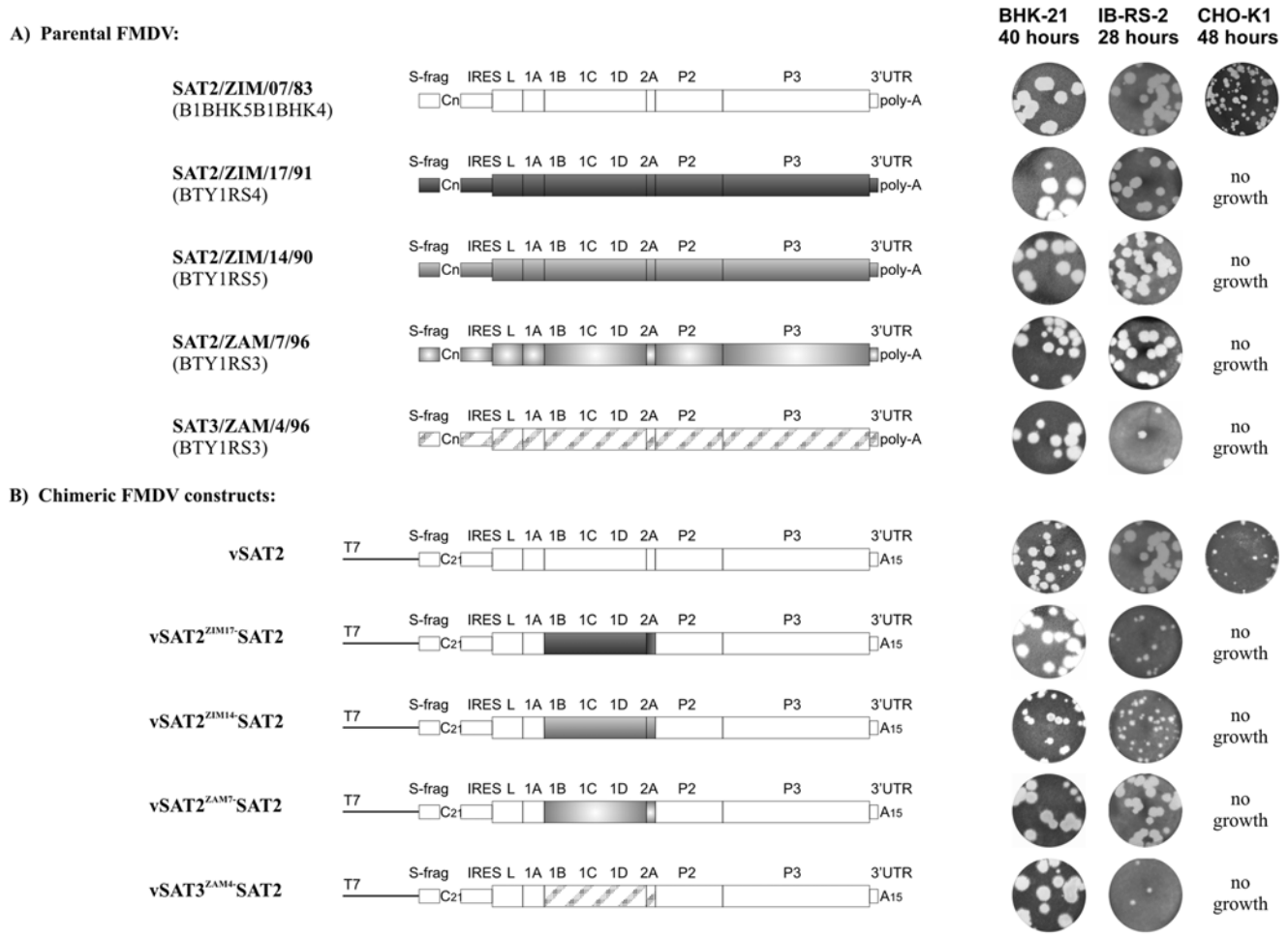

Figure 1. Schematic representation of (A) the genomes of the parental field viruses and (B) the chimeric FMDV constructs described in this study. Plaque morphologies of the parental and genetically engineered viruses obtained on monolayers of BHK-21, IB-RS-2 and CHO-K1 cells are shown. Cells infected with the respective viral strains were incubated for either 40 h (BHK-21 and CHO-K1) or 28 h (IB-RS-2).
doi:10.1371/journal.pone.0061612.g001

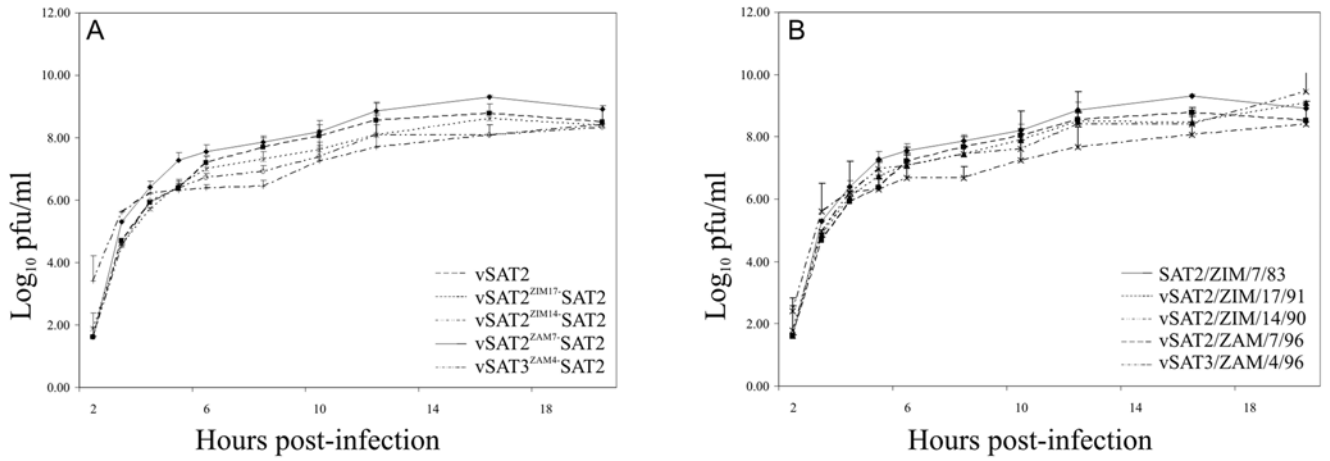

Figure 2. One-step growth kinetic studies were performed in BHK-21 cells. The average log virus titers are shown at different times p.i. with the vSAT2, vSAT2^{ZIM17}-SAT2, vSAT2^{ZIM14}-SAT2, vSAT2^{ZAM7}-SAT2 and vSAT3^{ZAM4}-SAT2 viruses (A) and the parental SAT2 and SAT3 viruses (B). For comparison of the relative release of virus particles from cells infected with the parental and chimeric viruses, the average virus titers were determined at different times p.i (2, 4, 6, 8, 10, 12, 16 and 20 h). The standard deviations of the titers determined from quadruple wells are indicated on the graph.
doi:10.1371/journal.pone.0061612.g002

Titration and kinetics of virus production

Titrations were performed at least in duplicate in standard plaque assays by infecting monolayer cells in 35 mm cell culture plates (Nunc^{TM}) with the respective viruses for 1 h, followed by the addition of a 2 ml tragacanth overlay [35]. Following incubation at 37°C for 28 or 40 h the overlayed infected monolayers were stained with 1% (w/v) methylene blue in 10% ethanol and 10% formaldehyde in phosphate buffered saline, pH 7.4.

One-step growth kinetic analyses were carried out in BHK-21 cells. Briefly, BHK-21 cells were infected with the virus strain for 1 h at a m.o.i. of 2–4 pfu/cell, washed with MBS-buffer (25 mM morpholine-ethanesulfonic acid, 145 mM NaCl, pH 5.5). Following incubation at 37°C for the indicated time intervals, the infected cells were harvested at 2, 4, 6, 8, 10, 12, 16 and 20 h post-infection (p.i.) and subsequently frozen at −70°C. Virus titers were determined and expressed as plaque forming units per millilitre (pfu/ml).

Monolayers of CHO-K1 or CHO-677 cells in 35 mm cell culture plates (Nunc^{TM}) were infected with an m.o.i. of 5–10 PFU/ml of the parental and recombinant viruses. After 1 h of adsorption, cells were washed with MBS-buffer and then incubated with virus growth medium (VGM; Ham's F-12 with 1% FCS) at 37°C for 1 h and 24 h for each CHO cell type and frozen at −70°C. Virus titers were determined in BHK-21 cells and viral growth was calculated by subtracting the 1 h titer results from the 24 h titer results. Positive titers were interpreted as an indication that the viruses were able to infect and replicate in the CHO cells.

Table 2. Comparison of the antigenicity of SAT2 parental and chimeric viruses as measured against reference SAT2 antisera.

Viruses	r-values[a]		
		SAT2 test antisera[b]	
	anti-KNP/19/89[c]	anti-ZIM/7/83	anti-ERI/12/89[d]
SAT2/KNP/19/89[c]	**1.00**	0.17±0.05	0.27±0.09
SAT2/ZIM/7/83	0.28±0.03	**1.00**	0.25±0.04
SAT2/ZIM/17/91	0.09±0.03	0.13±0.02	0.17±0.05
SAT2/ZIM/14/90	0.16±0.03	0.07±0.02	0.15±0.05
SAT2/ZAM/7/96	0.09±0.04	0.12±0.03	0.18±0.05
SAT3/ZAM/4/96[e]	-	-	-
vSAT2^{ZIM17}-SAT2	0.13±0.06	0.11±0.02	0.06±0.03
vSAT2^{ZIM14}-SAT2	0.06±0.01	0.08±0.04	0.05±0.02
vSAT2^{ZAM7}-SAT2	0.02±0.01	0.05±0.02	0.12±0.03
vSAT3^{ZAM4}-SAT2[e]	-	-	-

[a]r-values are expressed as the ratio between the heterologous/homologous end point serum titers of the last dilution of serum to neutralize 100 $TCID_{50}$ in 50% of the wells in VN assay. The average of two repeats is shown. The homologous r-values are in bold (n.d. = not done).
[b]The sera used in the VN assays were prepared by two consecutive vaccinations on day 0 and 28 and subsequently bled on day 38 with reference SAT2 viruses, i.e. SAT2/KNP/19/89, SAT2/ZIM/7/83 and SAT2/ERI/12/89.
[c]The SAT2/KNP/19/89 virus, belonging to SAT2 topotype 1 [25] and its homologous serum was included as a SAT2 control in the VN assay.
[d]SAT2/ERI/12/89 belong to the SAT2 topotype 12 [25] viruses from East Africa.
[e]VNT's were not performed against the SAT3 viruses using SAT2 antisera.
doi:10.1371/journal.pone.0061612.t002

RNA extraction, cDNA synthesis and construction of infectious, chimera cDNA clones

RNA was extracted from infected cell lysates with TRIzol® reagent (InVitrogen) according to the manufacturer's specifications and used as template for cDNA synthesis. Viral cDNA was synthesised with SuperScript III^{TM} (InVitrogen). The *ca.* 2.2 kb outer capsid-coding region of the SAT2 or SAT3 field isolates was obtained by PCR amplification. Unique *SspI* and *XmaI* sites were introduced at the 5′ and 3′ termini of the amplicons, respectively, to facilitate cloning into pSAT2 plasmid [15]. Briefly, the corresponding 2.2 kb fragment was excised from pSAT2 by digestion with *SspI* and *XmaI* restriction enzymes and the remaining fragment was ligated to the SAT2 and SAT3-specific amplicons. The resultant chimeric constructs, *i.e.* pSAT2^{ZIM17}-SAT2, pSAT2^{ZIM14}-SAT2, pSAT2^{ZAM7}-SAT2 and pSAT3^{ZAM4}-SAT2, were verified by sequencing using genome-specific oligonucleotides and the ABI PRISM^{TM} BigDye Terminator Cycle Sequencing Ready Reaction Kit v3.0 (Applied Biosystems).

In vitro RNA synthesis, transfection and virus recovery

RNA was synthesized from *SwaI*-linearised plasmid DNA templates with the MEGAscript^{TM} T7 kit (Ambion). The transcript RNAs were examined by agarose gel electrophoresis to evaluate their integrity and the RNA concentrations were determined spectrometrically. BHK-21 cell monolayers, in 35-mm cell culture wells (Nunc^{TM}), were transfected with the *in vitro*-generated RNA using Lipofectamine2000^{TM} (InVitrogen). The transfection medium was removed after 3–5 h and replaced with VGM, followed by incubation at 37°C for up to 48 h with a 5% CO_2 influx. After one freeze-thaw cycle, the transfection supernatants were used for serial passaging on BHK-21 cells. BHK-21 monolayers in 35-mm cell culture wells were infected using 1/10th of clarified infected supernatants and incubated for 48 h at 37°C. Viruses were subsequently harvested from infected cells by a freeze-thaw cycle and passaged four times on BHK-21 cells, using 10% of the supernatant from the previous passage. The recombinant viruses derived from the infectious chimeric cDNA clones were designated vSAT2^{ZIM14}-SAT2, vSAT2^{ZIM17}-SAT2, vSAT2^{ZAM7}-SAT2 and vSAT3^{ZAM4}-SAT2. Following the recovery of viable viruses, the presence of the inserts was verified once again with automated sequencing. Unless otherwise stated, viruses that were passaged four times were used for analysis.

Cell-binding assay

Cell-binding studies were essentially performed as described previously [36,37]. This entails the infection of COS-1 cells, transiently expressing the bovine integrin α_V subunit and either the β1, β3 or β6 subunits, with the vSAT2, pSAT2^{ZIM17}-SAT2 and pSAT2^{ZIM14}-SAT2 viruses, respectively. Sixteen hours after infection, cells were labelled with [^{35}S]methionine and viral protein synthesis analyzed by radio-immunoprecipitation (RIP) of equal amounts of trichloroacetic acid-precipitable counts per minute using a SAT2 polyclonal serum followed by sodium dodecyl sulphate-polyacrylamide gel electrophoresis (SDS-PAGE). Radio-labelled proteins from non-transfected COS-1 cells and BHK-21 cells infected with vSAT2 were included as controls.

Virus Neutralization test

The antigenic cross-reactivity of the SAT2/ZIM/7/83, SAT2/ZIM/17/91, SAT2/ZIM/14/90, SAT2/ZAM/7/96, vSAT2, pSAT2^{ZIM17}-SAT2, pSAT2^{ZIM14}-SAT2 and pSAT2^{ZAM7}-SAT2-viruses was determined using the micro-neutralization test essentially as described in the OIE Manual of Standards [38].

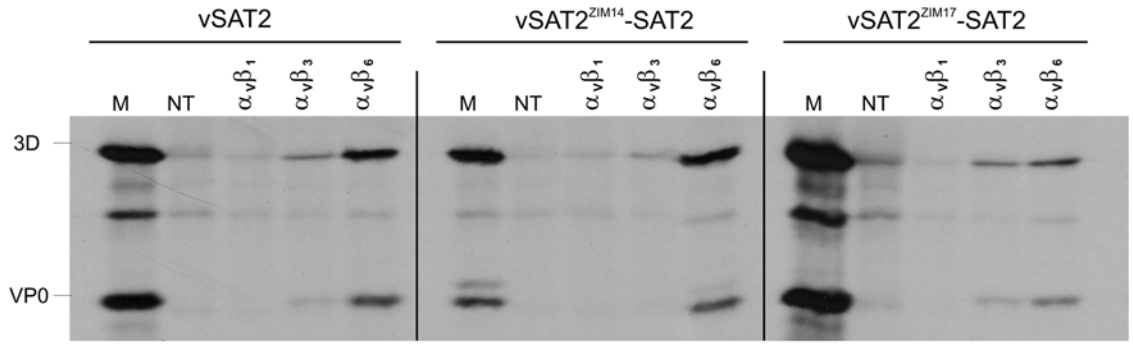

Figure 3. COS-1 cells were co-transfected with cDNA plasmids encoding the bovine integrin α_V subunit and either the β1, β3 or β6 subunits. Transfected cells were infected with the recombinant SAT2 viruses and proteins were radiolabelled with [^{35}S]methionine. Viral protein synthesis were analyzed by radiolabelled immune-precipitation and SDS-PAGE. Immune-precipitated proteins from non-transfected but infected cell-lysates are indicated by "NT", and the location of the viral structural proteins from lysates prepared from FMDV-infected BHK-21 cells is indicated by "M".
doi:10.1371/journal.pone.0061612.g003

Reference cattle sera were prepared by two consecutive vaccinations (vaccinated on day 0, boosted on day 28 and bled on day 38) with the SAT2/ZIM/7/83, SAT2/KNP/19/89 and SAT2/ERI/12/98 vaccines. Cattle were housed in the isolation facility at TADP and all procedures were approved by the Onderstepoort Veterinary Institute Animal Ethics Committee and were performed according to national and international guidelines. IB-RS-2 cells were used as the indicator system in the neutralization test. The end point titer of the serum against homologous (SAT2/ZIM/7/83) and heterologous (SAT2/KNP/19/89 and SAT2/ERI/12/98) viruses was calculated as the reciprocal of the last dilution of serum to neutralise 100 $TCID_{50}$ virus in 50% of the wells [39]. One-way antigenic relationships (r_1-values) of the field isolates and engineered viruses relative to the reference sera were calculated and expressed as the ratio between the heterologous/homologous serum titer. All neutralization titer determinations were repeated at least twice and presented as an average.

Sucrose density gradient purification

Culture fluids were harvested, clarified by centrifugation, concentrated with 8% PEG (w/v) and resolved on 10–50% (w/v) sucrose density gradients (SDG) by rate zonal centrifugation at 36,000 g for 16 h at 4°C. The gradients were fractionated and analysed spectrophotometrically by measuring the absorbancy at 260 nm. Fractions containing 146S virions were calculated using the extinction coefficient E_{259nm} = 79.9 [40] and pooled for analysis. The presence of the outer capsid proteins were verified using SDS-PAGE analysis, while the integrity of the RNA was verified by RT-PCR and sequencing of the 1D-coding region.

Capsid dissociation assays and measurements of rate constants

The wild-type and recombinant SAT virus particles present in the cell culture supernatants or SDG purified samples were prepared in TNE buffer (100 mM Tris pH 7.4, 10 mM EDTA, 150 mM NaCl) essentially as described [41]. Briefly, 10^6 to 10^7 pfu/ml of infectious particles were mixed with TNE buffer ranging from pH 5.6 to 9.0 (±0.02) at a ratio of 1:50 respectively. The mixtures were subsequently incubated for 30 min at room temperature. As a control, virus particles were also mixed with VGM at the same ratio as above. The samples were subsequently neutralised with 1 M Tris (pH 7.4), 150 mM NaCl and titrated on BHK-21 cells. Similarly, virus particles were treated for 30 min with TNE buffers with a constant pH of 7.4, containing NaCl

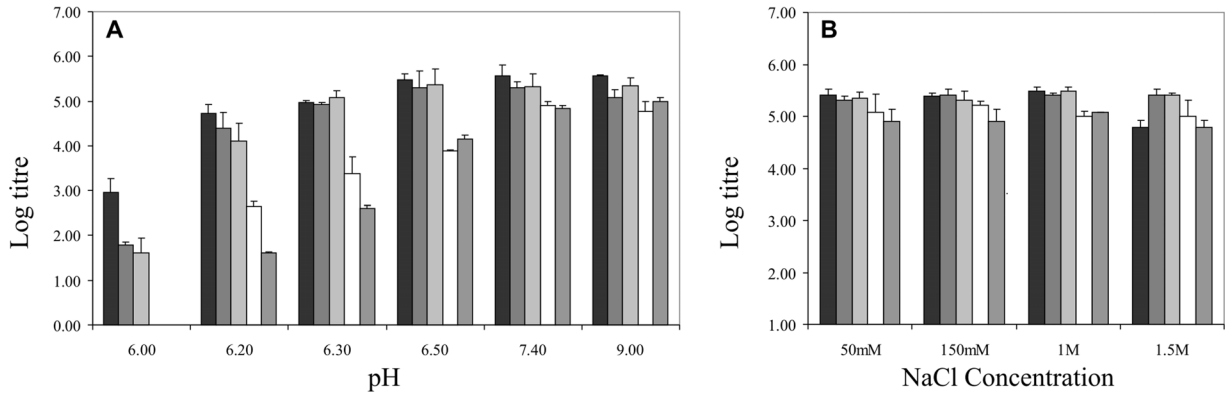

Figure 4. pH and ionic strength stability profiles of vSAT2 (black), vSAT2^{ZIM14}-SAT2 (dark grey), vSAT2^{ZIM17}-SAT2 (light grey), vSAT2^{ZAM7}-SAT2 (white) and vSAT3^{ZAM4}-SAT2 (medium grey). (A) Inactivation of SDG-purified virus particles following treatment with TNE (100 mM Tris, 150 mM NaCl, 10 mM EDTA) buffers ranging from pH 9.0 to 6.0 for 30 min. The average virus titers of two inactivation experiments at each pH are plotted. (B) The viruses were incubated in buffers with varying NaCl concentrations and the average log titers of two experiments are plotted.
doi:10.1371/journal.pone.0061612.g004

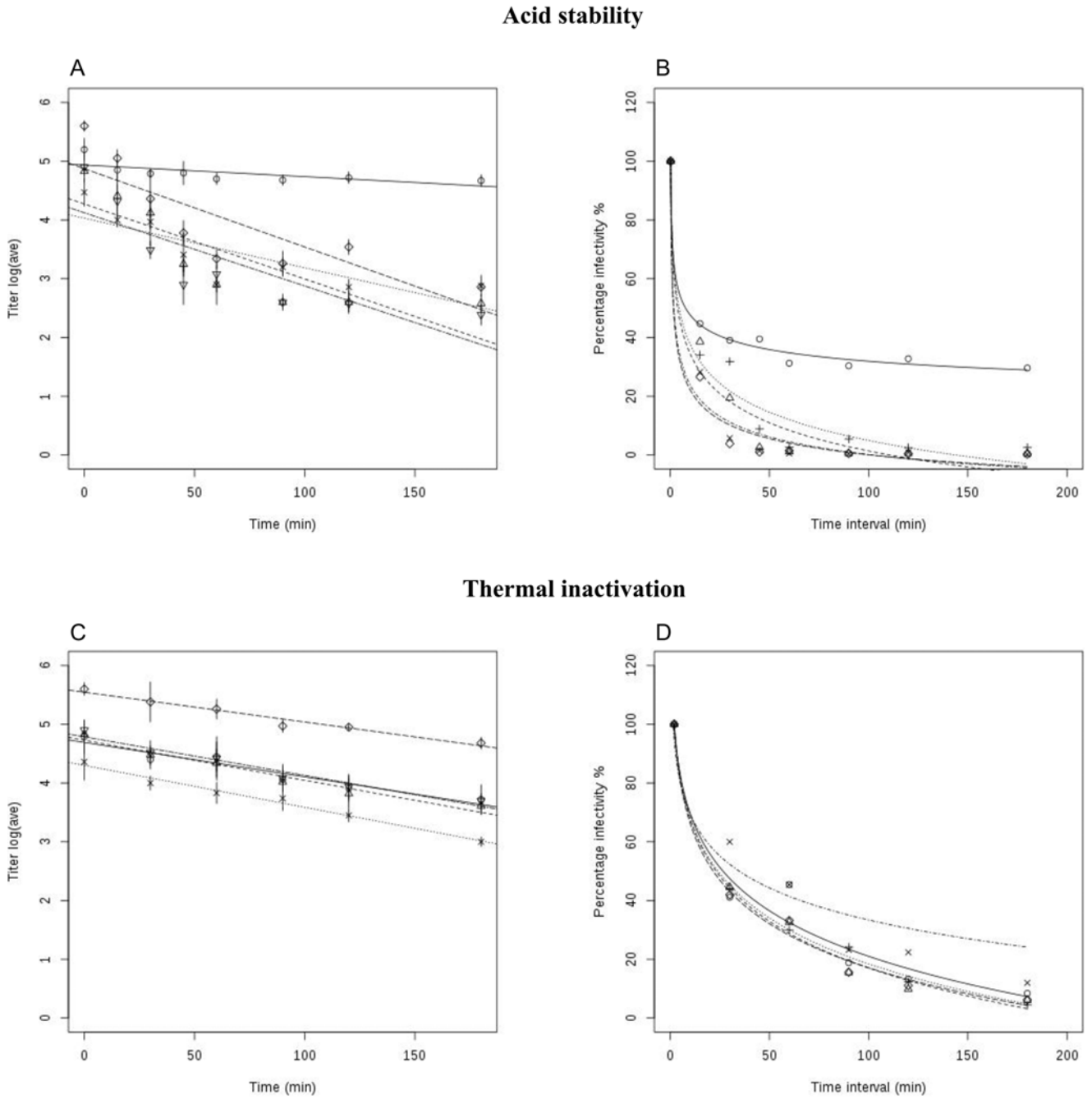

Figure 5. pH and thermal inactivation kinetics of vSAT2, vSAT2^{ZIM17}-SAT2, vSAT2^{ZIM14}-SAT2, vSAT2^{ZAM7}-SAT2 and vSAT3^{ZAM4}-SAT2 viruses. (A & C) Inactivation of SDG-purified vSAT2, vSAT2^{ZIM14}-SAT2, vSAT2^{ZIM17}-SAT2, vSAT2^{ZAM7}-SAT2, and vSAT3^{ZAM4}-SAT2 particles following treatment with TNE buffer at pH 6.0 (A) and heat treated at 42°C (C) for up to 3 h. The average $\log_{10}$ virus titers, as determined in two different inactivation experiments are shown. The respective logarithmic values of the virus titers at the different time points (0, 15, 30, 45, 60, 90, 120 and 180 min p.i.) were linearly fitted and the slopes were determined. (B & D) The average virus titers following pH treatment (B) or heat inactivation (D) were used to determine the percentage of residual infectivity over time.
doi:10.1371/journal.pone.0061612.g005

concentrations ranging from 0.05–1.5 M (1:50 virus particles to buffer), followed by titrations on BHK-21 cells. Alternatively the virus particles in TNE buffer (pH 7.4) were treated at temperatures of 25°C, 37°C, 45°C or 55°C for 30 minutes, after which the samples were cooled on ice and titrated. The 1:50 dilution of the SDG purified particles ensured that the stabilising effect of sucrose was negligible as it was calculated the viscosity was less than 1%. All assays were performed in duplicate and the average virus titers were determined.

In addition, SDG-purified particles with an approximate titer of $4–8\times10^6$ pfu/ml were either treated at pH 6.0, or heated at 42°C for different time intervals following a 1:50 dilution in the appropriate TNE buffer. The number of infectious particles remaining after treatment was determined by plaque titrations on BHK-21 cells. The respective logarithmic values of the virus titers

at the different time points (0, 15, 30, 45, 60, 90, 120 and 180 min p.i) were linearly fitted and the slopes were determined [42,43] using the R statistical software [44]. The percentage of remaining infectious particles was also calculated and plotted along with the exponential decline used to calculate the inactivation rate constant as described [14].

Structural analysis of variable amino acids in capsid subunits

Three-dimensional models of protomers comprising the four capsid proteins (1A, 1B, 1C and 1D) of the SAT2 viruses were constructed based on the crystallographic coordinates of O1BFS (1FOD) [45], while pentameric models were built using the capsid coordinates, $A_{10}61$ (1ZBE). The models were based on an optimal amino acid alignment of the capsid proteins. Sequence alignments were performed with ClustalX software [46] using the default parameter setting. The modelling scripts were generated using the structural module in the FunGIMS software pakage and models were built using the Modeller 9v1 programme [47]. The homology structure was calculated by the satisfaction of spatial restraints as described by empirical databases. Structures were visualised with PyMol v0.98 (DeLano Scientific LLC). A PROPKA [48] analysis of each protomer was carried out to identify major protonation states affected by a pH of 6.0. Yasara [49] was used to analyse any hydrogen bond networks that were present.

pH-dependent differences between pentamers were investigated using a molecular dynamics simulation for ~2.5 ns [49]. The simulation was performed at a pH of 6.0, water density of 0.997 g/ml and a NaCl concentration of 0.9% using the Amber99 force-field with periodic boundary conditions at a temperature of 298 K. A molecule consisting of two protomers (henceforth called the dimer) was also generated to analyse the interface between two pentamers.

Results

Construction and *in vitro* characterization of genetically engineered FMDV

To study the stability of SAT2 and SAT3 virions and the amino acid differences responsible for altered stabilities in a defined genetic background, we constructed infectious chimeric cDNA clones, containing the 1B/C/D/2A-coding region of SAT2 and SAT3 field isolates in the defined genetic background of an infectious pSAT2 genome-length clone (ZIM/7/83) [15]. Clones containing the capsid-coding region of southern Africa SAT2 isolates, *i.e.* SAT2/ZIM14/90, SAT2/ZIM/17/91 and SAT2/

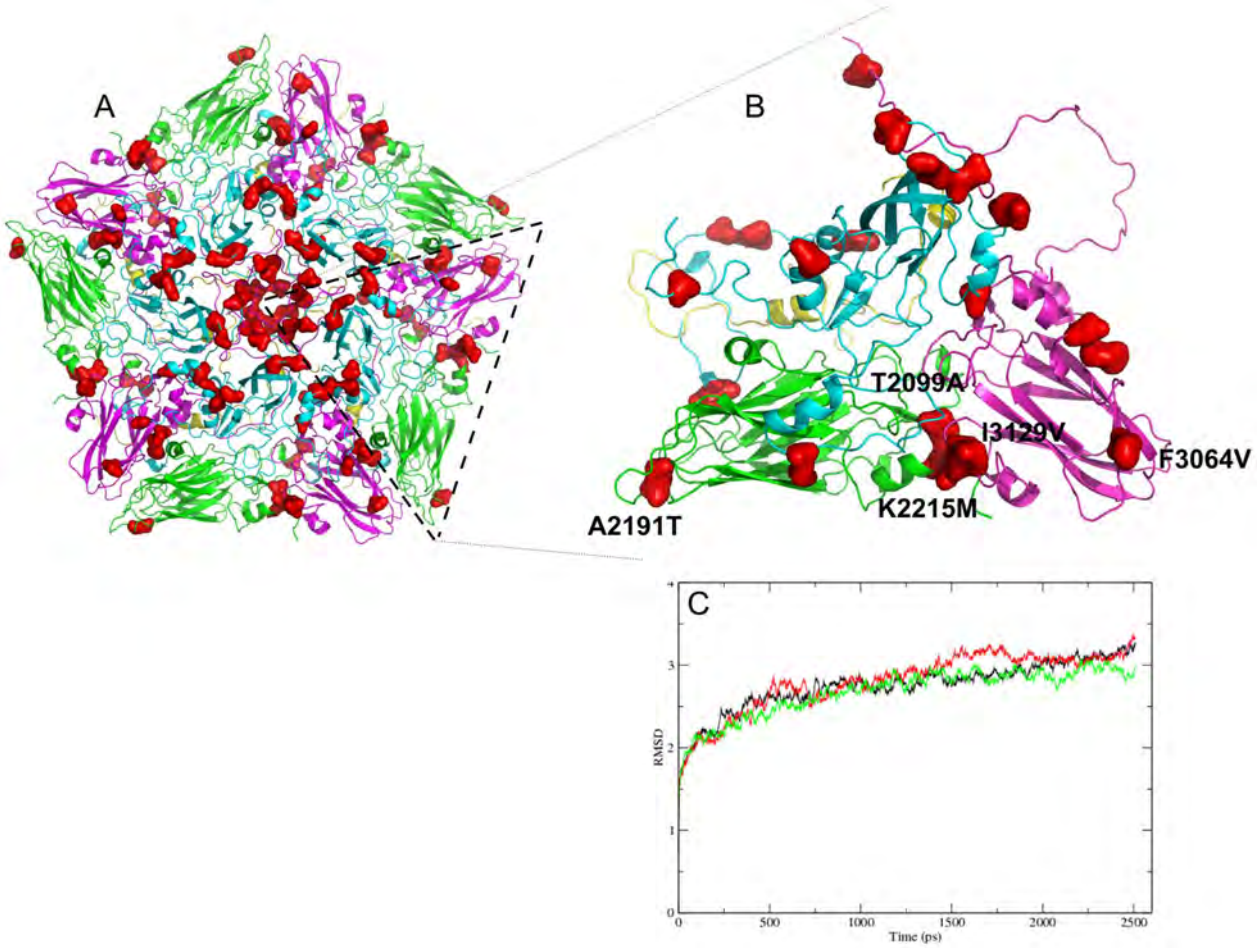

Figure 6. Variation observed in VP1-3 mapped to the structural models of the SAT2 (A) pentamers and (B) protomers. The amino alignment and effect of the variable residues is shown in Table S1. Residues predicted to play a role in the capsid stability are shown here. Variable positions are coloured in red, VP1 in cyan, VP2 in green, VP3 in magenta and VP4 in yellow. (C) The Cα RMSD variation of SAT2/ZIM/7/83 (in red), vSAT2 (in black) and $vSAT2^{ZAM7}$-SAT2 (in green) over the ~2.5 ns simulation time at pH 6.0 using the pentamers.
doi:10.1371/journal.pone.0061612.g006

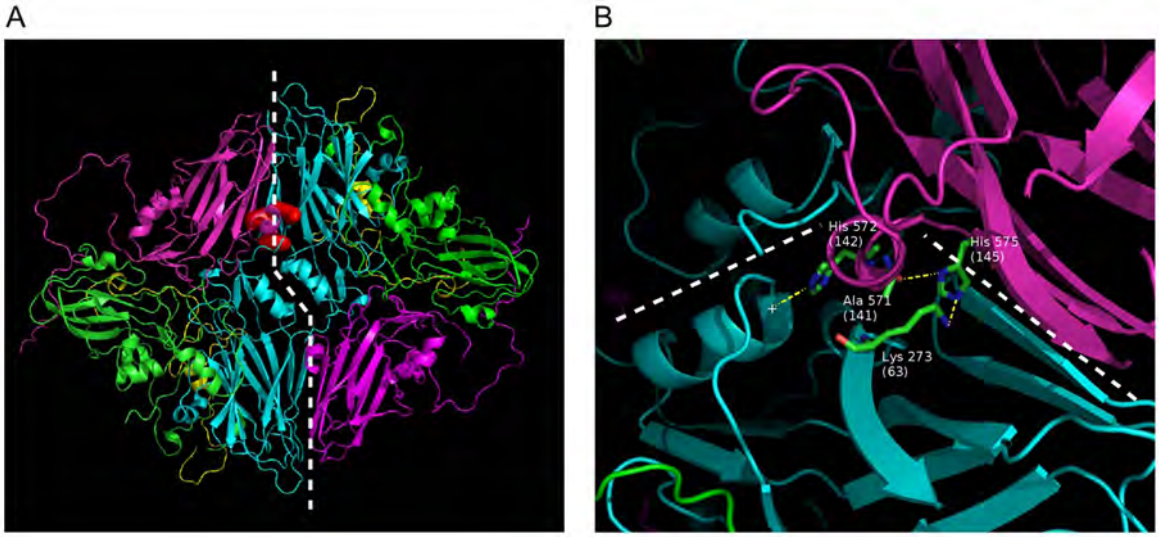

Figure 7. The interaction interface between two adjacent pentamers. (A) One protomer of each pentamer is shown. The dashed line indicates the interaction surface. VP3 residues H145, H142 and K63 using Van der Waals surfaces are coloured red. (B) The hydrogen bond network found in the pentamer interface. When VP3 H145 is neutral, it forms a hydrogen bond with VP2 K63 and VP3 A141. The neutral state seems to prevent pentamer association through H142 and H145. Yellow dashed lines indicate hydrogen bonds and the white dashed line indicates pentamer interface. The "+" indicates the charged dipole of the α-helix.
doi:10.1371/journal.pone.0061612.g007

ZAM/7/96, as well as a SAT3 virus, SAT3/ZAM/4/96, were selected to synthesize RNA. The transcript RNAs were transfected into BHK-21 cells and viable chimeric viruses recovered. The recombinant viruses derived from the infectious chimeric cDNA clones were designated vSAT2^{ZIM14}-SAT2, vSAT2^{ZIM17}-SAT2, vSAT2^{ZAM7}-SAT2 and vSAT3^{ZAM4}-SAT2, respectively (Fig. 1). The vSAT3^{ZAM4}-SAT2 is the only inter-serotype chimera containing the SAT3 outer capsid-coding region in a SAT2 genetic background.

Plaque morphologies, growth and antigenic properties of the recombinant viruses were examined to determine whether they resembled those of the parental viruses. As illustrated in Fig. 1, SAT2 and SAT3 field viruses, and the derived chimeric viruses produced large plaques (7–8 mm) on BHK-21 cells. The SAT2/ZIM/7/83 parental virus (passage history: B1BHK5B1) produced large plaques while its genetically-cloned derivative, vSAT2 (passage history: BHK3), produced a mixture of large and small (3–5 mm) plaques on BHK-21 cells. A porcine kidney cell line (IB-RS-2), known to express $\alpha_V\beta8$ [50], was also included in the analysis. The distribution of large plaques (7–8 mm) formed by the parental SAT2 and SAT3 viruses and vSAT2^{ZAM7}-SAT2 on IB-RS-2 cells were similar to those observed on BHK-21 cells (Fig. 1). The vSAT2^{ZIM14}-SAT2, vSAT2^{ZIM17}-SAT2 and vSAT3^{ZAM4}-SAT2 viruses formed medium plaques (3–5 mm) on IB-RS-2 cells (Fig. 1). In CHO-K1 (wild-type, glycosaminoglycan or GAG positive) cells, only the SAT2 vaccine strain, ZIM/7/83 and its derivative, vSAT2, were able to propagate, yielding small plaques (<2 mm) 48 h post-infection (p.i.) (Fig. 1). SAT2 and SAT3 field viruses, as well as their genetically-cloned derivatives, vSAT2-^{ZIM14}-SAT2, vSAT2^{ZIM17}-SAT2, vSAT2^{ZAM7}-SAT2 and vSAT3-^{ZAM4}-SAT2, were unable to produce plaques on CHO-K1 cells (Fig. 1). Subsequently, CHO-677 (GAG-deficient cell line) were also infected with the respective recombinant SAT viruses, but none of these viruses were able to replicate (not shown).

The growth kinetics of both field SAT2 and SAT3 and genetically-engineered intra- and inter-serotype viruses illustrates that the growth of the chimeric viruses, vSAT2^{ZIM14}-SAT2, vSAT2^{ZIM17}-SAT2, vSAT2^{ZAM7}-SAT2 and vSAT3^{ZAM4}-SAT2, were similar to that of the vSAT2 (Fig. 2A) and parental field viruses (Fig. 2B). Following infection of BHK-21 cells at a m.o.i. of 2–5 pfu/cell all viruses yielded high and comparable titers at 20 h p.i., after which their growth became indistinguishable.

Next we compared the antigenic profiles of the parental and the three intra-serotype chimeric viruses using SAT2 antisera from prototype strains in a virus neutralization (VN) assay (Table 2). The antigenic variation of the parental SAT2 isolates with the antisera was pronounced, returning r_1-values of lower than 0.2, even though SAT2/ZIM/7/83, SAT2/ZIM/14/90 and SAT2/ZIM/17/91 belonged to the same topotype [25]. Based on the VN assay results, the r_1-values of the chimeric viruses (Table 2) indicated that the sera reacted similarly to the recombinant SAT2 viruses, suggesting the absence of significant alterations in the structure of antigenic determinants on the chimeric virions. The r_1-values of SAT2/ZAM/7/96 and vSAT2^{ZAM7}-SAT2 against the reference sera were below 0.2. Hence, the results from the plaque morphology, growth kinetics and VN assays demonstrate that the immunological characteristics and receptor preferences of the parental field isolates were transferred to the chimeric viruses.

Analysis of receptor usage by the engineered SAT type FMDV

The receptor specificity of the chimeric SAT2 viruses was investigated using COS-1 cells, co-transfected with bovine α_V integrin subunit and either of the β1, β3 or β6 subunit cDNAs. Replication of vSAT2 and the SAT2 chimeric viruses, vSAT2-^{ZIM14}-SAT2 and vSAT2^{ZIM17}-SAT2, was demonstrated in cultured cells expressing $\alpha_V\beta6$ (Fig. 3). The bovine αvβ1 integrins were not able to sustain infection for any of these viruses. Only low level virus protein synthesis was detected in bovine αvβ3-expressing cells infected with vSAT2, vSAT2^{ZIM14}-SAT2 and vSAT2^{ZIM17}-SAT2.

Stability of SAT viruses to biophysical conditions

The stability of SAT2 and SAT3 chimeric viruses to different pH, ionic strength and temperature conditions was evaluated. Treatment of the SDG-purified SAT2 and SAT3 chimeric viruses to buffered solutions of varying pH revealed intra-serotype differences with respect to viral capsid stability in mild acidic pH (Fig. 4A). Both vSAT2^{ZIM17}-SAT2 and vSAT2^{ZIM14}-SAT2 chimeric infectious particles (western lineage) displayed a comparable decrease in titer when the pH of the buffers were reduced from 9.0 to 6.2, with 21–25% infectivity remaining after 30 minutes at pH 6.2 (Fig. 4A). This stability profile was comparable to vSAT2 where 23% infectivity remained at pH 6.2, with a sudden drop in titer at a pH <6.2 (Fig. 4A). For the chimeric SAT2 viruses, the pH_{50} values, defined as the pH where 50% of infectivity is measurable, were calculated as 6.46 and 6.48 for vSAT2^{ZIM14}-SAT2 and vSAT2^{ZIM17}-SAT2, respectively. The pH_{50} value vSAT2 was calculated to be 6.51.

Conversely, vSAT2^{ZAM7}-SAT2 revealed a significantly higher sensitivity in buffers at and below pH 6.5 as evidenced by a 260-fold decrease in infectious particles (1.5% infectivity remaining) within 30 min of incubation at pH 6.2, compared to the virus titer measured at pH 7.4 (Fig. 4A). At pH 6.0, no vSAT2^{ZAM7}-SAT2 infectious particles were detected, while vSAT2, vSAT2^{ZIM14}-SAT2 and vSAT2^{ZIM17}-SAT2 maintained a titer of 10^2 pfu/ml (Fig. 4A). The SAT3 inter-serotype chimera, vSAT3^{ZAM4}-SAT2, showed a >2000-fold drop in titer when the pH was lowered from 7.4 to 6.2 and it diminished rapidly with no infectious particles detected at pH 6.0 (Fig. 4A). The pH_{50} values for the infectious virus particles were calculated as 6.8 and 6.81 for vSAT2^{ZAM7}-SAT2 and vSAT3^{ZAM4}-SAT2, respectively.

The recombinant virions showed remarkable resilience in a series of buffers with increasing ionic strengths (0.05–1.5 M NaCl; Fig. 4B). Similar virus titers were observed for purified vSAT2, vSAT2^{ZIM14}-SAT2, vSAT2^{ZIM17}-SAT2 and vSAT2^{ZAM7}-SAT2 infectious 146 S particles in buffered solutions containing varying NaCl concentrations of between 0.05–1.5 M (Fig. 4B). Although differences in titers were observed, it is not believed to carry any biological relevance, with the exception of vSAT2 incubated in 1.5 M NaCl. A significant drop in titer was observed for vSAT2 after 30 min incubation in 1.5 M NaCl. It has been reported for A24 Cruzeiro empty capsids that increasing ionic strength (50 to 250 mM) destabilizes the capsids [12]. Although we did not investigate the effect of ionic strength on the SAT2 empty capsids, the destabilizing effect on infectious particles was observed at ten times the physiological salt concentration (1.5 M NaCl).

When incubated at temperatures ranging from 20°C to 55°C, the vSAT2, and the chimeric viruses, displayed similar thermostability with 6–14% residual infectivity remaining after incubation at 45°C for 30 min (data not shown). No infectious particles were detected after incubation at 55°C for 30 min.

Heat and pH inactivation of SAT2 and SAT3 viruses

The differences in the stability of the chimeric virions were further elucidated using pH and heat inactivation assays. These inactivation assays were done in a similar way, essentially SDG-purified chimeric particles at an approximate titer of 4–9×10^6 pfu/ml, were either treated in a pH 6.0 buffer or at 42°C in a pH 7.4 buffer for different time intervals as indicated in Fig. 5. The observed inactivation profiles of the particles in a pH 6.0-buffered solution did not conform to a linear, but rather a logarithmic decrease in the number of infectious viral particles (Fig. 5A). When plotting the logarithmic titers over time, the acid lability of the chimeric viruses was reflected by the inactivation rate constant values at pH 6.0, which were 0.002, 0.008, 0.013, 0.013 and 0.012 per minute (min^{-1}) for vSAT2, vSAT2^{ZIM14}-SAT2, vSAT2^{ZIM17}-SAT2, vSAT2^{ZAM7}-SAT2 and vSAT3^{ZAM4}-SAT2, respectively. The inactivation rates of vSAT2^{ZIM17}-SAT2, vSAT2^{ZAM7}-SAT2 and vSAT3^{ZAM4}-SAT2 were higher than that of vSAT2 and vSAT2^{ZIM14}-SAT2 viruses and were a reflection of the faster deterioration of the infectious particles following treatment in a pH 6.0 buffer (Fig. 5A). The vSAT2 virus showed the slowest rate of inactivation which resulted in *ca.* 24% of infectious particles remaining after 3 h treatment at pH 6.0 (Fig. 5B).

Contrary to the pH inactivation rates, no substantial differences with respect to thermostability were demonstrated between the vSAT2 and chimeric viruses (Fig. 5C). Temperature inactivation profiles can be drawn by plotting the decrease in virus logarithmic titers over time. The inactivation rate constants were then determined from the slope of the linear plots. The inactivation rate constant values at 42°C for vSAT2^{ZAM7}-SAT2 and vSAT2 were 0.013 and 0.015 min^{-1}, respectively, while the value for the remaining three chimeras was determined to be to be 0.018 min^{-1} (Fig. 5C). The decrease in the percentage of infectivity was similar to vSAT2 with 6–12% residual infectivity after 3 h at 42°C (Fig. 5D). Taken together, the results reveal that contrary to what we suspected, despite the variation in the outer capsid proteins the thermal stability of the FMDV particles was remarkably conserved.

Molecular dynamics and the role of variable amino acids in the FMDV interpentameric interactions

Structural mapping of variable amino acid residues within the outer capsid proteins of the chimeric SAT2 viruses that may play a role in the altered acid sensitivities was performed. The amino acid differences in the outer capsid proteins were mapped on the structure of a pentameric unit (Fig. 6) and their involvement in VP2–VP3 and VP2–VP2 pairwise contacts at the pentameric interface were analysed (Fig. S1, Table S1). The 50 amino acid differences that were observed between vSAT2 and the less acid-stable vSAT2^{ZAM7}-SAT2 may suggest that some of these residues play a critical role in virion stability (Table S1).

Alignment of the capsid proteins showed that 10.5% of the residues were variable. The internally located 1A protein of the chimeric viruses and the vSAT2 virus shared 100% identity, due to the cloning strategy followed (Fig. 1). Although 1A may be involved in protein-RNA interaction or exert a small effect on inter-protomer interactions, the overall effect of 1A in the stability of the SAT2 virions was not taken into consideration in this analysis. The variation within the outer capsid proteins could be categorised into three groups, *i.e.* those having no effects (surface-exposed variable residues with no change in the local structure or interactions); those affecting the intra-protomer association; and those affecting the inter-protomer interactions (Fig. 6A).

The majority of the variable residues were surface-exposed, suggesting that these changes may exert a minimal effect on the stability of the capsid. At least 17 of the observed differences appeared to have putative effects on protomer-protomer interactions based on the predicted models (Fig. 6A and B). Although six of the variable residues could be considered as neutral and did not appear to influence the structure significantly, at least 11 of the 17 variable residues appeared to result in the addition or loss of interactions. Five of these residues mapped to the protomer particularly at the pentameric interface and adjacent to the pores located at the 3-fold axis (Fig. 6A and B). These differences may indeed influence the capsid assembly and disassembly dynamics, but still needs to be confirmed experimentally.

Molecular dynamics simulations were performed for ~2.5 ns with the vSAT2, SAT2/ZIM/7/83 and vSAT2^{ZAM7}-SAT2 pentamers. The root mean-square deviation (RMSD) variation over time for each of the pentamers at pH 6.0 is shown in Fig. 6C. Contrary to the lower acid stability observed for the purified vSAT2^{ZAM7}-SAT2 infectious particles, there was no noteworthy difference in the RMSD of the pentamers of the viruses included in the study. Any significant difference between the infectious particles, such as pentamer dissociation, was expected to result in high RMSD values.

PROPKA analysis of the modelled FMDV protomer structures, however, indicated four His residues that play putative roles in capsid stability, *i.e.* H81 and H115 in VP2 and H145 and H172 in VP3. Of these, the His residue at position 145 of VP3 correlated with the residues at the pentameric interfaces that were previously identified and shown to contribute to virion stability [13]. These His residues are most likely involved in inter-pentamer interactions and are buried in the dimer interface, thereby concealing them from the aqueous phase. Changes in pKa values of the His residues in either a single protomer or two adjacent protomers (dimer) were determined with PROPKA analysis. The predicted pKa values of the protomers indicated that the four His residues changed protonation states in the region of pH 6.0. When the pattern of binding by these His residues was taken into consideration, it appeared as if none of the protomers of the SAT2 viruses, ZIM/7/83, vSAT2 or vSAT2^{ZAM7}-SAT2, gained or lost a nett amount of bonds. However, when the residues were mapped to the predicted protein models, bond changes occurring between adjacent VP3 chains in the pentamer interfaces were clearly observed.

Discussion

There is a large body of evidence suggesting that thermal stability of complete 146S FMDV particles and the immunogenicity of the particles could be linked to vaccine efficacy [1]. There is a common believe that SAT viruses are particularly unstable and very little is known about residues located at the SAT pentameric interfaces involved in structural stability. Consequently, we have investigated the biophysical stability of infectious virions generated from southern African isolates of the SAT2 and SAT3 serotypes under various controlled environmental conditions which are relevant during the vaccine production process.

We have demonstrated that chimeric viruses, containing the outer capsid of dissimilar viruses in a SAT2 genetic background, retained the plaque phenotypes, infectivity kinetics and immunological profiles of the parental strains (isolated during an outbreak) from which they were derived. With respect to cellular receptor preferences [50,51], the SAT2 and SAT3 viruses originating from buffalo grew in BHK-21 or IB-RS2 cells following amplification in cell culture, but were unable to infect and replicate in CHO-K1 cells, suggesting that these field viruses do not utilize GAG receptors for cell entry. The interaction of SAT2 viruses with three $\alpha_V\beta$-integrin molecules was demonstrated in this study by expressing these integrin molecules transiently in COS cells. The results indicated that not all the integrins are used with the same affinity for cell entry by the SAT2 viruses. Whereas the SAT2 viruses were able to infect and replicate in COS cells expressing the $\alpha_V\beta6$ integrins, we found that these viruses displayed a poor ability to infect cells expressing $\alpha_V\beta3$ integrins, the result of which is in agreement with previous findings. with regards to the low affinity of type O_1 viruses for $\alpha_V\beta3$ receptors [50,52,53]. This observation may be attributed to the G-H loop in VP1 that is structurally not optimal for binding to the $\alpha_V\beta3$ integrin [54]. Contrary to the ability of type O_1 viruses to utilize $\alpha_V\beta1$ and $\alpha_V\beta6$ with a high efficiency [50,52,53], the $\alpha_V\beta1$ integrins were not able to mediate infection of any of the SAT2 viruses under the experimental conditions.

We found that virus particles of the SAT2 serotype, which differ by less than 11% in the capsid protein amino acid sequences, are stable in mild acidic conditions from pH 6.5 to 7.0. However, their infectivity was rapidly lost in buffers with a pH below 6.5, although infectious particles could still be detected at pH 6.0. The range of pH_{50} variation for the SAT2 serotype was 0.4 pH units between pH 6.8 and 6.4, with vSAT2^{ZAM7}-SAT2 (SAT2/ZAM/7/96 derivative) being the least stable. The infectious vSAT3^{ZAM4}-SAT2 particles also displayed a pronounced sensitivity under acidic conditions, losing 50% of its infectivity at pH 6.81. This variation in pH sensitivity did not appear to hamper the growth properties of the SAT2 or SAT3 viruses in cultured cells, an attribute to be expected of a virus that depends on acidification within endosomes for RNA release and replication [32].

SAT2 and SAT3 chimeric infectious particles were sensitive to mild heating. Thermal dynamics indicated that the SAT infectious particles decreased at a rate fitted best to single first order kinetics that is consistent with simple dissociation and similar to the behavior of a type C virus under mild temperature conditions [14]. It is known that mild heating of FMDV virions leads to irreversible dissociation into stable pentamers or 12S particles [1,14]. Consequently, the first order kinetics observed for the SAT inactivation suggests similar dissociation of the infectious virions. The dissociation of virions in an acidic environment is considered to similarly lead to dissociation into pentamers and the observed inactivation rate was typified by a linear decrease of the logarithmic titer. Contrary to the thermal dynamics and acid lability of the SAT2 and SAT3 infectious particles, these particles were consistently stable in solutions with a high ionic strength and a pH as high as 9.0.

The stability of the FMD virion can be described as an equilibrium of multimeric electrostatic and hydrophobic interactions between the protein subunits and disruption of these interaction causes dissociation of the virion [11,55,56,14]. Two likely residues, *i.e.* H142 and H143 in VP3, responsible for the destabilization of serotype A viruses as a function of pH, have been described previously [57,58]. In an attempt to identify the relevant residues and side chain interaction that may cause the SAT2/ZAM/7/96 to be less stable in mild acidic conditions compared to the other SAT2 viruses, we mapped the amino acid variation to a modeled structure of the SAT2 capsid. While some of the amino acid variation was mapped to the surface of the virion, most of the variation was adjacent to the pore at the five fold axis of the virion (Table S1). These residues have the potential of interacting with VP4 or viral RNA at the inside of the pore [12]. When the variable surface-exposed residues were ignored on the basis that they may be involved in virus neutralisation or cell entry and, therefore, their effect on virion stability regarded to be minimal, at least 11 amino acid residues revealed potential protein-protein interaction. Five residues mapped to the pentamer interface, three (T2099A, K2215M and I3128V) of which shows interactions with residues at the C-terminus of the VP2 α-helix, responsible for interactions across the interface. A2191T and F3064V form hydrogen bonds across the interface at the 3-fold axis.

The pentamer models for vSAT2, SAT2/ZIM/7/83 and SAT2/ZAM/7/96 were built on the same template, therefore RMSD deviation after dynamic simulation could be directly compared. The molecular dynamics simulations of the related vSAT2 and SAT2/ZIM/7/83, and the distant SAT2/ZAM/7/96 showed that the pentamers were stable during the simulation as

seen from the RMSD curves in Fig. 6. This indicates that the effect on the stability of the virus particles should be seen at the level of pentamer assembly into virions and not at a level of protomers assembling into pentamers. We also could not detect any change in the protonation state in any of the residue changes among the SAT2 viruses.

The pKa predictions results for the protomers indicated four His residues which change protonation states around pH 6.0. H145 in VP3 is involved in inter-protomer interaction on the pentameric interfaces and hydrogen bond analysis of the dimer molecule showed that this residue interacts with A141 in VP3 and with K63 in VP2 of the adjacent protomer (Fig. 7). The PROPKA results for the dimer molecule show the pKa for VP3 H145 to be -1.12. Thus, from these results it appears that a pH below 6.0 would disrupt interactions at the pentamer interface. A significant proportion of VP3 H145 needs to be neutral for pentamers to assemble into a capsid. This confirms previous observations that VP3 H145 plays a role in capsid disassembly and vaccine stability [12,13,57]. The VP3 H142 residue was also shown to be important in the association between the pentamers. The hydrogen bond analysis showed that VP3 H145 made a hydrogen bond with the backbone of VP3 A141 (Fig. 7B). This backbone hydrogen bond seems to be important is helping to orientate the VP3 H142 containing loop correctly to form the association with the charged dipole of the alpha-helix. The VP3 H145 also makes a hydrogen bond with VP2 K63 in the adjacent pentamer, thus providing extra interaction and stabilization between the pentamers (Fig. 7B). The loss of the hydrogen bonds with either VP2 K63 or VP3 A141 would have a significant effect on the interaction interface.

Our study provides evidence that SAT2 viruses isolated from buffalo enters the cell host with a preference for $\alpha_V\beta6$ integrin receptors. Moreover, the SAT virus particles were shown to dissociate within a range of mild acidic conditions which does not significantly impact on viral functions or infectivity. Furthermore, chimeric SAT viruses containing the immunological outer capsid-coding region of an emerging virus in the genetic background of a stable vaccine strain are infectious. Together, the data demonstrate the utility of recombinant DNA technology to produce chimeric viruses as vaccine seed stock with desirable properties and thermal-stability for the improvement of virus immunogenicity and vaccine efficacy.

Supporting Information

Figure S1 Sequence alignment of the outer capsid proteins of the SAT2 viruses included in this study, i.e. ZIM/7/83, ZIM/14/90, ZIM/17/91 and ZAM/7/96.
(DOC)

Table S1 A summary of the variable amino acids in an alignment of the capsid proteins of the SAT2 viruses ZIM/7/83, ZIM/14/90, ZIM/17/91 and ZAM/7/96 and the possible interactions of the residues in the complete capsids.
(DOC)

Acknowledgments

The authors would like to express their gratitude to the personnel at the ARC-OVI (TADP) for their contributions to virus isolation and animal work. Many thanks to Jan Esterhuysen for his contribution with performing VNT's and Geoff Fosgate for the statistic performed in this study. We would also like to thank Drs Sonja Maree, Katherine Scott, Ben Mans and Jacques Theron for commenting and critical reading of the manuscript.

Author Contributions

Conceived and designed the experiments: FM TdB ER. Performed the experiments: FM BB TdB ER. Analyzed the data: FM TdB ER. Contributed reagents/materials/analysis tools: FM ER. Wrote the paper: FM TdB ER.

References

1. Doel TR, Baccarini PJ (1981) Thermal stability of foot-and-mouth disease virus. Arch Virol 70: 21–32.
2. Barnett PV, Carabin H (2002) A review of emergency foot-and-mouth disease (FMD) vaccines. Vaccine 20: 1505–14.
3. Doel TR (2003) FMD vaccines. Virus Res 91: 81–99.
4. Pay TWF, Rweyemamu MM, O'Reilly KJ (1978) Experiences with Type SAT 2 foot-and-mouth disease vaccines in Southern Africa. XVth Conference of the Office International Des Epizzoties Permanent Commision on foot-and-mouth disease. p1–25.
5. Preston KJ, Owens H, Mowat GN (1982) Sources of variations encountered during the selection and production of three strains of FMD virus for the development of vaccine for use in Nigeria. J Biol Stand 10: 35–45.
6. Amadori M, Berneri C, Archetti IL (1994) Immunogenicity of foot-and-mouth disease virus grown in BHK-21 suspension cells. Correlation with cell ploidy alterations and abnormal expression of the alpha 5 beta 1 integrin. Vaccine 12: 159–166.
7. Bachrach HL (1968) Foot-and-mouth disease. Annu Rev Microbiol 22: 201–244.
8. Pereira HG (1978) Antigenic variation in relation to epidemiology and control of foot and mouth disease. Br Vet J 35: 167–74.
9. Sobrino F, Saiz M, Jiménez-Clavero MA, Núñez JI, Rosas MF, et al. (2001) Foot-and-mouth disease virus: a long known virus, but a current threat. Vet Res 32: 1–30.
10. Domingo E, Baranowski E, Escarmís C, Sobrino F (2002) Foot-and-mouth disease virus. Comp Immunol Microbiol Infect Dis 25: 297–308.
11. Acharya R, Fry E, Stuart D, Fox G, Rowlands D, Brown F (1989) The three-dimensional structure of foot-and-mouth disease virus at 2.9 A resolution. Nature 337: 709–716.
12. Curry S, Fry E, Blakemore W, Abu-Ghazaleh R, Jackson T, et al. (1996) Perturbations in the surface structure of A22 Iraq foot-and-mouth disease virus accompanying coupled changes in host cell specificity and antigenicity. Structure 4: 135–145.
13. Ellard FM, Drew J, Blakemore WE, Stuart DI, King AM (1999) Evidence for the role of His-142 of protein 1C in the acid-induced disassembly of foot-and-mouth disease virus capsids. J Gen Virol 80: 1911–1918.
14. Mateo R, Díaz A, Baranowski E, Mateu MG (2003) Complete alanine scanning of intersubunit interfaces in a foot-and-mouth disease virus capsid reveals critical contributions of many side chains to particle stability and viral function. J Biol Chem 278: 41019–41027.
15. Van Rensburg HG, Henry T, Mason PW (2004) Studies of genetically defined chimeras of a European type A virus and a South African Territories type 2 virus reveal growth determinants for foot-and-mouth disease virus. J Gen Virol 85: 61–68.
16. Maree FF, Blignaut B, de Beer TAP, Visser N, Rieder E (2010) Mapping of amino acid residues responsible for adhesion of cell culture-adapted foot-and-mouth disease SAT type viruses. Virus Res 153: 82–91.
17. Liljas L (1986) The structure of spherical viruses. Prog Biophys Mol Biol 48: 1–36.
18. Rossmann MG, Johnson JE (1989) Icosahedral RNA virus structure. Annu Rev Biochem 58: 533–573.
19. Reguera J, Carreira A, Riolobos L, Almendral JM, Mateu MG (2004) Role of interfacial amino acid residues in assembly, stability, and conformation of a spherical virus capsid. Proc Natl Acad Sci USA 101: 2724–2729.
20. Reguera J, Grueso E, Carreira A, Sánchez-Martínez C, Almendral JM, et al. (2005) Functional relevance of amino acid residues involved in interactions with ordered nucleic acid in a spherical virus. J Biol Chem 280: 17969–77.
21. Mateo R, Luna E, Rincón V, Mateu MG (2008) Engineering viable foot-and-mouth disease viruses with increased thermostability as a step in the development of improved vaccines. J Virol 82: 12232–40.
22. Vosloo W, Kirkbride E, Bengis RG, Keet DF, Thomson GR (1995) Genome variation in the SAT types of foot-and-mouth disease viruses prevalent in buffalo (Syncerus caffer) in the Kruger National Park and other regions of southern Africa, 1986–93. Epidemiol Infect 114: 203–218.
23. Van Rensburg HG, Nel LH (1999) Characterization of the structural-protein-coding region SAT 2 type foot-and-mouth disease virus. Virus Genes 19: 229–233.
24. Bastos ADS, Haydon DT, Forsberg R, Knowles NJ, Anderson EC, et al. (2001) Genetic heterogeneity of SAT-1 type foot-an-d-mouth disease viruses in southern Africa. Arch Virol 146: 1537–1551.

25. Bastos ADS, Haydon DT, Sangare O, Boshoff CI, Edrich JL, et al. (2003) The implications of virus diversity within the SAT 2 serotype for control of foot-and-mouth disease in sub-Saharan Africa. J Gen Virol 84: 1595–1606.
26. Mateu MG (1995) Antibody recognition of picornaviruses and escape from neutralization: a structural view. Virus Res 38: 1–24.
27. Mateu MG, Valero ML, Andreu D, Domingo E (1996) Systematic replacement of amino acid residues within an Arg-Gly-Asp-containing loop of foot-and-mouth disease virus and effect on cell recognition. J Biol Chem 271: 12814–12819.
28. Samuel AR, Knowles NJ (2001) Foot-and-mouth disease virus: cause of the recent crisis for the UK livestock industry. Trends Genet 17: 421–424.
29. Rossmann MG, Greve JM, Kolatkar PR, Olson NH, Smith TJ, et al. (1997) in Structural Biology of Viruses (Chiu W, Garcea R, Burnette R, eds). 105–133, Oxford University, Press, Oxford.
30. Brown F, Cartwright (1963) Purification of radioactive foot-and-mouth disease virus. Nature 199: 1168–70.
31. Burroughs JN, Rowlands DJ, Sangar DV, Talbot P, Brown F (1971) Further evidence for multiple proteins in the foot-and-mouth disease virus particle. J Gen Virol 13: 73–84.
32. Carrillo EC, Giachetti C, Campos RH (1984) Effect of lysosomotropic agents on the foot-and-mouth disease virus replication. Virology 135: 542–545.
33. Curry S, Fry E, Blakemore W, Abu-Ghazaleh R, Jackson T, et al. (1997) Dissecting the roles of VP0 cleavage and RNA packaging in picornavirus capsid stabilization: the structure of empty capsids of foot-and-mouth disease virus. J Virol 71: 9743–9752.
34. Van Vlijmen HWT, Curry S, Schaefer M, Karplus M (1998) Titration calculations of foot-and-mouth disease virus capsid and their stabilities as a function of pH. J Mol Biol 275: 295–308.
35. Rieder E, Bunch T, Brown F, Mason PW (1993) Genetically engineered foot-and-mouth disease viruses with poly(C) tracts of two nucleotides are virulent in mice. J Virol 67: 5139–5145.
36. Duque H, Baxt B (2003) FMDV receptors: comparison of bovine αv integrin utilization by type A and O Viruses. J Virol 77: 2500–2511.
37. Duque H, LaRocco M, Golde WT, Baxt B (2004) Interactions of foot-and-mouth disease virus with soluble bovine αVβ3 and αVβ6 integrins. J Virol 78: 9773–81.
38. Office International des Epizooties (2009). In Manual of Diagnostic Tests and Vaccines for Terrestrial Animals 2009, Chapter 2.1.5. 1–25. Office International des Epizooties, Paris, France.
39. Rweyemamu MM, Ouldridge EJ, Head M, Ferrari R (1984) The effect of antiserum quality on strain specificity assessment of foot and mouth disease virus by the neutralization reaction. J Biol Stand 12: 295–303.
40. Doel TR, Mowat GN (1985) An international collaborative study on foot and mouth disease virus assay methods. 2. Quantification of 146S particles. J Biol Stand 13: 335–44.
41. Knipe T, Rieder E, Baxt B, Ward G, Mason P (1997) Characterization of synthetic foot-and-mouth disease virus provirions separates acid-mediated disassembly from infectivity. J Virol 71: 2851–2856.
42. Mateo R, Mateu MG (2007) Deterministic, compensatory mutational events in the capsid of foot-and-mouth disease virus in response to the introduction of mutations found in viruses from persistent infections. J Virol 81: 1879–87.
43. Mateo R, Luna E, Mateu MG (2007) Thermostable variants are not generally represented in foot-and-mouth disease virus quasispecies. J Gen Virol 88: 859–864.
44. R Development Core Team (2009) R: A Language and Environment for Statistical Computing.
45. Logan D, Abu-Ghazaleh R, Blakemore W, Curry S, Jackson T, et al. (1993) Structure of a major immunogenic site on foot-and-mouth disease virus. Nature 362: 566–568.
46. Thompson JD, Gibson TJ, Plewniak F, Jeanmougin F, Higgins DG (1997) The CLUSTAL_X windows interface: flexible strategies for multiple sequence alignment aided by quality analysis tools. Nucleic Acids Res 25: 4876–82.
47. Fiser A, Sali A (2003) Modeller: generation and refinement of homology-based protein structure models. Methods Enzymol 374: 461–491.
48. Li H, Robertson AD, Jensen JH (2005) Very fast empirical prediction and rationalization of protein pKa values. Proteins 61: 704–721.
49. Krieger E, Nielsen JE, Spronk CA, Vriend G (2006) Fast empirical pKa prediction by Ewald summation. J Mol Graph Model 25: 481–486.
50. Burman A, Clark S, Abrescia NG, Fry EE, Stuart DI, et al. (2006) Specificity of the VP1 GH Loop of foot-and-mouth disease virus for αv integrins. J Virol 80: 9798–9810.
51. Jackson T, Clarck SJ, Berryman S, Burman A, Cambier S, et al. (2004) Integrin αvβ8 functions as a receptor for foot-and-mouth disease virus: Role of the β-chain cytodomain in integrin-mediated infection. J Virol 78: 4533–4540.
52. Jackson T, Mould AP, Sheppard D, King AMQ (2002) Integrin αvβ1 is a receptor for foot-and-mouth disease virus. J Virol 76: 935–941.
53. Neff S, Mason PW, Baxt B (2000) High-efficiency utilization of the bovine integrin αvβ3 as a receptor for foot-and-mouth disease virus is dependent on the bovine β3 subunit. J Virol 74: 7298–7306.
54. Boettiger D, Lynch L, Blystone S, Huber F (2001) Distinct ligand-binding modes for integrin $\alpha_v\beta_3$-mediated adhesion to fibronectin versus vitronectin. J Biol Chem 276: 31684–90.
55. Lea S, Hernandez J, Blakemore W, Brocchi E, Curry S, et al. (1994) The structure and antigenicity of a type C foot-and-mouth disease virus. Structure 2: 123–139.
56. Lea S, Abu-Ghazaleh R, Blakemore W, Curry S, Fry E, et al. (1995) Structural comparison of two strains of foot-and-mouth disease virus subtype O_1 and a laboratory antigenic variant G67. Structure 3: 571–580.
57. Twomey T, France LL, Hassard S, Burrage TG, Newman JFE, et al. (1995) Characterization of an acid-resistant mutant of foot-and-mouth disease virus. Virology 206: 69–75.
58. Curry S, Abrams CC, FryE, Crowther JC, Belsham GJ, et al. (1995) Viral RNA modulates the acid sensitivity of Foot-and-mouth disease virus capsids. J Virol 69: 430–438.

Mechanisms of Foot-and-Mouth Disease Virus Tropism Inferred from Differential Tissue Gene Expression

James J. Zhu*, Jonathan Arzt, Michael C. Puckette, George R. Smoliga, Juan M. Pacheco, Luis L. Rodriguez*

Foreign Animal Disease Research Unit, Agricultural Research Unit, United States Department of Agriculture, Plum Island Animal Disease Research Center, Orient Point, New York, United States of America

Abstract

Foot-and-mouth disease virus (FMDV) targets specific tissues for primary infection, secondary high-titer replication (e.g. foot and mouth where it causes typical vesicular lesions) and long-term persistence at some primary replication sites. Although integrin αVβ6 receptor has been identified as primary FMDV receptors in animals, their tissue distribution alone fails to explain these highly selective tropism-driven events. Thus, other molecular mechanisms must play roles in determining this tissue specificity. We hypothesized that differences in certain biological activities due to differential gene expression determine FMDV tropism and applied whole genome gene expression profiling to identify genes differentially expressed between FMDV-targeted and non-targeted tissues in terms of supporting primary infection, secondary replication including vesicular lesions, and persistence. Using statistical and bioinformatic tools to analyze the differential gene expression, we identified mechanisms that could explain FMDV tissue tropism based on its association with differential expression of integrin αVβ6 heterodimeric receptor (FMDV receptor), fibronectin (ligand of the receptor), IL-1 cytokines, death receptors and the ligands, and multiple genes in the biological pathways involved in extracellular matrix turnover and interferon signaling found in this study. Our results together with reported findings indicate that differences in (1) FMDV receptor availability and accessibility, (2) type I interferon-inducible immune response, and (3) ability to clear virus infected cells via death receptor signaling play roles in determining FMDV tissue tropism and the additional increase of high extracellular matrix turnover induced by FMDV infection, likely via triggering the signaling of highly expressed IL-1 cytokines, play a key role in the pathogenesis of vesicular lesions.

Citation: Zhu JJ, Arzt J, Puckette MC, Smoliga GR, Pacheco JM, et al. (2013) Mechanisms of Foot-and-Mouth Disease Virus Tropism Inferred from Differential Tissue Gene Expression. PLoS ONE 8(5): e64119. doi:10.1371/journal.pone.0064119

Editor: Jagadeesh Bayry, Institut National de la Santé et de la Recherche Médicale U 872, France

Received December 20, 2012; **Accepted** April 11, 2013; **Published** May 28, 2013

This is an open-access article, free of all copyright, and may be freely reproduced, distributed, transmitted, modified, built upon, or otherwise used by anyone for any lawful purpose. The work is made available under the Creative Commons CC0 public domain dedication.

Funding: This work was funded by USDA-ARS project 1940-32000-057-00D. The funders had no role in study design, data collection and analysis, decision to publish, or preparation of the manuscript.

Competing Interests: The authors have declared that no competing interests exist.

* E-mail: james.zhu@ars.usda.gov (JJZ); luis.rodriguez@ars.usda.gov (LLR)

Introduction

Foot and mouth disease (FMD) is one of the most contagious and economically devastating viral animal diseases. It is caused by FMD virus (FMDV), a positive-sense, single stranded RNA virus member of the family Picornaviridae (genus *Aphtovirus*). Susceptible hosts include several domesticated (e.g. cattle, Asian buffalo, sheep, goats, and swine) and wild (e.g. African buffalo and wild boar) cloven-hoofed animals. The morbidity is very high but the mortality is generally low in adult hosts. The infection in cattle commonly occurs via the respiratory route by aerosolized virus [1]. After infection, the virus replicates locally in primary replication sites such as the nasopharynx and lung during the pre-viremic phase [2], [3], [4], [5]. The infection then spreads via the bloodstream (viremic phase) to secondary replication sites where the virus grows to high titers and causes typical blisters, erosions, and ulcers at specific regions of the oral cavity, feet, and occasionally other sites [1]. Persistent infection can occur for long periods (30 days –5 years) with virus persisting at certain primary infection sites (e.g. nasopharynx) in a subset of infected animals [6], [7]. The mechanisms that determine FMDV tissue tropism including target sites for primary, secondary, and persistent infection remain undetermined despite extensive research on this virus discovered over 100 years ago.

Several host integrins including αvβ1, αvβ3, αvβ5, αvβ6 and αvβ8 have been shown to be receptors for FMDV in cultured cells and the mechanism of binding has been shown to involve an Arg-Gly-Asp (RGD) amino acid sequence motif present on the FMDV VP1 [8], [9], [10], [11], [12], [13], [14]. However, several lines of evidence suggest that αvβ6 is the primary FMDV receptor in animals and this receptor expression is associated with FMDV tropism [15], [16], [17], [18]. Despite this evidence, the tissue expression patterns of the integrins do not fully explain the tropism and pathogenesis as many non-susceptible tissues also express the αvβ6 integrin [18]. Results from several studies using other piconaviruses also suggest that viral receptors are not the sole determinants of virus tropism [19]. Interestingly, the site-specific location of vesicular lesions is not unique to FMDV. Vesicular stomatitis virus, swine vesicular disease virus, and vesicular exanthema of swine virus have nearly identical lesion sites and clinical signs as FMD in cattle and swine, suggesting that these targeted tissues possess certain biological characteristics rendering them susceptible to a common pathway associated with these viral vesicular diseases.

Like other pathogenic viruses, the FMDV genome encodes several proteins that facilitate evasion of the innate immune response of infected cells. For example, the leader protease (Lpro) can inhibit host cap-dependent translation by cleaving translation initiator factor eIF4G but has no effects on viral cap-independent translation [20]. Lpro is also found to enter the cell nucleus and inhibit the induction of IFNβ and some interferon stimulated genes [21], [22]. Additionally, there are several reports showing that altering some host cellular factors such as Rab5 and RNA helicase A can inhibit FMDV replication [23], [24]. These findings indicate that host factors other than the virus receptors may be contributing to FMDV tissue tropism.

Because cells differentiate by alternating their gene expression, differential tissue gene expression may provide valuable insights into the molecular mechanisms involved in determining FMDV tissue tropism. We designed a custom bovine whole genome expression microarray and used microarray analysis to identify genes differentially transcribed among tissues targeted and not targeted by FMDV for primary, secondary, and persistent infection in infected and non-infected cattle. The bioinformatic analyses of the differentially expressed genes lead to the identification of several biological processes/pathways which activity could be affected by the differential expression. Based on the expression of the genes involved in these biological processes and on relevant findings from the literature, we propose molecular bases that help explain the mechanisms of FMDV tissue tropism.

Materials and Methods

Animal Inoculations, Tissue Collection, and RNA Preparation

All animal studies were conducted under an approved Institutional Animal Care and Use Committee protocol. Five Holstein steers weighing 225 to 300 kg were obtained from an accredited experimental-livestock provider (Thomas-Morris Inc, Reisterstown, MD). Two of the steers were aerosol-inoculated as previously described [5] with FMDV-A24-Cruzeiro and three were mock inoculated with sterile cell culture media. All steers were euthanized at 72 hours post infection which was coincident with the first observation of generalized FMD (vesicles) in the two infected animals. Necropsies and tissue collections were performed immediately after euthanasia as previously described [3]. For the sites with observed vesicular lesion, tissues with ~0.75 centimeter away from the vesicular lesion were sampled to avoid the impact of tissue necrosis on RNA quality. These tissues were immediately frozen in liquid nitrogen and stored in −70°C. Total tissue RNA was isolated from the frozen tissues using a Qiagen RNA isolation kit (Qiagen, Germantown, MD). The quantity and integrity of RNA samples were examined with a NanoDrop 1000 (Thermo Fisher Scientific, Waltham, MA) and a Bioanalyzer 2000 (Agilent Technologies, Santa Clara CA), respectively. Viral RNA in sera and nasal secretions was quantitated using real-time RT-PCR as previously described [3].

Description and Classification of Analyzed Tissues

Selected tissues were collected based on pathogenesis studies as previously described [3]. The dorsal soft palate (DSP), dorsal nasal pharynx (DNP), and mid anterior lung (LNG) have been shown to be the primary replication sites (PRS) based upon consistent localization of FMDV to these tissues when collected from previremic steers infected with FMDV [3]. The nasal turbinate epithelium (NTE), previously shown not to be infected during the early phase of FMD pathogenesis, was used individually as a negative control for PRS. The interdigital cleft skin (IDC), coronary band (CB), and tongue epithelium (TE) are secondary replication sites (SRS) where the virus can replicate to high titers and cause vesicular lesions. Despite close proximity to the feet, the metacarpal skin (MCS) has never been described as a FMD lesion site in cattle and was therefore chosen as a negative control for SRS. For data analyses, MCS and NTE were also grouped as not targeted sites (NTS) based on low or no viral replication compared to their corresponding targeted tissues. DSP and DNP were also grouped as persistent infection sites (PIS) to contrast all other tissues where FMDV persistence does not occur.

DNA Microarray Design

A bovine whole genome expression microarray was designed based on all bovine expressed sequence tags and RNA sequences from the NCBI database and assembled into unique sequences with the CAP3 program [25]. The assembled sequences were aligned to the bovine genome sequences and displayed with the UCSC genome browser [26]. Non-redundant bovine expressed sequences and sequences with homology to genes in other species but no bovine EST or RNA were selected for probe design. The custom bovine whole genome expression microarray comprised approximately 42,000 60-oligonucleaotide sense probes and was designed with ArrayDesigner 4.0 (PREMIER Biosoft International, Palo Alto CA) from the selected bovine sequences. The probes were designed with locations biased to the 3′-end of RNA sequences in order to produce high signal intensity for fluorescent labeling chemistry using poly-T priming. The annotation of the bovine microarray was based on the results of BLAST against human sequences, manual annotation based on the probe sequence alignments in the bovine genome sequence (Baylor 4.0/bosTau4 October 2007 release), and other genetic information displayed on the UCSC genome browser (http://genome.ucsc.edu/cgi-bin/hgGateway). The DNA probes for all available FMDV genome sequences were also designed and included in the array to detect FMDV RNA levels.

Microarray Analysis

The custom bovine microarrays used in this study were manufactured by Agilent technologies. Agilent Quick Amp RNA labeling kit (Agilent Technologies, Santa Clara CA) was used for the sample labeling. Total RNA prepared from a metacarpal skin sample was labeled with Cy5 and used as a universal control for cross-array data normalization, whereas all samples including 8 tissues from each animal (40 samples) were labeled individually with Cy3. Each Cy3 labeled sample together with the control was hybrided to a microarray. The entire procedure from RNA quality check to microarray hybridization and washing was conducted using reagents and protocols provided by Agilent Technologies. The microarrays were scanned at 5 μm resolution with Cy3:Cy5 signal ratio of between 0.9 to 1 using a GenePix 4000B scanner and GenePix Pro 6.0 program (Molecular Devices, Sunnyvale, CA).

Statistical and Bioinformatic Analyses

Microarray data were extracted from the signal intensity of Cy3 and Cy5 using GenPix Pro 6.0 program and data imported into a SQL database created with Microsoft SQL Server 2000 and Acuity® 4.0 Enterprise Microarray Informatics software (Molecular Devices, Sunnyvale, CA). The data of extracted gene expression signals were background-corrected with the average signals of nearby negative control features. All negative intensity readings were adjusted as 0. The expression data were normalized with the signal of Cy5-labeled universal control to have equal averaged signal intensity. After normalization, all expression data were added with an arbitrary small value of 1 as suggested in the EDGE program user manual (http://

www.genomine.org/edge/edgehelp.pdf) to avoid statistical analysis involved with division by zero. The normalized signal data were square-root-transformed and analyzed using t-test. Differentially expressed genes (DEG) were defined as having a difference of ≥75% or 1.75 fold with a *P* value of 0.05 or smaller in all pair-wise two tissue comparisons between tissue groups. The significant differences obtained from bovine sequences without known human homologous genes were not included in the gene sets and were excluded from further analysis. Eight gene sets including up- and down-regulated in non-targeted sites (NTS) vs targeted sites (SRS+PRS), up- and down-regulated in secondary replication sites (SRS) vs other tissues (NTS+PRS), up- and down-regulated in persistent infection sites (PIS) vs others (NTS+SRS+LNG), and up- and down-regulated in primary replication sites (PRS) vs nasal turbinate epithelium comparisons were created from data obtained from three not infected animals and identified as NTS-up, NTS-down, SRS-up, SRS-down, PIS-up, PIS-down, PRS-up, and PRS-down, respectively (Table 1).

The gene sets were submitted to a BIOBASE web site (http://explain30.biobase-international.com/cgi-bin/biobase/ExPlain_3.0/bin/start.cgi) using a subscribed account to identify the pathways/networks that can regulate the differential expression by analyzing over-represented transcription factor binding sites in the promoter sequences of the identified DEG and can be significantly affected by the differential gene expression using ExPlain™ program (BIOBASE, Wolfenbüttel, Germany). To identify over-represented transcription factor binding sites, all bovine gene sequences used to design the microarray probes were mapped to human genes based on the result of BLAST or annotation from the bovine genome sequence displayed in the UCSC genome browser. The promoter sequences in −500 and +100 bases of transcription starting sites of human genes homologous to the identified bovine DEG were compared to a human house-keeping gene set provided by BIOBASE as a control. The over-represented transcription factor binding sites not shared in compared gene sets were considered as the sites of interests, and signal transduction pathways that can activate transcription factors to bind to these sites are considered to regulate the differential expression. To detect biological networks that may be significantly affected by the differential gene expressions, the gene sets were analyzed to identify those with significant more DEG than that may occur randomly (false discover rate ≤0.05) using statistical tests included in the ExPlain™ program. Both up- and down-stream networks of key nodes were analysis to identify DEG regulating and regulated by the key nodes, respectively.

Biological Inferences

Once candidate pathways/networks were detected, all genes known to be involved in these biological processes were identified and their expression levels were examined in terms of up- or down-regulation and the magnitudes of the differences between tissue groups. Significant differences ($P=$ or <0.05) were analyzed with t-test. Biological impact of differential gene expression was evaluated based on known biological functions of the genes with an assumption that higher transcription levels are associated with higher biological activity of the genes. The tissue activity of indentified pathways/networks was determined based on the expression levels and functions of the genes in the pathways. Biological inferences were made according to the impact of predicted differences in the activity of the pathways on FMDV infection. The data from three non-infected and two infected animals were used to make the inferences.

Estimate of Integrin αVβ6 Receptor Level

RGD-binding integrins were selected based on Hynes [27], which include 1 α subunit (ITGAV) and 5 β subunits (ITGB1, ITGB3, ITGB5, ITGB6, and ITGB8). According to Hynes [27], ITGB1 also forms heterodimeric receptors with ITGA1, ITGA2, ITGA3, ITGA4, ITGA6, ITGA7, ITGA9, ITGA10, and ITGA11, and ITGB3 also binds to ITGA2B. The portion of ITGB1 that may binds to ITGAV (ITGB1_v) was estimated by multiplying the signal intensity of ITGB1 with the percentage of ITGAV intensity in the total intensity of all ITGB1-binding α subunits. Similarly, the portion of ITGB3 binding to ITGAV (ITGB3_v) was calculated by multiplying the level of ITGB3 with the percentage of ITGAV level in the sum of ITGAV and ITGA2B. Finally, the expression level of integrins αVβ6 was estimated based on the product of ITGAV and the percentage of ITGB6 in the sum of ITGB1_v, ITGB3_v, ITGB5, ITGB6, and ITGB8.

Results

Clinical Observations

Steers inoculated with sterile media did not develop fever, vesicular lesions, or any other signs of disease or complications from the aerosolization procedure. The two steers inoculated with FMDV-A24 had very similar clinical syndromes including fever

Table 1. The average microarray signal intensity of FMDV target sequences in the tissues of two infected animals collected at 72 hours post FMDV infection.

Infection sites	Tissues	Tissue tropism	Virus signal
Secondary replication sites	TE	High titer VR, VL, no PI	4445
	IDC		11928
	CB		871
Not targeted sites	MCS	Low VR, no VL, no PI	206
	NTE		39
Primary replication but not persistence site	LNG	Low VR, no VL, no PI	359
Primary replication and persistence sites	DSP	Low VR, no VL, PI	230
	DNP		134

CB: coronary band; DSP: distal soft palate; DSP: distal nasal pharynx; IDC: interdigital cleft skin; LNG: middle anterior lung; MCS: metacarpal skin (control for secondary replication sites); NTE: nasal turbinate (control for primary replication sites); TE: tongue epithelium; VR: FMDV replication; VL: vesicular lesion; PI: persistent infection.
doi:10.1371/journal.pone.0064119.t001

(rectal temperature >39.5C) at 2–3 days post infection and vesicles in the mouth and/or feet detected at 3 days post infection indicating that both animals were at the start of generalized FMDV infection when euthanized for tissue collection. Steer #1 had vesicles in the interdigital cleft of one foot and in the tongue, whereas steer #2 had vesicles on all 4 interdigital clefts. No other lesions were identified. Both animals were subsequently confirmed to have FMDV and viral RNA (8.36–9.08 log10 viral RNA copies/ml) in sera (viremia) and in nasal secretions at the time of euthanasia.

Signal Intensity of FMDV Target Sequences

Varying signal intensities of FMDV microarray features were observed in the infected tissues (Table 1), whereas the tissues of the non-infected animals displayed signal intensities nearly identical to the negative control. As expected, the signal intensities of FMDV RNA from the infected secondary replication sites (sampled away from vesicular lesions) were the highest among the tissues tested. There were also differences among the SRS tissues with significantly lower signals in the coronary band than other secondary replication tissues. Not targeted tissues such as the metacarpal skin and nasal turbinate epithelium displayed 3–4 fold lower FMDV RNA signal than their corresponding targeted tissues. The signal intensity of the metacarpal skin was more than 5 times higher than that of nasal turbinate epithelium. The interdigital cleft skin and lung had the highest signal intensity of the SRS and PRS, respectively; however, the viral RNA signal intensity in the interdigital cleft skin was over 33-fold higher than that in the lung. These results are consistent with viral titers and tissue distribution observed in infected animals in previous studies [2].

Differentially Expressed Genes

Whole genome gene expression profiles of the tissues from the three naïve animals were compared across four tissue categories selected according to their classification as not targeted sites, primary infection, secondary replication, or persistence sites. Tissue categories were based upon previously published studies describing tissue-specific FMDV loads as stated earlier. Eight gene sets were created from the tissue comparisons based on the statistical analysis described earlier (Table 2). In the tissue comparison of not targeted sites versus others, most of the DEG were up-regulated (n = 36) and only two genes were down-regulated (Table 2). Similarly, when comparing the persistent infection site versus other tissues, there were 73 up-regulated and only 4 down-regulated genes. When the SRS or PRS were compared to the rest of the tissues, there were 412 and 220 up-regulated and 103 and 360 down-regulated genes in the secondary and primary replication sites, respectively. These gene sets were statistically analyzed using the ExPlain™ program to infer the biological pathways that could be potentially involved in determining FMDV tissue tropism.

Expression of Integrins αVβ6 and Fibronectin

Integrin β subunits may compete with each other for ITGAV if the expression of ITGAV is a limiting factor. Our results show that the signal intensity of ITGAV was significantly lower than the total of all RGD-binding integrins β (Table 3). Therefore, differential expression of other integrins β besides ITGAV and ITGB6 may also affect the amount of heterodimeric integrins αVβ6 (FMDV receptor). Additionally, the binding between integrins αVβ6 and the ligand, fibronectin (FN1), may hinder the binding of FMDV to the receptors. Therefore, the expressions of integrin αVβ6 heterodimeric receptor and FN1 were examined to determine if the expression of the receptor could explain the mechanisms of FMDV tropism.

Table 2. The number of genes differentially expressed between tissues different in FMDV tropism in non-infected animals.

Gene set	Pair-wise tissue comparisons	Number of genes
NTS-up	MCS>IDC, TE, and CB	90
	NTE>DNP, DSP, and LNG	
NTS-down	MCS<IDC, TE, and CB,	2
	NTE<DNP, DSP, and LNG	
SRS-up	IDC>DNP, DSP, LNG, MCS, and NTE	103
	TE>DNP, DSP, LNG, MCS, and NTE	
	CB>DNP, DSP, LNG, MCS, and NTE	
SRS-down	IDC>DNP, DSP, LNG, MCS, and NTE	412
	TE>DNP, DSP, LNG, MCS, and NTE	
	CB>DNP, DSP, LNG, MCS, and NTE	
PIS-up	DNP> LNG, and NTE	73
	DSP> LNG, and NTE	
PIS-down	DNP< LNG, and NTE	4
	DSP< LNG, and NTE	
PRS-up	NTE<DNP, DSP, and LNG	220
PRS-down	NTE>DNP, DSP, and LNG	360

CB: coronary band; DSP: distal soft palate; DSP: distal nasal pharynx; IDC: interdigital cleft skin; LNG: middle anterior lung; MCS: metacarpal skin; NTE: nasal turbinate epithelium; TE: tongue epithelium; NTS: not FMDV targeted sites (MCS, NTE); PIS: persistent infection sites (DNP, DSP); PRS: primary replication sites (DNP, DSP, and LNG); SRS: secondary replication sites (TE, IDC, and CB); -up: up-regulated expression in the tissue group; and -down: down-regulated expression in the tissue group.
doi:10.1371/journal.pone.0064119.t002

Although the expression of ITGAV was not significantly different among tissues, the SRS expressed higher ITGB6 and lower FN1 than other tissues in infected and non-infected animals (Table 3). The expression of ITGB6 in the SRS increased after FMDV infection, while the expression of FN1 decreased when the infected and non-infected tissues were compared (Table 3). The total expression of RGD-binding integrin β subunits (ITGBs) was the lowest in the SRS of infected and not infected animals (Table 3). Among them, ITGB3 and ITGB8 were DEG in the SRS-down gene set. The estimated level of integrin αVβ6 dimeric receptor was significantly higher in the infected and non-infected SRS than that in other tissues (Table 3). However, the difference was not observed between primary replication sites and the control tissue. Thus, higher number of integrin αVβ6 heterodimeric receptor and lower expression of fibronectin in the SRS especially in the infected animals indicate that the expression levels of FMDV receptor and the ligand are determining factors of FMDV tropism in the secondary infection.

Bioinformatics of Differential Expression

Because there were less than 5 genes in the NTS-down and PIS-down gene sets, only other six gene sets were used in the bioinformatic analysis to infer biological mechanisms of FMDV tissue tropism. Analysis of the promoter sequences of the DEG identified 33 over-represented transcription factor binding sites (Table 4). Six of these binding sites (V$AP1_Q2_01, V$IRF_Q6, V$IRF2_01, V$ISRE_01, V$STAT_Q6, and V$STAT1_01) are known to play important roles in inducing antiviral innate immune

Table 3. Average expression signal intensity of integrins and fibronectin in the tissues of two infected and three non-infected animals.

Gene	SRS-i	SRS-c	MCS-i	MCS-c	PIS-i	PIS-c	LNG-i	LNG-c	NTE-i	NTE-c
ITGAV	241	134	258	152	279	207	212	176	253	171
ITGA2B	189	184	167	238	177	297	549	548	190	269
ITGAs**	3878	4826	7251	7888	4560	4778	11777	9257	5465	6848
ITGB1	429	297	2164	784	1055	619	3794	2224	1573	799
ITGB3	57*	55*	271	187	555	764	676	654	464	817
ITGB5	199	196	255	120	200	149	140	129	314	184
ITGB6	280*	175	165	115	88	102	151	225	183	168
ITGB8	35*	23*	143	101	93	85	93	85	84	86
ITGBs**	1000*	747*	2998	1307	1990	1719	4931	3414	2618	2054
ITGαVβ6***	68*	33	14	14	12	11	7	12	18	20
FN1	96*	232	595	349	727	842	1592	1437	566	704

MCS: metacarpal skin; LNG: lung; NTE: nasal turbinate epithelium; PIS: persistent infection site; SRS: secondary replication site; -c: not infected; -i: FMDV infected;
*statistically significantly different between SRS and the rests;
**the sum of the signal intensity of ITGB1-binding integrin α subunits (ITGAs) or RGD-binding integrin β subunits (ITGBs) according to cited reference [27]; and
***: estimated level of integrin αVβ6 heterodimeric receptor.
doi:10.1371/journal.pone.0064119.t003

response. V$ISRE_01 (a binding site for transcription factor complex activated by type 1 interferon signaling pathway) was found to be over-represented in the NTS-up, SRS-down, and PIS-up gene sets. V$IRF_Q6 and V$IRF2_01 (binding sites for interferon response factors) were more frequent in the SRS-down gene set, while AP1_Q2_01 (a binding site for transcription factors activated by IL-1cytokine family) appeared more in the SRS-up gene set. V$STAT1_01 (a binding site for STAT1 activated by IFNγ signaling) and V$STAT_Q6 (a site for STATs stimulated by the cytokine receptor-kinase complex) were over-represented in the PRS-up gene set. These results indicate that transcription factors binding to these binding sites may play roles in differential gene expression; therefore, pathways such as interferons and IL-1 cytokines that activate these transcription factors may be involved in determining FMDV tropism.

Using the ExPlain^{TM} program to identify networks that may be significantly affected by the differential expression, we detected several networks relevant to those identified using the promoter sequences of the DEG and to FMDV infection. Several network key nodes associated with type I interferon signaling were detected in the analysis using the SRS-down (PKR, IFNα, indole-acetaldehyde, Jak1), PRS-down (IFNα), and PRS-up (IFNα, Jak1) gene sets, whereas some involved in IL-1 signaling were found using the SRS-down (p38α, p38β2), PRS-down (p38α), and PRS-up (FOS, IκB-α, IKK-β:IκB-α, IL18, IL1B) gene sets (Table 5). In the SRS-up and SRS-down sets, significant numbers of DEG are in a network regulating uPAR-integrin pathways and a network associated with integrins, which may be relevant to FMDV receptors (Table 5). In the PIS-up gene set, 10 DEG are in a network up-stream of survivin (BRIC5, an inhibitor of apoptosis) and two DEG in the PIS-down gene set were in the down-stream of TNF-alpha regulated network, suggesting the involvement of clearing virus infected cells via inducing cell death. Based on the results of these bioinformatic analyses and their relevance to FMDV infection, we decided to further examine the expression of genes involved in extracellular matrix turnover and IL-1, interferon, and death receptor signaling to determine if the expression could explain the mechanisms of FMDV tropism (biological inferences).

Extracellular Matrix (ECM) Turnover

Cell attachment involves two types of interactions; cell-ECM and cell-cell adhesion. Cell-ECM interaction is mediated by RGD-binding integrins and regulated by urokinase plasminogen activator receptor (PLAUR or uPAR)-integrin pathways [28]. PLAUR and plasminogen (PLG), the activators of ECM degradation, were expressed significantly higher in the high-titer secondary replication sites, SRS, than those in the negative control tissue (Figure 1A and 1B). On the other hand, SERPINE and SERPINF, the inhibitors of urokinase plasminogen activator (PLAU) and PLG, respectively, were expressed at significantly lower levels in the SRS than those in the control. These differential expressions between the SRS and the control were observed in both infected and non-infected animals. Plasmin can also activate metalloproteases (MMPs) to degrade ECM. Although the average expression of MMPs in the SRS was 1.4 and 2 fold lower than that in the control, the expression of the inhibitors of MMPs (TIMPs) in the control was 2.6 and 5.3 fold higher than that in the SRS in not infected and infected animals, respectively (Figure 1A and 1B). Interestingly, SERPINE and SERPINF were also expressed significantly lower in the non-infected primary replication site, PRS, (3 fold in PIS and 4.6 fold in the lung) than those in the negative control, nasal turbinate epithelium, whereas PLAU, another activator of ECM degradation, was expressed at significantly higher level in both infected and not infected PRS (at least 2.6 fold in PIS and 10.6 fold in the lung) than that in the control (Figure 1A and 1B).

When the expression of these individual genes was normalized to be equally weighted, the SRS expressed significantly higher activators and lower inhibitors of ECM degradation than the negative control tissue, whereas the PRS had significantly lower expression of the inhibitors than their negative control tissue in the not infected animals and the activators were expressed significantly higher in the lung than the control in the infected and non-infected animals. These results indicate that tissues susceptible to primary and secondary infection have gene expression profiles promoting higher ECM turnover.

Table 4. Over-represented transcription factor binding sites in the promoters of genes differentially expressed between tissue groups of three non-infected animals.

Tropism	*Matrix name*	*Transcription factors*	*Gene set**
Target versus non- targeted site	V$AP2ALPHA_01	adaptor-related protein complex 2, alpha 1	NTS-up
	V$CRX_Q4	cone-rod homeobox	NTS-up
	V$EBF_Q6	early B-cell factors	NTS-up
	V$ETS_Q6	v-ets erythroblastosis virus E26 oncogene homolog	NTS-up
	V$HLF_01	hepatic leukemia factor	NTS-up
	V$HNF1_Q6	hepatocyte nuclear factor 1	NTS-up
	V$ISRE_01	signal transducer and activator of transcription 1,2, and IRF9	NTS-up
	V$OSF2_Q6	runt-related transcription factor 2	NTS-up
	V$PBX1_02	pre-B-cell leukemia homeobox 1	NTS-up
	V$SPZ1_01	spermatogenic leucine zipper 1	NTS-up
	V$WT1_Q6	Wilms tumor 1	NTS-up
	V$ZNF219_01	zinc finger protein 219	NTS-up
High titer replication	V$CRX_Q4	cone-rod homeobox	SRS-down
and vesicular lesion	V$HNF1_Q6	hepatocyte nuclear factor 1	SRS-down
site	V$IRF_Q6	interferon response factors	SRS-down
	V$IRF2_01	interferon response factor 2	SRS-down
	V$ISRE_01	signal transducer and activator of transcription 1,2, and IRF9	SRS-down
	V$NKX25_Q5	NK2 homeobox 5	SRS-down
	V$PBX1_02	pre-B-cell leukemia homeobox 1	SRS-down
	V$TGIF_01	TGFB-induced factor homeobox 1	SRS-down
	V$VMYB_02	myeloblastosis viral oncogene homolog	SRS-down
	V$AP1_Q2_01	Activating protein-1 transcription factors	SRS-up
	V$COUP_DR1_Q6	paired-like homeodomain transcription factor 2	SRS-up
	V$DR1_Q3	nuclear receptor subfamily 2, group F, member 2	SRS-up
	V$E2A_Q2	transcription factor 3	SRS-up
	V$PPAR_DR1_Q2	peroxisome proliferator-activated receptors	SRS-up
	V$YY1_Q6	YY1 transcription factor	SRS-up
Primary versus non-	V$TGIF_01	TGFB-induced factor homeobox 1	PRS-up
primary replication site	V$STAT_Q6	signal transducer and activator of transcription	PRS-up
	V$STAT1_01	signal transducer and activator of transcription 1	PRS-up
	V$ZIC3_01	Zic family member 3	SRS-up
Persistent versus non-	V$CRX_Q4	cone-rod homeobox	PIS-up
persistent infection site	V$E2F_03	E2F transcription factor	PIS-up
	V$E2F_Q6_01	E2F transcription factor	PIS-up
	V$HNF1_Q6	hepatocyte nuclear factor 1	PIS-up
	V$HSF2_01	heat shock transcription factor 2	PIS-up
	V$IRF_Q6	interferon response factors	PIS-up
	V$ISRE_01	signal transducer and activator of transcription 1,2, and IRF9	PIS-up
	V$NF1_Q6_01	neurofibromin 1	PIS-up
	V$NFY_01	nuclear transcription factor Y	PIS-up
	V$NFY_Q6_01	nuclear transcription factor Y	PIS-up
	V$PBX1_02	pre-B-cell leukemia homeobox 1	PIS-up
	V$SF1_Q6	splicing factor 1	PIS-up
	V$STAT1_01	signal transducer and activator of transcription 1	PIS-up

Table 4. Cont.

Tropism	*Matrix name*	*Transcription factors*	*Gene set**
	V$TGIF_01	TGFB-induced factor homeobox 1	PIS-up
	V$VMYB_02	myeloblastosis viral oncogene homolog	PIS-up

*NTS: not targeted site; PIS: persistent infection site; PRS: primary replication site; SRS: secondary replication site; -up: up-regulated in the groups; and -down: down-regulated in the group -up: up-regulated expression in the tissue group; and -down: down-regulated expression in the tissue group.
doi:10.1371/journal.pone.0064119.t004

IL-1 Gene Family

In order to evaluate the impact of differential IL-1 cytokine expression, we examined the expression ratios of agonist(s) vs their antagonist(s) instead of the individual genes according to Johnston et al. [29] because there are agonists and antagonist for several receptors and cytokines of the IL-1 gene family [30], [31]. The SRS had significantly higher ratios of IL1R1 vs IL1RII, IL18 vs IL18BP+IL18RN, and IL36 vs IL36RNs but expressed significantly less IL18R1 and IL33 than the negative control, MCS, in the infected and non-infected animals (Figure 2A and 2B). Similarly, primary replication sites had higher IL1 vs IL1RN ratio than their negative control tissue in the infected and non-infected animals (Figure 2A and 2B) and also expressed higher other agonists or have higher agonist vs antagonist ratios than the control in the non-infected animals (Figure 2A). In the infected animals, the differences between the lung and the control, NTE, were smaller and not significant (Figure 2B). When the gene expression was evaluated based on the average Log 2 ratio of targeted vs not targeted tissues, both SRS/MCS and PRS/NTE ratios were at least 1.4 (equivalent to ~2.6 fold difference between the SRS and MCS) and 0.7 (~1.6 fold) for IL-1 cytokines in the infected and not infected animals, respectively, and the differences for the receptors were much smaller than those for the cytokines, indicating that susceptibility to FMDV infection in the primary and secondary replication sites was associated with relatively higher local expression of IL-1 agonist cytokines.

Interferon Signaling

We examined the expression of genes in the interferon JAK-STAT and PI3K-AKT pathways (regulating transcription and translation, respectively) according to Kroczynska et al. [32] and found that four of the seven genes in the interferon JAK-STAT signaling pathway were expressed lower in the non-infected SRS than those in the control tissue (three were statistically different) (Figure 3A). Three of four genes known to enhance interferon signing [33] were also expressed significantly lower in the SRS than in the control tissue (Figure 3A). The differential expression was also observed in the infected animals (Figure 3B). The average signal intensity of these genes appeared to be lower in the SRS than the control in the not infected animal but was significantly smaller in the infected tissues. Unlike the SRS, the PRS especially the lung appeared to have higher expression in the genes involved in interferon signaling than their control tissue, NTE (Figure 3). Similarly, differential expression for the genes in the interferon PI3K-AKT signaling pathway was also obtained as those in the JAK-STAT pathway. Five kinases (PIK3CA, PIK3CG, PIK3R1, AKT3, and RPS6KB1) in the pathway were expressed lower in the SRS than those in the control tissue in both infected and non-infected animals. In contrast to the SRS, the expression in the PRS appeared to higher than that in their control tissue (Figure 4A and 4B).

To compare the status of interferon signaling pathways among tissues, 48 interferon-inducible antiviral effector genes were identified from the Gene Database (http://www.ncbi.nlm.nih.gov/sites/entrez?db = gene) based on the functions discussed by Saddler and Williams [34]. The average expression of these genes was significantly lower in the SRS than that in the control tissue in both infected and not infected animals (Figure 5A). There were no significant differences in overall expression of type I interferon between the SRS and metacarpal skin, though the SRS appeared to have higher type I interferons in the infected animals (Figure 5B), indicating that the differential expression of antiviral effectors between the SRS and the control tissue was mainly due to differences in genes involved in interferon signal transduction.

Table 5. FMDV receptor- or Immune-related biological networks detected based on the genes differentially expressed between tissue groups of three non-infected animals.

Gene set	Location of DEG	Key nodes of networks	Number of DEG	FDR
SRS-up	down-stream	uPAR:integrin	4	≤0.03
SRS-down	down-stream	Jak2, PKR, TGFB2, TLR4:Btk	≥21	≤0.03
	up-stream	IFNα, indole-acetaldehyde, integrins, Jak1, p38α, p38β2, SOCS-1	≥15	<0.01
PIS-up	down-stream	survivin{ubK48}{ubK63}	10	0.008
PIS-down	up-stream	(TNFα:TNFR1)3:(TRADD:traf2)2:(MEKK1)2	2	0.024
PRS-up	down-stream	FOS, IκB-α, IKK-β:IκB-α, IL18, IL1B,	≥27	<0.05
	Up-stream	IFNα, IL-10R, IL-2Rβ, IL-3R, IL-4R, IL-5R, IL-7R, Jak1, RANK	≥28	<0.03
PRS-down	Up-stream	p38α, SOCS-1, IL-7R, IL-4R, IL-2Rβ, IFNα	≥12	<0.05

DEG: differentially expressed genes; FDR: false discover rate produced by ExPlain program; NTS: not targeted site; PIS: persistent infection site; PRS: primary replication site; SRS: secondary replication site; -up: up-regulated expression in the tissue groups; and -down: down-regulated expression in the tissue group.
doi:10.1371/journal.pone.0064119.t005

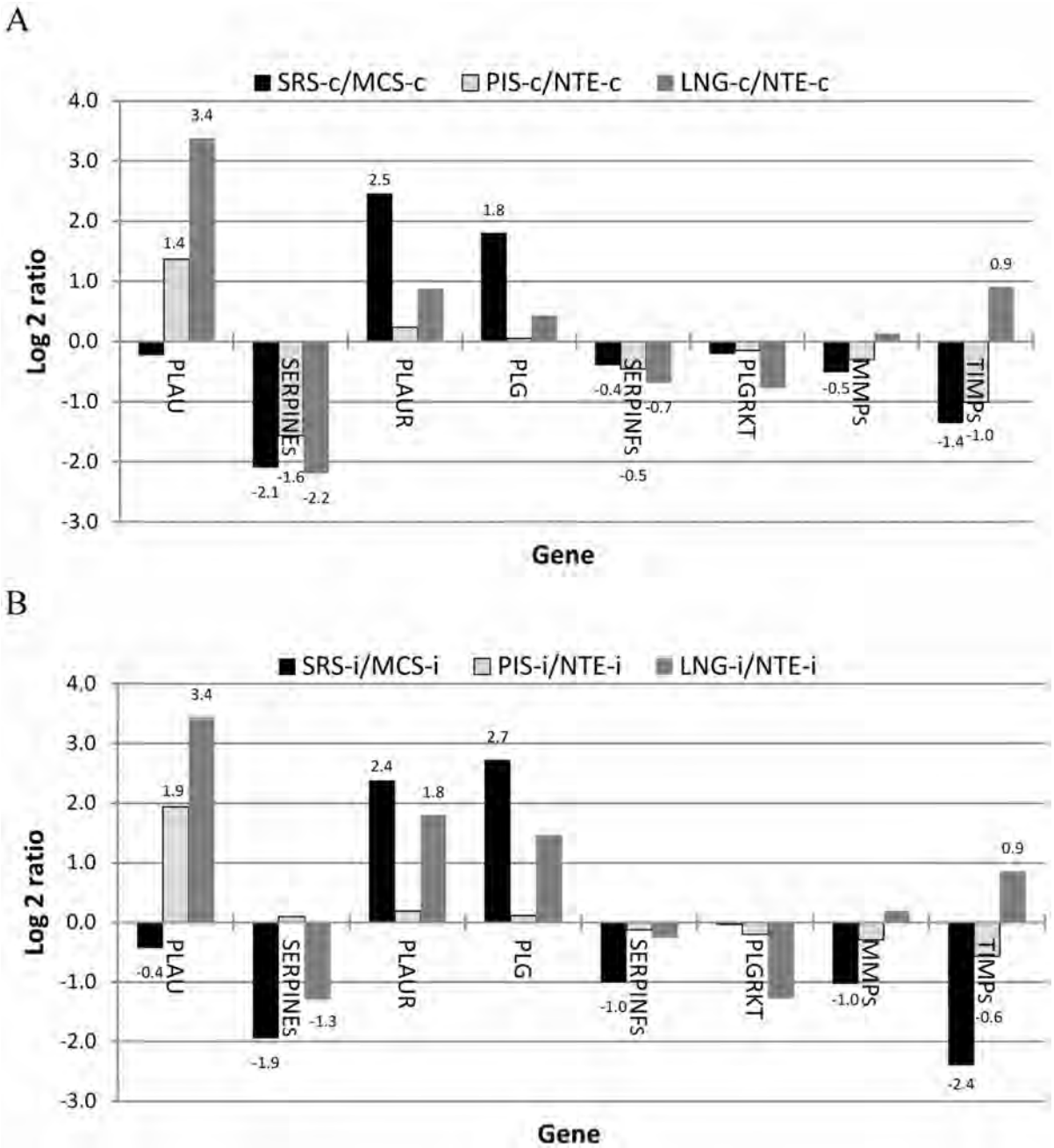

Figure 1. Differential expression of genes regulating extracellular matrix turnover. The log 2 expression ratios (FMDV-targeted tissues versus non-targeted tissue) in three non-infected (A) and two infected (B) animals. MCS: metacarpal skin; LNG: lung; NTE: nasal turbinate epithelium; PIS: persistent infection site; SRS: secondary replication site; -c: not infected; -i: FMDV infected; and data label indicating that the difference between two tissue groups is statistically significant.
doi:10.1371/journal.pone.0064119.g001

Unlike the SRS, there were no significant differences in the expression of interferon-inducible antiviral effectors between the PRS and the negative control in the non-infected animals (Figure 5A). However, the lung had higher type I interferon expression than the PIS and negative control (Figure 5B) in the not infected animals and expressed significantly higher antiviral effectors than the PIS and the control in the infected cattle (Figure 5A). As in the non-infected animals, the lung of the infected animals appeared to have higher type I interferon expression than the PIS and the control (Figure 5B), but the differences was not statistically significant. Interferons α and ω in non-infected animals and interferons β in the infected animals accounted for most of the observed differences (data not shown). Taken together with the results of genes involved in the interferon signaling, our results strongly suggest that high-titer FMDV replication and susceptibility to FMDV persistence in primary replication sites are associated with relatively weaker type I interferon signaling when targeted and not targeted tissues were compared.

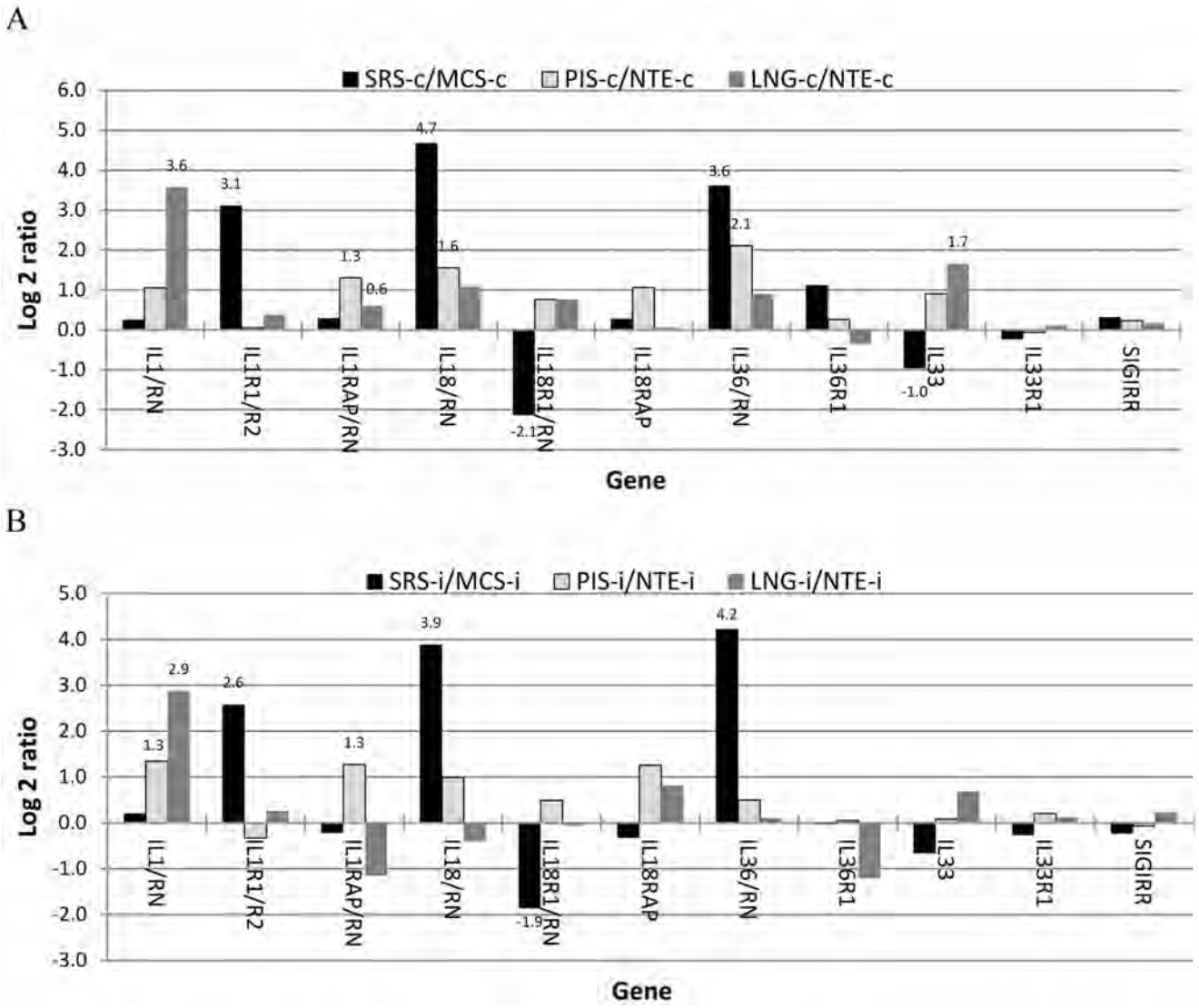

Figure 2. Differential expression of IL-1 family genes. The log 2 expression ratios (FMDV-targeted tissues versus non-target tissue) in three non-infected (A) and two infected (B) animals. MCS: metacarpal skin; LNG: lung; NTE: nasal turbinate epithelium; PIS: persistent infection site; SRS: secondary replication site; -c: not infected; -i: FMDV infected; and data label indicating that the difference between two tissue groups is statistically significant.
doi:10.1371/journal.pone.0064119.g002

Death Receptors and the Ligands

It is well known that several members of the TNF super family including LTA, TNF, FASLG, TNFSF10, TNFSF12, and TNFSF15 play important roles in clearing virus by inducing apoptosis and/or necrosis of infected cells via binding to death receptors such as TNFRSF1, FAS, TNFRSF10, TNFRSF21, and TNFRSF25 [35], [36], [37], [38]. There were significant differences in the expression of the death receptors and the ligands between the SRS and the negative control and between the PRS and the control (data not provided). Interestingly, TNFSF10 was the only ligand which expression was significantly induced by FMDV infection in all tissues tested and was significantly higher (5.6 fold in not infected and 7.7 in the infected animals) in the lung than that in those susceptible to persistent infection. When the expression of the receptors and the ligands was added together, the SRS had lower overall expression of death receptor ligands in both infected and not infected animals (Figure 6A) and lower death receptor expression (excluding TNFRSF10 and TNFRSF25, which probes were not in our microarray) in the infected animals (Figure 6B) than the negative control. The overall expression of the ligands in the lung was at least 5 fold higher than that in the PIS and nasal turbinate epithelium of both infected and not infected animals (Figure 6A). There was no difference in the ligand expression between the PIS and nasal turbinate epithelium; however, the PIS had significantly lower overall expression of death receptors tested than the lung and nasal turbinate epithelium in the non-infected cattle and remained lower in the infected animals (Figure 6B). These results suggest that FMDV tropism particularly at persistence sites is associated with relatively lower expression of death receptors and the ligands.

In summary, we found that a large number of genes were differentially expressed between tissues with different FMDV tropism. Analysis of the differentially expressed genes leads to identification of several biological processes that may be affected by the differential expression. Further examination focused on those relevant to FMDV infection according to reported findings

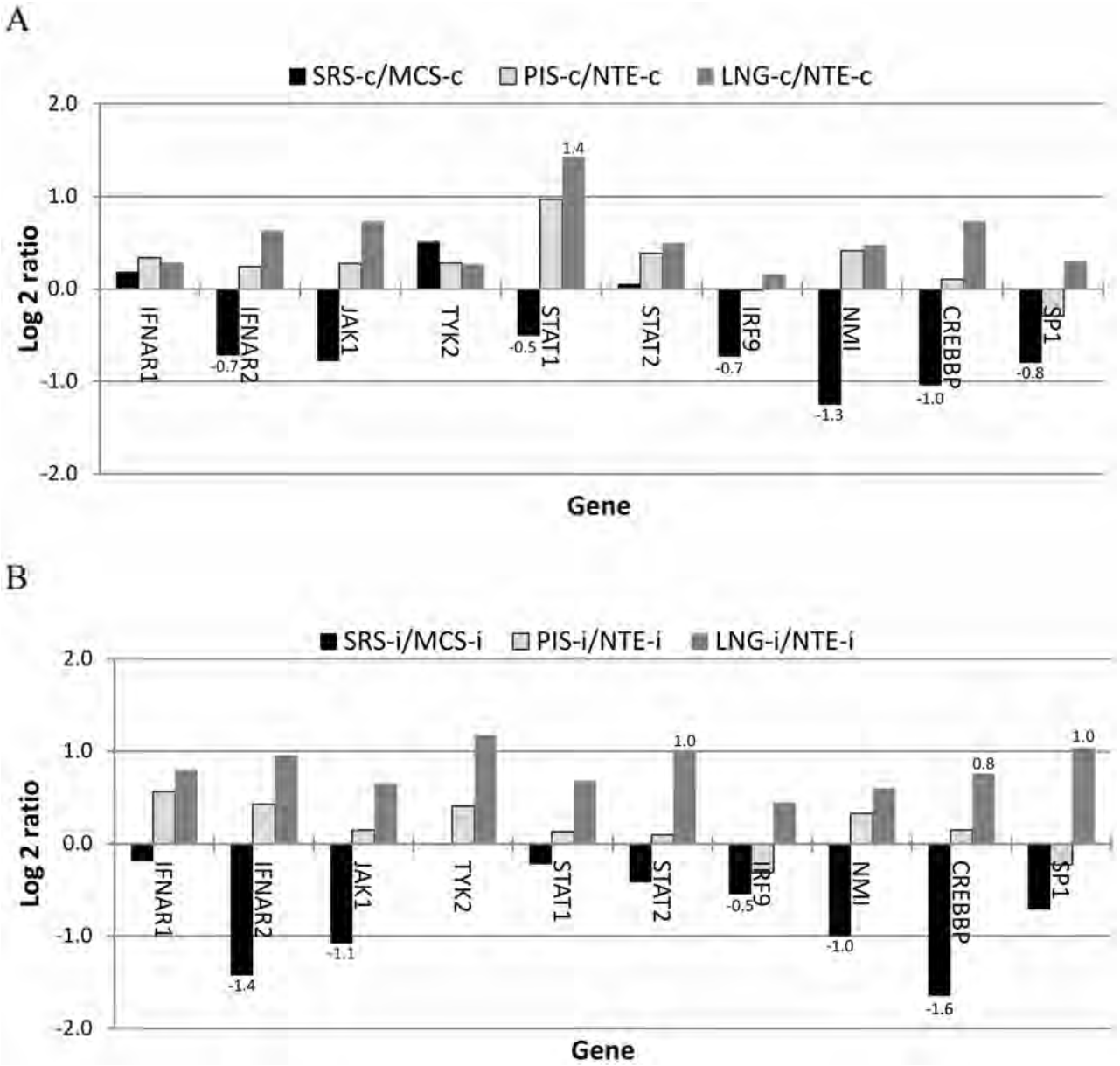

Figure 3. Differential expression of genes in the interferon JAK-STAT signal pathway. The log 2 expression ratios (FMDV-targeted tissues versus non-target tissue) in three non-infected (A) and to infected (B) animals. MCS: metacarpal skin; LNG: lung; NTE: nasal turbinate epithelium; PIS: persistent infection site; SRS: secondary replication site; -c: not infected; -i: FMDV infected; and data label indicating that the difference between two tissue groups is statistically significant.
doi:10.1371/journal.pone.0064119.g003

shows that FMDV tissue tropism was associated with significantly differential expression in integrin αVβ6 heterodimeric receptor, fibronectin, IL-1 cytokines, death receptors and the ligands, and multiple genes involved in ECM turnover and type I interferon signaling.

Discussion

FMDV tropism has been known for nearly half a century [39], [40]. However, the molecular basis for FMDV tissue tropism remains mostly unknown. The functional genomics approach used here allows for a systematic investigation of mechanisms involved. Our previous study demonstrated that data obtained with our custom microarray agreed with those measured using real-time PCR [41]. In this study, we used pair-wise two-tissue comparisons instead of tissue group comparisons in order to detect genes with consistent effects across the tissue tested. Various cut-offs ranging from 2 to 1.5 fold difference with $P<$ or $=0.05$ were tested. We found that the threshold of significantly differential expression at the 1.75 fold was a better cut-off in terms of balancing between false positives and false negatives and between detection power and biological impact of differential expression in order to create gene sets optimal for the pathway/network analysis. Threshold correction for multiple t-tests was not applied because it is too stringent to create the gene sets with adequate gene number for bioinformatic analysis due to diverse tissues within the tissue groups. For example, when we used threshold correction for

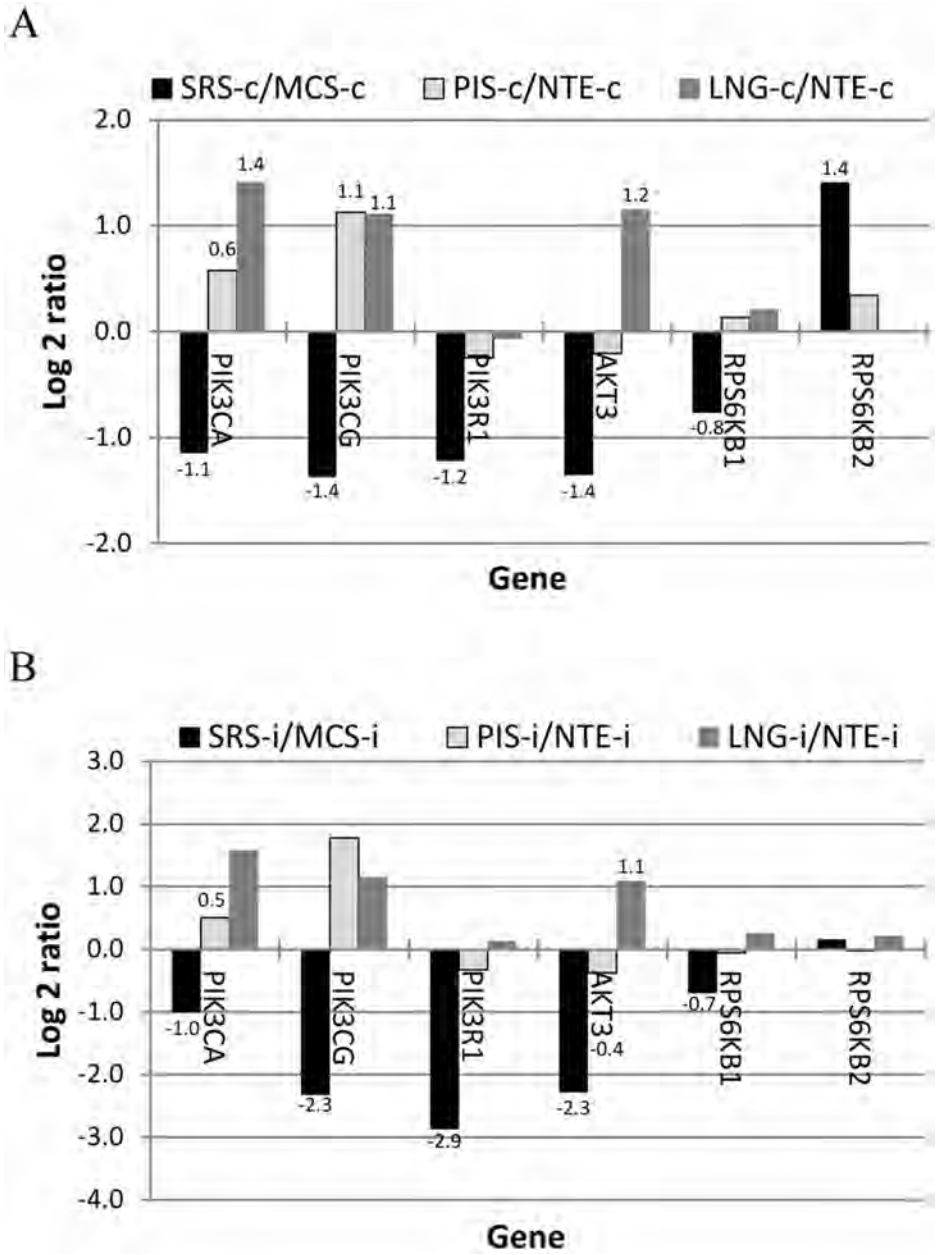

Figure 4. Differential expression of genes in the interferon PI3K-AKT signal pathway. The log 2 expression ratios (FMDV-targeted tissues versus non-target tissue) in three non-infected (A) and two infected (B) animals. MCS: metacarpal skin; LNG: lung; NTE: nasal turbinate epithelium; PIS: persistent infection site; SRS: secondary replication site; -c: not infected; -i: FMDV infected; and data label indicating that the difference between two tissue groups is statistically significant.
doi:10.1371/journal.pone.0064119.g004

multiple t-tests according to Leek et al. [42], less than 10 differentially expressed genes were identified (Data not shown).

We used different bioinformatic tools to analyze the gene sets to identify candidate pathways or networks. The results of different bioinformatic analyses support each other, and the results from non-infected animals mostly agree with those from infected animals. Because of substantial intrinsic differences among tissues, we do not expect that all DEG identified play roles in determining FMDV tropism. On the other hand, not all genes involved can be detected with the pair-wise tissue comparisons because differential expression of different genes can have same effect on a biological process as we found in this study. Some of detected biological processes may play roles in determining FMDV tropism but were not recognized in this study due to lack of knowledge. We used an approach based on published biological findings to interpret the gene expression results and focused on those relevant to virus/FMDV infection to make the biological inferences. The examination of gene expression in the detected biological processes revealed that the differential expression found could explain FMDV tropism under the widely accepted assumption of the correlation between gene expression level and the functional activity.

Differential expression in integrins αVβ6, fibronectin, and genes regulating ECM turnover appears to be the major factors

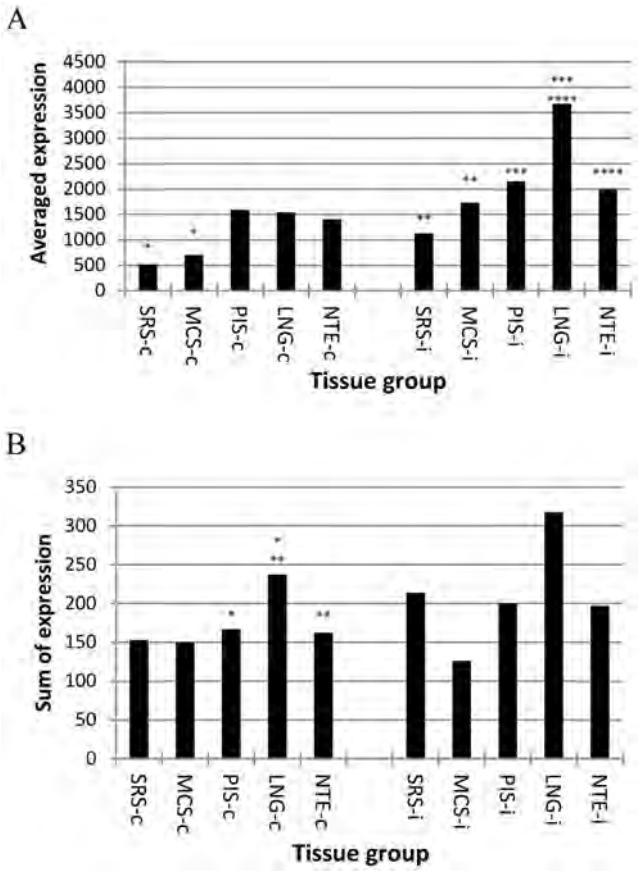

Figure 5. Differential expression of genes of Type I interferons and antiviral effectors. The average signal intensity of interferon-inducible antiviral effectors (A) and the sum of signal intensity of type I interferons (B) in three non-infected and two infected animals. MCS: metacarpal skin; LNG: lung; NTE: nasal turbinate epithelium; PIS: persistent infection site; SRS: secondary replication site; -c: not infected; -i: FMDV infected; and *: statistically significantly different grouped by the number of *.
doi:10.1371/journal.pone.0064119.g005

determining FMDV tropism based on the magnitude of the differences and the biological process involved. Our results of the estimated expression of integrins αVβ6 alone can only explain in part why SRS is more susceptible to FMDV infection than other tissues, but it cannot elucidate the difference between PRS and the negative control tissue. However, the results of combining the scale of the differential expression and the differentially expressed genes involved in regulating cell-ECM attachment could explain the susceptibility to both primary and secondary infections and the differences between primary and secondary replication sites in terms of virus replication titers and pathogenesis. It has been reported that ECM acts as a barrier against virus spread [43], [44], [45], [46], [47]. Because fibronectin is an ECM protein that binds to integrin αVβ6 receptor with the same RGD sequence motif as FMDV, it is reasonable to hypothesize that higher ECM turnover and the degradation and decreased expression of fibronectin make the receptors more accessible for FMDV to infect cells. Based on the known mechanisms involved in cell-ECM attachment, our results show that all FMDV-susceptible tissues examined here regarding both primary and secondary infection possess similar biological characteristics (high ECM turnover) by differentially expressing the same and/or different genes. Our results could also explain why cells isolated from non-targeted tissues become susceptible to FMDV infection in cell culture and why SRS tissues are susceptible to vesicular lesions caused by several viruses.

Our results show tissue susceptibility to primary and secondary FMDV infection was also associated with relatively higher local expression of IL-1 family agonist genes. IL-1 has been reported to be an important mediator of pemphigus vulgaris [48], which can induce an acantholysis process that resembles vesicular lesions seen in FMD, and the pathogenesis of acantholysis can be mediated via uPA system [49]. More interestingly, it has been reported that high IL-1 level in nasal lavage fluids before virus challenge was associated with the onset of rhinovirus infection in humans [50], indicating high IL-1 level is a susceptible factor of viral respiratory infections. The mechanisms of IL-1 signaling involved in susceptibility to respiratory diseases are unknown. However, IL-1 signaling can induce the expression of the activators of ECM degradation [51], [52], [53]. Therefore, we hypothesize that high expression of IL-1 agonists and high ECM turnover render tissues susceptible to viral infections and vesicular lesions. Our results show that significant differences in the estimated level of integrin αVβ6 heterodimeric receptor and fibronectin expression were observed only in the infected animals, indicating that IL-1 signaling triggered by FMDV infection may also play a key role in this differential expression.

Interferon pretreatment has been known to protect against FMDV infection by inducing expression of interferon-inducible antiviral effectors [54]. The data reported here show that the overall expression of interferon-inducible antiviral effector genes and several genes involved in interferon signaling were significantly lower in the SRS than that in other tissues tested. These results suggest that cells in the SRS tissues are more permissive for viral replication because of their decreased expression of antiviral effectors, which probably due to weaker response to interferon stimulation based on the lower expression of genes involved in the signaling found in this study. This agrees with a previous report showing that type 1 interferon response and the expression level of interferon-stimulated genes were the determining factors of tissue susceptibility to poliovirus infection [55]. The lungs (a primary replication site resistant to FMDV persistent infection) of the infected cattle had higher expression of interferon-inducible antiviral effectors, which was associated with higher expression of type I interferons and genes involved in interferon signaling, than the tissues of primary replication site susceptible to the persistent infection (i.e. pharynx), indicating that interferon signaling may also play roles in determining FMDV persistent infection.

Our bioinformatic analyses also led to the identification of a candidate mechanism that could explain, at least in part, why FMDV targets certain PRS for persistent infection. We have identified all bovine death receptors except TNFRSF10 and have found death domains in these receptors. TNFSF10, also named as tumor necrosis factor-related apoptosis-inducing ligand (TRAIL), has been reported to play critical roles in the clearance of viruses by specifically targeting infected cells to induce apoptosis and/or necrosis and by facilitating cell-mediated cytotoxic immune response [38], [56], [57], [58]. We found that the expression of this cytokine was significantly induced by FMDV infection and was several fold higher in the primary replication site (the lung) resistant to FMDV persistence than that in those susceptible. In addition, there were 10 genes in the survivin network significantly up-regulated in PIS compared to other tissues. Because survivin is an inhibitor of apoptosis [59], up-regulated expressions of genes in this network may render the cells more resistant to apoptosis, which may in turn facilitate persistent infection. Studies conducted

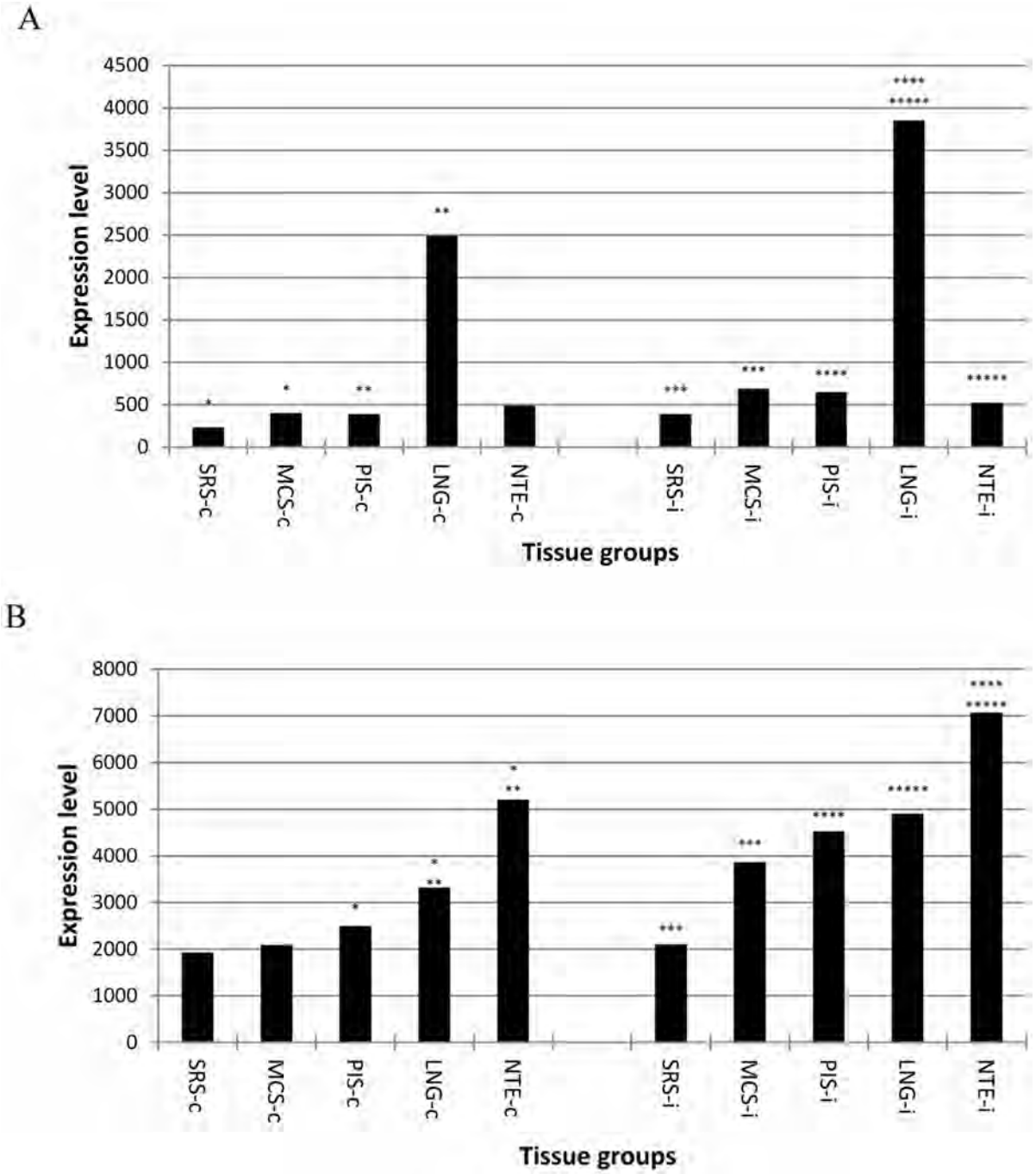

Figure 6. Total expression level of death receptor ligands (A) and death receptors (B) in three non-infected and two infected animals. MCS: metacarpal skin; LNG: lung; NTE: nasal turbinate epithelium; PIS: persistent infection site; SRS: secondary replication site; -c: not infected; -i: FMDV infected; and *: statistically significantly different grouped by the number of *.
doi:10.1371/journal.pone.0064119.g006

by Zhang and Alexandersen [60] and Zhang et al. [61] showed that declining rate of FMDV levels during early infection rather than the virus levels determined FMDV persistent infection. These authors proposed that either variations on the host's abilities to clear virus or differences in the support of virus replication may determine the establishment of FMDV persistent infection. Our results analyzing death receptor and interferon signaling genes provide molecular evidence supporting both hypotheses.

In conclusion, we have identified differential gene expression at a genomic scale between tissues with different FMDV tropism. FMDV tropism could not be explained by the differential expression of a single gene alone. The bioinformatic analysis of the genes differentially expressed led to identify a few biological processes or pathways. Further examination of genes in those relevant to FMDV infection according to reported findings provide the molecular basis that could explain, at least in part, the mechanisms of why FMDV targets specific tissues for primary,

high-titer secondary and persistent infection and causes vesicular lesions. Based on these results, we hypothesize that multiple contributory factors including increased FMDV receptor availability and accessibility resulted from high ECM turnover and differential FMDV receptor and the ligand expression, reduced antiviral innate immunity due to low type I interferon response and/or type I interferon production, and decreased ability to clear infected cells via death receptor signaling play roles in determining FMDV tropism. We also hypothesize that additional increase in already high tissue ECM turnover induced by FMDV infection, likely via triggering the signaling of highly expressed IL-1 cytokines, plays a key role in the pathogenesis of vesicular lesions. This work provides guidance for future research to rationally test these factors and further elucidate the molecular mechanisms of tissue tropism for FMDV. The approaches used in this study may also be applied to understanding tropism of other viral agents.

Acknowledgments

We wish to thank the PIADC Animal Resource Unit for their help and support in all animal experiments, Ethan Hartwig, Elizabeth Bishop and Meghan Tucker for technical assistance, and Drs. William Golde and Douglas Gladue for providing valuable comments and suggestions during manuscript preparation. We also thank Dr. Christine Elsik (Georgetown University) for her suggestions in EST sequence assembly.

Author Contributions

Conceived and designed the experiments: JJZ JA LLR. Performed the experiments: JJZ JA GRS JMP. Analyzed the data: JJZ JA MCP. Contributed reagents/materials/analysis tools: JJZ JA LLR. Wrote the paper: JJZ JA LLR MCP.

References

1. Alexandersen S, Mowat N (2005) Foot-and-mouth disease: host range and pathogenesis. Curr Top Microbiol Immunol 288: 9–42.
2. Arzt J, Pacheco JM, Rodriguez LL (2010) The early pathogenesis of foot-and-mouth disease in cattle after aerosol inoculation. Identification of the nasopharynx as the primary site of infection. Vet Pathol 47: 1048–1063.
3. Arzt J, Juleff N, Zhang Z, Rodriguez LL (2011) The Pathogenesis of foot-and-mouth disease I: viral pathways in cattle. Transbound Emerg Dis 58: 291–304.
4. Brown CC, Piccone ME, Mason PW, McKenna TS, Grubman MJ (1996) Pathogenesis of wild-type and leaderless foot-and-mouth disease virus in cattle. J Virol 70: 5638–5641.
5. Pacheco JM, Arzt J, Rodriguez LL (2010) Early events in the pathogenesis of foot-and-mouth disease in cattle after controlled aerosol exposure. Vet J 183: 46–53.
6. Burrows R (1966) Studies on the carrier state of cattle exposed to foot-and-mouth disease virus. J Hyg 64: 81–90.
7. Zhang ZD, Kitching RP (2001) The localization of persistent foot and mouth disease virus in the epithelial cells of the soft palate and pharynx. J Comp Pathol 124: 89–94.
8. Berinstein A, Roivainen M, Hovi T, Mason PW, Baxt B (1995) Antibodies to the vitronectin receptor (integrin alpha V beta 3) inhibit binding and infection of foot-andmouth disease virus to cultured cells. J Virol 69: 2664–2666.
9. Duque H, Baxt B (2003) Foot-and-mouth disease virus receptors: comparison of bovine alpha(V) integrin utilization by type A and O viruses. J Virol 77: 2500–2511.
10. Jackson T, Sheppard D, Denyer M, Blakemore W, King AM (2000) The epithelial integrin alphavbeta6 is a receptor for foot-and-mouth disease virus. J Virol 74: 4949–4956.
11. Jackson T, Mould AP, Sheppard D, King AM (2002) Integrin alphavbeta1 is a receptor for foot-and-mouth disease virus. J Virol 76: 935–941.
12. Jackson T, Clark S, Berryman S, Burman A, Cambier S, et al. (2004) Integrin alphavbeta8 functions as a receptor for foot-and-mouth disease virus: role of the beta-chain cytodomain in integrin-mediated infection. J Virol 78: 4533–4540.
13. Neff S, Baxt B (2001) The ability of integrin alpha(v)-beta(3) to function as a receptor for foot-and-mouth disease virus is not dependent on the presence of complete subunit cytoplasmic domains. J Virol 75: 527–532.
14. Neff S, Mason PW, Baxt B (2000) High-efficiency utilization of the bovine integrin alpha(v)beta(3) as a receptor for foot-and-mouth disease virus is dependent on the bovine beta(3) subunit. J Virol 74: 7298–7306.
15. Burman A, Clark S, Abrescia NG, Fry EE, Stuart DI, et al. (2006) Specificity of the VP1 GH loop of Foot-and-Mouth Disease virus for alphav integrins. J Virol 80: 9798–9810.
16. Dicara D, Burman A, Clark S, Berryman S, Howard MJ, et al. (2008) Foot-and-mouth disease virus forms a highly stable, EDTA-resistant complex with its principal receptor, integrin alphavbeta6: implications for infectiousness. J Virol 82: 1537–1546.
17. Monaghan P, Gold S, Simpson J, Zhang Z, Weinreb PH, et al. (2005) The alpha(v)beta6 integrin receptor for Foot-and-mouth disease virus is expressed constitutively on the epithelial cells targeted in cattle. J Gen Virol 86: 2769–2780.
18. O'Donnell V, Pacheco JM, Gregg D, Baxt B (2009) Analysis of foot-and-mouth disease virus integrin receptor expression in tissues from naïve and infected cattle. J Comp Pathol 141: 98–112.
19. Evans DJ, Almond JW (1998) Cell receptors for picornaviruses as determinants of cell tropism and pathogenesis. Trends Microbiol 6: 198–202.
20. Devaney MA, Vakharia VN, Lloyd RE, Ehrenfeld E, Grubman MJ (1988) Leader protein of foot-and-mouth disease virus is required for cleavage of the p220 component of the cap-binding protein complex. J Virol 62: 4407–4409.
21. De Los Santos T, de Avila Botton S, Weiblen R, Grubman MJ (2006) The leader proteinase of foot-and-mouth disease virus inhibits the induction of beta interferon mRNA and blocks the host innate immune response. J Virol 80: 1906–1914.
22. De los Santos T, Segundo FD, Zhu J, Koster M, Dias CC, et al. (2009) A conserved domain in the leader proteinase of foot-and-mouth disease virus is required for proper subcellular localization and function. J Virol 83: 1800–1810.
23. Johns HL, Berryman S, Monaghan P, Belsham GJ, Jackson T (2009). A dominant-negative mutant of rab5 inhibits infection of cells by foot-and-mouth disease virus: implications for virus entry. J Virol 83: 6247–6256.
24. Lawrence P, Rieder E (2009) Identification of RNA helicase A as a new host factor in the replication cycle of foot-and-mouth disease virus. J Virol. 83: 11356–1166.
25. Huang X, Madan A (1999) CAP3: A DNA sequence assembly program. Genome Res 9: 868–877.
26. Karolchik D, Hinrichs AS, Kent WJ (2009) The UCSC Genome Browser. Curr Protoc Bioinformatics. Chapter 1, Unit 1.4.
27. Hynes RO (2002) Integrins: bidirectional, allosteric signaling machines. Cell 110: 673–687.
28. Smith HW, Marshall CJ (2010) Regulation of cell signalling by uPAR. Nat Rev Mol Cell Biol 11: 23–36.
29. Johnston A, Xing X, Guzman AM, Riblett M, Loyd CM, et al. (2010) IL-1F5, -F6, -F8, and -F9: a novel IL-1 family signaling system that is active in psoriasis and promotes keratinocyte antimicrobial peptide expression. J Immunol 186: 2613–2622.
30. Dinarello CA (2009) Immunological and inflammatory functions of the interleukin-1 family. Annu Rev Immunol 27: 519–550.
31. van de Veerdonk FL, Stoeckman AK, Wu G, Boeckermann AN, Azam T, et al. (2012) IL-38 binds to the IL-36 receptor and has biological effects on immune cells similar to IL-36 receptor antagonist.Proc Natl Acad Sci USA 109: 3001–3005.
32. Kroczynska B, Kaur S, Platanias LC (2009) Growth suppressive cytokines and the AKT/mTOR pathway. Cytokine 48: 138–43.
33. Shuai K, Liu B (2003) Regulation of JAK-STAT signalling in the immune system. Nat Rev Immunol 3: 900–911.
34. Sadler AJ, Williams BR (2008) Interferon-inducible antiviral effectors. Nat Rev Immunol 8: 559–568.
35. Guicciardi ME, Gores GJ (2009) Life and death by death receptors. FASEB J 23: 1625–37.
36. Shepard BD, Badley AD (2009) The Biology of TRAIL and the Role of TRAIL-Based Therapeutics in Infectious Diseases. Antiinfect Agents Med Chem 8: 87–101.
37. Van Herreweghe F, Festjens N, Declercq W, Vandenabeele P (2010) Tumor necrosis factor-mediated cell death: to break or to burst, that's the question. Cell Mol Life Sci 67: 1567–79.
38. Warke RV, Martin KJ, Giaya K, Shaw SK, Rothman AL, et al. (2008) TRAIL is a novel antiviral protein against dengue virus. J Virol 82: 555–564.
39. Fracastorius H (1546) De alijs differentijs contagionis. De Sympathia et Antipathia Rerum Liber Unus. De Contagione et Contagiosis Morbis et Curatione (libri iii), 36–38. Heirs of L.A. Junta Book 1.
40. Sutmoller P, Gaggero A (1965) Foot-and mouth diseases carriers. Vet Rec 77: 968–969.
41. Zhu J, Weiss M, Grubman MJ, de los Santos T (2010) Differential gene expression in bovine cells infected with wild type and leaderless foot-and-mouth disease virus. J Virol 404: 32–40.
42. Leek JT, Monsen EC, Dabney AR, Storey JD (2006) EDGE: Extraction and analysis of differential gene expression. Bioinformatics 22: 507–508.
43. Kolodkin-Gal D, Zamir G, Edden Y, Pikarsky E, Pikarsky A, et al. (2008) Herpes simplex virus type 1 preferentially targets human colon carcinoma: role of extracellular matrix. J Virol 82: 999–1010.

44. Choi IK, Lee YS, Yoo JY, Yoon AR, Kim H, et al. (2010) Effect of decorin on overcoming the extracellular matrix barrier for oncolytic virotherapy. Gene Ther 17: 190–201.
45. Fanibunda SE, Modi DN, Gokral JS, Bandivdekar AH (2011) HIV gp120 binds to mannose receptor on vaginal epithelial cells and induces production of matrix metalloproteinases. PLoS One 6: e28014.
46. Yaacov B, Lazar I, Tayeb S, Frank S, Izhar U, et al. (2012) Extracellular matrix constituents interfere with Newcastle disease virus spread in solid tissue and diminish its potential oncolytic activity. J Gen Virol 93: 1664–1672.
47. Schuurhof A, Bont L, Hodemaekers HM, de Klerk A, de Groot H, et al. (2012) Proteins involved in extracellular matrix dynamics are associated with respiratory syncytial virus disease severity. Eur Respir J 39: 1475–1481.
48. Feliciani C, Toto P, Amerio P, Pour SM, Coscione G, et al. (2000) In Vitro and In Vivo Expression of Interleukin-1 and Tumor Necrosis Factor-mRNA in Pemphigus Vulgaris: Interleukin-1 and Tumor Necrosis Factor- are Involved in Acantholysis J Invest Dermat 114: 71–77.
49. Feliciani C, Toto P, Wang B, Sauder DN, Amerio P, et al. (2003) Urokinase plasminogen activator mRNA is induced by IL-1alpha and TNF-alpha in in vitro acantholysis. Exp Dermatol 12: 466–471.
50. Proud D, Gwaltney JM Jr, Hendley JO, Dinarello CA, Gillis S, et al. (1994) Increased levels of interleukin-1 are detected in nasal secretions of volunteers during experimental rhinovirus colds. J Infect Dis 169: 1007–1013.
51. Bryan L, Paugh BS, Kapitonov D, Wilczynska KM, Alvarez SM, et al.(2008) Sphingosine-1-phosphate and interleukin-1 independently regulate plasminogen activator inhibitor-1 and urokinase-type plasminogen activator receptor expression in glioblastoma cells: implications for invasiveness. Mol Cancer Res 6: 1469–1477.
52. Bechtel MJ, Reinartz J, Rox JM, Inndorf S, Schaefer BM, et al. (1996) Upregulation of cell-surface-associated plasminogen activation in cultured keratinocytes by interleukin-1 beta and tumor necrosis factor-alpha. Exp Cell Res 223: 395–404.
53. Schwab W, Schulze-Tanzil G, Mobasheri A, Dressler J, Kotzsch M, et al. (2004) Interleukin-1beta-induced expression of the urokinase-type plasminogen activator receptor and its co-localization with MMPs in human articular chondrocytes. Histol Histopathol 19: 105–112.
54. Diaz-San Segundo F, Moraes MP, de Los Santos T, Dias CC, Grubman MJ (2010) Interferon-induced protection against foot-and-mouth disease virus infection correlates with enhanced tissue-specific innate immune cell infiltration and interferon-stimulated gene expression. J Virol 84: 2063–2077.
55. Ida-Hosonuma M, Iwasaki T, Yoshikawa T, Nagata N, Sato Y, et al. (2005) The alpha/beta interferon response controls tissue tropism and pathogenicity of poliovirus. J Virol 79: 4460–4469.
56. Shrestha B, Pinto AK, Green S, Bosch I, Diamond MS (2012) CD8+ T cells use TRAIL to restrict West Nile virus pathogenesis by controlling infection in neurons. J Virol 86: 8937–8948.
57. Brincks EL, Gurung P, Langlois RA, Hemann EA, Legge KL, et al. (2011) The magnitude of the T cell response to a clinically significant dose of influenza virus is regulated by TRAIL. J Immunol 187: 4581–4588.
58. Varchetta S, Mele D, Mantovani S, Oliviero B, Cremonesi E, et al. (2012) Impaired intrahepatic natural killer cell cytotoxic function in chronic hepatitis C virus infection. Hepatology 56: 841–849.
59. Bongiovanni L, Müller EJ, Della Salda L (2011) Survivin in skin pathologies. Exp Dermatol 20: 457–463.
60. Zhang Z, Alexandersen S (2004) Quantitative analysis of foot-and-mouth disease virus RNA loads in bovine tissues: implications for the site of viral persistence. J Gen Virol. 85: 2567–2575.
61. Zhang Z, Murphy C, Quan M, Knight J, Alexandersen S (2004) Extent of reduction of foot-and-mouth disease virus RNA load in oesophageal-pharyngeal fluid after peak levels may be a critical determinant of virus persistence in infected cattle. J Gen Virol 85: 415–421.

Immunology Letters 152 (2013) 135–143

Contents lists available at SciVerse ScienceDirect

Immunology Letters

journal homepage: www.elsevier.com/locate/immlet

Review

Cell mediated innate responses of cattle and swine are diverse during foot-and-mouth disease virus (FMDV) infection: A unique landscape of innate immunity

Felix N. Toka[a,*], William T. Golde[b]

[a] Department of Preclinical Science, Faculty of Veterinary Medicine, Warsaw University of Life Science, Warsaw, Poland
[b] Plum Island Animal Disease Center, Agricultural Research Service, USDA, Greenport, New York 11944, USA

ARTICLE INFO

Article history:
Received 11 February 2013
Received in revised form 6 May 2013
Accepted 13 May 2013
Available online 30 May 2013

Keywords:
NK cells
Dendritic cells
Gamma delta T cells
TLR
FMDV
Innate immunity

ABSTRACT

Pathogens in general and pathogenic viruses in particular have evolved a myriad of mechanisms to escape the immune response of mammalian species. Viruses that cause acute disease tend to bear characteristics that make them very contagious, as survival does not derive from chronicity of infection, but spread of disease throughout the herd. Foot-and-mouth disease virus (FMDV) is one of the most contagious viruses known. Upon infection of susceptible species, cloven-hoofed animals, the virus proliferates rapidly and causes a vesicular disease within 2–4 days. Disease symptoms resolve by 10 days to 2 weeks and in most cases, virus can no longer be detected. Periods of fever and viremia are usually brief, 1–3 days. *In vivo* control of virus infection and clearance of the virus during and following acute infection is of particular interest. The interaction of this virus with cells mediating the early, innate immune response has been analyzed in a number of recent studies. In most reports, the virus has a distinct inhibitory effect on the response of cells early in infection. Here we review these new data and discuss the dynamics of the interaction of virus with different cell types mediating the immune response to infection.

© 2013 Elsevier B.V. All rights reserved.

1. Introduction

While evidence has been gathering pointing to the importance of innate immune responses in shaping overall immunity against infection, in large animal immunology, the subject is still in its infancy. Lessons learned from the mouse system are helpful in understanding the execution of innate immune responses in large animals and provide valuable insights applicable to many other species. For this reason throughout the review, we frequently refer to established facts in other species to indicate areas in large animal immunology where data is lacking. This review focuses on studies that are now available to advance the understanding of innate immune responses of cattle and pigs following infection with important pathogens, particularly FMDV.

2. Cells mediating innate immune responses

Development of the critical cellular components of the innate immune system in cattle and swine has not been fully described. These include natural killer cells, NK; dendritic cells, DC; gamma delta T cells, γδT; B cells, macrophages, Mϕ, and granulocytes. We can only assume that development of these cells probably takes place in a similar manner as has been described for the most studied system, the mouse. However, there are likely to be important differences.

One prominent example is the number of γδ T cells in ruminants versus that in humans or mice. As reported by Yasuda et al. [1], in cattle, γδ T cells initially increase significantly in the dome region of the Peyer's patches during prenatal development and decrease following birth, but the reverse is observed in the intestinal villi where a few γδ T cells are observed during the prenatal development but increase after birth. However, it remains to be proven if these developmental differences are translated into functional differences. Moreover, according to Hein and Dudler [2], in sheep, establishment of a normal γδ T cell repertoire in the periphery is developmentally regulated and dependent on the continual presence of a functional thymus during ontogeny.

The situation with porcine γδ T cells is no less complex. At least 12 subsets of γδ T cells have been reported that belong to two major groups, (1) cluster of differentiation 4 (CD4)-γδ thymocytes that are further subdivided based on CD2/CD8αα expression, and (2) $CD4^+$ γδ thymocytes that stably express CD1, CD2 and CD8αα, but are not exported to the periphery [3].

In the case of development of natural killer (NK) cells and dendritic cells (DC), until recently, we relied on the data derived in the mouse system since minimal data are available for the large animal

* Corresponding author at: Department of Preclinical Science, Faculty of Veterinary Medicine, Warsaw University of Life Science, Ciszewskiego 8, 02-786 Warsaw, Poland. Tel.: +48 22 593 6063; fax: +48 22 593 6066.
E-mail address: felix_toka@sggw.pl (F.N. Toka).

0165-2478/$ – see front matter © 2013 Elsevier B.V. All rights reserved.
http://dx.doi.org/10.1016/j.imlet.2013.05.007

species. However, since conditions of generating these cells *in vitro* have widely been described now [4,5], advancement in characterizing these cells in large animal species and understanding how these cells develop and function to protect the host is now possible. In large animals, we also face yet another unknown, that being, the precise role the innate immune cells play. For instance, data in both mouse and humans show that individuals genetically lacking NK cells suffer from severe and recurrent infections [6–8]. We do not have such an example in large animals or that such a condition leads to a similar situation as that observed in humans or mice.

More recent data [9–11] in humans and mice introduce a new group of cells referred to as innate lymphoid cells (ILC) which includes NK cells. Other members are lymphoid tissue inducer cells (LTi) and natural cytotoxicity receptor 22 cells (NCR22). The later have characteristics of both NK and LTi cells and are referred to as NK receptor-positive (NKR^+) LTi cells. ILC play a protective role in responses to infectious microorganisms, lymphoid tissue formation, tissue remodeling after injury or infection and homeostasis of tissue stromal cells. ILC appear to specialize in production of IFNγ (NK cells), IL-17 and/or IL-22 (LTi and NKR^+ LTi cells). Additionally, in mice "natural helper" (NH) cells have been described, which produce IL-5 and IL-13 associated with Th_2 helper cells. In large animals, we still do not have data suggesting the existence of the LTi cells or NKR^+ LTi cells and we will not discuss these cells further in this review.

Finally, there is also the contribution of macrophages and granulocytes that phagocytose particles including bacteria and cell debris, particularly in sites of inflammation. These cells also have a prominent role in the resolution of inflammation; however, for this review we will focus on the recent advances in the role of NK, DC and γδ T cell responses during infection of cattle and pigs by viral agents, and refer to other animal species. The humoral factors of innate responses such as the complement, acute phase proteins, defensins, cathelicidins, pentraxins and heat shock proteins play a significant role in bacterial infections, but are less understood in relation to viral infection, especially in livestock species. As such, these are not included in this review, but rather we maintain our focus on cellular innate responses to viral infection.

3. Role of NK cells in innate response to infection

Natural killer (NK) cells are part of the innate immune system responsible for early elimination of pathogen-infected cells and thus preventing dissemination within the host and transmission to other hosts. With the availability of an antibody against bovine CD335 (NKp46) [12], the biology of bovine NK cells and their direct role in vaccination or infection with various animal pathogens has been analyzed.

Bovine NK cells are found in peripheral blood, spleen, lung, liver, lymph nodes and bone marrow [12,13]. As in other species, bovine NK cells also express natural cytotoxicity receptors like CD335, produce IFNγ, lyse sensitive targets and appear to have a $CD335^+/CD2^{+/-}/CD8^{+/-}/CD3^-$ phenotype [12,14,15]. Evidence that bovine NK cells are capable of lysing an infected target was initially demonstrated by Boysen et al. [16] and later by Klevar et al. [17], in their studies with *Neospora caninum*. Similar observations have been made by others regarding activation of NK cells by other microorganisms [18,19]. Bovine NK cells also express a short form of natural-killer group 2, member D protein (NKG2D, an activating receptor found on NK and $CD8^+$ T cells) which associates with signaling adaptors such as DNAX activation proteins of 10 kDa (DAP10) and 12 kDa, DAP12 [20]. Furthermore, NKG2D expressed on $CD335^+$ cells in peripheral blood, mesenteric lymph nodes and intraepithelial cells binds to bovine MIC1 (bovine leukocyte antigen-like molecule 1) and MIC4. *In vitro* culture of bovine peripheral blood $CD335^+$ cells with soluble MIC1 or MIC4, showed increased NK cell response in form of IFNγ production, indicating that bovine MIC1 and MIC4 are ligands for NK cell-expressed NKG2D [21]. A review by Boysen and Storset [22] tabulates many more receptors and cell markers expressed by bovine NK cells.

Unlike T cells, NK cells recognize their targets without the need for prior exposure and activation, in an antigen independent manner. Once activated, they show increased cytolytic, secretory and proliferative functions [23]. Besides the cytolytic activity against target cells, NK cells are important mediators of immune responses e.g., participating in immune responses controlled by dendritic cells [24]. These effector functions of NK cells are highly regulated by a balance between inhibiting and activating signals mediated through receptors harboring immunoreceptor tyrosine-based inhibitory motif (ITIM) or immunoreceptor tyrosine-based activation motif (ITAM), respectively, in their cytoplasmic tails [25].

During transportation of cattle, the stress response of these animals is characterized by activation of NK cells indicating that these play a role in innate response [26,27]. In other infections of cattle such as *N. caninum* [17], an initial decrease in peripheral blood NK cells is observed in the early times of infection (4–6 days post infection). However, NK cells significantly increase later, at 11–15 days post infection, acting as early responders to invasion with this parasite. This study did not report if this increase affected the clearance of the parasite. According to Dennis et al. [18], NK cells are directly involved in the elimination of *Mycobacterium bovis* infected macrophages (MΦ). The NK cells interact with and enhance the capability of infected MΦ to produce IL-12 and nitric oxide (NO) and induce apoptosis in the infected cells and as such limit the replication of the intracellular bacteria. Inhibition of NK cell functions appears to be a common feature of viral infections in pigs. Mendoza [28] also found a similar characteristic of NK cells when mononuclear cells were cultured with African swine fever virus (ASFV). Similarly, porcine respiratory and reproduction syndrome virus infection affects the innate immune response of young pigs by inhibiting the function of peripheral blood NK cells [29].

The present experimental data about how NK cells function in the mouse show that this innate cell type may also elicit memory based antigen specific responses [30]. Such cells have not been described in large animal species to date. Depending on results of future studies, NK cells may be targeted to enhance the innate response while priming them for antigen specific memory responses. Recently, Thierry et al. [31] have described invariant NK T (iNKT) cells in porcine peripheral blood, which reside in the $CD4^-/CD8^+$ and $CD4^-/CD8^-$ T cell compartments. They have an activated memory phenotype indicated by SLA-DR+, CD45RA(-) and produce considerable amounts of IFNγ. Porcine iNKT cells expand in the presence of IL-2, IL-15 and IL-33 following activation with α-galactoceramide (α-GC), but expansion is restricted to $CD3^-$αGC-$CD1dTT^+$ cell population. The role of these cells in infection remains to be determined.

3.1. NK cells in FMDV infection

Although information is becoming available about the bovine NK cell response in bacterial and parasitic infections, data are not widely available regarding the function of bovine NK cells in viral infections. To learn if there is a possible role for bovine NK cells in a viral infection, we studied bovine $CD335^+$ NK cells originating from cattle infected with FMDV.

Infection of cattle with FMDV causes an acute disease associated with development of lesions on the hooves and buccal area. Although the infection is rarely fatal in adult animals, it leads to significant economic losses resulting from reduced productivity of infected animals, or losses due to culling of infected animals or even the whole herd in areas of disease outbreak. Such losses are

more pronounced, particularly in industrialized countries that are free of disease and thus do not practice vaccination against FMDV. Therefore, understanding how NK cells function during infection with FMDV is conducive to rational strategies of augmenting the innate immunity against this devastating disease of cloven-hoofed animals.

We have now shown that NK cells originating from FMDV infected animals have an elevated level of cytotoxicity against bovine derived target cells *in vitro* (Patch, Dar, Waters, Toka & Golde, manuscript submitted). NK cells were also described as having low cytotoxicity for bovine non-infected target cells but were able to efficiently lyse parainfluenza 3 virus (PI-3) infected target cells following addition of anti-PI-3 virus antibodies, indicating a role for NK-mediated antibody dependent cell cytotoxicity [32].

In swine, NK cells are identified as $CD2^+/CD8^+/CD3^-$ cells [33] which show characteristics of NK cells described in other species. *In vitro* data show that, at rest, porcine NK cells are minimally cytotoxic even towards target cells infected with FMDV. However, following stimulation with cytokines such as IL-2, IL-12, IL-15, IL-18 or interferon alpha (IFNα), their cytotoxicity significantly increased [34,35] including cytotoxicity against FMDV infected target cells. However, NK cells isolated from swine infected with FMDV are dysfunctional because of the suppressive nature of the virus infection *in vivo* [36]. Porcine NK cells isolated during acute FMDV infection do not secrete IFNγ and are not cytotoxic for NK-sensitive targets such as the human lymphocytic cell line, K562 or FMDV infected porcine fibroblasts. Such a status of NK cells may preclude their protective role in the early phase of infection of pigs with FMDV.

4. Gamma/delta T cells

In young ruminants and swine, T cells expressing γδ T cell receptors (TCR) account for 20–50% of circulating T cells. Although not much is known about the character of antigens recognized by these cells in any mammalian species, antigen recognition is predicted to be MHC independent. In addition, the role of these cells in immune responses to virus infections is not clear. γδ T cells express innate immune functions such as production of proinflammatory cytokines and non-MHC restricted cytolytic activity, i.e., NK-like activity [37]. Further, reports have described a role in wound healing through production of the insulin-like growth factor 1 (IGF-1) [38]. Hoek et al. [39] recently described bovine γδ T cells that likely are regulatory T cells expressing the workshop cluster 1 molecule (WC1) as well as a γδ TCR. These authors propose that these cells may have regulatory functions instead of $CD4^+/CD25^{high/}FoxP3^+$, but the results were limited to WC1 cells expressing mRNA for IL-10. More detailed studies are necessary to confirm a Treg-like function of $WC1^+$ γδ T cells.

In cattle, there are two major populations of γδ T cells differentiated on the expression of WC1, which belongs to the cystein-rich scavenger receptor family of proteins. These are the $WC1^+/CD3^+/CD5^+/CD2^-/CD6^-/CD8^-$ and $WC1^-/CD3^+/CD5^+/CD2^+/CD6^+/CD8^+$ subsets as reported by Wijnaard et al. [40] and Aruffo et al. [41]. The later, $WC1^-$ γδ T cell subset has been reported to express perforin in American bison [42]. The $WC1^+$ subpopulation is further divided into $WC1.1^+$ and $WC1.2^+$ cells; however, the significance of this division is not yet clear. In addition this division relied on monoclonal antibody reactivity. Studies by Baldwin and colleagues [43] show that at least 13 genes located on chromosome 5 within two loci, encode the WC1 molecules. Extensive alternative splicing of transcripts of this family of genes is probably the reason we have a large diversity among this type of scavenger receptor. Moreover, such diversity may contribute to the functional difference observed between γδ T cells in cattle.

Swine γδ T cells appear early in the thymus as CD3ε high cells during the gestation period [44]. As many as 12 different populations of γδ T cell in thymus of pigs have been found by Sinkora et al. [45] based on the expression of CD1, CD2, CD4, CD8 and CD45RC. Two major groups can be defined based on CD4 expression, but these cells do not have counterparts in periphery. However, it suggested that the $CD4^-$ group gives rise to all γδ T cells found in the periphery [3]. Further studies by Sinkora [46] reveal that the peripheral blood harbours the most $CD2^-/CD8^-$ γδ T cells while $CD2^+/CD8^+$ are frequently found in solid tissues and $CD2^+/CD8^-$ are enriched in the spleen and thymus, but the proportions of these cell subsets vary with age.

There is constitutive expression of CD25 on γδ T cells from germ-free pigs with almost all $CD2^-/CD8^-$ cells expressing high levels whereas $CD2^+/CD8^+$ and $CD2^+/CD8^-$ cells have low levels. Expression of CD25 can be increased by PMA and IL-2 stimulation although IL-2 is less potent and only effective for $CD2^-/CD8^-$ γδ T cells. While γδ T cells from germ-free pigs express CD11b, albeit at variable levels, almost none of the $CD2^-/CD8^-$ γδ T cells in conventional animals express CD11b and enhancement of expression in such animals could not be achieved even when cells were stimulated with PMA [46]. The majority of $CD2^+/CD8^+$ γδ T cells express MHC II molecules unlike $CD2^+/CD8^-$ or $CD2^-/CD8^-$. Stimulation of blood γδ T cells with PMA increases MHC II expression. Additionally, γδ T cells may express swine workshop cluster 1 (SWC1, CD52) [47], CD45RA, CD45RC and SWC7, albeit at varied levels and varied tissue distribution. Despite the differential characterization of porcine γδ T cells, it is still far from providing a functional definition of these different phenotypic profiles. Only recently, have porcine γδ TCR^+ cells been reported to be one of the major producers of IL-17 [48], indicating that these cells are bona fide participants in innate immune responses.

Experimental infection of and re-exposure to porcine reproductive and respiratory syndrome virus (PRRSV) increased the number of γδ T cells in circulation between 14 and 70 days post virus stimulation. *In vitro* assays measuring cell proliferation and IFNγ synthesis indicated increased activity of these cells at least between the 14th and 50th day post stimulation [49]. Although this may suggest response of porcine γδ T cells to virus infection, other functional assays such as cytotoxicity were not shown. Moreover, γδ T cells in swine share a phenotype with that of antigen presenting cells, since they are able to take up antigen and present it to $CD4^+$ T cells *via* MHC class II molecules [37,50], therefore connecting the innate to adaptive immunity. Activation of γδ T cells has been described in other infections such as mycobacteria [51] and leptospira in swine [52].

4.1. Gamma delta T cells in FMDV infection

The knowledge available so far on the interaction of FMDV with the immune system has been largely generated in the pig. Even then, not much has been described about the role of the various components of the innate immune response during infection or vaccination. The observation that naive porcine γδ T cells are stimulated to transcribe mRNA of various cytokines and chemokines when treated with a high potency emergency vaccine against FMDV, indicates a role for these cells in innate responses to vaccination or infection [37].

In a study perfomed by Amadori et al. [53] a population of cells with a phenotype and function similar to the human or murine large granular lymphocytes/NK lineage was indicated. Those cells, isolated from peripheral blood of cattle vaccinated against FMDV, could lyse target cells infected with virus in an MHC-independent manner. Later, in another experiment with murine raised antibodies, a similar population was identified as γδ T cells. Amadori et al. [54], isolated γδ T cells from FMDV vaccinated cattle and showed

that they exhibited cytotoxic or cytostatic capabilities against target cells infected with different viruses. Moreover, in a different experiment Amadori et al. [54] infected heifers with bovine herpesvirus 1 and observed an increase in γδ T cells within the peripheral blood mononuclear cell population within the first days of infection. The γδ T cells also inflitrated the tongue and palate mucosae and was more pronounced in animals vaccinated against FMDV. Therefore, γδ T cells in cattle respond to FMDV antigens.

We have recently reported that $WC1^+$ γδ T cells may be involved in the innate response to infection with FMDV in cattle [55]. These cells show a transiently activated phenotype characterized by increased expression of CD25, reduced expression of CD62L and CD45RO, and increased production of IFNγ. Most interestingly, $WC1^+$ γδ T cells acquire NK-like capabilities to kill an *in vitro* target, shown by increased storage of perforin and expression of CD335. Data from these studies also indicated that bovine γδ T cells might act as antigen presenting cells due to increased expression of major histocompatibility class II molecule (MHC II) and CD13, and the ability to ingest and process exogenous proteins. Gamma delta T cells have been previously shown to act as antigen presenting cells [56]. Whether this activation indicates direct interaction of γδ T cells with virus or a bystander effect, is not yet known. Further studies should precisely define particular phenotypes responsible for both NK-like behavior and antigen presenting properties and particularly if these cells are able to activate $CD4^+$ T cells in an antigen-dependent manner. Our data support the earlier findings of Amadori et al. [53,54] and suggest an important role of γδ T cells in the innate immune response against FMDV. In cattle persistently infected with bovine leukemia virus (BLV), administration of recombinant IFNγ increased the number of γδ T cells in circulation and suppressed the replication of BLV *in vivo*, although no mechanisms were suggested by these authors on how the γδ T cells eliminated the IgM^+ cells harboring the virus [57].

5. Dendritic cells initiate innate responses

A critical role of dendritic cells is to scan for antigen (including vaccine antigen) in the periphery and then migrate to the T cell areas of lymph nodes to initiate the immune response. Antigen presenting cell maturation results in amplified antigen uptake and presentation of antigen as peptides through MHC class I or II complexes [58,59]. The late Dr. Ralph M. Steinman first described the function of DC in linking the innate to adaptive immunity as follows; "They are sentinels, able to capture, process and present antigen and migrate to lymphoid tissue to select rare antigen-reactive T cell clones. They are sensors responding to a spectrum of environmental cues by extensive differentiation and maturation" [60].

Apart from being the cells that initiate primary immune responses, DCs are efficient producers of type I interferons, and as such, powerful mediators of innate immune responses. Stephens et al. [61] have described two DC populations $CD172^+/CD13^-$ ($SIRP^+/CC18Ag^-$) and $CD172a^-/CD13^+$ ($SIRP^-/CC18Ag^+$), in afferent lymph of cattle. These two DC populations have different patterns of cytokine production. Of the two populations, $CD13^+$ produced more IL-12, although prolonged stimulation of both populations produced comparable amounts of IL-12. The early response of the $CD13^-$ cells was characterized by IL-10 secretion. However, both populations of DC did not produce type I interferon (IFNα or β). It is difficult to assess what role these DC may play in innate immunity to vaccination or infection since the cytokine profile arising from prolonged stimulation appears to promote Th1 type (both cell types produced IL-12) of immune response, i.e., suited to activation of adaptive rather than innate immune responses. There is a level of plasticity retained in these DC populations that may allow them to stimulate either Th1 or Th2 responses depending on the conditions of the initial stimulatory signals or these subsets of DCs may be integral to one or the other T helper cell response. A firm conclusion in this paradigm awaits more definitive data.

Protection through innate immune responses may be mediated through production of IFNα by natural interferon producing cells (NIPC) (an early name for plasmacytoid dendritic cells (pDC)) as has been reported in pigs by Charley et al. [62] during experimental influenza or coronavirus infections. The precise role of DC in generating antiviral innate responses that are protective in swine remains controversial. Several groups have shown that FMDV can replicate in pDC, MoDC and bone marrow-derived DCs [63–65] and yet other groups have reported the refractory nature of skin DCs to infection with FMDV [66]. In fact, many viruses induce type I IFN yet are quite sensitive to this antiviral cytokine. However, many viruses have also evolved various mechanisms to evade this powerful innate control of pathogens. Summerfield [67,68] outlines the mechanisms certain viruses may engage in order to evade the innate immune responses mediated through type I IFN.

5.1. Dendritic cells in FMDV infection

Recently, Reid et al. [69] have identified a population of dendritic cells in cattle with high capability to produce type I interferon. $CD3^-/CD14^-/CD21^-/CD11c^-/NK^-/TCR\gamma^-/CD4^+/MHCII^+/CD45RB^+/CD172a^+/CD32^+$ pDCs accounted for 0.1% of the total lymphocyte population in peripheral blood, pseudoafferent lymph and lymph nodes. High levels of type I IFN were produced after stimulation of the cells with the TLR9 agonist CpG and FMDV immune complexes. Depletion of $CD4^+$ cells *in vivo* reduced the level of type I IFN in the serum of animals following infection with FMDV. These data likely indicate that these pDCs may be critical in generating protective immunity in animals already vaccinated, because the production of type I IFN was dependent on the presence of FMDV-antibody complexes in *in vivo* experiments. Interestingly, mesenteric lymph nodes yielded DCs with particularly high capacity to produce type I IFN, suggesting a role for these cells in lymph nodes. However, the results reported in the study by Reid et al. [69] do not indicate a role for type I IFN in early phases of infection since no effect on clinical disease was observed following depletion of $CD4^+$ type I IFN producing cells. Further, monocyte-derived DC (MoDC) complexed with dead virus stimulated FMDV-specific $CD4^+$ memory T cells, suggesting a possibility that such complexes could be used to target FMDV in vaccine formulations [65].

In a study by Nfon et al. [70], porcine DC were readily stimulated to produce IFN type I when exposed to FMDV *in vitro*. However, moDC and skin DC derived from swine infected with FMDV, failed to produce IFNα, constitutively or following *in vitro* stimulation, and this inability to produce IFNα coincides with the rising titers of FMDV in the blood. The mechanism of how production of IFNα is inhibited was described recently. Data suggests the leader protease (Lpro) of FMDV disrupts the integrity of NF-κB therefore, discontinuing NF-κB-dependent gene transcription [71,72]. Of note is a recent study by Lannes et al. [73], showing IFNα production by pDCs can be enhanced by both neutralizing and opsonizing anti-FMDV antibodies.

DC also secretes type III IFN [74]. Antiviral activity of type III interferon against FMDV was detected in cattle vaccinated with an adenovirus vector encoding a gene for bovine IFNλ3. The IFNλ3 induced upregulation of IFN regulated genes [75]. In cattle, it is not entirely clear whether DC are the primary source of IFNλ3, moreover, no challenge experiments have been performed to conclusively determine the *in vivo* efficacy of IFNλ3 as an antiviral agent. Similarly, IFNλ1 has also antiviral activity against FMDV [76].

6. Interplay between cells of the innate immune response

Lessons from the rodent models show that the innate immune system accomplishes activation and initiation of inflammatory responses through interaction of cellular components. DCs initiate the interaction upon encounter with the pathogen or upon receiving inflammatory signals from the periphery. They secrete cytokines such as interleukin 1 (IL-1), IL-2, IL-12, IL-15 and IL-18 that activate NK cells. This activation leads to increased proliferation, cytotoxicity and expression of NK cell receptors [77] that in turn may control the activation and maturation of DC. Also involved at this stage of activation are cytokines produced by NK cells such as tumor necrosis factor alpha (TNFα), interferon gamma (IFNγ) and granulocyte-macrophage colony-stimulating factor (GM-CSF) that up-regulate expression of MHC I molecules on DC. Apparently, as part of DC-NK crosstalk, NK cells may lyse immature DC (iDC), most likely to limit the immune response or to protect from induction of tolerance towards pathogens, as reported in the mouse [78]. Most recently, Siddiqui and Hope [79] showed that bovine $CD335^+/CD2^-$ NK cells migrate towards *M. bovis* infected DC that abundantly expressed chemokines such as CCL3, 4, 5, 20 and CXCL8. In this scenario, DCs produced IL-12 that activated NK cells to produce IFNγ, and in turn, $CD335^+/CD2^-$ NK cells induced an increase in the intensity of MHC II expression on the DCs. This observation clearly demonstrates the interaction between DC and NK cells.

However, it is not clear where in the tissue this interaction occurs. A study by Buentke et al. [80] showed that in the dermis of healthy humans, only scattered NK cells could be observed, however, in human skin biopsies positive for the *Malassezia* atopy-patch-test, NK cells were found in close proximity with $CD1a^+$ DC, indicating that inflammatory sites are likely to be sites where interaction may occur. The second possibility is the lymph node. In humans and mice, both DC and $CD56^{bright}$ NK cells can express chemokine receptors such as chemokine (C–C motif) receptor 7 (CCR7) and chemokine (X-C motif) receptor 3 (CXCR3) [81,82], that are responsible for immune cell trafficking to lymph nodes. Thus NK cells and DCs are in close proximity for interactions that lead to activation [83]. Moreover, in humans NK cells secrete the high mobility group B1 (HMGB1) inflammatory cytokine that protects DC from lysis by NK cells. Further, DC secrete IL-18, a cytokine that is leaderless and hence restricted to the synaptic cleft, promoting cell-cell contact of NK and DC [84].

There is also a level of interaction between γδ T cells and DC. Conti et al. [85] showed that human DC are induced to up-regulate the expression of CD86 and MHC I molecules by γδ (Vδ2) T cells and these cells secrete TNFα and IFNγ, all following stimulation with non-peptide phosphoantigens. Human NK cells positively regulate γδ T cells by interaction through CD54 and secretion of TNFα and GM-CSF but not IFNγ. In turn γδ T cells respond by vigorous proliferation to microbial antigen [86]. Because there is still lack of knowledge about the nature of antigens recognized by γδ T cells we still do not know if γδ T cells interact with DC during viral infection, in which transient activation of these cells has been observed [55]. It is highly possible that the interplay between DC, NK and γδ T cells in large animal species constitutes the stronghold of the innate immune response to infection. Fig. 1 depicts possible ways of how these cells may interact.

6.1. Implication for FMDV in the cellular interaction pathways

There is a distinct difference in the manner of response of cattle and swine to infection with FMDV. In swine DC are incapacitated and secretion of critical cytokines is disrupted by the infection. Subsequently, the lack of cytokine support and a non-productive interaction of NK cells with virus renders these cells dysfunctional. Although swine γδ T cells favourably respond to vaccination with FMDV antigens, no reliable data is available on their reactivity to infection with FMDV. Considering the dysfunction of DCs, it can be speculated that γδ T cells from swine may be dysfunctional as well. Conversely, in cattle, γδ T cells are transiently activated during the initial phase of infection with FMDV and acquire a level of cytotoxicity against *in vitro* target cells. Additionally, γδ T cells produce IFNγ which probably influences the activity of NK cells originating from infected cattle as shown in *in vitro* assays (unpublished data Patch, Dar, et al.). These responses could be initiated by DC. Appearance of antibodies could disrupt this interaction because formation of antibody/FMDV complexes appear to alter tropism of FMDV and dendritic cells are killed when such complexes are internalized through Fc receptors [65].

7. The role of Toll-like receptors in innate responses

Expression of receptors on innate immune cells defines the function of those cells. Therefore, a thorough understanding of pathogen recognition receptors (PRR) in particular Toll-like receptors (TLRs) expressed by DC, NK and γδ T cells and their agonists (pathogen associated molecular patterns, PAMP, [87]) is required in order to design proper stimulatory formulations of vaccines or immunotherapeutics. Since innate immunity plays a critical role in orchestrating interaction between different host cells, and those cells and the pathogen, modulation of the response through PRR may afford the means to enhance immunity against viruses. The pattern recognition receptors including TLRs appear to be modulated by the presence of pathogens [88].

As depicted in Fig. 1, the innate immune cell types can respond to stimulation through TLR. Although not all information is complete on the expression of TLR in large animals, bovine DC express TLR2 and 4 [89,90]. TLR7 and TLR8 are expressed by $CD14^+$ cells in the peripheral blood and respond by secreting IL-12 when treated with TLR7 and TLR8 agonists [91]. Reid et al. [69] reported the response of DC to TLR9 agonist by production of type I IFN. Microarray data compiled by Hedges et al. [92] showed transcription of TLR1, 2, 3, 4, 5, 8, 9 and other PRR in bovine γδ T cells treated with LPS. However, to date no reliable data in the literature is available indicating TLR expression on bovine NK cells.

In studies done by Lee et al. [93], bovine monocytes exposed to bovine viral diarrhea virus (BVDV), differentially transcribed TLR3 mRNA. The cytopathic strain of the virus did not significantly increase the transcription of TLR3 mRNA, while both cytopathic and non-cytopathic strains upregulated the transcription of TLR7 only after 24 h of infection. Surprisingly, this increased expression of TLR7 did not lead to enhanced type I IFN response in infected monocytes, suggesting that monocytes may play a minor role in overall synthesis of type I IFNs during infection with BVDV. The same authors had earlier shown that infection of macrophages with BVDV did not influence expression of TLR2, 3 and 4. Moreover, TLR signalling detected in these studies was not attributed to increases in TNFα or IL-1β. Persistent infection that usually occurs with BVDV is likely established due to the virus' ability to suppress the innate immune response components, in this case monocytes, by inhibiting expression of pro-inflammatory cytokines production.

Infection of cattle with FMDV up regulates expression of TLR4 but not TLR3 in nasal associated lymphoid tissue (NALT) during the acute phase of disease [94]. Studies by Zhang [94] indicate a role for the increased expression of TLR4, since mRNA level of type I IFNs concurrently increased. This may be surprising because FMDV is an RNA virus, more likely to provide ligands for TLR3 (dsRNA, a replication intermediate in many RNA viruses) than for TLR4 which transduces signals after recognizing LPS from Gram-positive bacteria.

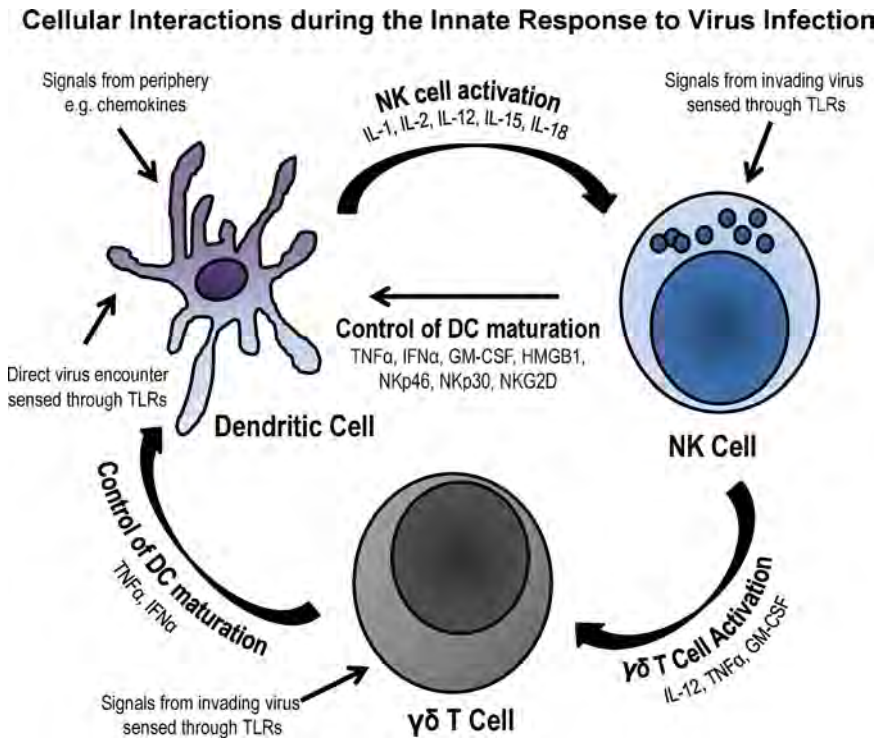

Fig. 1. Possible interaction of DC, NK and γδ T cells in an innate immune response. The figure shows three major cellular components of the innate immune system. It appears that each of the cellular components might initiate innate responses individually. Mostly because all the cell types express TLR, hence are capable of sensing pathogens. DC, upon encounter with pathogens or receiving signals from the periphery through chemokines, produce cytokines such as IL-1, IL-2, IL-12, IL-15 and IL-18, which are important activators of NK cells. NK cells in turn respond by secreting more cytokines, particularly TNFα, IFNγ, GM-CSF and HMGB1 that have a regulatory effect on DC and an activating effect on γδ T cells. Further, the NK cells proliferate in response to DC cytokines and enhance cytotoxicity against virus infected cells. In addition to cytokines secreted by NK cells γδ T cells also, secrete TNFα and GM-CSF that affect the DC activation leading to maturation and enhanced expression of MHC class I and II molecules and subsequent antigen presentation. The interplay depicted here account for the effective role played by these cells to counteract infection before it spreads within the host. However, the efficacy with which these mechanisms are executed remains largely unknown in large animal species, since viruses such as FMDV manage to efficiently replicate in swine and cause immunosuppression.

In swine, we have reported expression of TLR7 and TLR8 by NK cells. The activation of these cells to enhanced killing is partially dependent on DCs, as removing the DCs resulted in low levels of cytotoxicity following treatment with TLR7/8 agonists [95]. Others have found TLR4, 5, 7 and 9 expressed by MoDCs [96,97]. In swine, an interferon response to the TLR9 agonist, CpG, was detected in plasmacytoid DCs, Langerhans cells and B cells [98]. Zhang et al. [99] reported that swine TLR7 is stimulated by RNA oligonucleotides found in FMDV leading to expression of IFNα and Th1 cytokine induction. Taken together, this leads to the possibility of targeting these TLRs in order to modulate the function of innate immune cells to fight viral infections.

Besides TLRs, another group of PRRs called RIG-I-like receptors (RLRs) participate in innate responses [100]. TLRs are expressed either on the cell surface or in endosomes, but RLRs are found in the cytoplasm and may more be suited to detecting virus nucleic acids. Husser et al. [100] found that in PK-15 cells (porcine kidney cell line), FMDV is detected by MDA-5, while classical swine fever virus was detected by MDA-5, RIG-I and TLR3 which led to induction of IFN-β. The evidence that FMDV preferentially signals through MDA-5 is supported by data from Wang et al. [101] that L^{pro} of FMDV, a shorter form of L^{pro} (Leader protease), significantly inhibits ubiquitination of RIG-I, likely leading to inhibition of type I IFNs induction.

8. Conclusion

Many reports have emphasized the critical role of antibodies in clearance of virus following FMDV infection and protection against FMDV challenge following vaccination. A minimal amount of research has been performed to understand mechanisms of innate immune responses that possibly contribute to early responses to FMDV. In our studies as well as studies by Salt and colleagues, and Summerfield and colleagues [102–107], it is clearly demonstrated that early protection is achieved amidst very little antibody production. These data indicate that other mechanisms besides humoral immunity are in play at early time points of infection. We have recently shown that infection with FMDV in cattle induces a rapid although transient activation of γδ T cells [55]. Notably, the activation of the innate immune system in the cattle following FMDV infection is the opposite result from what we have reported in swine. Within 24 h following inoculation of pigs with FMDV, DCs stop secreting type I IFN and their numbers are reduced [108,109]. Further, NK cells isolated from FMDV infected pigs 24–96 h after infection do not produce IFNγ and fail to spontaneously lyse target cells *in vitro* [36], all indicating that the swine innate response is inhibited by the virus.

The cause of differences in response to FMDV infection between cattle and pigs is not clear. Rapid replication of FMDV in pigs leads to production of large amounts of virus. Additionally, the initial, high IFNα production is curtailed abruptly leading to high levels of viraemia and subsequent lymphopenia. A combination of these two factors may lead to immunosuppression of these innate responses in pigs. Conversely, although vireamia is observed in cattle, levels of IFNα are much lower than those in pigs and neither lymphopenia nor immunosuppression of NK cells or γδ T cells occurs in cattle [110]. Taken together, a new emphasis is required to focus investigations on the innate immune mechanisms that may be exploited in design of new interventions to control FMDV outbreaks.

Acknowledgements

The authors thank Ms. Raisa Glabman for assistance in preparing the illustration. This work was funded by CRIS #1940-32000-057-00D from the Agricultural Research Service, USDA (WTG) and by an interagency agreement (60-1940-8-037) between the Department of Homeland Security, Science and Technology Directorate, and the USDA, Agricultural Research Service (WTG). This work was also supported by the Polish National Science Centre (NCN) grant NN308566040 (FNT) and USDA Specific Cooperative Agreement 58-1940-0-088F (WTG & FNT).

References

[1] Yasuda M, Ogawa D, Nasu T, Yamaguchi T, Murakami T. Kinetics and distribution of bovine γδ T-lymphocyte in the intestine: γδ T cells accumulate in the dome region of Peyer's patch during prenatal development. Dev Comp Immunol 2005;29:555–64.
[2] Hein WR, Dudler L. Divergent evolution of T cell repertoires: extensive diversity and developmentally regulated expression of the sheep γδ T cell receptor. EMBO J 1993;12:715–24.
[3] Sinkora M, Sinkorova J, Cimburek Z, Holtmeier W. Two groups of porcine TCR γδ$^+$ thymocytes behave and diverge differently. J Immunol 2007;178:711–9.
[4] Bautista EM, Nfon C, Ferman GS, Golde WT. IL-13 replaces IL-4 in development of monocyte derived dendritic cells (MoDC) of swine. Vet Immunol Immunopathol 2007;115:56–67.
[5] Renjifo X, Howard C, Kerkhofs P, Denis M, Urbain J, Moser M, et al. Purification and characterization of bovine dendritic cells from peripheral blood. Vet Immunol Immunopathol 1997;60:77–88.
[6] Kaiko GE, Phipps S, Angkasekwinai P, Dong C, Foster PS. NK cell deficiency predisposes to viral-induced Th2-type allergic inflammation via epithelial-derived IL-25. J Immunol 2010;185:4681–90.
[7] Carr DJJ, Wuest T, Ash J. An increase in herpes simplex virus type 1 in the anterior segment of the eye is linked to a deficiency in NK cell infiltration in mice deficient in CXCR3. J Interferon Cytokine Res 2008;28:245–51.
[8] Eidenschenk C, Jouanguy E, Alcais A, Mention J-J, Pasquier B, Fleckenstein IM, et al. Familial NK cell deficiency associated with impaired IL-2- and IL-15-dependent survival of lymphocytes. J Immunol 2006;177:8835–43.
[9] Spits H, Cupedo T. Innate lymphoid cells: emerging insights in development, lineage relationships, and function. Annu Rev Immunol 2012;30:647–75.
[10] Spits H, Di Santo JP. The expanding family of innate lymphoid cells: regulators and effectors of immunity and tissue remodeling. Nat Immunol 2011;12:21–7.
[11] Vivier E, Spits H, Cupedo T. Interleukin-22-producing innate immune cells: new players in mucosal immunity and tissue repair. Nat Rev Immunol 2009;9:229–34.
[12] Storset AK, Kulberg S, Berg I, Boysen P, Hope JC, Dissen E. NKp46 defines a subset of bovine leukocytes with natural killer cell characteristics. Eur J Immunol 2004;34:669–76.
[13] Goff WL, Storset AK, Johnson WC, Brown WC. Bovine splenic NK cells synthesize IFN-γ in response to IL-12-containing supernatants from Babesia bovis-exposed monocyte cultures. Parasitol Immunol 2006;28:221–8.
[14] Bastos RG, Johnson WC, Mwangi W, Brown WC, Goff WL. Bovine NK cells acquire cytotoxic activity and produce IFN-γ after stimulation by *Mycobacterium bovis* BCG- or Babesia bovis-exposed splenic dendritic cells. Vet Immunol Immunopathol 2008;124:302–12.
[15] Boysen P, Olsen I, Berg I, Kulberg S, Johansen G, Storset A. Bovine CD2$^-$/NKp46$^+$ cells are fully functional natural killer cells with a high activation status. BMC Immunol 2006;7:10.
[16] Boysen P, Klevar S, Olsen I, Storset AK. The protozoan *Neospora caninum* directly triggers bovine NK cells to produce gamma interferon and to kill infected fibroblasts. Infect Immun 2006;74:953–60.
[17] Klevar S, Kulberg S, Boysen P, Storset AK, Moldal T, Bjorkman C, et al. Natural killer cells act as early responders in an experimental infection with *Neospora caninum* in calves. Int J Parasitol 2007;37:329–39.
[18] Denis M, Keen DL, Parlane NA, Storset AK, Buddle BM. Bovine natural killer cells restrict the replication of *Mycobacterium bovis* in bovine macrophages and enhance IL-12 release by infected macrophages. Tuberculosis 2007;87:53–62.
[19] Hope JC, Sopp P, Howard CJ. NK-like CD8(+) cells in immunologically naive neonatal calves that respond to dendritic cells infected with *Mycobacterium bovis* BCG. Journal of Leukocyte Biology 2002;71:184–94.
[20] Fikri Y, Nyabenda J, Content J, Huygen K. Cloning, sequencing, and cell surface expression pattern of bovine immunoreceptor NKG2D and adaptor molecules DAP10 and DAP12. Immunogenetics 2007;59:653–9.
[21] Guzman E, Birch JR, Ellis SA. Cattle MIC is a ligand for the activating NK cell receptor NKG2D. Vet Immunol Immunopathol 2010;136:227–34.
[22] Boysen P, Storset AK. Bovine natural killer cells. Vet Immunol Immunopathol 2009;130:163–77.
[23] Albertsson PA, Basse PH, Hokland M, Goldfarb RH, Nagelkerke JF, Nannmark U, et al. NK cells and the tumour microenvironment: implications for NK-cell function and anti-tumour activity. Trends Immunol 2003;24:603–9.
[24] Cerundolo V, de la Salle H. Description of HLA class I- and CD8-deficient patients: insights into the function of cytotoxic T lymphocytes and NK cells in host defense. Sem Immunol 2006;18:330–6.
[25] Moretta A, Biassoni R, Bottino C, Moretta L. Surface receptors delivering opposite signals regulate the function of human NK cells. Sem Immunol 2000;12:129–38.
[26] Ishizaki H, Kariya Y. Road transportation stress promptly increases bovine peripheral blood absolute NK cell counts and cortisol levels. J Vet Med Sci 2010;72:747–53.
[27] Riondato F, D'Angelo A, Miniscalco B, Bellino C, Guglielmino R. Effects of road transportation on lymphocyte subsets in calves. Vet J 2008;175:364–8.
[28] Mendoza C, Videgain SP, Alonso F. Inhibition of natural killer activity in porcine mononuclear cells by African swine fever virus. Res Vet Sci 1991;51:317–21.
[29] Jung K, Renukaradhya GJ, Alekseev KP, Fang Y, Tang Y, Saif LJ. Porcine reproductive and respiratory syndrome virus modifies innate immunity and alters disease outcome in pigs subsequently infected with porcine respiratory coronavirus: implications for respiratory viral co-infections. J Gen Virol 2009;90:2713–23.
[30] Sun JC, Lopez-Verges S, Kim CC, DeRisi JL, Cells Lanier LLNK. Immune memory. J Immunol 2011;186:1891–7.
[31] Thierry A, Robin A, Giraud S, Minouflet S, Barra A, Bridoux F, et al. Identification of invariant natural killer T cells in porcine peripheral blood. Vet Immunol Immunopathol 2012;149:272–9.
[32] Bradford HEL, Adair BM, Foster JC. Antibody-dependent killing of virus-infected targets by NK-like cells in bovine blood. J Vet Med B 2001;48:637–40.
[33] Denyer MS, Wileman TE, Stirling CMA, Zuber B, Takamatsu H-H. Perforin expression can define CD8 positive lymphocyte subsets in pigs allowing phenotypic and functional analysis of natural killer, cytotoxic T, natural killer T and MHC un-restricted cytotoxic T-cells. Vet Immunol Immunopathol 2006;110:279–92.
[34] Pintaric M, Gerner W, Saalmuller A. Synergistic effects of IL-2, IL-12 and IL-18 on cytolytic activity, perforin expression and IFN-γ production of porcine natural killer cells. Vet Immunol Immunopathol 2008;121:68–82.
[35] Toka FN, Nfon CK, Dawson H, Estes DM, Golde WT. Activation of porcine natural killer cells and lysis of foot-and-mouth disease virus infected cells. J Interf Cytok Res 2009;29:179–92.
[36] Toka FN, Nfon C, Dawson H, Golde WT. Natural killer cell dysfunction during acute infection with foot-and-mouth disease virus. Clin Vaccine Immunol 2009;16:1738–49.
[37] Takamatsu HH, Denyer MS, Stirling C, Cox S, Aggarwal N, Dash P, et al. Porcine γδ T cells: possible roles on the innate and adaptive immune responses following virus infection. Vet Immunol Immunopathol 2006;112:49–61.
[38] Toulon A, Breton L, Taylor KR, Tenenhaus M, Bhavsar D, Lanigan C, et al. A role for human skin-resident T cells in wound healing. J Exp Med 2009;206:743–50.
[39] Hoek A, Rutten VPMG, Kool J, Arkesteijn GJA, Bouwstra RJ, van Rhijn I, et al. Subpopulations of bovine WC1$^+$ γδ T cells rather than CD4$^+$CD25^{high} Foxp3$^+$ T cells act as immune regulatory cells ex vivo. Vet Res 2009;40:06.
[40] Wijngaard PL, Metzelaar MJ, MacHugh ND, Morrison WI, Clevers HC. Molecular characterization of the WC1 antigen expressed specifically on bovine CD4$^-$CD8$^-$ γδ T lymphocytes. J Immunol 1992;149:3273–7.
[41] Aruffo A, Bowen MA, Patel DD, Haynes BF, Starling GC, Gebe JA, et al. CD6-ligand interactions: a paradigm for SRCR domain function. Immunol Today 1997;18:498–504.
[42] Skyberg JA, Thornburg T, Rollins M, Huarte E, Jutila MA, Murine Pascual DW. Bovine γδ T cells enhance innate immunity against *Brucella abortus* infections. PLoS ONE 2011;6:e21978.
[43] Herzig CT, Baldwin CL. Genomic organization and classification of the bovine WC1 genes and expression by peripheral blood γδ T cells. BMC Genomics 2009;10:191.
[44] Sinkora M, Sinkora J, Rehakova Z, Butler JE. Early ontogeny of thymocytes in pigs: sequential colonization of the thymus by T cell progenitors. J Immunol 2000;165:1832–9.
[45] Sinkora M, Sinkorova J, Holtmeier W. Development of γδ thymocyte subsets during prenatal and postnatal ontogeny. Immunology 2005;115:544–55.
[46] Stepanova K, Sinkora M. The expression of CD25, CD11b, SWC1, SWC7, MHC-II, and family of CD45 molecules can be used to characterize different stages of γδ T lymphocytes in pigs. Dev Comp Immunol 2012;36:728–40.
[47] Leitner J, Reutner K, Essler SE, Popow I, Gerner W, Steinberger P, et al. Porcine SWC1 is CD52 – final determination by the use of a retroviral cDNA expression library. Vet Immunol Immunopathol 2012;146:27–34.
[48] Stepanova H, Mensikova M, Chlebova K, Faldyna M. CD4$^+$ and γδTCR$^+$ T lymphocytes are sources of interleukin-17 in swine. Cytokine 2012;58:152–7.
[49] Olin M, Batista L, Xiao Z, Dee S, Murtaugh M, Pijoan C, et al. γδ Lymphocyte response to porcine reproductive and respiratory syndrome virus. Viral Immunol 2005;18:490–9.
[50] Takamatsu HH, Denyer MS, Wileman TE. A sub-population of circulating porcine γδ T cells can act as professional antigen presenting cells. Vet Immunol Immunopathol 2002;87:223–4.
[51] Olin MR, Hwa Choi K, Lee J, Molitor TW. γδ T-lymphocyte cytotoxic activity against *Mycobacterium bovis* analyzed by flow cytometry. J Immunol Methods 2005;297:1–11.
[52] Wang F, Herzig CTA, Chen C, Hsu H, Baldwin CL, Telfer JC. Scavenger receptor WC1 contributes to the γδ T cell response to Leptospira. Mol Immunol 2011;48:801–9.

[53] Amadori M, Archetti IL, Verardi R, Berneri C. Isolation of mononuclear cytotoxic cells from cattle vaccinated against foot-and-mouth disease. Arch Virol 1992;122:293–306.
[54] Amadori M, Archetti IL, Verardi R, Berneri C. Role of a distinct population of bovine γδ T cells in the immune response to viral agents. Viral Immunol 1995;8:81–91.
[55] Toka FN, Kenney MA, Golde WT. Rapid and transient activation of γδ T cells to IFN-γ production, NK cell-like killing, and antigen processing during acute virus infection. J Immunol 2011;186:4853–61.
[56] Collins RA, Werling D, Duggan SE, Bland AP, Parsons KR, Howard CJ. γδ T cells present antigen to CD4+ αβ T cells. J Leukocyte Biol 1998;63:707–14.
[57] Murakami K, Sentsui H, Inoshima Y, Inumaru S. Increase in γδ T cells in the blood of cattle persistently infected with Bovine Leukemia Virus following administration of recombinant bovine IFN-gamma. Vet Immunol Immunopathol 2004;101:61–71.
[58] Steinman RM. Dendritic cells in vivo: a key target for a new vaccine science. Immunity 2008;29:319–24.
[59] Steinman RM. Dendritic cells and vaccines. Proceedings (Bayl Univ Med Cent) 2008;21:3–8.
[60] Steinman RM. Linking innate to adaptive immunity through dendritic cells. Novart Fdn Symp 2006;279:101–9 [discussion 9–13, 216–219].
[61] Stephens SA, Brownlie J, Charleston B, Howard CJ. Differences in cytokine synthesis by the sub-populations of dendritic cells from afferent lymph. Immunology 2003;110:48–57.
[62] Charley B, Riffault S, van Reeth K. Porcine innate and adaptative immune responses to influenza and coronavirus infections. Ann NY Acad Sci 2006;1081:130–6.
[63] Guzylack-Piriou L, Bergamin F, Gerber M, McCullough KC, Summerfield A. Plasmacytoid dendritic cell activation by foot-and-mouth disease virus requires immune complexes. Eur J Immunol 2006;36:1674–83.
[64] Harwood LJ, Gerber H, Sobrino F, Summerfield A, McCullough KC. Dendritic cell internalization of foot-and-mouth disease virus: influence of heparan sulfate binding on virus uptake and induction of the immune response. J Virol 2008;82:6379–94.
[65] Robinson L, Windsor M, McLaughlin K, Hope J, Jackson T, Charleston B. Foot-and-mouth disease virus exhibits an altered tropism in the presence of specific immunoglobulins, enabling productive infection and killing of dendritic cells. J Virol 2011;85:2212–23.
[66] Bautista EM, Ferman GS, Gregg D, Brum MC, Grubman MJ, Golde WT. Constitutive expression of alpha interferon by skin dendritic cells confers resistance to infection by foot-and-mouth disease virus. J Virol 2005;79:4838–47.
[67] Summerfield A. Viewpoint factors involved in type I interferon responses during porcine virus infections. Vet Immunol Immunopathol 2012;148:168–71.
[68] Fiebach AR, Guzylack-Piriou L, Python S, Summerfield A, Ruggli N. Classical swine fever virus Npro limits type i interferon induction in plasmacytoid dendritic cells by interacting with interferon regulatory factor 7. J Virol 2011;85:8002–11.
[69] Reid E, Juleff N, Gubbins S, Prentice H, Seago J, Charleston B. Bovine plasmacytoid dendritic cells are the major source of type I interferon in response to foot-and-mouth disease virus in vitro and in vivo. J Virol 2011;85:4297–308.
[70] Nfon CK, Ferman GS, Toka FN, Gregg DA, Golde WT. Interferon-α production by swine dendritic cells is inhibited during acute infection with foot-and-mouth disease virus. Viral Immunol 2008;21:68–77.
[71] de los Santos T, de Avila Botton S, Weiblen R, Grubman MJ. The leader proteinase of foot-and-mouth disease virus inhibits the induction of beta interferon mRNA and blocks the host innate immune response. J Virol 2006;80:1906–14.
[72] de los Santos T, Diaz-San Segundo F, Grubman MJ. Degradation of nuclear factor kappa b during foot-and-mouth disease virus infection. J Virol 2007;81:12803–15.
[73] Lannes N, Python S, Summerfield A. Interplay of foot-and-mouth disease virus, antibodies and plasmacytoid dendritic cells: virus opsonization under non-neutralizing conditions results in enhanced interferon-alpha responses. Vet Res 2012;43:64.
[74] Iversen MB, Ank N, Melchjorsen J, Paludan SR. Expression of type III interferon (IFN) in the vaginal mucosa is mediated primarily by dendritic cells and displays stronger dependence on NF-κB than type I IFNs. J Virol 2010;84:4579–86.
[75] Diaz-San Segundo F, Weiss M, Perez-Martin E, Koster MJ, Zhu J, Grubman MJ, et al. Antiviral activity of bovine type III interferon against foot-and-mouth disease virus. Virology 2011;413:283–92.
[76] Wang D, Fang L, Liu L, Zhong H, Chen Q, Luo R, et al. Foot-and-mouth disease virus (FMDV) leader proteinase negatively regulates the porcine interferon-λ-1 pathway. Mol Immunol 2011;49:407–12.
[77] Wai L-E, Garcia JA, Martinez OM, Krams SM. Distinct roles for the NK cell-activating receptors in mediating interactions with dendritic cells and tumor cells. J Immunol 2011;186:222–9.
[78] Cooper MA, Fehniger TA, Fuchs A, Colonna M, Caligiuri MA. NK cell and DC interactions. Trends Immunol 2004;25:47–52.
[79] Siddiqui N, Hope J. Differential recruitment and activation of natural killer cell sub-populations by *Mycobacterium bovis*-infected dendritic cells. Eur J Immunol 2013;43:159–69.
[80] Buentke E, Heffler LC, Wilson JL, Wallin RPA, Lofman C, Chambers BJ, et al. Natural killer and dendritic cell contact in lesional atopic dermatitis skin-Malassezia-influenced cell interaction. J Invest Derm 2002;119:850–7.
[81] Campbell JJ, Qin S, Unutmaz D, Soler D, Murphy KE, Hodge MR, et al. Unique subpopulations of CD56+ NK and NK-T peripheral blood lymphocytes identified by chemokine receptor expression repertoire. J Immunol 2001;166:6477–82.
[82] Palucka K, Banchereau J. How dendritic cells and microbes interact to elicit or subvert protective immune responses. Curr Opin Immunol 2002;14:420–31.
[83] Fehniger TA, Cooper MA, Nuovo GJ, Cella M, Facchetti F, Colonna M, et al. CD56bright natural killer cells are present in human lymph nodes and are activated by T cell-derived IL-2: a potential new link between adaptive and innate immunity. Blood 2003;101:3052–7.
[84] Semino C, Angelini G, Poggi A, Rubartelli A. NK/iDC interaction results in IL-18 secretion by DCs at the synaptic cleft followed by NK cell activation and release of the DC maturation factor HMGB1. Blood 2005;106:609–16.
[85] Conti L, Casetti R, Cardone M, Varano B, Martino A, Belardelli F, et al. Reciprocal activating interaction between dendritic cells and pamidronate-stimulated γδ T Cells: role of CD86 and inflammatory cytokines. J Immunol 2005;174:252–60.
[86] Zhang R, Zheng X, Li B, Wei H, Tian Z. Human NK cells positively regulate γ T cells in response to mycobacterium tuberculosis. J Immunol 2006;176:2610–6.
[87] Janeway CJ. Approaching the asymptote? Evolution and revolution in mmunology. Cold Spring Harb SympQuant Biol 1989;54:1–13.
[88] Rohmann K, Tschernig T, Pabst R, Goldmann T, Dromann D. Innate immunity in the human lung: pathogen recognition and lung disease. Cell Tissue Res 2011;343:167–74.
[89] Werling D, Hope JC, Howard CJ, Jungi TW. Differential production of cytokines, reactive oxygen and nitrogen by bovine macrophages and dendritic cells stimulated with Toll-like receptor agonists. Immunology 2004;111:41–52.
[90] Werling D, Piercy J, Coffey TJ. Expression of Toll-like receptors (TLR) by bovine antigen-presenting cells – potential role in pathogen discrimination. Vet Immunol Immunopathol 2006;112:2–11.
[91] Buza J, Benjamin P, Zhu J, Wilson HL, Lipford G, Krieg AM, et al. CD14+ cells are required for IL-12 response in bovine blood mononuclear cells activated with Toll-like receptor (TLR) 7 and TLR8 ligands. Vet Immunol Immunopathol 2008;126:273–82.
[92] Hedges JF, Lubick KJ, Jutila MA. γδ T cells respond directly to pathogen-associated molecular patterns. J Immunol 2005;174:6045–53.
[93] Lee SR, Pharr GT, Boyd BL, Pinchuk LM. Bovine viral diarrhea viruses modulate Toll-like receptors, cytokines and co-stimulatory molecules genes expression in bovine peripheral blood monocytes. Comp Immunol Microbiol Infect Dis 2008;31:403–18.
[94] Zhang Z, Bashiruddin JB, Doel C, Horsington J, Durand S, Alexandersen S. Cytokine and Toll-like receptor mRNAs in the nasal-associated lymphoid tissues of cattle during foot-and-mouth disease virus infection. J Comp Pathol 2006;134:56–62.
[95] Toka FN, Nfon CK, Dawson H, Golde WT. Accessory-cell-mediated activation of porcine NK cells by Toll-like receptor 7 (TLR7) and TLR8 agonists. Clin Vaccine Immunol 2009;16:866–78.
[96] Alves MP, Neuhaus V, Guzylack-Piriou L, Ruggli N, McCullough KC, Summerfield A. Toll-like receptor 7 and MyD88 knockdown by lentivirus-mediated RNA interference to porcine dendritic cell subsets. Gene Ther 2007;14:836–44.
[97] Raymond CR, Wilkie BN. Toll-like receptor, MHC, II, B7 and cytokine expression by porcine monocytes and monocyte-derived dendritic cells in response to microbial pathogen-associated molecular patterns. Vet Immunol Immunopathol 2005;107:235–47.
[98] Alves MP, Guzylack-Piriou L, Juillard V, Audonnet JC, Doel T, Dawson H, et al. Innate immune defenses induced by CpG do not promote vaccine-induced protection against foot-and-mouth disease virus in pigs. Clin Vaccine Immunol 2009;16:1151–7.
[99] Zhang Y, Guo Y, Lv K, Wang K, Sun S. Molecular cloning and functional characterization of porcine Toll-like receptor 7 involved in recognition of single-stranded RNA virus/ssRNA. Mol Immunol 2008;45:1184–90.
[100] Husser L, Alves MP, Ruggli N, Summerfield A. Identification of the role of RIG-I, MDA-5 and TLR3 in sensing RNA viruses in porcine epithelial cells using lentivirus-driven RNA interference. Virus Res 2011;159:9–16.
[101] Wang D, Fang L, Li P, Sun L, Fan J, Zhang Q, et al. The leader proteinase of foot-and-mouth disease virus negatively regulates the type I interferon pathway by acting as a viral deubiquitinase. J Virol 2011;85:3758–66.
[102] Golde WT, Pacheco JM, Duque H, Doel T, Penfold B, Ferman GS, et al. Vaccination against foot-and-mouth disease virus confers complete clinical protection in 7 days and partial protection in 4 days: use in emergency outbreak response. Vaccine 2005;23:5775–82.
[103] Pacheco JM, Brum MCS, Moraes MP, Golde WT, Grubman MJ. Rapid protection of cattle from direct challenge with foot-and-mouth disease virus (FMDV) by a single inoculation with an adenovirus-vectored FMDV subunit vaccine. Virology 2005;337:205–9.
[104] Cox SJ, Barnett PV, Dani P, Salt JS. Emergency vaccination of sheep against foot-and-mouth disease: protection against disease and reduction in contact transmission. Vaccine 1999;17:1858–68.
[105] Doel TR, Williams L, Barnett PV. Emergency vaccination against foot-and-mouth disease: rate of development of immunity and its implications for the carrier state. Vaccine 1994;12:592–600.
[106] Rigden RC, Carrasco CP, Barnett PV, Summerfield A, McCullough KC. Innate immune responses following emergency vaccination against foot-and-mouth disease virus in pigs. Vaccine 2003;21:1466–77.

[107] Salt JS, Barnett PV, Dani P, Williams L. Emergency vaccination of pigs against foot-and-mouth disease: protection against disease and reduction in contact transmission. Vaccine 1998;16:746–54.
[108] Nfon CK, Ferman GS, Toka FN, Gregg DA, Golde WT. Interferon-alpha production by swine dendritic cells is inhibited during acute infection with foot-and-mouth disease virus. Viral Immunol 2008;21:68–77.
[109] Nfon CK, Toka FN, Kenney M, Pacheco JM, Golde WT. Loss of plasmacytoid dendritic cell function coincides with lymphopenia and viremia during foot-and-mouth disease virus infection. Viral Immunol 2010;23:29–41.
[110] Windsor M, Carr BV, Bankowski B, Gibson D, Reid E, Hamblin P, et al. Cattle remain immunocompetent during the acute phase of foot-and-mouth disease virus infection. Vet Res 2011;42:108.

Provided for non-commercial research and educational use only.
Not for reproduction, distribution or commercial use.

This chapter was originally published in the book *Handbook of Proteolytic Enzymes*, published by Elsevier, and the attached copy is provided by Elsevier for the author's benefit and for the benefit of the author's institution, for non-commercial research and educational use including without limitation use in instruction at your institution, sending it to specific colleagues who know you, and providing a copy to your institution's administrator.

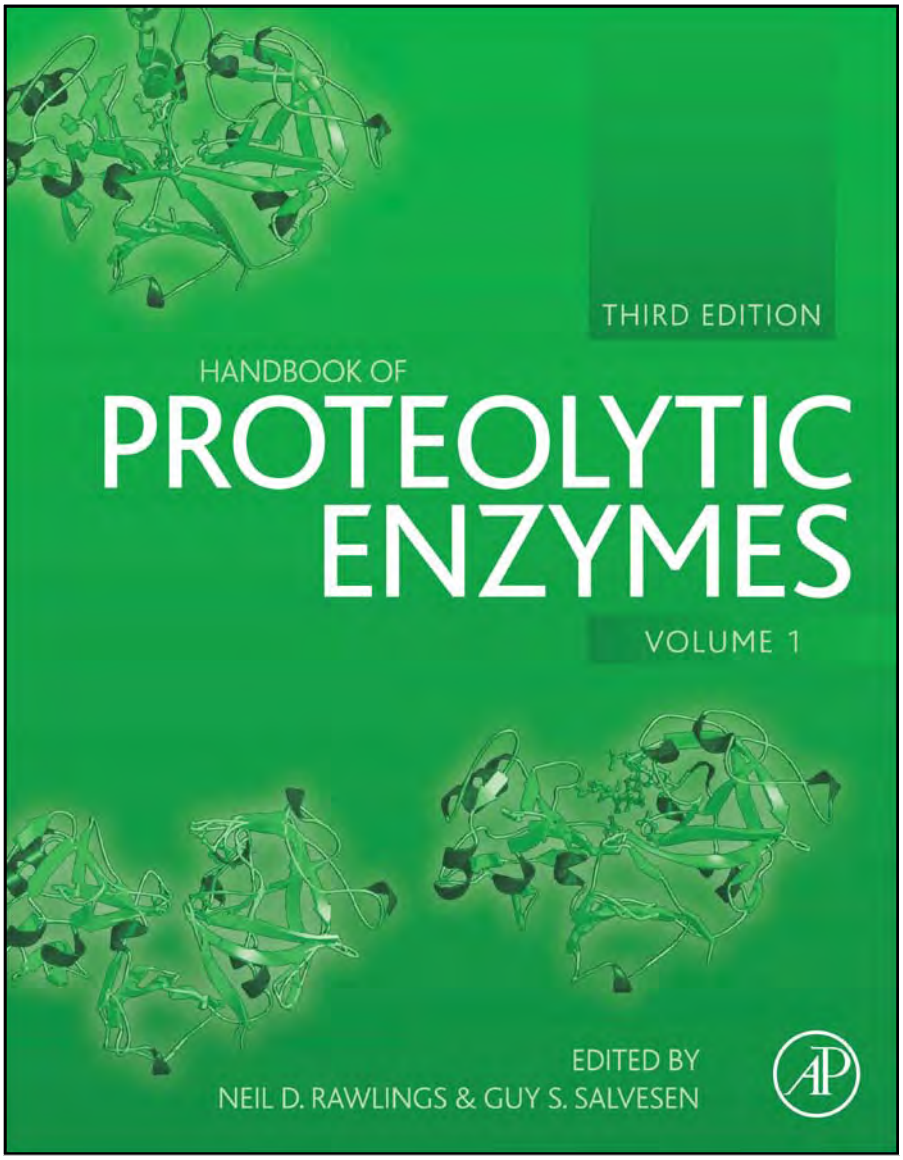

All other uses, reproduction and distribution, including without limitation commercial reprints, selling or licensing copies or access, or posting on open internet sites, your personal or institution's website or repository, are prohibited. For exceptions, permission may be sought for such use through Elsevier's permissions site at:
http://www.elsevier.com/locate/permissionusematerial

From Marvin J. Grubman, Foot-and-Mouth Disease Virus L-Peptidase. In: Neil D. Rawlings and Guy S. Salvesen, editors, Handbook of Proteolytic Enzymes. Oxford: Academic Press, 2013, pp. 2183-2186.
ISBN: 978-0-12-382219-2
Copyright © 2013 Elsevier Ltd.
Academic Press.

Author's personal copy

Chapter 491

Foot-and-Mouth Disease Virus L-Peptidase

Databanks

MEROPS name: foot-and-mouth disease virus L-peptidase
MEROPS classification: clan CA, family C28, peptidase C28.001
IUBMB: EC 3.4.22.46 (BRENDA)
Tertiary structure: Available
Species distribution: known only from foot-and-mouth disease virus
Reference sequence from: foot-and-mouth disease virus

Name and History

Foot-and-mouth disease virus (FMDV), equine rhinitis A virus (ERAV), and bovine rhinitis B virus (BRBV) comprise the genus *Aphthovirus* within the family Picornaviridae [1]. Seven genera within this family, the *Aphthoviruses*, *Cardioviruses*, *Erbovirus*, *Kobuvirus, Senecavirus, Sapelovirus*, and *Teschovirus* encode a leader (L)-protein [1]. However, only the *Aphthoviruses* and *Erbovirus* L-protein have proteolytic activity [1,2]. FMDV L-protein has been identified as a peptidase by sequence homology with papain and functional studies [3–6]. The ERBV L-protein also has *peptidase* activity whereas the *Cardiovirus*, *Kobuvirus*, *Senecavirus*, *Sapelovirus*, and *Teschovirus* L-proteins are proteolytically inactive [7]. The current nomenclature for picornavirus proteins was adopted at the third meeting of the European Study Group on the Molecular Biology of Picornaviruses and formalized by Rueckert & Wimmer [8]. A uniform nomenclature was devised at that time because of the complex cleavage pathways of these proteins and the additional variability of the numerous virus species within the family. The L-protein is defined as that region of the polyprotein preceding the capsid precursor protein, and the name was chosen because of its location in the polyprotein and to minimize possible confusion with other viral proteins.

For FMDV there are two in-frame AUG codons separated by 84 nucleotides at the beginning of the viral genome open reading frame, resulting in the synthesis of two L-proteins, Lab and Lb. Lb, the smaller of the two proteins, is the major species synthesized. The L sequence is highly variable among FMDV subtypes and serotypes that have been examined, but all retain the active site residues [9,10]. The BRBV genome also possesses two in-frame AUG codons but separated by 69 nucleotides and current evidence suggests that similar to FMDV the smaller Lb protein is the predominant

Author's personal copy

product [11]. In the case of ERAV there are two AUG pairs separated by 57 nucleotides and *in vitro* results with ERAV bicistronic plasmids suggest that the second AUG of the first pair appears to be the dominant start site [12–14].

Strebel & Beck [15] were the first to demonstrate that the L-protein of FMDV has proteolytic activity, and autocatalytically cleaves itself from the growing viral polypeptide chain. Subsequently it was demonstrated that the L-protein is also involved in the cleavage of a host protein, eIF4G, which is required for the initiation of cap-dependent protein synthesis [4,5]. By a number of criteria, including limited sequence alignment, inhibitor studies and genetic analysis, the L-protein has been defined as one of the 'papain-like' viral proteinases [3,16–18]. Recently, Wang *et al*. [19] showed by sequence alignment and structural bioinformatic analyses that the FMDV L protein displays similarity to cellular and viral ubiquitin-proteinases. Furthermore, the authors demonstrated that *in vitro* FMDV Lb has de-ubiquitinase activity on cellular targets. ERAV L has maintained the key catalytic residues and predicted secondary structure of FMDV L [20]. Both ERAV and BRBV L retain the autocatalytic and eIF4G cleavage activities [7].

Activity and Specificity

Kirchweger *et al*. [6] purified the Lb form of the L-peptidase and demonstrated that it cleaves the host initiation factor eIF4G (later termed eIF4GI) at the Gly674-Arg675 bond. Subsequently it was demonstrated that there are two forms of eIF4G, I and II, which are functionally equivalent [6,21]. Both forms are cleaved very rapidly in FMDV infected cells and *in vitro* by Lb and the cleavage sites have been mapped [22]. Cleavage of eIF4GII occurs between Gly700 Ser701. This site differs from the cleavage site of eIF4GI and the L-peptidase from its precursor polyprotein P1 because a Ser residue replaces a basic amino acid at the scissile peptide bond. However, it has been speculated that Arg702 may provide the positive charge required for Lb substrate binding [22]. Cleavage sites are: L-VP4, Val-Gln-Arg-Lys-Leu-Lys↓Gly-Ala-Gly-Gln-Ser-Ser; eIF4GI, Ser-Phe-Ala-Asn-Leu-Gly↓Arg-Thr-Thr-Leu-Ser-Thr; eIF4GII, Pro-Leu-Leu-Asn-Val-Gly↓Ser-Arg-Arg-Ser-Gln-Pro.

Ziegler *et al*. [23] found that purified L-peptidase cleaved the translation products of a number of reporter genes, but no significant pattern of sequence conservation was apparent when the different cleavage sites were compared. L-Peptidase autocatalytic activity at the L-VP4 scissile bond is blocked by E-64 in a cell-free system and by E-64d, a membrane-permeable analog, in infected cells [16]. Likewise, cleavage of eIF4G is inhibited by E-64d in infected cells.

Structural Chemistry

The Lab protein contains 201 amino acids with a size of approximately 23 kDa and a pI of about 4.7, while the smaller Lb-peptidase is a 173 amino acid protein of approximately 21 kDa and pI of 4.8. The crystal and solution structures of Lb have been determined at high resolution and showed that it comprises a globular catalytic domain similar to that of the cysteine proteinases of the papain superfamily with active-site residues Cys51 and His148 on opposite sides of a cleft separating two subdomains, but with a unique flexible C-terminal extension [24–27]. This extension has been developed to enable C-terminal self-processing from the viral polypeptide, a reaction that is likely intramolecular under physiological conditions [24,25]. In contrast to the majority of papain-like proteinases, the L-peptidase has evolved a mechanism for stabilizing and orienting its active site that involves the presence of an electrostatic charge at position 164 (Asp) [28]. Studies of hydrolytic properties and substrate specificity using FRET peptides revealed that the FMDV leader protease has unusual characteristics in comparison to the class prototypes, papain and cathepsins, including a high sensitivity to salt and a very specific substrate binding site that extends to seven amino acids from the cleavage site [29]. In addition residues Leu178 and Leu143 contribute to the architecture of more than one substrate binding pocket giving specificity and explaining why Lb is one of the smallest, albeit one of the most specific papain-like enzymes [29,30]. Additionally, residues Asp184 and Glu186 are required for binding and proper processing of eIF4G independently of self-cleavage functions [31].

Preparation

The Lb gene has been expressed in *Escherichia coli* either under the control of the inducible λPL promoter or a T7 RNA polymerase promoter [6,32,33]. In the latter two cases, because of the toxicity of the Lb-peptidase in *E. coli*, the protein can be reliably expressed only in a plasmid in which the basal level of T7 RNA polymerase is tightly controlled. The Lb-peptidase was purified to homogeneity from an *E. coli* expression system and this material or derivatives of it have been utilized to determine its three-dimensional structure [6,24,26].

Biological Aspects

A major function of the Lb-peptidase in infected cells appears to be the cleavage of eIF4G, which is a subunit of the cap-binding protein complex required for the translation of cap-dependent mRNAs. Cleavage of this component correlates with the shut-off of most host cell protein synthesis. However, translation of FMDV mRNA occurs by a

Author's personal copy

cap-independent mechanism and is not impaired. A genetically altered variant of FMDV, which lacks the coding region for the Lb-peptidase, was constructed [34]. This virus is significantly attenuated in cattle and swine as compared to wild-type virus, suggesting that the Lb-peptidase may be required for rapid viral growth and for the dramatic cytopathic effects associated with FMDV infection [35,36]. Studies in cell culture indicate that leaderless virus is attenuated because it allows translation of viral-induced type I interferon (IFN) mRNA, while wild-type virus infection blocks the translation of this capped mRNA [37].

de los Santos *et al.* [38,39] demonstrated that Lb-peptidase translocates to the nucleus of infected cells and in this compartment it becomes involved in the cleavage of the p65 subunit of the transcription factor nuclear factor kappa B (NF-κB). As a result, induction of IFNβ mRNA and IFN-stimulated genes are reduced in comparison to cells infected with leaderless virus [38]. Degradation of NF-κB requires L peptidase catalytic activity although no direct interaction has been demonstrated between L and NF-κB [40]. Bioinformatic analyses suggest that Lb-peptidase contains a SAP (for SAF-A/B, Acinus and PIAS) domain, a protein structure associated with nuclear retention of molecules [41,42]. Mutation of this domain prevents retention of Lb-peptidase in the nucleus and subsequently NF-κB is not degraded resulting in the induction of NF-κB-dependent mRNAs. Mutation of the SAP domain does not significantly affect degradation of eIF4G [40]. More recently, it was shown that FMDV Lb is also involved in degradation of the transcription factors IFN regulatory factors 3 and 7 which, like NF-κB, are required for IFN and IFN stimulated gene induction [43]. Sequence alignment and comparison with other genomes have shown that the L protein is a ubiquitin (Ub)-proteinase responsible for removal of Ub moieties from cellular targets [19]. To this end deubiquitination (DUB) upon over-expression of L, has been demonstrated in key molecules which are sensors or inducers of the type I IFN response, including retinoic acid-inducible gene I, TANK-binding kinase 1, tumor necrosis factor receptor associated factor 6 (TRAF6) and TRAF1. Interestingly, residues important in catalysis (Cys51 or Asp163) or embedded in the SAP domain (Ile83 or Leu86) are required for DUB activity [43]. In summary, these results suggest that FMDV L has evolved multiple mechanisms to block the host response to viral infection.

Distinguishing Features

The Lb-peptidase may be blocked at its N-terminus, since microsequencing of this protein was only possible after acetylation was inhibited [44]. Rabbit polyclonal antisera have been prepared against the Lb-peptidase from types C1 and A12 expressed in *E. coli* [32,33].

References

[1] Knowles, N.J., Hovi, T., King, A.M., Stanway, G. (2010). Overview of taxonomy, in: *The Picornaviruses*, 1st edn, Ehrenfeld, E., Domingo, E., R.P. Roos, R.P., eds. Washington, DC: ASM Press, pp. 19–32.

[2] Martinez-Salas, E., Ryan, M.D. (2010). Translation and protein processing, in: *The Picornaviruses*, 1st edn, Ehrenfeld, E., Domingo, E., R.P. Roos, R.P., eds. Washington, DC: ASM Press, pp. 141–161.

[3] Gorbalenya, A.E., Koonin, E.V., Lai, M.M.-C. (1991). Putative papain-related thiol proteases of positive-strand RNA viruses: identification of rubi- and aphthovirus proteases and delineation of a novel conserved domain associated with proteases of rubi, α-and coronaviruses. *FEBS Lett.* 288, 201–205.

[4] Devaney, M.A., Vakharia, V.N., Lloyd, R.E., Ehrenfeld, E., Grubman, M.J. (1988). Leader protein of foot-and-mouth disease virus is required for cleavage of the p220 component of the cap-binding protein complex. *J. Virol.* 62, 4407–4409.

[5] Medina, M., Domingo, E., Brangwyn, J.K., Belsham, G.J. (1993). The two species of the foot-and-mouth disease virus leader protein expressed individually, exhibit the same activities. *Virology* 194, 355–359.

[6] Kirchweger, R., Ziegler, E., Lamphear, B.J., Waters, D., Liebig, H.-D., Sommergruber, W., Sobrino, F., Hohenadl, C., Blaas, D., Rhoads, R.E., Skern, T. (1994). Foot-and-mouth disease virus leader proteinase: purification of the Lb form and determination of its cleavage site on eIF-4γ. *J. Virol.* 68, 5677–5684.

[7] Hinton, T.M., Ross-Smith, N., Warner, S., Belsham, G.J., Crabb, B.S. (2002). Conservation of L and 3C proteinase activities across distantly related aphthoviruses. *J. Gen. Virol.* 83, 3111–3121.

[8] Rueckert, R.R., Wimmer, E. (1984). Systematic nomenclature of picornavirus proteins. *J. Virol.* 50, 957–959.

[9] van Rensburg, H., Haydon, D., Joubert, F., Bastos, A., Heath, L., Nel, L. (2002). Genetic heterogeneity in the foot-and-mouth disease virus leader and 3C proteinases. *Gene* 289, 19–29.

[10] Carrillo, C., Tulman, E.R., Delhon, G., Lu, Z., Carreno, A., Vagnozzi, A., Kutish, G.F., Rock, D.L. (2005). Comparative genomics of foot-and-mouth disease virus. *J. Virol.* 79, 6487–6504.

[11] Hollister, J.R., Vagnozzi, A., Knowles, N.J., Rieder, E. (2008). Molecular and phylogenetic analyses of bovine rhinovirus 2 shows it is closely related to foot-and-mouth disease virus. *Virology* 373, 411–425.

[12] Li, F., Browning, G.F., Studdert, M.J., Crabb, B.S. (1996). Equine rhinovirus 1 is more closely related to foot-and-mouth disease virus than to other picornaviruses. *Proc. Natl. Acad. Sci. USA* 93, 990–995.

[13] Wutz, G., Auer, H., Nowotny, N., Grosse, B., Skern, T., Kuechler, E. (1996). Equine rhinovirus serotypes 1 and 2: relationship to each other and to aphthoviruses and cardioviruses. *J. Gen. Virol.* 77, 1719–1730.

[14] Hinton, T.M., Li, F., Crabb, B.S. (2000). Internal ribosomal entry site-mediated translation initiation in equine rhinitis A virus: similarities to and differences from that of foot-and-mouth disease virus. *J. Virol.* 74, 11708–11716.

[15] Strebel, K., Beck, E. (1986). A second protease of foot-and-mouth disease virus. *J. Virol.* 58, 893–899.

[16] Kleina, L.G., Grubman, M.J. (1992). Antiviral effects of a thiol protease inhibitor on foot-and-mouth disease virus. *J. Virol.* 66, 7168–7175.

Author's personal copy

[17] Piccone, M.E., Zellner, M., Kumosinski, T.F., Mason, P.W., Grubman, M.J. (1995). Identification of the active-site residues of the L proteinase of foot-and-mouth disease virus. *J. Virol.* 69, 4950–4956.

[18] Roberts, P.J., Belsham, G.J. (1995). Identification of critical amino acids within the foot-and-mouth disease virus leader protein, a cysteine protease. *Virology* 213, 140–146.

[19] Wang, D., Fang, L., Li, P., Sun, L., Fan, J., Zhang, Q., Luo, R., Liu, X., Li, K., Chen, H., Chen, Z., Xiao, S. (2011). The leader proteinase of foot-and-mouth disease virus negatively regulates type I interferon pathway by acting as a viral deubiquitinase. *J. Virol.* 85(8), 3758–3766.

[20] Skern, T., Fita, I., Guarńe, A. (1998). A structural model of picornavirus leader proteinases based on papain and bleomycin hydrolase. *J. Gen. Virol.* 79, 301–307.

[21] Gradi, A., Imataka, H., Svitkin, Y.V., Rom, E., Raught, B., Morino, S., Sonenberg, N. (1998). A novel functional human eukaryotic translation initiation factor 4G. *Mol. Cell. Biol.* 18, 334–342.

[22] Gradi, A., Foeger, N., Strong, R., Svitkin, Y.V., Sonenberg, N., Skern, T., Belsham, G.J. (2004). Cleavage of eukaryotic translation initiation factor 4GII within foot-and-mouth disease virus-infected cells: identification of the L-protease cleavage site *in vitro*. *J. Virol.* 78, 3271–3278.

[23] Ziegler, E., Borman, A.M., Kirchweger, R., Skern, T., Kean, K.-M. (1995). Foot-and-mouth disease virus Lb proteinase can stimulate rhinovirus and enterovirus IRES-driven translation and cleave several proteins of cellular and viral origin. *J. Virol.* 69, 3465–3474.

[24] Guarné, A., Tormo, J., Kirchweger, R., Pfistermueller, D., Fita, I., Skern, T. (1998). Structure of the foot-and-mouth disease virus leader protease: a papain-like fold adapted for self-processing and eIF4G recognition. *EMBO J.* 17, 7469–7479.

[25] Glaser, W., Cencic, R., Skern, T. (2001). Foot-and-mouth disease leader proteinase: involvement of C-terminal residues in self-processing and cleavage of eIF4GI. *J. Biol. Chem.* 276, 35473–35481.

[26] Guarné, A., Hampoelz, B., Glaser, W., Carpena, X., Tormo, J., Fita, I., Skern, T. (2000). Structural and biochemical features distinguish the foot-and-mouth disease virus leader proteinase from other papain-like enzymes. *J. Mol. Biol.* 302, 1227–1240.

[27] Cencic, R., Mayer, C., Juliano, M.A., Juliano, L., Konrat, R., Kontaxis, G., Skern, T. (2007). Investigating the substrate specificity and oligomerisation of the leader protease of foot-and-mouth disease virus using NMR. *J. Mol. Biol.* 373, 1071–1087.

[28] Schlick, P., Kronovetr, J., Hampoelz, B., Skern, T. (2002). Modulation of the electrostatic charge at the active site of the foot-and-mouth disease virus leader proteinase, an unusual papain-like enzyme. *Biochem.* 363, 493–501.

[29] Santos, J.A., Gouvea, I.E., Júdice, W.A., Izidoro, M.A., Alves, F.M., Melo, R.L., Juliano, M.A., Skern, T., Juliano, L. (2009). Hydrolytic properties and substrate specificity of the foot-and-mouth disease leader protease. *Biochemistry* 48, 7948–7958.

[30] Mayer, C., Neubauer, D., Nehinda, A.T., Cencic, R., Trompf, K., Skern, T. (2008). Residue L143 of the foot-and-mouth disease virus leader proteinase is a determinant of cleavage specificity. *J. Virol.* 82, 4656–4659.

[31] Foeger, N., Kuehnel, E., Cencic, R., Skern, T. (2005). The binding of foot-and-mouth disease virus leader proteinase to eIF4G involves conserved ionic interactions. *FEBS J.* 272, 2602–2611.

[32] Strebel, K., Beck, E., Strohmaier, K., Schaller, H. (1986). Characterization of foot-and-mouth disease virus gene products with antisera against bacterially synthesized fusion proteins. *J. Virol.* 57, 983–991.

[33] Piccone, M.E., Sira, S., Zellner, M., Grubman, M.J. (1995). Expression in *Escherichia coli* and purification of biologically active L proteinase of foot-and-mouth disease virus. *Virus Res.* 35, 263–275.

[34] Piccone, M.E., Rieder, E., Mason, P.W., Grubman, M.J. (1995). The foot-and-mouth disease virus leader proteinase gene is not required for viral replication. *J. Virol.* 69, 5376–5382.

[35] Brown, C.C., Piccone, M.E., Mason, P.W., McKenna, T.S.-C., Grubman, M.J. (1996). Pathogenesis of wild-type and leaderless foot-and-mouth disease virus in cattle. *J. Virol.* 70, 5638–5641.

[36] Chinsangaram, J., Mason, P.W., Grubman, M.J. (1998). Protection of swine by live and inactivated vaccines prepared from a leader proteinase-deficient serotype A12 foot-and-mouth disease virus. *Vaccine* 16, 1516–1522.

[37] Chinsangaram, J., Piccone, M.E., Grubman, M.J. (1999). Ability of foot-and-mouth disease virus to form plaques in cell culture is associated with suppression of alpha/beta interferon. *J. Virol.* 73, 9891–9898.

[38] de los Santos, T., de Avila Botton, S., Weiblen, R., Grubman, M.J. (2006). The leader proteinase of foot-and-mouth disease virus inhibits the induction of beta interferon mRNA and blocks the host innate immune response. *J. Virol.* 80, 1906–1914.

[39] de los Santos, T., Diaz-San Segundo, F., Grubman, M.J. (2007). Degradation of nuclear factor kappa B during foot-and-mouth disease virus infection. *J. Virol.* 81, 12803–12815.

[40] de los Santos, T., Diaz-San Segundo, F., Zhu, J., Koster, M., Dias, C., Grubman, M.J. (2009). A conserved domain in the leader proteinase of foot-and-mouth disease virus is required for proper sub-cellular localization and function. *J. Virol.* 83, 1800–1810.

[41] Aravind, L., Koonin, E.V. (2000). SAP: a putative DNA-binding motif involved in chromosomal organization. *Trends Biochem. Sci.* 25, 112–114.

[42] Shuai, K. (2006). Regulation of cytokine signaling pathways by PIAS proteins. *Cell Res.* 16, 196–202.

[43] Wang, D., Fang, L., Luo, R., Ye, R., Fang, Y., Xie, L., Chen, H., Xiao, S. (2010). Foot-and-mouth disease virus leader proteinase inhibits dsRNA-induced type I interferon transcription by decreasing interferon regulatory factor 3/7 in protein levels. *Biochem. Biophys. Res. Commun.* 399, 72–78.

[44] Robertson, B.H., Grubman, M.J., Weddel, G.N., Moore, D.M., Welsh, J.D., Fischer, T., Dowbenko, D.J., Yansura, D.G., Small, B., Kleid, D.G. (1985). Nucleotide and amino acid sequence coding for polypeptides of foot-and-mouth disease virus type A12. *J. Virol.* 54, 651–660.

Marvin J. Grubman

USDA, ARS, NAA, Plum Island Animal Disease Center, PO Box 848, Greenport, NY 11944, USA. Email: marvin.grubman@ars.usda.gov

Teresa de los Santos

USDA, ARS, NAA, Plum Island Animal Disease Center, PO Box 848, Greenport, NY 11944, USA. Email: teresa.delossantos@ars.usda.gov

VIRAL IMMUNOLOGY
Volume 26, Number 4, 2013
© Mary Ann Liebert, Inc.
Pp. 1–11
DOI: 10.1089/vim.2013.0011

Characterization of Cytotoxic T Lymphocyte Function After Foot-and-Mouth Disease Virus Infection and Vaccination

Jared R. Patch, Mary Kenney, Juan M. Pacheco, Marvin J. Grubman, and William T. Golde

Abstract

The induction of neutralizing antibodies specific for foot-and-mouth disease virus (FMDV) has been the central goal of vaccination efforts against this economically important disease of cloven-hoofed animals. Although these efforts have yielded much success, challenges remain, including little cross-serotype protection and inadequate duration of immunity. Commonly, viral infections are characterized by induction of cytotoxic T lymphocytes (CTL), yet the function of CTL in FMDV immunity is poorly defined. We developed an assay for detection of CTL specific for FMDV and reported that a modified adenovirus-vectored FMDV vaccine could induce CTL activity. This allowed us to determine whether FMDV-specific CTL responses are induced during infection and to test further whether vaccine-induced CTL could protect against challenge with FMDV. We now show the induction of antigen-specific CTL responses after infection of swine with FMDV strain A24 Cruizero. In addition, we developed a vaccination strategy that induces FMDV-specific CTL in the absence of significant neutralizing antibody. Animals vaccinated using this protocol showed delayed clinical disease and significantly suppressed viremia compared to control animals, suggesting a role for CTLs in the control of virus shedding. These results provide new insights showing induction of CTL responses to FMDV following infection or vaccination, and create the potential for improving vaccine performance by targeting cellular immunity.

Introduction

Foot-and-mouth disease virus (FMDV) causes a viral disease of cloven-hoofed animals that remains a threat to livestock throughout the world. The disease is characterized by fever, lameness, lethargy, vesicles on the feet and in the mouth, and loss of meat and milk productivity (reviewed in (18)). This highly acute infection induces clinical signs for only a few days and these resolve by 7 to 10 days following exposure. Clinical disease in swine is associated with immunopathology that includes lymphopenia (3), blocking dendritic cell (DC) production of type I interferons (IFN) (35,36), and loss of natural killer (NK) cell function (54) (reviewed in (17)).

FMDV is a picornavirus with the genome consisting of single-stranded positive-sense RNA. This is translated as a single polyprotein that is subsequently cleaved into mature proteins by virus encoded proteases, especially 3C ($3C^{pro}$) (2,10,26,56). The leader protease (L^{pro}) (13) blocks host protein synthesis by cleaving initiation factor 4G (eIF4G) eliminating cap-dependent mRNA translation, and the combined actions of viral proteins 2B and 2C serve to disrupt vesicular transport (30,31). Virus RNA translation then co-opts the ribosomes as the 5′ UTR of the virus contains an internal ribosome entry site (IRES) which does not require intact eIF4G (4, 27).

Although many countries are largely free of FMD, the persistence of disease in parts of the world, and its highly infectious nature, require vigilance on the part of FMD-free countries. Agricultural concerns are focused primarily on cattle, swine, sheep, and goats. However, many wild ruminant and cloven-hoofed species are also susceptible to infection, though severity of clinical disease can vary from severe to inapparent (34). Routine control of FMD is maintained primarily through trade practices that limit the exportation of animal products from countries reporting FMD (18). Acute outbreaks have been controlled through vaccination or mass culling of susceptible animals (24,49,52,57). The adverse economic consequences of FMD outbreaks highlight the need for preventive measures, including effective vaccines.

Current vaccines consist of killed virus in adjuvant and are effective at generating protective neutralizing antibodies (14,45). However, the inability to differentiate infected from vaccinated animals (DIVA) makes deploying vaccines problematic for maintaining trade status. In addition, vaccine production requires the growth of large amounts of virus requiring expensive, high containment facilities for manufacture, thus

Plum Island Animal Disease Center, Agricultural Research Service, USDA, Greenport, New York.

providing an incentive for the exploration of alternative FMDV vaccines. A leading candidate DIVA vaccine for FMDV is vectored by a replication-defective human adenovirus 5 (Ad5). This construct delivers the coding regions for the P1 capsid precursor and $3C^{pro}$ to cells. Once expressed, $3C^{pro}$ cleaves the P1 polyprotein into the mature capsid proteins, which then form "empty capsids" (19). This approach to vaccination has been shown to protect both pigs and cattle (28,29,33,37,42). However, like the traditional killed virus vaccine, serotype and strain matching are required because the elicited neutralizing antibodies are type specific and cross-react poorly with other serotypes, and subtypes within serotypes (45).

Cytotoxic T lymphocytes (CTLs) are a CD8-expressing subset of T cells that can directly kill virus-infected cells in an antigen-specific manner. In contrast to antibodies, which recognize complex antigens, CTLs recognize processed antigens that are cleaved by the proteasome into short peptides of 8 to 12 amino acids, loaded into major histocompatibility complex (MHC) class I molecules in the lumen of the endoplasmic reticulum (ER), and then transported to the cell surface (43,58). The ability of CTLs to recognize peptides derived from all regions of the viral proteome makes their induction one potential way to bridge the gap of cross-serotype protection. Variation between serotypes of FMDV is located within the structural proteins forming the capsid (7), which is likely a consequence of immune selective pressure exerted by neutralizing antibodies specific for the capsid (23).

In contrast, the nonstructural proteins are very highly conserved (7), which increases the likelihood of different serotypes containing identical peptides that can be recognized by CTLs. However, *in vitro*, FMDV infection inhibits synthesis of new class I MHC proteins (47), which would block induction of CTLs if the same process occurs within virus infected cells *in vivo*. Further, the relatively rapid resolution of disease likely contributes to a dampened CTL response due to insufficient duration of antigen exposure. Despite their prominent role as part of the adaptive immune system and considering the lack of MHC expression predicted for infected cells, analysis of CTL responses to FMDV infection or vaccination has seldom been reported. This lack of data has led to the opinion that CTL do not play a role in the response to FMD (14).

CTLs are one component of cellular immunity, which refers to the more general response of multiple T cell subsets and the multiple functions those T cells exert during immune responses. Analysis of the response in cattle following vaccination with the commercial, killed virus vaccine has demonstrated CD8 T cells producing interferon gamma (IFNγ) (22). The peptide specificity of the response to vaccination has also been reported, analyzing proliferation and IFNγ secretion by CD4 T cells (16) or IFNγ secretion by CD8 T cells (16, 21). We have also reported IFNγ production by both CD4 and CD8 T lymphocytes following vaccination of cattle with the Ad5-FMDV vaccine (32). These results illustrate that there are multiple cell populations capable of producing IFNγ, especially within the CD8 T lymphocyte populations studied. Thus, these previous studies highlight the need to analyze CTL killing of virus-infected target cells and not assume that detected production of IFNγ is from virus-specific CTLs.

In part, the limited knowledge of CTL responses to FMDV is due to the technical difficulties of establishing reliable assays for CTL responses for this virus. FMDV is a highly cytopathic virus and therefore the experimental target cells for a CTL response cannot be infected with live virus (9,22). Further, the assay requires MHC class I matching of the responding animals and the target cells and intact expression of those MHC proteins. We previously reported the establishment of a CTL killing assay that utilizes the Ad5 expression system for the production of FMDV proteins that induces little cytopathic effect. Using this assay, we showed that vaccination of swine with an Ad5 construct lacking efficient processing of the P1 polyprotein resulted in the induction of anti-FMDV CTLs and that multiple vaccinations were needed in order to generate significant neutralizing antibody titers. The presence of $CD8^+$ MHC-restricted CTLs was confirmed by swine leukocyte antigen (SLA)-1 tetramer staining. The companion parental vaccine construct, that processes the polypeptide into components that assemble into capsids, failed to induce a CTL response and required a single vaccination to induce a significant B cell response exhibited by neutralizing antibody titers (33,41). We refer to these vaccine constructs as Ad5-FMDV-T and Ad5-FMDV-B, respectively, for convenience and to signify the arm of the adaptive immune system preferentially stimulated.

These results provided an experimental system with which to test the contribution of CTL immunity to protection against infection with FMDV following challenge with live, virulent virus. This design was solely to address the experimental question of whether each can contribute to overall immunity to virus. Clearly, this is not an optimal vaccine design as maximizing both responses is the goal for an effective vaccine.

We now report the induction of CTL responses in naïve, infected pigs, the first demonstration of antigen-specific class I MHC-mediated killing of virus-infected target cells by $CD8^+$ CTLs from FMDV-infected livestock. Further, we tested the efficacy of the CTL-inducing vaccine to protect swine against live virus challenge in the absence of significant neutralizing antibodies. Swine that received the T cell vaccine mounted a CTL response and developed delayed clinical disease with reduced/no viremia. Although insufficient to protect against challenge with FMDV under these designed experimental conditions, induction of CTL immunity under more optimal conditions, specifically while also inducing the well characterized humoral response to the virus, is likely to improve the performance of the Ad5-FMDV vaccination approach.

Materials and Methods

Cell lines

Porcine kidney [PK(15)] cells (ATCC CCL-33) and PK(15)-EGFP cells (41) were maintained in minimal essential medium (MEM) (Invitrogen, Carlsbad, CA), and baby hamster kidney (BHK-21) cells (ATCC CCL-10) were maintained in basal medium Eagle (BME) (Invitrogen). All media contained 10% fetal bovine serum (FBS) (Thermo Fisher Scientific, Waltham, MA) along with other supplements, as described previously (41).

Viruses

Viruses Ad5-A24-3C-mut (Ad5-FMDV-T), Ad5-A24 (Ad5-FMDV-B), and Ad5-VSV-G (Ad5 expressing the glycoprotein

of vesicular stomatitis virus) have been described previously (33,41). Ad5-FMDV-T and Ad5-FMDV-B differ in that the 3C protease of the former is a mutant that is inefficient at P1 processing. For *in vitro* assays, FMDV, strain A24 Cruzeiro, was propagated in BHK-21 cells. A swine-derived isolate of the same strain was used for animal inoculation, prepared as previously described (40).

Animals

All animal experiments were performed in a secure biosafety level three laboratory on Plum Island Animal Disease Center (PIADC) following the protocol approved by the Institutional Animal Care and Use Committee following the guidelines of the United State Public Health Service, Department of Health and Human Services and the Animal Plant Health Inspection Service (APHIS) of the US Department of Agriculture (USDA). Sixteen National Institute of Health miniature (NIH mini) pigs, homozygous for MHC haplotype 4a.0/4a.0 (*0401 for all class I genes), also published as $NIH^{d/d}$ (51), were generously provided by Scott Arn and David Sachs (Transplantation Biology Research Center, Massachusetts General Hospital, Boston, MA). Animals ranged in age between 10 and 14 months, and weighed approximately 100 lbs.

Vaccination and challenge

Twelve NIH mini pigs were divided into three groups and vaccinated with either Ad5-FMDV-T (seven pigs), Ad5-FMDV-B (two pigs), or Ad5-VSV-G (three pigs). Animals were separated by gender with the Ad5-FMDV-T vaccinated animals (all male) kept in a separate room. The naïve animals (Ad5-VSV-G) were female, and the two animals vaccinated with Ad5-FMDV-B were a male and a female. The vaccine was delivered intradermally using the Derma-Vac® needle-free system (Merial Animal Health, Duluth, GA) at four sites on the neck for a total dose of 5×10^9 plaque forming units (pfu)/pig. All animals were boosted on the same day with 5×10^9 pfu of their respective immunogen 10 weeks (FMDV-B and VSV-G) or 12 weeks (FMDV-T) postvaccination. Eight days following the boost, all animals were challenged with 10^5 $TCID_{50}$ of FMDV, strain A24 Cruzeiro, by intradermal needle inoculation in the heel bulb (39).

PBMC preparation

Vacutainer® tubes containing heparin were used to collect porcine blood. After dilution with PBS, the blood was underlain with Lymphoprep (Axis-Shield, Oslo, Norway), and then centrifuged at 1400 *g* for 20 min at room temperature. The resulting band of peripheral blood mononuclear cells (PBMCs) was harvested, washed with PBS three times, and then suspended Roswell Park Memorial Institute (RPMI)-1640 medium (Invitrogen, Carlsbad, CA).

Cytotoxic T lymphocyte killing assay

CTLs were sorted, and killing activity was measured as described previously (41). Briefly, PBMCs were cultured in the presence of PK(15) cells infected with Ad5-FMDV-T for 3 days, after which cells were purified on Lymphoprep and positively sorted for CD6 expression in order to reduce MHC unrestricted killing (12). $CD6^+$ cells were sorted by incubating with anti-CD6 antibody (clone MIL8, AbD Serotec, Raleigh, NC) and then goat anti-mouse microbeads, followed by passage through LS columns using a MidiMACS magnetic separator (Miltenyi Biotec, Gladbach, Germany).

Following CD6 purification, effector cells were incubated for 4 h with PK(15)-EGFP target cells that were infected with Ad5-FMDV-T, Ad5-VSV-G, or mock-infected at E:T ratios of 50:1, 25:1, and 12:1 in the presence of 7-amino-actinomycin D (7-AAD) (BD Biosciences, San Jose, CA). The percent cell killing was determined by flow cytometry using a FACS-Calibur flow cytometer with a high-throughput sampler (HTS) (BD Biosciences, San Jose, CA) by gating on the $EGFP^+$ cell population and determining the percent $7\text{-}AAD^+$ cells. Background lysis of target cells alone was subtracted from all samples. In order to eliminate noise of day-to-day variability in the CTL killing assays, the greatest mean lysis of control target cells (mock infected or Ad5-VSV-G infected) was subtracted from mean lysis of the antigen-specific target cells at each time point (see Fig. 2A–C). Unadjusted data are shown in Supplementary Figure S1 (supplementary data are available online at www.liebertpub.com/vim).

Serum neutralization assay

Four-fold dilutions of heat inactivated serum were incubated with 100 $TCID_{50}$ FMDV A24 for 1 h at 37°C, and then incubated for 3 days with BHK-21 cells, which were scored for cytopathic effect. Endpoint serum neutralization titers (SNT) were calculated as previously described (38) and comparison of induction of neutralizing and total anti-FMDV antibody titers has been reported (29).

Serum virus titration

Frozen serum samples were thawed and used to make a series of 10-fold dilutions. Each dilution was added to a microtiter plate in quadruplicate, after which 10^4 BHK-21 cells were added to each well. Following 3 days of incubation at 37°C, wells were scored for presence of CPE and the $TCID_{50}$ was calculated.

FMDV RNA detection

RNA was extracted from 50 μL of serum as previously described (1), and then detected by real-time RT-PCR according to the method of Callahan and co-workers (6). Cycle thresholds <45 were considered positive and converted to RNA copies/mL by comparison to a standard curve generated by real-time RT-PCR of known concentrations of *in vitro* synthesized FMDV RNA, as described (1).

Clinical evaluation

Scoring of clinical disease was based on appearance of vesicles, as previously described (39). A maximum score of 20 was possible based on the presence of vesicles on each digit, the snout, tongue, lower lip, or carpal/tarsal area of at least one leg. Clinical scores were cumulative through the period of evaluation.

Statistics

Statistical significance of CTL killing activity based on comparison between target cell groups was determined using a one-tailed, paired Student's *t* test. Statistical significant

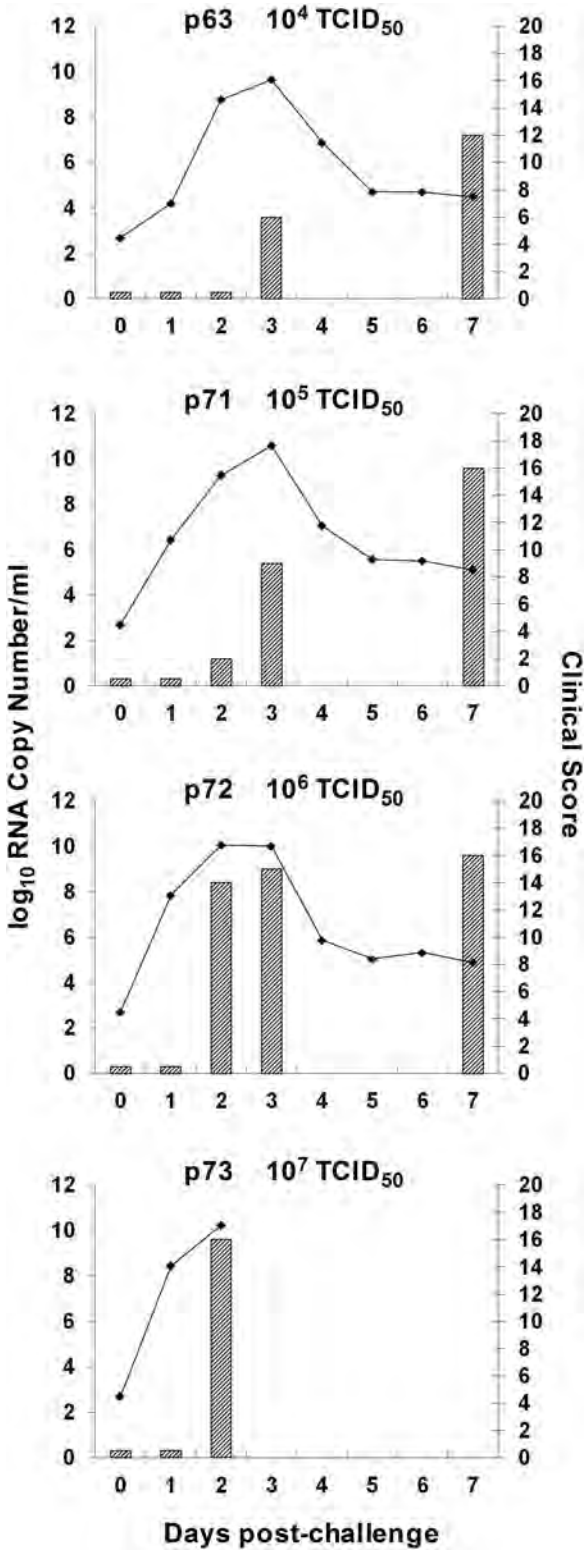

FIG. 1. Clinical evaluation of pigs used to determine challenge dose. Individual pigs were challenged with the indicated dose of FMDV and evaluated for clinical signs on days 1, 2, 3, and 7 (*bars*), as described in Materials and Methods. Although no clinical evaluation occurred on days 4 through 6, scoring is cumulative over the course of disease, which implies a score no lower than that of day 3. Sera were collected daily and viremia was measured using real-time RT-PCR (*lines*). Severe disease necessitated euthanasia of pig 73.

elevation of antigen-specific CTL killing compared to baseline was determined using repeat-measures one-way ANOVA with Dunnett's post test. CTL killing was considered statistically significant only if both comparisons gave p values of 0.05 or less. Statistically significant differences in serum antibody and viremia were determined using one-tailed unpaired Student's t test.

Results

Titration of challenge virus in genetically defined swine

Analysis of CTL function requires an assay to measure lysis of virus-infected target cells in an antigen-specific, MHC-restricted fashion. This requires MHC class I matching between the effector T cells and target cells. We had

availability of National Institutes of Health (NIH) miniature pigs (NIH mini pigs) homozygous for MHC for such studies. However, infection of this strain of pigs with FMDV, particularly animals that are 1 year old and weighing 100 lbs, had not been demonstrated. Therefore, we conducted a preliminary trial to determine an appropriate challenge dose of FMDV by inoculating four pigs with 10-fold dilutions of virus ranging from 10^4 to 10^7 $TCID_{50}$, and then evaluating them for clinical signs on days 1, 2, 3, and 7 following infection. Viremia was confirmed by real-time RT-PCR. All pigs developed clinical disease and detectable viremia (Fig. 1). Severity of clinical disease increased with challenge dose such that the pig that received the highest dose, 10^7 $TCID_{50}$, required euthanasia 2 days post challenge. The pigs with the two lowest doses had comparable clinical signs and viremia. Based on these data, we chose a challenge dose of 10^5 $TCID_{50}$, assuring inoculation would result in clinical disease in the naïve animals.

Humoral and cellular immune response following vaccination with Ad5 FMDV vectored vaccines

In order to test the ability of FMDV-specific CTLs to protect against disease, seven pigs were vaccinated with Ad5-FMDV-T, which expresses unprocessed P1 polyprotein. An additional two pigs were vaccinated with the standard empty capsid vaccine, Ad5-FMDV-B, the original vaccine vector containing the wild-type 3C protease. This virus-vectored vaccine has been shown to protect against homologous virus strain challenge of pigs with virulent FMDV as early as 7 days and for as long as 42 days (11,33). An irrelevant Ad5 vectored vaccine, Ad5-VSV-G (expressing the glycoprotein of vesicular stomatitis virus, VSV-G) was used to vaccinate three pigs and these animals served as FMDV naïve controls. Prior to vaccination and at several time points following vaccination, peripheral blood mononuclear cells (PBMCs) from all pigs were isolated and tested for FMDV-specific CTL killing activity as described in Materials and Methods. For pigs vaccinated with Ad5-FMDV-T, we observed an increase in CTL activity ($p<0.01$) 21 days after vaccination that returned to background levels by day 31 (Fig. 2A). There was minimal, statistically insignificant specific CTL activity detected using cells isolated from either the Ad5-FMDV-B or Ad5-VSV-G control vaccinated pigs (Fig. 2B and C). The lack of a VSV-G specific CTL response in the Ad5-VSV-G vaccinated animals (Supplementary Fig. S1C; supplementary data available on website www.liebertpub.com/vim) may indicate that the replication defective, Ad5 vector is not the optimal way to vaccinate for CD8 T cell responses to VSV-G. CTL reactivity with the adenovirus vector itself was not expected nor detected as these are replication defective adenoviruses providing no source of

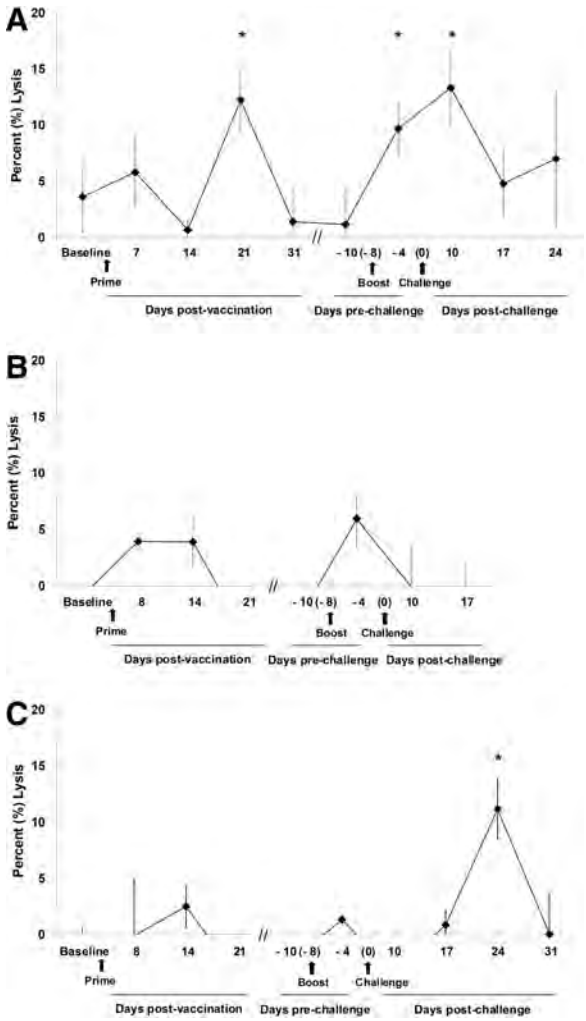

FIG. 2. CTL killing activity induced by vaccination and challenge. PBMCs were collected from pigs at various time points relative to vaccination with **(A)** Ad5-FMDV-T ($n=7$), **(B)** Ad5-FMDV-B ($n=2$), or **(C)** Ad5-VSV-G ($n=3$), and subsequent challenge. CTL killing of target cells infected with Ad5-FMDV-T, Ad5-VSV-G, or mock infected, was determined by flow cytometry as described in Materials and Methods. Results represent percent lysis of Ad5-FMDV-T-infected target cells relative to the control target cells exhibiting the greatest lysis (mock infected or Ad5-VSV-G infected), as described in Materials and Methods. Means. Standard deviations of 50:1 E:T ratio are shown, with statistical significance indicated by *asterisks*.

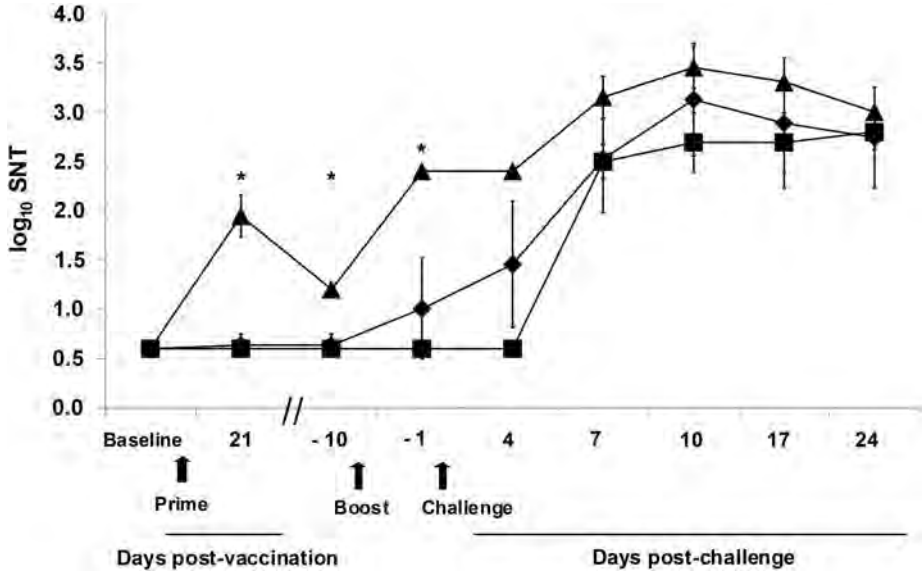

FIG. 3. Serum neutralizing antibody titers. Sera were collected at indicated times relative to prime, boost, and challenge. Dilutions of sera were tested for neutralization of 100 $TCID_{50}$ FMDV A24, as described in Materials and Methods. Geometric -mean neutralization titer is shown for vaccination groups (▲, Ad5-FMDV-B ($n=2$); ◆, Ad5-FMDV-T ($n=7$); ■, Ad5-VSV-G ($n=3$)) with standard deviation. *Asterisks* indicate statistically significant difference ($p<0.01$) between Ad5-FMDV-B and Ad5-FMDV-T groups.

newly synthesized virus proteins and subsequent peptides for binding by class I MHC proteins.

The presence of neutralizing antibodies was detected 21 days post-vaccination in sera from pigs vaccinated with Ad5-FMDV-B, but not in either the Ad5-FMDV-T or Ad5-VSV-G vaccine groups (Fig. 3). This initial dichotomy between induction of CTLs and neutralizing antibodies is consistent with our previous observations and allowed for analysis of the relative role of humoral and cellular immunity in protection against disease.

All animals were simultaneously boosted, 10 weeks following vaccination for the FMDV-B and VSV-G groups and 12 weeks following vaccination for the FMDV-T animals. PBMC from all animals were analyzed for CTL responses before challenging all animals with virulent FMDV, strain A24. We observed elevated CTL killing activity by cells derived from pigs vaccinated with Ad-FMDV-T ($p<0.01$), compared to 2 days before the boost (Fig. 2A). We also observed a small rise in CTL activity by cells derived from pigs vaccinated with Ad5-FMDV-B (Fig. 2B), although it did not

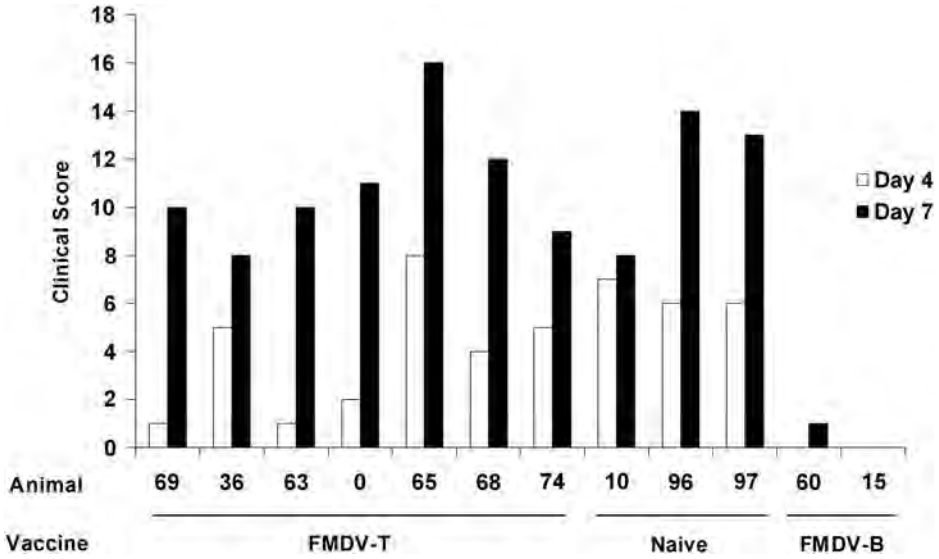

FIG. 4. Clinical scores of individual animals challenged with FMDV. All animals were scored for presence of vesicles on days 4 and 7 postchallenge, as described in Materials and Methods. Scoring is cumulative over the course of disease, which implies a score no lower than that of day 4 on subsequent days.

reach statistical significance. Evaluation of serum samples taken 7 days following the boost (1 day before challenge) showed an increased neutralizing antibody titer in Ad5-FMDV-B-vaccinated pigs compared to levels prior to the vaccine boost (Fig. 3). Although neutralizing antibodies were detected in some of the pigs vaccinated with Ad5-FMDV-T, the titers were uniformly lower than Ad5-FMDV-B-vaccinated pigs (Fig. 3 and Supplementary Fig. S2A and B). The highest individual titer in this vaccine group was 1.8 $\log_{10}$ and three pigs from this group had no detectable serum neutralizing antibodies (Supplementary Fig. S2A). Control pigs vaccinated with Ad5-VSV-G showed no evidence of FMDV-specific CTL activity (Fig. 2C) or serum neutralizing antibodies (Fig. 3 and Supplementary Fig. S2B), as expected.

Clinical disease following challenge of vaccinated animals with FMDV

All animals in the study were challenged with 10^5 $TCID_{50}$ of FMDV strain A24 Cruzero, and animals were evaluated for clinical disease on days 4 and 7. One of the animals vaccinated with Ad5-FMDV-B remained completely clear of vesicles, while the second developed a single vesicle on one digit by day 7 (Fig. 4). Animals vaccinated with Ad5-FMDV-T exhibited clinical signs of disease. However, with the exception of one animal, the clinical scores at day 4 were lower than the naïve controls, suggesting a delay in disease progression. By day 7 after challenge, clinical scores of the group vaccinated with Ad5-FMDV-T were very similar to the naïve controls (Fig. 4).

Detection of viremia by virus isolation was greatly reduced in pigs vaccinated with Ad5-FMDV-T by a mean difference of almost 3 logs compared to the naïve controls (day 3 following challenge, Fig. 5A). The highest viremia detected in the Ad5-FMDV-T-vaccinated pigs was in animal 65, which had peak viremia on day 5 of $\log_{10}$ 3.75, 1 log lower and 2 days delayed from the peak for all naïve animals (Supplementary Fig. S3A and B). The balance of the Ad5-FMDV-T-vaccinated pigs had either no detectable viremia

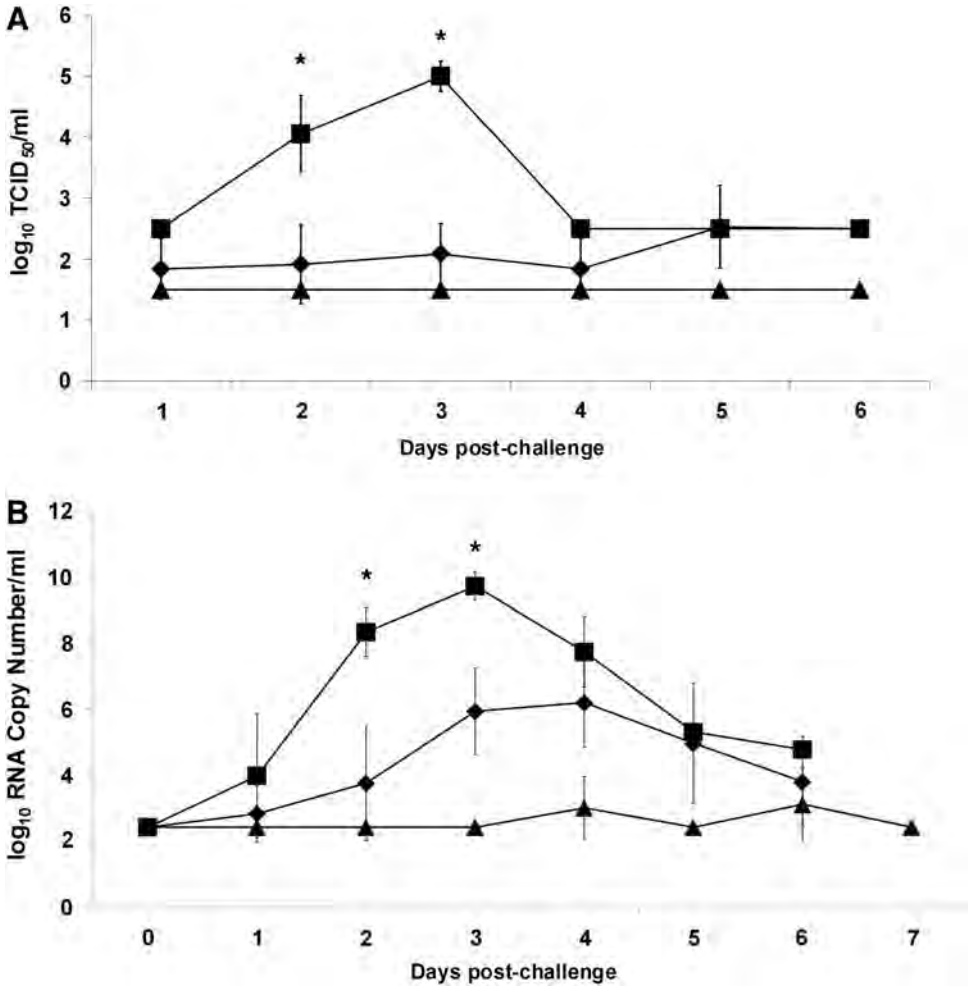

FIG. 5. Quantification of viremia. Daily sera were collected from animals following challenge. **(A)** Serum was diluted and plated in the presence of BHK-21 cells. Following 3 days of incubation, wells were scored for presence of CPE and the $TCID_{50}$/mL was determined. **(B)** FMDV RNA in serum was quantified by real-time RT-PCR. Plotted data represent geometric means for vaccination groups (▲, Ad5-FMDV-B ($n=2$); ◆, Ad5-FMDV-T ($n=7$); ■, Ad5-VSV-G ($n=3$)) with standard deviation. *Asterisks* indicate statistically significant difference ($p<0.01$) between Ad5-VSV-G and Ad5-FMDV-T groups.

following infection ($\log_{10}$ 1.5 being the lower limit of the assay) or viremia that was 2 to 3 logs lower than controls. No viremia was detected in pigs given the standard vaccine, Ad5-FMDV-B (Fig. 5A).

Real-time RT-PCR detection of FMDV RNA present in serum yielded similar results (Fig. 5B). Again, pig number 65 showed FMDV RNA levels intermediate between the rest of the vaccine cohort and the naïve controls. In this assay, pig 68 also showed higher presence of FMDV RNA than the rest of the cohort but still an order of magnitude less than the naïve controls (Supplementary Fig. S4A and B). All other animals vaccinated with the FMDV-T construct had lower FMDV titers using the PCR assay. The average peak titer of this cohort of animals was log 6.19 on day 4 compared to an average titer of log 9.72 on day 3 for naïve, Ad5 VSV-G vaccinated animals. As in the virus isolation assay, the PCR assay showed reduced FMDV titers peaking in a delayed manner (Fig. 5). This assay detects presence of RNA viral genome resulting in signal combining presence of live virus genome and residual RNA from killed virus, yet relative results between these three treatment groups are the same as that of virus isolation.

CTL responses following challenge of vaccinated animals with FMDV

PBMCs were isolated and tested for CTL killing activity beginning 10 days after challenge. Cells from pigs vaccinated with Ad5-FMDV-T displayed an increase in CTL activity 10 days post challenge relative to preboost ($p < 0.01$) that returned to background levels by 17 days post challenge (Fig. 2A). We attempted to evaluate CTL activity on day 4 but failed to obtain enough cells for the assay. We attribute this to the lymphopenia and immunopathology induced by FMDV (3).

Although we had observed a slight elevation in CTL activity in PBMCs derived from pigs vaccinated with Ad5-FMDV-B during the vaccination phase of the experiment, no CTL activity was observed following challenge with FMDV (Fig. 2B). However, serum neutralizing titers of these pigs continued to rise following challenge (Fig. 3A), suggesting a low level of virus replication *in vivo*. This was also observed in the Ad5-FMDV-T vaccinated animals following challenge, although pig 68 continued to lack detectable neutralizing antibodies as late as 4 days following challenge.

The pigs given the irrelevant vaccine, Ad5-VSV-G, served as FMDV naïve controls. These animals showed a statistically significant anti-FMDV CTL response at 24 days post-challenge ($p < 0.05$). CTL killing of Ad5-FMDV infected target cells was no longer detectable 31 days following challenge (Fig. 2C). This followed similar kinetics to that observed for vaccination of animals with Ad5-FMDV-T, where significant killing was observed 21 days after vaccination and no longer detectable by 31 days (Fig. 2A). This represents the first report of porcine CTL killing activity following infection with FMDV.

Discussion

Historically, analysis of immune responses to FMDV vaccination and/or infection has focused on measurement of serum antibody, yielding an informative and widely reported assessment of humoral immunity to the virus. Defining the role of cellular immune responses to FMDV in controlling this acute viral disease has been difficult as this highly cytopathic virus does not allow for classical analysis of the killing of virus infected target cells using *in vitro* assays. Previous reports have analyzed surrogate responses for CTL killing such as proliferation or production of IFNγ by CD8 expressing cells (9,21,22,25,44,46). These data have been informative, but far from definitive, as many CD8-expressing lymphocytes that are not CTLs produce IFNγ, including NK cells and subsets of $\gamma\delta$ T cells (5,53,55). Further, none of these reports sufficiently define the cell populations being assayed as CTLs such as detecting activation of perforin/granzyme expression and secretion of these proteins by αß T cell receptor expressing (TCR^+), CD8 T lymphocytes.

We previously tested the hypothesis that inhibiting proteolytic processing of FMDV capsid proteins would enhance induction of CTLs, presumably by increasing the pool of antigenic peptides available for class I MHC presentation and stimulation of cognate CTLs (41). In those studies, we developed methodology to analyze antigen-specific, virus-infected cell killing and confirmed our results by showing MHC tetramer staining of the CD8 T cells correlates to target cell killing. The response we measured was generated in the artificial setting created by infecting the MHC matched target cells with the same replication-defective Ad5 virus, Ad5-FMDV-T, as was used for the vaccination. In the present study, we now show FMDV specific CTLs are induced following infection with live, virulent FMDV. Thus, we confirm that the CTL killing assay used in all of these studies can detect cellular immune responses to FMDV following infection, not solely in the case of immunization with the same Ad5 vector that is used in the CTL assay.

FMDV infection of cells *in vitro* was reported to mediate inhibition of MHC class I cell surface expression (47). Data presented here now indicate such inhibition *in vivo* is partial at best, as MHC class I expression by virus-infected cells is required to induce the CTL response we detected. This novel observation confirms that a primary CTL response is a characteristic of swine immunity to FMDV infection. Further, the kinetics of this response are comparable to the primary response of animals vaccinated with Ad5-FMDV-T, where CTL activity was detected 21 days following vaccination. This naturally induced CTL response is likely not robust, an inference that is supported by the rapid loss of CTL killing that we observed under experimental conditions more favorable for CTL induction.

We were able to design an experimental strategy that resulted in anti-FMDV antibody mediated immunity in the absence of CTL induction and alternatively, anti-FMDV CTL immunity in the absence of a significant neutralizing antibody response. This allowed testing of whether these respective immune responses would protect swine against FMD. During the challenge phase of this study, space limitations required that the cohort of pigs vaccinated with the standard Ad5 vectored vaccine (Ad5-FMDV-B), one male and one female, be housed in the same room as the naïve animals, which were all female. The pigs were allowed to comingle, except for the male, who was sequestered by gating in a separate pen. Analysis of the CTL response of the two Ad5-FMDV-B vaccinated animals showed no statistically significant induction of anti-FMDV CTL, as we reported previously (41).

Following primary vaccination with Ad5-FMDV-B, the neutralizing titers were approaching the titer of antibody response that is predictive of protection, 2.0 $\log_{10}$, and were both over 2.0 $\log_{10}$ after the secondary application of this vaccine. The development of neutralizing antibodies to this vaccine following priming has been repeatedly observed and reported (28,29,33,42). Following challenge, the sequestered male animal showed no signs of disease throughout the experiment. The female pig that received the Ad5-FMDV-B vaccine developed a vesicle on one toe. We attribute this result to overwhelming secondary challenge from the naïve animals in the same pen because pigs are prolific shedders of virus (15,50).

Although little or no CTL killing activity was detected in animals following priming with the standard or irrelevant vaccines, a significant CTL response was detected 21 days following primary immunization in animals given the CTL targeting vaccine, Ad5-FMDV-T,. This response rapidly returned to background by day 31. This result is consistent with the general response window of 2 to 4 weeks for porcine T cells (8). A similar result has been observed in cattle, with CD8 T cells detected by ELISPOT measuring IFNγ at 14 days following vaccination and returning to undetectable levels by day 21 (21). After secondary vaccination of these animals with Ad5-FMDV-T, the recall CTL response was detected within 4 days, which is suggestive of a memory response. Anti-FMDV neutralizing antibody was detected after this vaccine boost in 4 of the 7 animals in this group. This is consistent with our previous observation (41), and is presumably a result of residual $3C^{pro}$ activity of the mutated $3C^{pro}$ gene product in this construct (20). Nevertheless, the Ad5-FMDV-T-vaccinated pigs were not protected from disease.

Although neutralizing antibodies may have played a role in clinical outcome in some cases, three of the seven pigs did not have measurable neutralizing antibodies prior to challenge and one of those (pig 68) remained negative for neutralizing antibodies until at least day 4 postchallenge. Although this pig had the highest level of serum viral RNA of animals in the cohort, it was still reduced compared to the naïve controls, and there was a marked reduction in viremia as measured by virus isolation. Thus, although the presence of low levels of neutralizing antibodies in this vaccine cohort precludes a definitive interpretation, these data suggest that CTLs played a role in controlling disease in these vaccinated animals. The duration of CTL activity was limited and waned by 17 days following challenge. This is comparable to previous results obtained following a third inoculation of Ad5-FMDV-T (41).

These results may be interpreted as evidence that CTL immunity is of limited value in protecting swine from FMDV infection. However, an important caveat should be considered. Because the Ad5 expression system is nonreplicating, the expression of P1 antigen and 3C protease is relatively limited in duration and this may not provide sufficient stimulation to generate CTL activity robust enough to withstand viral challenge under these conditions. Thus, this may be a limitation in the delivery of peptide antigens that stimulate CTL responses, not the ability of CTL-mediated immunity to protect against infection. Further, the present Ad5 construct only immunizes with structural proteins. CTLs specific for nonstructural proteins are likely to be induced following infection, and vaccination with constructs expressing the additional nonstructural proteins may provide more effective protection. Though these possibilities remain to be investigated, data presented here show that even under these suboptimal conditions, disease was reduced and delayed and viral spread *in vivo* controlled. These factors strongly indicate that the results reported here do not represent the maximum possible contribution of CTLs to controlling virus propagation and disease during an infection, and optimizing vaccination for induction of CTL could be a highly effective vaccine formulation.

In previous studies, Sanz-Parra and co-workers immunized swine with the FMDV P1 capsid precursor using an Ad5 vector and observed partial protection based on clinical evaluation, and similar results were obtained in cattle (46,48). However, the presence of a cell-mediated response was inferred by lack of neutralizing antibodies and by *in vitro* lymphocyte proliferation in response to stimulation with virus. The results described here support and extend those findings by demonstrating the presence of killing activity of CTLs at the time of challenge corresponds to reduction of viremia and delay of disease progression compared to control animals lacking FMDV-specific CTL responses.

A vaccine that induces both neutralizing antibodies and a robust CTL response may be predicted to approach sterile immunity, the ultimate goal for vaccine performance. Minimally, a strong CTL response could reduce the effective antibody titer required to protect against clinical disease. Combined humoral and CTL immunity may therefore be able to slow outbreaks of FMDV, with CTLs especially important when the infecting viruses are poorly matched serologically to the vaccine strains available. Thus, if CTLs can be induced without compromising the efficacy of neutralizing antibody responses in new vaccine vectors, targeting CTL immunity may play an important role in FMDV vaccine strategies.

Acknowledgments

The authors would like to thank Ms. Raisa Glabman, Ms. Mital Pandya, and Mr. Ethan Hartwig for their support and assistance with these studies. We thank Scott Arn and Dr. David Sachs of the Transplantation Biology Research Center, Massachusetts General Hospital, Boston, MA, for providing the NIH mini pigs used in these studies. We would also like to thank the staff of the Animal Resources Unit (Plum Island Animal Disease Center, Department of Homeland Security) for their professional work with the animals used in these experiments. This work was funded by CRIS #1940-32000-057-00D from the Agricultural Research Service, USDA (MJG and WTG).

Author Disclosure Statement

No competing financial interests exist.

References

1. Arzt J, Pacheco JM, and Rodriguez LL. The early pathogenesis of foot-and-mouth disease in cattle after aerosol inoculation: Identification of the nasopharynx as the primary site of infection. Vet Pathol 2010;47:1048–1063.
2. Bablanian GM, and Grubman MJ. Characterization of the foot-and-mouth disease virus 3C protease expressed in Escherichia coli. Virology 1993;197:320–327.

3. Bautista EM, Ferman GS, and Golde WT. Induction of lymphopenia and inhibition of T cell function during acute infection of swine with foot and mouth disease virus (FMDV). Vet Immunol Immunopathol 2003;92:61–73.
4. Belsham GJ, and Brangwyn JK. A region of the 5′ noncoding region of foot-and-mouth disease virus RNA directs efficient internal initiation of protein synthesis within cells: Involvement with the role of L protease in translational control. J Virol 1990;64:5389–5395.
5. Boysen P, and Storset AK. Bovine natural killer cells. Vet Immunol Immunopathol 2009;130:163–177.
6. Callahan JD, Brown F, Osorio FA, *et al*. Use of a portable real-time reverse transcriptase-polymerase chain reaction assay for rapid detection of foot-and-mouth disease virus. J Am Vet Med Assoc 2002;220:1636–1642.
7. Carrillo C, Tulman ER, Delhon G, *et al*. Comparative genomics of foot-and-mouth disease virus. J Virol 2005;79: 6487–6504.
8. Charerntantanakul W, and Roth JA. Biology of porcine T lymphocytes. Anim Health Res Rev 2006;7:81–96.
9. Childerstone A, Cedillo-Baron L, Foster-Cuevas M, and Parkhouse R. Demonstration of bovine CD8+ T-cell responses to foot-and-mouth disease virus. J Gen Virol 1999;80:663–669.
10. Clarke BE, and Sangar DV. Processing and assembly of foot-and-mouth disease virus proteins using subgenomic RNA. J Gen Virol 1988;69:2313–2325.
11. de Avila Botton S, Brum MC, Bautista E, Koster M, Weiblen R, Golde WT, and Grubman MJ. Immunopotentiation of a foot-and-mouth disease virus subunit vaccine by interferon alpha. Vaccine 2006;24:3446–3456.
12. Denyer MS, Wileman TE, Stirling CM, Zuber B, and Takamatsu HH. Perforin expression can define CD8 positive lymphocyte subsets in pigs allowing phenotypic and functional analysis of natural killer, cytotoxic T, natural killer T and MHC un-restricted cytotoxic T-cells. Vet Immunol Immunopathol 2006;110:279–292.
13. Devaney MA, Vakharia VN, Lloyd RE, Ehrenfeld E, and Grubman MJ. Leader protein of foot-and-mouth disease virus is required for cleavage of the p220 component of the cap-binding protein complex. J Virol 1988;62:4407–4409.
14. Doel TR. FMD vaccines. Virus Res 2003;91:81–99.
15. Donaldson AI, Herniman KA, Parker J, and Sellers RF. Further investigations on the airborne excretion of foot-and-mouth disease virus. J Hyg (Lond) 1970;68:557–564.
16. Gerner W, Hammer SE, Wiesmuller KH, and Saalmuller A. Identification of major histocompatibility complex restriction and anchor residues of foot-and-mouth disease virus-derived bovine T-cell epitopes. J Virol 2009;83:4039–4050.
17. Golde WT, de Los Santos T, Robinson L, Grubman MJ, Sevilla N, Summerfield A, and Charleston B. Evidence of activation and suppression during the early immune response to foot-and-mouth disease virus. Transbound Emerg Dis 2011;58:283–290.
18. Grubman MJ, and Baxt B. Foot-and-mouth disease. Clin Microbiol Rev 2004;17:465–493.
19. Grubman MJ, Moraes MP, Schutta C, *et al*. Adenovirus serotype 5-vectored foot-and-mouth disease subunit vaccines: The first decade. Future Virol 2010;5:51–64.
20. Grubman MJ, Zellner M, Bablanian G, Mason PW, and Piccone ME. Identification of the active-site residues of the 3C proteinase of foot-and-mouth disease virus. Virology 1995;213:581–589.
21. Guzman E, Taylor G, Charleston B, and Ellis SA. Induction of a cross-reactive CD8(+) T cell response following foot-and-mouth disease virus vaccination. J Virol 2010;84: 12375–12384.
22. Guzman E, Taylor G, Charleston B, Skinner MA, and Ellis SA. An MHC-restricted CD8+ T-cell response is induced in cattle by foot-and-mouth disease virus (FMDV) infection and also following vaccination with inactivated FMDV. J Gen Virol 2008;89:667–675.
23. Haydon DT, Bastos AD, Knowles NJ, and Samuel AR. Evidence for positive selection in foot-and-mouth disease virus capsid genes from field isolates. Genetics 2001;157:7–15.
24. Hutber AM, Kitching RP, Fishwick JC, Bires J. Foot-and-mouth disease: The question of implementing vaccinal control during an epidemic. Vet J 2011;188:18–23.
25. Joshi G, Sharma R, and Kakker NK. Phenotypic and functional characterization of T-cells and in vitro replication of FMDV serotypes in bovine lymphocytes. Vaccine 2009;27: 6656–6661.
26. Klump W, Marquardt O, and Hofschneider PH. Biologically active protease of foot and mouth disease virus is expressed from cloned viral cDNA in Escherichia coli. Proc Natl Acad Sci USA 1984;81:3351–3355.
27. Kuhn R, Luz N, and Beck E. Functional analysis of the internal translation initiation site of foot-and-mouth disease virus. J Virol 1990;64:4625–4631.
28. Mayr GA, Chinsangaram J, and Grubman MJ. Development of replication-defective adenovirus serotype 5 containing the capsid and 3C protease coding regions of foot-and-mouth disease virus as a vaccine candidate. Virology 1999;263: 496–506.
29. Mayr GA, O'Donnell V, Chinsangaram J, Mason PW, and Grubman MJ. Immune responses and protection against foot-and-mouth disease virus (FMDV) challenge in swine vaccinated with adenovirus-FMDV constructs. Vaccine 2001; 19:2152–2162.
30. Moffat K, Howell G, Knox C, Belsham GJ, Monaghan P, Ryan MD, and Wileman T. Effects of foot-and-mouth disease virus nonstructural proteins on the structure and function of the early secretory pathway: 2BC but not 3A blocks endoplasmic reticulum-to-golgi transport. J Virol 2005;79:4382–4395.
31. Moffat K, Knox C, Howell G, *et al*. Inhibition of the secretory pathway by foot-and-mouth disease virus 2BC protein is reproduced by coexpression of 2B with 2C, and the site of inhibition is determined by the subcellular location of 2C. J Virol 2007;81:1129–1139.
32. Moraes MP, Diaz-San Segundo F, Dias CC, Pena L, and Grubman MJ. Increased efficacy of an adenovirus-vectored foot-and-mouth disease capsid subunit vaccine expressing nonstructural protein 2B is associated with a specific T cell response. Vaccine 2011;29:9431–9440.
33. Moraes MP, Mayr GA, Mason PW, and Grubman MJ. Early protection against homologous challenge after a single dose of replication-defective human adenovirus type 5 expressing capsid proteins of foot-and-mouth disease virus (FMDV) strain A24. Vaccine 2002;20:1631–1639.
34. Murphy FA, Gibbs EPJ, Horzinek MC, and Studdert MJ. Picornaviridae *Veterinary Virology.* Third ed. Academic Press, New York, NY, 1999;417–532.
35. Nfon CK, Ferman GS, Toka FN, Gregg DA, and Golde WT. Interferon-alpha production by swine dendritic cells is inhibited during acute infection with foot-and-mouth disease virus. Viral Immunol 2008;21:68–77.
36. Nfon CK, Toka FN, Kenney M, Pacheco JM, and Golde WT. Loss of plasmacytoid dendritic cell function coincides with

lymphopenia and viremia during foot-and-mouth disease virus infection. Viral Immunol 2010;23:29–41.
37. Pacheco JM, Brum MC, Moraes MP, Golde WT, and Grubman MJ. Rapid protection of cattle from direct challenge with foot-and-mouth disease virus (FMDV) by a single inoculation with an adenovirus-vectored FMDV subunit vaccine. Virology 2005;337:205–209.
38. Pacheco JM, Butler JE, Jew J, Ferman GS, Zhu J, and Golde WT. IgA antibody response of swine to foot-and-mouth disease virus infection and vaccination. Clin Vaccine Immunol 2010;17:550–558.
39. Pacheco JM, and Mason PW. Evaluation of infectivity and transmission of different Asian foot-and-mouth disease viruses in swine. J Vet Sci 2010;11:133–142.
40. Pacheco JM, Tucker M, Hartwig E, Bishop E, Arzt J, and Rodriguez LL. Direct contact transmission of three different foot-and-mouth disease virus strains in swine demonstrates important strain-specific differences. Vet J 2012;193:456–463.
41. Patch JR, Pedersen LE, Toka FN, *et al*. Induction of foot-and-mouth disease virus-specific cytotoxic T cell killing by vaccination. Clin Vaccine Immunol 2011;18:280–288.
42. Pena L, Moraes MP, Koster M, *et al*. Delivery of a foot-and-mouth disease virus empty capsid subunit antigen with nonstructural protein 2B improves protection of swine. Vaccine 2008;26:5689–5699.
43. Rock KL, Farfan-Arribas DJ, and Shen L. Proteases in MHC class I presentation and cross-presentation. J Immunol 2010; 184:9–15.
44. Rodriguez A, Ley V, Ortuno E, *et al*. A porcine CD8+ T cell clone with heterotypic specificity for foot-and-mouth disease virus. J Gen Virol 1996;77:2089–2096.
45. Rodriguez LL, and Grubman MJ.Foot and mouth disease virus vaccines. Vaccine 2009;27:D90–94.
46. Sanz-Parra A, Jimenez-Clavero MA, Garcia-Briones MM, Blanco E, Sobrino F, and Ley V. Recombinant viruses expressing the foot-and-mouth disease virus capsid precursor polypeptide (P1) induce cellular but not humoral antiviral immunity and partial protection in pigs. Virology 1999;259:129–134.
47. Sanz-Parra A, Sobrino F, and Ley V. Infection with foot-and-mouth disease virus results in a rapid reduction of MHC class I surface expression. J Gen Virol 1998;79:433–436.
48. Sanz-Parra A, Vazquez B , Sobrino F, Cox SJ, Ley V, and Salt JS. Evidence of partial protection against foot-and-mouth disease in cattle immunized with a recombinant adenovirus vector expressing the precursor polypeptide (P1) of foot-and-mouth disease virus capsid proteins. J Gen Virol 1999; 80:671–679.
49. Scudamore JM, and Harris DM. Control of foot and mouth disease: Lessons from the experience of the outbreak in Great Britain in 2001. Rev Sci Tech 2002;21:699–710.
50. Sellers RF, and Parker J. Airborne excretion of foot-and-mouth disease virus. J Hyg (Lond) 1969;67:671–677.
51. Smith DM, Lunney JK, Martens GW, *et al*. Nomenclature for factors of the SLA class-I system, 2004. Tissue Antigens 2005;65:136–149.
52. Sutmoller P, Barteling SS, Olascoaga RC, and Sumption KJ. Control and eradication of foot-and-mouth disease. Virus Res 2003;91:101–144.
53. Toka FN, Kenney MA, and Golde WT. Rapid and transient activation of gammadelta T cells to IFN-gamma production, NK cell-like killing, and antigen processing during acute virus infection. J Immunol 2011;186:4853–4861.
54. Toka FN, Nfon C, Dawson H, and Golde WT. Natural killer cell dysfunction during acute infection with foot-and-mouth disease virus. Clin Vaccine Immunol 2009;16:1738–1749.
55. Toka FN, Nfon CK, Dawson H, Estes DM, and Golde WT. Activation of porcine natural killer cells and lysis of foot-and-mouth disease virus infected cells. J Interferon Cytokine Res 2009;29:179–192.
56. Vakharia VN, Devaney MA, Moore DM, Dunn JJ, and Grubman MJ. Proteolytic processing of foot-and-mouth disease virus polyproteins expressed in a cell-free system from clone-derived transcripts. J Virol 1987;61:3199–3207.
57. Yang PC, Chu RM, Chung WB, and Sung HT. Epidemiological characteristics and financial costs of the 1997 foot-and-mouth disease epidemic in Taiwan. Vet Rec 1999;145:731–734.
58. Yewdell JW, and Haeryfar SM. Understanding presentation of viral antigens to CD8+ T cells in vivo: The key to rational vaccine design. Annu Rev Immunol 2005;23:651–682.

Address correspondence to:
Dr. William T. Golde
Foreign Animal Disease Research Unit
Plum Island Animal Disease Center
Agricultural Research Service, USDA
P.O. Box 848
Greenport, NY 11944

E-mail: william.golde@ars.usda.gov

Transboundary and Emerging Diseases

Transboundary and Emerging Diseases

ORIGINAL ARTICLE

Heterogeneity in the Antibody Response to Foot-and-Mouth Disease Primo-vaccinated Calves

S. Di Giacomo[1,*], B. P. Brito[2,*], A. M. Perez[2,3], D. Bucafusco[1,3], J. Pega[1,3], L. Rodríguez[4], M. V. Borca[4] and M. Pérez-Filgueira[1,3]

[1] Instituto de Virología, Centro de Investigaciones en Ciencias Veterinarias y Agronómicas (CICVyA), Instituto Nacional de Tecnología Agropecuaria, Hurlingham, Argentina
[2] Department of Medicine and Epidemiology, Center for Animal Diseases Modeling and Surveillance, School of Veterinary Medicine, University of California, Davis, CA, USA
[3] Consejo Nacional de Investigaciones Científicas y Técnicas, Buenos Aires, Argentina
[4] Plum Island Animal Disease Center, Agricultural Research Service, USDA, Greenport, NY, USA

Keywords:
foot-and-mouth disease; antibody response; vaccine; cattle; breed

Correspondence:
M. Pérez-Filgueira. Instituto de Virología, Centro de Investigaciones en Ciencias Veterinarias y Agronómicas (CICVyA), Instituto Nacional de Tecnología Agropecuaria, N. Repetto y De Los Reseros S/N, Hurlingham (1686), Argentina.
Tel.: +54 11 4481 6684;
Fax: +54 11 4621 1743;
E-mail: mperez@cnia.inta.gov.ar

*Authors contributed equally to this report.

Received for publication March 15, 2013

doi:10.1111/tbed.12130

Summary

Foot-and-mouth disease (FMD) vaccines are routinely used as effective control tools in large regions worldwide and to limit outbreaks during epidemics. Vaccine-induced protection in cattle has been largely correlated with the FMD virus (FMDV)-specific antibodies. Genetic control of cattle immune adaptive responses has been demonstrated only for peptide antigens derived from FMDV structural proteins. Here, we quantify the heterogeneity in the antibody response of cattle primo-vaccinated against FMD and study its association with the genetic background in Holstein and Jersey sires. A total of 377 FMDV-seronegative calves (122 and 255 calves from 16 and 15 Holstein and Jersey sires, respectively) were included in the study. Samples were taken the day prior to primo-vaccination and 45 days post-vaccination (dpv). Animals received commercial tetravalent FMD single emulsion oil vaccines formulated with inactivated FMDV. Total FMDV-specific antibody responses were studied against three viral strains included in the vaccine, and antibody titres were determined by liquid-phase blocking ELISA. Three linear hierarchical mixed regression models, one for each strain, were formulated to assess the heterogeneity in the immune responses to vaccination. The dependent variables were the antibody titres induced against each FMDV strain at 45 dpv, whereas sire's 'breed' was included as a fixed effect, 'sire' was included as a random effect, and 'farm' was considered as a hierarchical factor to account for lack of independence of within herd measurements. A significant association was found between anti-FMDV antibody responses and sire's breed, with lower immune responses found in the Jersey sires' offspring compared with those from Holstein sires. No significant intrabreed variation was detected. In addition, farm management practices were similar in this study, and results of the serological assays were shown to be repeatable. It therefore seems plausible that differences in the immune response may be expected in the event of a mass vaccination campaigns.

Introduction

Foot-and-mouth disease (FMD) is a highly contagious and acute viral disease affecting all ruminants and cloven-footed animals. Domestic species typically infected by the FMD virus (FMDV) include cattle, swine, sheep and goats; numerous susceptible wildlife species may act as reservoirs for FMDV under certain ecological conditions (Alexandersen et al., 2003). Fatal cases are usually restricted to young animals and certain FMDV strains; however, the high

© 2013 Blackwell Verlag GmbH • Transboundary and Emerging Diseases.

morbidity rate and indirect losses associated with FMD outbreaks result in severe and far-reaching economic losses to the livestock industry (Yang et al., 1999; Thompson et al., 2002).

Disease outbreaks in FMD-free regions are controlled using a combination of mitigation strategies, such as control of animal movements and, in some cases, killing of infected and exposed animals and/or vaccination. In recent decades, social, economic and environmental concerns have increasingly favoured the use of vaccination to control FMD outbreaks (Mackay et al., 2004; Poulin and Christianson, 2006). Moreover, vaccination is routinely used in countries and large regions recognized as free from the disease by the World Organization for Animal Health (OIE), to prevent FMDV incursions (Saraiva and Darsie, 2004).

Current commercial vaccines are based on chemically inactivated whole virus particles formulated in oil or hydroxide–saponine adjuvanted formulations (Doel, 2003). Good quality vaccines prevent the development and transmission of the disease and decrease the incidence of persistently infected animals (Anderson et al., 1974; Orsel et al., 2005; Cox et al., 2006). Protection provided by FMD vaccines is serotype (and in many cases strain specific) specific and closely related to the induction of specific antibody responses (Pay and Hingley, 1987). Moreover, *in vitro* assays such as liquid-phase blocking ELISA (LPB-ELISA) or virus neutralization tests (VNT) may be used to assess vaccine potency based on statistical correlations between antibody titres and OIE-recognized *in vivo* protection assays, such as the 'protection against podal generalization'(PPG) test (Maradei et al., 2008).

Immune responses elicited by commercial FMD vaccines vary between different hosts (Doel et al., 1994; Patil et al., 2002; Barnett et al., 2004; Parida et al., 2007), and thus, formulations should be tailored to affected animal species. Variations are also observed depending on the age of the animal (Spath et al., 1995; Samina et al., 1998) and the pre-existence of vaccine-induced passive maternal immunity (Nicholls et al., 1984; Sadir et al., 1988). Genetic factors involved have also been investigated in laboratory animal models and natural hosts, mainly through the study of specific immune responses elicited by discrete FMDV-derived peptide sequences(Francis et al., 1987; Glass et al., 1991, 2000; Glass and Millar, 1994; Van Lierop et al., 1995; Garcia-Briones et al., 2000; Baxter et al., 2009; Leach et al., 2010). However, to the authors' knowledge, only one early report has included some observations on the association between genetic factors and immune responses against whole inactivated FMDV particles within vaccines (Samina et al., 1998).

The hypothesis assessed in the study here was that the antibody response to FMD primo-vaccination in cattle varies in association with sire's breed, which is suggestive of genetic-borne variation in the response. This was tested using data from total anti-FMDV serum antibody titres induced 45 days post-vaccination (dpv) against three FMDV vaccine strains. A significant association ($P < 0.05$) was found between humoral responses and sire's breed, with offspring from Jersey sires exhibiting less of an immune response than Holstein sires. No significant intra-breed variation was identified. Results presented here provide supporting evidence of genetic-borne influence on the immune response to FMD vaccination.

Materials and Methods

Animals

Four to seven months old naïve calves ($n = 606$) raised in four dairy farms in Buenos Aires Province, Argentina, were screened during a twelve-month period. As all the animals were born to FMD-vaccinated dams, only calves without detectable anti-FMDV colostral antibodies at the time of vaccination (62.2%, $n = 377$) were included in the study. Calves included in the study were from Holstein (16 sires, 122 calves) and Jersey (15 sires, 255 calves) breeds, and all sires analysed presented at least three calves in their progeny. Two of the farms (referred to as farms No. 1 and 2) included only Holstein calves and another farm included only Jersey calves (farm No. 4), whereas the remaining farm included both Holstein and Jersey calves (farm No. 3).

Samples and vaccination

Paired whole blood samples were obtained from the 377 calves. Samples were taken the day prior to primary vaccination and 45 days later. Vaccinations were performed in the frame of the national FMD campaigns in Argentina using officially approved commercial tetravalent FMD single oil emulsion vaccines from same manufacturer. Formulations contained inactivated FMDV from A24 Cruzeiro/Brazil/55 (A24 Cruzeiro), A/Argentina/2001 (A/Arg/01), O1/Campos/Brazil/58 (O1 Campos) and C3/Indaial/Brazil/71 (C3 Indaial) strains. Vaccines were provided, handled and applied by trained professionals authorized by the national sanitary authority (SENASA) following current regulations (SENASA, 2002, 2006, 2011). Whole blood samples taken at 0 and 45 dpv were centrifuged to separate plasma from cells, and both fractions were stored at −20°C until used.

Serological assays

Total FMDV-specific antibody responses were determined against three vaccine strains (A24/Cruzeiro, A/Arg/01 and O1/Campos) belonging to serotypes with recent circulation in South America. Anti-FMDV antibody titres

 © 2013 Blackwell Verlag GmbH • Transboundary and Emerging Diseases.

were studied by means of a liquid-phase blocking ELISA (LPB-ELISA) performed under ISO standards and utilized by the regional OIE FMD Reference Laboratory in Argentina to assess herd immunity and vaccine efficacy (Periolo et al., 1993; Maradei et al., 2008). Briefly, serial dilutions of plasma samples were incubated with inactivated whole FMDV particles corresponding to these three vaccine strains. Plasma–virus mixtures were transferred to ELISA plates previously coated with strain-specific rabbit polyclonal sera to capture non-associated virus. Captured virus was finally detected using panels of MAb specific for each of these three strains and anti-mouse Ig sera HRP-conjugated. Antibody titres were expressed as the reciprocal $\log_{10}$ of serum dilutions giving the 50% of the absorbance recorded in the virus control wells without plasma. Calves carrying FMDV-specific colostral antibodies prior to primary vaccination were also identified using this test and removed from the study. Thirty-five randomly selected samples were retested to evaluate repeatability of the assay by computing the concordance correlation coefficient (ρc) (Lin, 1989), using an online application (National Institute of Water and Atmospheric Research, 2011).

Statistical analysis

Differences in the serotype-specific responses were assessed using a Student's *t*-test, and the correlation of immune responses between individuals was assessed using an *R*-Spearman test (Zar, 1972).

Association of the antibody responses with sire's breed was assessed using three linear hierarchical mixed regression models (Goldstein, 2011), one for each virus strain. The dependent variable was antibody titre induced against FMDV O1/Campos, A24/Cruzeiro and A/Arg/01 at 45 dpv, whereas sire's breed was included as a fixed effect, sire was taken as a random effect, and farm was considered as a hierarchical factor to account for intraherd lack of independence in the observations. The fixed effect (breed) was tested for significance, and the random effect (sire) was evaluated based on their contribution to the model improvement as indicated by the value of Akaike's information criterion (AIC) (Akaike, 1974).

Table 2. Mean and standard deviation of antibody titres[a] in calves at 45 dpv per farm and sire breed

		A24/Cruzeiro		O1/Campos		A/Arg/01	
Sire breed	*n*	Mean	SD	Mean	SD	Mean	SD
Holstein	122	2.782	0.515	2.592	0.573	2.817	0.534
Jersey	255	2.229	0.425	2.122	0.488	2.279	0.469

[a]Mean FMDV-specific antibody responses were measured by LPB-ELISA expressed as described in Materials and Methods.

Results

Antibody titres against three of the vaccine strains (A24/Cruzeiro, O1/Campos and A/Arg/01) were measured by a validated and controlled LPB-ELISA utilized by the regional OIE FMD Reference Laboratory in Argentina. However, because samples were obtained and processed during a 12-month period, we studied the repeatability of the LPB-ELISA by retesting a subset of 35 randomly selected samples after analysing the whole set of plasma. The assay used here demonstrated good repeatability of results, as indicated by the high values of ρc estimated, which were (95% CI) ρc = 0.94 (0.88, 0.97), ρc = 0.92 (0.85, 0.96) and ρc = 0.87 (0.76, 0.94) for O1/Campos, A24/Cruzeiro and A/Arg/01, respectively.

A total of 377 FMDV-seronegative naïve calves from 31 different Holstein or Jersey sires distributed throughout four farms were primary vaccinated with commercial tetravalent FMD vaccines and included in this study. As it is shown in Table 1, 45 days after primary vaccination, titres of antibodies against A/Arg/01 were on average 0.04 log10 higher ($P < 0.05$) than those against A24/Cruzeiro, which in turn were 0.14 log10 higher ($P < 0.05$) than those against the O1/Campos strain (Table 1). Also, correlation between strain-specific antibody responses was high for all strains studied ($R = 0.85$–0.9). Moreover, primary FMD vaccination in all these groups of calves was efficient, inducing mean antibody titres against each of the strains at 45 dpv above the 75% of expected protection, based on the correlation with the *in vivo* potency tests (Maradei et al., 2008). (Table 2).

Table 1. Mean antibody titres[a]at 45 dpv per FMDV strain and mean difference between strains

FMDV strain	Mean Ab response at 45 dpv[a]	Compared to	Mean difference	Paired t-test significance	Pearson's correlation	Pearson's significance
O1/Campos	2.27	A24/Cruzeiro	−0.13	<0.01	0.85	<0.01
A24/Cruzeiro	2.41	A/Arg/01	−0.04	<0.01	0.87	<0.01
A/Arg/01	2.45	O1/Campos	0.18	<0.01	0.9	<0.01

[a]Mean FMDV-specific antibody responses were measured by LPB-ELISA expressed as described in Materials and Methods.

The whole set of mean antibody titres detected for each virus strain, grouping calves according to their sire and breed, is shown in Fig. 1. Intrabreed differences were negligible, as indicated by the similar averages and overlapping intervals estimated for specific sires (Fig. 1).

Results of the linear hierarchical mixed regression models are depicted in Table 3. The intercept in the model represents the overall mean antibody response of the reference breed value (Jersey), taking into account the herd correlated data. The estimate of the breed represents the mean increase in antibody titre increase of Holstein breed compared with Jersey, and the standard error (SE) measures data dispersion from the expected (mean) values based on the sampling distribution. A greater standard error indicates less statistical precision of the estimate, which will be reflected in wider confidence intervals. Analyses using the regression models indicated that sire's breed was significantly associated ($P < 0.05$) with the immune response for the three strains (Table 3), resulting in an antibody response to FMD vaccination at 45 dpv significantly lower ($P < 0.01$) for the progeny of Jersey compared with those of Holstein (Table 2). Addition of sire as a random effect did not improve the fit of the model for any of the three virus strains, suggesting that individual factors other than differences in sire breed were negligible.

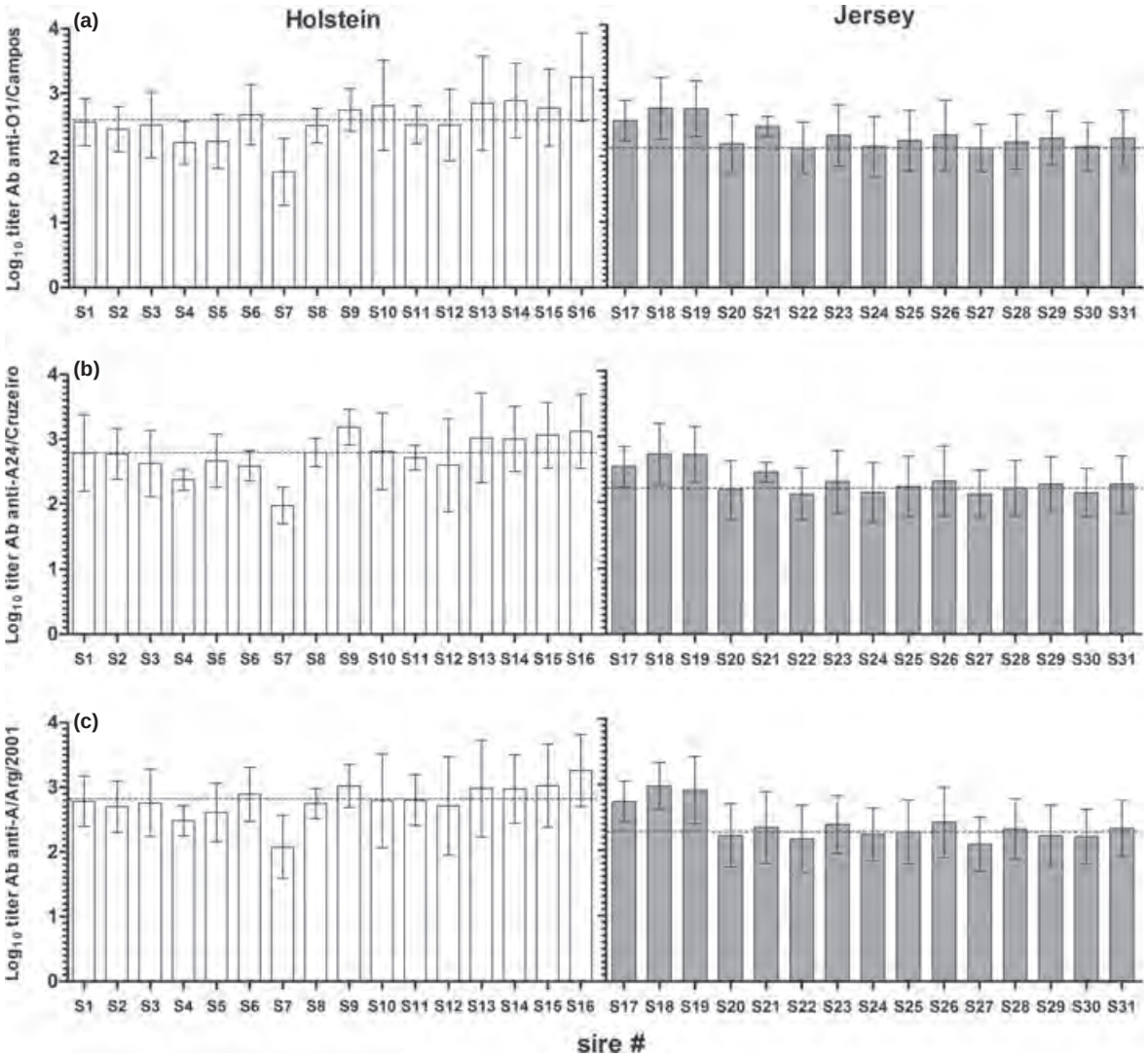

Fig. 1. Mean antibody titres against FMDV O1/Campos (a), A24/Cruzeiro (b) and A/Arg/01 (c) in calves at 45 dpv. Calves were grouped by breed and sire from which they derived. Antibody titres were measured by LPB-ELISA and expressed as the reciprocal $\log_{10}$ of serum dilutions giving the 50% of the absorbance recorded in the virus control wells without serum. Error bars represent the standard deviation of the mean titres, and dotted lines indicate average values for each breed and virus strain. Sires S1-S7 correspond to farm 1; S8–S15 to farm 2; S16–S19 to farm 3; and S20–S31 to farm 4.

 © 2013 Blackwell Verlag GmbH • Transboundary and Emerging Diseases.

Table 3. Hierarchical linear model results for antibody titres[a] at 45 dpv against O1/Campos, A24/Cruzeiro and A/Arg/01

	Estimate	SE	95% CI	Sig.
O1 Campos				
Intercept	2.24	0.21	1.71–2.78	<0.01
Breed[b]	0.45	0.18	0.09–0.81	0.02
A24/Cruzeiro				
Intercept	2.39	0.16	1.98–2.79	<0.01
Breed	0.42	0.16	0.10–0.73	0.01
A/Arg/01				
Intercept	2.49	0.18	2.02–2.96	<0.01
Breed	0.35	0.17	0.01–0.70	0.04

[a]Mean FMDV-specific antibody responses were measured by LPB-ELISA expressed as described in Materials and Methods. SE, standard error.
[b]Indicates the fixed effect analysed in the regression model.

Discussion

The induction of neutralizing antibodies is the mechanism most frequently related to protection against FMDV (Barnett and Carabin, 2002; Golde et al., 2005; Orsel et al., 2005; Cox et al., 2006, 2007; Maradei et al., 2008; Robiolo et al., 2010), and a number of reports have provided in-depth information about the genetic control of humoral responses in cattle (O'Neill et al., 2006; Minozzi et al., 2010; Glass et al., 2011; Leach et al., 2012). Previous work has shown MHC-based restrictions to FMDV-derived antigens in cattle. Early studies focused on the genetic restrictions imposed on T-cell recognition via major histocompatibility complex class II (MHC II) polymorphism (Francis et al., 1987; Glass et al., 1991; Van Lierop et al., 1995). Some alleles of the MHC II system in cattle (Glass et al., 2000) have been associated with both the magnitude (Glass and Millar, 1994) and the quality (Garcia-Briones et al., 2000; Baxter et al., 2009) of humoral responses induced against FMDV peptides. Only recently, whole genome analyses also revealed quantitative trait loci (QTL) which controlled both humoral and cellular immunity against FMDV peptides in regions outside the BoLA genes (Leach et al., 2010).

Complexity of the associations between genetic-related factors and immune responses to FMDV runs in parallel with that of the immunizing antigen. Some important aspects of the anti-FMDV responses observed in cattle, such as T-independent antibody responses (Juleff et al., 2009), are tightly associated with structural features of the intact particle. Consequently, they do not follow the same immune pathways as for peptide antigens and cannot be explained as the addition of independent responses to an array of discrete peptides. Two other factors add difficulties to the FMDV model in cattle: the genetic variability associated with outbreed bovine populations and the fact that FMDV antigens included in vaccines are not antigenically homogenous but rather a mix of multiple variants produced during virus replication (Piatti et al., 1995).

Only one early report presented results about the influence of the genetic background on the immune response to FMD vaccines (Samina et al., 1998). In that paper, groups of cattle ($n = 10$) deriving from four different sires were compared. Animals received three vaccinations with a trivalent FMD aqueous vaccine formulated with aluminium hydroxide and saponine and were tested 1 year after the last vaccination. The authors indicate that the sire effect was significant for daughters' antibody responses against the vaccine strains, although there was no association between the bulls' own response and their daughter's responses for any of the serotypes, thus hindering interpretation of the results.

With this background, we decided to use FMDV vaccines as model antigens. Humoral responses raised against three strains used in commercial tetravalent vaccines at 45 days after primo-vaccination were measured by a reliable serological assay and associated with sire and breed effects. Highest mean antibody titres were found for A/Arg/01 strain, followed by A24/Cruzeiro and O1/Campos, 0.04 and 0.18 Log_{10} titre units below A/Arg/01, respectively ($P < 0.01$). As previously described, these differences between strains could be related to different antigenic payloads for each particular strain included in the vaccine (Rweyemamu et al., 1984) and also to the differential capsid stability among FMDV strains (Doel and Baccarini, 1981) which may impact on the immunogenicity of the viral antigens (Doel and Chong, 1982). In any case, it is important to note that all of these average values were above the LPB-ELISA titres determined to confer 75% of expected protection to the viral challenge (Maradei et al., 2008). As a whole, our results demonstrated that antibody responses induced after primo-vaccination were homogenously high for all calves assayed, with a good inter-strain correlation between titres.

Significant differences found between antibody responses against each vaccine strain reinforce the idea of the poor inter-strain cross-reactivity (Alexandersen et al., 2003) and the independence of the pathways involved in the induction of antibodies against each virus. Thus, we decided to study all three humoral immune responses independently.

Associations of the humoral responses elicited in calves with sire or breed effects were analysed by three linear hierarchical mixed regression models. Design of the experiment included animals from different farms. The possible impact of environmental factors was reduced by including dairy farms with identical management and similar environmental characteristics. The potential bias introduced by this

variability was also addressed by including farms as a hierarchy in the statistical model, so the final immune response attributed to the sire characteristics was unbiased. Also, although the number of calves per breed was uneven between both groups (122 Holstein and 255 Jersey), using herd as a hierarchical factor controls for correlated data, in this case, regarding breed and other factors related with within herd similarities. This model deals with the potential for overestimation of the estimate precision when similar (correlated) data are represented with large sample sizes.

We found no significant intrabreed differences in the antibody responses obtained in calves grouped by sire for any of the three strains. Moreover, mean antibody titres grouped by sire followed a similar pattern among strains. This lack of intrabreed differences may be in part explained by the within-farm genetic homogeneity; however, the vigorous humoral responses induced by these vaccines may also have an impact. Good quality vaccines are quite efficient in inducing FMDV-specific antibodies, and thus, they might be hiding or compensating some of the inherent, genetically driven, immunological differences between individuals.

Sire's breed, however, significantly affected the outcome of the antibody responses registered here, as indicated by the results of the regression models. Progeny of Jersey sires developed a post-vaccination immune response significantly lower ($P < 0.05$) than progeny from Holstein sires for the three FMDV strains analysed at 45 dpv. Titre values differed from 2.24- (for A/Arg/01) to 2.82-fold (for O1/Campos) between these two breeds. These observations are also in agreement with the idea that less potent humoral responses, in this case those induced against the O1/Campos strain, may be better than high potency vaccines in revealing small differences in humoral responses related to the genetic background of the animals.

Results presented here provide evidence that the immune response to primo-vaccination in cattle is affected by the genetic background of the calves, as indicated by the association detected between sire's breed and immune response. These results suggest that additional exploration into the limitations and potentials of genetic markers may help to predict immune responses to FMDV immunization and other vaccines in cattle.

Acknowledgements

This work was funded by the Agricultural Research Service Collaborative Agreement No. 58-1940-8-111F and the Instituto Nacional de Tecnología Agropecuaria FMD Project No. AESA-201721. Authors want to acknowledge to Dr Sol Juncos for her expert veterinary assistance along the project, Dr Martin Peluca Ygartua for his assistance during sampling procedures and Dr Alejandra Capozzo for helpful discussions. Authors also thank Ms Melanie Prarat for critical reading and editing of the manuscript. Finally, our extended thanks to Mr Mariano Tuculet and Mr Francisco Furlong for their support and interest towards the project.

References

Akaike, K., 1974: A new look at the statistical model identification. *IEEE Trans. Autom. Control* 19, 716–723.

Alexandersen, S., Z. Zhang, A. I. Donaldson, and A. J. Garland, 2003: The pathogenesis and diagnosis of foot-and-mouth disease. *J. Comp. Pathol.* 129, 1–36.

Anderson, E. C., W. J. Doughty, and J. Anderson, 1974: The effect of repeated vaccination in an enzootic foot-and-mouth disease area on the incidence of virus carrier cattle. *J. Hyg. (Lond.)* 73, 229–235.

Barnett, P. V., and H. Carabin, 2002: A review of emergency foot-and-mouth disease (FMD) vaccines. *Vaccine* 20, 1505–1514.

Barnett, P. V., P. Keel, S. Reid, R. M. Armstrong, R. J. Statham, C. Voyce, N. Aggarwal, and S. J. Cox, 2004: Evidence that high potency foot-and-mouth disease vaccine inhibits local virus replication and prevents the "carrier" state in sheep. *Vaccine* 22, 1221–1232.

Baxter, R., S. C. Craigmile, C. Haley, A. J. Douglas, J. L. Williams, and E. J. Glass, 2009: BoLA-DR peptide binding pockets are fundamental for foot-and-mouth disease virus vaccine design in cattle. *Vaccine* 28, 28–37.

Cox, S. J., C. Voyce, S. Parida, S. M. Reid, P. A. Hamblin, G. Hutchings, D. J. Paton, and P. V. Barnett, 2006: Effect of emergency FMD vaccine antigen payload on protection, subclinical infection and persistence following direct contact challenge of cattle. *Vaccine* 24, 3184–3190.

Cox, S. J., S. Parida, C. Voyce, S. M. Reid, P. A. Hamblin, G. Hutchings, D. J. Paton, and P. V. Barnett, 2007: Further evaluation of higher potency vaccines for early protection of cattle against FMDV direct contact challenge. *Vaccine* 25, 7687–7695.

Doel, T. R., 2003: FMD vaccines. *Virus Res.*, 91, 81–99.

Doel, T. R., and P. J. Baccarini, 1981: Thermal stability of foot-and-mouth disease virus. *Arch. Virol.* 70, 21–32.

Doel, T. R., and W. K. Chong, 1982: Comparative immunogenicity of 146S, 75S and 12S particles of foot-and-mouth disease virus. *Arch. Virol.* 73, 185–191.

Doel, T. R., L. Williams, and P. V. Barnett, 1994: Emergency vaccination against foot-and-mouth disease: rate of development of immunity and its implications for the carrier state. *Vaccine* 12, 592–600.

Francis, M. J., G. Z. Hastings, A. D. Syred, B. McGinn, F. Brown, and D. J. Rowlands, 1987: Non-responsiveness to a foot-and-mouth disease virus peptide overcome by addition of foreign helper T-cell determinants. *Nature* 330, 168–170.

Garcia-Briones, M. M., G. C. Russell, R. A. Oliver, C. Tami, O. Taboga, E. Carrillo, E. L. Palma, F. Sobrino, and E. J. Glass, 2000: Association of bovine DRB3 alleles with immune

 © 2013 Blackwell Verlag GmbH • Transboundary and Emerging Diseases.

response to FMDV peptides and protection against viral challenge. *Vaccine* 19, 1167–1171.

Glass, E. J., and P. Millar, 1994: Induction of effective cross-reactive immunity by FMDV peptides is critically dependent upon specific MHC-peptide-T cell interactions. *Immunology* 82, 1–8.

Glass, E. J., R. A. Oliver, T. Collen, T. R. Doel, R. Dimarchi, and R. L. Spooner, 1991: MHC class II restricted recognition of FMDV peptides by bovine T cells. *Immunology* 74, 594–599.

Glass, E. J., R. A. Oliver, and G. C. Russell, 2000: Duplicated DQ haplotypes increase the complexity of restriction element usage in cattle. *J. Immunol.* 165, 134–138.

Glass, E. J., R. Baxter, R. J. Leach, and O. C. Jann, 2011: Genes controlling vaccine responses and disease resistance to respiratory viral pathogens in cattle. *Vet. Immunol. Immunopathol.* 148, 90–99.

Golde, W. T., J. M. Pacheco, H. Duque, T. Doel, B. Penfold, G. S. Ferman, D. R. Gregg, and L. L. Rodriguez, 2005: Vaccination against foot-and-mouth disease virus confers complete clinical protection in 7 days and partial protection in 4 days: use in emergency outbreak response. *Vaccine* 23, 5775–5782.

Goldstein, H., 2011: Multilevel Statistical Models, 4th edn. Wiley, London.

Juleff, N., M. Windsor, E. A. Lefevre, S. Gubbins, P. Hamblin, E. Reid, K. McLaughlin, P. C. Beverley, I. W. Morrison, and B. Charleston, 2009: Foot-and-mouth disease virus can induce a specific and rapid CD4 + T-cell-independent neutralizing and isotype class-switched antibody response in naive cattle. *J. Virol.* 83, 3626–3636.

Leach, R. J., S. C. Craigmile, S. A. Knott, J. L. Williams, and E. J. Glass, 2010: Quantitative trait loci for variation in immune response to a Foot-and-Mouth Disease virus peptide. *BMC Genet.* 11, 107.

Leach, R. J., R. G. O'Neill, J. L. Fitzpatrick, J. L. Williams, and E. J. Glass, 2012: Quantitative trait loci associated with the immune response to a Bovine Respiratory Syncytial Virus vaccine. *PLoS ONE* 7, e33526.

Lin, L. I., 1989: A concordance correlation coefficient to evaluate reproducibility. *Biometrics* 45, 255–268.

Mackay, D., S. Parida, D. Paton, and J. Anderson, 2004: Making a vaccinate-to-live policy a reality in foot-and-mouth disease. *Dev. Biol. (Basel)* 119, 261–266.

Maradei, E., J. La Torre, B. Robiolo, J. Esteves, C. Seki, A. Pedemonte, M. Iglesias, R. D'Aloia, and N. Mattion, 2008: Updating of the correlation between lpELISA titers and protection from virus challenge for the assessment of the potency of polyvalent aphtovirus vaccines in Argentina. *Vaccine* 26, 6577–6586.

Minozzi, G., L. Buggiotti, A. Stella, F. Strozzi, M. Luini, and J. L. Williams, 2010: Genetic loci involved in antibody response to *Mycobacterium avium* ssp. paratuberculosis in cattle. *PLoS ONE* 5, e11117.

Nicholls, M. J., L. Black, M. M. Rweyemamu, J. Genovese, R. Ferrari, C. A. Hammant, E. de Silva, and O. Umehara, 1984: The effect of maternally derived antibodies on the response of calves to vaccination against foot and mouth disease. *J. Hyg. (Lond.)* 92, 105–116.

National Institute of Water and Atmospheric Research, 2011: Statistical calculators. Available at http://www.niwa.co.nz/online-services/statistical-calculators/concordance (accessed 20 February 2012).

O'Neill, R. G., J. A. Woolliams, E. J. Glass, J. L. Williams, and J. L. Fitzpatrick, 2006: Quantitative evaluation of genetic and environmental parameters determining antibody response induced by vaccination against bovine respiratory syncytial virus. *Vaccine* 24, 4007–4016.

Orsel, K., A. Dekker, A. Bouma, J. A. Stegeman, and M. C. de Jong, 2005: Vaccination against foot and mouth disease reduces virus transmission in groups of calves. *Vaccine*, 23, 4887–4894.

Parida, S., L. Fleming, Y. Oh, M. Mahapatra, P. Hamblin, J. Gloster, C. Doel, S. Gubbins, and D. J. Paton, 2007: Reduction of foot-and-mouth disease (FMD) virus load in nasal excretions, saliva and exhaled air of vaccinated pigs following direct contact challenge. *Vaccine* 25, 7806–7817.

Patil, P. K., J. Bayry, C. Ramakrishna, B. Hugar, L. D. Misra, and C. Natarajan, 2002: Immune responses of goats against foot-and-mouth disease quadrivalent vaccine: comparison of double oil emulsion and aluminium hydroxide gel vaccines in eliciting immunity. *Vaccine* 20, 2781–2789.

Pay, T. W., and P. J. Hingley, 1987: Correlation of 140S antigen dose with the serum neutralizing antibody response and the level of protection induced in cattle by foot-and-mouth disease vaccines. *Vaccine* 5, 60–64.

Periolo, O. H., C. Seki, P. R. Grigera, B. Robiolo, G. Fernandez, E. Maradei, R. D'Aloia, and J. L. La Torre, 1993: Large-scale use of liquid-phase blocking sandwich ELISA for the evaluation of protective immunity against aphthovirus in cattle vaccinated with oil-adjuvanted vaccines in Argentina. *Vaccine* 11, 754–760.

Piatti, P., S. Hassard, J. F. Newman, and F. Brown, 1995: Antigenic variants in a plaque-isolate of foot-and-mouth disease virus: implications for vaccine production. *Vaccine* 13, 781–784.

Poulin, M. C., and W. T. Christianson, 2006: On-farm eradication of foot-and-mouth disease as an alternative to mass culling. *Vet. Rec.* 158, 467–472.

Robiolo, B., J. La Torre, E. Maradei, C. P. Beascoechea, A. Perez, C. Seki, E. Smitsaart, N. Fondevila, E. Palma, N. Goris, K. De Clercq, and N. Mattion, 2010: Confidence in indirect assessment of foot-and-mouth disease vaccine potency and vaccine matching carried out by liquid phase ELISA and virus neutralization tests. *Vaccine* 28, 6235–6241.

Rweyemamu, M. M., L. Black, A. Boge, A. C. Thorne, and G. M. Terry, 1984: The relationship between the 140S antigen dose in aqueous foot-and-mouth disease vaccines and the serum antibody response of cattle. *J. Biol. Stand.* 12, 111–120.

Sadir, A. M., A. A. Schudel, O. Laporte, M. Braun, and R. A. Margni, 1988: Response to foot-and-mouth disease vaccines

in newborn calves. Influence of age, colostral antibodies and adjuvants. *Epidemiol. Infect.* 100, 135–144.

Samina, I., Z. Zakay-Rones, J. I. Weller, and B. A. Peleg, 1998: Host factors affecting the homologous and heterologous immune response of cattle to FMDV: genetic background, age, virus strains and route of administration. *Vaccine* 16, 335–339.

Saraiva, V., and G. Darsie, 2004: The use of vaccines in South American foot-and-mouth disease eradication programmes. *Dev. Biol. (Basel)* 119, 33–40.

SENASA, 2002: Regulation 623/2002. FMD eradication plan. Provides that the local health entities must adjust the structure and functioning of the Task Force. SENASA, 623/2002. Available at http://www.senasa.gov.ar/contenido.php?to=n&in=1077&io=4531 (accessed 29 January 2013).

SENASA, 2006: Regulation 799/2006. Manual of Procedures for Implementation of FMD vaccines. SENASA, 799/2006. Available at http://www.senasa.gov.ar/contenido.php?to=n&in=1029&io=5036 (accessed 29 January 2013).

SENASA, 2011: Regulation 368/2011. National Programme for Control of Foot and Mouth Disease. Inclusion of private veterinarians. SENASA, 368/2011. Available at http://www.senasa.gov.ar/contenido.php?to=n&in=1501&io=18755 (accessed 29 January 2013).

Spath, E. J., E. Smitsaart, A. P. Casaro, N. Fondevila, F. Fernandez, M. R. Leunda, D. Compaired, M. Buffarini, and H. Pessi, 1995: Immune response of calves to foot-and-mouth disease virus vaccine emulsified with oil adjuvant. Strategies of vaccination. *Vaccine* 13, 909–914.

Thompson, D., P. Muriel, D. Russell, P. Osborne, A. Bromley, M. Rowland, S. Creigh-Tyte, and C. Brown, 2002: Economic costs of the foot and mouth disease outbreak in the United Kingdom in 2001. *Rev. Sci. Tech.* 21, 675–687.

Van Lierop, M. J., P. R. Nilsson, J. P. Wagenaar, J. M. Van Noort, J. D. Campbell, E. J. Glass, I. Joosten, and E. J. Hensen, 1995: The influence of MHC polymorphism on the selection of T-cell determinants of FMDV in cattle. *Immunology* 84, 79–85.

Yang, P. C., R. M. Chu, W. B. Chung, and H. T. Sung, 1999: Epidemiological characteristics and financial costs of the 1997 foot-and-mouth disease epidemic in Taiwan. *Vet. Rec.* 145, 731–734.

Zar, J. H., 1972: Significance testing of the spearman rank correlation coefficient. *J Am Statist Assoc* 339, 578–580.

 © 2013 Blackwell Verlag GmbH • Transboundary and Emerging Diseases.

Virology 447 (2013) 172–180

Contents lists available at ScienceDirect

Virology

journal homepage: www.elsevier.com/locate/yviro

Characterization of a chimeric foot-and-mouth disease virus bearing a bovine rhinitis B virus leader proteinase

Sabena Uddowla, Juan M. Pacheco, Christopher Larson [1], Elizabeth Bishop, Luis L. Rodriguez, Devendra K. Rai, Jonathan Arzt, Elizabeth Rieder *

Foreign Animal Disease Research Unit, United States Department of Agriculture, Agricultural Research Service, Plum Island Animal Disease Center, Greenport, NY 11944, United States

ARTICLE INFO

Article history:
Received 10 June 2013
Returned to author for revisions 10 July 2013
Accepted 29 August 2013
Available online 1 October 2013

Keywords:
Chimeric foot-and-mouth disease virus (FMDV)
FMDV pathogenesis
Bovine rhinitis B virus (BRBV) leader proteinase

ABSTRACT

Bovine rhinitis B virus (BRBV) shares many motifs and sequence similarities with foot-and-mouth disease virus (FMDV). This study examined if the BRBV leader proteinase (L^{pro}) could functionally replace that of FMDV. A mutant $A_{24}L_{BRV}3D_{YR}$ FMDV engineered with the BRBV L^{pro} and an antigenic marker in the 3D polymerase exhibited growth properties and eIF4G cleavage similar to parental A_{24}WT virus. The $A_{24}L_{BRV}3D_{YR}$ type I interferon activity in infected bovine cells resembled that of A_{24}LL virus that lacks L^{pro}, but this effect was less pronounced for $A_{24}L_{BRV}3D_{YR}$ infected porcine cells. *In vivo* studies showed that the $A_{24}L_{BRV}3D_{YR}$ virus was attenuated in cattle, and exhibited low virulence in pigs exposed by direct contact. The mutant virus induced protective immunity in cattle against challenge with parental A_{24}WT. These results provide evidence that L^{pro} of different *Aphthoviruses* are not fully functionally interchangeable and have roles that may depend on the nature of the infected host.

Published by Elsevier Inc.

Introduction

Foot-and-Mouth Disease Virus (FMDV) is an extremely contagious disease of domestic cloven-hoofed animals including cattle, pigs, sheep, goats, buffalo and more than 70 wildlife species. The disease is manifested in infected animals by fever, lameness, and appearance of vesicular lesions of the epithelium of the mouth, tongue, teats and feet. The virus rapidly spreads *via* aerosol and replicates in susceptible animal populations with disease appearance in 2–14 days following virus exposure and can last for 7–10 days. Recently, a new species, bovine rhinitis B virus (BRBV) within the *Aphthovirus* genus has been described (Hollister et al., 2008). BRBV causes upper respiratory infections in cattle characterized by elevated body temperature, increased respiration, serous nasal discharge, and macroscopic lesions in the lungs.

FMDV contains a positive-sense, single-stranded RNA of 8500 nucleotides that is surrounded by an icosahedral capsid composed of 60 copies of each of the structural proteins (Grubman and Baxt, 2004). It codes for a single polyprotein that undergoes post-translational cleavage resulting in four structural proteins (VP1, VP2, VP3, and VP4), and ten non-structural proteins (L^{pro}, 2A, 2B, 2C, 3A, $3B_{1-3}$, $3C^{pro}$, and $3D^{pol}$).

The N-terminus of the polyprotein region of FMDV encodes the leader protease (L^{pro}). L^{pro} is a papain-like proteinase (Kleina and Grubman, 1992; Roberts and Belsham, 1995; Skern et al., 1998) that has been shown to be dispensable for virus replication *in vitro* but is a virulence determinant at the host-pathogen level. It is responsible for cleaving itself from the nascent polyprotein as well as cleaving the eukaryotic initiation factor 4G (eIF4G) resulting in the shut-off of cap-dependent host cell translation machinery. Subsequently, a second cleavage of eIF4G occurs during infection that is mediated by the viral $3C^{pro}$ (Belsham et al., 2000). The L^{pro} has been shown to relocate to the nucleus of FMDV-infected cells and to induce degradation of nuclear factor kappa B (NF-κB) with the consequent inhibition of host innate immune response (de Los Santos et al., 2006; de Los Santos et al., 2007). Two different forms of FMDV-L^{pro} (Lab and Lb) are observed depending on usage of first or second AUG start codon. Translation from the first site results in Lab form of L^{pro}, which contains 201 amino acids while the second site produces the predominant, 173 amino acids long Lb form (Cao et al., 1995; Piccone et al., 1995). Deletion of the L^{pro}-coding region in the context of an infectious clone yielded viable virus progeny only when FMDV polyprotein was translated from second AUG site suggesting that the Lb is the biologically relevant form of the L^{pro} protein (Cao et al., 1995; Piccone et al., 1995). Genetically engineered serotype A FMDV viruses which lack L^{pro} have been shown to be infectious, grow more slowly in cell culture

* Correspondence to: Plum Island Animal Disease Center, USDA/ARS/NAA PO Box 848 Greenport, NY 11944-0848. Fax: +1 631 323 3006.
E-mail address: Elizabeth.Rieder@ars.usda.gov (E. Rieder).
[1] Present address: Arthropod-Borne and Infectious Diseases Laboratory, Department of Microbiology, Immunology, and Pathology, Colorado State University, Fort Collins, CO 80523, United States.

0042-6822/$ - see front matter Published by Elsevier Inc.
http://dx.doi.org/10.1016/j.virol.2013.08.035

(Piccone et al., 1995; Uddowla et al., 2012), and are highly attenuated in both cattle and swine (Brown et al., 1996; Chinsangaram et al., 1998; Mason et al., 1997; Uddowla et al., 2012). Marker FMDVs lacking the L^{pro} and harboring negative antigenic sites in 3B and 3D (based on the FMD-LL3B3D virus, Uddowla et al. 2012) were shown to induce low neutralizing antibody titers in these host species, which limited their potential use as live attenuated vaccines. Studies have shown that one of the reasons for the attenuation of the leaderless (L^{pro} deleted) virus was its inability to inhibit cellular translation, specifically translation of type I alpha/beta interferon (IFN α/β) that resulted in increased antiviral effects (Chinsangaram et al., 1999). A recent study has identified a sequence motif, SAP (SAF-A/B, Acinus, and PIAS) in FMDV L^{pro} that when mutated does not alter self-processing and eIF4G cleavage activities but prevents inhibition of NF-κB dependent transcription and confers an *in vivo* attenuated phenotype (de los Santos et al., 2009).

Although the functions of the BRBV L^{pro} are poorly understood, preliminary work suggests that regardless of the sequence divergence (36% amino acid identity), BRBV L^{pro} is likely to play a role and perform similar functions as the FMDV counterpart in viral pathogenesis (Hollister et al., 2008). In this study, we have used oligonucleotide site directed mutagenesis and reverse genetics to construct a mutant FMDV containing $BRVL^{pro}$ and a negative antigenic marker encoded in $3D^{pol}$ ($A_{24}L_{BRV}3D_{YR}$) using a full-length cDNA clone of a highly virulent FMDV strain A_{24}WT (Rieder et al., 2005). This mutant was used to investigate if FMDV L^{pro} can be exchanged with the closely related BRBV L^{pro} both *in vitro* and *in vivo*. We found that the $A_{24}L_{BRV}3D_{YR}$ rescued virus exhibited growth characteristics in BHK-21 cells similar to A_{24}WT, that L_{BRV} released itself at the L/VP4 junction, and induced the cleavage of eukaryotic translation initiation factor eIF4G at early times during infection. Interestingly, BRBV L^{pro} in the context of the chimeric virus was defective at blocking IFN response, with levels comparable to that induced by the L^{pro} deleted mutant FMDV in infected bovine cells, but this effect was less significant in cells of porcine origin. Furthermore, we found that the $A_{24}L_{BRV}3D_{YR}$ virus was attenuated in cattle challenged by aerosolization, and showed mild disease in pigs infected by direct contact with infected pigs.

Results

Derivation and in vitro characterization of $A_{24}L_{BRV}3D_{YR}$

In order to examine whether the BRBV and FMDV L^{pro} proteins were functionally interchangeable, we derived a chimeric $pA_{24}L_{BRV}3D_{YR}$ cDNA clone by exchanging the FMDV L^{pro} for that of BRV (Fig. 1A). In addition, two mutations, $H_{27}Y$ and $N_{31}R$ in the $3D^{pol}$ were introduced to function as a negative antigenic marker (as described in our previous studies, (Uddowla et al., 2012). This clone was linearized, transcribed into RNA, electroporated and the virus phenotype was studied following passages in BHK-21 cells. The chimeric virus produced cytopathic effects (CPE) comparable to A_{24}WT during the early passages. Moreover, full virus sequence analysis of the $A_{24}L_{BRV}3D_{YR}$ virus recovered from passage 5 showed the presence of the BRBV L^{pro} with the engineered marker mutation in the $3D^{pol}$ region without additional changes. For phenotypic characterization of the chimeric virus, we also examined a previously described $A_{24}L_{FMDV}3D_{YR}$ virus carrying the FMDV L^{pro}, and mutations in $3D^{pol}$ that creates a negative antigenic marker (Uddowla et al., 2012). This particular marker virus has been shown to be similar to the parental A_{24}WT virus in plaque morphology, growth kinetics, and pathogenicity in cattle (Uddowla et al., 2012) (Fig. 1).

First, the plaque morphologies of the mutant and wild-type (WT) viruses were found to be similar (Fig. 1B). Secondly, a multi-step growth kinetics performed using a high multiplicity of infection (MOI=5) in BHK-21, LFBK, and IBRS-2 cells (Fig. 2A) showed no significant difference in the growth pattern in all three cell lines. Third, in Western blot analysis, the A_{24}WT and $A_{24}L_{BRV}3D_{YR}$ viruses exhibited similar kinetics of cleavage of eIF4G. In particular, both viruses exhibited partial cleavage of eIF4G by 3 h post-infection (hpi) with complete cleavage by 6 hpi (Fig. 2B). Moreover, the presence of another non-structural viral protein, 3B, was similarly detected in both virus-infected cell extracts at 3 hpi. As expected, Western blot analysis showed only a positive reaction with the parental A_{24}WT virus, but not with the marker virus using a 3D-specific monoclonal antibody (mAb) that recognizes the $3D^{pol}$ epitope mutated in the $A_{24}L_{BRV}3D_{YR}$ chimera (Fig. 2B) (Uddowla et al., 2012). This negative marker can serve as a useful tool to antigenically distinguish the chimeric virus from FMDV field strains. Consistent with the *in vitro* growth patterns, the VP1 capsid protein was detected by Western blot with both viruses by 6 hpi suggesting that the chimeric virus was able to undergo viral protein synthesis and processing with similar kinetics as the A_{24}WT virus (Fig. 2C).

Induction of antiviral activity by $A_{24}L_{BRV}3D_{YR}$

Previous work has shown that supernatants from cells infected with leaderless (LL) mutant FMDV induce higher levels of type I interferon (IFN α/β) activity when compared to supernatants from WT infected cells (Chinsangaram et al., 1999). Experiments were

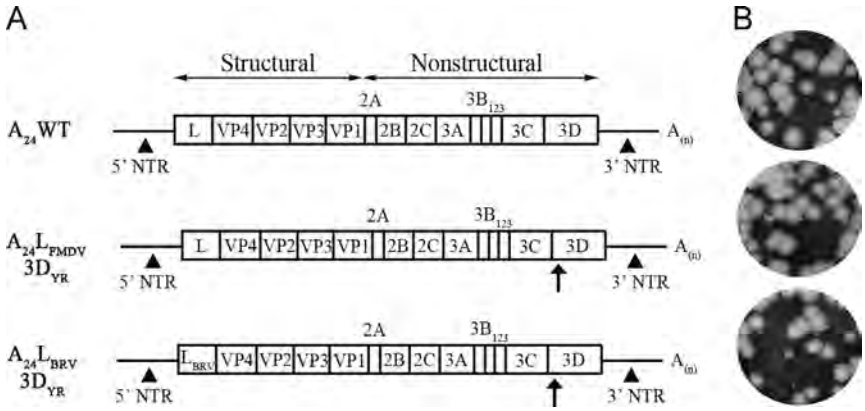

Fig. 1. Schematic representation of viral constructs used in this study. The $A_{24}L_{FMDV}3D_{YR}$ virus contains the FMDV L^{pro} as well as a mutation in $3D^{pol}$ that introduces a negative antigenic site marker (see arrow). In the $A_{24}L_{BRV}3D_{YR}$ virus, the. FMDV L^{pro} is replaced by the corresponding coding sequence of BRBV. In addition, the mutation in $3D^{pol}$ is also present in the chimeric $A_{24}L_{BRV}3D_{YR}$ virus. (B) Plaque size assessment of A_{24}WT, $A_{24}L_{FMDV}3D_{YR}$, and $A_{24}L_{BRV}3D_{YR}$ viruses in BHK-21 cells. Cells were infected and after 1 h adsorption, 0.6% gum tragacanth overlay was added, followed 48 h later with crystal violet staining.

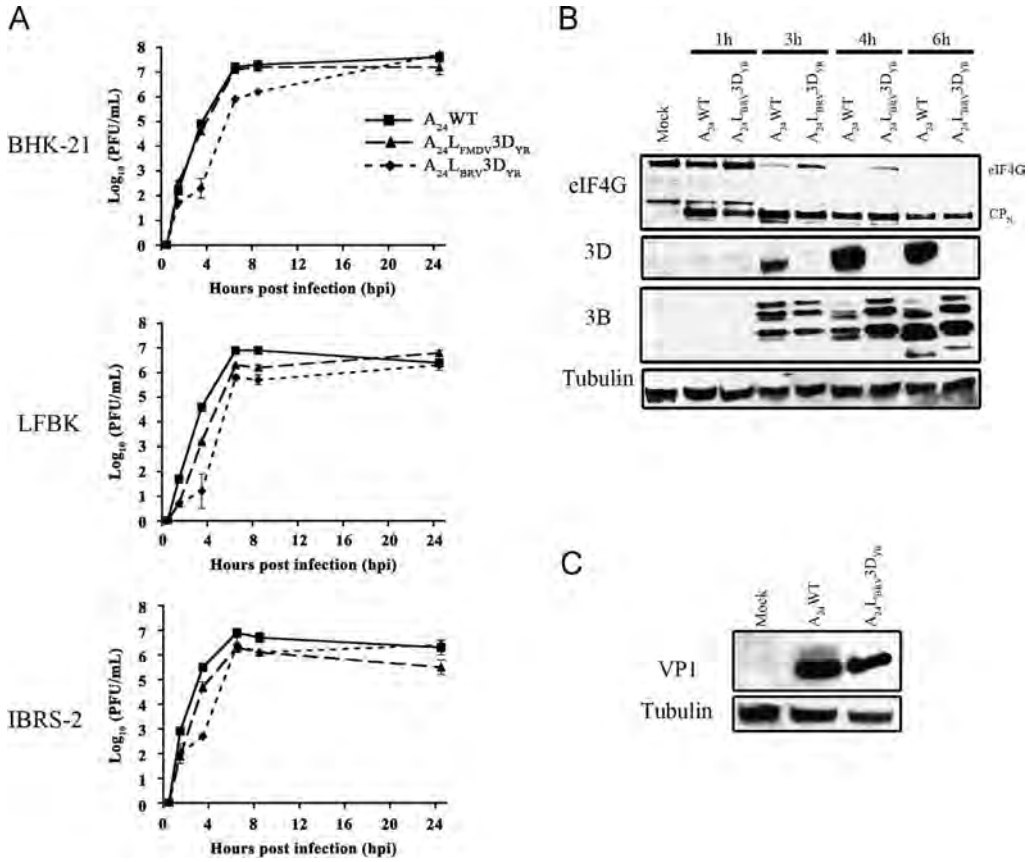

Fig. 2. *In vitro* characterization of $A_{24}L_{BRV}3D_{YR}$. (A) Multi-step growth kinetics of A_{24}WT, $A_{24}L_{FMDV}3D_{YR}$, and $A_{24}L_{BRV}3D_{YR}$ viruses in BHK-21, LFBK and IBRS-2 cell lines infected at a MOI of 5. (B) Detection of eIF4G intact and cleavage product. Lysates of LFBK cells infected with either A_{24}WT or $A_{24}L_{BRV}3D_{YR}$ viruses were separated on SDS-PAGE. Western blot analysis was performed using anti-FMDV 3B and $3D^{pol}$ as well as anti-eIF4G antibodies. The N-terminus eIF4GI cleavage product (CP_N) that is recognized by the rabbit polyclonal sera used in this experiment is indicated. (C) Capsid processing by $A_{24}L_{BRV}3D_{YR}$. Lysates of LFBK cells infected with either A_{24}WT or $A_{24}L_{BRV}3D_{YR}$ viruses were analyzed by Western blot using anti-VP1 antibody.

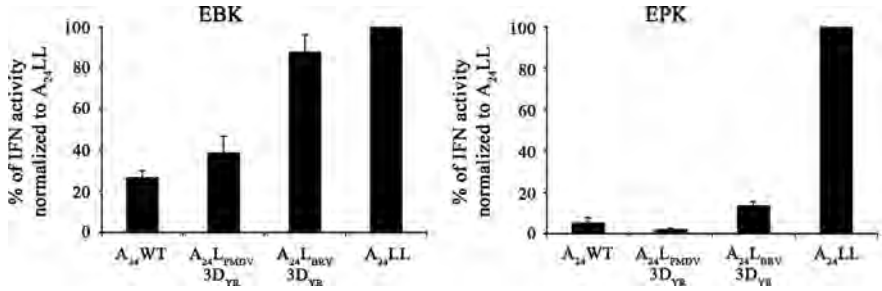

Fig. 3. Antiviral activity of $A_{24}L_{BRV}3D_{YR}$ virus. Biologically active type I IFN was measured by *Mx*/CAT ELISA. Bovine (EBK) and porcine (EPK) cells were infected with A_{24}WT, $A_{24}3D_{YR}$, $A_{24}L_{BRV}3D_{YR}$ and A_{24}LL viruses at a MOI of 5. Supernatants were used to treat MDBK-t2 cells, and CAT binding was measured after 24 h. Results are expressed as percent (%) of IFN activity normalized to the activity of A_{24}LL virus. Note that the net values for porcine IFN were ten times lower than those observed in bovine cells.

designed to examine $A_{24}L_{BRV}3D_{YR}$-induced antiviral activity by using an *Mx*/CAT ELISA reporter system that has been validated to measure biologically active type I IFN (Chinsangaram et al., 1999; Fray et al., 2001). To this end, embryonic bovine and porcine cells (EBK and EPK, respectively) were infected with A_{24}WT, A_{24}LL, $A_{24}L_{FMDV}3D_{YR}$, and $A_{24}L_{BRV}3D_{YR}$ viruses at a MOI of 5, and supernatants were collected 24 hpi to determine Mx promoter mediated expression of CAT, using CAT ELISA, as a measure of type I IFN activity. A mutant of A_{24}WT virus that lacks the L^{pro} coding region so-called A_{24}LL, recently characterized (Uddowla et al., 2012) was used as a positive control since the absence of L^{pro} has been implicated in increased antiviral activity in cells (Chinsangaram et al., 1999). Embryonic kidney cells were used in this experiment as other FMDV-susceptible established cell lines have been shown to exhibit impaired type I IFN response (Chinsangaram et al., 2001; Chinsangaram et al., 1999). Fig. 3 shows that EBK cells infected with A_{24} $L_{BRV}3D_{YR}$ produced similar levels of antiviral activity as in A_{24}LL (virus lacking L^{pro}) in infected cells. Although the overall levels of IFN obtained in EPK cells were 10 times lower than those observed in EBK, A_{24} $L_{BRV}3D_{YR}$ exhibited a significantly reduction on type I IFN activity when these values were compared to those of the A_{24}LL virus in EPK cells (Fig. 3). These results suggest that the chimeric virus induced lower levels of type I IFN production in cells of bovine and porcine origin. It suppressed antiviral activity in EPK cells similarly to A_{24}WT while it induced higher IFN activity in EBK cells when compared to the A_{24}WT virus.

Virulence and protection study in cattle

In order to investigate the infectivity and virulence of $A_{24}L_{BRV}3D_{YR}$ in cattle, two steers (#37 and #38) were infected *via* a simulated natural (aerosol) inoculation route that has been successfully utilized previously (Arzt et al., 2010; Pacheco et al., 2010). During the course of 21 days post-infection (dpi) neither steer had fever, vesicles, or other clinically detectable abnormalities consistent with FMD (Fig. 4). Despite the absence of clinical signs, there was evidence of sub-clinical infection in both steers although the infection dynamics was quite different between the two animals as judged by measurements of viral RNA in blood, saliva, and nasal swab samples. In particular, steer #37 had minimal and intermittent detectable $A_{24}L_{BRV}3D_{YR}$ RNA in secretions (maximum 3 logs RNA CN/ml), and all swab samples were negative by virus isolation (VI) (data not shown). Similarly, sera were RNA-negative and VI-negative at all times. At the time of challenge with virulent FMDV (21 dpi), this animal exhibited a serum neutralizing antibody titer (SN) of 1.2 $\log_{10}$ (Table 1). Despite the lack of clinical signs (Fig. 4), substantially more $A_{24}L_{BRV}3D_{YR}$ RNA and infectious virus were recovered from steer #38. Viral RNA was detected in nasal and oral swabs from 5–9 dpi (maximum RNA CN/ml = 5.86, 8 dpi, oral). Steer #38 exhibited viremia from 4–8 dpi as determined by rRT-PCR and 4–7 dpi by VI (Fig. 4, data not shown). At the time of challenge with virulent FMDV (21 dpi), the SN titer of steer #38 was 2.4 $\log_{10}$.

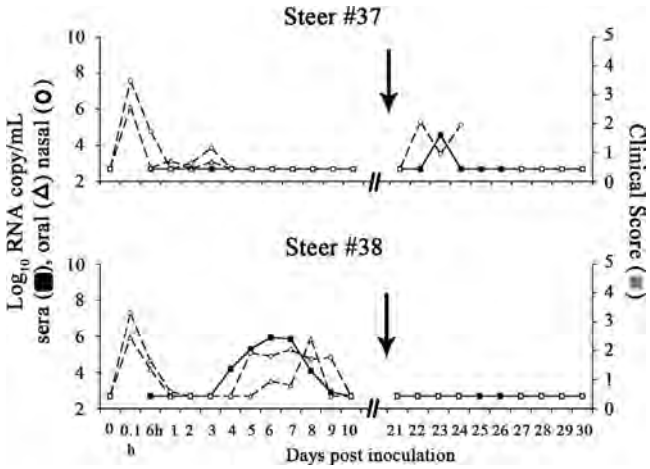

Fig. 4. Assessment of $A_{24}L_{BRV}3D_{YR}$ virus virulence in cattle. Animals were inoculated with aerosol containing 1.7×10^6 $TCID_{50}$ of $A_{24}L_{BRV}3D_{YR}$ virus and were monitored for clinical disease for 21 days. On day 21 post inoculation (arrows), both animals were challenged with 10^4 $TCID_{50}$ of FMDV A_{24}WT virus. Viral RNA in serum (■), oral (Δ) and nasal (○) samples are expressed in the left axes; clinical scores (bars) are expressed in the right axes.

Table 1
Specific neutralizing antibody response and protection against challenge with FMDV A_{24}WT strain after aerosol infection with $A_{24}L_{BRV}3D_{YR}$ virus in cattle.

Bovine #	Neutralization titer (days post inoculation)							Protection[c]
	0	7	14	21[b]	28	35	42	
37	< 0.9[a]	< 0.9	< 0.9	1.2	3.0	3.0	3.0	Yes
38	< 0.9	< 0.9	2.4	2.4	3.0	3.3	3.0	Yes

[a] Virus neutralizing titers of serum antibody responses ($\log_{10}$ of reciprocal of the last serum dilution to neutralize 100 $TCID_{50}$ of virus in 50% of the wells). Sensitivity > 0.9.
[b] Day of challenge.
[c] Cattle were challenged by intradermolingual inoculation of 4 $\log_{10}$ bovine tongue infectious doses of FMDV A_{24}WT.

Based on the immune response observed in cattle experimentally infected with $A_{24}L_{BRV}3D_{YR}$ in the absence of clinical FMD signs, an investigation was pursued to determine whether these animals could be protected against challenge with the parental A_{24} WT virus at 21 dpi *via* intradermolingual route (IDL). For 21 days post challenge (dpc), neither steer had any fever or vesicles beyond the inoculation site (Fig. 4, Table 1). Despite the lack of clinical scores, the challenged steers exhibited limited systemic dissemination of challenge virus with some variation. Detailed examination of steer #37 (limited subclinical $A_{24}L_{BRV}3D_{YR}$ infection; challenge SN = 1.2) indicated that this animal had lingual vesicles at 1 dpc, exhibited viremia at 2 dpc (23 dpi), and shed virus in nasal secretions from 1–3 dpc (22–24 dpi). In contrast, steer #38 (milder subclinical $A_{24}L_{BRV}3D_{YR}$ infection; challenge SN = 2.4) never developed lingual vesicles; only blanching of lingual epithelium was apparent at 2 dpc (23 dpi), which was more evident at 4 dpc (25 dpi) when the affected epithelium began to slough. Moreover, steer #38 was never viremic subsequent to challenge. Both steers were euthanized at 42 dpi/21 dpc for necropsy and tissue collection. Viral RNA and infectious virus were recovered from the nasopharyngeal mucosa and draining lymph nodes of both animals (Arzt et al., manuscript in progress).

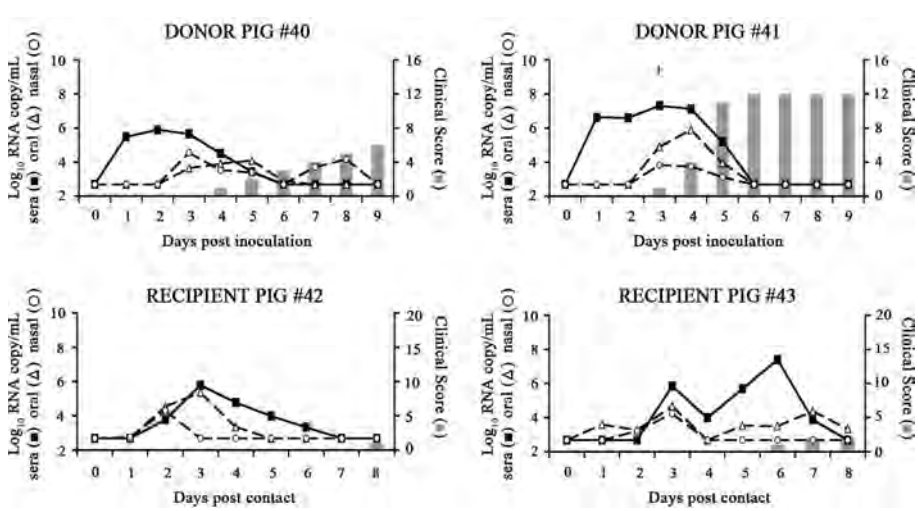

Fig. 5. Assessment of $A_{24}L_{BRV}3D_{YR}$ virus virulence in swine. Two donor pigs (#40 and #41) were directly inoculated into the foot bulb with 10^6 $TCID_{50}$ of $A_{24}L_{BRV}3D_{YR}$. After 24 h, two recipient pigs (#42 and #43) were brought into contact with donor animals and housed in the same room for the next eight days. Viral RNA in serum (■), oral (Δ) and nasal (○) samples are expressed in the left axes; clinical scores (bars) are expressed in the right axes + denotes fever (> 40 °C).

Although the distribution of viral RNA was similar in both steers, infectious virus was recovered from more tissues of steer #37.

Virulence study in pigs

Next, we carried out experiments to investigate the pathogenic characteristics of $A_{24}L_{BRV}3D_{YR}$ in swine by direct contact infection that simulates a natural route of exposure. To this end, two donor pigs (#40 and #41) were inoculated in the heel bulb of the rear feet with the chimeric virus, brought into contact with two naïve pigs 24 h later (recipient pigs, #42 and #43), and subsequently all animals were monitored for 9 dpi/8 dpc for clinical signs of disease and characterizing virus dynamics. The clinical signs in donor pigs were moderately attenuated compared to what we have previously observed in animals infected with the parental A_{24}WT virus using this route and similar dose (Fig. 5) (Dias et al., 2011; Pacheco et al., 2012). One donor pig developed fever only on day 2, but both animals exhibited lesions at non-inoculation sites, with pig #40 showing lower clinical score. Both animals were viremic at 1 dpi and first developed vesicles at non-inoculation sites at 3–4 dpi. The clinical manifestations of disease in recipient (contact-challenged) pigs were substantially milder (score 1–2) and delayed compared to the donor directly inoculated pigs (score 6–12). These recipient pigs showed RNA in blood at 2–3 dpc and vesicles appeared not earlier than 6–8 dpc. Maximum detection of virus in swab samples occurred at 3–4 dpi for donor pigs and 3 dpc for both contact-exposed pigs.

Homology modeling of BRBV L^{pro}

In our previous studies, we showed that the FMD and BRBV virus L^{pro} exhibits only 24% invariable amino acids including key catalytic residues necessary for cleavage at the L/VP4 junction and of eIF4G (Hollister et al., 2008). We therefore examined the structural elements that distinguish the BRBV L^{pro} from the FMDV counterpart using computer-modeling software. A homology model was built for BRBV L^{pro} using 173 amino acids of a type O FMDV Lb^{pro} for a template (PDB 1QOL, Chain A). As shown in Fig. 6A, BRBV Lb^{pro} (pink) had high homology with FMDV L^{pro} (olive) in terms of its overall three dimensional structure. Despite overall homology, at the N-terminus, the β1- and β2 strands of BRBV L^{pro} are connected by a long disordered loop, ELGFNNTLV-TADLDGNE (Fig. 6Ai). In contrast, the loop connecting β1- and β2 strands in FMDV L^{pro} is formed by the tripeptide, LYN for serotype O, which is LHN in A_{24}WT. Fig. 6 Aii shows critical C-terminal residues of the two proteases where significant differences were observed. In particular, a stretch of nine amino acids at the C-terminus of BRBV L^{pro} forms an uncharged hydrophobic surface (AEFFKQVYL, Fig. 6 Aii shown in pink). In contrast, the corresponding region of FMDV L^{pro} consists of charged residues (KAKVQRKLK, Fig. 6 Aii shown in olive); the abundance of uncharged residues being 67% and 33% in BRBV and FMDV L^{pro}, respectively. In addition, BRBV L^{pro} is rich in aromatic and non-polar amino acid side chains at the surface while FMDV L^{pro} has higher percentage of charged and polar side chains at the surface. In spite of these differences and relatively low sequence conservation between FMDV and BRBV L^{pro}, the proteases have identical active sites (Fig. 6 Aiii) and conserved key domain residues necessary for interaction with eIF4G within the L^{pro} C-terminal extension (data not shown, (Foeger et al., 2002)). Fig. 6B shows the electrostatic surfaces of the two proteases with peptide entry channels depicted with green arrows. The floor of the peptide channel is more positively charged in BRBV L^{pro} while it is comparatively neutral in FMDV L^{pro}. The peptide exit channel of BRBV protease is narrower in comparison to that of FMDV and flanked by lysine.

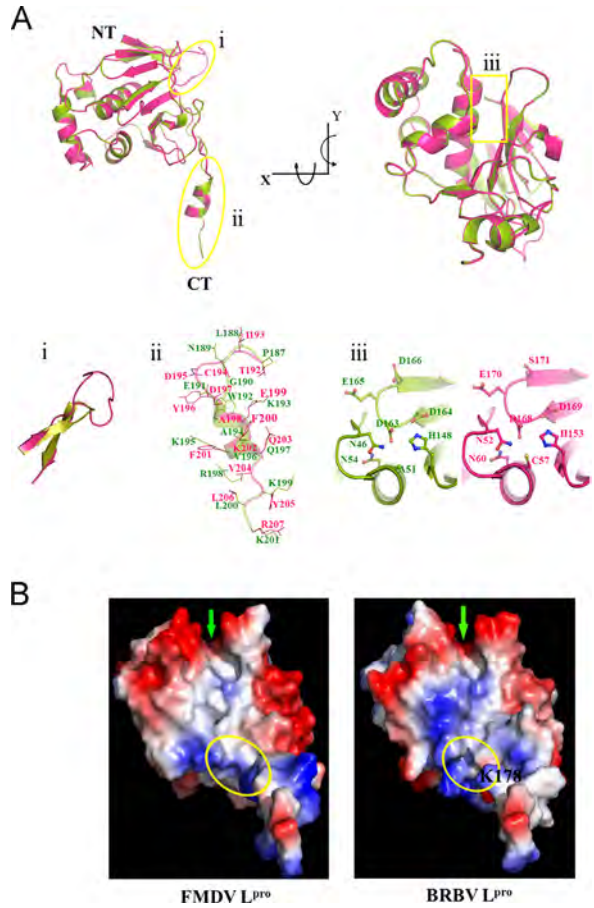

Fig. 6. Structure of BRBV L^{pro} homology model. (A) BRBV L^{pro} (pink) superimposed onto FMDV L^{pro} (olive). In order to highlight the key regions showing structural differences the two protease structures were rotated as indicated in comparison to the initial description of the FMDV leader protease structure showing left and right half formed by α-helical and β-sheet structures and active site in top view, see right panel (Guarne et al., 1998). Inset i shows large long disordered loop, ELGFNNTLV-TADLDGNE connecting N-terminal β1- and β2 strands of BRBV L^{pro} in comparison with small tripeptide, LYN that connects β1- and β2 strands in FMDV L^{pro} crystal structure. Inset ii describes the C-terminus of the two proteases. The amino acid residues of the two proteases are marked with the text in same color (pink for BRBV L^{pro} and olive for FMDV Lpro). Inset iii highlights the conservation of catalytically important amino acid residues (shown as ball and stick) and their positioning in two proteases. The carbon atoms of the sticks are colored as parent chain (pink for BRBV and olive for FMDV L^{pro}), whereas oxygen, nitrogen and sulfer are colored red, blue and yellow, respectively. (B) Electrostatic surface of the FMDV and BRBV L^{pro}. Peptide exit channel is encircled by lysine side chain (K178) in BRBV L^{pro} (yellow oval), whereas FMDV L^{pro} has open peptide exit channel. The peptide entry channel is shown by green arrow. Blue–white–red colors represent most positive, neutral and negatively charged surfaces, respectively.

Discussion

Picornavirus-encoded proteinases are known to perform critical functions in the cleavage of the polyprotein precursor as well as of cellular proteins targeted in a very regulated fashion. Currently, the L^{pro} has been firmly implicated in pathogenesis of FMDV. Genetic studies with a leaderless FMD mutant virus have shown that L^{pro} is not required for viral replication in cell culture, but cattle and swine inoculated with the mutant virus exhibited significant attenuation in both species (Brown et al., 1996; Chinsangaram et al., 1998; Mason et al., 1997; Piccone et al., 1995; Uddowla et al., 2012). Moreover, earlier studies have shown that aerosol exposure of cattle with the leaderless virus failed to spread systemically and resulted in limited replication in the lungs (Brown et al., 1996). *In vitro* evidence also suggested that this attenuation is most likely due to the inability of the leaderless

virus to inhibit IFN production in the host. In fact, a type A leaderless mutant virus has been shown to be unable to prevent host translation of IFN α/β mRNAs and secretion of type I IFN products, thus facilitating the rapid clearance of the virus from the host (Chinsangaram et al., 1999).

In this study, we sought to generate a chimeric FMD virus to investigate the extent by which FMDV L^{pro} can be exchanged with the closely related BRBV L^{pro} (Hollister et al., 2008) and assess its applicability to a live attenuated vaccine. *In vitro* characterization of the chimeric $A_{24}L_{BRV}3D_{YR}$ virus provided evidence of partial functional replacement between FMDV and BRBV L^{pro}. In particular, the chimeric virus carrying L_{BRV} displayed similar plaque phenotype and titer in BHK-21 cells as well as comparable growth kinetics as the A_{24}WT in hamster, bovine and porcine cell lines (BHK-21, LFBK and IBRS-2, respectively). Moreover, BRBV L^{pro} in the context of a FMDV backbone exhibited the same protease activity as FMDV L^{pro}, and was able to cleave eIF4G in a similar fashion without significant detrimental effects on downstream viral polyprotein processing (Fig. 2). This was evident regardless of the sequence differences present at the L^{pro}-VP4 junctions (A_{24}WT:QKLK↓GAGQSSP; BRBV:VYLR↓GAGSSKP and $A_{24}L_{BRV}3D_{YR}$: VYLR↓GAGQSSP). On the other hand, we sought to determine if BRBV L^{pro} could block host innate immunity just like the FMDV counterpart, and based on *Mx*/CAT ELISA results, we found that $A_{24}L_{BRV}3D_{YR}$ elicited an antiviral activity in bovine cells that resembles that found with an attenuated, leader deleted FMDV mutant (Fig. 3). Specifically, EBK cells (bovine origin) infected with $A_{24}L_{BRV}3D_{YR}$ virus secreted similar levels of type I IFN as A_{24}LL-infected cells using a *Mx*/CAT ELISA reporter system. The high levels of type I IFN was in sharp contrast to A_{24}WT and cells infected with FMDV-containing L^{pro} and a marker in $3D^{pol}$ ($A_{24}L_{FMDV}3D_{YR}$) where the IFN response was more limited. The type I IFN response obtained with the control A_{24}WT virus in infected bovine cells was consistent with reports showing lower levels of antiviral activity in cells infected with a type A FMDV compared to supernatants from LL-mutant infected cells (Chinsangaram et al., 1999). For reasons we cannot explain, it is noteworthy that in infected porcine cells the type I IFN values were lower (by approximately 10 fold) than those observed in bovine cells. Despite this fact, and in contrast with the observations in bovine cells, the levels of IFN induced by the chimeric $A_{24}L_{BRV}3D_{YR}$ virus in EPK cells (porcine origin) were significantly lower to those of the A_{24}LL virus.

Recently, a controlled aerosol inoculation system to deliver virus in cattle has been described, which mimics a natural route of exposure (Pacheco et al., 2010). In the current study, a preliminary experiment using this delivery method in cattle with 10^6 $TCID_{50}$ of chimeric $A_{24}L_{BRV}3D_{YR}$ virus did not show any clinical signs of disease including vesicular lesions and fever. Examination of two cattle following virus exposure showed detectable viral RNA in both nasal and oral swabs within 10 min of inoculation, (as shown in Fig. 4), indicating that the virus was successfully delivered. Although sub-clinical in both cases, the dynamics of viral replication showed differences between the two infected animals. For instance, one animal had minimal levels of viral RNA in sera and swab samples with low serum neutralization titer (1.2 at 21 dpi), while the second animal had more significant levels of viral RNA in blood oral and nasal swaps and higher serum neutralization titer (2.4 at 21 dpi) prior to challenge. We believe the low virulence of $A_{24}L_{BRV}3D_{YR}$ chimera is most likely due to the contribution of BRBV L^{pro} and not to the mutations engineered in 3D, based on studies in our laboratory showing that aerosol inoculation with 10^6 $TCID_{50}$ of 3D mutant $A_{24}L_{FMDV}3D_{YR}$ virus (carrying the FMDV L^{pro}) in cattle, resulted in classical FMD disease (Uddowla et al., 2012). The immune response induced by the chimeric virus resulted in protection of both animals against an IDL challenge with A_{24}WT, following the OIE recommendations protocol for vaccine trials. Viral RNA was recovered from the lungs and nasopharynx of cattle following exposure and challenge with $A_{24}L_{BRV}3D_{YR}$ and A_{24}WT, respectively (data not shown). Therefore, further studies are being carried out to identify and characterize the distribution of the virus in tissues collected during necropsy. Nevertheless, the sites of viral recovery are consistent with the profiles previously observed in cattle that received aerosol inoculation with parental FMDVs and attenuated L^{pro} mutant viruses (Arzt et al., 2010; Brown et al., 1996).

To determine if the $A_{24}L_{BRV}3D_{YR}$ virus induces disease in other susceptible species, a contact transmission experiment in pigs was also investigated. Inoculation of two donor pigs *via* the intradermal route (heel bulb) with the chimeric virus resulted in viremia and signs of clinical disease by days 3 and 4 (Fig. 5). In these animals, the extent of the clinical disease and dynamics of the viral infection were moderately attenuated relative to previous studies using this route of inoculation in pigs and doses of 10^5–10^7 $TCID_{50}$ of parental A_{24}WT-virus (full-blown FMD) (Dias et al., 2011; Pacheco et al., 2012). For instance, the levels of viral RNA in secretions were significantly lower to those previously observed in A_{24}WT inoculated animals. In addition, these donor animals did not exhibit fever during the entire course of the experiment, and had clinical scores of 6–12 at the end of 9 dpi. The contact challenged pigs (recipient pigs #42 and #43) exhibited a significant delay in the manifestation of clinical symptoms and a milder form of FMD. The low virulence observed in recipient pigs could be the result of the additive effect of reduced virus replication and shedding, resulting from limited transmission of the virus and a reduced virulence of the chimeric virus expressing the BRBV L^{pro} in this species. Together, the data suggest that the FMDV L^{pro} might be more effective or better fit to the environment within the FMDV-targeted cells in the host, than the BRBV L^{pro}, in agreement with the fact that FMDV grows faster, produces higher titers, and spreads more rapidly than BRBV. The observed disease caused by the chimeric virus in directly inoculated pigs, could be the result of the high susceptibility of this species combined with the intradermal route of inoculation, which bypasses most of the primary mechanisms of defense against viral infections. In contrast, swine in direct contact with these animals, a more natural route of infection, showed very limited clinical disease. Although evidence for intertypic and intratypic recombination has been described for FMDV (Simmonds, 2006), to the best of our knowledge, there are no reports documenting naturally occurring recombination between the closely related FMDV and BRBV. Since swine are not a natural host for BRVB it is unlikely that a recombination event with FMDV could occur in this species. Additionally, the low transmission profile and reduced *in vivo* replication kinetics shown by the engineered $A_{24}L_{BRV}3D_{YR}$ virus described here suggests less favorable conditions for natural selection with respect to field FMDV isolates.

In an effort to determine if sequence motifs and/or structural elements of the BRBV and FMDV L^{pro} are significantly different, we performed model predictions for L_{BRV} and compared them to the known features and three-dimensional structure of FMDV L^{pro}. Specifically, the analysis revealed that the active site of BRBV L^{pro} is very similar to FMDV L^{pro}. The catalytic triad in BRV proteinase is formed by C57, H153 and D158, which correspond to C51, H148 and D163 in FMDV L^{pro}. Despite this similarity, the N-terminus of BRBV L^{pro} has a long disordered loop, which is absent on the FMDV L^{pro}. The entire loop is surface-exposed on the BRBV L^{pro} indicating its possible role in interaction with other protein(s) or importance in maintaining the structure/function of the protein during the infection of the host cell. Future studies will investigate the role of this loop by mutational analysis in BRBV L^{pro} and FMDV L^{pro}. Interestingly, the C-terminus of BRBV L^{pro} is highly hydrophobic in

contrast to highly charged C-terminus of FMDV L^{pro}. This was also consistent with our observations that expression of recombinant BRBV L^{pro} in *Escherichia coli* was purified from insoluble fraction whereas similar expression system used for FMDV L^{pro} purified this protein from soluble fractions (data not shown). This suggests possible alterations in BRBV L^{pro} behavior in the intracellular membranous web, which is the primary site of replication of picornaviruses. It is important to note that BRBV L^{pro} in the context of the chimeric virus was self-processed and produced eIF4G cleavage products similar to the FMDV counterpart but we observed a less efficient IFN blocking activity in cells of bovine origin when compared with A_{24}WT virus. A recent study by Pineiro et al. (2012) calls for more investigation into the proteins that interact with/processed by Leader protease in the cell. Nogueira Santos et al. (2012) performed FMDV L^{pro} cleavage of a number of synthetic peptides and concluded that although L^{pro} recognizes its substrate very specifically, it is the presence not the order of positively charged (K/R) and small amino acids (G/A) that is critical to L^{pro} activity. The observed differences in N and C-terminus of the BRBV and FMDV L^{pro} as well as the relatively high abundance of positive charge at the floor of peptide binding cleft of BRBV L^{pro} suggests that this differences may have impacted L^{pro} interaction with host-specific factor/s.

The pathogenic outcome of FMDV infection in the natural host is determined by the complex interplay between highly regulated functions performed by the virus and the host counteracting response. In the current study, we demonstrated the feasibility to exchange the FMDV L^{pro} by the BRBV counterpart, and confirmed previous reports that pathogenic properties of the virus directly correlates with the ability of L^{pro} to modulate the innate immune response. Our observations of partial functional correspondence among related L^{pro} also suggest that within the *Aphthovirus* genus, the L^{pro} might have evolved to adapt to the different replication fitnesses of the respective viruses.

Materials and methods

Viruses, cell lines and plasmids

A baby hamster kidney cell line (BHK-21) (ATCC, catalog number CCL-10) was maintained in Eagle's basal medium (BME) (Gibco) supplemented with 10% bovine calf serum (BCS) (Hyclone), 10% Tryptose phosphate broth (Sigma), and antibiotic/antimycotic (Gibco). Monolayers of a bovine kidney cell line (LFBK) (Swaney, 1988) and a porcine kidney cell line (IBRS-2) (de Castro, 1964) were grown in Eagle's minimal essential medium (EMEM) and Dulbecco's modified Eagle's medium (DMEM), respectively, containing 10% fetal calf serum (FCS) (Hyclone) and antibiotic/antimycotic. Embryonic bovine and porcine kidney cell lines (EBK and EPK, respectively) were kindly provided by Dr. S. Wessman, USDA, APHIS, Ames, Iowa. EBK and EPK cells were maintained in EMEM supplemented with 20% FBS, antibiotics and nonessential amino acids. Madin-Darby bovine kidney (MDBK-t2) cells transfected with plasmid expressing the human *MxA* promoter linked to a chloramphenicol acetyltransferase (CAT) reporter were kindly provided by B. Charleston (Institute for Animal Health, Pirbright, United Kingdom). MDBK-t2 cells were maintained in DMEM supplemented with 10% FBS, antibiotics, glutamine, sodium pyruvate (Invitrogen), and 10 μg/mL blasticidin (Invitrogen). All cells were grown at 37 °C in a humidified chamber with 5% CO_2 atmosphere. FMDV type A_{24} Cruzeiro was derived from the infectious cDNA clone pA_{24}Cru (called here for simplicity A_{24}WT (Rieder et al., 2005)). A plasmid containing the bovine rhinovirus type 2 (pBRBV, accession number EU236594) sequence from poly(C) to poly(A) described previously (Hollister et al., 2008) was used as a source of bovine rhinovirus genetic material. In order to derive $pA_{24}L_{BRV}$, gene fragments were amplified using primers P1325 (5′-CCAACTGACACAAACCGTGCAATT) and P1328 (5′-GAAGTCTCTCATAGTCATTCCTGTGGCTCGTGGTAGG) from pA_{24} Cru template and P1327 (5′-CCTACCACGAGCCACAGGAATGACTACT-GAGAGACTTC) and P1326 (5′- CTGGATTGGCCGGCCCCTCTCAAGTA-CACTTGTTTGA) from pBRBV.

The two PCR products were subsequently used as templates to generate a 1000 bp fragment using P1325 and P1326 that contained the complete BRBV leader sequence. The product was then inserted into a LL pA_{24} using *XbaI* and *FseI* restriction sites in order to generate $pA_{24}L_{BRV}$. In addition, mutations at codons 27 and 31 of protein $3D^{pol}$ were introduced by PCR utilizing mutagenic oligonucleotides P1266 (5′-ACCGTTGCGTACGGTGTGTTCCGTCCTGAGTTCGGG) and P1267 (5′-CCCGAACTCAGGACGGAACACACCGTACGCAACGGT). The derivation of $pA_{24}3D_{YR}$ ($pA_{24}L_{FMDV}3D_{YR}$) was described previously (Uddowla et al., 2012). The generated plasmids pA_{24}Cru, $pA_{24}L_{FMDV}3D_{YR}$, and $pA_{24}L_{BRV}3D_{YR}$ all contain a T7 promoter sequence in front of a hammerhead ribozyme at the 5′ terminus of the S fragment of the FMDV genome, and terminates with a poly (A) tract of 15 residues. Full-length genomic clones were linearized with *SwaI* and *in vitro* transcribed using the T7 Megascript system (Ambion, Austin, TX). Transcript RNAs were transfected into BHK-21 cells by electroporation as previously described (Rieder et al., 1993). The electroporated cells were seeded in 6-well plates and incubated for 24–48 h at 37 °C and 5% CO_2. Viruses were serially passaged up to 4 times in BHK-21 and were stored at −70 °C. All viruses were sequenced entirely, and titers were determined by plaque assays as described below.

Viral growth and plaque assays

For virus growth curves, BHK-21, LFBK and IBRS-2 cells were infected with A_{24}WT, $A_{24}L_{FMDV}3D_{YR}$ or $A_{24}L_{BRV}3D_{YR}$ at a multiplicity of infection (MOI) of 5 plaque forming units (PFU/cell). After 1 h of adsorption at 37 °C, cells were rinsed with MES buffer (Morpholine Ethane Sulfonic acid 25 mM, 145 mM NaCl, pH 5.5), then twice with PBS, followed by addition of fresh BME without serum. At 1, 3, 6, 8, and 24 hpi, viral titers were determined by inoculating BHIK-21 cells with dilutions of each virus. After 1 h of adsorption, tragacanth gum overlay (0.6%) was added, and the cells were further incubated for 48 h at 37 °C. Plates were fixed, stained with crystal violet (0.3% in Histochoice; Amresco, Solon, Ohio), and the plaques were counted. The assay was performed in triplicate, and titers were expressed as $\log_{10}$ of PFU per milliliter (PFU/mL).

Western blot

LFBK cells were mock-or infected with A_{24}WT or $A_{24}L_{BRV}3D_{YR}$ at a MOI of 5. At 1, 3, 4 and 6 hpi, infected cells were lysed with RIPA buffer (1 × phosphate buffered solution supplemented with 1% NaDOC, 0.1% SDS and protease inhibitors) and stored at −70 °C until further use. Eight microliters of cell lysates were run under denaturing conditions in 12% Bis-Tris SDS-PAGE gels (Invitrogen) and transferred onto nitrocellulose membranes using XCell II™ transfer system (Invitrogen). The blots were probed with FMDV-specific monoclonal antibodies (mAbs) 6HC4 (1:8) (Robertson et al., 1984), 40C8 (1:750) and F32-44 (1:200) to detect VP1, 3B and presence or absence of mutations in the 3D region, respectively. mAbs 40C8 and F32-44 were kindly provided by Dr. Alfonso Clavijo (TVMDL, Texas A&M, College Station, TX). Cell lysates were also run in a 3–8% Tris–Acetate SDS-PAGE gel (Invitrogen) and blotted against rabbit polyclonal eIF4G specific for the N-terminus (1:1000, Bethyl Laboratories) to evaluate the cleavage capabilities of the viruses. Alpha-tubulin (1:1000, Abcam) was used as a loading control.

Antiviral activity of $A_{24}L_{BRV}3D_{YR}$ virus

A *Mx* promoter-chloramphenicol acetyltransferase (*Mx*/CAT) reporter gene assay used to determine biologically active type I IFN was previously described (Fray et al., 2001). EBK and EPK cells were infected with A_{24}WT, $A_{24}L_{FMDV}3D_{YR}$, $A_{24}L_{BRV}3D_{YR}$ and A_{24}LL viruses at a MOI of 5. The A_{24}LL virus has been previously described and characterized (Uddowla et al., 2012). At 24 h post-infection, supernatants were collected, and the assay was performed in MDBK-t2 cells as previously described (Perez-Martin et al., 2012). CAT binding was determined using a commercially available enzyme linked immunosorbent assay (ELISA) kit (Roche Applied Sciences) according to manufacturer's protocol.

Virulence and protection study in cattle

All animal experiments were performed in BSL-3 containment facility under animal experimentation protocols approved by the facility's Institutional Animal Care and Use Committee. Two 250–300 kg Holstein steers (ID #37 and #38) were each infected with 1.7×10^6 $TCID_{50}$ of $A_{24}L_{BRV}3D_{YR}$ *via* the aerosol route as previously described (Pacheco et al., 2010). At 21 days post-infection (dpi), these steers were challenged with 10^4 $TCID_{50}$ of the parental A_{24}WT *via* intradermolingual injection (O.I.E and O.I.D. 2012). Discussions of timing of the events in the following passages are described relative to the initial inoculation of $A_{24}L_{BRV}3D_{YR}$ or relative to challenge with A_{24}WT [days post challenge (dpc)], as appropriate. Steers were housed in separate containment rooms for the entire duration of the procedures described. Clinical evaluation and sampling (sera, nasal and oral secretions) were performed on the following schedule: 0–10, 14, 22–31 dpi. Neutralizing antibody titers in cattle sera were determined as described elsewhere (Golde et al., 2005).

Virulence study in pigs

Two 25–30 kg Yorkshire-cross pigs (ID #40 and #41) were each inoculated with 2×10^6 $TCID_{50}$ per pig of $A_{24}L_{BRV}3D_{YR}$ *via* heel bulb intraepithelial injection as previously described (Pacheco and Mason, 2010). At 1 dpi, 2 additional pigs (#42 and #43) were brought into direct contact with the inoculated pigs, and the four animals co-habitated with direct contact for the duration of the study. Clinical evaluation and sampling (sera, nasal and oral swabs) were performed from 0–9 dpi. Clinical evaluation consisted of monitoring rectal temperature and lesion scoring as described (Pacheco and Mason, 2010). Maximum achievable lesion score was 20 for contact-exposed pigs and 16 for inoculated pigs since the inoculated foot was not used for scoring. Cotton tipped swabs were used to detect virus from oral and nasal secretions; swabs were immersed in 2 mL of minimum essential medium with 25 mM HEPES, and were stored at −70 °C from the time of collection until processing.

FMDV RNA detection

FMDV RNA was measured in sera and swab samples by rRT-PCR as previously described (Arzt et al., 2010; Pacheco and Mason, 2010). Virus isolation of samples was performed as previously described (Pacheco et al., 2010; Swaney, 1988).

Homology model of bovine rhinovirus leader protease

The structure of BRBV L^{pro} was modeled based on L^{pro} of FMDV using PDB file 1Q0L as template on SWISSMODEL workspace (Arnold et al., 2006; Peitsch, 1995; Schwede et al., 2003). The modeled BRBV L^{pro} was refined using the GROMOS96 43B1 force field *in-vacuo* (Schmid et al., 2011). The sterochemical quality of the model was further validated with verify3D (Eisenberg et al., 1997) and PROCHECK (Laskowski et al., 1993). Electrostatic surfaces of the FMDV and BRBV L^{pro} were generated using adaptive Poisson–Boltzman algorithm (APBS) (Baker et al., 2001). Figures were generated with pymol 1.3. rc.

Acknowledgments

We thank Dr. Alfonso Clavijo for the gift of mAbs against the FMDV $3D^{pol}$ and Drs. Marvin Grubman and Paul Lawrence for fruitful discussions. This research was supported by CRIS Project no. 1940-32000-053-00D, 1940-32000-057-00D, Agricultural Research Service (ARS), U.S. Department of Agriculture (Dr. Elizabeth Rieder). Dr. Sabena Uddowla, Dr. Devendra K. Rai and Mr. Christopher Larson were the recipient of a fellowship by the Plum Island Animal Disease Research Participation Program administered by the Oak Ridge Institute for Science and Education through an interagency agreement between the U.S. Department of Energy and the U.S. Department of Agriculture.

References

Arnold, K., Bordoli, L., Kopp, J., Schwede, T., 2006. The SWISS-MODEL workspace: a web-based environment for protein structure homology modelling. Bioinformatics (Oxford, England) 22, 195–201.
Arzt, J., Pacheco, J.M., Rodriguez, L.L., 2010. The early pathogenesis of foot-and-mouth disease in cattle after aerosol inoculation. Identification of the nasopharynx as the primary site of infection. Vet. Pathol. 47, 1048–1063.
Baker, N.A., Sept, D., Joseph, S., Holst, M.J., McCammon, J.A., 2001. Electrostatics of nanosystems: application to microtubules and the ribosome. Proc. Natl. Acad. Sci. USA. 98, 10037–10041.
Belsham, G.J., McInerney, G.M., Ross-Smith, N., 2000. Foot-and-mouth disease virus 3C protease induces cleavage of translation initiation factors eIF4A and eIF4G within infected cells. J. Virol. 74, 272–280.
Brown, C.C., Piccone, M.E., Mason, P.W., McKenna, T.S., Grubman, M.J., 1996. Pathogenesis of wild-type and leaderless foot-and-mouth disease virus in cattle. J. Virol. 70, 5638–5641.
Cao, X., Bergmann, I.E., Fullkrug, R., Beck, E., 1995. Functional analysis of the two alternative translation initiation sites of foot-and-mouth disease virus. J. Virol. 69, 560–563.
Chinsangaram, J., Koster, M., Grubman, M.J., 2001. Inhibition of L-deleted foot-and-mouth disease virus replication by alpha/beta interferon involves double-stranded RNA-dependent protein kinase. J. Virol. 75, 5498–5503.
Chinsangaram, J., Mason, P.W., Grubman, M.J., 1998. Protection of swine by live and inactivated vaccines prepared from a leader proteinase-deficient serotype A12 foot-and-mouth disease virus. Vaccine 16, 1516–1522.
Chinsangaram, J., Piccone, M.E., Grubman, M.J., 1999. Ability of foot-and-mouth disease virus to form plaques in cell culture is associated with suppression of alpha/beta interferon. J. Virol. 73, 9891–9898.
de Castro, M.P., 1964. Comportamiento do virus aftoso em cultura de celulas: susceptibilidade da linhagem de celulas suinas IB-RS-2. Arq. Inst. Biol. (Sao Paulo) 31, 63–78.
de Los Santos, T., de Avila Botton, S., Weiblen, R., Grubman, M.J., 2006. The leader proteinase of foot-and-mouth disease virus inhibits the induction of beta interferon mRNA and blocks the host innate immune response. J. Virol. 80, 1906–1914.
de Los Santos, T., Diaz-San Segundo, F., Grubman, M.J., 2007. Degradation of nuclear factor kappa B during foot-and-mouth disease virus infection. J. Virol. 81, 12803–12815.
de los Santos, T., Segundo, F.D., Zhu, J., Koster, M., Dias, C.C., Grubman, M.J., 2009. A conserved domain in the leader proteinase of foot-and-mouth disease virus is required for proper subcellular localization and function. J. Virol. 83, 1800–1810.
Dias, C.C., Moraes, M.P., Segundo, F.D., de los Santos, T., Grubman, M.J., 2011. Porcine type I interferon rapidly protects swine against challenge with multiple serotypes of foot-and-mouth disease virus. J. Interferon Cytokine Res. 31, 227–236.
Eisenberg, D., Luthy, R., Bowie, J.U., 1997. VERIFY3D: assessment of protein models with three-dimensional profiles. Methods Enzymol. 277, 396–404.
Foeger, N., Glaser, W., Skern, T., 2002. Recognition of eukaryotic initiation factor 4G isoforms by picornaviral proteinases. J. Biol. Chem. 277, 44300–44309.
Fray, M.D., Mann, G.E., Charleston, B., 2001. Validation of an Mx/CAT reporter gene assay for the quantification of bovine type-I interferon. J. Immunol. Methods 249, 235–244.
Golde, W.T., Pacheco, J.M., Duque, H., Doel, T., Penfold, B., Ferman, G.S., Gregg, D.R., Rodriguez, L.L., 2005. Vaccination against foot-and-mouth disease virus confers

complete clinical protection in 7 days and partial protection in 4 days: Use in emergency outbreak response. Vaccine 23, 5775–5782.
Grubman, M.J., Baxt, B., 2004. Foot-and-mouth disease. Clin. Microbiol. Rev. 17, 465–493.
Guarne, A., Tormo, J., Kirchweger, R., Pfistermueller, D., Fita, I., Skern, T., 1998. Structure of the foot-and-mouth disease virus leader protease: a papain-like fold adapted for self-processing and eIF4G recognition. EMBO. J. 17, 7469–7479.
Hollister, J.R., Vagnozzi, A., Knowles, N.J., Rieder, E., 2008. Molecular and phylogenetic analyses of bovine rhinovirus type 2 shows it is closely related to foot-and-mouth disease virus. Virology 373, 411–425.
Kleina, L.G., Grubman, M.J., 1992. Antiviral effects of a thiol protease inhibitor on foot-and-mouth disease virus. J. Virol. 66, 7168–7175.
Laskowski, R.A., MacArthur, M.W., Moss, D.S., Thornton, J.M., 1993. PROCHECK-a program to check the stereochemical quality of protein structures. J. Appl. Crystallogr. 26, 283–291.
Mason, P.W., Piccone, M.E., McKenna, T.S., Chinsangaram, J., Grubman, M.J., 1997. Evaluation of a live-attenuated foot-and-mouth disease virus as a vaccine candidate. Virology 227, 96–102.
Nogueira Santos, J.A., Assis, D.M., Gouvea, I.E., Judice, W.A., Izidoro, M.A., Juliano, M.A., Skern, T., Juliano, L., 2012. Foot and mouth disease leader protease (Lbpro): Investigation of prime side specificity allows the synthesis of a potent inhibitor. Biochimie 94, 711–718.
O.I.E., O.I.D., 2012. Foot and mouth disease. Commission, O.S. (Ed.), Manual of Standards for Diagnostic Tests and Vaccines. Paris, pp. 145–173 (chapter 2.1.5).
Pacheco, J.M., Arzt, J., Rodriguez, L.L., 2010. Early events in the pathogenesis of foot-and-mouth disease in cattle after controlled aerosol exposure. Vet. J. 183, 46–53.
Pacheco, J.M., Mason, P.W., 2010. Evaluation of infectivity and transmission of different Asian foot-and-mouth disease viruses in swine. J. Vet. Sci. 11, 133–142.
Pacheco, J.M., Tucker, M., Hartwig, E., Bishop, E., Arzt, J., Rodriguez, L.L., 2012. Direct contact transmission of three different foot-and-mouth disease virus strains in swine demonstrates important strain-specific differences. Vet. J.
Peitsch, M.C., 1995. Protein modeling by E-mail. Nat. Biotechnol. 13, 658–660.
Perez-Martin, E., Weiss, M., Diaz-San Segundo, F., Pacheco, J.M., Arzt, J., Grubman, M.J., de los Santos, T., 2012. Bovine type III interferon significantly delays and reduces the severity of foot-and-mouth disease in cattle. J. Virol. 86, 4477–4487.
Piccone, M.E., Rieder, E., Mason, P.W., Grubman, M.J., 1995. The foot-and-mouth disease virus leader proteinase gene is not required for viral replication. J. Virol. 69, 5376–5382.
Pineiro, D., Ramajo, J., Bradrick, S.S., Martinez-Salas, E., 2012. Gemin5 proteolysis reveals a novel motif to identify L protease targets. Nucleic Acids Res. 40, 4942–4953.
Rieder, E., Bunch, T., Brown, F., Mason, P.W., 1993. Genetically engineered foot-and-mouth disease viruses with poly(C) tracts of two nucleotides are virulent in mice. J. Virol. 67, 5139–5145.
Rieder, E., Henry, T., Duque, H., Baxt, B., 2005. Analysis of a foot-and-mouth disease virus type A24 isolate containing an SGD receptor recognition site in vitro and its pathogenesis in cattle. J. Virol. 79, 12989–12998.
Roberts, P.J., Belsham, G.J., 1995. Identification of critical amino acids within the foot-and-mouth disease virus leader protein, a cysteine protease. Virology 213, 140–146.
Robertson, B.H., Morgan, D.O., Moore, D.M., 1984. Location of neutralizing epitopes defined by monoclonal antibodies generated against the outer capsid polypeptide, VP1, of foot-and-mouth disease virus A12. Virus. Res. 1, 489–500.
Schmid, N., Allison, J.R., Dolenc, J., Eichenberger, A.P., Kunz, A.P., van Gunsteren, W.F., 2011. Biomolecular structure refinement using the GROMOS simulation software. J. Biomol. NMR. 51, 265–281.
Schwede, T., Kopp, J., Guex, N., Peitsch, M.C., 2003. SWISS-MODEL: an automated protein homology-modeling server. Nucleic Acids Res. 31, 3381–3385.
Simmonds, P., 2006. Recombination and selection in the evolution of picornaviruses and other Mammalian positive-stranded RNA viruses. J. Virol. 80, 11124–11140.
Skern, T., Fita, I., Guarne, A., 1998. A structural model of picornavirus leader proteinases based on papain and bleomycin hydrolase. J. Gen. Virol. 79 (Pt 2), 301–307.
Swaney, L.M., 1988. A continuous bovine kidney cell line for routine assays of foot-and-mouth disease virus. Vet. Microbiol. 18, 1–14.
Uddowla, S., Hollister, J., Pacheco, J.M., Rodriguez, L.L., Rieder, E., 2012. A safe foot-and-mouth disease vaccine platform with two negative markers for differentiating infected from vaccinated animals (Diva). J. Virol 86, 11675–11685.

Virology 446 (2013) 260–267

Contents lists available at ScienceDirect

Virology

journal homepage: www.elsevier.com/locate/yviro

A partial deletion in non-structural protein 3A can attenuate foot-and-mouth disease virus in cattle

Juan M. Pacheco [a,1], Douglas P. Gladue [a,c,1], Lauren G. Holinka [a], Jonathan Arzt [a], Elizabeth Bishop [a], George Smoliga [a], Steve J. Pauszek [a], Alexa J. Bracht [b], Vivian O'Donnell [a,c], Ignacio Fernandez-Sainz [a], Paige Fletcher [a], Maria E. Piccone [a], Luis L. Rodriguez [a], Manuel V. Borca [a,*]

[a] Agricultural Research Service, U.S. Department of Agriculture, Plum Island Animal Disease Center, Greenport, NY, USA
[b] Plum Island Animal Disease Center, APHIS, U.S. Department of Agriculture, Greenport, NY, USA
[c] Department of Pathobiology and Veterinary Science, University of Connecticut, Storrs, CT, USA

ARTICLE INFO

Article history:
Received 26 April 2013
Returned to author for revisions
25 July 2013
Accepted 5 August 2013

Keywords:
FMDV
Virus
Pathogenesis
3A

ABSTRACT

The role of non-structural protein 3A of foot-and-mouth disease virus (FMDV) on the virulence in cattle has received significant attention. Particularly, a characteristic 10–20 amino acid deletion has been implicated as responsible for virus attenuation in cattle: a 10 amino acid deletion in the naturally occurring, porcinophilic FMDV O1 Taiwanese strain, and an approximately 20 amino acid deletion found in egg-adapted derivatives of FMDV serotypes O1 and C3. Previous reports using chimeric viruses linked the presence of these deletions to an attenuated phenotype in cattle although results were not conclusive. We report here the construction of a FMDV O1Campos variant differing exclusively from the highly virulent parental virus in a 20 amino acid deletion between 3A residues 87–106, and its characterization *in vitro* and *in vivo*. We describe a direct link between a deletion in the FMDV 3A protein and disease attenuation in cattle.

Published by Elsevier Inc.

Introduction

Foot-and-mouth disease (FMD) is an infectious viral disease that affects cloven-hoofed animals, including cattle, sheep, swine, goats, camelids and deer. Its wide host range and rapid spread make FMD an international animal health concern, since all countries are vulnerable to accidental or intentional trans-boundary introduction (Grubman and Baxt, 2004; Rowlands, 2003). The disease is caused by foot-and-mouth disease virus (FMDV), an *Aphthovirus* within the viral family *Picornaviridae* that exists as seven immunologically distinct serotypes: O, A, C, Asia 1, and South African Territories (SAT) type 1, SAT2 and SAT3. The viral genome consists of a single-stranded, positive-sense RNA of about 8200 nucleotides (nt). The open reading frame (ORF) encodes a single polyprotein that is post-translationally processed by virus-encoded proteases into four structural proteins (VP1 through 4) and eight non-structural proteins (L, 2A, 2B, 2C, 3A, 3B, 3C and 3D) (Belsham, 1993). While the contribution of each of these proteins to virulence during infection of the natural host is not clear, the role of non-structural protein 3A in virulence has been the focus of several studies.

FMDV 3A is a conserved protein of 153 amino acids (aa) in most FMDVs examined to date. Changes in 3A have been associated with altered host range as reviewed by Knowles et al. (2001) in the hepatoviruses (Graff et al., 1994a, 1994b; Lemon et al., 1991; Morace et al., 1993), rhinoviruses (Heinz and Vance, 1996) and enteroviruses (Lama et al., 1998). The 3A protein in FMDV is substantially larger than the 3A proteins of other picornaviruses being 50% larger than the 87 aa 3A of poliovirus (Kitamura et al., 1981). The first half of the 3A coding region, which encodes an N-terminal hydrophilic domain and a hydrophobic domain capable of binding membranes, is highly conserved among all FMDVs (Knowles et al., 2001). It was previously demonstrated that amino acid substitution Q44 to R in 3A was sufficient to give FMDV the ability to exacerbate virulence of FMDV strain C-S8c1 adapted to guinea pigs (Nunez et al., 2001). In FMDV, deletions in the C-terminal half of 3A has been associated with decreased virulence in cattle. Thus, FMDV strains that were attenuated through serial passages in chicken embryos for the development of vaccines in South America had reduced virulence in cattle and contained 19- to 20-codon deletions in the 3A coding region (Giraudo et al., 1990). A deletion in the same 3A region consisting of 10 amino acids, was also observed (Beard and Mason, 2000) in the FMDV

* Correspondence to: Plum Island Animal Disease Center, USDA/ARS/NAA, P.O. Box 848, Greenport 11944-0848, NY, USA. Fax: +1 631 323 3006.
E-mail address: manuel.borca@ars.usda.gov (M.V. Borca).
[1] These authors have equally contributed to the results presented in this report.

0042-6822/$ - see front matter Published by Elsevier Inc.
http://dx.doi.org/10.1016/j.virol.2013.08.003

isolate responsible for an outbreak of FMD in Taiwan in 1997 (O/TAW/97) that severely affected swine, but did not spread to cattle (Dunn and Donaldson, 1997; Yang et al., 1999). Thus, a region of the FMDV 3A protein located downstream of the hydrophobic domain is altered in O/TAW/97 virus and in the egg-adapted FMDVs. An association was therefore established between the presence of a specific deletion in this particular area of 3A and attenuation of virus virulence in cattle. However, this association was speculative, as these attenuated strains also contain numerous additional genome-wide amino acid substitutions when compared with virulent related or parental strains, and it cannot be ruled out that these other amino acid substitutions have some influence on the phenotype observed.

In the previous study by Beard and Mason (2000), the direct involvement of these deletions in the induction of attenuation was tested using reverse genetics with infectious clone chimeras. Chimeric viruses were created using the genomic backbone of FMDV strains virulent in cattle (A12 and O1Campos) containing the 3A protein of the porcinophilic O/TAW/97 isolate. When this chimeric virus was intradermally inoculated into the tongue of cattle, it produced less severe local lesions than parental A12 virus, yet still progressed to systemic FMD. Conversely, a chimeric virus harboring 3A of the A12 virus in the context of O/TAW/97 structural proteins produced severe local lesions in the inoculated tongue, yet failed to produce a systemic form of the disease. Thus, exchanging the 3A genomic area of parental virus strains altered the severity of lesions, but did not conclusively define virulence in cattle or the role of 3A. The possible contribution of genome-wide amino acid changes, in addition to the 3A deletions, to the observed patterns of virulence in cattle remained largely unclear. In fact, it should be noted that no complete genomic sequence was determined for the chimeric viruses constructed in that study.

To clarify the role of the 3A deletions in FMDV virulence in cattle, we developed a virus lacking 20 amino acids between residue positions 87 and 106 of 3A (O1CaΔ3A) using a full-length infectious cDNA clone derived from the FMDV O1Campos/Bra/58 strain (Borca et al., 2012) and evaluated its ability to replicate in cell cultures and its virulence profile in cattle and swine in comparison to its parental virus (O1Ca). Results demonstrated that while both viruses grow equally well in primary porcine cell cultures, O1CaΔ3A exhibited a significantly decreased replication ability in primary bovine cell cultures. Similarly, while O1Ca caused typical generalized disease in cattle and swine, O1CaΔ3A produced fulminant FMD in swine, but was completely attenuated in cattle. Therefore, this report presents direct evidence showing that a deletion within the 3A protein is responsible for attenuation of a highly virulent FMDV strain in cattle.

Results

Generation and characterization of pO1Ca

The full-length cDNA clone pO1Ca was constructed by overlapping PCR fragments flanked by unique restriction enzymes as described previously (Borca et al., 2012). The full-length cDNA was preceded by the T7 polymerase promoter and two additional G residues to improve transcription efficiency and followed by a polyA tail of 15 residues and a unique EcoRV site. Plasmid O1CaΔ3A (pO1CaΔ3A) containing the deletion of amino acid residues between positions 87 and 106 in non-structural protein 3A (Fig. 1) derived from the infectious clone pO1Ca was constructed as described in Materials and methods.

RNA transcripts derived from pO1Ca or pO1CaΔ3A were used to transfect BHK-21 cells by electroporation, and then subjected to serial passage in LF-BK cells expressing the bovine integrin αVβ6 (LF-BK-αVβ6) (Larocco et al., 2013) to amplify the clone-derived viruses. Sequencing of the entire genome of recovered viruses (O1Ca and O1CaΔ3A) verified that they were identical to the parental DNAs, confirming that only the predicted mutations were incorporated into the viruses.

Cell tropism of viruses O1Ca and O1CaΔ3A assessed in primary cell cultures

To evaluate the species-specific tropism of viruses O1Ca and O1CaΔ3A, multistep growth curves were performed using different cell substrates to comparatively assess *ex vitro* growth characteristics (Fig. 2). Different cells were infected at a multiplicity of infection (MOI) of 0.01 using virus titers determined on LF-BK-αVβ6, the cells used to amplify the viruses. Samples were collected at regular intervals between 4 and 48 h post-infection (hpi).

Results demonstrated that viruses O1Ca and O1CaΔ3A exhibited similar growth characteristics and reached comparable titers in LF-BKαVβ6 (Fig. 2A). The ability of these viruses to replicate in bovine and swine primary fetal kidney cell (FBK and FPK, respectively) cultures was assessed under similar experimental conditions as those described for LF-BK-αVβ6. The ability of either virus to replicate in FPK cell cultures showed a slight delay for O1CaΔ3A at 24 h although both viruses reached the same maximal titer at

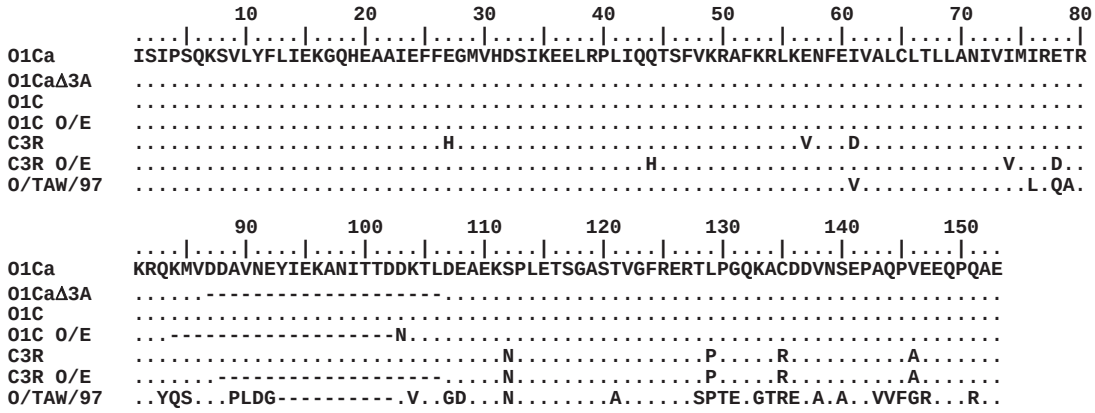

Fig. 1. Alignment of the amino acid sequence obtained from full length FMDV non-structural protein 3A from: O1Campos/Bra/58 (O1Ca) (Borca et al., 2012); O1Campos Bra/55 (O1C) (Parisi et al., 1985); O1Campos B/55 O/E (O1C O/E) (Parisi et al., 1985); C3 Resende (C3R) (Sagedahl et al., 1987); C3 Resende O/E (C3R O/E) (Sagedahl et al., 1987); O1 Taiwan 97 (O/TAW/97) (Beard and Mason, 2000); and the constructed virus used in this study O1Campos Δ3A (O1CaΔ3A).

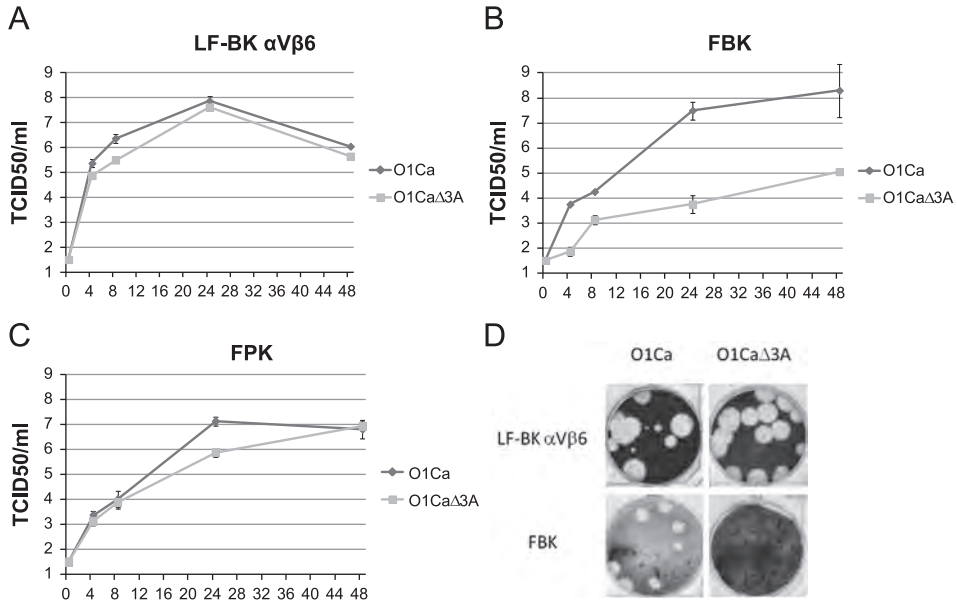

Fig. 2. Growth characteristics of FMDV O1Ca and O1CaΔ3A. *In vitro* growth curves of O1Ca and O1CaΔ3A viruses (MOI 0.01) in LF-BK-αVβ6 (A), FBK (B) and FPK (C) cells. Samples obtained at indicated time points were titrated in LF-BK-αVβ6 cells and virus titers expressed as TCID50/ml. (B) Plaques corresponding to O1Ca and O1CaΔ3A viruses in LF-BK-αVβ6 and FBK cell**s.** Infected cells were incubated at 37 °C under a tragacanth overlay and stained with crystal violet at 48 hpi. Plaques from appropriate dilutions are shown.

48 h (Fig. 2C). However, O1CaΔ3A had substantially decreased its ability to replicate in FBKs when compared to virus O1Ca. Differences of approximately 1000-fold were observed in the titer values of samples harvested at 24 and 48 hpi (Fig. 2B).

The decreased ability of virus O1CaΔ3A to replicate in primary bovine cells was further analyzed in a standard plaque assay performed in LF-BK-αVβ6 and FBK cell cultures (Fig. 2D). Results demonstrated that virus O1Ca and O1CaΔ3A both produced a similar large plaque size in LF-BK-αVβ6 cells. However, while virus O1Ca produced smaller plaques in FBK cells than those produced in LF-BK-αVβ6 cells, virus O1CaΔ3A was completely unable to produce any visible plaques. Thus, the deletion in 3A harbored by O1CaΔ3A virus determined the ability of the virus to replicate in primary cells of bovine origin but did not significantly affect replication in swine primary cells.

Assessment of FMDV O1Ca and O1CaΔ3A virulence in cattle

Virulence of both viruses, O1Ca and O1CaΔ3A, in cattle was assessed utilizing an aerosol inoculation method developed in our laboratory (Pacheco et al., 2010a). This method was chosen since it appears to more closely simulate the natural route of infection as compared to the intradermolingual route. Three steers (each 300–400 kg) were infected with approximately 10^7 PFU/cattle of O1Ca or O1CaΔ3A virus, diluted in MEM, and infection and clinical signs were monitored daily as described previously (Pacheco et al., 2010a). Results demonstrated that the three animals (animals #72–74) inoculated with the O1Ca virus developed severe clinical FMD. Lesions typical of FMD appeared by 3 or 4 day post-infection (dpi) and reached the maximum clinical score (mouth and four feet affected with vesicles) by 4 or 5 dpi (Fig. 3). All three animals had fever (> 40 °C) from 3 to 7 dpi (results not shown). Viremia lasted 4–6 day, starting at 2 dpi. Virus shedding was detected in nasal swabs from all animals beginning at 1 dpi and was undetectable by 10 or 14 dpi; virus shedding was detected in oral swabs from 1 to 3 dpi until, at least, 10 dpi (Fig. 3).

Interestingly, cattle inoculated with O1CaΔ3A (animals #66–68) showed no clinical signs of FMD, including no hyperthermia, throughout the experimental period (Fig. 3). Neither viremia nor virus shedding was detected in any of these animals at any sampling time after the noculum virus was cleared. Additionally, no serum neutralizing antibodies nor antibodies to the non-structural 3ABC protein were detected throughout the experimental period (Table 1), which indicates very limited, if any, virus replication. Despite lack of detection of O1CaΔ3A from antemortem samples, infectious virus and viral RNA were detected in tissue samples of the pharyngeal area (dorsal soft palate, dorsal nasal pharynx and retropharyngeal lymph node) at 21 dpi in animals inoculated with either O1Ca or O1CaΔ3A virus (Table 1). Interestingly, while viral RNA was easily found in the interdigital cleft skin in all animals infected with O1Ca, it was absent in these tissues from all animals inoculated with O1CaΔ3A. These results clearly indicate that after aerosol inoculation with O1CaΔ3A virus there is only local replication in the bovine nasopharynx, with a clear absence of viremia, lack of spread to other organs and absence of clinical signs. Virus that was recovered from the dorsal soft palate of these O1CaΔ3A infected animals was amplified in LF-BK-αVβ6 to obtain the complete sequence of 3A and all of the recovered viruses maintained the deletion in 3A. While animal 67 was identical to the O1CaΔ3A inoculum, point mutations occurred in animal 66 (G118D), and 68 (G118D, R54H).

Virulence assessment of FMDV O1Ca and O1CaΔ3A in swine

To examine the effect of the deletion in the 3A protein on virus virulence in swine, virulence studies were performed utilizing a direct-inoculation and direct-contact exposure methodology (Pacheco and Mason, 2010; Pacheco et al., 2012). Briefly, two animals were intradermally inoculated in the heel bulb with approximately 10^6 PFU/animal of O1Ca (Fig. 4) and after 48 h were placed into co-habitation with two naïve pigs. In a separate room, the same intradermal inoculation and comingling was performed with O1CaΔ3A. All animals were monitored for the presence of clinical disease and sampled to characterize viral dynamics.

Both animals intradermally inoculated with O1Ca (#23 and #24) developed classic FMD (Fig. 4A). At 2 dpi animals became febrile, depressed, lame and developed lesions in the non-inoculated feet and mouth. Pig #24 was euthanized at 4 dpi due

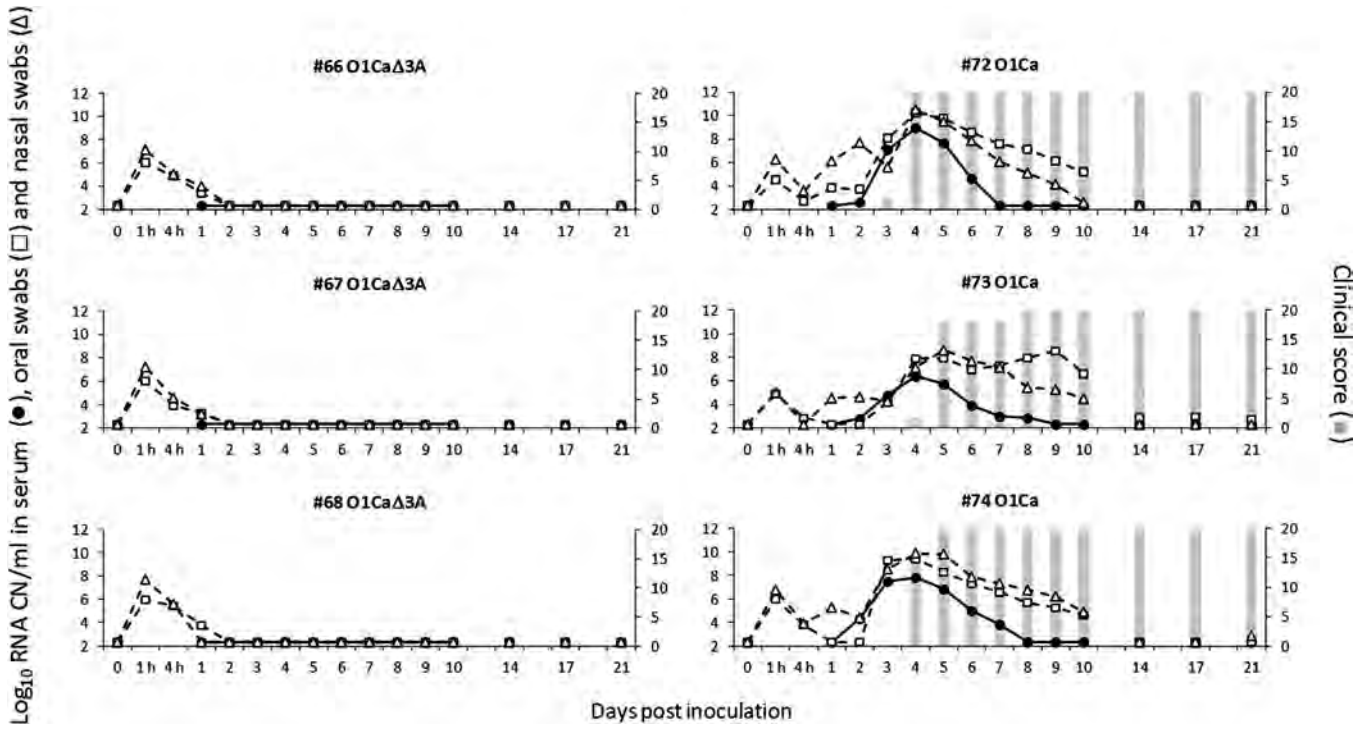

Fig. 3. Assessment of O1Ca and O1CaΔ3A virus virulence in cattle. Steers were inoculated with 10^7 TCID50 of either O1Ca (animals #72–74) or O1CaΔ3A (animals #66–68) as per the aerosol inoculation method. Presence of clinical signs (clinical scores), and virus yield (quantified as $\log_{10}$ of viral RNA copies/ml of sample) in serum, oral and nasal swabs were determined daily during a 10 day observational period, and twice a week up to 21 dpi.

Table 1
Tissue-specific distribution of FMDV and viral RNA at 21 dpi in different tissues of cattle inoculated with either O1Ca or O1CaΔ3A virus.

	O1CaΔ3A			O1Ca		
Animal #	**66**	**67**	**68**	**72**	**73**	**74**
Dorsal soft palate	4.68[a]/Pos[b]	4.30/Pos	3.64/Pos	2.93/Neg	3.98/Pos	4.08/Pos
Dorsal nasal pharynx	4.40/Pos	Neg/Pos	3.34/Pos	3.47/Neg	4.68/Pos	2.05/Neg
RPLN[c]	3.14/Pos	Neg/Neg	Neg/Pos	2.66/Neg	4.82/Neg	2.93/Neg
Interdigital cleft	Neg/Neg	Neg/Neg	Neg/Neg	3.96/Neg	2.98/neg	3.12/Neg
VNA[d]	< 0.9	< 0.9	< 0.9	3.6	3.6	3.6
3ABC antibodies[e]	Neg	Neg	Neg	Pos	Pos	Pos

[a] Maximum RNA CN/mg (copy number, expressed as $\log_{10}$, per mg of tissue) obtained from two different samples collected from the indicated tissue.
[b] Virus isolation performed with the same two tissues used for RNA isolation above, on T-25 flask pre-seeded with LF-BK-αvb6 cells as previously described (Arzt et al., 2010).
[c] RPLN = retropharyngeal lymph node.
[d] VNA: titers of virus-neutralizing antibodies in sera titers were determined as previously described (Pacheco et al., 2010b).
[e] Antibodies against FMDV 3ABC were detected using the prionics PrioCHECK FMDV NS ELISA.

to severe clinical disease. Viremia (detected by rRT-PCR) started at 1 dpi and peaked at 2 dpi coincident with onset of clinical disease. Virus was also detected by rRT-PCR in oral (tonsil) and nasal swabs of both animals starting as early as 1 dpi and peaking at 2–4 dpi.

Animals exposed by direct-contact (#25 and #26) developed disease with all classical symptoms described above and severe lesions in mouth and feet (Fig. 4C) At 3 day post challenge (dpc) both animals had clinical signs of congestive heart failure; on that day #25 died and #26 was euthanized due to respiratory distress. Real-time RT-PCR analysis demonstrated the presence of virus in blood as well as in oral and nasal swabs of both animals starting at 1 dpc.

Similar to what was observed in animals inoculated with O1Ca, both swine intradermally inoculated with O1CaΔ3A (#19 and #20) developed classic FMD, with severity and kinetics similar from the disease caused by O1Ca (Fig. 4B). Viremia and virus shedding also resembled that observed in O1Ca-infected animals. Animals infected by co-habitation (#21 and #22) developed a highly virulent disease with the classical signs described above, including lesions in the mouth and feet (Fig. 4D). Progression of vesiculation and viral dynamics in swine caused by O1CaΔ3A did not significantly differ from those caused by the parental virus O1Ca, when pigs were inoculated intradermally or by co-habitation. Virus recovered from vesicles of the contact-inoculated animals was sequenced to confirm they maintained the deletion, and no other mutations in 3A were observed. These results clearly indicate that the effect of deletion within non-structural protein 3A does not significantly affect virulence in swine.

Discussion

The molecular basis of FMDV virulence during infection in natural hosts is incompletely understood (reviewed in references (Arzt et al., 2010; Mason et al., 2003a)). Although much research has been devoted to discovering virulence factors within the

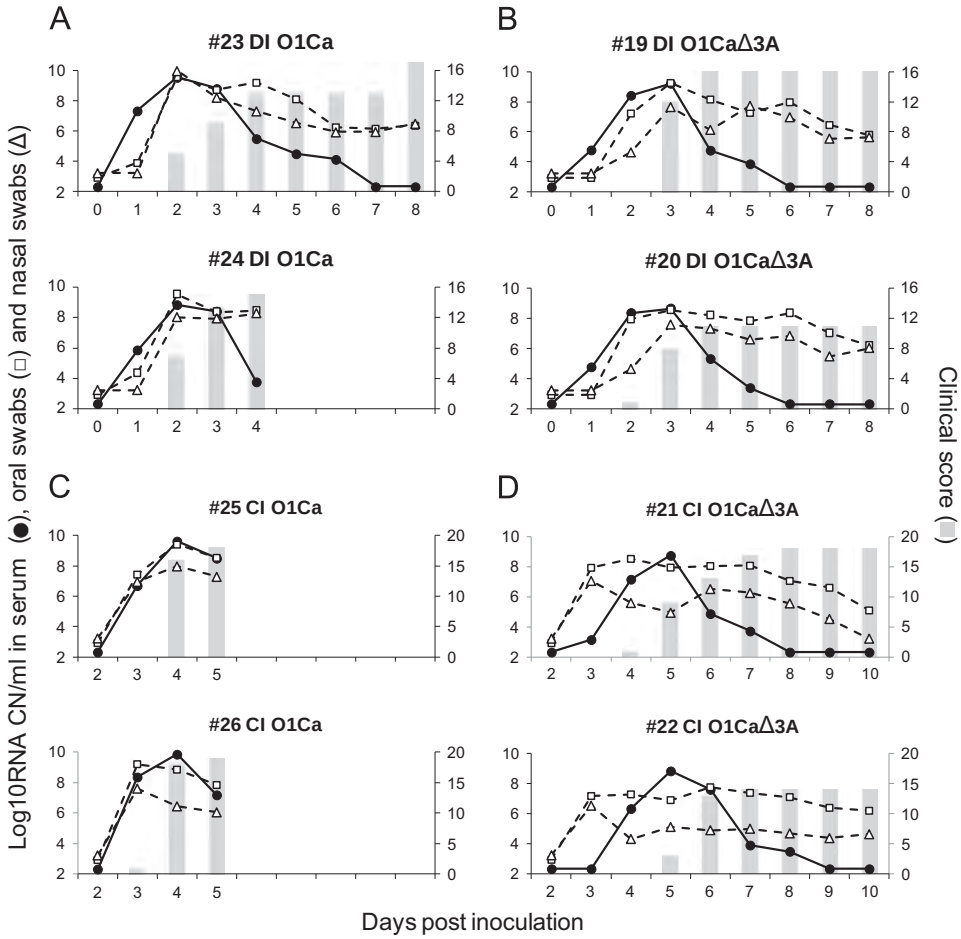

Fig. 4. Assessment of O1Ca and O1CaΔ3A virus virulence in swine. Two swine were intradermally inoculated into the foot bulb with 10^6 TCID50 of either O1Ca (animals #23 and #24) or O1CaΔ3A (animals #19 and #20). After 48 hpi, inoculated animals #23 and #24 were put in co-habitation with naïve swine #25 and #26, while animals #19 and #20 were put into co-habitation with naïve swine #25 and #26. Presence of clinical signs (clinical scores) and virus yield (quantified as $\log_{10}$ of viral RNA copies/ml of sample) in blood and nasal swabs were determined daily during an 8 day observational period after direct- or contact-inoculation. Animal #24 was humanely sacrificed at 4 dpi due to severe disease. Animals #25 and 26 were affected by FMDV induced cardiomyopathy. Day post inoculation indicates day of heel bulb inoculation of the first two pigs on each group.

FMDV genome, very few genomic determinants have been unquestionably identified. Besides the well established role of virulence in cattle and swine of the leader proteinase (Brown et al., 1996), the role of residue Arg56 in VP3 (Borca et al., 2012), the importance of virus structural proteins complex (Botner et al., 2011; Lohse et al., 2012) and the 3′ untranslated region (Rodriguez Pulido et al., 2009), no other area of the virus genome has conclusively been associated with production of viral attenuation in the natural host.

FMDV non-structural protein 3A has been known to influence virulence since the report of an approximately 20 amino acid deletion within the central area of 3A found in two South American viruses adapted to growth in chicken embryos (residues 84–102 in O1Campos O/E, and residues 88–106 in C3 Resende/Brasil55) (Giraudo et al., 1990, 1987; Sagedahl et al., 1987). These viruses were attenuated in cattle but not in swine. Further support came from the 1997 Taiwanese FMD outbreak strain (O/TAW/97) that devastated the country's pig industry, but did not spread to cattle (Dunn and Donaldson, 1997; Yang et al., 1999). Sequencing of O/TAW/97 indicated that the epidemic virus contained a 10 amino acid deletion between amino acid residues 93 and 102 of 3A, similar to the South American viruses described above (Beard and Mason, 2000). However, FMDV strain O/SKR/AS/2002, isolated from the South Korean outbreak of 2002, is phenotypically indistinguishable from O/TAW/97 in terms of its virulence pattern (highly virulent in swine but fails to produce generalized disease in cattle). Interestingly, partial sequencing of O/SKR/AS/2002 demonstrated the presence of a full-length version of 3A without any of the deletions characteristic of the O1 PanAsia lineage (Oem et al., 2008), indicating that attenuated phenotype in cattle is not always associated with 3A deletions. Another PanAsia topotype strain, O/TAW/2/99, originally avirulent in cattle was highly virulent in cattle but only after undergoing two passages in swine. This strain harbors a full-length 3A and changes in virulence were attributed to other changes in the genome, and not to 3A deletions (Mason et al., 2003b).

Due to the aforementioned conflicting reports, it was difficult to establish a clear relationship between the presence of the deletion within the 3A protein and an attenuated phenotype in cattle. Genomic comparisons between viruses that have an attenuated phenotype in cattle and their putative parental viruses are quite difficult since the presence of the 3A deletion is always associated with several additional simultaneous mutations within the 3A genomic area as well as in many other areas of the virus genome.

Previous attempts to obtain direct evidence of the role of 3A in determining host specific virulence were inconclusive. In fact, there is only one report that used reverse genetics to explore the role of the 3A deletion in cattle (Beard and Mason, 2000). Specifically, Beard and Mason, investigated a chimeric virus

composed of the untranslated region and most of the non-structural proteins of A12, the structural proteins of O1Campos, and the carboxyl half of 3A along with the 3Bs and part of 3C of O/TAW/97. They determined that when this virus was intradermally inoculated into the tongue of cattle, mild local lesions appeared at inoculation sites, then progressed to systemic disease (Beard and Mason, 2000). Conversely, another chimeric virus composed of the untranslated region and the carboxy end of 2C along with 3A, 3Bs, 3C and the amino end of 3D of FMDV A12, and the structural proteins and carboxyl end of 3D from O/TAW/97, produced severe local lesions when intradermally inoculated in the tongue but failed to produce a systemic form of the disease. It is possible that the chimeric nature of the viruses constructed in their study masked the functional role of 3A. In addition, the strategy based on the swap of 3A areas between O/TAW/97 and A12 virus included, in addition to the deletion, at least 26 other substituted residues in 3A, as well as additional changes in other adjacent non-structural proteins as described above.

The current study is based upon a mutant virus that differs from its highly virulent parental virus exclusively in the particular genetic area under study, the 20 amino acid deletion between residues 87 and 106 of the non-structural protein 3A.

The role of this deletion in defining host range in cell culture remains controversial. As previously reported (Knowles et al., 2001), O/TAW/97 and closely related viruses obtained from swine in South East Asia since 1970, bearing a deletion between amino acid residues 93 and 102 of 3A, grew approximately 10- to 100-fold less in bovine-derived keratinocyte cultures than in cultures prepared from swine tissue. However, as reported by the same authors, viruses isolated before 1983 that have the same deletion grew very well in bovine cells (Knowles et al., 2001). On this basis, these authors proposed that the 93–102 deletion in this region of 3A cannot, alone, account for the inability to replicate in bovine cells, and that other mutations in the genome of this virus lineage, possibly generated in response to the 3A deletion, may be responsible for the host range of O/TAW/97. More recently, it was reported that an Asia 1 recombinant virus, developed by reverse genetics, containing the 93–102 amino acid residues deletion within 3A failed to replicate in primary bovine kidney cells while replicating as efficiently as its parental virus in the hamster cell line BHK or swine cell line PK15 (Li et al., 2010).

Our results indicate that the 3A deletion although does not significantly alter replication in primary swine cells, it severely affected virus yield in primary cells of bovine origin. The discrepancies between the complete lack of plaque formation by O1CaΔ3A virus on FBK cells virus versus the residual replication ability showed in the one step growth curve in those cells may be explained by utilizing LF-BK-αvβ6 as the substrate for determining titers in the growth curve assays.

The recovery of O1Ca and O1CaΔ3A from bovine nasopharyngeal tissues is consistent with previous works that have demonstrated tropism of FMDV for these regions in acute (Arzt et al., 2010; Pacheco et al., 2010a) and persistent (Zhang and Kitching, 2001) phases of FMD in cattle. It is intriguing that at 21 dpi similar levels of viral RNA were detected in the pharynx of cattle inoculated with either O1Ca or O1CaΔ3A. This indicates that O1CaΔ3A was able to infect bovine cells *in vivo* at the primary site of infection but failed to establish viremia, generalized in the infected animal and caused clinical disease. Sequencing of 3A in the recovered viruses demonstrated, in all three cases, that the 3A deletion remained unaltered. In addition, a single (G118D), and a double (G118D, R54H) amino acid substitution occurs in 3A of two of animals. We cannot rule out the possibility that these mutations may actually contribute to the attenuation caused by the 3A deletion. It is also possible that these point mutations were incorporated during the amplification of the clinical sample in cell culture due to the low levels of virus that were recovered from the animals.

Our results demonstrate a direct correlation between the deletion of residues 87–106 of the 3A protein and the virus' ability to replicate in bovine primary cell cultures with no significant effect on replication in porcine cells. Importantly, this partial deletion of 3A led to a completely attenuated phenotype in cattle by aerosol inoculation with no significant effect on virulence for swine. Overall, these data provide evidence implicating the central region of FMDV 3A as a virulence factor in cattle and host range determinant of FMDV.

Materials and methods

Cell lines and virus

Baby hamster kidney cell line (BHK-21, ATCC, catalog number CCL-10) was used as previously described (Borca et al., 2012). A derivative cell line obtained from bovine kidney, LF-BK (Swaney, 1988), expressing the bovine αVβ6 integrin (LF-BK-αVβ6) (Larocco et al., 2013), and primary cell cultures of fetal bovine and porcine kidney (FBK and FPK, respectively) were grown and maintained in D-MEM containing 10% fetal calf serum. Growth kinetics and plaque assays were performed as described previously (Pacheco et al., 2010b). The FMDV strain O1Campos/Bra/58 was obtained from the Institute of Virology at the National Agricultural Technology Institute, Argentina (Borca et al., 2012).

Construction of the FMDV O1Ca full-length cDNA infectious clone and mutant O1CaΔ3A

The highly virulent FMDV strain O1Campos/Bra/58 was the template virus used to construct a cDNA infectious clone (IC). Construction of the pO1Ca full-length cDNA IC has been previously described in detail (Borca et al., 2012). pO1CaΔ3A is a derivative of pO1Ca that contains a 20 amino acid deletion (between residue positions 87 and 106) within 3A that was introduced by site-directed mutagenesis using full-length pO1Ca as a template using the Quick Change XL Site-Directed Mutagenesis kit (Stratagene, Cedar Creek, TX) performed per manufacturer's instructions. Primers were designed using the manufacturer's primer design program (https://www.genomics.agilent.com/CollectionSubpage.aspx?PageType=Tool&SubPageType=ToolQCPD&PageID=15). The primers used were 5′-caagaggcagaaaatggtggatgaggcggagaag-3′ as the foreword primer and 5'-cttctccgcctcatccaccattttctgcctcttg-3′ as the reverse primer. pO1Ca and pO1CaΔ3A were completely sequenced to confirm the presence of expected modifications and absence of unwanted substitutions.

Transfection and recovery of the infectious clone-derived viruses

Plasmid pO1Ca and its derivative, pO1CaΔ3A, were linearized at the EcoRV site following the poly(A) tract for RNA synthesis using the MegaScript T7 kit (Ambion, Austin, TX) according to the manufacturer's protocols. BHK-21 cells were transfected with these synthetic RNAs by electroporation (Electrocell Manipulator 600; BTX, San Diego, CA) as previously described (Borca et al., 2012). Briefly, 0.5 ml of BHK-21 cells at a concentration of 3×10^7 cells/ml in phosphate-buffered saline (PBS) were mixed with 10 μg of RNA in a 4-mm gap BTX cuvette. The cells were then pulsed once at 330 V, maximum resistance, and a capacitance of 1000 μF, followed by dilution in cell growth medium and attachment to a T-25 flask. After 4 h (h), the medium was removed, fresh medium was added and the cultures were incubated at 37 °C, 5% CO_2 for up to 24 h.

The supernatants from transfected cells were passed in LF-BK-αVβ6 cells until the cytopathic effect (CPE) appeared. After successive passages in these cells, virus stocks were prepared and the viral genome completely sequenced using the Prism 3730xl automated DNA sequencer (Applied Biosystems) as previously described (Piccone et al., 2010).

Viruses derived from plasmid pO1Ca and the derived mutant plasmid encoding the 3A deletion are referred to as O1Ca and O1CaΔ3A, respectively.

Comparative ability of viruses to grow in cells of different origin

Comparative growth curves between O1Ca and O1CaΔ3A viruses were performed in LF-BK-αVβ6, FBK and FPK cells. Preformed monolayers were prepared in 24-well plates and infected with the two viruses at MOI of 0.01 (based on TCID50 previously determined in LF-BK-αVβ6 cells). After 1 h of adsorption at 37 °C the inoculum was removed and the cells were rinsed two times with ice-cold 145 mM NaCl, 25 mM MES (pH 5.5) to remove residual virus particles. The monolayers were then rinsed with media containing 1% fetal calf serum and 25 mM Hepes (pH 7.4) and incubated for 0, 4, 8, 24 and 48 h at 37 °C. At appropriate times post-infection, the cells were frozen at −70 °C and the thawed lysates were used to determine titers by TCID50/ml on LF-BK-αVβ6 cells. All samples were run simultaneously to avoid inter-assay variability. Plaque assays in LF-BK-αVβ6 and FBK were performed as previously described (Pacheco et al., 2010b).

Virulence of O1Ca and O1CaΔ3A viruses in cattle and swine

Animal experiments were performed under biosafety level 3 conditions in the animal facilities at PIADC following a protocol approved by the Institutional Animal Care and Use Committee. Three steers (each 300–400 kg) were infected as per the aerosol inoculation method (Pacheco et al., 2010a) with approximately 10^7 PFU/steer of O1Ca or O1CaΔ3A virus, diluted in MEM containing 25 mM Hepes. Different viruses were inoculated in different animal rooms. Rectal temperatures and clinical exam with sedation looking for secondary site replication (vesicles) were performed daily. Clinical score was based on presence of vesicles in the mouth and feet, with a maximum of 20 was performed as previously described (Pacheco et al., 2010a). Antemortem sample collection consisted of blood (to obtain serum), nasal and oral swabs collected daily up to 10 dpi, and at 14, 17 and 21 dpi. Postmortem sample acquisition, performed at 21 dpi, consisted of collection of tissues as previously described (Pacheco et al., 2010a) from dorsal soft palate, dorsal nasal pharynx, retropharyngeal lymph node and interdigital cleft.

Four 20 kg pigs were infected intradermally in the heel bulb (Pacheco and Mason, 2010) with 10^6 PFU/pig of either O1Ca or O1CaΔ3A (two pigs per virus and one virus per room), diluted in MEM containing 25 mM Hepes. At 48 hpi, two naïve pigs were introduced to each room. The four animals remained cohabitating for the rest of the experimental period. For 8 day after inoculation, animals were clinically examined, including rectal temperature recordings and serum and nasal swab collections. Clinical score was based on severity of affected digits and/or snout with a maximum of 16 for direct inoculated animals (inoculated foot was not considered for scoring) and 20 for contact inoculated animals was performed as previously described (Pacheco and Mason, 2010).

After collection, clinical samples were aliquotted and frozen at ≤ −70 °C. One serum and one swab aliquot, collected each day from each animal, were used to perform viral titration by rRT-PCR as described previously (Pacheco et al., 2010a).

FMDV RNA quantitation by real time RT-PCR

FMDV real time RT-PCR (rRT-PCR) was performed as previously described (Pacheco et al., 2010a). RNA copy numbers per ml of fluids (antemortem samples) or per mg of tissue (postmortem samples) were calculated based on a O1Campos specific calibration curve developed with *in vitro* synthesized RNA obtained from pO1Ca. For this, a known amount of FMDV RNA was 10-fold serial diluted in nuclease-free water and each dilution was tested in triplicate by FMDV rRT-PCR. Ct values from triplicates were averaged and plotted against FMDV RNA copy number.

Acknowledgments

We wish to acknowledge Ethan Hartwig for assistance in processing samples. We also thank the Plum Island Animal Resource Unit personnel for their excellent assistance with the animal experiments. We also thank Melanie Prarat for the editing of this manuscript.

References

Arzt, J., Pacheco, J.M., Rodriguez, L.L., 2010. The early pathogenesis of foot-and-mouth disease in cattle after aerosol inoculation. Identification of the nasopharynx as the primary site of infection. Vet. Pathol. 47, 1048–1063.
Beard, C.W., Mason, P.W., 2000. Genetic determinants of altered virulence of Taiwanese foot-and-mouth disease virus. J. Virol. 74, 987–991.
Belsham, G.J., 1993. Distinctive features of foot-and-mouth disease virus, a member of the picornavirus family; aspects of virus protein synthesis, protein processing and structure. Prog. Biophys. Mol. Biol. 60, 241–260.
Borca, M.V., Pacheco, J.M., Holinka, L.G., Carrillo, C., Hartwig, E., Garriga, D., Kramer, E., Rodriguez, L., Piccone, M.E., 2012. Role of arginine-56 within the structural protein VP3 of foot-and-mouth disease virus (FMDV) O1 Campos in virus virulence. Virology 422, 37–45.
Botner, A., Kakker, N.K., Barbezange, C., Berryman, S., Jackson, T., Belsham, G.J., 2011. Capsid proteins from field strains of foot-and-mouth disease virus confer a pathogenic phenotype in cattle on an attenuated, cell-culture-adapted virus. J. Gen. Virol. 92, 1141–1151.
Brown, C.C., Piccone, M.E., Mason, P.W., McKenna, T.S., Grubman, M.J., 1996. Pathogenesis of wild-type and leaderless foot-and-mouth disease virus in cattle. J. Virol. 70, 5638–5641.
Dunn, C.S., Donaldson, A.I., 1997. Natural adaption to pigs of a Taiwanese isolate of foot-and-mouth disease virus. Vet. Rec. 141, 174–175.
Giraudo, A.T., Sagedahl, A., Bergmann, I.E., La Torre, J.L., Scodeller, E.A., 1987. Isolation and characterization of recombinants between attenuated and virulent aphthovirus strains. J. Virol. 61, 419–425.
Giraudo, A.T., Beck, E., Strebel, K., de Mello, P.A., La Torre, J.L., Scodeller, E.A., Bergmann, I.E., 1990. Identification of a nucleotide deletion in parts of polypeptide 3A in two independent attenuated aphthovirus strains. Virology 177780–783
Graff, J., Kasang, C., Normann, A., Pfisterer-Hunt, M., Feinstone, S.M., Flehmig, B., 1994a. Mutational events in consecutive passages of hepatitis A virus strain GBM during cell culture adaptation. Virology 204, 60–68.
Graff, J., Normann, A., Feinstone, S.M., Flehmig, B., 1994b. Nucleotide sequence of wild-type hepatitis A virus GBM in comparison with two cell culture-adapted variants. J. Virol. 68, 548–554.
Grubman, M.J., Baxt, B., 2004. Foot-and-mouth disease. Clin. Microbiol. Rev. 17, 465–493.
Heinz, B.A., Vance, L.M., 1996. Sequence determinants of 3A-mediated resistance to enviroxime in rhinoviruses and enteroviruses. J. Virol. 70, 4854–4857.
Kitamura, N., Semler, B.L., Rothberg, P.G., Larsen, G.R., Adler, C.J., Dorner, A.J., Emini, E.A., Hanecak, R., Lee, J.J., van der Werf, S., Anderson, C.W., Wimmer, E., 1981. Primary structure, gene organization and polypeptide expression of poliovirus RNA. Nature 291, 547–553.
Knowles, N.J., Davies, P.R., Henry, T., O'Donnell, V., Pacheco, J.M., Mason, P.W., 2001. Emergence in Asia of foot-and-mouth disease viruses with altered host range: characterization of alterations in the 3A protein. J. Virol. 75, 1551–1556.
Lama, J., Sanz, M.A., Carrasco, L., 1998. Genetic analysis of poliovirus protein 3 A: characterization of a non-cytopathic mutant virus defective in killing Vero cells. J. Gen. Virol. 79 (Pt 8), 1911–1921.
Larocco, M., Krug, P.W., Kramer, E., Ahmed, Z., Pacheco, J.M., Duque, H., Baxt, B., Rodriguez, L.L., 2013. A continuous bovine kidney cell line constitutively expressing bovine alphaVss6 integrin has increased susceptibility to foot and mouth disease virus. J. Clin. Microbiol..
Lemon, S.M., Murphy, P.C., Shields, P.A., Ping, L.H., Feinstone, S.M., Cromeans, T., Jansen, R.W., 1991. Antigenic and genetic variation in cytopathic hepatitis A virus variants arising during persistent infection: evidence for genetic recombination. J. Virol. 65, 2056–2065.

Li, S., Gao, M., Zhang, R., Song, G., Song, J., Liu, D., Cao, Y., Li, T., Ma, B., Liu, X., Wang, J., 2010. A mutant of infectious Asia 1 serotype foot-and-mouth disease virus with the deletion of 10-amino-acid in the 3A protein. Virus Genes 41, 406–413.
Lohse, L., Jackson, T., Botner, A., Belsham, G.J., 2012. Capsid coding sequences of foot-and-mouth disease viruses are determinants of pathogenicity in pigs. Vet. Res. 43, 46.
Mason, P.W., Grubman, M.J., Baxt, B., 2003a. Molecular basis of pathogenesis of FMDV. Virus Res. 91, 9–32.
Mason, P.W., Pacheco, J.M., Zhao, Q.Z., Knowles, N.J., 2003b. Comparisons of the complete genomes of Asian, African and European isolates of a recent foot-and-mouth disease virus type O pandemic strain (PanAsia). J. Gen. Virol. 84, 1583–1593.
Morace, G., Pisani, G., Beneduce, F., Divizia, M., Pana, A., 1993. Mutations in the 3A genomic region of two cytopathic strains of hepatitis A virus isolated in Italy. Virus Res. 28, 187–194.
Nunez, J.I., Baranowski, E., Molina, N., Ruiz-Jarabo, C.M., Sanchez, C., Domingo, E., Sobrino, F., 2001. A single amino acid substitution in nonstructural protein 3A can mediate adaptation of foot-and-mouth disease virus to the guinea pig. J. Virol. 75, 3977–3983.
Oem, J.K., Yeh, M.T., McKenna, T.S., Hayes, J.R., Rieder, E., Giuffre, A.C., Robida, J.M., Lee, K.N., Cho, I.S., Fang, X., Joo, Y.S., Park, J.H., 2008. Pathogenic characteristics of the Korean 2002 isolate of foot-and-mouth disease virus serotype O in pigs and cattle. J. Comp. Pathol.138, 204–214.
Pacheco, J.M., Mason, P.W., 2010. Evaluation of infectivity and transmission of different Asian foot-and-mouth disease viruses in swine. J. Vet. Sci. 11, 133–142.
Pacheco, J.M., Arzt, J., Rodriguez, L.L., 2010a. Early events in the pathogenesis of foot-and-mouth disease in cattle after controlled aerosol exposure. Vet. J. 183, 46–53.
Pacheco, J.M., Piccone, M.E., Rieder, E., Pauszek, S.J., Borca, M.V., Rodriguez, L.L., 2010b. Domain disruptions of individual 3B proteins of foot-and-mouth disease virus do not alter growth in cell culture or virulence in cattle. Virology 405, 149–156.
Pacheco, J.M., Tucker, M., Hartwig, E., Bishop, E., Arzt, J., Rodriguez, L.L., 2012. Direct contact transmission of three different foot-and-mouth disease virus strains in swine demonstrates important strain-specific differences. Vet. J. 193, 456–463.
Parisi, J.M., Costa Giomi, P., Grigera, P., Auge de Mello, P., Bergmann, I.E., La Torre, J. L., Scodeller, E.A., 1985. Biochemical characterization of an aphthovirus type 0 (1) strain campos attenuated for cattle by serial passages in chicken embryos. Virology 147, 61–71.
Piccone, M.E., Pacheco, J.M., Pauszek, S.J., Kramer, E., Rieder, E., Borca, M.V., Rodriguez, L.L., 2010. The region between the two polyprotein initiation codons of foot-and-mouth disease virus is critical for virulence in cattle. Virology 396, 152–159.
Rodriguez Pulido, M., Sobrino, F., Borrego, B., Saiz, M., 2009. Attenuated foot-and-mouth disease virus RNA carrying a deletion in the 3′ noncoding region can elicit immunity in swine. J. Virol. 83, 3475–3485.
Rowlands, D.J., 2003. Special issue—foot-and-mouth disease—preface. Virus Res. 91, 1.
Sagedahl, A., Giraudo, A.T., De Mello, P.A., Bergmann, I.E., La Torre, J.L., Scodeller, E. A., 1987. Biochemical characterization of an aphthovirus type C3 strain Resende attenuated for cattle by serial passages in chicken embryos. Virology 157, 366–374.
Swaney, L.M., 1988. A continuous bovine kidney cell line for routine assays of foot-and-mouth disease virus. Vet. Microbiol. 18, 1–14.
Yang, P.C., Chu, R.M., Chung, W.B., Sung, H.T., 1999. Epidemiological characteristics and financial costs of the 1997 foot-and-mouth disease epidemic in Taiwan. Vet. Rec. 145, 731–734.
Zhang, Z.D., Kitching, R.P., 2001. The localization of persistent foot and mouth disease virus in the epithelial cells of the soft palate and pharynx. J. Comp. Pathol. 124, 89–94.

Antiviral Research 101 (2014) 30–36

Contents lists available at ScienceDirect

Antiviral Research

journal homepage: www.elsevier.com/locate/antiviral

Pore-forming activity of pestivirus p7 in a minimal model system supports genus-specific viroporin function

Eneko Largo [a], Douglas P. Gladue [b], Nerea Huarte [a], Manuel V. Borca [b], José L. Nieva [a,*]

[a] Biophysics Unit (CSIC-UPV/EHU) and Biochemistry and Molecular Biology Department, University of the Basque Country (UPV/EHU), P.O. Box 644, 48080 Bilbao, Spain
[b] Plum Island Animal Disease Center, ARS, USDA, Greenport, NY 11944, USA

ARTICLE INFO

Article history:
Received 20 August 2013
Revised 3 October 2013
Accepted 22 October 2013
Available online 2 November 2013

Keywords:
Pestivirus
Classical swine fever virus
Viroporin
Viroporin inhibition
Channel blocker
Pore-forming protein

ABSTRACT

Viroporins are small integral membrane proteins functional in viral assembly and egress by promoting permeabilization. Blocking of viroporin function therefore constitutes a target for antiviral development. Classical swine fever virus (CSFV) protein p7 has been recently regarded as a class II viroporin. Here, we sought to establish the determinants of the CSFV p7 permeabilizing activity in a minimal model system. Assessment of an overlapping peptide library mapped the porating domain to the C-terminal hydrophobic stretch (residues 39–67). Pore-opening dependence on pH or sensitivity to channel blockers observed for the full protein required the inclusion of a preceding polar sequence (residues 33–38). Effects of lipid composition and structural data further support that the resulting peptide (residues 33–67), may comprise a bona fide surrogate to assay p7 activity in model membranes. Our observations imply that CSFV p7 relies on genus-specific structures–mechanisms to perform its viroporin function.
© 2013 Elsevier B.V. All rights reserved.

1. Introduction

The *Flaviviridae* family comprises of positive-strand RNA viruses, classically classified into three genera: Flavivirus, Pestivirus, and Hepacivirus (Lindenbach et al., 2007). These genera include highly diverse viruses with increasing relevance as both human and animal pathogens. Pestiviruses and hepaciviruses show a high similarity in genome structure and replication mechanisms, and to a lesser extent similarity to flaviviruses (Lindenbach et al., 2007). All viruses belonging to this family translate their RNA into a single polyprotein precursor, which is subsequently cleaved by a combination of host and viral proteases to render structural and non-structural proteins. Specific to the Pestivirus and Hepacivirus genera is the existence of an α-helix-turn-α-helix integral membrane hairpin that connects the structural proteins encoded in the N-terminal portion of the polyprotein with the C-terminal non-structural proteins. After full proteolytic processing of the precursor, the released product, termed p7 (Fig. 1A), remains associated to membranes as an integral membrane protein of approximately 60–70 amino acids (Harada et al., 2000; Lin et al., 1994).

In the last decade an intense research effort has focused on the p7 protein derived from hepatitis C virus (HCV) (reviewed in Steinmann and Pietschmann 2010). This protein is required for production of infectious viruses, but dispensable for viral entry or RNA replication (Steinmann et al., 2007a; Steinmann and Pietschmann, 2010). Moreover, HCV p7 is a viroporin, whose membrane-permeabilizing activity has been proven essential for viral propagation (Jones et al., 2007; Nieva et al., 2012; Wozniak et al., 2010). Consistent with this idea, several compounds have been shown to block HCV p7 pores and inhibit virus production (Foster et al., 2011; Griffin et al., 2003; Steinmann et al., 2007b).

Similarly to hepaciviruses, p7 plays an essential role in the life cycle of pestiviruses and contributes to their pathogenicity (Gladue et al., 2012; Griffin et al., 2004; Luscombe et al., 2010). It has been argued that the pestivirus p7 constitutes a general model for the HCV p7 viroporin, therefore making it useful in the characterization of anti-HCV compounds (Griffin et al., 2004; Luscombe et al., 2010). Here, we have aimed at establishing the determinants of the pestivirus p7 pore-forming activity in a liposome-based model system. Accordingly, we first sought to establish the minimal CSFV p7 sequence required for a pH-dependent pore-forming activity that could be inhibited by channel blockers. Establishment of a shorter active sequence, more amenable for synthesis and purification than the full-length protein, subsequently allowed determining the lipid dependence of the process, and the structural characterization of the pore-forming domain. Together, our data disclose the

Abbreviations: BVDV, bovine viral diarrhea virus; CD, circular dichroism; Chol, cholesterol; CL, cardiolipin; CSFV, classical swine fever virus; HCV, hepatitis C virus; PC, phosphatidylcholine; PE, phospahtidylethanolamine; PS, phosphatidylserine; PI, phosphatidylinositol; SM, sphingomyelin.

* Corresponding author. Tel.: +34 94 6013353; fax: +34 94 6013360.
E-mail address: gbpniesj@lg.ehu.es (J.L. Nieva).

0166-3542/$ - see front matter © 2013 Elsevier B.V. All rights reserved.
http://dx.doi.org/10.1016/j.antiviral.2013.10.015

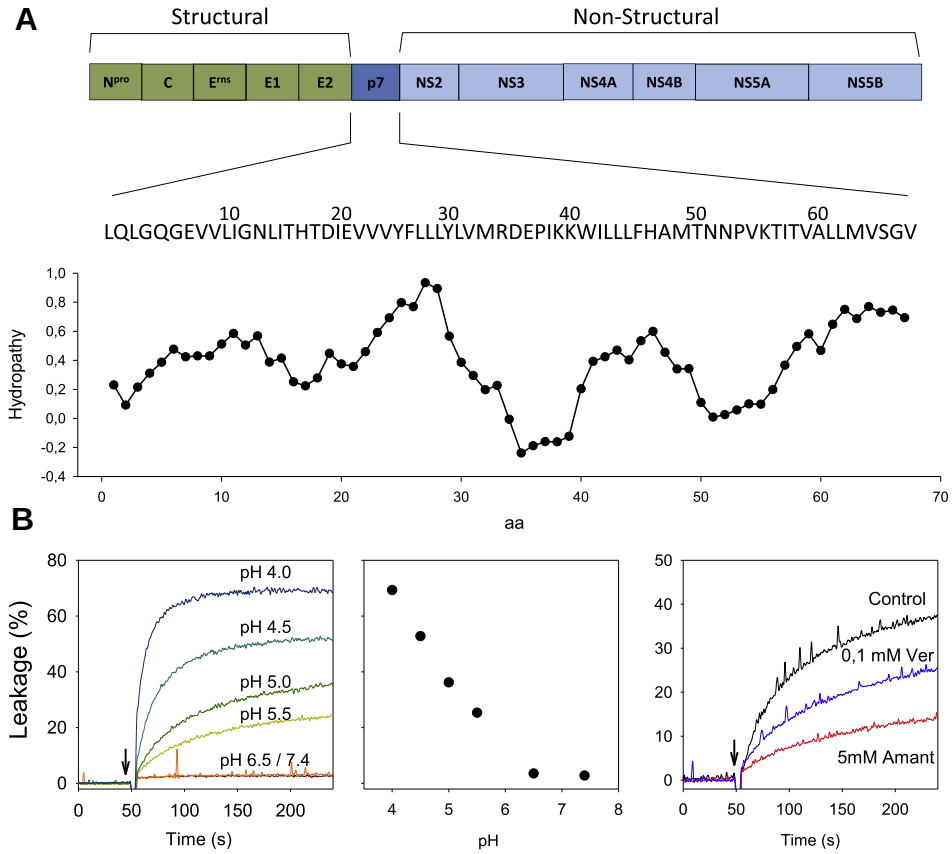

Fig. 1. CSFV p7 sequence and pore-forming activity. (A) Direct translation of pestivirus ssRNA genome gives rise to a single, large polyprotein, which is processed into individual viral proteins. Membrane-integral p7 originates from processing by the host signal peptidase (Top). The hydropathy plot below CSFV p7 sequence is based on the Eisenberg scale. Plotted values represent means for a sliding window of 11 amino acids. (B) Membrane permeabilization induced by p7 (ANTS/DPX assay). The protein dissolved in DMSO was injected (indicated by the arrow) into stirring solutions of PC:PE:PI (5:3:2 mol ratio) liposomes at a protein-to-lipid ratio of 1:100 (mol:mol). Leakage of vesicular internal aqueous contents was monitored as a function of time. Lipid concentration was 100 μM. The effect of lowering the pH from 7.4 to 4.0 is illustrated in the left and central panels. In the latter the levels of permeabilization after 200 s was plotted as a function of the assayed pH values. Addition of peptide solvent alone did not have any effect on vesicle stability (not shown). The right panel shows the effect of adding amantadine (5 mM) or verapamil (100 μM) on pore-forming activity (red and blue curves, respectively) at pH 5.0. The black curve corresponds to the control without inhibitor. (For interpretation of the references to colour in this figure legend, the reader is referred to the web version of this article.)

determinants of the p7 permeabilizing activity, and suggest a new potential means for isolation of antivirals targeting p7.

2. Materials and methods

The p7 protein and derived peptides displayed in Table 1 were produced and assayed as previously described (Gladue et al., 2012). Phosphatidylcholine (PC), phospahtidylethanolamine (PE), phosphatidylinositol (PI), phosphatidylserine (PS), sphingomyelin (SM), cardiolipin (CL) and cholesterol (Chol) were purchased from Avanti Polar Lipids (Birmingham, AL, USA). Dodecylphosphocholine (DPC) was from Anatrace (Maumee, OH, USA). The 8-aminonaphtalene-1,3,6-trisulfonic acid sodium salt (ANTS) and *p*-xylenebis(pyridinium)bromide (DPX) were obtained from Molecular Probes (Junction City, OR, USA).

Large unilamellar vesicle (LUV) production, ANTS/DPX leakage assays, and circular dichroism (CD) measurements, were essentially conducted as previously reported (Sanchez-Martinez et al., 2008). The leakage assay protocol was adapted as described (Gladue et al., 2012).

Penetration into lipid monolayers was measured to estimate the capacity of p7 peptides for inserting into membranes that mimic different target organelles. In brief, changes in surface pressure were monitored as a function of time in a fixed-area circular trough (μTrough S system, Kibron, Helsinki) measuring 2 cm in diameter and with a volume of 1 ml. The aqueous phase consisted of 1 ml of 5 mM Hepes, 100 mM NaCl (pH 7.4). Lipids, dissolved in chloroform, were spread over the surface and the desired initial surface pressure (π_0) was attained by changing the amount of lipid applied to the air–water interface. Peptides were injected into the subphase with a Hamilton microsyringe (Fig. S1).

Table 1
Peptide sequences used in this study.

Name	Sequence[a]	CSFV p7 numbering[a]
p7	LQLGQGEVVLIGNLITHTDIEVVVYFLLLYLVMRDEPIKK WILLLFHAMTNNPVKTITVALLMVSGV	1–67
p7-1	LQLGQGEVVLIGNLITHTDIE	1–21
p7-2	THTDIEVVVYFLLLWLVMRDEPIKK-KK	16–40-KK
p7-3	MRDEPIKKWILLLFHAMTNNPVK	33–55
p7-4	KK-KKWILLLFHAMTNNPVKTITVALLMVSGV	KK-39–67
p7-N	LQLGQGEVVLIGNLITHTDIEVVVYFLLLYLVMRDEPIKK	1–32
p7-C	MRDEPIKKWILLLFHAMTNNPVKTITVALLMVSGV	33–67

[a] Sequences and numbering based on Brescia strain. Underlined residues correspond to the polar turn proposed to connect the two transmembrane domains.

3. Results

3.1. Membrane permeabilizing activity of the full-length CSFV p7 protein

Fig. 1A displays the CSFV p7 sequence and the hydrophobicity distribution within. The presence of two mainly hydrophobic regions (residues 1–32 and 41–67), intervened by polar residues (33–40) suggests that p7 can form an integral hairpin in membranes (Monne et al., 1999). Furthermore, consistent with a viroporin-like function, a synthetic p7 protein was capable of establishing permeabilizing pores upon addition to a suspension of liposomes that emulate the endoplasmic reticulum (ER) membrane (Fig. 1B). Underscoring the functional relevance of the process, liposome permeabilization was elicited at low pH, the leakage level increasing from virtually 0% to 70% upon lowering the pH value from 7.4 to 4.0 (Fig. 1B left-hand and central panels). Moreover, the process was inhibited by addition of the generic channel blockers amantadine and verapamil (Fig. 1B, right-hand panel). Thus, this assay provides a suitable means to establish sequence determinants and lipid dependence of pore formation by p7.

3.2. Pore-forming activity dependence on sequence

A library of overlapping synthetic peptides was produced to map the minimal p7 sequence required for pore formation (Table 1 and Fig 2A). To ensure membrane-spanning capacity, the minimal length of these peptides was primarily set to 20 residues. Then, the actual sequence range was established attending to the presence of polar p7 residues with tendency to form turns in membranes (Monne et al., 1999) (Fig. 2A). Thus, the polar sequences overlapping peptides p7–1/p7–2 and p7–2/p7–3 were ^{16}THTDIE^{21} and ^{33}MRDEPIKK^{40}, respectively. The sequence overlapping peptides p7–3 and p7–4 was longer (residues 39–55). In this case, p7–4 boundaries were selected to span the hydrophobic C-terminal section of p7. The resulting sequence was long enough to transverse the membrane, although interrupted by the turn-promoting ^{49}MTNNPVK^{55} polar sequence. Finally, to keep the solubility of the synthetic peptides comparable, a Lys-tag were also added to p7–2 and p7–4 as described (Madan et al., 2007).

We have previously reported mutagenesis results indicating that the conserved polar residues within the connection between the potential CSFV p7 transmembrane domains were required for virus production, but not for RNA replication or polyprotein processing (Gladue et al., 2012). Thus, we added to the analysis p7-C, designed to include the turn-promoting residues and the C-terminal transmembrane domain, and an overlapping p7-N, based on the N-terminal section of the protein (Table 1).

Liposome permeabilization levels induced by the different p7-derived peptides are compared in Fig. 2B. Given the activation at low pH observed for the full-length protein and the potential relevance of such effect (Fig. 1), the peptide-library was assayed at pH 5.0. Addition of p7–4 permeabilized the liposomes efficiently, whereas the rest of the peptides were largely inactive. This observation underpins the C-terminal transmembrane section as the p7 pore-forming domain. Data displayed in this figure further indicates that p7-C was also an effective pore-forming peptide, while p7-N was devoid of activity.

To determine the involvement of the conserved ^{33}MRDEPIKK^{40} turn in pore-forming activity, we further compared in the liposomal system pore-forming activities of p7-C and p7–4 (Fig. 3). Of note, the latter peptide was devoid of the turn-promoting residues, but bore comparable solubility due to the Lys-tag (Table 1). The p7–4 peptide showed higher pore-forming activity as a function of the peptide dose (panel A, right). However, as compared to p7-C, p7–4 activity was not dependent on pH (panel B) or inhibited by addition of the channel blockers amantadine (panel C) or verapamil (panel D). Inhibition of p7-C activity by the latter compounds was actually observed within the same range of concentrations that blocked pore formation by the full-length protein (Fig. 1).

These data would be consistent with pore-forming activity residing at the C-terminal transmembrane section, and with the N-terminal turn residues playing a role at regulating the process. According to this view, p7-C would recreate more precisely than p7–4 the viroporin activity of the full p7 protein.

3.3. Pore-forming activity dependence on lipid

We used p7-C as a minimal version of the full protein to determine the lipid dependence of pore-forming activity. Data displayed in Fig. 4 compare p7-C insertion induced permeabilization of membranes that emulate different target organelles. Fig. 4A shows results of p7-C-induced permeabilization of ER-like liposomes upon lowering the pH (left panel), and its insertion into monolayers at pH 5.0 and 7.4 (center and right panels). The lipid monolayer technique provides information at the molecular level on peptide interactions with lipid membranes (for a comprehensive review on this method and its application to peptides see: Maget-Dana 1999). In the penetration experiments, p7 peptide insertion into a monolayer of constant area was monitored by following the increase of surface pressure as a function of time (Fig. S1). Induction of high final pressure values, and/or capacity for increasing the surface pressure of highly compressed monolayers (i.e., insertion at high initial pressure values) is consistent with efficient peptide insertion into membranes.

Kinetic traces in the center panel of Fig. 3A disclosed p7-C capacity for increasing the surface pressure of an ER-like lipid monolayer initially compressed at ca. 20 mN/m (π_0), the process being more efficient at pH 5.0 than at pH 7.4. The right-hand panel discloses the critical pressures (π_c-s) for membrane insertion (i.e., the surface pressure at which the peptide was excluded from the lipid monolayer (Fig. S1)). At both pHs, p7-C was capable of penetrating into ER-like monolayers above surface pressures of unstressed natural membranes ($\pi_c \geqslant 30$ mN/m, Marsh 2007). However, as compared to pH 5.0 (filled symbols), the lower slope observed at pH 7.4 (empty symbols) for the increase in pressure as a function of π_0, suggests that reduced amounts of peptide associated with the monolayer under this condition.

The analogous HCV p7 protein has been localized primarily to the ER, but also to the plasma membrane and mitochondria (Carrere-Kremer et al., 2002; Griffin et al., 2005, 2004; Haqshenas et al., 2007), which has led the proposal that the p7 product may modify the functions of distinct organelles (Steinmann and Pietschmann, 2010). Thus, we next analyzed the dependence of p7-C pore-forming activity and insertion on the composition of additional target membranes (Table 2). Data displayed in Fig. 4B-top confirmed a pH-dependent permeabilization of membranes emulating the Golgi compartment, but not of those emulating the plasma membrane. Membranes emulating mitochondria were also permeabilized after peptide addition, but the pH effect was less pronounced, and an optimum pH of 6.0 was observed. The source and/or relevance of this difference with respect to the Golgi-like membranes are presently unknown. The corresponding π_c-s (Fig. 4B, bottom) denoted more effective insertion into Golgi or mitochondria membranes at pH 5.0. Notably, the peptide could also insert above 30 mN/m into monolayers made of the plasma membrane lipids at both pH's, i.e., under conditions not leading to pore formation. This observation suggests that pore-formation by p7-C inserted into membranes is dependent on the lipid composition, and optimal in membranes emulating secretory compartments.

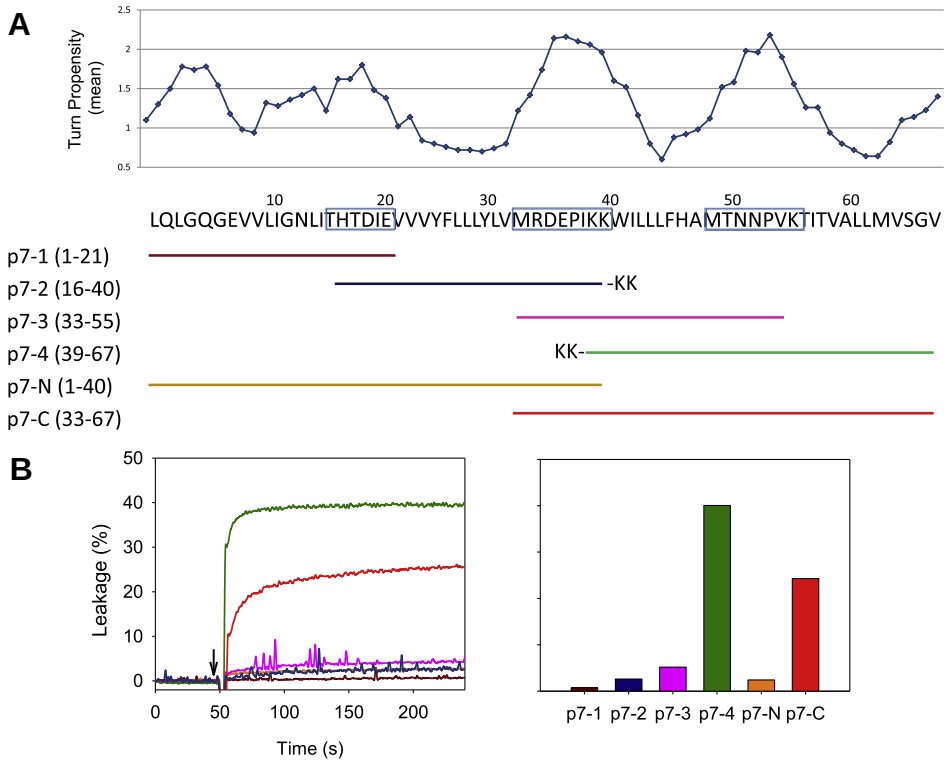

Fig. 2. Analysis of membrane-permeabilizing activity in a peptide library. (A) Propensity for establishing turns in membranes within p7 amino acid sequence and derived peptide library below. Plotted values are the average of normalized turn potentials described by Monne et al. 1999, calculated within sliding windows of 5 amino acids. Boxes designate potential turns within p7 sequence. (B) Left: kinetics of peptide-induced liposome permeabilization. Peptides were added to vesicles at a peptide-to-lipid ratio of 1:250 (mol:mol) and pH 5.0. Right: Bars correspond to permeabilization levels after incubation of peptides with liposomes for 200 s. Conditions otherwise as in previous Fig. 1B.

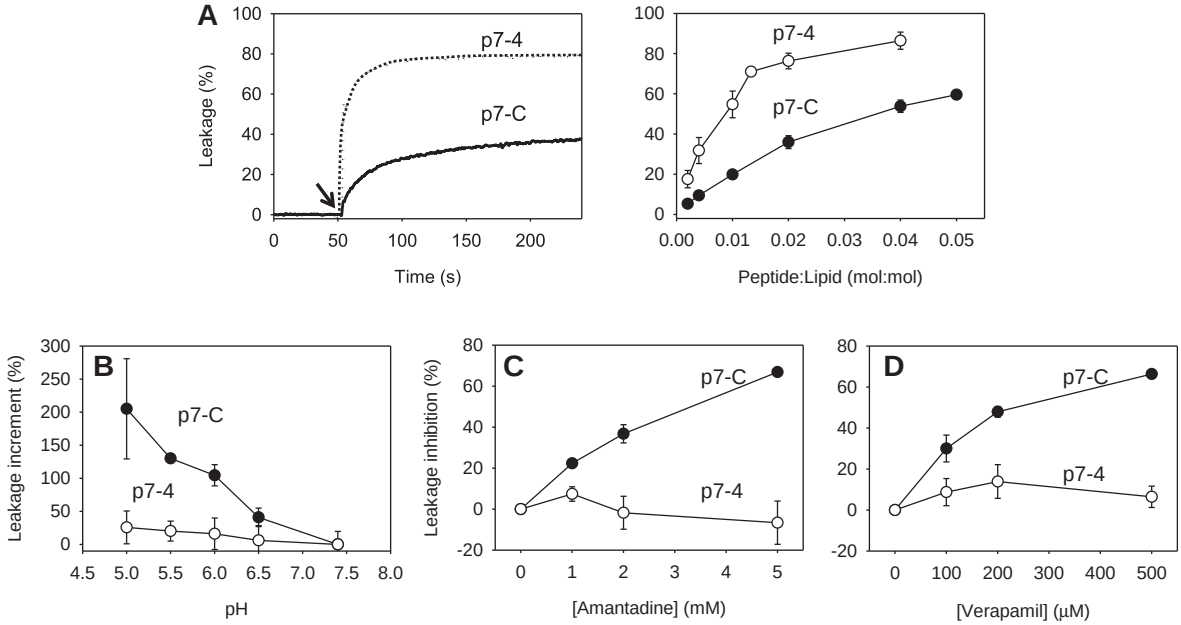

Fig. 3. Effect of turn-promoting ^{33}MRDEPI^{38} residues on pore-forming activity. (A) Comparison of leakage levels induced by p7-C and p7–4. Left: Leakage of vesicle contents induced as a function of time by p7-C and p7–4 peptides (solid and dotted lines, respectively) at pH 7.4. The peptide-to-lipid ratio was 1:50 and the lipid concentration 100 μM. Right: lytic activity as a function of p7-C and p7–4 dose (filled and empty symbols, respectively). The plotted values correspond to extents of leakage measured 200 s after peptide addition. (B) Dependence of leakage on pH. Percentage increase of the extent of leakage at each pH was calculated with respect to the value obtained at pH 7.4. Peptide was added at a peptide-to-lipid ratio of 1:250 and leakage values determined as in the previous panel. (C and D) Inhibition of leakage by Amantadine and Verapamil, respectively. Extents of leakage in the presence of increasing amounts of inhibitor were determined 200 s after peptide addition. Conditions otherwise as in panel A. Means ± S.D. of three values are represented in panels A-right, B–D.

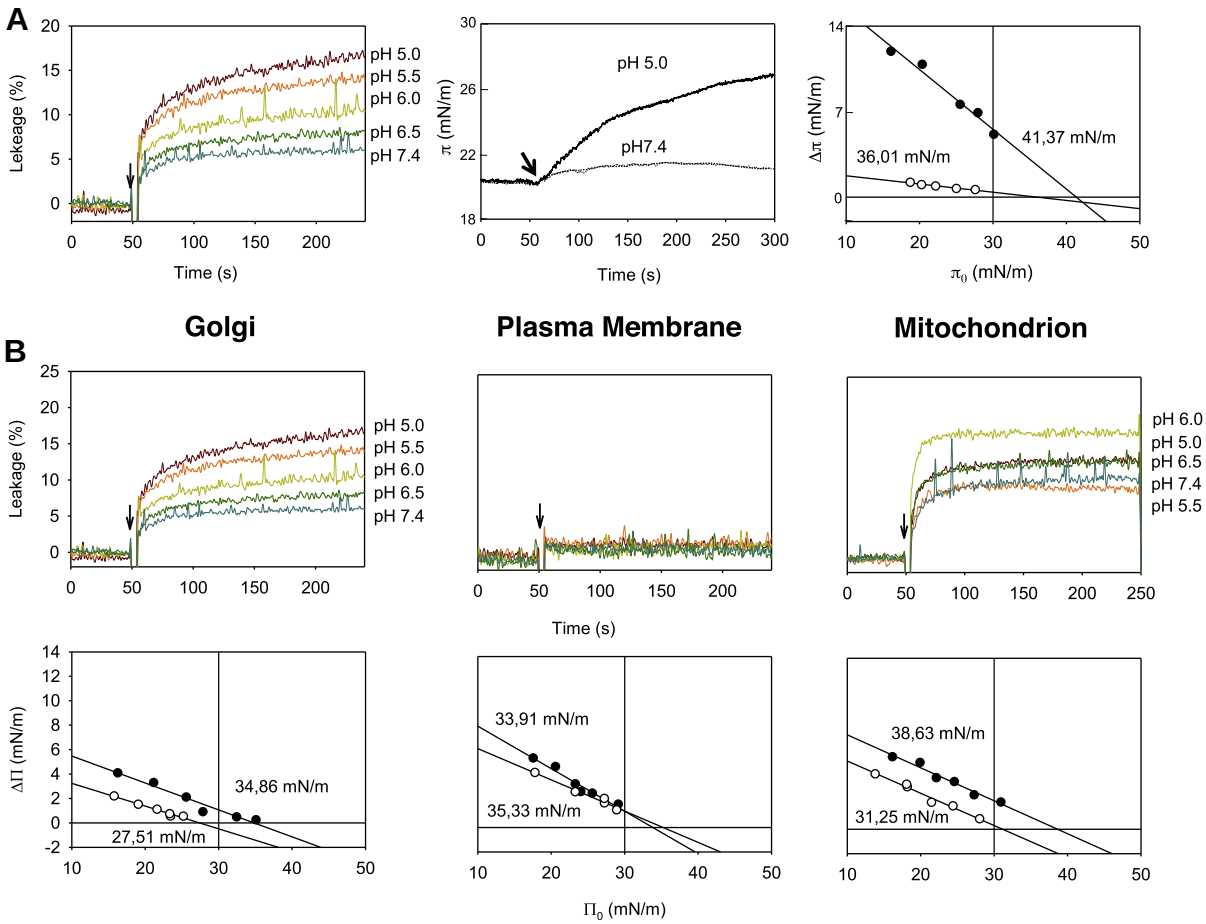

Fig. 4. Interactions of p7-C peptide with membranes emulating the lipid composition of different cell compartments. (A) Interactions with membranes emulating the ER composition (Table 2). Left: membrane permeabilization (ANTS/DPX assay). The peptide was injected (addition time indicated by the arrow) into stirring solutions of liposomes at the pHs indicated in the panel. The lipid and peptide concentrations were 100 and 0.4 μM, respectively. Center: Insertion into lipid monolayers. Surface pressure increase was measured in time upon injection of peptide (indicated by the arrow) in the subphase (final peptide concentration: 0.4 μM). The initial pressure of the monolayer was fixed at ≈20 mN/m, and the pH was 7.4 or 5.0 (dotted and solid lines, respectively). Right: Maximum increase in surface pressure induced by the peptide, measured as a function of the initial surface pressure of the phospholipid monolayers incubated at pH 7.4 or 5.0 (empty and filled symbols, respectively). The dotted lines begin at 30 mN/m. The critical pressures for insertion (π_c-s) are indicated in the panels. (B) Interactions of p7-C with membranes emulating the lipid composition of the Golgi apparatus, plasma membrane and mitochondria (Table 2). Measuring conditions for membrane permeabilization (top) and insertion into lipid monolayers (bottom) as described in the previous panel.

Table 2
Lipid mixtures used in vesicle and monolayer assays.

	PC	PE	PI	PS	SPM	CL	Chol
ER[a]	50	30	20	–	–	–	–
Golgi	50	20	10	–	20	–	–
Plasma membrane	20	12.5	–	5	12.5	–	50
Mitochondria	40	35	10	–	–	15	–

[a] Mole percentages based on those reported by van Meer et al. (2008).

3.4. Secondary structure determination

Sequence features and functional results so far suggest that the p7-C peptide may embody a transmembrane helical pore, putatively intervened by a short turn. To test this possibility further, we measured p7-C secondary structure in diverse non-polar media and membrane mimics, and compared it with that adopted by the reverting helix represented by p7-N (Fig. 5A). The structural components of both peptides were obtained after deconvolution of CD spectra using the CDPro software package (Sreerama and Woody, 2000). p7-N and p7-C peptides adopted main α-helical conformations in 50% 1,1,1,3,3,3-hexafluoro-2-propanol (HFIP). In this medium p7-C was slightly more helical than p7-N, albeit not significantly (top-left). Comparatively higher amounts of p7-C helical conformers were also observed in the presence of SDS micelles (top-right), or when dispersed in the membrane-mimic DPC at neutral pH (bottom-left). However, in DPC at pH 5.0 the fraction of p7-N helices decreased significantly, while β-sheet and non-periodic conformers of this peptide increased. In sharp contrast, a subtle increase of p7-C helical structures could be observed under these conditions. Thus, in the presence of DPC phospholipid and acidic pH, the CD data were compatible with stability of the helical structure adopted by the p7-C sequence, while a certain degree of p7-N disorganization seemed to take place. Nonetheless, turn and unordered structures accounted for approximately 30% of the p7-C conformers in DPC under both conditions, consistent with the predicted turn formation in membranes by residues ^{33}MRDEPIKK^{40} and ^{49}MTNNPVK^{55} (Fig. 2A).

Together, the previous CD results are consistent with adoption of a main helical conformation by the C-terminal hydrophobic domain of CSFV p7 in the membrane milieu under conditions of optimal pore-forming activity, while non-periodic structures would contribute significantly more to the conformation adopted by the N-terminal sequence. These data support a model for the CSFV p7 channel in membranes in which the C-terminal bipartite

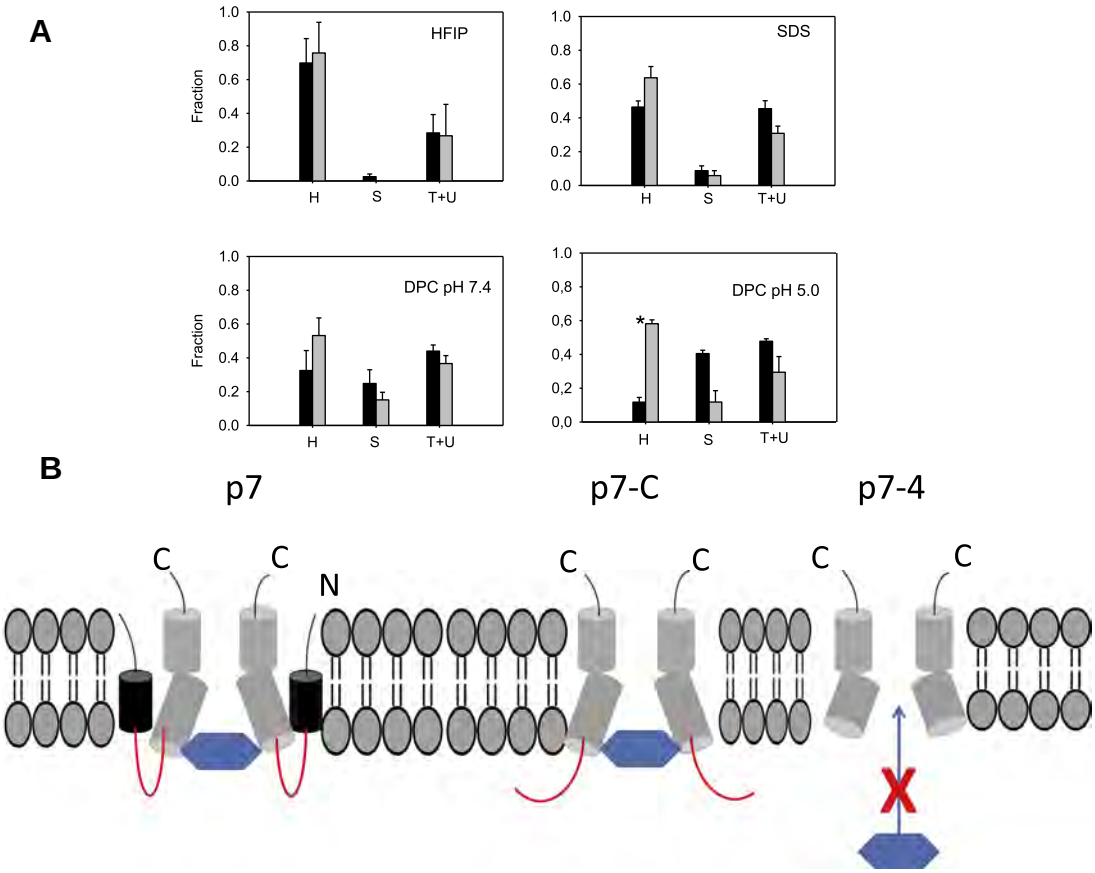

Fig. 5. Secondary structure of the CSFV p7 hydrophobic regions and proposed architecture within membranes. (A) The structural components were calculated for the CD spectra obtained in different non-polar media and membrane mimics, as indicated in the panels. Means ± S.D. for the fraction values estimated with CONTIN-LL, CDSSTR and SELCON3 programs are plotted for p7-N (black bars) and p7-C (gray bars) peptides. H, helix; S, strand; T + U, turns + unordered. (B) Models for the membrane pores established by the full-length p7 protein (left), and the peptide surrogates p7-C (center) and p7-4 (right). The hexagon represents the channel blockers used in this study (amantadine and verapamil).

helix forms the actual permeating pore (Fig 5B-left). This pore could be recreated in the liposomal system by p7-C, a peptide devoid of the N-terminal hydrophobic domain (Fig 5B-center). In the absence of the ^{33}MRDEPI^{38} turn, pores could be efficiently formed by p7–4, but were not dependent on pH or inhibited by amantadine or verapamil (Fig. 5B-right).

4. Discussion

In essence, our findings here and the previous report (Gladue et al., 2012) support similar viroporin activities for the p7 products of the members of the *Flaviviridae* family. However, despite the fact that hepacivirus and pestivirus p7 proteins share a similar class IIA viroporin architecture in membranes (Nieva et al., 2012), the low sequence similarity (Fig. S1A) and the experimental evidence presented here indicate that determinants of the pore-forming function in both proteins might be different.

Our approach in this work identifies the CSFV p7 C-terminal hydrophobic sequence as a pore-forming bipartite helix (Figs. 2, 3 and 5). According to our results, this domain inserted into membranes of the secretory pathway would display pore-forming activity in the ER and Golgi (Fig. 4). In addition, boosting of the process at acidic pH supports a putative role in alkalinizing the lumen of the Golgi apparatus, in line with the proposed function for other viroporins (Nieva et al., 2012; Wozniak et al., 2010). Structural and biochemical evidence suggests a comparable overall organization for the HCV p7 protein, consisting of two transmembrane segments connected by a short interhelical loop (Carrere-Kremer et al., 2002; Cook et al., 2013; Cook and Opella, 2011; Patargias et al., 2006). However in contrast to our observations, in the hepaciviral p7 protein the N-terminal section has been shown to embody the pore-forming domain (Chew et al., 2009; Montserret et al., 2010; Steinmann and Pietschmann, 2010). Thus, as inferred from computational models (Luik et al., 2009; Patargias et al., 2006; StGelais et al., 2009) and recently reported high-resolution NMR structural data (OuYang et al., 2013), in the prevailing structural model for the HCV p7 pore in lipid bilayers the N-terminal domains form the channel interior, while the reverting chains face the lipid.

Moreover, determinants of amantadine sensitivity seem to be different in both proteins. In the case of HCV p7, mutagenesis identifies a poly-Leu sequence within the reverting C-terminal helix as a main determinant of amantadine sensitivity (StGelais et al., 2009). Consistent with this observation, the binding site has been recently mapped to a hydrophobic pocket between the pore-forming and reverting helices (OuYang et al., 2013). Thus, our finding that the connecting turn determines sensitivity to amantadine in the absence of the reverting helix (Fig. 3) suggests that membrane pores are formed and regulated by different structures–mechanisms in the case of the CSFV p7.

Consistently with the pore-forming activity, the CD results sustain the stability of the p7-C helical conformation in a membrane milieu at low pH, while the conformation adopted by the preceding N-terminal sequence included a majority of flexible conformers (Fig. 5A). Thus, the organization inferred for CSFV-p7 (S2B-left) is

opposite to the organization postulated for the analogous HCV p7 inserted into membranes, which consists of a predominantly helical domain at the N-terminus, and a (short)helix-loop motif at the C-terminus (Montserret et al., 2010; OuYang et al., 2013) (Fig. S2 B-right).

Finally our data has implications for the development of antivirals targeting the flavivirus p7 viroporin function. As previously suggested for HCV p7 (Gervais et al., 2011; StGelais et al., 2007), reconstitution of CSFV p7 viroporin function in a liposomal system may be useful for identifying and characterizing new potential antiviral compounds. However, the poor yield of synthesis, owing to the length and hydrophobicity of the sequence, restricts the potential application of the complete protein to systematic experimentation. It has been argued that peptides representing a single transmembrane domain may retain the capacity to assemble ion channels and pores in membranes, and often comprise bona fide surrogates of the full protein sequences (Shai, 1995). Our identification of a shorter version of CSFV p7, more amenable to synthesis, but otherwise retaining its pH-dependent pore-forming activity in a liposomal system, may help in establishing the methodological basis for future antiviral high-throughput screenings.

Overall our observations also imply the existence of essentially different determinants of pore-forming activity in hepaciviruses and pestiviruses. Thus, our experimental data support common inhibition of viroporin function by generic channel blockers such as adamantane or verapamil, but cautions that development of more specific (and likely more potent) inhibitory ligands requires the use of genus-specific sequences-structures.

Acknowledgements

This study was in part supported by Spanish MINECO and Basque Government Grants (BIO2011-29792 and IT838-13 to J.L.N.)

Appendix A. Supplementary data

Supplementary data associated with this article can be found, in the online version, at http://dx.doi.org/10.1016/j.antiviral.2013.10.015.

References

Carrere-Kremer, S., Montpellier-Pala, C., Cocquerel, L., Wychowski, C., Penin, F., Dubuisson, J., 2002. Subcellular localization and topology of the p7 polypeptide of hepatitis C virus. J. Virol. 76, 3720–3730.
Chew, C.F., Vijayan, R., Chang, J., Zitzmann, N., Biggin, P.C., 2009. Determination of pore-lining residues in the hepatitis C virus p7 protein. Biophys. J. 96, L10–L12.
Cook, G.A., Opella, S.J., 2011. Secondary structure, dynamics, and architecture of the p7 membrane protein from hepatitis C virus by NMR spectroscopy. Biochim. Biophys. Acta-Biomembr. 1808, 1448–1453.
Cook, G.A., Dawson, L.A., Tian, Y., Opella, S.J., 2013. Three-dimensional structure and interaction studies of hepatitis C virus p7 in 1,2-dihexanoyl-sn-glycero-3-phosphocholine by solution nuclear magnetic resonance. Biochemistry 52, 5295–5303.
Foster, T.L., Verow, M., Wozniak, A.L., Bentham, M.J., Thompson, J., Atkins, E., Weinman, S.A., Fishwick, C., Foster, R., Harris, M., Griffin, S., 2011. Resistance mutations define specific antiviral effects for inhibitors of the hepatitis C virus p7 ion channel. Hepatology 54, 79–90.
Gervais, C., Do, F., Cantin, A., Kukolj, G., White, P.W., Gauthier, A., Vaillancourt, F.H., 2011. Development and validation of a high-throughput screening assay for the hepatitis C virus p7 viroporin. J. Biomol. Screen. 16, 363–369.
Gladue, D.P., Holinka, L.G., Largo, E., Fernandez Sainz, I., Carrillo, C., O'Donnell, V., Baker-Branstetter, R., Lu, Z., Ambroggio, X., Risatti, G.R., Nieva, J.L., Borca, M.V., 2012. Classical swine fever virus p7 protein is a viroporin involved in virulence in swine. J. Virol. 86, 6778–6791.
Griffin, S.D., Beales, L.P., Clarke, D.S., Worsfold, O., Evans, S.D., Jaeger, J., Harris, M.P., Rowlands, D.J., 2003. The p7 protein of hepatitis C virus forms an ion channel that is blocked by the antiviral drug, Amantadine. FEBS Lett. 535, 34–38.
Griffin, S.D., Harvey, R., Clarke, D.S., Barclay, W.S., Harris, M., Rowlands, D.J., 2004. A conserved basic loop in hepatitis C virus p7 protein is required for amantadine-sensitive ion channel activity in mammalian cells but is dispensable for localization to mitochondria. J. Gen. Virol. 85, 451–461.
Griffin, S., Clarke, D., McCormick, C., Rowlands, D., Harris, M., 2005. Signal peptide cleavage and internal targeting signals direct the hepatitis C virus p7 protein to distinct intracellular membranes. J. Virol. 79, 15525–15536.
Haqshenas, G., Mackenzie, J.M., Dong, X., Gowans, E.J., 2007. Hepatitis C virus p7 protein is localized in the endoplasmic reticulum when it is encoded by a replication-competent genome. J. Gen. Virol. 88, 134–142.
Harada, T., Tautz, N., Thiel, H.J., 2000. E2–p7 region of the bovine viral diarrhea virus polyprotein: processing and functional studies. J. Virol. 74, 9498–9506.
Jones, C.T., Murray, C.L., Eastman, D.K., Tassello, J., Rice, C.M., 2007. Hepatitis C virus p7 and NS2 proteins are essential for production of infectious virus. J. Virol. 81, 8374–8383.
Lin, C., Lindenbach, B.D., Pragai, B.M., McCourt, D.W., Rice, C.M., 1994. Processing in the hepatitis C virus E2-NS2 region: identification of p7 and two distinct E2-specific products with different C termini. J. Virol. 68, 5063–5073.
Lindenbach, B.D., Thiel, H.-J., Rice, C.M., 2007. Flaviviridae: the viruses and their replication. In: Knipe, D.M., Howley, P.M. (Eds.), Fields Virology, fifth ed. Lippincott Williams & Wilkins, Philadelphia, pp. 1102–1152.
Luik, P., Chew, C., Aittoniemi, J., Chang, J., Wentworth, P., Dwek, R.A., Biggin, P.C., Venien-Bryan, C., Zitzmann, N., 2009. The 3-dimensional structure of a hepatitis C virus p7 ion channel by electron microscopy. Proc. Nat. Acad. Sci. USA 106, 12712–12716.
Luscombe, C.A., Huang, Z., Murray, M.G., Miller, M., Wilkinson, J., Ewart, G.D., 2010. A novel Hepatitis C virus p7 ion channel inhibitor, BIT225, inhibits bovine viral diarrhea virus in vitro and shows synergism with recombinant interferon-alpha-2b and nucleoside analogues. Antiviral Res. 86, 144–153.
Madan, V., Sanchez-Martinez, S., Vedovato, N., Rispoli, G., Carrasco, L., Nieva, J.L., 2007. Plasma membrane-porating domain in poliovirus 2B protein. A short peptide mimics viroporin activity. J. Mol. Biol. 374, 951–964.
Maget-Dana, R., 1999. The monolayer technique: a potent tool for studying the interfacial properties of antimicrobial and membrane-lytic peptides and their interactions with lipid membranes. Biochim. Biophys. Acta 1462, 109–140.
Marsh, D., 2007. Lateral pressure profile, spontaneous curvature frustration, and the incorporation and conformation of proteins in membranes. Biophys. J. 93, 3884–3899.
Monne, M., Nilsson, I., Elofsson, A., von Heijne, G., 1999. Turns in transmembrane helices: determination of the minimal length of a "helical hairpin" and derivation of a fine-grained turn propensity scale. J. Mol. Biol. 293, 807–814.
Montserret, R., Saint, N., Vanbelle, C., Salvay, A.G., Simorre, J.P., Ebel, C., Sapay, N., Renisio, J.G., Bockmann, A., Steinmann, E., Pietschmann, T., Dubuisson, J., Chipot, C., Penin, F., 2010. NMR structure and ion channel activity of the p7 protein from hepatitis C virus. J. Biol. Chem. 285, 31446–31461.
Nieva, J.L., Madan, V., Carrasco, L., 2012. Viroporins: structure and biological functions. Nat. Rev. Microbiol. 10, 563–574.
OuYang, B., Xie, S., Berardi, M.J., Zhao, X., Dev, J., Yu, W., Sun, B., Chou, J.J., 2013. Unusual architecture of the p7 channel from hepatitis C virus. Nature 498, 521–525.
Patargias, G., Zitzmann, N., Dwek, R., Fischer, W.B., 2006. Protein-protein interactions: modeling the hepatitis C virus ion channel p7. J. Med. Chem. 49, 648–655.
Sanchez-Martinez, S., Huarte, N., Maeso, R., Madan, V., Carrasco, L., Nieva, J.L., 2008. Functional and structural characterization of 2B viroporin membranolytic domains. Biochemistry 47, 10731–10739.
Shai, Y., 1995. Molecular recognition between membrane-spanning polypeptides. Trends Biochem. Sci. 20, 460–464.
Sreerama, N., Woody, R.W., 2000. Estimation of protein secondary structure from circular dichroism spectra: comparison of CONTIN, SELCON, and CDSSTR methods with an expanded reference set. Anal. Biochem. 287, 252–260.
Steinmann, E., Pietschmann, T., 2010. Hepatitis C virus P7-A viroporin crucial for virus assembly and an emerging target for antiviral therapy. Viruses-Basel 2, 2078–2095.
Steinmann, E., Penin, F., Kallis, S., Patel, A.H., Bartenschlager, R., Pietschmann, T., 2007a. Hepatitis C virus p7 protein is crucial for assembly and release of infectious virions. PLoS Pathog. 3, 962–971.
Steinmann, E., Whitfield, T., Kallis, S., Dwek, R.A., Zitzmann, N., Pietschmann, T., Bartenschlager, R., 2007b. Antiviral effects of amantadine and iminosugar derivatives against hepatitis C virus. Hepatology 46, 330–338.
StGelais, C., Tuthill, T.J., Clarke, D.S., Rowlands, D.J., Harris, M., Griffin, S., 2007. Inhibition of hepatitis C virus p7 membrane channels in a liposome-based assay system. Antiviral Res. 76, 48–58.
StGelais, C., Foster, T.L., Verow, M., Atkins, E., Fishwick, C.W., Rowlands, D., Harris, M., Griffin, S., 2009. Determinants of hepatitis C virus p7 ion channel function and drug sensitivity identified in vitro. J. Virol. 83, 7970–7981.
van Meer, G., Voelker, D.R., Feigenson, G.W., 2008. Membrane lipids: where they are and how they behave. Nat. Rev. Mol. Cell Biol. 9, 112–124.
Wozniak, A.L., Griffin, S., Rowlands, D., Harris, M., Yi, M., Lemon, S.M., Weinman, S.A., 2010. Intracellular proton conductance of the hepatitis C virus p7 protein and its contribution to infectious virus production. PLoS Pathog. 6, e1001087.

Virus Research 178 (2013) 328–339

Contents lists available at ScienceDirect

Virus Research

journal homepage: www.elsevier.com/locate/virusres

Pathogenesis of highly virulent African swine fever virus in domestic pigs exposed via intraoropharyngeal, intranasopharyngeal, and intramuscular inoculation, and by direct contact with infected pigs

Erin B. Howey[a,b], Vivian O'Donnell[a,c], Helena C. de Carvalho Ferreira[a,b], Manuel V. Borca[a], Jonathan Arzt[a,*]

[a] Plum Island Animal Disease Center, Foreign Animal Disease Research Unit, Agricultural Research Service, United States Department of Agriculture, Greenport, NY 11944, USA
[b] Oak Ridge Institute for Science and Education, PIADC Research Participation Program, Oak Ridge, TN 37831, USA
[c] Department of Pathobiology and Veterinary Science, University of Connecticut at Storrs, Storrs, CT 06269, USA

ARTICLE INFO

Article history:
Received 9 July 2013
Received in revised form
13 September 2013
Accepted 13 September 2013
Available online 26 September 2013

Keywords:
African swine fever
ASFV
Transmission
Challenge
Pathogenesis
Domestic pig

ABSTRACT

To investigate the pathogenesis of African swine fever virus (ASFV), domestic pigs ($n = 18$) were challenged with a range (10^2–10^6 50% hemadsorbing doses (HAD_{50})) of the highly virulent ASFV-Malawi strain by inoculation via the intraoropharyngeal (IOP), intranasopharyngeal (INP), or intramuscular (IM) routes. A subsequent contact challenge experiment was performed in which six IOP-inoculated donor pigs were allowed to have direct contact (DC) with six naïve pigs for exposure times that varied from 24 to 72 h. All challenge routes resulted in clinical progression and postmortem lesions similar to those previously described in experimental and natural infection. The onset of clinical signs occurred between 1 and 7 days post inoculation (dpi) and included pyrexia with variable progression to obtundation, hematochezia, melena, moribundity and death with a duration of 4–11 days. Viremia was first detected between 4 and 5 dpi in all inoculation groups whereas ASFV shedding from the nasal cavity and tonsil was first detected at 3–9 dpi. IM and DC were the most consistent modes of infection, with 12/12 (100%) of pigs challenged by these routes becoming infected. Several clinical and virological parameters were significantly different between IM and DC groups indicating dissimilarity between these modes of infection. Amongst the simulated natural routes, INP inoculation resulted in the most consistent progression of disease across the widest range of doses whilst preserving simulation of natural exposure and therefore may provide a superior system for pathogenesis and vaccine efficacy investigation.

Published by Elsevier B.V.

1. Introduction

African swine fever (ASF) is a highly contagious, often fatal, transboundary disease of domestic and wild suids caused by ASF virus (ASFV) (Tulman et al., 2009). It is the sole member of the *Asfarviridae* family and is a large, double stranded DNA virus with a 170–190 kb genome. Due to the lack of a commercial or experimental vaccine or treatment, large economical losses are associated with ASFV outbreaks (Sánchez-Vizcaíno et al., 2012). Such an event occurred in 2007, when ASFV was introduced into the Republic of Georgia which has subsequently led to spread to Russia, Armenia, Azerbaijan, Ukraine, and most recently to Belarus (WAHID, 2013), with the range of the virus progressively extending west toward Europe (Costard et al., 2013).

In domestic swine, it is generally accepted that under natural conditions, ASFV is primarily transmitted via direct contact with excreted viral particles through nuzzling and/or ingestion (Sánchez-Vizcaíno et al., 2012; Wardley et al., 1983). However, the detailed mechanism of this mode of transmission has yet to be explicitly defined. Arthropod-borne transmission via *Ornithodoros* spp. ticks, which is a relevant means of transmission of ASFV within the wild suid population and from wild suids to domestic swine, is a minor method of transmission between domestic pigs (Arzt et al., 2010; Jori et al., 2013; Penrith, 2009).

An extensive portion of in vivo ASF research has utilized the intramuscular (IM) route of inoculation (Ballester et al., 2010; Carrasco et al., 1996, 1997; Childerstone et al., 1998; Fernández de Marco et al., 2007; Gómez-Villamandos et al., 1995a, 1995b,

* Corresponding author at: Foreign Animal Disease Research Unit, USDA/ARS Plum Island Animal Disease Center, P.O. Box 848, Greenport, NY 11944, USA. Tel.: +1 631 323 3336; fax: +1 631 323 3006.
E-mail addresses: Erin.Howey@ars.usda.gov (E.B. Howey), Vivian.ODonnell@ars.usda.gov (V. O'Donnell), Helena.Ferreira@ars.usda.gov (H.C. de Carvalho Ferreira), Manuel.Borca@ars.usda.gov (M.V. Borca), Jonathan.Arzt@ars.usda.gov (J. Arzt).

0168-1702/$ – see front matter. Published by Elsevier B.V.
http://dx.doi.org/10.1016/j.virusres.2013.09.024

1997a, 1997b, 1998; Oura et al., 1998; Pan and Hess, 1984; Salguero et al., 2004). This method results in highly reproducible clinical disease. However, since IM inoculation does not result in viral interaction with the oral and upper respiratory mucosal surfaces, it bypasses many of the innate defense mechanisms the virus would normally encounter through natural infection. Therefore, it may be a suboptimal inoculation method to examine the early pathogenesis and previremic stages of disease. Similarly, these limitations make IM challenge, an unnatural model for vaccine assessment.

The conventional pathogenesis of ASF has been investigated in vivo using simulated natural routes of inoculation including intranasal (IN) (de Carvalho Ferreira et al., 2012, 2013a; Greig, 1972; Greig and Plowright, 1970; Heuschele, 1967; Plowright et al., 1968), intraoral (IO) (Boulanger et al., 1967; Colgrove et al., 1969), combined oronasal (ON) (Boinas et al., 2004; Hamdy and Dardiri, 1984; McVicar, 1984; Mebus et al., 1978; Mebus and Dardiri, 1979, 1980) and direct contact/aerosol (DC) (de Carvalho Ferreira et al., 2013b; Wilkinson and Donaldson, 1977; Wilkinson et al., 1977, 1981). Within all of the studies noted, the main route of virus detection was through virus isolation and was usually performed only on the blood, serum or a limited number of tissues. Few have focused on virus detection within the secretions (de Carvalho Ferreira et al., 2012; Greig and Plowright, 1970; McVicar, 1984; Wilkinson et al., 1983; Ekue et al., 1989). While these reports have contributed to current understanding of the viral dynamics and pathogenesis of ASF, they fail to capture some specific information which may contribute to develop the next generation of rationally designed countermeasures. Specifically, confirmation of the primary site(s) of infection and elucidation of virus–host interactions during early pathogenesis would facilitate the process of developing and validating effective prophylaxis. Furthermore, variability in methodologies including virus strain, dose, and route of challenge has confounded comparison across studies. The importance of standardizing experimental models including the description and interpretation of clinical and pathologic findings in experimental ASF has recently been emphasized (Galindo-Cardiel et al., 2013). The goal of such standardization is to facilitate comparison of studies across research groups for the purpose of advancing ASF vaccine development whilst avoiding redundancy of research activities.

In the current study, we compared four routes of challenge of domestic pigs with ASFV in order to characterize route- and dose-dependent viral dynamics and the transmission of ASFV via direct contact. This was done to determine how different means of exposure/inoculation alter the pathogenesis of ASFV in swine and to determine which route most closely simulates natural infection with optimum experimental reproducibility.

2. Materials and methods

2.1. Virus

The highly pathogenic ASFV isolate Malawi Lil-20/1 was originally isolated from *Ornithodoros* sp. ticks during a field outbreak in Malawi in 1983 and obtained from L. Dixon (Institute of Animal Health, Pirbright Laboratory, Woking, Surrey, United Kingdom) (Borca et al., 1998). The stock virus was passaged once in primary porcine macrophages derived from heparinized swine blood. The tissue culture supernatant was then stored as 10^8 50% hemadsorbing dose (HAD_{50}) aliquots at −70 °C.

The inoculum was prepared by initially diluting stock virus 10-fold in Dulbeco's Modified Eagle's Medium (DMEM) (Gibco; Invitrogen, NY) containing 1% antibiotic/antimycotic (10,000 units/mL of penicillin, 10,000 μg/mL of streptomycin, and 25 μg/mL of Fungizone®) (Gibco; Invitrogen, NY) and subsequently performing additional dilution to achieve the desired viral dose in 2 ml of media.

2.2. Animals

Conventional castrated male Yorkshire pigs from a herd that is demonstrated to be free of porcine reproductive and respiratory syndrome virus were used for all experiments. Animals were dewormed and vaccinated for common porcine pathogens including porcine circovirus 2 prior to arrival at our facility. Pigs were approximately 3–4 months old and 22–27 kg upon arrival. All animal procedures were performed following Protocol 225-10-R approved by the Plum Island Animal Disease Center Institutional Animal Care and Use Committee (IACUC), which ensured ethical and humane treatment of experimental animals. The animal experiments were carried out in BSL-3 Ag isolation rooms at Plum Island Animal Disease Center. Animals were kept within the housing facilities 7 days prior to the start of the experiments to allow for acclimation to the new environment. All animals were fed daily and had unlimited access to water.

All animals except for donors in the DC study were allowed to survive until terminal disease. Severely moribund animals were humanely euthanized intravenously with 85.8 mg/kg of sodium pentobarbital. Animals without clinical disease were humanely euthanized at the end of the study as described above.

2.3. Study design

2.3.1. Direct inoculation studies

Experiments were performed to compare three routes of direct inoculation. Eighteen pigs were used in these experiments. Six pigs were assigned to each of the three inoculation route groupings: intramuscular (IM), intranasopharyngeal (INP) and intraoropharyngeal (IOP). Inoculation route groupings were further subdivided into three inoculation dosage groups: low dose 10^2 HAD_{50} ($n = 2$), mid dose 10^4 HAD_{50} ($n = 2$) and high dose 10^6 HAD_{50} ($n = 2$). IM-inoculated pigs received a 2 mL injection of inoculum within the right semimembranosus muscle. Pigs assigned to INP inoculation were sedated with an intramuscular injection of telazol (3 mg/kg), ketamine (8 mg/kg), xylazine (4 mg/kg), placed in sternal recumbency and 2 mL inoculum was instilled through the nares into the nasopharynx via a 15 gauge silicon catheter (Abbott Laboratories, IL). Pigs assigned to IOP inoculation received 2 mL of the inoculum perorally via syringe with an attached 6 in. sterile metal cannula. Animals were sedated, placed in dorsal recumbency and 2 mL of the inoculum was deposited in the ventral portion of the soft palate and palatine tonsil.

2.3.2. Direct contact (DC) transmission studies

Additional experiments were performed to characterize ASFV transmission from IOP-inoculated pigs and viral dynamics in pigs challenged by direct contact. Donor ($n = 6$) and naïve pigs ($n = 6$) were initially housed in two separate rooms. Donor pigs were inoculated via the intraoropharyngeal method as described above with 2 mL of inoculum at a dose of 10^5 HAD_{50} of the same ASFV Malawi Lil-20/1 described above. Upon detection of pyrexia (rectal temperature greater than or equal to 40 °C) in at least 4 donor pigs (6 days post inoculation (dpi)), contact pigs were transferred into the donor room and allowed to comingle with inoculated pigs. Feed was withheld for approximately 4 h to encourage contact between pigs. After 24 h (1 day post contact (dpc)), two contact animals were removed and isolated into a separate room and two donor animals were euthanized to maintain the donor/naïve pig ratio. This process was repeated at 48 and 72 h (2 and 3 dpc). Contact-exposed animals were then monitored for onset and progression of clinical disease.

Table 1
Clinical signs and scoring value for ASF.

Characteristic	Score	
Behavior and mentation	0	Normal, alert, responsive
	1	Mildly obtunded. Slightly reduced liveliness, stands up unassisted, resists restraint or rectal thermometer
	2	Obtunded. Reluctant to stand but will do so when assisted; decreased resistance to restraint or rectal thermometer
	3	Intermittent ataxia, disorientation, can still stand/walk or will not stand/walk even when assisted, still conscious
	4	Moribund. Nonambulatory, unconscious/nonresponsive
Neurologic signs	0	Normal
	2	Unambiguous neurologic signs (e.g. convulsions, seizures)
Defecation	0	Normal to mildly soft stools
	1	Profuse watery diarrhea, ±mild hematochezia or melena
	2	Severe to marked hematochezia/melena
Body temperature[a]	0	38–40 °C
	1	Temperature greater than or equal to 40 °C at any point of study
	2	Temperature greater than or equal to 40 °C for at least 2 subsequent days
	3	Temperature greater than or equal to 41 °C
	4	Temperature less than 38 °C

[a] Temperature scores are never reduced.

2.4. Clinical evaluation

Incidence proportion of ASF was calculated for each dose/route combination as [(number of successfully infected pigs for that dose and route) ÷ (all pigs subjected to that dose and route)]. For all studies, clinical evaluations were performed on all animals until death or termination of the experiment. Clinical signs used to characterize progression of ASF are listed in Table 1. These clinical signs were assigned a numerical value based on severity and significance. The sum of the scores of all clinical signs present for each pig was recorded daily.

2.5. Sample collection and processing

Sample collection including whole blood with EDTA, clotted blood for the collection of serum, swab specimens from the nasal cavity and superficial scrapings from the tonsil of the soft palate were performed on the day of inoculation at 0 days post inoculation (dpi) followed by sample collection every other day. Pigs were manually restrained for sample collection. Whole blood and serum were collected via the jugular vein. Tonsil scrapings were collected with a sterile spoon by gently scraping along the surface of the tonsil of the soft palate, exfoliating superficial epithelial cells while making sure to not disrupt the mucosa. Nasal swabs were collected bilaterally using sterile cotton swabs extended just caudal to the alar fold. Following collection, nasal swabs and tonsil scrapings were immediately immersed in 1 mL of DMEM with 5% antibiotic/antimycotic; then, all samples were transferred on ice to the laboratory for processing. All samples were transferred to cryovials and stored at −70 °C until they were analyzed by virus isolation (VI).

Necropsies were performed as soon as possible following euthanasia or natural death. Tissues collected during postmortem examination included: tonsil of the soft palate, lingual tonsil, nasal tonsil, dorsal soft palate (rostral and caudal), dorsal nasopharynx, caudal nasal turbinate, epiglottis, trachea, bronchial mucosa, lung, thymus, liver, spleen, kidney, adrenal gland, thyroid, pancreas, small intestine, large intestine, bone marrow, and lymph nodes including: retropharyngeal, submandibular, hilar, gastrohepatic, renal, inguinal and popliteal. Urine was also taken via direct aspiration from the urinary bladder at the time of necropsy. Tissue samples collected were placed in cryovials as described above and cryomolds, embedded in Optimal Cutting Temperature (OCT) medium (Tissue-Tek O.C.T. compound, Sakura Finetek, CA) and then frozen in liquid nitrogen. Detailed description of tissues from these animals will appear in a separate manuscript (Howey et al., in progress).

2.6. Virus isolation and titration

Blood, serum, nasal swabs, tonsil scrapings, urine (postmortem only) and tissues from infected pigs were screened for ASFV by virus isolation and titration (VI) on primary porcine blood macrophage cell cultures prepared from defibrinated swine blood as previously described (Zsak et al., 2005). Presence of virus was determined by identification of infected cells by rosette formation (hemadsorption) and titers expressed as doses calculated by the Spearman–Karber method (Mahy and Kangro, 1996).

2.7. Immunomicroscopy

Microscopic localization of the virus in tissues positive for ASFV via VI was performed via immunohistochemistry (IHC). Immunofluorescence (IFA) was used to detect virus in combination with other cellular markers in order to further determine/characterize phenotypes of infected cells. All primary antibodies were extensively tested prior to this study in sections of tissue from ASFV infected or non-infected pigs, using IHC, to ensure specificity.

OCT-embedded tissue samples for IHC and IFA were cryosectioned onto electrostatically charged glass slides and fixed for 10 min in acetone at −20 °C. Slides were blocked for 2 h at 20 °C with Phosphate buffered saline with Tween (PBST) containing 6% mixed serum and 2% powdered non-fat milk. A mouse monoclonal primary antibody 1D9, targeting the ASFV VP30 (Cuesta-Geijo et al., 2012; Galindo et al., 2012) (kindly provided by Javier Dominguez Juncal, Departamento de Biotecnología, Instituto Nacional de Investigación y Tecnología Agraria y Alimentaria (INIA)), was diluted 1:250 in blocking buffer and applied to tissue sections that were then incubated for 20 h at 4 °C.

For IHC, specific anti-ASFV immunoreactivity was detected using a commercial micropolymer alkaline phosphatase detection system (Mach 3 AP kit; Biocare, CA) as per manufacturers' recommendation with an alkaline phosphatase substrate (Vector Red; Vector Laboratories, CA). Slides were counterstained with Gill's hematoxylin and cover slipped using routine methods. A duplicate serial section of each tissue screened was treated with a mouse monoclonal anti-foot and mouth disease virus (FMDV) antibody (10GA4, targeting FMDV O1-Brugge (Arzt et al., 2009)) serving as a negative control.

Table 2
Clinical characteristics of pigs infected with ASFV by different routes and dosages.

Group	No. infected/total no.	Total days survival (±SD)	Pyrexia	Clinical signs	
			Days to onset (±SD)	Days to onset (±SD)	Maximum clinical score (±SD)
IM					
Overall	6/6	8.5 (±1.8)[c]	5.2 (±1.2)[c]	4.5 (±1.2)[c]	6.3 (±1.4)[c]
10^2 (n = 2)	2/2	10.5 (±0.3)	5.5 (±0.7)	5.5 (±0.7)	7.0 (±1.4)
10^4 (n = 2)	2/2	8.0 (±1.4)	5.5 (±0.7)	5.0 (±0.0)	6.5 (±2.1)
10^6 (n = 2)	2/2	7.0 (±0.0)	4.5 (±2.1)	3.0 (±0.0)	5.5 (±0.7)
INP					
Overall	5/6	10.3 (±1.9)[c]	5.0 (±2.7)[c]	2.6 (±2.5)[c]	6.2 (±2.8)[c]
10^2 (n = 2)	1/2	11.0 (±1.4)	7.0 (±0.0)[a]	7.0 (±0.0)[a]	9.0 (±0.0)[a]
10^4 (n = 2)	2/2	11.0 (±1.4)	7.0 (±0.0)	1.5 (±0.7)	5.0 (±1.4)
10^6 (n = 2)	2/2	9.0 (±2.8)	2.0 (±0.0)	1.5 (±0.7)	6.0 (±4.2)
IOP					
Overall	4/6	10.5 (±2.4)[c]	5.8 (±1.3)[c]	4.3 (±2.4)[c]	4.8 (±4.0)[c]
10^2 (n = 2)	0/2	13.0 (±0.0)	–	–	–
10^4 (n = 2)	2/2	10.0 (±2.8)	6.5 (±0.7)	3.5 (±3.5)	6.5 (±5.0)
10^6 (n = 2)	2/2	8.5 (±0.7)	5.0 (±1.4)	5.0 (±1.4)	3.0 (±0.0)
DC					
Overall	6/6	10.3 (±1.2)[c]	5. (±1.8)[c]	5.0 (±1.9)[c]	6.8 (±2.0)[c]
1 dpc (n = 2)	2/2	10.5 (±0.7)	5.0 (±0.0)	4.5 (±0.7)	7.5 (±0.7)
2 dpc (n = 2)	2/2	10.5 (±2.1)	3.5 (±2.1)	3.5 (±2.1)	8.0 (±1.4)
3 dpc (n = 2)	2/2	10.0 (±1.4)	7.0 (±0.0)	7.0 (±0.0)	5.0 (±2.8)
IOP donor					
Overall	4/6	–[b]	3.6 (±0.6)	4.0 (±1.7)	4.0 (±2.5)

–, not detected; SD, standard deviation.
[a] One animal affected within group.
[b] Survival not calculated due to predetermined euthanasia.
[c] No statistical difference between group overall values (IM, INP, IOP and DC).

Multichannel IFA was performed similarly as described for IHC, except ASFV antigen detection was performed in combination with primary antibodies with specificity for host cellular markers including pancytokeratin (180059, Zymed, Invitrogen, NY) for epithelium, CD163 and CD172a for macrophages (MCA 2311, and MCA2312GA, respectively AbD Serotec, UK). After incubation of primary antibodies for 20 h at 4 °C, isotype-specific secondary antibodies labeled with fluorescent dyes (AF 350, 488, 594, and 647, AlexaFluor; Molecular Probes Inc., OR) were applied and slides were incubated for 1 h at 37 °C. Images were obtained using a Nikon Eclipse 90i multichannel epi-fluorescent microscope equipped with 350, 488, 594, and 647 excitation filter cubes and digital camera.

2.8. Statistical analyses

All statistical analyses were performed using R statistical program (R core Team, 2013)), employing different R packages (explained in detail below). Statistical significance was considered as $p < 0.05$. All data reported herein is not statistically significant unless explicitly stated.

2.8.1. Survival analysis

Duration of survival for each pig was calculated as the total number of days from inoculation/exposure to natural death or euthanasia due to moribundity. Survival functions were calculated for pigs belonging to the IM, INP, IOP and DC groups and compared through a Cox proportional hazard regression model using the package "Survival" for R software (Therneau, 2013). Multiple comparisons were made: (1) between inoculation/infection routes (IM, INP, IOP and DC), (2) within inoculated groups (IM, INP and IOP) comparing type of inoculation route and dose, (3) within each dose (comparing different inoculation routes), (4) within each route (comparing doses), and (5) within the DC pigs (comparing exposure length). Survival was not calculated for donor pigs (IOP donor group) from the contact experiment since these pigs were euthanized at predetermined times regardless of clinical disease.

2.8.2. Clinical signs, viremia and shedding

For all clinical and virological parameters examined, the mean ± standard deviation (SD) for each infection group/dose combination was calculated using data values collected per individual animal per time point. The effect of the inoculation/infection route used to establish infection was compared across groups (both within the direct inoculation studies and between direct inoculation and contact studies) for the outcome variables present in Tables 2 and 3. These comparisons were made using regression analysis, using a linear model, considering the 4 types of inoculation/infection route as categorical explanatory variables: intramuscular (IM), intranasopharyngeal (INP), intraoropharyngeal (IOP) and direct contact (DC). A linear model was also used to assess the effects of different exposure levels applied in the pigs infected by direct contact, with exposure as explanatory variable (with 3 exposure levels – 1 day, 2 days and 3 days) and variables present in Tables 2 and 3 as outcome. Linear model assumptions were confirmed through visual inspection of the residual plots. The statistical power of these experiments was analyzed retrospectively using the package "pwr" (Champely, 2012). The study did not have enough power to test for possible interactions of type of inoculation route and dose used for inoculation. The power of the analysis using only the explanatory variable type of inoculation/infection route (determining differences between inoculation/infection groups) varied from 0.58 to 0.31, depending on the number of missing values.

3. Results

3.1. Direct inoculation studies

3.1.1. Inoculation and infectivity

Successful infection of individual pigs was determined by the presence of characteristic clinical signs combined with detection of ASFV within the blood components (viremia). In the IM group, all animals regardless of dose were successfully infected (2/2 high dose, 2/2 mid dose, and 2/2 low dose (100% incidence)). In the INP

Table 3
Virologic parameters of pigs infected with ASFV by different routes and dosages.

Group	No. infected/ total no.	Viremia			Shedding			
		Days to onset (±SD)	Duration (±SD)	Maximum titer (±SD)[b,c,g]	Days to onset of tonsil shedding (±SD)	Maximum titer (±SD)[b]	Days to onset of nasal shedding (±SD)	Maximum titer (±SD)[b]
IM								
Overall	6/6	4.3 (±1.6)[e]	5.2 (±1.3)[e]	6.5 (±0.6)[c]	8.0 (±1.2)[e]	2.4 (±0.4)[e]	9.0 (±0.0)[a,e]	2.1 (±0.0)[a,e]
10^2 ($n=2$)	2/2	6.0 (±1.4)	5.5 (±0.7)	6.1 (±0.0)[c]	9.0 (±0.0)[a]	2.8 (±0.0)[a]	9.0 (±0.0)[a]	2.1 (±0.0)[a]
10^4 ($n=2$)	2/2	4.0 (±1.4)	5.0 (±2.8)	6.4 (±0.9)[c]	8.0 (±1.4)	2.4 (±0.5)	–	–
10^6 ($n=2$)	2/2	3.0 (±0.0)	5.0 (±0.0)	6.9 (±0.2)[c]	7.0 (±0.0)[a]	2.1 (±0.0)[a]	–	–
INP								
Overall	5/6	5.4 (±1.1)[e]	5.6 (±1.7)[e]	7.0 (±1.2)	7.5 (±1.7)[e]	3.3 (±1.0)[e]	7.7 (±3.5)[e]	4.2 (±1.7)[e,f]
10^2 ($n=2$)	1/2	5.0 (±0.0)[a]	6.0 (±0.0)[a]	5.8 (±0.0)[a]	9.0 (±0.0)[a]	2.8 (±0.0)[a]	–	–
10^4 ($n=2$)	2/2	5.0 (±1.4)	7.0 (±0.0)	8.3 (±0.0)[c]	6.0 (±0.0)	4.0 (±0.7)	6.0 (±2.8)	5.2 (±0.5)
10^6 ($n=2$)	2/2	6.0 (±1.4)	4.0 (±1.4)	6.3 (±0.4)	9.0 (±0.0)[a]	2.3 (±0.0)[a]	11.0 (±0.0)[a]	2.3 (±0.0)[a]
IOP								
Overall	4/6	5.0 (±1.2)[e]	5.3 (±1.7)[e]	8.5 (±0.1)	5.5 (±1.9)[e,f]	5.3 (±1.7)[f]	6.5 (±1.0)[e]	5.2 (±1.1)[f]
10^2 ($n=2$)	0/2	–	–	–	–	–	–	–
10^4 ($n=2$)	2/2	6.0 (±0.0)	5.0 (±2.8)	8.6 (±0.0)	7.0 (±1.4)	4.4 (±0.5)	7.0 (±1.4)	4.7 (±0.2)
10^6 ($n=2$)	2/2	4.0 (±0.0)	5.5 (±0.7)	8.4 (±0.2)	4.0 (±0.0)	6.2 (±2.3)	6.0 (±0.0)	5.8 (±1.4)
DC								
Overall	6/6	5.2 (±1.5)[e]	6.2 (±1.7)[e]	8.8 (±0.3)	3.5 (±2.4)[f]	5.2 (±0.8)[f]	7.7 (±0.6)[e]	4.7 (±0.1)[f]
1 dpc ($n=2$)	2/2	4.0 (±1.4)	7.5 (±2.1)	8.7 (±0.2)	1.5 (±0.7)	4.7 (±0.5)	8.0 (±0.0)	4.6 (±0.4)
2 dpc ($n=2$)	2/2	5.0 (±1.4)	6.5 (±0.7)	8.8 (±0.4)	4.0 (±2.8)	5.8 (±0.0)	7.5 (±0.7)	4.7 (±0.2)
3 dpc ($n=2$)	2/2	6.5 (±0.7)	4.5 (±0.7)	8.9 (±0.5)	5.0 (±2.8)	5.2 (±1.2)	7.5 (±0.7)	4.8 (±0.0)
IOP donor								
Overall	4/6	4.8 (±2.2)	–[d]	7.4 (±3.2)	2.8 (±1.5)	4.1 (±1.2)	6.5 (±1.3)	4.6 (±1.3)

–, not detected; SD, standard deviation.
[a] One animal affected within group.
[b] $Log_{10}HAD_{50}$/mL.
[c] All titers derived from whole blood except 'c' below (serum derived).
[d] Duration of viremia not calculated due to predetermined euthanasia.
[e] Group overall values (IM, INP, IOP and DC) with a common superscript are not significantly different ($p > 0.05$).
[f] Group overall values (IM, INP, IOP and DC) with a common superscript are not significantly different ($p > 0.05$).
[g] No statistical differences were calculated for this group.

and IOP groups, incidence was 100% within the mid (2/2) and high dose (2/2) groups; however amongst low dose animals, 1/2 pigs in the INP group and the entire (0/2) IOP group did not become infected (low dose incidence = 50%, 0% respectively).

3.1.2. Survival

The IM-inoculated pigs had the shortest overall survival (mean 8.5 ± 1.8 dpi, $n = 6$) (Table 2, Figs. 1A and 2), however, no statistically significant differences were found between the IM, INP and IOP groups in the Cox proportional hazard analysis. IM-inoculated pigs also had the shortest survival following onset of pyrexia (mean 4.3 ± 1.9 days, $n = 6$). Mean survival after pyrexia was longest within the low dose group (6 ± 0.0 days, $n = 2$) and equal within the mid and high dose groups (3.5 ± 2.1 days, $n = 2$ per group). Amongst the INP-inoculated pigs, overall mean survival was 10.3 ± 1.9 dpi with 5.5 ± 1.8 days survival following the onset of pyrexia. Survival was shortest within the high dose group (9.0 ± 2.8 days, $n = 2$) compared to the mid and low dose groups (11.0 ± 1.4 days, $n = 2$ per group). Overall survival within the intraoropharyngeal group was the longest compared to all other routes with a mean of 10.5 ± 2.4 dpi ($n = 6$). Survival following onset of pyrexia was 4.5 ± 2.1 days; however, the number of days to onset of pyrexia was the longest (5.8 ± 1.3 dpi).

The dose used for inoculation had a significant effect on the pig's survival, with pigs inoculated with the low dose (10^2 HAD_{50} ASFV) having a significantly longer survival ($p = 0.02$) than pigs inoculated with a higher dose (10^6 HAD_{50} ASFV). However, when groups were compared within the same dose (i.e. across route), there were no statistical differences between the different inoculation routes.

3.1.3. Clinical signs

For all route-dose combinations, the most consistent and commonly earliest detected clinical sign was pyrexia ranging from 40 to 41.9 °C. Diarrhea, hematochezia and melena were common in all groups during the late stages of infection, except the contact experiment donors. Less consistent clinical signs included obtundation, oculonasal discharge, coughing, and dermal hyperemia which were often transient and variable throughout all groups. Terminal stage ASF was characterized by moribundity including a rapid and substantial decrease in body temperature, lack of response to stimulus, inability to stand or ambulate, and occasionally, seizure-like behavior. There were no statistically significant differences ($p > 0.05$) between the IM, INP, IOP and DC routes for total days of survival, days to onset of pyrexia and clinical signs, and maximum clinical score (Table 2).

Amongst the IM-inoculated pigs, the onset of clinical signs was shortest within the high dose group (Table 2, Fig. 2) including pyrexia (4.5 ± 2.1 days) and obtundation (6.0 ± 0.0 days) which occurred in all pigs ($n = 6$). Melena/hematochezia was observed in one animal from the mid and high dose groups, with the shortest onset (5.0 ± 0.0 days) within the high dose. The overall highest mean clinical score was 6.3 ± 1.4 with the highest mean clinical score observed within the low dose group ($n = 2$). The IM-inoculated pigs, had significantly earlier onset of obtundation and onset of melena/hematochezia ($p < 0.05$) in comparison to every group, or in comparison to the DC and INP routes individually.

The lowest overall number of days to the onset of clinical signs was amongst the INP-inoculated pigs (mean 2.6 ± 2.5 dpi, 5/6

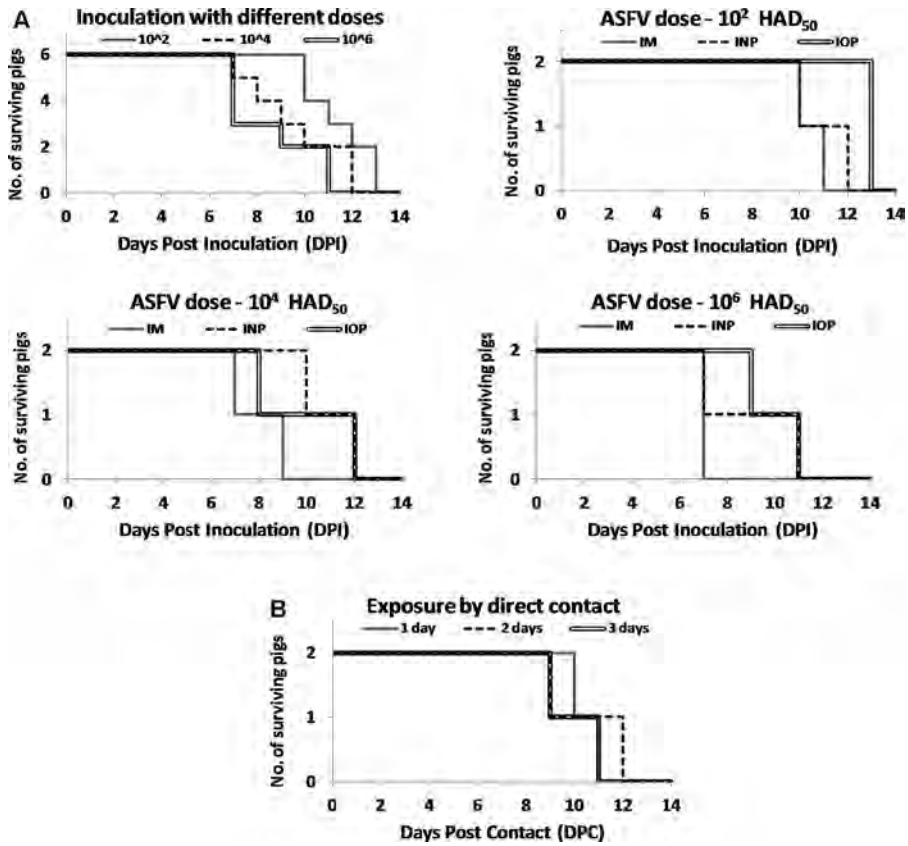

Fig. 1. Descriptive survival analyses for ASFV-exposed pigs relating dose/exposure length to survival duration within the direct inoculation studies (A) and direct contact study (B).

pigs). However, onset within the low dose group was substantially longer (7 days) than the mid and high dose groups (1.5 ± 0.7 days) (Fig. 2D–F). The lowest overall number of days to onset of pyrexia was amongst the INP-inoculated pigs (mean 5.0 ± 2.7 dpi, $n = 2$) with the high dose group having the shortest onset (2.0 ± 0.0 days, $n = 2$) compared to the low (1/2 pigs) and mid dose (2/2 pigs) groups (7.0 ± 0.0 days). Obtundation and melena/hematochezia occurred in 4 out of 6 pigs with respective means to onset of 9.5 ± 1.0 and 10.0 ± 0.8 days. The mean maximum clinical score amongst the INP-inoculated pigs was 6.2 ±;2.8 with the highest clinical score occurring within the low dose group (9.0 ± 0.0).

The mean maximum clinical score for the IOP groups was 4.8 ± 4.0 (4/6 pigs) with the lowest clinical score found within the high dose group. Clinical signs consistent with ASF were not observed in pigs from the low dose group. Onset of pyrexia occurred within the mid and high dose groups at 6.5 ± 0.7 and 5.0 ± 1.4 days respectively ($n = 2$ per group). Obtundation and melena/hematochezia were detected only in one mid dose IOP-inoculated animal starting at 10 and 11 dpi respectively.

3.1.4. Viremia and ASFV shedding

The IM-inoculated pigs ($n = 6$) had the shortest overall period to onset of viremia (mean 4.3 ± 1.6 dpi) and number of days of viremia (5.2 ± 1.3 days) (Table 3). Amongst the IM-inoculated pigs, the low dose group had both the longest time before onset and longest duration of viremia (Fig. 2A, Table 3). The highest mean titer of ASFV in serum was detected within the high dose group (6.9 ± 0.2 $\log_{10}$HAD$_{50}$/mL). Onset to detection of ASFV from the tonsil was shortest within the high dose group. Nasal shedding was only detected in 1 pig within the low dose IM group which occurred at 9 dpi. There was an overall mean of 4.0 ± 1.6 days from onset of viremia to detection of ASFV in secretions. IM-inoculated pigs had significantly different results in comparison with pigs infected by DC. Specifically these pigs had longer days to onset of tonsil shedding, and lower maximum ASFV titers in tonsil and nasal swabs (Table 3).

The overall number of days to onset of viremia was the longest in the INP groups at 5.4 ± 1.1 dpi (5/6 pigs). The number of days of viremia averaged 5.6 ± 1.7 days with the high dose group having the shortest length of viremia (Fig. 2C, Table 3). The overall mean maximum serum/whole blood titer was 7.0 ± 1.2 $\log_{10}$HAD$_{50}$/mL. Tonsillar ASFV was detected in 4 out of 6 INP-inoculated animals with a mean onset of 7.5 ± 1.7 days and a max titer of 3.3 ± 1.0 $\log_{10}$HAD$_{50}$/mL. Nasal shedding was detected in 3 out of 6 animals with a mean onset of 7.7 ± 3.5 dpi and a max titer of 4.2 ± 1.7 $\log_{10}$HAD$_{50}$/mL. The mean difference between the onset of viremia and onset of ASFV detection in secretions was 1.5 ± 1.9 days. In comparison to DC-exposed pigs, the INP-inoculated pigs had significantly longer days to onset of tonsil shedding (for INP), and significantly lower maximum titers in tonsil.

Within the IOP groups, overall onset of viremia was detected at 5.0 ± 1.2 dpi with overall duration of viremia for 5.3 ± 1.7 days for 4 out of 6 pigs inoculated (Table 3). The high dose group had both the shortest onset to viremia and shortest duration. The mean maximum titer from whole blood was 8.5 ± 0.1 $\log_{10}$HAD$_{50}$/mL. Tonsil and nasal shedding was detected within all infected animals (4/6) with a mean onset of shedding at 5.5 ± 1.9 and 6.5 ± 1.0 dpi respectively. The mean maximum titers for tonsil and nasal swabs for IOP-inoculated pigs were 5.3 ± 1.7 and 5.2 ± 1.1 $\log_{10}$HAD$_{50}$/mL. The period between onset of viremia and viral shedding was the shortest of all routes at 0.5 ± 1.2 days. There were no statistical significant differences in any of the outcome variables between the IOP and the DC groups.

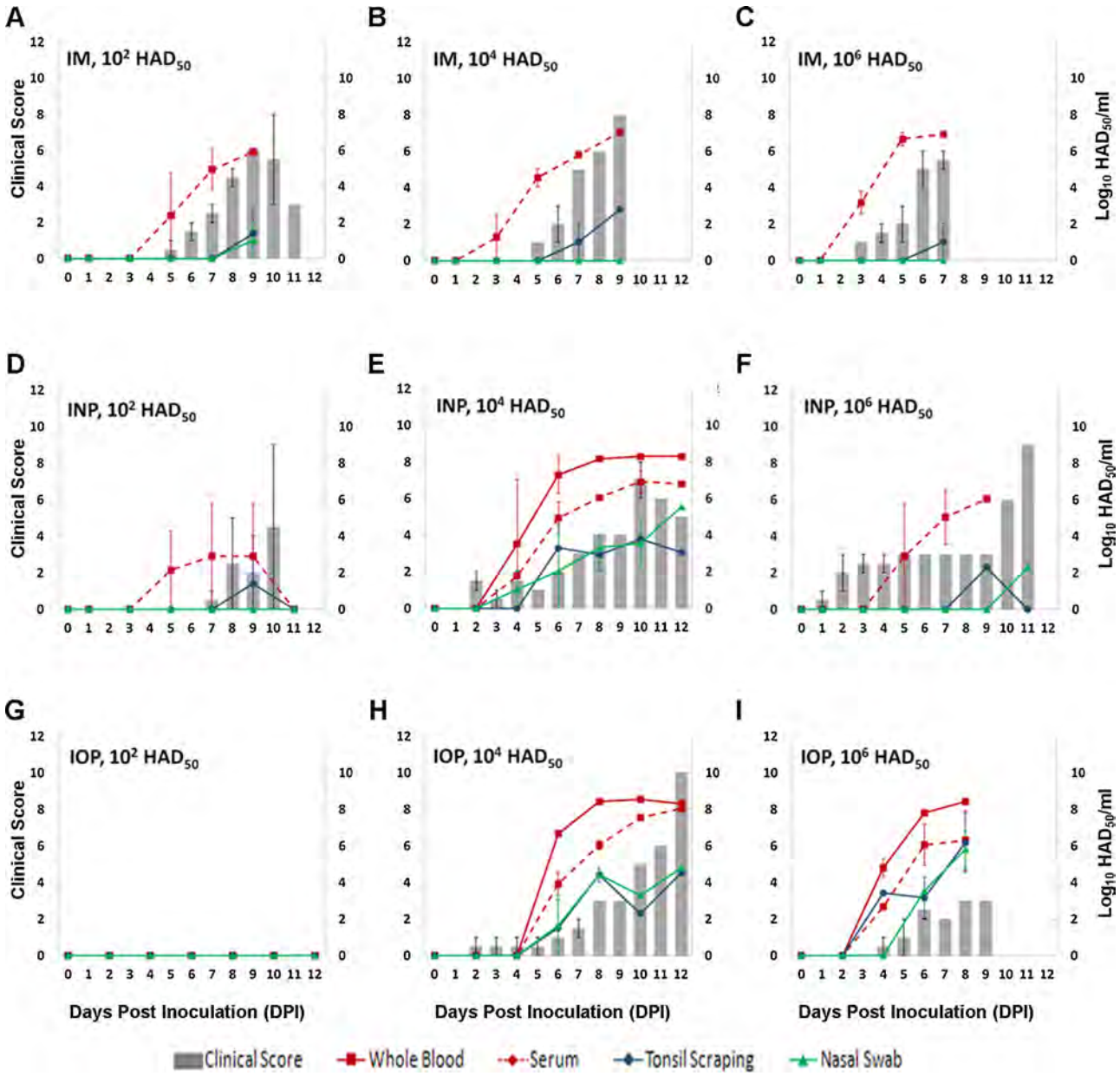

Fig. 2. Relationship between clinical score and virus shedding in pigs inoculated IM (A–C), INP (D–F), and IOP (G–I) with ASFV Malawi at 10^2, 10^4 and 10^6 HAD_{50}. Lines indicating viral titer in whole blood, serum, tonsil swabs and nasal swabs are expressed on the right *Y*-axis. The daily clinical score (bars) are expressed on the left *Y*-axis.

3.2. Direct contact experiment

3.2.1. Inoculation and infectivity

For the IOP-inoculated donor pigs from the contact experiment, the overall incidence of ASFV infection was 66% (4/6 pigs), identical to the incidence in IOP-inoculated animals from the direct inoculation studies. Within DC groups, all animals, regardless of exposure time, were successfully infected (incidence = 100%) (Table 2).

3.2.2. Survival

All donor animals were euthanized between 7 and 9 dpi in accordance with the predetermined scheme to maintain 1:1 ratio with contact pigs. Naïve pigs were exposed to IOP-inoculated donors for 1, 2, or 3 days. Overall mean survival for all three exposure groups ($n = 6$) was 10.3 ± 1.2 dpc with the longest onset of survival following onset of pyrexia (5.9 ± 2.0 days) compared to direct infection routes (Table 2, Fig. 1B). Animals exposed to donors for 3 dpc had the shortest overall survival compared to the 1 dpc and 2 dpc-exposure groups. However, there were no statistical differences in the survival according to the Cox proportional analysis between different exposure durations.

3.2.3. Clinical signs

Among the IOP-inoculated donors, the mean number of days to onset of pyrexia was 3.6 ± 0.6 dpi. The mean duration to onset of clinical signs was 4.0 ± 1.7 dpi (Table 2). Two animals were pyrexic for 1–2 days but their temperature returned to within normal limits before euthanasia. These two pigs did not become viremic nor was shedding detected. One pig was not pyrexic by the time of euthanasia, but was viremic and shed virus nasally on the day of euthanasia (8 dpi). Four out of six pigs were obtunded with a mean onset of 4.0 ± 2.5 dpi. Donor animals did not have melena or hematochezia.

Amongst the DC-exposed pigs, onset of clinical signs began with pyrexia that was detected first within the 2 dpc-exposure group (3.5 ± 2.1 dpc, $n = 2$) followed by the 1 dpc-exposure (4.5 ± 0.7 dpc, $n = 2$) and 3 dpc-exposure (7.0 ± 0.0 dpc, $n = 2$) groups. Obtundation

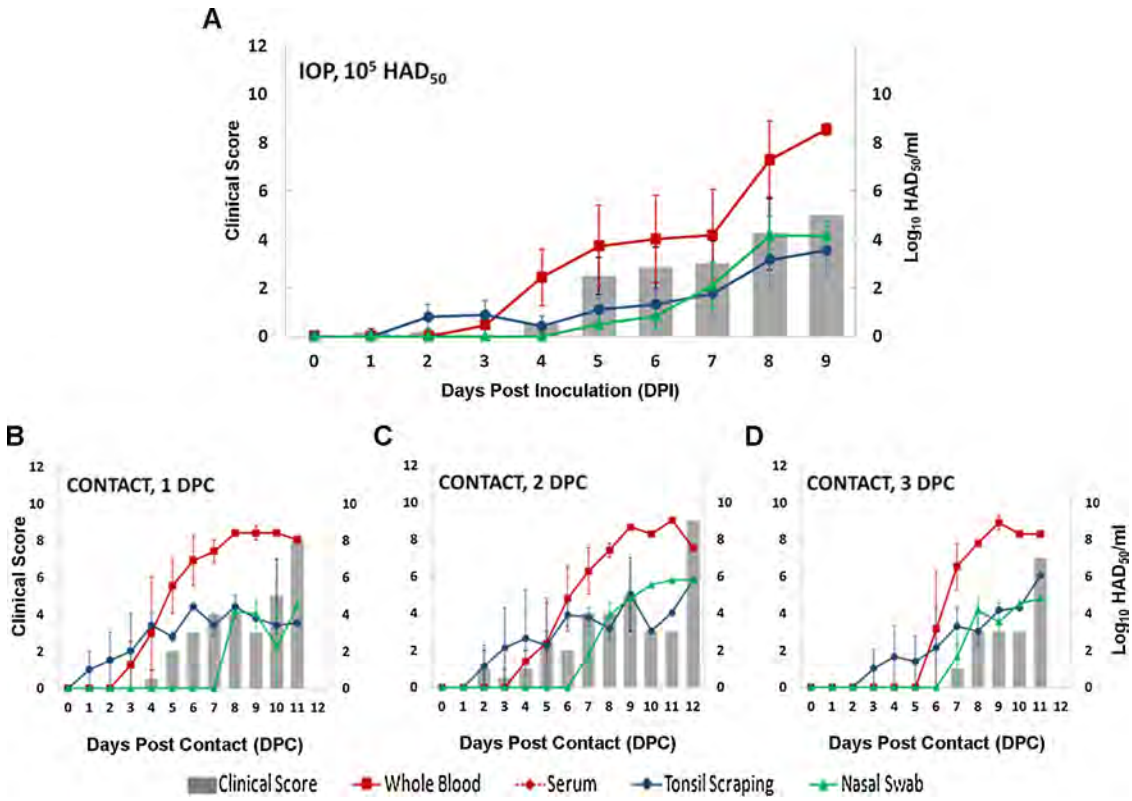

Fig. 3. Relationship between clinical score and virus shedding in donor pigs inoculated IOP (A) with ASFV Malawi at 10^5 HAD_{50} and pigs exposed via Direct Contact (DC) for 24 h (B), 48 h (C) and 72 h (D). Lines indicating viral titer in whole blood, serum, tonsil swabs and nasal swabs are expressed on the right *Y*-axis. The daily clinical score (bars) are expressed on the left *Y*-axis.

was detected within 5 out of 6 pigs with a mean onset of 10.6 ± 1.1 dpc. Melena/hematochezia was detected in 2 of 6 pigs with a mean onset of 11.5 ± 0.7 dpc. The DC-exposed pigs had the highest overall maximum clinical score (6.8 ± 2.0); with the highest score in the 2 dpc group followed by the 1 dpc and 3 dpc groups.

3.2.4. Viremia and ASFV shedding

The mean detection of onset of viremia occurred within 4 out of 6 of the donor group pigs at 4.8 ± 2.2 dpi with the mean maximum whole blood titer of 7.4 ± 3.2 $\log_{10}HAD_{50}$/mL. The onset of tonsil shedding was detected prior to viremia in 2 pigs. Onset of tonsil and nasal shedding was detected at 2.8 ± 1.5 and 6.5 ± 1.3 dpi respectively. Maximum titers for tonsil and nasal swabs were 4.1 ± 1.2 and 4.6 ± 1.3 $\log_{10}HAD_{50}$/mL respectively (Fig. 3A, Table 3). The difference between onset of viremia and shedding averaged 1.3 ± 0.6 days.

Amongst contact-exposed pigs, mean onset of viremia was 5.2 ± 1.5 dpc and was detected first within the 1 dpc-exposure group (4.0 ± 1.4 dpc, $n = 2$) followed by the 2 dpc and 3 dpc-exposure groups (5.0 ± 1.4 and 6.5 ± 0.7 dpc, $n = 2$ per group). The overall mean highest whole blood titer was 8.8 ± 0.3 $\log_{10}HAD_{50}$/mL, which was the highest amongst all routes (Table 3). Tonsillar detection of ASFV occurred prior to viremia in 4 pigs. The mean onset of tonsil and nasal shedding was detected at 3.5 ± 2.4 and 7.7 ± 0.6 dpc respectively, with mean maximum titers of 5.2 ± 0.8 and 4.7 ± 0.1 $\log_{10}HAD_{50}$/mL. The difference between onset of viremia and shedding averaged 1.7 ± 1.7 days.

3.3. Postmortem lesions

All four routes produced comparable gross and histologic lesions in pigs at terminal stages of disease. The most consistent lesion amongst pigs was enlarged and often hemorrhagic lymph nodes. The most severe lymphadenomegaly commonly involved the gastrohepatic lymph nodes. Splenomegaly ranged from mild to severe enlargement. Renal lesions varied from mild cortical petechia to renomegaly with diffuse hemorrhage and congestion.

Histologically, lymphoid organs of all animals examined had perifollicular regions expanded by cellular debris, extensive hemorrhage, and distinct fragmented nuclear remnants, most consistent with lymphocyte apoptosis (Fig. 4A and B). Lymphoid follicles were still identifiable but less distinct compared to normal lymphoid architecture in naïve pigs.

3.4. Immunohistochemical localization of ASFV antigens

Examination of the distribution of virus and its association with specific cellular markers was performed on tissues collected from pigs of each inoculation route. Within lymphoid tissues of pigs with fulminant ASF, there was extensive cell-associated labeling with the anti-ASFV-VP30 antibody. Localization was predominately within interfollicular regions with few immunopositive cells within follicles (Fig. 4C). Within the tonsil of the soft palate, labeling was most prominent surrounding tonsillar crypts, with few labeled cells within the tonsillar crypt epithelium. This VP30-positive labeling did not colocalize with pancytokeratin.

Within all positive tissues, immunoreactive cells were morphologically consistent with large mononuclear cells (interpreted as macrophages). Combined multichannel immunofluorescence demonstrated that cells immunopositive for ASFV were also commonly positive for monocyte/macrophage cellular markers such as CD163 (Fig. 4D–G) and CD172a (not shown).

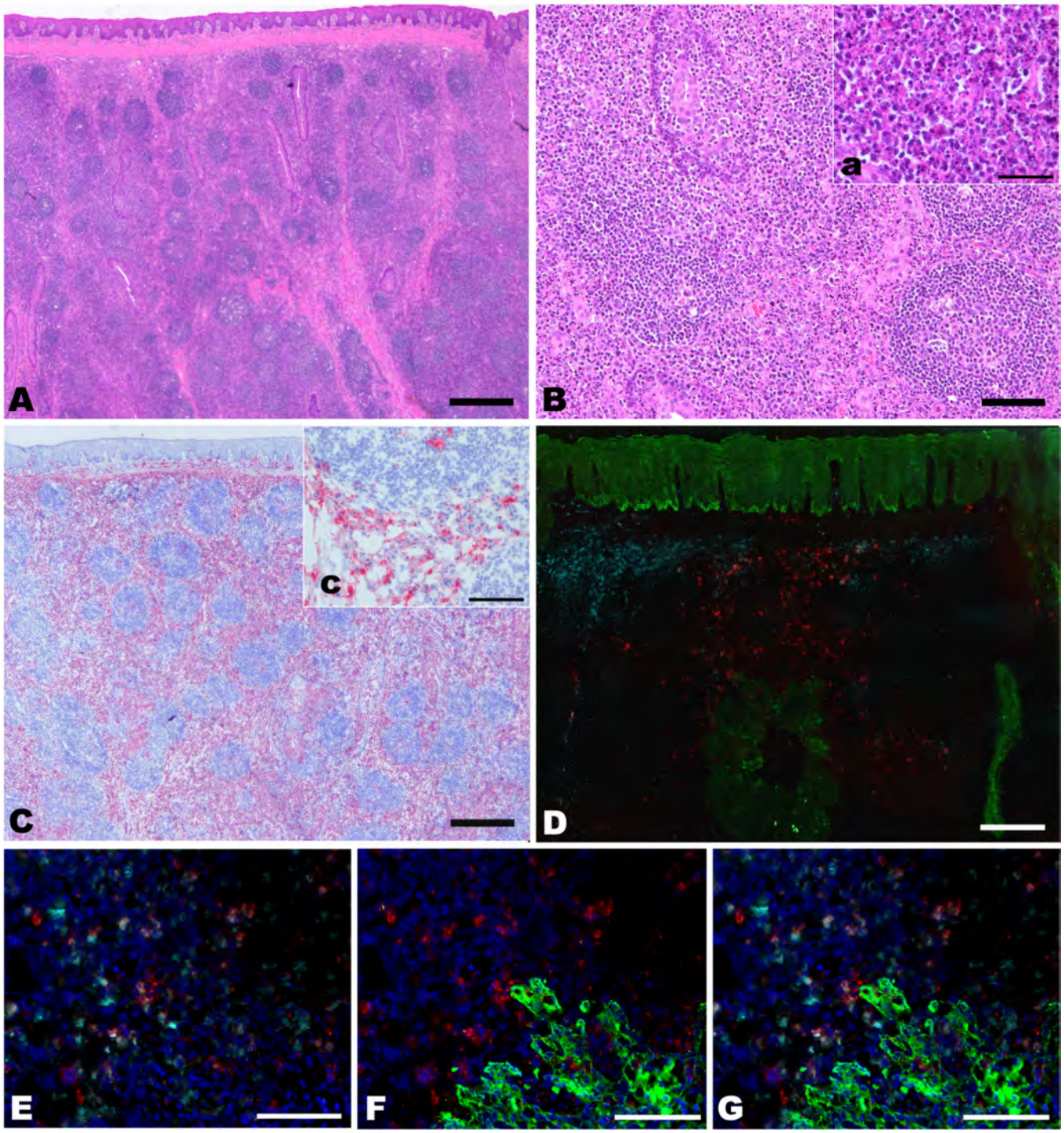

Fig. 4. Histopathology of lesions from pigs infected with ASFV-Malawi. Palatine tonsil, animal #38, INP ASFV-Malawi 10^2 HAD_{50}/mL; Lymphoid tissues including tonsil of the soft palate (A and B), lymph nodes, and spleen displayed loss of lymphocytes and karyorrhectic debris. Scale bars: (A) 500 μm, (B) 100 μm immunohistochemical staining (C) via Alkaline phosphatase polymer kit with anti-ASFV VP30 (1D9). Positive labeling extensively throughout interfollicular regions. Scale bar 500 μm. Inset (c), region of interest at higher magnification. Multichannel immunofluorescence (D–G). (D) Low magnification three channel image containing anti-ASFV (red), pancytokeratin (green), and macrophage marker CD163 (aqua). Scale bar 500 μm. (E) Three channel image containing Anti-ASFV (red), leukocyte marker macrophage marker CD163 (aqua) and nuclear staining with DAPI (blue). (F) Three channel image containing anti-ASFV (red), pancytokeratin (green), and nuclear staining with DAPI (blue). (G) Four channel merged image with colocalization of anti-ASFV (red) and leukocyte marker macrophage marker CD163 (aqua), pancytokeratin (green), and nuclear staining with DAPI (blue). Scale bar (E–G) 100 μm.

4. Discussion

The goal of the investigation described herein was to evaluate dose- and route-dependent effects on the clinical course of ASF and viral dynamics of ASFV within domestic pigs. This work serves to clarify and/or challenge previous conclusions derived from a collection of pathogenesis studies whose work is not directly comparable due to variability of virus strain, dose, inoculation technique, and detection methods. In addition, this work contributes to the establishment of challenge model systems for ASF which closely simulate

natural infection. The goals of the model systems were to achieve modes of challenging pigs that were (1) consistent with previous accounts of ASF, (2) consistent across experimental subjects, (3) compatible with the current understanding of natural routes of direct pig-to-pig transmission, (4) allowed control of dose and timing of challenge, and (5) provided natural engagement of host immune defenses. Recent studies have led toward standardization of clinical scoring systems for ASF (de Carvalho Ferreira et al., 2012; Galindo-Cardiel et al., 2013), and the current work demonstrates adaptation of these systems where appropriate.

Four routes of challenge (IM, IOP, INP, DC) resulted in a similar clinical course of ASF that was consistent with previously described field cases (Ayoade and Adeyemi, 2003; Detray, 1963; Sánchez Botija, 1982) and experimental models (Boulanger et al., 1967; Colgrove et al., 1969; Greig, 1972; Greig and Plowright, 1970; Heuschele, 1967; McVicar, 1984; Mebus et al., 1978; Mebus and Dardiri, 1979, 1980; Plowright et al., 1968; Wilkinson and Donaldson, 1977; Wilkinson et al., 1977, 1980). Clinical signs did not vary substantially according to route of inoculation. The greatest consistency was achieved similarly by IM and DC challenge which both had 100% incidence of infection. However, these systems suffer from unnatural delivery of virus (IM) and inability to precisely control dose and timing of challenge (DC). All pigs challenged via DC became infected with ASFV regardless of length of exposure, thereby demonstrating that only 24 h of exposure to shedding animals is required for infection with ASFV. This finding is consistent with the previous works that demonstrated transmission after 24 h (Greig and Plowright, 1970) or 6 h (Ekue et al., 1989) of exposure to donor pigs. However, other studies have concluded that the quantity of virus shed 24 h following pyrexia was inadequate to ensure infection in pigs exposed via direct contact (Heuschele, 1967; Plowright et al., 1968). INP inoculation had higher incidence whilst maintaining a natural exposure route and allowing control of dose and timing of challenge. Additionally, the shortest time to onset of clinical signs was observed within the INP groups, however this difference was not statistically significant.

Precise determination of pig infectious dose 50% ([PID_{50}], i.e. the minimum dose necessary to infected 50% of pigs) for the distinct inoculation routes was not possible due to logistical constraints which dictated some aspects of experimental design. However, the data herein suggests that the required dose of ASFV to establish infection is lowest for IM, intermediate for INP, and highest for IOP delivery of ASFV to domestic swine. Specifically, low dose inoculation ($10^2 HAD_{50}$) incidence proportions were 100% (IM), 50% (INP), and 0% (IOP). Yet, at 10^4 HAD_{50} all routes had 100% incidence of infection. This is consistent with previous studies that have demonstrated low ASFV IM dose (lower than 10^5 $TCID_{50}$) (Pan and Hess, 1984; McVicar, 1984) and high IOP dose (PID_{50} higher than 10^3 $TCID_{50}$) (de Carvalho Ferreira et al., 2012; Greig, 1972; McVicar, 1984). Additionally, Maurer et al. demonstrated that a minimal infectious dose of 10^5 HAD_{50} was necessary to infect pigs orally with ASFV (Maurer and Griesemer, 1958). The precise manner by which specific routes of inoculation of ASFV correlate with variable PID_{50} via distinct pathogenesis mechanisms remains to be elucidated.

The route-specific clinical and virological characteristics described herein are likely to be the result of distinct route-determined, unique pathogenesis events in early ASFV infection. Pigs inoculated IM had the shortest mean survival duration; however the difference was not statistically significant. Shortest onset to viremia amongst IM-inoculated pigs was statistically significant. This may be due to more direct access to the vascular system associated with deposition within the muscle as compared to contact with intact mucosa as occurred with simulated natural challenge routes. Furthermore, the finding of several statistically significant differences in the viremia and shedding parameters between the intramuscular and the direct contact route suggests that the intramuscular route is a poor simulator of natural infection. As a result, inoculation via IM should be avoided in experimental studies trying to mimic a natural course of disease. Contrastingly, both the IOP and INP inoculated pigs had comparable (i.e. not significantly different) results compared to the DC exposed pigs suggesting that IOP and INP are more likely to closely simulate natural infection.

The implied superior infectivity of ASFV via INP inoculation as compared to IOP was reflected in slightly higher incidence proportion and delayed onset of pyrexia and longer survival time seen among INP-inoculated pigs in comparison with all successfully IOP-inoculated pigs (including donors in DC experiment). However, IOP led to significantly higher shedding titers in the tonsil compared with INP inoculation. This effect may have been due to anatomic and physiological factors currently under investigation in our laboratory. IOP inoculation directly deposits the inoculum along the tonsil of the soft palate. While this tonsil has been documented as an early site of viral replication (Heuschele, 1967; Plowright et al., 1968), to our knowledge, specific virus–host interactions in ASFV primary infection in vivo have never been explicitly described. Thus, the lower incidence of infection by the IOP route compared to INP-inoculation could be explained by lack of establishment of systemic disease subsequent to primary infection within the tonsil of the soft palate and other oropharyngeal tissues. Since low-dose INP-inoculated pigs had a higher incidence of successful infection than IOP, the nasopharynx may provide more permissive conditions for establishing systemic ASFV infection. INP inoculation targets nasopharyngeal tissues, including nasal tonsil, dorsal soft palate and walls/roof of the nasopharynx. The data presented in this study suggest that sites targeted by INP inoculation, or other tissues in the respiratory tract, may provide important portals for ASFV infection.

Increased inoculation dose of ASFV was associated with a significant decrease in survival duration of pigs. Animals inoculated with 10^6 HAD_{50}, regardless of route, had a decreased mean number of days to onset of clinical signs (pyrexia, obtundation, hematochezia/melena) and survival compared to the mid and low dosage groups. The number of days to onset of viremia and shedding was decreased compared to mid and low doses as well, suggesting that a higher viral dose resulted in overwhelming primary replication and faster systemic dissemination of the virus. Paradoxically, the high-dose pigs had lower mean maximum clinical scores because of the rapidity of progression to death before the full severity of disease had occurred. Thus, maximum clinical score does not (in itself) describe the severity of disease but must be evaluated in context with duration of survival, virological characteristics, and pathologic findings.

During the clinical phase of infection, ASFV was variably detected in whole blood, serum and tonsil and nasal swabs. Amongst all challenge routes, viremia and shedding commonly either coincided with the onset of pyrexia or it occurred 2 days before or after pyrexia, which is in agreement with other studies (Greig and Plowright, 1970; McVicar, 1984). The DC-exposed pigs had the highest mean ASFV titer within whole blood. Throughout the course of this study whole blood samples had titers of almost 2 log_{10} higher than serum samples. This is consistent with previous studies that has described greater number of mature virus particles associated with erythrocytes and within circulating monocytes in whole blood, in comparison to free virions within serum (Genovesi et al., 1988; Wardley and Wilkinson, 1977).

Detection of ASFV within secretions (tonsil scraping and nasal swabs) varied across infection routes and dosage groups. ASFV titers in tonsil scrapings and nasal swabs were generally quite similar, suggesting that virus was released from both regions and/or

virus quantities equilibrate between nasal and oral secretions. One noteworthy exception to this trend was amongst DC-exposed pigs wherein ASFV was consistently detected in tonsil scrapings (for 1–6 days) prior to detection in nasal swabs. Across all three inoculation routes, initial detection of ASFV shedding occurred at the same time, or subsequent to, virus detection in whole blood and serum. However within the contact challenge study, ASFV was detected in tonsil scraping samples 1–4 days prior to detection in blood of IOP-inoculated donors and DC-exposed pigs. This indicates that, under these distinct conditions, it was uniquely possible to detect local viral replication and shedding within the oral cavity prior to systemic dissemination. This is consistent with previous studies in which ASFV could be detected within oral and pharyngeal swabs 1–2 days prior to viremia and pyrexia (Greig and Plowright, 1970) or as early as 24 h post inoculation (hpi) in lymphoid and respiratory tract tissues (Heuschele, 1967; Plowright et al., 1968).

Gross and histologic changes in pigs in the late stages of disease were similar regardless of route of infection and were consistent with postmortem findings described in field and experimental cases of ASF. Systemic hemorrhages affecting the kidney and heart and pulmonary congestion and edema are similar to previously described lesions (Detray, 1963; Mebus, 1988). Amongst individual pigs, severity of lesions varied from mild to severe based upon recently published recommendations for standardization of pathologic findings for ASF (Galindo-Cardiel et al., 2013). The hallmark depletion and apoptosis of lymphocytes throughout the lymphoid tissue with subsequent infiltration of macrophages commonly described for ASF (Gómez-Villamandos et al., 2003) was observed histologically within this study. Detailed pathological description will be forthcoming in a separate manuscript (Howey et al., in preparation).

Immunohistochemical visualization of ASFV antigen was demonstrated in tonsil of the soft palate of pigs in terminal stages of ASF, further confirming the presence and characterizing the distribution of virus within tissues. Immunoreactive cells were large mononuclear cells and colocalization with monocyte/macrophage cellular antigen suggested that the predominate infected cell type is of monocytic origin. Colocalization of ASFV with CD163 supports previous suggestions that this molecule may serve as an important ASFV receptor (Alonso et al., 2013; Sánchez-Torres et al., 2003). Additionally, this is consistent with numerous reports indicating monocytotropism of ASFV (Detray, 1963; Tulman et al., 2009; Wardley and Wilkinson, 1978).

5. Conclusions

The current study has demonstrated that four modes of challenging pigs with ASFV result in similar ASF syndromes with slight variations. The IM route may be advantageous for the study of late stage ASF events; however several significant differences from DC indicated this is not an optimal system to simulate natural infection. DC would be preferable when simulating a natural manner of transmission was utmost priority; however this system is expensive due to the inclusion of additional (donor) animals in each experiment and does not allow control of dose quantity and timing. The two simulated natural manners of inoculation, IOP and INP, allowed precise control of timing and dose of ASFV delivery and had similar incidence of successful infection of pigs. Overall, the slightly lower minimum infectious dose and slightly higher incidence of infection subsequent to INP inoculation in these experiments suggest that INP may be the preferred route of inoculation for pathogenesis and vaccine challenge studies of pigs with ASFV. Further validation of these techniques with larger sample sizes would contribute to stronger conclusions regarding the differences between the infection systems described herein.

Conflict of interests

The authors do not have any financial or personal conflict of interests.

Acknowledgements

EH planned and carried out the live animal experiments, virus isolation, immunomicroscopy and drafted the manuscript. VO provided expertise in conceptual design, as well as optimization and troubleshooting of techniques. HF performed the statistical analysis and helped with manuscript revisions. MB consulted and contributed on all aspects of study design and implementation; also provided critical review of manuscript. JA conceived the study, oversaw the implementation of experiments, helped draft and revised the manuscript. All authors read and approved the final manuscript.

We wish to thank Meghan Tucker, George Smoliga and Ethan Hartwig for superb technical support. Luis Rodriguez and Carolina Stenfeldt are acknowledged for critical review of the manuscript. Juan Pacheco supported data manipulation and consulted regarding VI technique. In addition, we would like to thank the staff of the Animal Resource Branch for their support in collecting data during animal experiments.

This research was funded, in part, by Agricultural Research Service–Current Research Information System project No. 1940-32000-056-00D. Additional funds came from an interagency agreement with the Science and Technology Directorate of the U.S. Department of Homeland Security under Award Number HSHQPM-12-X-00005. Erin Howey's position is funded through the Plum Island Animal Disease Research Participation Program administered by the Oak Ridge Institute for Science and Education through an interagency agreement between the U.S. Department of Energy and the U.S. Department of Agriculture.

References

Alonso, C., Galindo, I., Cuesta-Geijo, M.A., Cabezas, M., Hernaez, B., Muñoz-Moreno, R., 2013. African swine fever virus–cell interactions: from virus entry to cell survival. Virus Res. 173 (1), 42–57.

Arzt, J., Gregg, D.A., Clavijo, A., Rodriguez, L.L., 2009. Optimization of immunohistochemical and fluorescent antibody techniques for localization of foot-and-mouth disease virus in animal tissues. J. Vet. Diagn. Invest. 21 (6), 779–792.

Arzt, J., White, W.R., Thomsen, B.V., Brown, C.C., 2010. Agricultural diseases on the move early in the third millennium. Vet. Pathol. 47 (1), 15–27.

Ayoade, G., Adeyemi, I., 2003. African swine fever: an overview. Rev. Élev. Méd. Vét. Pays Trop. 56 (3–4), 129–134.

Ballester, M., Galindo-Cardiel, I., Gallardo, C., Argilaguet, J.M., Segalés, J., Rodríguez, J.M., Rodríguez, F., 2010. Intranuclear detection of African swine fever virus DNA in several cell types from formalin-fixed and paraffin-embedded tissues using a new in situ hybridisation protocol. J. Virol. Methods 168 (1–2), 38–43.

Boinas, F.S., Hutchings, G.H., Dixon, L.K., Wilkinson, P.J., 2004. Characterization of pathogenic and non-pathogenic African swine fever virus isolates from *Ornithodoros erraticus* inhabiting pig premises in Portugal. J. Gen. Virol. 85 (8), 2177–2187.

Borca, M.V., Carrillo, C., Zsak, L., Laegreid, W.W., Kutish, G.F., Neilan, J.G., Burrage, T.G., Rock, D.L., 1998. Deletion of a CD2-like gene, 8-DR, from African swine fever virus affects viral infection in domestic swine. J. Virol. 72 (4), 2881–2889.

Boulanger, P., Bannister, G.L., Gray, D.P., Ruckerbauer, G.M., Willis, N.G., 1967. African swine fever. II. Detection of the virus in swine tissues by means of the modified direct complement-fixation test. Can. J. Comp. Med. Vet. Sci. 31 (1), 7–11.

Carrasco, L., Chacon, M.d.L.F., Martin de Las Mulas, J., Gómez-Villamandos, J.C., Sierra, M.A., Villeda, C.J., Wilkinson, P.J., 1997. Ultrastructural changes related to the lymph node haemorrhages in acute African swine fever. Res. Vet. Sci. 62 (3), 199–204.

Carrasco, L., de Lara, F.C., Martín de las Mulas, J., Gómez-Villamandos, J.C., Hervás, J., Wilkinson, P.J., Sierra, M.A., 1996. Virus association with lymphocytes in acute African swine fever. Vet. Res. 27 (3), 305–312.

Champely, S., 2012. pwr: Basic functions for power analysis. R package version 1.1.1. http://CRAN.R-project.org/package=pwr

Childerstone, A., Takamatsu, H., Yang, H., Denyer, M., Parkhouse, R.M., 1998. Modulation of T cell and monocyte function in the spleen following infection of pigs with African swine fever virus. Vet. Immunol. Immunopathol. 62 (4), 281–296.

Colgrove, G.S., Haelterman, E.O., Coggins, L., 1969. Pathogenesis of African swine fever in young pigs. Am. J. Vet. Res. 30 (8), 1343–1359.
Costard, S., Mur, L., Lubroth, J., Sánchez-Vizcaíno, J.M., Pfeiffer, D.U., 2013. Epidemiology of African swine fever virus. Virus Res. 173 (1), 191–197.
Cuesta-Geijo, M.A., Galindo, I., Hernáez, B., Quetglas, J.I., Dalmau-Mena, I., Alonso, C., 2012. Endosomal maturation, Rab7 GTPase and phosphoinositides in African swine fever virus entry. PLoS ONE 7 (11), e48853.
de Carvalho Ferreira, H.C., Weesendorp, E., Elbers, A.R., Bouma, A., Quak, S., Stegeman, J.A., Loeffen, W.L., 2012. African swine fever virus excretion patterns in persistently infected animals: a quantitative approach. Vet. Microbiol. 160 (3–4), 327–340.
de Carvalho Ferreira, H.C., Weesendorp, E., Quak, S., Stegeman, J.A., Loeffen, W.L., 2013a. Quantification of airborne African swine fever virus after experimental infection? Vet. Microbiol. 165 (3–4), 243–251.
de Carvalho Ferreira, H.C., Backer, J.A., Weesendorp, E., Klinkenberg, D., Stegeman, J.A., Loeffen, W.L., 2013b. Transmission rate of African swine fever virus under experimental conditions. Vet. Microbiol. 165 (3–4), 296–304.
Detray, D.E., 1963. African swine fever. Adv. Vet. Sci. Comp. Med. 19, 299–333.
Ekue, N.F., Wilkinson, P.J., Wardley, R.C., 1989. Infection of pigs with the Cameroon isolate (Cam/82) of African swine fever virus. J. Comp. Pathol. 100 (2), 145–154.
Fernández de Marco, M., Salguero, F.J., Bautista, M.J., Núñez, A., Sánchez-Cordón, P.J., Gómez-Villamandos, J.C., 2007. An immunohistochemical study of the tonsils in pigs with acute African swine fever virus infection. Res. Vet. Sci. 83 (2), 198–203.
Galindo-Cardiel, I., Ballester, M., Solanes, D., Nofrarías, M., López-Soria, S., Argilaguet, J.M., Lacasta, A., Accensi, F., Rodríguez, F., Segalés, J., 2013. Standardization of pathological investigations in the framework of experimental ASFV infections. Virus Res. 173 (1), 180–190.
Galindo, I., Hernáez, B., Muñoz-Moreno, R., Cuesta-Geijo, M.A., Dalmau-Mena, I., Alonso, C., 2012. The ATF6 branch of unfolded protein response and apoptosis are activated to promote African swine fever virus infection. Cell Death Dis. 3 (7), e341.
Genovesi, E.V., Knudsen, R.C., Whyard, T.C., Mebus, C.A., 1988. Moderately virulent African swine fever virus infection: blood cell changes and infective virus distribution among blood components. Am. J. Vet. Res. 49 (3), 338.
Gómez-Villamandos, J.C., Bautista, M.J., Carrasco, L., Caballero, M.J., Hervás, J., Villeda, C.J., Wilkinson, P.J., Sierra, M.A., 1997a. African swine fever virus infection of bone marrow: lesions and pathogenesis. Vet. Pathol. 34 (2), 97–107.
Gómez-Villamandos, J.C., Bautista, M.J., Carrasco, L., Chacón-Manrique de Lara, F., Hervás, J., Wilkinson, P.J., Sierra, M.A., 1998. Thrombocytopenia associated with apoptotic megakaryocytes in a viral haemorrhagic syndrome induced by a moderately virulent strain of African swine fever virus. J. Comp. Pathol. 118 (1), 1–13.
Gómez-Villamandos, J.C., Carrasco, L., Bautista, M.J., Sierra, M.A., Quezada, M., Hervás, J., Chacón, M.de L., Ruiz-Villamor, E., Salguero, F.J., Sónchez-Cordón, P.J., Romanini, S., Núñez, A., Mekonen, T., Méndez, A., Jover, A., 2003. African swine fever and classical swine fever: a review of the pathogenesis. Dtsch. Tierarztl. Wochenschr. 110 (4), 165–169.
Gómez-Villamandos, J.C., Hervás, J., Méndez, A., Carrasco, L., Martín de las Mulas, J., Villeda, C.J., Wilkinson, P.J., Sierra, M.A., 1995a. Experimental African swine fever: apoptosis of lymphocytes and virus replication in other cells. J. Gen. Virol. 76 (Pt. 9), 2399–2405.
Gómez-Villamandos, J.C., Hervás, J., Méndez, A., Carrasco, L., Villeda, C.J., Wilkinson, P.J., Sierra, M.A., 1995b. Ultrastructural study of the renal tubular system in acute experimental African swine fever: virus replication in glomerular mesangial cells and in the collecting ducts. Arch. Virol. 140 (3), 581–589.
Gómez-Villamandos, J.C., Hervás, J., Moreno, C., Carrasco, L., Bautista, M.J., Caballero, J.M., Wilkinson, P.J., Sierra, M.A., 1997b. Subcellular changes in the tonsils of pigs infected with acute African swine fever virus. Vet. Res. 28 (2), 179–189.
Greig, A., 1972. Pathogenesis of African swine fever in pigs naturally exposed to the disease. J. Comp. Pathol. 82 (1), 73–79.
Greig, A., Plowright, W., 1970. The excretion of two virulent strains of African swine fever virus by domestic pigs. J. Hyg. (Lond.) 68 (4), 673–682.
Hamdy, F.M., Dardiri, A.H., 1984. Clinical and immunologic responses of pigs to African swine fever virus isolated from the Western Hemisphere. Am. J. Vet. Res. 45 (4), 711.
Heuschele, W.P., 1967. Studies on the pathogenesis of African swine fever. I. Quantitative studies on the sequential development of virus in pig tissues. Arch. Gesamte Virusforsch. 21 (3), 349–356.
http://www.oie.int/wahis_2/public/wahid.php/Wahidhome/Home (accessed 3.09.13). Jori, F., Vial, L., Penrith, M.L., Perez-Sanchez, R., Etter, E., Albina, E., Michaud, V., Roger, F., 2013. Review of the sylvatic cycle of African swine fever in sub-Saharan Africa and the Indian Ocean. Virus Res. 173 (1), 212–227.
Mahy, B.W.J., Kangro, H.O. (Eds.), 1996. Virology Methods Manual. Academic Press, San Diego.
Maurer, F.D., Griesemer, R.A., 1958. The pathology of African swine fever; a comparison with hog cholera. Am. J. Vet. Res. 19 (72), 517–539.
McVicar, J.W., 1984. Quantitative aspects of the transmission of African swine fever. Am. J. Vet. Res. 45 (8), 1535–1541.
Mebus, C.A., Dardiri, A.H., 1979. Additional characteristics of disease caused by the African swine fever viruses isolated from Brazil and the Dominican Republic. Proc. Annu. Meet. U. S. Anim. Health Assoc. (83), 227–239.
Mebus, C.A., Dardiri, A.H., 1980. Western hemisphere isolates of African swine fever virus: asymptomatic carriers and resistance to challenge inoculation. Am. J. Vet. Res. 41 (11), 1867–1869.
Mebus, C.A., Dardiri, A.H., Hamdy, F.M., Ferris, D.H., Hess, W.R., Callis, J.J., 1978. Some characteristics of African swine fever viruses isolated from Brazil and the Dominican Republic. Proc. Annu. Meet. U. S. Anim. Health Assoc. (82), 232–236.
Mebus, C.A., 1988. African swine fever. Adv. Virus Res. 35, 251–269.
Oura, C.A., Powell, P.P., Parkhouse, R.M., 1998. Detection of African swine fever virus in infected pig tissues by immunocytochemistry and in situ hybridisation. J. Virol. Methods 72 (2), 205–217.
Pan, I.C., Hess, W.R., 1984. Virulence in African swine fever: its measurement and implications. Am. J. Vet. Res. 45 (2), 361–366.
Penrith, M.L., 2009. African swine fever. Onderstepoort J. Vet. Res. 76 (1), 91–95.
Plowright, W., Parker, J., Staple, R.F., 1968. The growth of a virulent strain of African swine fever virus in domestic pigs. J. Hyg. (Lond.) 66 (1), 117–134.
R Core Team, 2013. R: A Language and Environment for Statistical Computing. R Foundation for Statistical Computing, Vienna, Austria http://www.R-project.org/
Salguero, F.J., Sánchez-Cordón, P.J., Sierra, M.A., Jover, A., Núñez, A., Gómez-Villamandos, J.C., 2004. Apoptosis of thymocytes in experimental African Swine Fever virus infection. Histol. Histopathol. 19 (1), 77–84.
Sánchez-Torres, C., Gómez-Puertas, P., Gómez-del-Moral, M., Alonso, F., Escribano, J.M., Ezquerra, A., Domínguez, J., 2003. Expression of porcine CD163 on monocytes/macrophages correlates with permissiveness to African swine fever infection. Arch. Virol. 148 (12), 2307–2323.
Sánchez-Vizcaíno, J.M., Mur, L., Martínez-López, B., 2012. African swine fever: an epidemiological update. Transbound Emerg. Dis. 59 (s1), 27–35.
Sánchez Botija, C., 1982. African Swine Fever. New developments. Rev. Sci. Tech. Off. Int. Epiz. 1 (4), 1065–1094.
Tulman, E.R., Delhon, G.A., Ku, B.K., Rock, D.L., 2009. African swine fever virus. Curr. Top. Microbiol. Immunol. 328, 43–87.
Therneau, T., 2013. A Package for Survival Analysis in S. R package version 2.37-4. http://CRAN.R-project.org/package=survival
Wardley, R.C., de, M.A.C., Black, D.N., de Castro Portugal, F.L., Enjuanes, L., Hess, W.R., Mebus, C., Ordas, A., Rutili, D., Sánchez-Vizcaíno, J., Vigário, J.D., Wilkinson, P.J., Moura Nunes, J.F., Thomson, G., 1983. African swine fever virus. Brief review. Arch. Virol. 76 (2), 73–90.
Wardley, R.C., Wilkinson, P.J., 1978. The growth of virulent African swine fever virus in pig monocytes and macrophages. J. Gen. Virol. 38 (1), 183–186.
Wardley, R.C., Wilkinson, P.J., 1977. The association of African swine fever virus with blood components of infected pigs. Arch. Virol. 55 (4), 327–334.
Wilkinson, P.J., Donaldson, A.I., 1977. Transmission studies with African swine fever virus. The early distribution of virus in pigs infected by airborne virus. J. Comp. Pathol. 87 (3), 497–501.
Wilkinson, P.J., Donaldson, A.I., Greig, A., Bruce, W., 1977. Transmission studies with African swine fever virus. Infections of pigs by airborne virus. J. Comp. Pathol. 87 (3), 487–495.
Wilkinson, P.J., Lawman, M.J., Johnston, R.S., 1980. African swine fever in Malta, 1978. Vet. Rec. 106 (5), 94–97.
Wilkinson, P.J., Wardley, R.C., Williams, S.M., 1981. African swine fever virus (Malta/78) in pigs. J. Comp. Pathol. 91 (2), 277–284.
Wilkinson, P.J., Wardley, R.C., Williams, S., 1983. Studies in pigs infected with African swine fever virus (Malta/78). In: Wilkinson, P.J. (Ed.), CEC/FAO Expert Consultation on African Swine Fever Research. September 1981, Sardinia.
Zsak, L., Borca, M.V., Risatti, G.R., Zsak, A., French, R.A., Lu, Z., Kutish, G.F., Neilan, J.G., Callahan, J.D., Nelson, W.M., Rock, D.L., 2005. Preclinical diagnosis of African swine fever in contact-exposed swine by a real-time PCR assay. J. Clin. Microbiol. 43 (1), 112–119.

AUTHOR INDEX

Section 1: Lawrence, P., Larocco, M.A., Schafer, E.A., Baxt, B., Rieder, A.E. 2013. Examination of soluble integrin resistant mutants of foot-and-mouth disease virus (FMDV). Virology Journal. 10(1):2.

Section 2: Ehizibolo, D.O., Perez, A.M., Carrillo, C., Pauszek, S.J., Al Khamis, M., Ajogi, I., Umoh, J.U., Kazeem, H.M., Ehizibolo, P.O., Fabian, A., Berninger, M., Moran, K., Rodriguez, L.L., Metwally, S.A. 2013. Epidemiological analysis, serological prevalence, and genotypic analysis of foot-and-mouth disease in Nigeria 2008-2009. Transboundary and Emerging Diseases. DOI:10.1111/tbed.12054.

Section 3: Loughran, G., Libbey, J.E., Uddowla, S., Scallan, M.F., Ryan, M.D., Fujinami, R.S., Rieder, A.E., Atkins, J.F. 2013. Theiler's murine encephalomyelitis virus contrasts with encephalomyocarditis and foot-and-mouth disease viruses in its functional utilization of the StopGo non-standard translation mechanism. Journal of General Virology. 94(2):348-353.

Section 4: Diaz San Segundo, F.C., Dias, C.C., Moraes, M.P., Weiss, M., Perez-Martin, E., Owens, G., Custer, M., Kamrud, K., De Los Santos, T.B., Grubman, M.J. 2013. Venezuelan Equine Encephalitis Virus replicon particles can induce rapid protection against Foot-and-Mouth Disease Virus. Journal of Virology. 87(10):5447-5460.

Section 5: Alejo, D.M., Moraes, M.P., Liao, X., Dias, C.C., Tulman, E.R., Diaz San Segundo, F.C., Rood, D., Grubman, M.J., Silbart, L.K. 2013. An adenovirus vectored mucosal adjuvant augments protection of mice immunized intranasally with an adenovirus-vectored foot-and-mouth disease virus subunit vaccine. Vaccine. 313(18):2302-2309.

Section 6: Larocco, M.A., Krug, P.W., Kramer, E., Ahmed, Z., Pacheco Tobin, J., Duque, H., Baxt, B., Rodriguez, L.L. 2013. A continuous bovine kidney cell line constitutively expressing bovine alpha v beta 6 integrin has increased susceptibility to foot-and-mouth disease virus. Journal of Clinical Microbiology. 51(6):1714-1720.

Section 7: Rai, D.K., Schafer, E.A., Singh, K., Mcintosh, M., Sarafianos, S., Rieder, A.E. 2013. Repeated exposure to 5D9, an inhibitor of 3D polymerase, effectively limits the replication of Foot-and-Mouth Disease Virus in host cells. Antiviral Research. 98(3):380-385.

Section 8: Gladue, D.P., O'Donnell, V., Baker-Branstetter, R., Holinka-Patterson, L.G., Pacheco Tobin, J., Fernandez Sainz, I.J., Lu, Z., Brocchi, E., Piccone, M.E., Fletcher, P., Ambroggio, X., Rodriguez, L.L., Borca, M.V. 2013. Foot-and-mouth disease virus modulates cellular vimentin for virus survival. Journal of Virology. 87(12):6794-6803.

AUTHOR INDEX

Section 9: Maree, F.F., Blignaut, B., De Beer, T.A., Rieder, A.E. 2013. Analysis of SAT type foot-and-mouth disease virus capsid proteins and the identification of putative amino acid residues in virus stability. PLoS One. 8(5):e61612.

Section 10: Zhu, J.J., Arzt, J., Puckette, M.C., Smoliga, G.R., Pacheco Tobin, J., Rodriguez, L.L. 2013. Mechanisms of foot-and-mouth disease virus tropism inferred from differential tissue gene expression. PLoS One. 8(5):e64119.

Section 11: Toka, F.N., Golde, W.T. 2013. Cell mediated innate responses of cattle and swine are diverse during foot-and-mouth disease virus (FMDV) infection: A unique landscape of innate immunity. Immunology Letters. 152(2):135-143.

Section 12: Grubman, M.J., De Los Santos, T.B. 2013. Foot-and-mouth disease virus L peptidase. In: Neil D. Rawlings and Guy S. Salvesen, editors. Handbook of Proteolytic Enzymes. 3rd Edition. Oxford,UK:Academic Press. p.2183-2186.

Section 13: Patch, J.R., Kenney, M.A., Pacheco Tobin, J., Grubman, M.J., Golde, W.T. 2013. Characterization of cytotoxic T lymphocyte function following foot-and-mouth disease virus infection and vaccination. Viral Immunology. 26(4):239-249.

Section 14: Di Giacomo, S., Brito, B.P., Perez, A.M., Bucafusco, D., Pega, J., Rodriguez, L.L., Borca, M.V., Perez-Filgueira, M. 2013. Heterogeneity in the antibody response to foot-and-mouth disease primo-vaccinated calves. Transboundary and Emerging Diseases. DOI:10.1111/tbed.12130.

Section 15: Uddowla, S., Pacheco Tobin, J., Larson, C., Bishop, E.A., Rodriguez, L.L., Rai, D., Arzt, J., Rieder, A.E. 2013. Characterization of a chimeric foot-and-mouth disease virus bearing bovine rhinitis B virus leader proteinase. Virology. 447(1-2):172-180.

Section 16: Pacheco Tobin, J., Gladue, D.P., Holinka-Patterson, L.G., Arzt, J., Bishop, E.A., Smoliga, G.R., Pauszek, S.J., Bracht, A.J., O'Donnell, V., Fernandez-Sainz, I., Fletcher, P., Piccone, M.E., Rodriguez, L.L., Borca, M.V. 2013. A partial deletion in non-structural protein 3A can attenuate foot-and-mouth disease virus in cattle. Virology. 446(1-2):260-267.

Section 17: Largo, E., Gladue, D.P., Huarte, N., Borca, M.V., Nieva, J.L. 2013. Pore-forming activity of pestivirus p7 in a minimal model system supports genus-specific viroporin function. Antiviral Research. 101:30-36.

Section 18: Howey, E.B., O'Donnell, V., De Carvalho Ferreira, H.C., Borca, M.V., Arzt, J. 2013. The pathogenesis of highly virulent African Swine Fever virus in domestic pigs exposed

via intraoropharyngeal, intranasopharyngeal, and intramuscular inoculation, and by direct contact with infected pigs. Virus Research. 178(2):328-339.